# SEQUENCE STRATIGRAPHY AND PROCESS SEDIMENTOLOGY OF THE CAMBRIAN OF SW WALES

By

ANDREW JAMES REES

A thesis submitted to
The University of Birmingham for the degree of
DOCTOR OF PHILOSOPHY

School of Geography, Earth, and Environmental Sciences,
The University of Birmingham,
May 2005

UNIVERSITY OF
BIRMINGHAM

## University of Birmingham Research Archive

### e-theses repository

This unpublished thesis/dissertation is copyright of the author and/or third parties. The intellectual property rights of the author or third parties in respect of this work are as defined by The Copyright Designs and Patents Act 1988 or as modified by any successor legislation.

Any use made of information contained in this thesis/dissertation must be in accordance with that legislation and must be properly acknowledged. Further distribution or reproduction in any format is prohibited without the permission of the copyright holder.

## ABSTRACT

Avalonian-Cadomian and related terranes of the circum-North Atlantic constitute portions of an accretionary orogen that developed on an active Gondwanan margin at the periphery of the Neoproterozoic supercontinent Vendia. These peri-Gondwanan terranes are defined by their Neoproterozoic evolution on an active continental margin, and by the peri-Gondwanan "Acado-Baltic" fauna of their Cambrian–Ordovician overstep sequence. Unlike most recent studies on the early evolution of Avalonia, this contribution focuses on the Cambrian overstep sequence (the Dyfed Supergroup) exposed in SW Wales (East Avalonia).

High-resolution sequence-stratigraphic techniques are applied to the Dyfed Supergroup across southern Britain to facilitate the integration of a revised lithostratigraphy into a unified Avalonian chronostratigraphy based on successions in Atlantic Canada (West Avalonia). The relative ease of integration reflects the shared epeirogenic history, sediment sources and accumulation history of a microcontinent unified by the Early Cambrian. The occurrence of lithologically similar and coeval depositional sequences may be relied upon to determine the limits of the Avalonian Superterrane in the Acadian-Caledonian orogen.

A broad subdivision of Cambrian stratigraphy into tectonically active and passive phases of sedimentation is recognized. Megasequence 1, which constitutes all of the Lower Cambrian and most of the Middle Cambrian, records transform termination of Avalonian subduction following oblique convergence, and the accretion of island arcs to the northern periphery of Gondwana. Under transpressional regimes, late Precambrian arc-related basins were inverted and recycled into Lower and Middle Cambrian pull-apart successor basins dominated, at their margins, by alluvial fan and fan-delta depositional systems. Megasequence 2 (Upper Cambrian to Lower Ordovician) reflects passive margin sedimentation, with Avalonia acting as a sediment sink to vast quantities of fine-grained sediment transferred off Gondwana by large, mature fluvial systems. This marked the culmination of the Avalonian-Cadomian orogenic cycle.

*For my parents and stepfather…….*

## AKNOWLEDGEMENTS

I am gratefully indebted to many people for their generous assistance during the course of this project. Firstly, completion would not have been possible without the help and encouragement of my supervisors Alan Thomas, Peter Turner and Paul Smith. An extended thanks to Alan for just being great all the time and always being so understanding, even when sometimes I probably didn't deserve it.

Many thanks are owed to Paul Hands, for preparing all the thin sections for the project, and for taking my mind off work with endless discussions on our shared passion, Liverpool FC. Aruna Mistry and John Clatworthy are thanked for being on hand for all kinds of problems, most of them well beyond the call of duty.

A huge thank you is extended to Dr. Adrian Rushton (Natural History Museum), who's help and endless e-mails have contributed so much to my understanding of Cambrian stratigraphy, without his endless enthusiasm and patience, I would surely have gone mad with frustration.

A number of people gave their time in productive conversation that considerably improved the content of this thesis. They include my Ph.D. panel members, Ken Thomson and Phil Donoghue, Mark Williams and Nigel Smith (BGS), Paul Myrow, Bill Arnott, Emiliano Mutti, Arne Nielson (for unpublished Cambrian sea level curves), and Gorden Baird.

Thanks to my fellow Ph.D. students for making the last 4 years just about bearable! These include: Big Ben, Brian, Liam, Big Jules (Mad' Ed), Neil (also a bit mad), the Wilson Twins, Nick, Dirk, Blum, Cockney John, Mike (G-S), Abdul no: 1 (aka harassed Abdul) and Abdul no: 2 (aka Happy Abdul), all true friends, I feel blessed!!!!!

My love and thanks go to my parents, to whom I have dedicated this thesis. Without their support, generosity and understanding, this work could not have been completed.

Last, but by no means least, I thank Vicky for being amazing and so understanding, writing up would have been even worse without you.

This project was funded by a University of Birmingham Studentship with an additional AAPG Grants-in-Aid Award for 2001.

# CONTENTS

Table of contents i
List of figures vi
List of tables xiv

*Chapter 1:*
**Introduction** 1

*Chapter 2:*
**Stratigraphy, sedimentology and sequence stratigraphy of the Dyfed Supergroup in SW Wales: Implications for a unified Avalonian chronostratigraphy**

2.1. Introduction 4
2.2. Stratigraphy
2.2.1. Caerfai Group 7
2.2.1.1. Ogof Golchfa Formation 11
2.2.1.2. St Non's Formation 16
2.2.1.3. Caerfai Bay Formation 19
2.2.1.4. Caerbwdy Formation 22
2.2.1.5. Newgale Formation 24
2.2.1.5.1. Trwyncynddeiriog Member 26
2.2.1.5.2. Pen-y-Cyffrwy Member 29
2.2.1.5.3. Cwm Mawr Member 31
2.2.1.6. Porth Clais Formation 34
2.2.2. Porth-y-rhaw Group 40
2.2.2.1. Whitesand Bay Formation 43
2.2.2.2. Menevia Formation 46
2.2.2.3. Aber Llong Formation 50
2.2.2.4. Ogof Velvet Formation 54
2.2.2.5. Treffgarne Bridge Formation 59
2.3. The concept of a unified Avalonian chronostratigraphy 60
2.4. Sequence stratigraphy 63
2.4.1. Depositional sequences
2.4.1.1. Sequence 3 63
2.4.1.2. Sequence 4 65
2.4.1.3. Sequence 5 70
2.4.1.4. Sequence 6 71

2.4.1.5. Sequence 7 76
2.4.1.6. Sequence 8 79
2.5. Tectonostratigraphy, provenance and basin analysis 89
2.5.1. Megasequence 1 90
2.5.2. Megasequence 2 93
2.6. Conclusions 97

*Chapter 3:*

**Basin margin sedimentology and tectonic implications of Early Cambrian rifting in Eastern Avalonia (Southern Britain): Transtensional successor basin development in the Lower Cambrian (Caerfai Group) of SW Wales, UK.**

3.1. Introduction 99
3.2. Basin margin sedimentology and lithofacies associations
3.2.1. Lithofacies Association A 103
3.2.1.1. Facies A1: unstratified, tabular, clast-supported conglomerate
3.2.1.1.1. Description 103
3.2.1.1.2. Interpretation 106
3.2.1.2. Facies A2: muddy-matrix-supported conglomerate
3.2.1.2.1. Description 110
3.2.1.2.2. Interpretation 110
3.2.1.3. Facies A3: unstratified, lenticular sand-matrix-supported conglomerate
3.2.1.3.1. Description 111
3.2.1.3.2. Interpretation 111
3.2.1.4. Facies A4: purple and red silty mudstone
3.2.1.4.1. Description 113
3.2.1.4.2. Interpretation 113
3.2.2. Lithofacies Association B 114
3.2.2.1. Facies B1: graded pebble conglomerate
3.2.2.1.1. Description 114
3.2.2.1.2. Interpretation 115
3.2.2.2. Facies B2: stratified pebble conglomerate
3.2.2.2.1. Description 116
3.2.2.2.2. Interpretation 118
3.2.2.3. Facies B3: stratified lenticular sandstone and massive silty mudstone
3.2.2.3.1. Description 119
3.2.2.3.1. Interpretation 120
3.2.3. Lithofacies Association C
3.2.3.1. Facies C1: well segregated pebble conglomerate and coarse sandstone
3.2.3.1.1. Description 120
3.2.3.1.2. Interpretation 122
3.2.3.2. Facies C2: trough cross-stratified coarse sandstone
3.2.3.2.1. Description 126
3.1.3.2.2. Interpretation 126
3.2.3.3. Facies C3: hummocky cross-stratified fine sandstone
3.2.3.3.1. Description 127

3.2.3.3.2. Interpretation 129
3.3. Palaeoenvironment and implications for basin margin evolution
3.3.1. Facies Association A 131
3.3.2. Facies Association B 135
3.3.3. Facies Association C 137
3.4. Petrography and provenance analysis
3.4.1. Methodology 140
3.4.2. Framework grains
3.4.2.1. Texture 143
3.4.2.2. Quartz 144
3.4.2.3. Feldspar 146
3.4.2.4. Lithics 146
3.4.2.5. Accessory minerals 148
3.4.3. Petrofacies discrimination 149
3.4.4. Petrofacies
3.4.4.1. Petrofacies A1: volcanic lithic petrofacies
3.4.4.1.1. Description 151
3.4.4.1.2. Interpretation 151
3.4.4.2. Petrofacies A2: metasedimentary lithic petrofacies
3.4.4.2.1. Description 152
3.4.4.2.2. Interpretation 153
3.4.4.3. Petrofacies B: high quartz petrofacies
3.4.4.3.1. Description 155
3.4.4.3.2. Interpretation 155
3.4.5. Quartz type 156
3.4.6. Controls on sandstone composition
3.4.6.1. Compositional variations due to diagenetic alteration 157
3.4.6.2. Compositional variations due to climate and relief in the source area 157
3.4.7. Source area 160
3.5. Tectonostratigraphy
3.5.1. Stratal architecture and controlling mechanisms 162
3.5.2. Tectonosedimentary model and basin margin evolution 167
3.5.2.1. Stage 1: syn-extension (phases 1–4) 168
3.5.2.2. Stage 2: transitional extension (phase 5) 170
3.5.2.3. Stage 3: post-extension (phase 6) 170
3.5.3. The extensional regime
3.5.3.1. General 171
3.5.3.2. The basin-fill 171
3.6. Conclusions: Implications for the late Neoproterozoic–Cambrian tectonostratigraphic evolution of Eastern Avalonia 173

***Chapter 4:***

**The anatomy of a flood-dominated fan-delta from the Middle Cambrian (St Davids Series) of SW Wales, UK: Processes, facies and classification**

4.1. Introduction 176
4.2. Geological setting 179
4.3. Terminology and definition of processes
4.3.1. Fan-deltas 181
4.3.2. Hyperconcentrated flow 184

4.3.3. High-density turbidity currents 186
4.4. Lithofacies and process sedimentology
4.4.1. Facies Association A: alluvial fan
4.4.1.1. Facies A1: unstratified, tabular pebbly sandstone
4.4.1.1.1. Description 189
4.4.1.1.2. Interpretation 193
4.4.1.2. Facies A2: unstratified, lenticular pebbly sandstone
4.4.1.2.1. Description 194
4.4.1.2.2. Interpretation 196
4.4.1.3. Palaeoenvironment and process sedimentology 197
4.4.2. Facies Association B: fan-delta plain
4.4.2.1. Facies B1: wavy and flaser bedded silty mudstone
4.4.2.1.1. Description 201
4.4.2.1.1. Interpretation 201
4.4.2.3. Facies B2: unstratified, lenticular pebbly sandstone
4.4.2.2.1. Description 203
4.4.2.2.2. Interpretation 203
4.4.2.4. Facies B3: unstratified, tabular sandstone
4.4.2.3.1. Description 206
4.4.2.3.2. Interpretation 206
4.4.2.5. Facies B4: muddy-matrix-supported conglomerate
4.4.2.4.1. Description 207
4.4.2.4.2. Interpretation 208
4.4.2.5. Palaeoenvironment and process sedimentology 209
4.4.3. Facies Association C: channel–lobe transition
4.4.3.1. Facies C1: tabular, unstratified pebbly sandstone
4.4.3.1.1. Description 211
4.4.3.1.2. Interpretation 212
4.4.3.2. Facies C2: massive to normal, and inversely graded, unstratified sandstone
4.4.3.2.1. Description 214
4.4.3.2.2. Interpretation 214
4.4.3.3. Palaeoenvironment and process sedimentology 216
4.4.4. Facies Association D: flood-generated delta-front sandstone lobe
4.4.4.1. Facies D1: inverse to normal, and inversely graded unstratified sandstone
4.4.4.1.1. Description 217
4.4.4.1.2. Interpretation 217
4.4.4.2. Facies D2: cross-stratified, well sorted sandstone
4.4.4.2.1. Description 219
4.4.4.2.2. Interpretation 219
4.4.4.3. Facies D3: graded sandstone with hummocky cross-stratification and climbing ripple lamination
4.4.4.3.1. Description 221
4.4.4.3.2. Interpretation 223
4.4.4.4. Facies D4: graded, stratified, tabular sandstone
4.4.4.4.1. Description 228
4.4.4.4.2. Interpretation 229
4.4.4.5. Facies D5: weakly graded, bioturbated silty mudstone
4.4.4.5.1. Description 229
4.4.4.5.2. Interpretation 230
4.4.4.6. Palaeoenvironment and process sedimentology 230
4.4.5. Facies Association E: prodelta–outer shelf
4.4.5.1. Facies E1: stratified fine-grained sandstone and siltstone
4.4.5.1.1. Description 235

4.4.5.1.2. Interpretation 236
4.4.5.2. Facies E2: homogenized silty mudstone with discontinuous limestone
4.4.5.2.1. Description 236
4.4.5.2.2. Interpretation 236
4.4.5.3. Facies E3: graded and banded siltstone and black mudstone
4.4.5.3.1. Description 238
4.4.5.3.2. Interpretation 238
4.4.5.4. Facies E4: laminated black mudstone
4.4.5.4.1. Description 240
4.4.5.4.2. Interpretation 240
4.4.5.5. Palaeoenvironment and process sedimentology 241
4.5. Sediment dispersal processes defined by facies tracts
4.5.1. Hyperpycnal underflows: spatial and temporal evolution of quasi-steady turbidity currents 243
4.5.1.1. Fully turbulent phase (flow waxing) 245
4.5.1.2. Density-stratified phase (peak discharge) 247
4.5.1.3. Turbulent diffusion phase (flow waning) 247
4.5.1.4. Channel backfilling phase (flow waning) 248
4.5.1.5. Temporal and spatial evolution 249
4.5.2. Hypopycnal surface plumes: formation and distribution of hemiturbidite 251
4.5.3. Homopycnal plumes: cloud collapse or double diffusive convection 254
4.5.4. Mass emplacement and textural inversion 255
4.6. Fan-delta classification based on alluvial feeder system and flow efficiency 256
4.7. Conclusion 260
Appendix A: AMS in detrital sediments
A1. Methodology 262
A2. Properties of the magnetic fabric 263

*Chapter 5*

**Processes, dynamics, and facies on a muddy storm-dominated Cambrian shelf: New perspectives on the bypass-zone tempestite model**

5.1. Introduction 267
5.2. Tempestite model: proximality trends and published accounts 271
5.3. Lithofacies associations of the Ogof Velvet Formation
5.3.1. Facies Association A: silt-dominated nearshore
5.3.1.1. Facies A1: description 275
5.3.1.2. Facies A1: interpretation 277
5.3.1.3. Facies A2: description 278
5.3.1.4. Facies A2: interpretation 279
5.3.1.5. Facies A3: description 281
5.3.1.6. Facies A3: interpretation 282
5.3.1.7. Summary 285
5.3.2. Facies Association B: sand-dominated inner to mid shelf
5.3.2.1. Facies B1: description 286
5.3.2.2. Facies B1: interpretation 286
5.3.2.3. Facies B2: description 291
5.3.2.4. Facies B2: interpretation 292
5.3.2.5. Facies B3: description 294

5.3.2.6. Facies B3: interpretation 296
5.3.2.7. Summary 298
5.3.3. Facies Association C: mud-dominated outer shelf
5.3.3.1. Facies C1: description 299
5.3.3.2. Facies C1: interpretation 299
5.3.3.3. Facies C2: description 301
5.3.3.4. Facies C2: interpretation 301
5.3.3.5. Summary 302
5.4. Shelf dynamics
5.4.1. Palaeoshoreline orientation 302
5.4.2. Current flow forcing mechanisms and the force balance equation 304
5.4.3. Palaeoflow and grain fabric analysis 306
5.4.3.1. AMS in detrital sediments 307
5.4.3.2. Properties of the magnetic fabric 309
5.4.4. Shelf hydrodynamics
5.4.4.1. Facies Association A: zone of nearshore bypass 312
5.4.4.2. Facies Association B: zone of inner–mid shelf deposition 316
5.4.4.3. Facies Association C: zone of outer-shelf condensation 317
5.4.5. Combined-flow characteristics: the role of storm type and fetch 318
5.4.6. Temporal and spatial evolution of storm-induced combined flow
5.4.6.1. The acceleration matrix 321
5.4.6.2. Depletive waxing flow 324
5.4.6.3. Depletive steady flow 324
5.4.6.4. Depletive waning flow 325
5.4.6.5. Uniform waning flow 325
5.4.6.6. Erosion and sediment bypass 326
5.4.6.7. Accumulative waning flow 327
5.4.6.8. Storm-flow evolution in the Ogof Velvet Formation 327
5.4.7. Shelf dynamics: concluding remarks 330
5.5. The bypass-zone tempestite model: environmental significance
5.5.1. Depositional setting 332
5.5.1.1. Early transgressive and late highstand carbonate platforms 332
5.5.1.2. Fine-grained subaqueous delta platforms 334
5.5.2. The Ogof Velvet Formation: palaeoenvironment and palaeogeography 335
5.5.2.1. Transgressive systems tract 339
5.5.2.2. Early highstand systems tract 339
5.5.2.3. Late highstand systems tract 341
5.5.2.4. Sediment source and dispersal patterns 342
5.6. Conclusions 344

*Chapter 6:*

**Conclusions** 346

**References** 351

# LIST OF FIGURES

**Chapter 2:**
**Stratigraphy, sedimentology and sequence stratigraphy of the Dyfed Supergroup in SW Wales: Implications for a unified Avalonian chronostratigraphy**

**Fig. 2.1.** Avalonia: stratigraphy and palaeogeography
**Fig. 2.2.** Lithological features of the Caerfai Group and Porth-y-rhaw Group exposed on the eastern cliffs of Caerfai Bay
**Fig. 2.3.** Lithological characteristics of the Ogof Golchfa Formation and the St Non's Formation
**Fig. 2.4.** Lithofacies, depositional processes and environments of the Dyfed Supergroup in SW Wales
**Fig. 2.5.** Lithological characteristics of the Newgale Formation
**Fig. 2.6.** Lithological characteristics of the Cwm Mawr Member
**Fig. 2.7.** Lithological features of the Porth Clais Formation
**Fig. 2.8.** Lithological characteristics of the Whitesand Bay Formation at the type locality of Whitesand Bay
**Fig. 2.9.** Sedimentological and stratigraphic features of the Porth-y-rhaw Group exposed from Ogof y Ffôs to Aber Llong
**Fig. 2.10.** Lithological characteristics of the Menevia Formation at the type locality of Porth-y-rhaw
**Fig. 2.11.** Sedimentological and stratigraphical features of the Aber Llong Formation
**Fig. 2.12.** Lithological features of the Ogof Velvet Formation
**Fig. 2.13.** Avalonian sequence stratigraphy.
**Fig. 2.14.** Sequence stratigraphy of the Dyfed Supergroup exposed in SW Wales
**Fig. 2.15.** Definition of megasequences based on palaeocurrent data, magnetic susceptibility and petrography
**Fig. 2.16.** Structural model to account for facies distribution, sequence architecture and location of unconformities in the successions in SW Wales, Shropshire, Malvern and Nuneaton

**Fig. 2.17.** Cross section and depositional sequence stratigraphy of the succession exposed at Comley, Shropshire
**Fig. 2.18.** Depositional model and systems tract linkage between SW Wales and North Wales during the formation of sequence boundary 3–4
**Fig. 2.19.** Chronostratigraphic chart for the upper Middle Cambrian and Upper Cambrian of SW Wales and North Wales
**Fig. 2.20.** Lithofacies, processes and depositional model for the Maentwrog through Dolgellau exposed at Fairbourne, North Wales
**Fig. 2.21.** Depositional model for the Maentwrog and Ffestiniog Flags formations in North Wales
**Fig. 2.22.** Megasequence definition based on tectonics setting and basin characterization
**Fig. 2.23.** Tectonostratigraphy of the late Precambrian to Ordovician succession exposed in SW Wales
**Fig. 2.24.** The subaqueous delta platform of the Upper Cambrian Welsh Basin: its palaeogeography as a sediment sink on the northern periphery of Gondwana

**Chapter 3:**
**Basin margin sedimentology and tectonic implications of Early Cambrian rifting in Eastern Avalonia (Southern Britain): Transtensional successor basin development in the Lower Cambrian (Caerfai Group) of SW Wales, UK.**

**Fig. 3.1.** (A) Early Mesozoic reconstruction of the North Atlantic showing the location of Avalonia and related peri-Gondwanan terranes of the Neoproterozoic. (B) Geological map of Wales showing terrane assemblage and Precambrian/Cambrian outcrops. (C) Geological map of NW Pembrokeshire showing locations of Cambrian outcrops and study areas discussed in the text
**Fig. 3.2.** Stratigraphy and detailed sedimentary log of the coastal section between Ogof Golchfa and Porthselau
**Fig. 3.3.** Sedimentological features of Facies Association A sediments (alluvial fan) exposed at Ogof Golchfa
**Fig. 3.4.** Plot of maximum particle size (MPS) against bed thickness (BTh) from conglomerate lithofacies of Facies Association A
**Fig. 3.5.** Palaeocurrent data from the Ogof Golchfa Formation and lower St Non's Formation exposed between Ogof Golchfa and Porthselau

**Fig. 3.6.** Schematic cross sectional representation of basal Cambrian overstep sequence in NW Pembrokeshire
**Fig. 3.7.** Sedimentary log of braided stream facies exposed at Ogof Golchfa
**Fig. 3.8.** Zonation of beach conglomerate above braided stream sediments at Ogof Goch
**Fig. 3.9.** Textural zonation of beach gravels at Sker Point, Wales (from Bluck 1967)
**Fig. 3.10.** Sedimentological features of Facies Association C sediments
**Fig. 3.11.** Sedimentological features of Facies C2 at Ogof Golchfa
**Fig. 3.12.** Storm flow hydrodynamics on a high-energy gravelly reflective shoreline based on features present in Facies Association C
**Fig. 3.13.** Ternary diagrams from Facies Associations A, B and C describing sandstone composition and interpreting tectonic setting
**Fig. 3.14.** Photomicrographs of principle grain types present in the Ogof Golchfa and St Non's formations
**Fig. 3.15.** Summary of sandstone compositional data and petrofacies discrimination
**Fig. 3.16.** Semi-quantitative weathering index based on semi-quantitative estimates for climate and relief
**Fig. 3.17.** Tectonosedimentary model for syn-extensional alluvial fan deposits of the Ogof Golchfa Formation
**Fig. 3.18.** Tectonosedimentary model for transitional and post extensional sedimentation in the Ogof Golchfa Formation and St Non's Formation
**Fig. 3.19.** Schematic cross sectional representation of basin margin evolution

**Chapter 4:**
**The anatomy of a flood-dominated fan-delta from the Middle Cambrian (St Davids Series) of SW Wales, UK: Processes, facies and classification**

**Fig. 4.1.** Different modes of interaction between sediment-laden river water and basin water, determined by the relative density of the water bodies
**Fig. 4.2.** Lithostratigraphy and sequence stratigraphy of the Middle Cambrian (St David's Series) exposed in NW Pembrokeshire
**Fig. 4.3.** (A) Early Mesozoic reconstruction of the North Atlantic showing the location of Avalonia and related peri-Gondwanan terranes of the Neoproterozoic (modified from Nance and Murphy 1994). (B) Geological map of Wales showing terrane assemblage. (C) Geological map of NW Pembrokeshire showing locations of Cambrian outcrops and study areas discussed in the text

**Fig. 4.4.** Stratigraphic framework and tectono-depositional features of late Precambrian to Ordovician strata exposed in NW Pembrokeshire
**Fig. 4.5.** Component elements of flood-dominated fan-deltas (modified from Schumm (1977) and Mutti *et al.* (1996))
**Fig. 4.6.** Classification of coarse-grained deltas based on feeder system, water depth and alluvial fan processes
**Fig. 4.7.** Flow properties in single phase and 2-phase flows, and differences between turbulent and inertia regimes
**Fig. 4.8.** Classification of turbidites based on grain size and sedimentary structures
**Fig. 4.9.** Stratigraphic correlation and large scale stacking patterns across the NW Pembrokeshire coast
**Fig. 4.10.** Palaeocurrent data from primary sedimentary structures evident in the Caerfai and Porth-y-rhaw groups
**Fig. 4.11.** Sedimentological characteristics of Facies Association A (alluvial fan) and B (fan-delta plain) at Newgale
**Fig. 4.12.** Inferred mechanism for deposition of hyperconcentrated flood-flow deposits based on characteristics present in Facies A2
**Fig. 4.13.** The acceleration matrix (after Kneller 1995) for quasi-steady turbidity currents, with illustrative bed sequences for each field showing downstream and vertical changes in relative grain size
**Fig. 4.14.** Sedimentological characteristics of Facies Association B (fan-delta plain) at Pen-y-Cyffrwy
**Fig. 4.15.** Evolutionary phase in the downstream maturity of a high-density turbidity current, and mechanism for the formation of massive sandstone by direct suspension sedimentation
**Fig. 4.16.** Sedimentological characteristics of Facies Association C (channel-lobe transition) at Porth Clais
**Fig. 4.17.** Forestepping and backstepping of facies during a single flood event controlled by the flood hydrograph
**Fig. 4.18.** Sedimentological characteristics of Facies Association D (delta-front sandstone lobe) sediments at Newgale
**Fig. 4.19.** Sedimentological features of Facies D3
**Fig. 4.20.** Grain long axis alignment determined from the anisotropy of magnetic susceptibility
**Fig. 4.21.** The generation of combined flow on flood-dominated fan-delta fronts
**Fig. 4.22.** Vertical variations in magnetic susceptibility from sandstones that appear ungraded and unstratified in outcrop

**Fig. 4.23.** Sedimentary characteristics of Facies Association E (pro-delta) at Porth-y-rhaw
**Fig. 4.24.** Model for pro-delta sedimentation based on the characteristics of Facies Association E
**Fig. 4.25.** Facies tracks reconstructed from lateral facies changes evident in the Caerfai and Porth-y-rhaw groups
**Fig. 4.26.** Temporal and spatial phases of flow evolution during a single flood event in response to waxing and waning of the flood hydrograph
**Fig. 4.27.** Temporal and spatial changes in flow evolution during a discrete flood event
**Fig. 4.28.** Mechanism for the formation of hemiturbidite through suspension sedimentation out of buoyant plume associated with a flooding event
**Fig. 4.29.** Mechanisms for homopycnal dispersion through positively buoyant plumes during flood discharge events
**Fig. 4.30.** Classification of fan-deltas based on flow efficiency
**Fig. 4.A1.** Basic principle of magnetic susceptibility
**Fig. 4.A2.** Graphical illustration of the shape of AMS ellipsoids in an L/F-plot

**Chapter 5:**
**Processes, dynamics, and facies on a muddy storm-dominated Cambrian shelf: New perspectives on the bypass-zone tempestite model**

**Fig. 5.1.** (A) Stratigraphy of the Upper Cambrian Lingula Flags Group in NW Pembrokeshire. (B) Early Mesozoic reconstruction of the North Atlantic showing location of Avalonia and related peri-Gondwanan terranes of the Neoproterozoic. (C) Geological map of Wales (inset) and NW Pembrokeshire showing location of Cambrian outcrops discussed in the text.
**Fig. 5.2.** Stratigraphic expression and proximality trends on prograding storm-dominated coastlines
**Fig. 5.3.** Bypass-zone tempestite model and proximality trends for the Ogof Velvet Formation
**Fig. 5.4.** Characteristic features of Facies Association A sediments
**Fig. 5.5.** Mechanism for the formation of pot and gutter casts through storm-tide interaction based on characteristics of Facies A2
**Fig. 5.6.** Detailed field sketch of the amalgamated channel complex displayed in Fig. 3A

**Fig. 5.7.** Sedimentological features of Facies Association B sediments
**Fig. 5.8.** Lithological features of Facies Association B sediments
**Fig. 5.9.** Representative stratification sequences from Facies B2 plotted in a bed configuration stability diagram for combined-flow in fine sand (diagram modified after Myrow and Southard 1991)
**Fig. 5.10.** Soft sediment deformation and process-response model for sediments of Facies B3
**Fig. 5.11.** Sedimentological features of Facies Association C
**Fig. 5.12.** Palaeohydraulic and environmental reconstruction of the Ogof Velvet Formation
**Fig. 5.13.** Storm induced current flow forcing mechanism over the lower shoreface and shelf in the northern hemisphere (modified from Duke 1990)
**Fig. 5.14.** Idealized diagram of motion in the coastal ocean during a downwelling event (modified after Swift *et al.* 1985)
**Fig. 5.15.** Basic principle of magnetic susceptibility
**Fig. 5.16.** Graphical illustration of the shape of AMS ellipsoids in an L/F-plot
**Fig. 5.17.** q value vs $k_{max}$ imbrication angle plotted as means of determining the likely depositional process
**Fig. 5.18.** (A) AMS data presented as lower hemisphere equal area stereoplots for facies associations A, B, and C. (B), (C), (D), (E) illustration of grain alignment and the expected stereographic representation for depositional process discussed in this study.
**Fig. 5.19.** Schematic position of the sub-tropical high pressure zone in the Northern Hemisphere and inferred hurricane and winter storm paths for: (A) Late Albian and (B) Early Maastrichtian palaeogeography (modified from Barron 1989)
**Fig. 5.20.** Acceleration matrix with illustrative bed sequences for each field showing downstream and vertical changes in relative grain size and sedimentary structures (modified from Kneller 1995)
**Fig. 5.21.** Temporal and spatial evolution of storm-induced combined-flow experienced during Ogof Velvet deposition
**Fig. 5.22.** Summary flow chart illustrating the main controls on the storm system during deposition of the Ogof Velvet Formation
**Fig. 5.23.** Nearshore bypass on carbonate platforms
**Fig. 5.24.** Temporal phases of subaqueous delta platform evolution within the controlling parameters of sediment flux and relative sea level change
**Fig. 5.25.** Lithological features of the Aber Llong Formation

**Fig. 5.26.** Mechanism for the formation of starved hummocks displaying HCS under oscillatory dominant combined flows, based on characteristics evident in the upper part of the Aber Llong Formation

**Fig. 5.27.** The subaqueous delta platform of the Upper Cambrian Welsh Basin: its palaeogeography as a sediment sink on the northern periphery of Gondwana

# LIST OF TABLES

**Chapter 2:**

**Stratigraphy, sedimentology and sequence stratigraphy of the Dyfed Supergroup in SW Wales, UK: Implications for a unified Avalonian chronostratigraphy**

**Table 2.1.** Selected developments in Cambrian stratigraphic nomenclature in SW Wales

**Table 2.2.** Summary of the main characteristics of large fine-grained subaqueous delta platforms.

**Table 2.3.** Depositional features of delta-fed submarine ramp systems after Heller and Dickinson (1985) and Surlyk (1987), and their occurrence in the Maentwrog and Ffestiniog Flags formations in North Wales.

**Chapter 3:**

**Basin margin sedimentology and tectonic implications of Early Cambrian rifting in Eastern Avalonia (Southern Britain): Transtensional successor basin development in the Lower Cambrian (Caerfai Group) of SW Wales, UK**

**Table 3.1.** Contrasting features of beachface and alluvial fan facies.

**Table 3.2.** Framework grains and recalculated parameters used in this study.

**Table 3.3**. Recalculated parameters used for composition and provenance analysis.

**Table 3.4.** Specific source rock indicates yielded from the main tectono-metamorphic units associated with the Berw and Llyn shear zones on Anglesey.

**Chapter 4:**

**The anatomy of a flood-dominated fan-delta from the Middle Cambrian (St Davids Series) of SW Wales, UK: Processes, facies and classification**

**Table A1.** Parameters used in the study to define the magnetic anisotropy and fabric.
**Table A2.** Fabric tests that describe the response of grains to flowing water.

**Chapter 5:**
**Processes, dynamics, and facies on a muddy storm-dominated Cambrian shelf: New perspectives on the bypass-zone tempestite model**

**Table 5.1.** Selected published examples of storm-dominated, tide-influenced coastlines where shore normal gutter casts and channels dissect the nearshore.
**Table 5.2.** Parameters used in the study to define the magnetic anisotropy and fabric.
**Table 5.3.** Fabric tests that describe the response of grains to flowing water.
**Table 5.4.** Sediment accumulation rates from three well studied modem subaqueous deltas.

# *CHAPTER 1*

# INTRODUCTION

Avalonian-Cadomian and related terranes of the circum-North Atlantic constitute portions of an accretionary orogen that developed on an active Gondwanan margin at the periphery of the Neoproterozoic supercontinent Vendia (Murphy *et al.* 2000). These peri-Gondwanan terranes are defined by their Neoproterozoic evolution on an active continental margin, and by the peri-Gondwanan "Acado-Baltic" fauna of their Cambrian–Ordovician overstep sequence (Nance *et al.* 1991; Landing 1996). They include: (1) the Avalonian Superterrane of southern Britain (e.g. Thorpe *et al.* 1984; Pharaoh *et al.* 1987; Gibbons and Horák 1996; Pharaoh and Carney 2000), referred to as "East Avalonia"; (2) the pre-drift continuation of this superterrane in New England and Atlantic Canada (e.g. Murphy and Nance 1989; Nance 1991; Nance *et al.* 1991, 2002), referred to as "West Avalonia"; and (3) the North Armorican Superterrane in the Cadomian orogenic belt of northwestern France and Bohemia (e.g. Chaloupsky 1990; Dupret *et al.* 1990).

Cambrian strata exposed in SW Wales forms part of the Dyfed Supergroup (Woodcock 1990), a lithostratigraphic unit that encompasses all Cambrian and Tremadoc rocks in southern Britain. These conglomerates, sandstones and mudstones were deposited on the southern margin of the Welsh Basin (Jones 1932), a NE–SW trending structural intra-shelf basin of uncertain origin (Crimes 1970a). The tectonostratigraphic evolution of the Avalonian Superterrane provides a record of Neoproterozoic subduction along an active continental margin of Gondwana until Avalonian rifting in the Early Ordovician (Prigmore *et al.* 1997) led to the inception of Iapetus subduction and oblique collision with Laurentia during the Early Silurian (Nance *et al.* 2002). In East Avalonia, the late Neoproterozoic (ca 700–570) history is characterized by voluminous arc-related volcanic and cogenetic plutonic rocks, by coeval sedimentary successions deposited in a variety of volcanic arc basins (Thorpe *et al.* 1984; Gibbons and Horák 1996; Compston *et al.* 2000), and by latest Neoproterozoic (ca 570–550) intra- and inter-arc extension and the development of arc-related successor basins (e.g. Reedman *et al.* 1984; Pauley 1990). This transition, as well as its

diachroniety across Avalonia (Gibbons and Horák 1996) is consistent with the evolution from orthogonal to increasingly oblique subduction.

Unlike most recent studies on the early evolution of Avalonia, this contribution focuses on the Cambrian overstep (platform) succession. Historically, the base of the Cambrian in southern Britain is taken at a regionally extensive basal conglomerate that typically rests with slight angular discordance on Precambrian arc-related rocks (Rushton 1974). The almost universal interpretation of this conglomerate as a transgressive shoreface sequence deposited during sea level encroachment across a stable, tectonically quiescent platform, has led to a view of Precambrian and Cambrian rocks as two mutually exclusive lithotectonic packages, a perception reinforced by the prominence of the sub-Cambrian unconformity. The transition from active subduction to stable cratonic platform has been variously termed the Avalonian or Cadomian orogeny (Rast 1979; Rast and Skehan 1983), a perception of collision upheld despite the lack of compelling evidence for regional orogenesis, crustal shortening/thickening, and widespread metamorphism (Nance 1991, Nance *et al.* 1991; Gibbons and Horák 1996).

This simple view of the late Neoproterozoic–Cambrian evolution of Avalonia has been recently challenged, with the extensive documentation of strike-slip tectonics in both the latest Proterozoic (Murphy and Nance 1989; Nance 1991) and Lower and Middle Cambrian (Murphy *et al.* 1985; Keppie and Murphy 1988; Landing 1996) successions in West Avalonia, and the realization that in northwest Wales at least, there is no prominent break between latest Precambrian events and Lower Cambrian sedimentation (Gibbons and Horák 1996). In addition, a number of basal Cambrian "nearshore marine" conglomerates have been reinterpreted as alluvial fan and fan-delta complexes, which are depositional systems with strong genetic ties to various syn-tectonic frameworks (McPherson *et al.* 1988; Massari and Colella 1988; Blair and McPherson 1994). Although the importance of regional strike-slip tectonics in the Precambrian succession of East Avalonia is now well documented (Pauley 1990; Gibbons and Horák 1996), no study has yet demonstrated any influence on Cambrian sedimentation patterns. This is surprising if one consults the extensive "local" literature (see review in Rushton 1974), which consistently demonstrates a number of characteristics compatible with local phases of transtension and transpression (Reading 1980).

The aims of this study are two-fold. The overlying theme is to chart the tectonostratigraphic evolution of East Avalonia from active island arc setting of the late

Neoproterozoic to passive continental margin in the early Tremadoc. This is accomplished by integrating a revised lithostratigraphy for the Cambrian of SW Wales into a unified Avalonian chronostratigraphy based on high-resolution sequence stratigraphic principles. The second part is mutually inclusive, and forms a detailed analysis of the depositional environments, processes, stratal architecture and provenance of the Dyfed Supergroup exposed in SW Wales. Particular topics discussed include:

- the sedimentary facies, stratal architecture and depositional processes on debris flow-dominated ("dry") and hyperconcentrated flood-flow-dominated ("wet") alluvial fans and fan-deltas
- the details of an alluvial fan to braided stream transition within a temporal framework of evolving tectonic and morphological constraints
- an examination of some of the classic tenets of the relationship between tectonic movement and sedimentary response, with particular reference to "anti-tectonic cycles"
- the processes, facies and classification of flood-dominated fan-delta systems defined by facies tracts and flow efficiency
- an assessment of the processes, dynamics and facies on fine-grained storm-dominated shelves utilising the bypass-zone tempestite model
- the environmental significance of this tempestite model with respect to carbonate platforms and fine-grained subaqueous delta platforms
- and an assessment of the temporal and spatial evolution of storm-induced combined-flow using detailed analysis of vertical stratification sequences in tempestites combined with magnetic grain fabric measurements utilising the anisotropy of magnetic susceptibility (AMS).

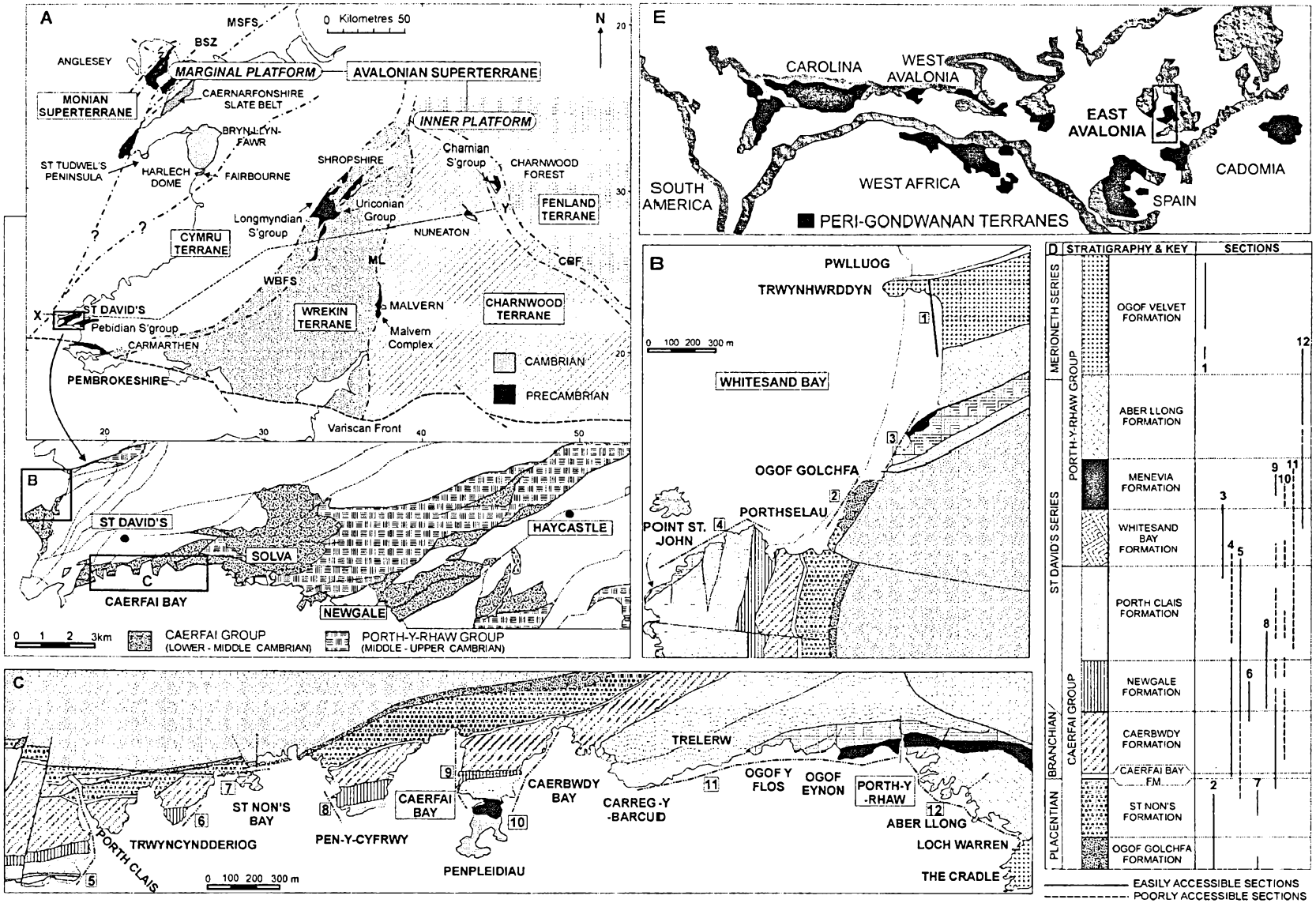
*CHAPTER 2*

# STRATIGRAPHY, SEDIMENTOLOGY AND SEQUENCE STRATIGRAPHY OF THE DYFED SUPERGROUP IN SW WALES, UK: IMPLICATIONS FOR A UNIFIED AVALONIAN CHRONOSTRATIGRAPHY

## 2.1. INTRODUCTION

Cambrian strata exposed in SW Wales (Fig. 2.1A) forms part of the Dyfed Supergroup (Woodcock 1990), a lithostratigraphic unit that encompass all Cambrian and Tremadoc rocks in southern Britain. The earliest Geological Survey maps of SW Wales, produced in 1857, distinguished a lower unit of "Cambrian Grits" overlain by the dominantly argillaceous "Lingula Flags". This two-fold division was upheld by Salter (1864) (Table 2.1) who noted the similarity between the succession exposed in NW Pembrokeshire (Fig. 2.1A) and the type-Cambrian sections of the Harlech Dome described by Sedgwick (in Sedgwick and Murchison 1835). The proliferation of more detailed stratigraphic schemes in both North Wales (see review in Allen *et al.* 1981) and South Wales (Table 2.1) in the latter part of Nineteenth Century and early Twentieth Century on one hand refined stratal packages to a resolution that facilitated detailed local correlation but on the other, clouded the most obvious regional two-fold division of Cambrian strata in Wales. A major remapping program undertaken by the Geological Survey throughout North and Mid Wales in the last 25 years has seen a shift back to this two-fold classification, with the erection above the Harlech Grits Group of the dominantly argillaceous Mawddach Group (Allen *et al.* 1981; Allen and Jackson 1985; Pratt 1995; Pratt *et al.* 1995).

The first part of this study is a contribution to Cambrian stratigraphy and sedimentology in SW Wales, and focuses on the classic outcrops of the St Davis's Peninsula and Haycastle inlier of NW Pembrokeshire (Fig. 2.1A). A fairly complete succession from the Placentian Series of the Lower Cambrian to the Merioneth Series of the Upper Cambrian is exposed (Fig. 2.1D), representing a total stratigraphic thickness in excess of 1250 m. The lithostratigraphy as it is recognized today owes much to the researchers of the Nineteenth Century (Table 2.1), with little


A
MSFS
BSZ
ANGLESEY
MARGINAL PLATFORM
AVALONIAN SUPERTERRANE
MONIAN SUPERTERRANE
CAERNARFONSHIRE SLATE BELT
INNER PLATFORM
BRYN-LLYN-FAWR
ST TUDWEL'S PENINSULA
HARLECH DOME
FAIRBOURNE
SHROPSHIRE
Charnian S'group
CHARNWOOD FOREST
Uriconian Group
Longmyndian S'group
FENLAND TERRANE
NUNEATON
CYMRU TERRANE
ML
CDF
WBFS
WREKIN TERRANE
MALVERN
CHARNWOOD TERRANE
ST DAVID'S
Pebidian S'group
Malvern Complex
CARMARTHEN
PEMBROKESHIRE
CAMBRIAN
PRECAMBRIAN
Variscan Front
0 Kilometres 50
N
B
HAYCASTLE
SOLVA
C
CAERFAI BAY
NEWGALE
0 1 2 3km
CAERFAI GROUP (LOWER - MIDDLE CAMBRIAN)
PORTH-Y-RHAW GROUP (MIDDLE - UPPER CAMBRIAN)
E
CAROLINA
WEST AVALONIA
EAST AVALONIA
CADOMIA
SOUTH AMERICA
WEST AFRICA
SPAIN
PERI-GONDWANAN TERRANES
B
PWLLUOG
TRWYNHWRDDYN
WHITESAND BAY
OGOF GOLCHFA
PORTHSELAU
POINT ST. JOHN
0 100 200 300 m
C
TRELERW
OGOF Y FLOS
OGOF EYNON
PORTH-Y-RHAW
CAERBWDY BAY
CARREG-Y-BARCUD
CAERFAI BAY
ST NON'S BAY
TRWYNCYNDDERIOG
PEN-Y-CYFRWY
PENPLEIDIAU
PORTH CLAIS
ABER LLONG
LOCH WARREN
THE CRADLE
0 100 200 300 m
D
STRATIGRAPHY & KEY
SECTIONS
MERIONETH SERIES
ST DAVID'S SERIES
PORTH-Y-RHAW GROUP
BRANCHIAN/
CAERFAI GROUP
PLACENTIAN
OGOF VELVET FORMATION
ABER LLONG FORMATION
MENEVIA FORMATION
WHITESAND BAY FORMATION
PORTH CLAIS FORMATION
NEWGALE FORMATION
CAERBWDY FORMATION
CAERFAI BAY FM.
ST NON'S FORMATION
OGOF GOLCHFA FORMATION
EASILY ACCESSIBLE SECTIONS
POORLY ACCESSIBLE SECTIONS

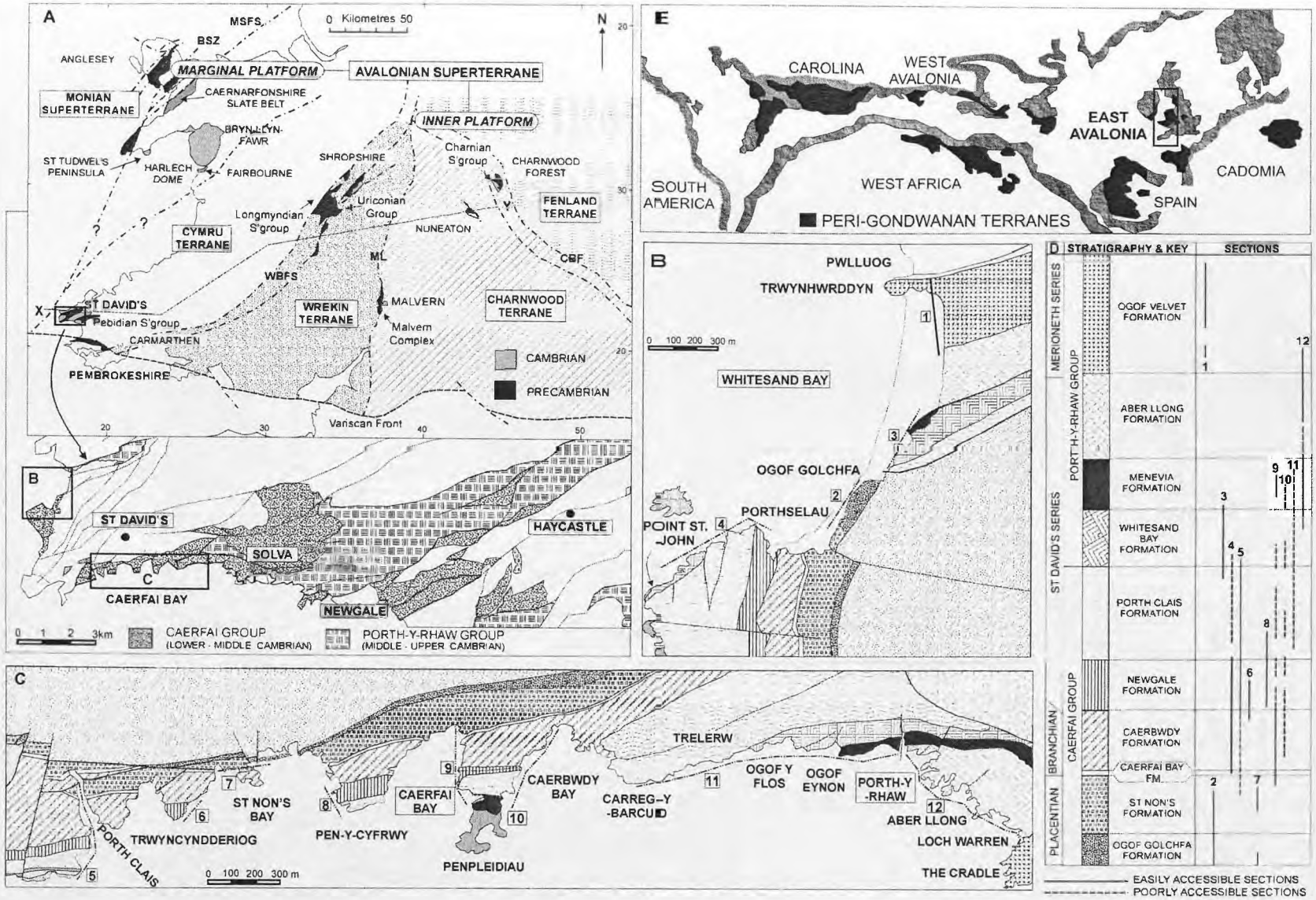

A
MSFS
BSZ
ANGLESEY
MARGINAL PLATFORM
AVALONIAN SUPERTERRANE
MONIAN SUPERTERRANE
CAERNARFONSHIRE SLATE BELT
INNER PLATFORM
BRYN-LLYN-FAWR
ST TUDWEL'S PENINSULA
HARLECH DOME
FAIRBOURNE
SHROPSHIRE
Charnian S'group
CHARNWOOD FOREST
FENLAND TERRANE
Uriconian Group
Longmyndian S'group
NUNEATON
CYMRU TERRANE
MF
CBF
WBFS
ST DAVID'S
Pebidian S'group
CARMARTHEN
WREKIN TERRANE
MALVERN
Malvern Complex
CHARNWOOD TERRANE
PEMBROKESHIRE
CAMBRIAN
PRECAMBRIAN
Variscan Front
0 Kilometres 50
N
B
ST DAVID'S
HAYCASTLE
SOLVA
C
CAERFAI BAY
NEWGALE
0 1 2 3km
CAERFAI GROUP (LOWER - MIDDLE CAMBRIAN)
PORTH-Y-RHAW GROUP (MIDDLE - UPPER CAMBRIAN)
E
CAROLINA
WEST AVALONIA
EAST AVALONIA
CADOMIA
SOUTH AMERICA
WEST AFRICA
SPAIN
PERI-GONDWANAN TERRANES
B
PWLLUOG
TRWYNHWRDDYN
0 100 200 300 m
WHITESAND BAY
OGOF GOLCHFA
PORTHSELAU
POINT ST. JOHN
C
TRELERW
OGOF Y FLOS
OGOF EYNON
PORTH-Y-RHAW
CAERBWDY BAY
CARREG-Y-BARCUD
CAERFAI BAY
ST NON'S BAY
PEN-Y-CYFRWY
TRWYNCYNDDERIOG
PORTH CLAIS
PENPLEIDIAU
ABER LLONG
LOCH WARREN
THE CRADLE
0 100 200 300 m
D
STRATIGRAPHY & KEY
SECTIONS
MERIONETH SERIES
ST DAVID'S SERIES
PORTH-Y-RHAW GROUP
BRANCHIAN
CAERFAI GROUP
PLACENTIAN
OGOF VELVET FORMATION
ABER LLONG FORMATION
MENEVIA FORMATION
WHITESAND BAY FORMATION
PORTH CLAIS FORMATION
NEWGALE FORMATION
CAERBWDY FORMATION
CAERFAI BAY FM.
ST NON'S FORMATION
OGOF GOLCHFA FORMATION
EASILY ACCESSIBLE SECTIONS
POORLY ACCESSIBLE SECTIONS

**Fig. 2.1.** Avalonia: stratigraphy and palaeogeography. (A) The Avalonian Superterrane in southern Britain (inset, modified after Pharaoh and Carney 2000) and general details of the Dyfed Supergroup in SW Wales. Cross section X–Y displayed in Fig. 2.16. Fault abbreviations: BSZ - Berw Shear Zone, CBF – Charnwood Boundary Fault (postulated), ML – Malvern Line, MSFS – Menai Straits Fault System, WBFS – Welsh Borderlands Fault System. (B) Geological map of Whitesand Bay (after Stead and Williams 1971) showing key sections discussed in the text. (C) Geological map of the coastline south of St David's showing key sections discussed in the text. (D) Lithostratigraphy and range of sections discussed in the text. (E) Early Mesozoic reconstruction of the North Atlantic showing location of Avalonian and related peri-Gondwanan terranes of the Neoproterozoic (modified after Nance and Murphy 1994).

work having been published since. This contribution presents a detailed and revised lithostratigraphy of the Dyfed Supergroup that aims to rationalize an outdated stratigraphy while retaining as many of the original and well known formational subdivisions as possible. At formational level, these boundaries follow, with only minor exception, those partly formalized by Cowie *et al.* (1972) based on the stratigraphical scheme proposed by Harkness and Hicks (1871) (Table 2.1).

The previous grouping of these formations into a four-fold arrangement (in ascending order: the "Caerfai", "Solva" and "Menevian" groups and the "Lingula Flags") is in most instances unworkable and overly complex. Conglomerates, pebbly sandstones and brightly coloured fine- to coarse-grained sandstones characterize both the "Caerfai" and "Solva" groups of Hicks (1881) (Table 2.1), and are here treated as a single unit, the Caerfai Group. By excluding the silt-dominated Upper Solva of Hicks (1881) from the Caerfai Group, the unit is readily defined by a basal and upper conglomerate/pebbly sandstone division, with intervening brightly coloured sandstones, siltstones and pebbly sandstones. The "Menevian Group" and "Lingula Flags" of Harkness and Hicks (1871) along with "Upper Solva" form the newly erected Porth-y-rhaw Group, a 687 m thick unit of fine-sandstones, siltstones, blue silty mudstone and black laminated mudstone. This two-fold division of the Dyfed Supergroup is comparable both lithologically and chronologically with the Harlech Grits Group and Mawddach Group in North and Mid Wales, and is also broadly coeval with the first lithostratigraphic scheme for SW Wales proposed by Salter in 1864.

In the second part of this investigation, high-resolution sequence stratigraphic techniques are applied to the Dyfed Supergroup, which facilitates comparisons with other Cambrian successions that define the Avalonian Superterrane in the Acadian-Caledonian orogen. Particular reference is made to the concept of a unified Avalonian chronostratigraphy (See Brasier 1989, Landing 1996), with the integration of the depositional sequence stratigraphy of Dyfed Supergroup into a

chronostratigraphic framework defined from Cambrian successions in Atlantic Canada (Landing 1996). An understanding of the controls on sequence development and internal architecture and the spatial and temporal evolution of facies belts are applied to basin analysis and the evolving tectonostratigraphic regime during terminal phases of the Avalonian-Cadomian orogeny.

## 2.2. STRATIGRAPHY OF THE DYFED SUPERGROUP

### 2.2.1. CAERFAI GROUP (revised)

*General:* The revised boundaries of the Caerfai Group (Table 2.1) incorporate strata previously assigned by Hicks (1881) to both the Caerfai Group and Solva Group. The latter term is now considered obsolete. These boundaries approximate those of the "Cambrian Grits" and "Longmyndian Group" proposed respectively by Salter (1864) and Harkness and Hicks (1871). The "Grey rocks" of Harkness and Hicks (1871) (= Upper Solva of Cowie *et al.* 1972) form the basal division of the overlying Porth-y-rhaw Group (new term).

*Name:* From Caerfai Bay (SM 7616 2438–7616 2417, Fig. 2.1C and 2.2) situated south of the city of St David's.

*Subdivisions:* The divisions of the Caerfai Group (*sensu* Hicks 1881) proposed by Cowie *et al.* (1972) are retained (Table 2.1), and given formal status (in ascending order): Ogof Golchfa Formation, St Non's Formation, Caerfai Bay Formation and Caerbwdy Formation. Strata previously assigned to the Lower and Middle Solva by Hicks (1881) are given formal status as the Newgale Formation and Porth Clais Formation respectively.

*Type locality:* The formation is best exposed and most accessible in the bays and headlands south of St David's extending from Porth Clais (SM 74292364) in the west to Ogof-y-Ffôs (SM 7770 2432) in the east (Fig. 2.1C). The most complete exposure occurs on the west side of Porth Clais and on the east side of Caerfai Bay (Fig. 2.1C and 2.2). Neither section expose the Ogof Golchfa Formation or the lowermost part of the overlying St Non's Formation. Good exposure of these lower formations exists at a reference section situated at the southernmost tip of Whitesand Bay (Fig. 2.1B) between Ogof Golchfa (SM 7305 2646) and Porthselau (SM 7275 2620).

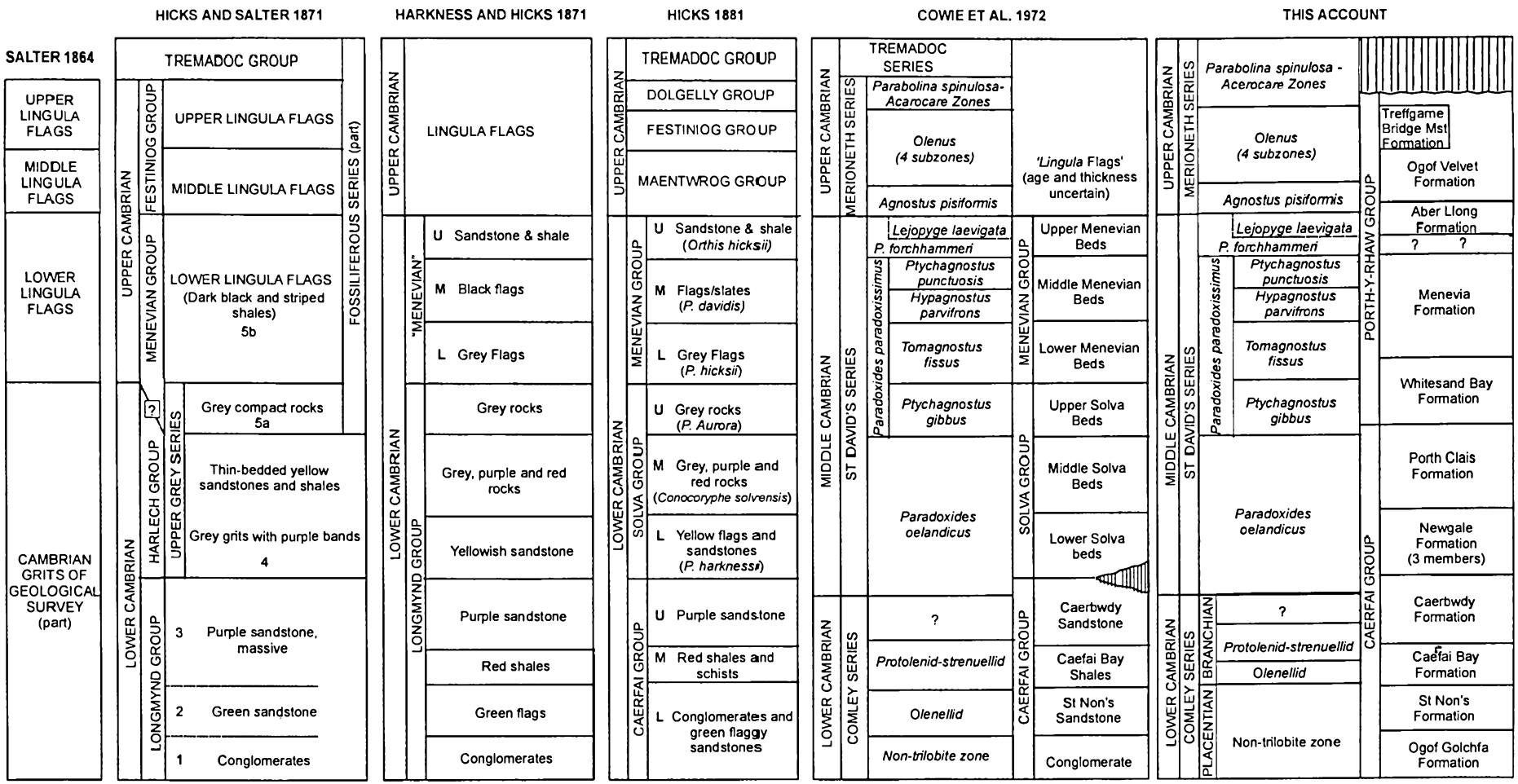



**Table 2.1.** Selected developments in Cambrian stratigraphic nomenclature in SW Wales.

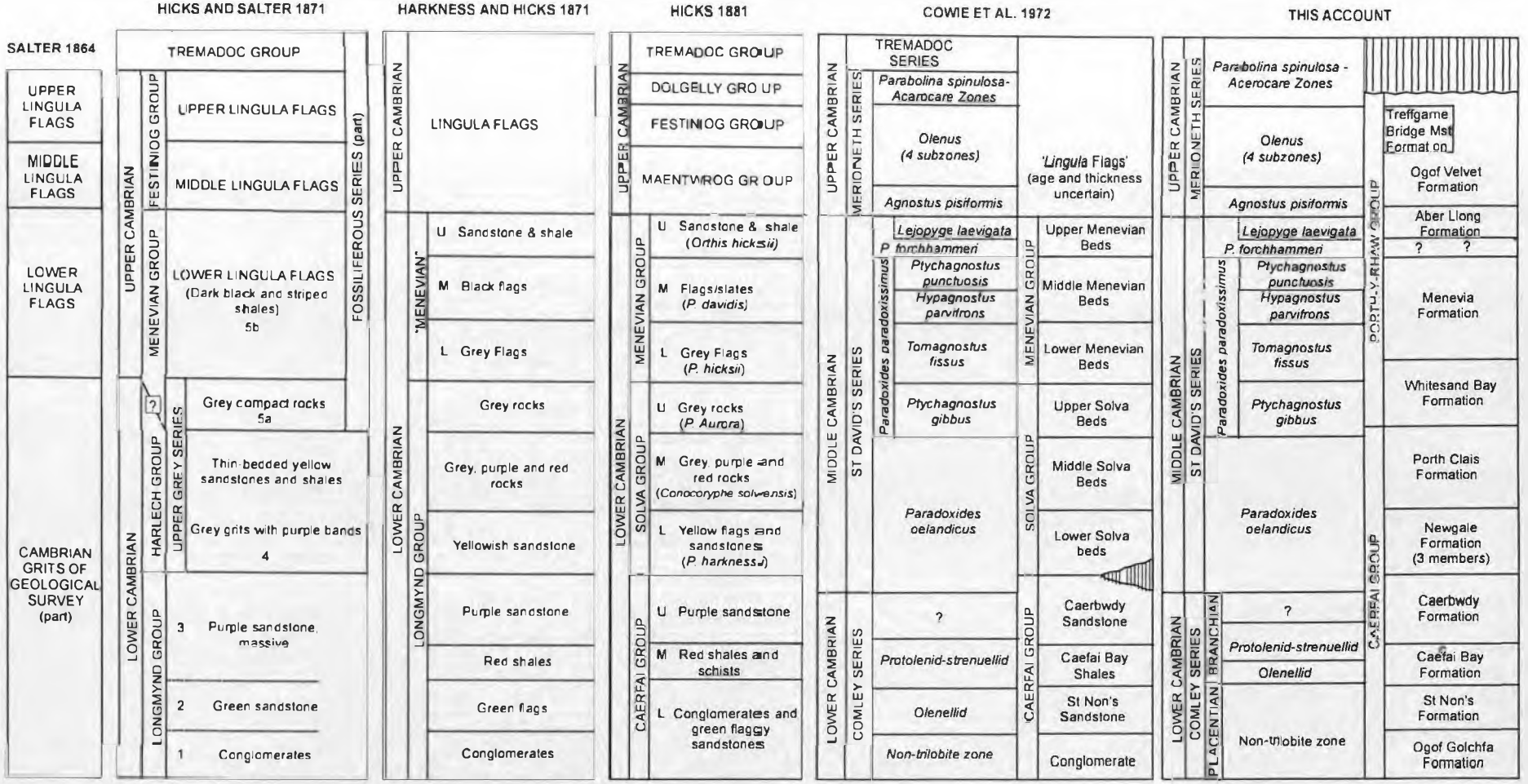



**Table 2.1.** Selected developments in Cambrian stratigraphic nomenclature in SW Wales.

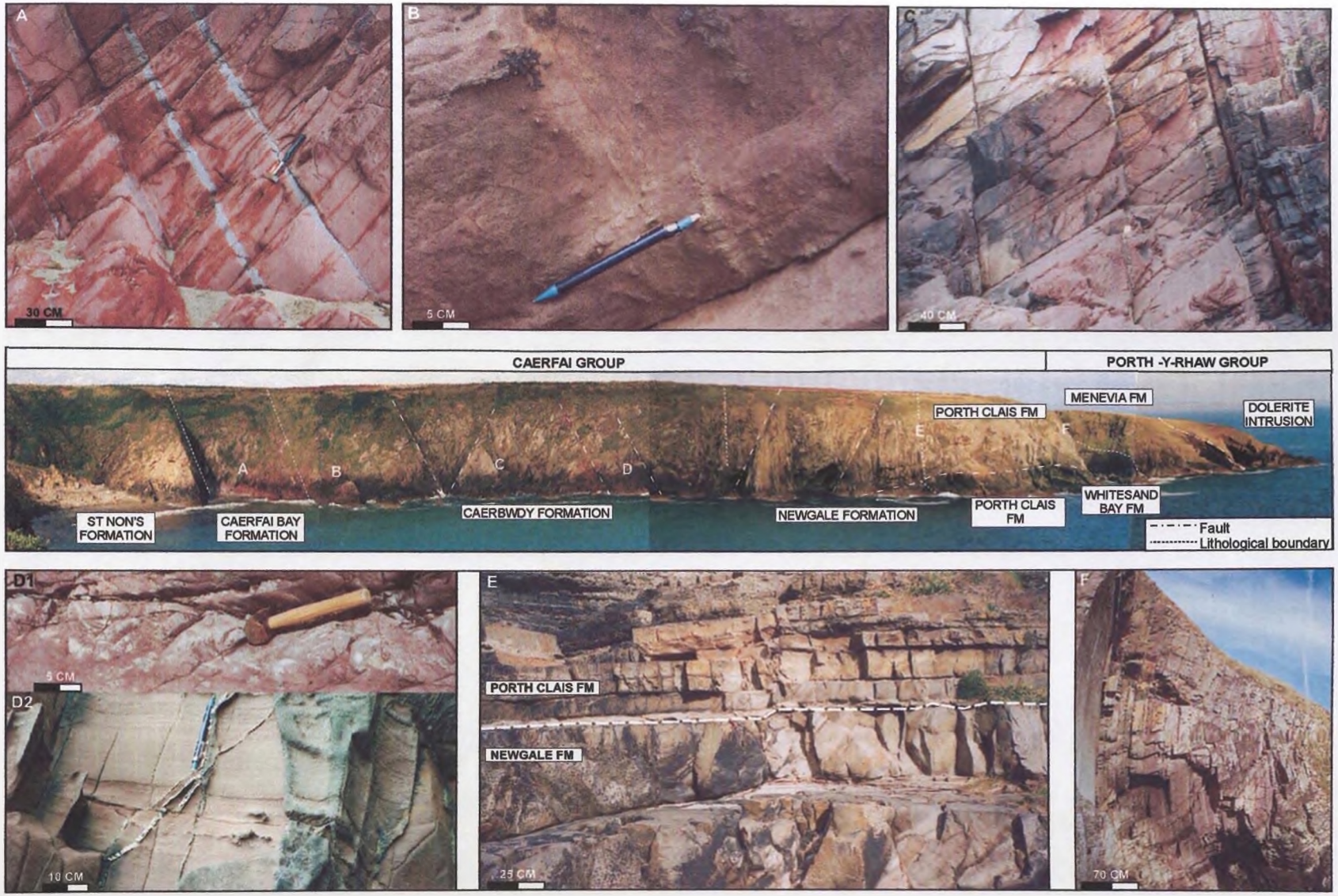

A
30 CM
B
5 CM
C
40 CM
CAERFAI GROUP
PORTH -Y-RHAW GROUP
MENEVIA FM
PORTH CLAIS FM
DOLERITE INTRUSION
E
F
A
B
C
D
ST NON'S FORMATION
CAERFAI BAY FORMATION
CAERBWDY FORMATION
NEWGALE FORMATION
PORTH CLAIS FM
WHITESAND BAY FM
Fault
Lithological boundary
D1
5 CM
D2
10 CM
E
PORTH CLAIS FM
NEWGALE FM
25 CM
F
70 CM

**Fig. 2.2.** Lithological features of the Caerfai, and Porth-y-rhaw groups exposed on the eastern side of Caerfai Bay. (A) Caerfai Bay Formation – red silty mudstone with bentonite horizons. (B) Caerbwdy Formation – purple sandstone homogenized by burrowing organisms. This is the cause of the thick bedding typical of the formation. (C) Caerbwdy Formation – bedding planes are only typically developed when bioturbated sandstone is separated by bentonite, as the latter is only rarely completely homogenized. (D) Caerbwdy Formation – lower flow regime parallel lamination. Contrary to previous interpretation, most of the Caerbwdy Formation is considered a suspension rather than traction deposit, and thus may be considered a condensed sequence. (E) Transitional contact between the Newgale Formation (Cwm Mawr Member) and the Porth Clais Formation. (F) Porth Clais Formation – diagenetic purple, green and grey sandstones in a well developed fining-upward sequence.

*Thickness:* The group has a thickness in excess of 564 m, this being a conservative figure compiled from a number of stratigraphic logs. The Caerbwdy, Newgale, and Porth Clais formations all display a marked thickening towards the east, thus the most complete section at Porth Clais must be considered relatively condensed.

*Lower boundary:* The Caerfai Group rests unconformably on various members of the Precambrian Pebidian Supergroup (Hicks 1877, Green 1908, Patchett and Jocelyn 1979). At Ogof Golchfa, where the contact is best displayed, it overlies the Ogof Golchfa Group, the uppermost division of the Pebidian Supergroup, while in Caerbwdy Valley, having apparently overstepped the Ramsey Sound Group, it comes to rest on the Caerbwdy Group (Green 1908, p. 376). The small divergence between the strike of the Precambrian and adjacent Cambrian suggests that the former had undergone only gentle warping prior to deposition of the Cambrian sequence. Most of the junctions with Dimetian rocks are faulted, but the unconformable relationship of the Cambrian basal conglomerate to the Dimetian granophyre was proven in a trench (SM 73950 24275) just west of the gas works (now demolished) at Porth Clais (Green 1908). A photograph showing details of the junction was reproduced by Green (1911, pl. 30). The trench has apparently become badly decomposed and overgrown and is now of historic rather than scientific interest (Owen *et al.* 1971, p. 21).

*Dominant lithology:* The group is predominantly composed of red, green and grey medium-grained sandstone with reoccurring units of conglomerate, pebbly sandstone and shale. Comparable lithologies occur at similar stratigraphic positions in the Harlech Grits Group in North Wales (Matley and Wilson 1946; Allen and Jackson 1985).

*Distribution:* As well as in the bays and headlands south of St David's and at Whitesand Bay, the Caerfai Group is also exposed west of the city on the coast north of Porthstinian (SM 7241 2526), although this section have been considerably affected by faulting and relationships between the various units are complicated. The subdivisions of the Caerfai Group have been traced eastwards across the St David's outcrops and into the Brawdy–Haycastle area (Fig. 2.1A), being very well exposed on the northern cliffs of Newgale Sands. Outcrops around the Haycastle anticline have been previously referred to as "Welsh Hook Beds" (Thomas and Jones 1912) and Ford Beds (Williams 1934, p. 46), a distinction not upheld here due to lithological similarities with the Caerfai Group. Small outcrops occur also north and west of Granston and Trecredston (Cox 1930, p. 278; Rushton 1974).

*Biota and age:* Fossils from the Caerfai Group are rare, but include Lower Cambrian (Branchian Series) bradoriids in the Caerfai Bay Formation (Siveter and Williams 1995), and a variety of Middle Cambrian trilobites from the Newgale and Porth Clais formations. The trilobites may be integrated within the biozonal framework employed by Westergård (1946) from Scandinavian sequences. Implementing this zonal scheme, the Newgale and Porth Clais formations are Middle Cambrian (St David's Series) in age, and range from *Paradoxides oelandicus* in the Newgale Formation to *Ptychagnostus gibbus* towards the top of the Porth Clais Formation. Sections at the northern end of Newgale Sands have also yielded acritarchs of possible Middle Cambrian age (Davies and Downie 1964).

Above the basal conglomerate of the Ogof Golchfa Formation, trace fossils are both varied and abundant. Although most are not age diagnostic, the ubiquitous occurrence of *Teichichnus* in silty mudstone at the base of the St Non's Formation places the unit above the *Phycodes pedum* trace fossil zone (see Fig. 2.13) either in the *Rusophycus avalonensis* Biozone or the *Teichichnus* Interval of the Placentian Series. The latter is considered most likely as *Teichichnus*-churned purple and green silty mudstones occur throughout this ichnozone in SE Newfoundland and the English Midlands (Landing 1992, 1996; Brasier 1992), and is a level more consistent with the lower Branchian age for the overlying Caerfai Bay Formation (discussed below).

#### 2.2.1.1. Ogof Golchfa Formation (new)

*History:* The Ogof Golchfa Formation is a new term that replaces the informal "Conglomerate" division of Hicks and Salter (1866), Harkness and Hicks (1871), and Cowie *et al.* (1972).

*Name:* From the Ogof Golchfa cliff section (SM 7305 2646) at the southernmost tip of Whitesand Bay northwest of St David's.

*Type locality:* The type section is a well exposed coastal section between Ogof Golchfa and Porthselau (SM 7275 2620), beginning at the southern end of Whitesand Bay (Fig. 2.1B). This is the only complete section through the formation.

*Thickness:* At the type locality, the formation is 46 m thick. All other sections are incomplete.

*Lower boundary:* The lower boundary is placed at the unconformable junction between the volcaniclastic sediments and volcanics of the Pebidian Supergroup and a boulder conglomerate with some included Pebidian clasts.

*Lithology and process sedimentology:* At the type locality the formation is dominated by reddish to brown polymictic conglomerates and pebbly sandstones. Clast size ranges from small pebbles to boulders, set in a poorly sorted coarse-grained sandy matrix (Fig. 2.3B, C, F). Clast shape is typically sub-rounded but varies to sub-angular. Matrix content is extremely variable but commonly forms less than 15%. Red colouration of this matrix is due to haematite staining, particularly of quartz. Clast composition is dominated by low and medium grade metasedimentary rocks that cannot be matched with local source rocks. Exotic clasts including quartzite, slate, schistose quartzite, schistose greywacke, banded chert (possibly mylonite), greenschist, phyllite, and jasper. Felsic volcanics and tuffaceous material occur up to 6 m above the unconformable contact with the Pebidian Supergroup, a source from which these clasts are easily matched. Beds are generally thick (30–210 cm) but do thin towards the junction with the St Non's Formation.

Based on bed geometry, grain size, and internal fabric and texture, four semi-distinct units are recognized in the type section that form an overall fining- and bed thinning-upward sequence. "Unit A" is developed in the basal 6 m of the section and comprises unstratified, lenticular sand-matrix-supported conglomerates (Fig. 2.3B). This amalgamated channelized sequence cuts deeply into the underlying Pebidian Supergroup, with multiple channel margins attaining relief of up to 1.9 m. Poor

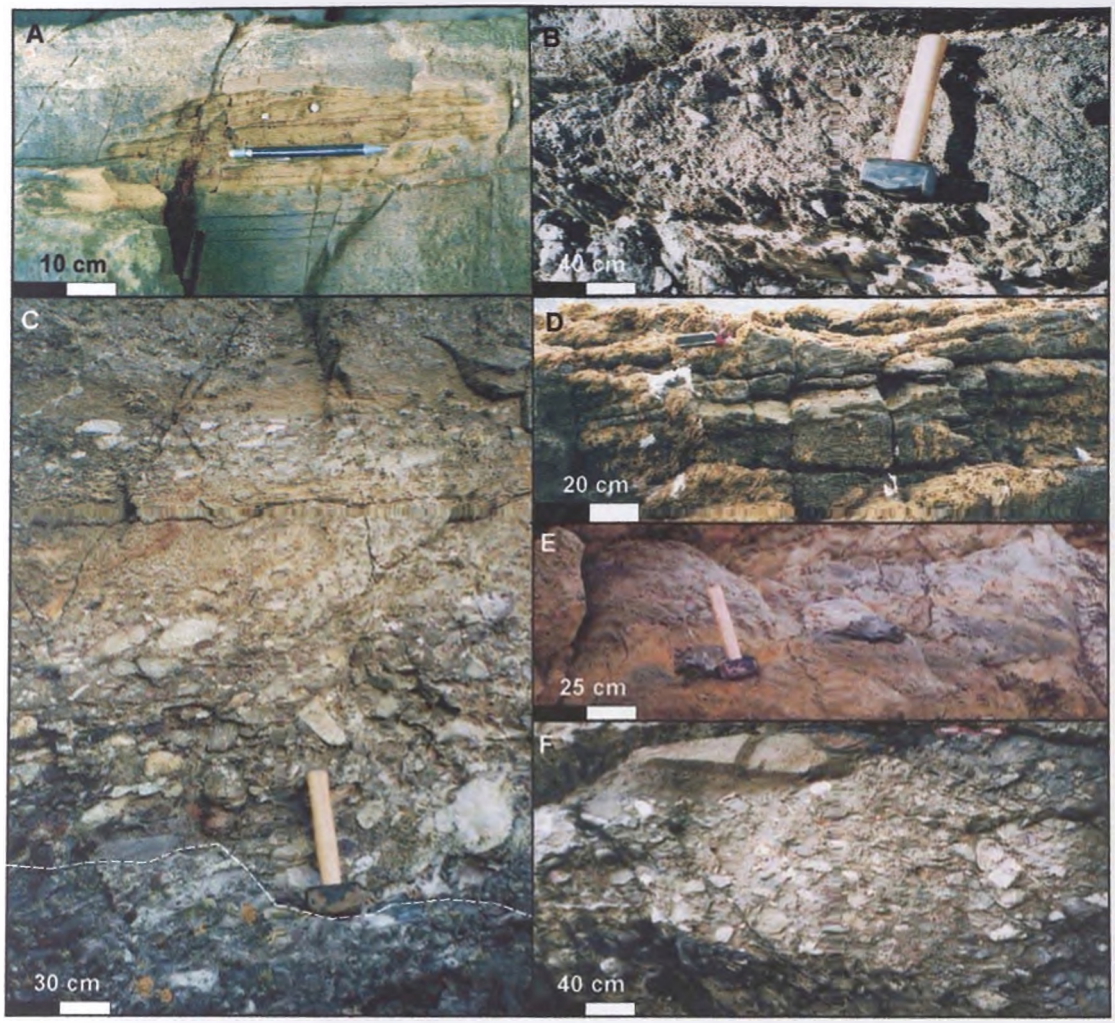



**Fig. 2.3.** Lithological characteristics of the Ogof Golchfa Formation and the St Non's Formation. Apart from C, all photos are from the section extending from Ogof Golchfa to Porthselau. (A) St Non's Formation - accretionary hummocky cross-stratification in fine-grained quartzose sandstone. (B) Ogof Golchfa Formation - highly channelized sand-matrix-supported conglomerates interpreted as hyperconcentrated flood-flow deposits (C) Ogof Golchfa Formation (Ogof Goch) – well rounded clast- to matrix-supported conglomerate passing upwards into crudely stratified pebbly sandstone. This sequence is interpreted as a beachface deposit overlying a wave ravinement surface (transgressive surface of erosion). (D) Ogof Golchfa Formation - trough cross-bedded pebbly sandstones. (E) St Non's Formation - gutter casts incised into bioturbated silty mudstones. (F) Ogof Golchfa Formation - imbricated clast– to matrix-supported conglomerate with an overlying coarse-grained sandstone wedge. These are interpreted as channel conglomerates deposited in a high-energy braided stream during flood stages.

sorting, significant erosive capabilities, a(p)a(i) clast imbrication (notation after Walker 1975), lack of internal stratification and massive to inversely graded profiles are typical features of strongly shearing hyperconcentrated flows (Nemec and Steel 1984; Smith 1986; Todd 1989; Granville and White 2003). The upward transition into "unit B" (20.5 m thick) occurs over 2 m, and is marked by a decrease in lenticular beds, an increase in tabular mud- and sand-matrix-supported conglomerates, and occasional thin (2–12 cm thick) interbedded purple siltstones. Bed boundaries are difficult to identify due to poorly organized texture and fabric, but where visible are planar and non-erosive. Despite evidence for clast rounding, traction influenced sedimentation is an unlikely depositional process due to a lack of stratification, matrix support, poor sorting, well developed inverse grading, a(p)a(i) clast imbrication, insignificant basal erosion, and unstable pebble orientations. These features instead suggest a sediment gravity flow origin as either cohesive (mud-matrix) or non-cohesive (sand-matrix) debris flows (Lowe 1982; Massari 1984; Kim *et al.* 1995).

"Unit C" (12.5 m thick) is composed of numerous small scale (1-1.6 m) fining upwards sequences. Each sequence begins with a clast-supported conglomerate lag, passing upward into a stratified clast-supported conglomerate with a cross-stratified coarse-grained sandstone cap (Fig. 2.3F). A tractional a(t)b(i) clast fabric, better sorting, erosive base, parallel and cross-stratification in both conglomerates and sandstone, and the broadly channelized geometry suggest fully turbulent flow. "Unit D" (4 m thick) is separated from the unit below by a conspicuous erosion surface (Fig. 2.3C), upon which lie large pebbles, cobbles and rarely boulders. This unit is characterized by very well rounded clasts, trough cross-bedding (Fig. 2.3D), and the first sign of bioturbation (*Skolithus* burrows and rare unidentifiable horizontal burrows). The accumulation of "unit D" in a shallow marine environment is unquestionable in the light of palaeontological evidence. The presence of *Skolithus* suggests shallow, well-oxygenated water affected by persistent, relatively high-energy currents above a mobile substrate (Frey and Pemberton 1984).

The interbedded assemblage of hyperconcentrated flows and debris flows in units A and B is consistent with deposition on an alluvial fan (Blair and McPherson 1994) (Fig. 2.4.). The crudely stratified conglomerates of "Unit C" are interpreted as braided stream channel lags and longitudinal bars (Rust 1978; Nemec and Postma 1993), while "Unit D" is a transgressive beach and shoreface sequence (Bourgeis and Leithold 1984; Nemec and Steel 1984) separated from continental deposits below by a wave ravinement surface (Cattaneo and Steel 2003). Crimes (1970a) previously interpreted the entire succession as a beach and shoreface setting based

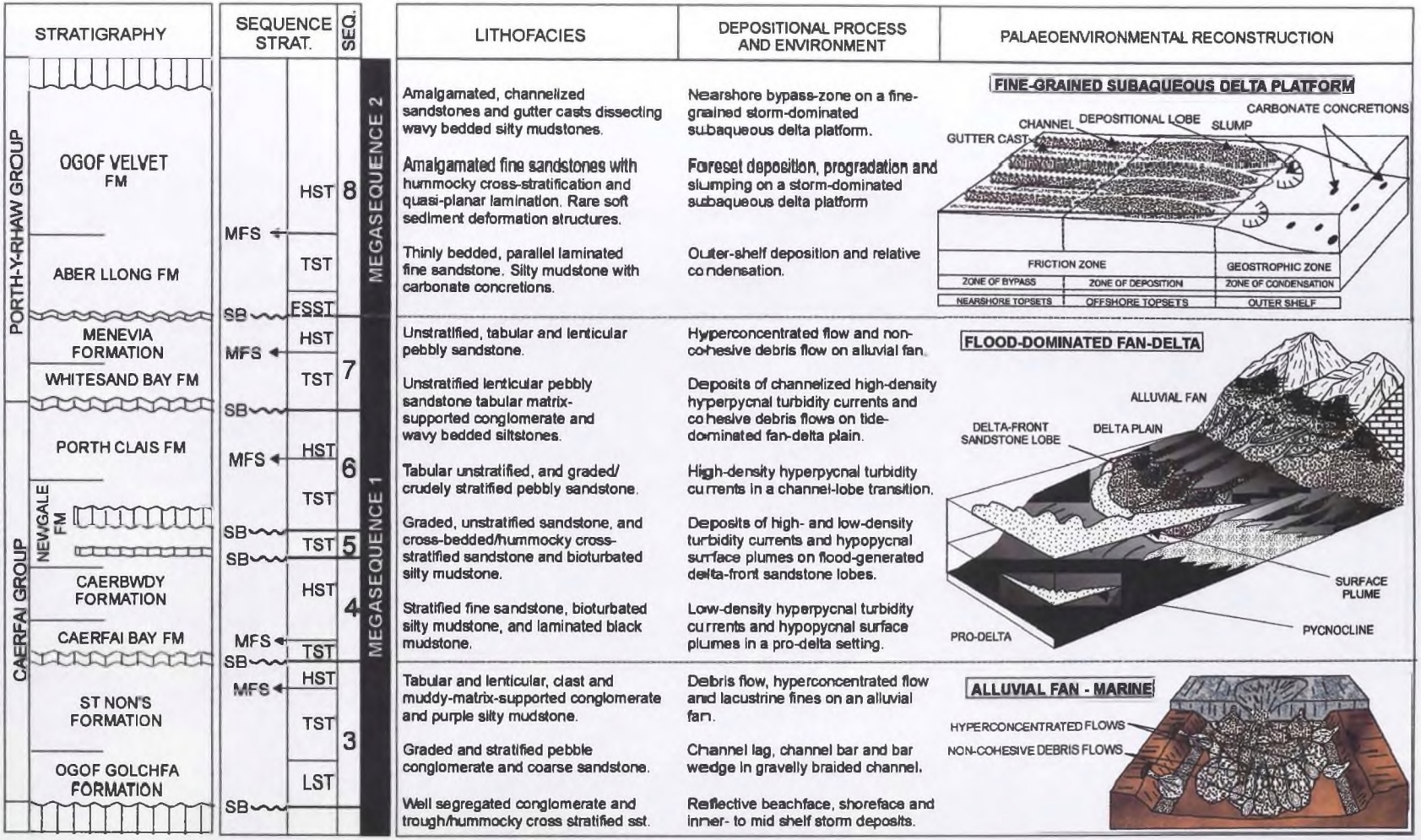



**Fig. 2.4.** Lithofacies, depositional processes and environments of the Dyfed Supergroup in SW Wales.

on *Skolithus*, but failed to specify where in the sequence bioturbation first occurs. In fact, the lower 40 m (units A, B and C) contain no evidence of biogenic activity.

*Distribution:* The Ogof Golchfa Formation is exposed on both sides of Caerbwdy Valley, 150–200 m north of the site of Melin Caer-Bwdy (Caerbwdy Mill), but both lower and upper junctions of the unit are obscured by vegetation. Although not exposed in the eastern Caerfai Bay section, boulders of conglomerate on the shore at the head of the inlet indicate close proximity to the unit (Fig. 2.1C). The unit passes just south of Caerfai Farm, from where it forms an easily mappable topographic feature extending westwards to St Non's Bay. Good exposures around the coastal path, approximately 250 m SE of St Non's Retreat, from where W. Jones (1911) recorded the presence of a cross-stratified lenticular body of detrital titaniferous haematite, c. 16 cm thick (at SM 75362 24250). On the western side of St Non's Bay, the conglomerate forms a prominent E–W trending ridge on the foreshore and can be seen to the east on several sea stacks. All of the outcrops in the vicinity of St Non's Bay correspond to "Unit D" of the type locality. The base is sharp, overturned to the north, and with slight angular discordance on Pebidian tuffs of the Caerbwdy Group. The tuffs are stained a reddish colour for at least 2 m below the junction and it has been suggested (Green and Jones 1911, p. 226; Owen *et al.* 1971, p. 24) that this possibly represents an original erosion surface or is an effect caused by the percolation of fluids along the plane of contact.

At Ogof-Llesugn (SM 7355 2350), west of Porth Clais, a mass of conglomerate with underlying stained Pebidian is faulted between Dimetian granophyre and vertical sediments of the Porth Clais Formation (new). In the arch at Ogof Goch, 900 m south of the St David's Lifeboat House on Ramsey Sound, the conglomerate rests with planar contact on reddish stained Pebidian rocks of the Ramsey Sound Group. Units C and D are readily identified at that locality, although the lower unit is highly attenuated. Green (1908, p. 380) described large blocks of Cambrian conglomerate incorporated as xenoliths within an unclassified mafic intrusive body west of Carn-ar-wig on Ramsey Sound.

### 2.2.1.2. St Non's Formation

*History:* The term "St Non's Sandstone" (Table 2.1) was introduced by Cowie *et al.* (1972, p. 31) for the succession of predominantly dark-green, buff-weathering sandstones overlying the basal conglomerate, and previously referred to as "green

sandstone" by Salter and Hicks (1866) and "green flags" by Harkness and Hicks (1871).

*Name:* From St Non's Bay on the coast south of St David's (Fig. 2.1C).

*Type locality:* The type section is at Porthselau (SM 7275 2620), where the formation is well exposed in an easily accessible coastal section at medium to low tide (Fig. 2.1B). There is no complete section through the St Non's Formation, but a composite section can be constructed from two further reference sections: (1) the northernmost part of the eastern cliff section, Caerfai Bay (Fig. 2.2), and (2) the western cliff section and wave cut platform at Porth Coch-bach, on the west side of St Non's Bay (SM 7502 2421 to SM 7504 2416).

*Thickness:* At the type locality, the formation reaches a thickness of 79 m, which defines a minimum value. The cumulative thickness from the three reference localities is 149 m, close to the value of 140 m proposed by Rushton (1974).

*Lower boundary:* The junction with the Ogof Golchfa Formation is only exposed at Porthselau and is transitional with no sharp sedimentological boundary. The base is drawn at the first coarse-grained sandstone bed that overlies the last pebble grade conglomerate bed. This roughly coincides with a colour change in interbedded sandstones from reddish-brown to green.

*Lithology and process sedimentology:* In general, the formation comprises dark green, buff weathering, fine- to medium-grained quartz-rich sandstones, with occasional pebbly sandstones that are confined to 4–6 m above the lower boundary. In the reference section at Caerfai Bay the uppermost 5–7 m is tinted purple and was distinguished by Hicks (1894, p. 7) as one of a fivefold division then adopted for the Caerfai Group. This subdivision has never gained formal acceptance with subsequent authors and is not recognized herein. The purple colouration is related to that of the overlying Caerfai Bay Formation, and is probably of diagenetic origin (Turner 1979).

The formation is stratified towards the base but this is lost higher up through intense bioturbation. The latter results in a marked increase in apparent bed thickness, which may reach up to 2 m in sections exposed at Caerfai Bay. The salient characteristics of the St Non's Formation are better studied at the type locality, where bioturbation is considerably less. There, the section comprises

amalgamated weakly graded sandstones or interbedded sandstones and silty mudstones. Bed thickness ranges from 5–33 cm, basal surfaces are typically planar-erosional or elliptical-erosional, gutter casts are particularly common (Fig. 2.3E), and stratification is well developed. Trough cross-bedding dominates the lowermost 12 m, which is replaced up-section by hummocky cross-stratification (Fig. 2.3A), parallel lamination, and quasi-planar lamination (Arnott 1993). Wave ripples are well developed throughout, while current ripples occur towards the base.

Interbedded silty mudstones are often completely homogenized, and are best analyzed on the wave cut platform at Porth Coch-bach. Flaser, wavy and lenticular bedding is pronounced, and dissected by small channels and gutter casts filled with either parallel lamination or hummocky cross-stratification. Large horizontal burrows occur in the caves at Porthstinian, along with dense *Skolithus* and *Teichichnus* burrows. Higher in the sequence, bioturbation is intense and individual burrows are not preserved. An exception are the eastern cliffs of Caerfai Bay where examples of dense *Skolithus* occur at the transition into the Caerfai Bay Formation.

Sedimentological and palaeontological evidence from the St Non's Formation is consistent with deposition on a high-energy wave-dominated coastline that was periodically affected by large storms (Harms *et al.* 1975; Hamblin and Walker 1979; Dott and Bourgeois 1982; Brenchley 1985). The upward evolution from trough cross-bedded pebbly sandstones at the base, through hummocky cross-stratified medium-grained sandstones in the middle, to homogenized muddy sandstones towards the top are common facies gradations from both modern and ancient transgressive storm-dominated coastlines (Bourgeois 1980; Aigner and Reineck 1882). Densely populated *Skolithus* burrows in the purple tinted uppermost 7 m of the formation may record a return to shallow water conditions but without the typical facies associated with this water depth as developed in the lower part of the formation. This rather unusual scenario suggests extremely rapid shallowing at a rate exceeding that of facies change (discussion further below).

*Distribution:* In addition to the exposures outlined above, the St Non's Formation also forms extensive but largely inaccessible cliff sections at Maes Bachau (SM 7225 2455) approximately 500 m south of Porthstinian. A small fault-bounded inlier occurs on the foreshore at Cwm Bach (SM 8415 2307) at the northern most point of Newgale Sands, in Caerbwdy Valley (SM 7678 2452) and to the west of Pen-y-Cwm (SM 8335 2364). Olive-green fine-grained sandstones and siltstones located immediately north of Ogof Golchfa were mapped by Williams (in Owen *et al.* 1971, p. 30) and Stead and Williams (1971, p.195) as St Non's Sandstone and by the B.G.S.

as "Solva Beds" (undifferentiated). Based on lithological and stratigraphical evidence, these beds are "Upper Solva" (Cowie *et al.* 1972) and form the type section for the Whitesand Bay Formation (new). This is in agreement with Jones (in Green 1911, p. 216, 217) who assigned the succession "to the top of the Solva (Lower Paradoxidian) beds", and highlights the problem of defining lithostratigraphic units entirely on diagenetic colouration.

### 2.2.1.3. Caerfai Bay Formation

*History:* The purple sandstones at the top of the St Non's Formation pass rapidly upwards into the "Caerfai Bay Shale" – a term introduced by Cowie *et al.* (1972, p. 27). Previous authors referred to this unit as being composed of "Red Shales" (Harkness and Hicks 1871; Cox *et al.* 1930b; Owen *et al.* 1971) despite the fact that it predominantly comprises a succession of dull siltstones that grade upwards in the St David's area into red mudstones. The term "shale" has presumably been applied because the mudstones in particular tend to be very strongly cleaved.

*Name:* From Caerfai Bay, situated on the coastal section south of St David's.

*Type locality:* The type area of the formation is the eastern side of Caerfai Bay (SM 7615 2434), but important reference sections also exist on the western side of the bay (although some minor faulting is evident) and at Cwm Bach (SM 8415 2307). The section at Cwm Bach assumed importance when biostratigraphically important ostracodes were collected by Pringle and George (1948) and Siveter and Williams (1995).

*Thickness:* In the type area, the Caerfai Bay Formation attains a thickness of 19 m. The formation appears to be uniformly developed throughout the entire district.

*Lower boundary:* The top of the St Non's Formation passes sharply into the Caerfai Bay Formation. This transition is marked by a group of purple-coloured siltstones, 4–9 cm thick, which are extensively bioturbated and represent the top of the St Non's Formation (Turner 1979). The bioturbation is frequently associated with *Skolithus* burrows. Although all earlier workers reported a gradational contact, Landing *et al.* (1998) suggested that the extensive bioturbation at the top of the St Non's Formation is a caliche horizon and interpreted the contact with the Caerfai Bay Formation as

unconformable. This surface was then correlated with an unconformity at the base of the Branchian in southeastern Newfoundland (see Fig. 2.13), although no evidence was found for caliche in this study, or that of Prigmore and Rushton (2000). Based on an apparent facies dislocation across the contact (discussed below), this surface is interpreted as a paraconformity.

*Lithology and process sedimentology:* The formation at Caerfai Bay and at several other localities along the south and west coasts of the St David's peninsula can be subdivided informally into two lithologically distinct units. The lower unit ("unit A") consists of about 4 m of dull-purple micaceous siltstones which exhibit cross-lamination, wave ripples, convolute bedding, micro-hummocky cross-stratification, load casts, flute casts, gutter casts, and bioturbation features such as the feeding burrow *Teichichnus* (Williams and Stead 1982), *Skolithus*, and unidentifiable escape burrows. Bioturbation is made evident particularly by the disturbance of thin horizons composed of coarse, well sorted silt cemented by calcite (Turner 1979). These siltstones grade into "unit B" which is a distinctive brick-red sequence of strongly cleaved mudstones roughly 15 m thick (Fig. 2.2A). Very little structure is evident due to intense homogenisation of the sediment by burrowing organisms (Prigmore and Rushton 2000).

Towards the junction with the overlying Caerbwdy Formation, the unit develops thin (2–6 cm), graded, very fine-grained sandstones with planar upper and lower contacts that exhibit cross-lamination, flute casts and load casts. The siltstones and mudstones contain illite, kaolinite, chlorite and smectite, and the red colouration appears to have been produced entirely by diagenetic alteration of iron silicates and volcanic ash (Turner 1979). Apart from the distinctive colouration, the presence of at least 17 water-laid, pale grey to purplish feldspathic crystal tuff horizons (Fig. 2.2A) makes the Caerfai Bay Formation a distinctive marker horizon across much the St David's Peninsula. Internally, these well graded volcanic ashes are cross-laminated, commonly deformed into convolute lamination, have sharp erosive bases, often with load casts and a coarse gravel lag containing intraclasts of red mudstone.

Like the St Non's Formation below, the salient characteristics of the Caerfai Bay Formation are consistent with deposition on a storm-influenced shelf. Although the formation is relatively thin, a number of fairly rapid changes in water depth are documented. The most distinctive occurs over the basal 2–3 m which records extremely rapid deepening from well above wave-base at the top of the St Non's Formation (as indicated by dense *Skolithus* burrows) to graded parallel laminated siltstones typical of B/C tempestites deposited below storm wave-base (Reineck and

Singh 1972). Evidence for rapid deepening as well as equally rapid shallowing in the uppermost St Non's Formation (see above) may record the tectonic event postulated by Landing *et al.* (1998) but without the development of a caliche. Their correlation of this junction based on radiometric dates with the major unconformity at the base of the Branchian is validated but is considered more cryptic than the caliche horizon suggested by those authors. This tectonic event is also consistent with the numerous volcanic ash layers which, considering their thickness and grain size, must have been sourced fairly locally.

*Distribution:* The Caerfai Bay Formation forms a distinctive unit across much of the southern and western coastlines of St David's Peninsula, and both eastern and western outcrops of the Haycastle inlier. It is particularly well exposed in all of the bays and headlands between and including Caerfai Bay and Porth Clais. The upper part of the formation and the transition into the overlying Caerbwdy Sandstone is well exposed at Porthstinian (SM 7241 2526) and immediately west of Porthselau (SM 7263 2607), but access is more restricted.

*Biota and age:* Fossils from the Caerfai Bay Formation are rare, and were once thought to be biostratigraphically undiagnostic (see Cowie *et al.* 1972, p. 26; Rushton 1974, p. 54). Hicks (1881) described the brachiopod *Lingulella primaeva* and the ostracode *Leperditia? cambrensis* from Porth Clais and recorded trilobite fragments from southeast of Rhosson (SM 7244 2461) in Ramsey Sound. Some fragments originally identified by Hicks as *Leperditia? cambrensis* were subsequently considered to be cephalic fragments of *Ollenellus* because they displayed a reticulate surface ornamentation (Hicks 1892, p. 21; Jones in Cox *et al.* 1930a, p. 250). In the summary of Progress of the Geological Survey for 1928 (p. 24) it was stated that a specimen collected by Pringle from the red shales at Cwm Bach, near Newgale in 1908 had been identified as the hypostoma of an *Olenellus* or closely allied genus. This "hypostoma", however, has subsequently been identified as an ostracode (Pringle and George 1948, p. 19).

Re-investigating Pringle's locality at Cwm Bach, Siveter and Williams (1995) collected some 50, mostly fragmentary, specimens of an ostracode species, a probable trilobite fragment, and a specimen of *Coleoloides?* sp. The fragments of ostracode were considered conspecific with 22 specimens collected by Pringle, and all were assigned to *Leperditia (?) lentiformis* Cobbold (*Indiana).* This identification affords an important point of correlation between the Caerfai Bay Formation and the Red *Callavia* Sandstone (division Ac2 of Cobbold 1933) of the basal Lower Comley

Sandstone, at Comley, Shropshire, and proves a lower Cambrian age for most, of not all, of the Caerfai Group. The presence of a trilobite fragment, and correlation with the Red *Callavia* Sandstone places the Caerfai Bay Formation in the trilobitic Olenellid Biozone of Cowie *et al.* (1972), a position consistent with the chronostratigraphy presented by Landing (1998) and a U–Pb data for the formation of 519 ± 1 Ma.

#### 2.2.1.4. Caerbwdy Formation

*History:* "Purple, or Caerbwdy Sandstone" (Table 2.1) was introduced by Jones (in Cox *et al.* 1930a, p. 251) as an alternative name for the uppermost "Purple Sandstone" division of the Caerfai Group as then recognised by Hicks (1881). Stubblefield (1959, p. 15) used the term "Caerbwddy Sandstones" and gave the type locality as "Caerbwddy Bay".

*Name:* From Caerbwdy Bay situated on the coastline south of St David's (Fig. 2.3C).

*Type locality:* Although a good section through the Caerbwdy Formation exists in Caerbwdy Bay (retained as an important reference section), the most easily accessible and complete succession occurs on the eastern side of Caerfai Bay (Fig. 2.2), which is considered the best candidate for stratotype.

*Thickness:* The Caerbwdy Formation was estimated by Harkness and Hicks (1871) to be 1000 ft (300 m) thick and by Green (1908, p. 365) to be 900 ft (275 m). Jones (in Cox *et al.* 1930a, p. 365) considered a thickness of 500 ft (150 m) as more probable. The logged thickness as exposed on the eastern side of Caerfai Bay is 136 m once fault bounded repetitions of relatively small sections have been removed. The Caerbwdy Formation shows a marked thinning to the east, with equivalent beds (formerly the "Welsh Hook Beds") in the Haycastle area attaining a maximum thickness of 80 m (Thomas and Jones 1912, p. 392).

*Lower boundary:* The lower junction with the Caerfai Bay Formation is entirely gradational and marked by the appearance of maroon sand grade detritus thinly interbedded with bright red cleaved mudstone. The base of the formation is defined at the point where sandstone beds account for more than 50% of rock volume.

*Lithology and process sedimentology:* In the St David's area the Caerbwdy Formation is a fairly uniform deposit of fine- to medium-grained micaceous, and somewhat argillaceous sandstone, dull purple in colour and generally poorly sorted. Beds may range up to 1.5 m in thickness (Fig. 2.2C) and are typically massive in appearance, although parallel lamination (Fig. 2.2D2), cross-stratification and grading sometimes occur. Individual beds exhibit planar tops and bases, and appear extensively bioturbated (Fig. 2.2B and D1). In most cases homogenization is so intense that discrete burrows are no longer preserved, although rare bedding parallel forms and *Skolithus* have been documented (Prigmore and Rushton 2000). The origin of these thick-bedded sandstones is uncertain (Rushton 1974). Crimes (1970a) suggested that deposition took place below storm wave-base, and that the whole Caerfai Group represents a transgressive sequence and thus a deepening sea. Prigmore and Rushton (2000) highlighted the presence of *Skolithus* and inferred rapid deposition from traction currents in a high-energy environment, and therefore a regressive state with respect to the Caerfai Bays. Critical to this argument is the almost complete absence of internal stratification, which on face value precludes traction-influenced sedimentation.

There are three possible mechanisms that can explain the observed characteristics: (1) deposition from a large surge-type tractional flow or long duration quasi-steady flow, followed by intensive bioturbation, (2) suspension sedimentation but in relatively shallow water, or (3) deposition from a form of non-Newtonian (and thus non-tractional) sediment gravity flow. Although traction structures are noted in the succession, they are extremely rare, and tend to occur only on upper bed surfaces suggesting formation during post-depositional reworking rather than during emplacement of the whole bed. It is also considered unlikely that bioturbation could destroy all stratification in a bed greater than 2 m thick as it was deposited, or once it had been emplaced. Although sediment gravity flows cannot be ruled out, the dominance of parallel lamination without parting lineation (therefore of the lower flow regime) is more consistent with suspension sedimentation. Deposition principally out of suspension would also allow time for thorough bioturbation.

Thin planar-bedded tuffaceous horizons identical to those seen in the Caerfai Bay Formation occur throughout but with greater vertical spacing. Bioturbation in these bands is also far more intense than that recorded previously, with many ash layers almost completely homogenized (Fig. 2.2D1). At Caerfai Bay, on the western side of Caerbwdy Bay and the western side of Porth Clais (70–80 m south of the harbour wall), there exists a brick red sequence some 80 m above the base of the formation (Jones in Cox *et al.* 1930a). Bedding in this sequence is better defined and

stratification preserved. Discrete beds up to 20 cm thick occur displaying rare bi-directional cross-bedding. These solitary sets display mud-draped reactivation surfaces and current ripple crests in the opposite direction to megaripple toesets. Bi-polar palaeocurrents and reactivation surfaces are typically associated with tidal action (Visser 1980), which may suggest a regressive phase during deposition of this unit. Above this sequence, the style of sedimentation normally associated with the Caerbwdy Formation returns. The uppermost beds of this formation are reduced in thickness and become much coarser where they pass gradationally into pebbly sandstones of the Newgale Formation (= "Lower Solva" of Hicks 1881). This coarsening upwards defines a regressive motif that continues into the overlying Newgale Formation.

*Distribution:* The Caerbwdy Formation is well developed in all the cliffs from Porth Clais to the eastern side of Caerbwdy Bay (Fig. 2.1C) where the highest sandstones and basal beds of the Newgale Formation are involved in a spectacularly exposed, southward verging, thrust-related monoclinal fold (see frontispiece in Holland 1974). South of the St David's Lifeboat Station on Ramsey Sound outcrops of the Caerbwdy Formation are much faulted and largely inaccessible. Minor exposures occur immediately west of Porthselau where the transitional contact with the Caerfai Bay Formation is seen, at Cwm Bach, Dinas Fawr (SM 8285 2290) and both eastern and western outcrops of the Haycastle inlier.

### 2.2.1.5. Newgale Formation (new)

*General:* The Newgale Formation (Table 2.1) is equivalent to the Lower Solva of Hicks (1881).

*Name:* From the northern cliffs of Newgale Sands.

*Type locality:* The formation is fully exposed at Porth Clais and immediately east of Porthstinian, but these sections are relatively condensed and partly inaccessible. Well exposed sections at Cwm Mawr and Ogof Blawd Ceirch (7554 2401) are faulted against the Caerbwdy Formation but in the former only a metre or so of section appears to be lost. Cwm Mawr is therefore designated stratotype, and in terms of lithology offers by far the most representative section through the Newgale Formation.

*Thickness:* A marked thinning of the Newgale Sands Formation is recorded from Cwm Mawr in the east, where it attains a minimum thickness of 55 m, to Porthstinian in the west, which measures 29 m. Sections at Porth Clais and Ogof Blawd Ceirch measure 38 m and 40 m respectively.

*Subdivisions:* The formation is divided into 3 members (Table 2.1), the boundaries of which are those defined by Stead and Williams (1971). In ascending order their "Lower pebbly sandstone member", "Sandstone-shale member", and "Upper pebbly sandstone member" are formally defined as the Trwyncynddeiriog Member, Pen-y-Cyffrwy Member, and the Cwm Mawr Member respectively.

*Lower Boundary:* The boundary between the Caerbwdy Formation and the Newgale Formation is well exposed in the eastern cliffs of Caerfai Bay, at Trwyncynddeiriog, Caerbwdy Bay, Dinas Fawr, Porth Clais, and west of Porthselau. Apart from at Caerfai Bay, all other localities display a simple gradation from coarse grained dull purple sandstones of the Caerbwdy Formation into pebbly sandstones typical of the Newgale Formation (Stead and Williams 1971; Rushton 1974; Prigmore and Rushton 2000). Although historically, the base of the Newgale Formation (previously the base of the Solva Group) is drawn at the first pebbly sandstone (Hicks 1894, p. 10), subsequent authors (e.g. Stead and Williams 1971; Prigmore and Rushton 2000) have preferred a more arbitrary contact defined by a diagenetic colour change from purple Caerbwdy Formation to greenish Newgale Formation. The first pebbly bed is a distinctive mappable horizon from Dinas Fawr in the east to Porthselau in the west, while the green/purple colouration differs quite significantly immediately above and below this pebbly bed. The definition by Hicks (1894) is therefore preferred although this marker bed may be purple or have a metre or so of purple beds above or below it.

At Caerfai Bay, the Newgale Formation was interpreted by Jones (1940) to rest disconformably upon eroded Caerbwdy Sandstone. To the east of the Haycastle Anticline, Jones (1940) also claimed a similar stratigraphic break between the green sandstones overlying the Caerbwdy Formation and the "Lower Solva" Musland Grit, and correlated this break with pre-"Solva" erosion at Caerfai Bay. A detailed analysis of this contact at Caerfai Bay by Stead and Williams (1971, p. 191) concluded that the offset interpreted as an unconformity is in fact a faulted contact. Higher in the cliff face, the same fault runs through the Caerbwdy Formation, revealing a transitional gradation into the Newgale Formation.

*Distribution:* Traced eastwards from Porth Clais, the Newgale Formation intersects and traverses the Trwyncynddeiriog, Pen-y-Cyffrwy, Caerfai and Caerbwdy headlands (Fig. 2.1C). Continuing eastwards, exposure occurs on the headland of Dinas Fawr (SM 8119 2281), and in the Haycastle anticline at Cwm Mawr. Complete, but largely inaccessible sections occur to the north of Porthstinian and to the west of Porthselau (Fig. 2.1B). Both sections terminate near Point St John. A small exposure of the upper part of the formation occurs in a small quarry (SM 8064 2447) on the roadside opposite Solva Harbour car park.

*Age and biota:* Fossils have only been recovered from the Pen-y-Cyffrwy Member on the extreme headland of Trwyncynddeiriog and indicate a late *Paradoxides oelandicus (P. pinus* Biozone*)* age (Middle Cambrian). The interval between the *Indiana* in the Caerfai Bay Formation and the paradoxidid fauna is therefore represented only by approximately 180 m, but is a time interval that spans the whole Moroccan Tissafinian Stage (with three trilobite zones). According to Rushton (pers. comm. 2003) this is too long an interval to be represented by the measured thickness if the sediment had been rapidly deposited, as had previously been assumed. Following considerations by early authors, Rushton (1974 and *op. cit.*) also inferred, based on this biostratigraphic evidence, that there must exist a cryptic hiatus some where between the Caerfai Bays and the Pen-y-Cyffrwy Member, preferring somewhere near the very base of the Newgale Formation. Detailed logging of this interval at 4 different locations found no evidence for a hiatus, and it is considered more likely that both the Caerfai Bay Formation and the Caerbwdy Formation are condensed sections, a conclusion consistent with the sedimentological characteristics of both formations.

*2.2.1.5.1. Trwyncynddeiriog Member (new)*

*Type locality:* The type locality is the headland of Trwyncynddeiriog (SM 7488 2392) on the western side of St Non's Bay (Fig. 2.1C). An important reference section occurs at Cwm Mawr, an exposure that demonstrates lithological characteristics not represented elsewhere.

*Thickness*: At the type locality, the Trwyncynddeiriog Member attains a thickness of 21 m. This increase eastwards attaining a minimum thickness at Newgale of 23 m, and decreases westwards, where less than 15 m can be demonstrated west of Porthselau.




**Fig. 2.5.** Lithological characteristics of the Newgale Formation. (A) Trwyncynddeiriog Member (Cwm Mawr) – pebbly mudstones and mud-matrix-supported conglomerates interpreted as cohesive debris flows. (B) Trwyncynddeiriog Member (Trwyncynddeiriog) – massive coarse-grained sandstones interpreted as the deposits of high-density turbidity currents. The upper part of the turbidite has been reworked by tidal currents into planar cross-stratification. (C) Trwyncynddeiriog Member (Cwm Mawr) – slump horizon. A similar horizon is also evident in coeval strata on the Trwyncynddeiriog headland. (D) The sharp contact between pebbly sandstones of the Trwyncynddeiriog Member and planar-laminated siltstones of Pen-y-Cyffrwy Member at Pen-y-Cyffrwy. This abrupt deepening occurs throughout the study area and is interpreted as a marine flooding surface. (E). Details of the contact outlined in (D).




**Fig. 2.5.** Lithological characteristics of the Newgale Formation. (A) Trwyncynddeiriog Member (Cwm Mawr) – pebbly mudstones and mud-matrix-supported conglomerates interpreted as cohesive debris flows. (B) Trwyncynddeiriog Member (Trwyncynddeiriog) – massive coarse-grained sandstones interpreted as the deposits of high-density turbidity currents. The upper part of the turbidite has been reworked by tidal currents into planar cross-stratification. (C) Trwyncynddeiriog Member (Cwm Mawr) – slump horizon. A similar horizon is also evident in coeval strata on the Trwyncynddeiriog headland. (D) The sharp contact between pebbly sandstones of the Trwyncynddeiriog Member and planar-laminated siltstones of Pen-y-Cyffrwy Member at Pen-y-Cyffrwy. This abrupt deepening occurs throughout the study area and is interpreted as a marine flooding surface. (E). Details of the contact outlined in (D).

*Lithology and process sedimentology:* The member consists essentially of poorly sorted grey-green to pale-yellow coarse to pebbly sandstones with thin mudstone interbeds. Mudstones typically constitute less than 20% of the member, which is in part due to intense amalgamation of coarser beds. Pebbly mudstones and mud-matrix-supported conglomerates (Fig. 2.5A) with a chaotic internal fabric and non-erosive bases are subordinate and confined to exposures at Cwm Mawr. Pebbly sandstones become coarser-grained, more frequent and thicker towards the east, where they attain their highest values at Cwm Mawr. Bedding is generally thick and tabular in geometry, with highly erosive bases that typically display load casts and flute casts. Grading is extremely variable, and includes normally graded, inversely graded, inverse to normally graded, and ungraded beds. Many beds display a clear bipartite structure, the most common being a simple pebbly sandstone-coarse sandstone couplet. Outsized rip-up clasts of mudstone are common, and are often found aligned between the two divisions or apparently "floating" in coarse sandy matrix. These intraclasts, as well as pebbles, typically display a(p)a(i) imbrication (notation after Walker 1975). Desiccation cracks have been reported from the type locality (Rushton 1974).

The amount of stratification also displays great variation from east to west. At Cwm Mawr, stratification is completely absent in sandstones and matrix-supported conglomerates, but is well developed in intercalated mudstones, where flaser and wavy bedding dominates. Elsewhere, mudstones are extensively bioturbated, although remnant fabric can still, in some case, be discerned. At Pen-y-Cyffrwy and Trwyncynddeiriog, stratification in sandstones is more common, with trough cross-bedding, herringbone cross-bedding, reactivation surfaces, and ripple cross-lamination documented. Hummocky cross-stratification and wave ripples also occur, but are extremely rare and very poorly developed. Stratification is generally confined to the upper 20 cm of graded or massive divisions (Fig. 2.5B). These upper portions are invariably better sorted, although pebbles are still common, often found aligned on megaripple foresets.

Upper contacts of sandstones and pebbly sandstones may be sharp or gradational. The upper 4–6 cm often consists of small overturned fold structures while bedding planes record irregular ripple-like forms. The latter resemble the kinneyia ripples described by Martinson (1965) and Dzulynski and Simpson (1966). Dish structures are common in all coarse sandstones, being particularly well developed at Pen-y-Cyffrwy. Larger scale soft sediment deformation structures occur at Cwm Mawr, including a 3 m thick slump horizon (Fig. 2.5C). The degree of bioturbation increases dramatically from Cwm Mawr to Porth Clais, being absent in

the former and ubiquitous in the latter. *Skolithus* burrows are the only identifiable traces. At all localities, beds display a typical regressive motif with coarsening and bed thickening upward. This trend is mirrored by a decrease in stratification upward through the section, a trend particularly pronounced at Pen-y-Cyffrwy.

Poor sorting, a(p)a(i) clast orientations, hydraulic sorting of pebbles, granules and sand into discrete couplets, lack of stratification, kinneyia ripples, erosive bases, dish structures, floating rip-up clasts, and massive and inverse grading are all typical of density-stratified, psuedo-laminar, coarse-grained high-density turbidity currents (Lowe 1982; Postma *et al.* 1988; Mulder and Alexander 2001). (Note: the term "turbidity current" is used here purely in a non-environmentally specific sense, and simply describes a mode of sediment transport in which motion is achieved by excess density). Both the S-sequence and R-sequence defined by Lowe (1982) for coarse-grained turbidites occur. Normal grading suggests fully Newtonian conditions and may represent deposition from low-density turbidity currents (Shanmugam 1997 2000). Mud-matrix-supported conglomerates and pebbly mudstones display characteristics consistent with deposition from cohesive debris flows where the cohesive matrix is the main clast support mechanism (Lowe 1982; Nemec and Steel 1984). The presence of cross-bedded tops to graded beds reflect subtidal reworking and partial redistribution of sediment emplaced by high-density turbidity currents. The presence of flaser and wavy bedding confirms the modulating effect of tidal currents on deposition (Visser 1980).

The interbedded assemblage of coarse-grained turbidites, cohesive debris flows, and fine-grained nearshore heterolithics is a commonly recorded facies association on flood-dominated fan-delta plains and fan-delta fronts (Prior and Bornhold 1989, 1990; Folk and Dorsey 1995; Mutti *et al.* 1996, 2000) (Fig. 2.4). The generation and ignition of high-density turbidity currents is directly related to flood episodes on coastal alluvial fans that discharge huge quantities of sediment into the nearshore generating quasi-steady turbidity currents of sufficient density to underflow sea water.

*2.2.1.5.2. Pen-y-Cyffrwy Member (new)*

*Type section:* The type section is located on the headland of Pen-y-Cyffrwy (SM 7553 2403 to SM 7554 2401) on the western side of Caerfai Bay (Fig. 2.1C). An important reference section occurs on the extreme headland of Trwyncynddeiriog. Although extensively faulted, this exposure offers the lowest horizon from which Middle Cambrian fossils have been found in Wales.

*Thickness:* The member is 13 m thick in the type section but thins dramatically east attaining only 1.5 m at Cwm Mawr.

*Lithology:* The Pen-y-Cyffrwy Member is composed predominantly of dark or medium brown-weathering, light-grey or green, finely laminated siltstone and mudstone (Fig. 2.5E), but includes well sorted beds of fine- to coarse- grained sandstone up to 50 cm thick in all sections apart from Cwm Mawr. This east–west lateral facies change also includes an increase in sandstone bed thickness up to the eastern side of Caerfai Bay, followed by a decrease in bed thickness and grain size at Porth Clais and west of Porthselau. The member is best displayed in the type section where it comprises two lithologically distinct units. The lower unit, about 2 m thick, consists of microlaminated mudstones and siltstones that display no structure other than discontinuous planar laminations and some bioturbation features (Fig. 2.5E). This closely resembles typical rhythmite facies documented from modern and ancient tide- and storm-influenced depositional systems (Reineck and Singh 1973; Johnson and Baldwin 1996).

The upper unit, approximately 11 m thick, consists predominantly of bioturbated silty mudstone interbedded with fine- to coarse-grained well graded sandstone. These sandstones often display either Bouma divisions Ta–Td, or more rarely tabular cross-bedding (particularly well developed at Porth Clais) and hummocky cross-stratification. Like the previous member, wave ripples are extremely rare while flute casts and load casts are common and well developed. Bioturbation throughout this upper unit is intense, with *Planolites*, *Sinusites* and *Teichichnus*-type burrows being particularly dominant. *Skolithus* burrows occur towards the junction with the overlying Cwm Mawr Member. In terms of depositional processes, most of the characteristics of this member can be reconciled with distal emplacement by similar currents that deposited the underlying member. The lower unit is difficult to interpret but is probably a rhythmite associated with distal turbidity currents as there no evidence for cyclicity, temporary exposure or wave action, features typical of tidal rhythmites. The upper unit with sandstones exhibiting Bouma divisions are more readily reconciled with low-density turbidity current deposition. This transition into more proximal facies as well as the presence of *Skolithus* towards the top of the member implies a shallowing-upward regressive motif after very sudden deepening at the base of the sequence.

*Lower boundary:* At all localities where the lower boundary may be examined, the contact is extremely sharp and marked by an instantaneous cut off of pebbly sandstone typical of the regressive Trwyncynddeiriog Member and very rapid deepening (Fig. 2.5D and E). Considering these characteristics, this junction may be referred to as a marine flooding surface, one that forms an important marker horizon throughout the area.

*Biota and age:* The discovery of fossils from this member was first reported by Salter (in Salter and Hicks 1869, footnote p. 52). Hicks (in Harkness and Hicks 1871) described the fauna as having been collected from a "headland near Nun's well"; it comprised *Paradoxides harknessi* Hicks, *Microdiscus sculptus* Hicks, *Bailiella* ("*Conocoryphe*") *lyellii* (Hicks), *Paradoxides* (*Plutonia*) *sedgewickii* (Hicks) and *Condylopyge* ("*Agnostus*") *cambrensis* (Hicks). Non-trilobite species described and/or illustrated by Hicks in the same paper were *Protospongia ? major* Hicks and "*Theca*" *antiqua* Hicks and *Lingulella ferruginea* Salter. The trilobites indicate a late *P. oelandicus* (*P. pinus* Biosubzone) age (Rushton 1974). The lowest Swedish Middle Cambrian Biosubzone, that of *P.* (*Eccaparadoxides*) *pinus*, is not proven in Britain, and may well be represented in part by the underlying Caerbwdy Formation.

*2.2.1.5.3. Cwm Mawr Member (new)*

*Type locality:* The type locality is at Cwm Mawr. Very different facies assemblages are recorded at important reference sections at Ogof Blawd Ceirch (SM 7554 2401 to 7555 2400) on the extreme headland of Pen-y-Cyffrwy and at Porth Clais.

*Thickness:* The member attains a minimum thickness of 19 m in the type locality, but this figure decreases to 12 m at Ogof Blawd Ceirch and 8 m at Porth Clais.

*Lithology:* In general, the member is composed of dull grey to yellow coarse-grained pebbly sandstones of polymictic composition. Beds are up to 2 m thick (Fig. 2.6D) and often form amalgamated units up to 3.2 m thick (Fig. 2.6A1). Geometrically, bedding is either tabular (Fig. 2.6D) with planar erosive or non-erosive surfaces, or highly channelized (Fig. 2.6A1, A2 and B) with multiple concave-up profiles (Fig. 2.6C) displaying a relief of up to 1.2 m, and a stepwise configuration reflecting channels with deeper and shallower parts. Smaller scale asymmetrical scours on these basal surfaces are occasionally filled with crude trough cross-bedding. General features include poor sorting, polymodal texture, massive, inverse, massive to

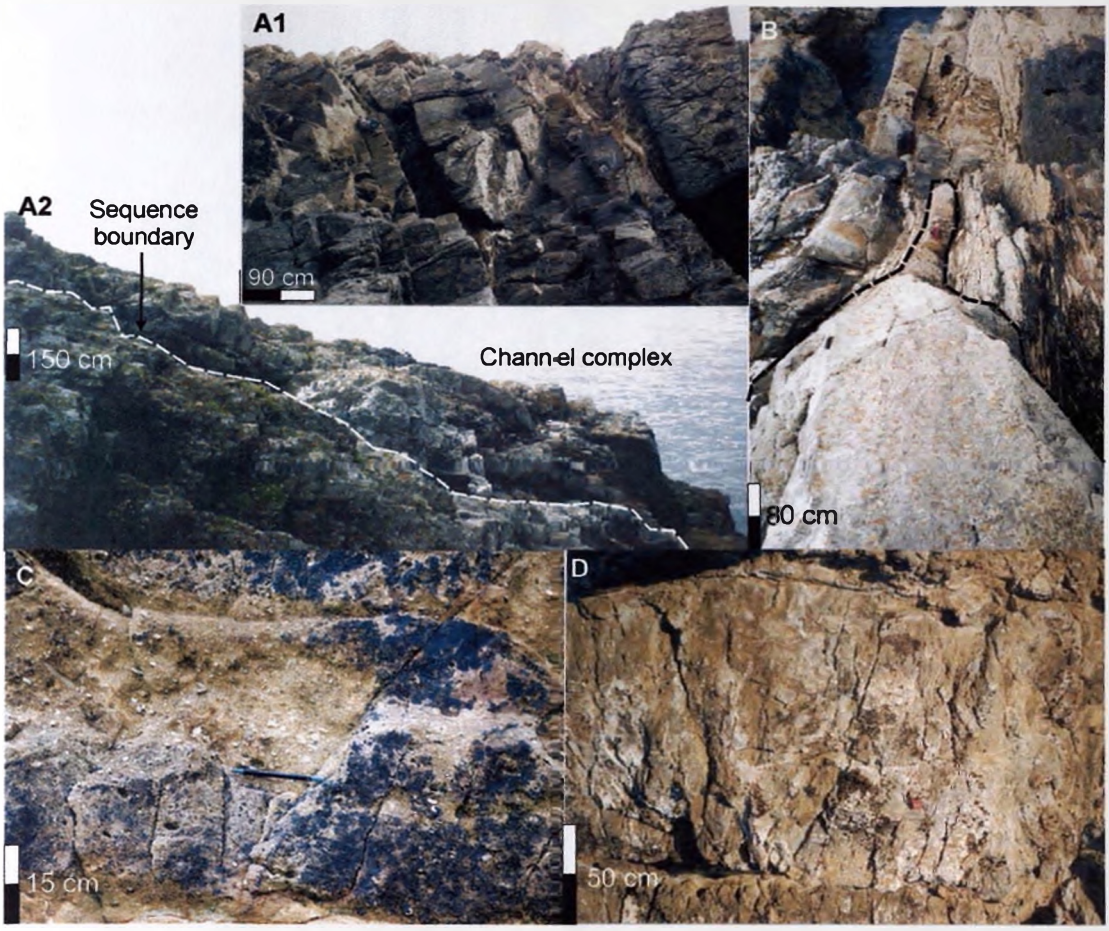



**Fig. 2.6.** Lithological characteristics of the Cwm Mawr Member. (A1/A2) Pen-y-Cyffrwy - amalgamated channel complex lying unconformably upon the Pen-y-Cyffrwy Member. (B) Cut and fill channel from the unit illustrated in (A). (C) Cwm Mawr - hyperconcentrated flow. Note the a(p)a(i) clast fabric and increase in imbrication angle upwards through the bed. (D) Cwm Mawr – thickly bedded, massive pebbly sandstone interpreted as a cohesionless debris flow.

inverse (Fig. 2.6C) or inverse to normal grading, floating rip-up clasts (many of which are highly deformed), rip-up clasts aligned upon internal shear planes, poorly organized texture and fabric, lack of internal stratification, and angular to subrounded pebbles set in a poorly sorted coarse-grained sandy matrix.

Clast fabric is dominantly a(p)a(i) but some examples either show no consistent imbrication, with clasts in unstable positions, or imbrication angles that increase upwards through the bed (Fig. 2.6C). The latter is associated with a "late stage" inversely graded profile that only affects the upper 30–40 cm of the bed. Coarse sandstones, usually less than 20 cm thick, commonly cap the pebbly sandstones. These sandstones are often highly lenticular, cut out by the succeeding sandstone unit. Internally, these sandstones are massive but often contain markedly outsized intraclasts up to 14 cm long apparently suspended in the sand. Clasts always display a well developed a(p)a(i) fabric.

The unit exhibits an east–west lateral facies variation between Cwm Mawr and Porth Clais. Pebbly sandstones become thinner, finer, and develop graded silty mudstone interbeds as the member is traced westwards. The degree of channel incision also varies quite dramatically, peaking at Ogof Blawd Ceirch (Fig. 2.6A), and becoming tabular at Porth Clais and west of Porthselau. This variation coincides with a marked increases in basal sole structures associated with tabular geometries. Mudstone interbeds are typically flaser and wavy bedded. Evidence for bioturbation is restricted to a few *Skolithus* burrows at Porth Clais and the section west of Porthselau.

Many of the features recorded in the Cwm Mawr Member are present also in the Trwyncynddeiriog Member and, likewise, the mode of emplacement is inferred to have occurred from structurally bipartite sediment gravity flows. Pebbly sandstones interbedded with tidal heterolithics may be interpreted as the deposits of high-density turbidity currents, a conclusion consistent with deformed intraclasts and clasts aligned along internal shear planes (Nemec 1990a). The transition from lenticular beds at Ogof Blawd Ceirch to tabular beds at Porth Clais and west of Porthselau is typical of the channel lobe transition often documented from fan-delta and deep-sea fan successions (Mutti and Ricci Lucchi 1972; Mutti *et al.* 1999). The record of tidal modulation and *Skolithus* burrows precludes deep marine sedimentation. Channelized units of coarser grained pebbly sandstones with a(p)a(i) imbrication at Cwm Mawr (Fig. 2.6C) are more difficult to interpret as there is no evidence to suggest subaqueous emplacement. They occur immediately (and conformably) above tidal heterolithics and record many features typical of the structurally bipartite hyperconcentrated flood flows documented on alluvial fans (Smith 1986; Mutti *et al.*

1996; Sohn *et al.* 1999, Manville and White 2003) (Fig. 2.4). Interbedded tabular pebbly sandstone (Fig. 2.6D) with disorganized texture and fabric, and clasts in unstable positions are characteristic of non-cohesive debris flow deposits (Lowe 1982; Nemec and Steel 1984; Kim *et al.* 1995).

*Lower boundary:* The lower boundary of the Cwm Mawr Member is interpreted as unconformable (Fig. 2.6A2) at all localities based on: the sharp erosive contact, deep channel incision (in excess of 5 m at Pen-y-Cyffrwy), abrupt grain size increase, intraclasts of the preceding member in basal beds, and the marked facies dislocation (Myers and Milton 1996, p. 39) at this surface. The latter is extremely prominent at Porth Clais and Pen-y-Cyffrwy, where coarse-grained turbidites interbedded with tidal heterolithics erosively overlie silty mudstones emplaced close to storm wave base. In the type locality at Cwm Mawr, the exact nature and position of the unconformity is complicated by lateral facies changes and difficulties in distinguishing major incision and abrupt basinward shifts in facies from localized channel scour (Posamentier and Weimer 1993; Wescott 1993). Thus one particular surface is difficult to determine precisely, especially as lateral exposure is severely limited.

### 2.2.1.6. Porth Clais Formation (new)

*General:* The Porth Clais Formation (Table 2.1) is a new term to replace the "Middle Solva" division of Hicks (1881) and subsequent authors. Stead and Williams (1971) divided the "Middle Solva" of Hicks (op. cit.) into a lower "Grey sandstone member" and an upper "Purple sandstone member" but defined no limits to these units. The divisions were based purely on secondary diagenetic colouration (presence or absence of purple and green beds), which they assumed affected all beds in the upper reaches of the "Middle Solva". While this simple two-fold division occurs in the type section at Porth Clais, the cliff sections immediately south of Trelerw between Carreg-y-Barcud (SM 7750 2410) and Ogof-y-Flôs (SM 7770 2432), and between Porthselau and Point St John (SM 7195 2597) (both sections are only accessible from the sea) cannot be distinguished by colour or any other lithological characteristics. Thus following Hicks's original classification and Rushton (1974), these beds are regarded as belonging to a single formation.

*Name:* From Porth Clais.

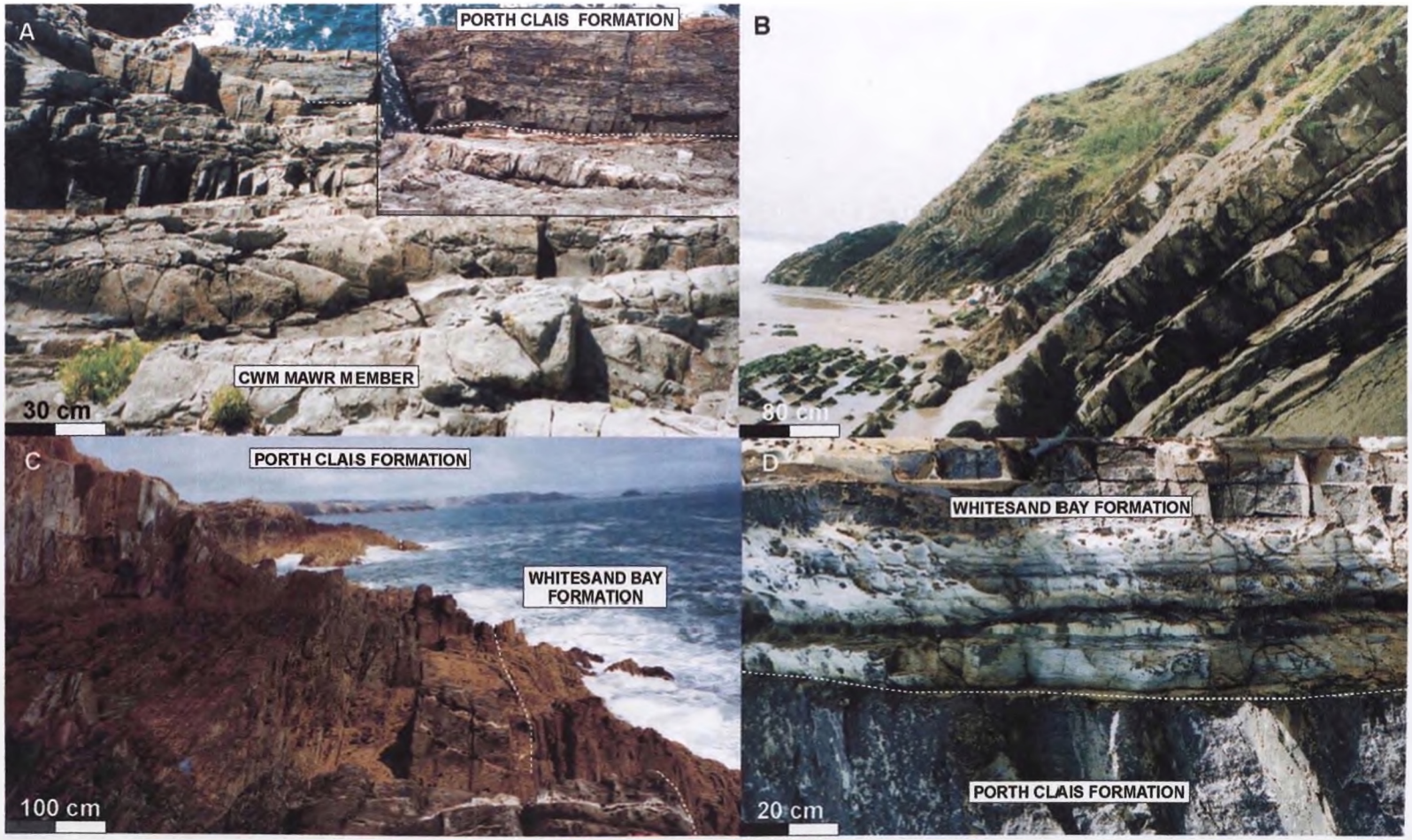



**Fig. 2.7.** Lithological features of the Porth Clais Formation, and the contact with the Whitesand Bay Formation. This junction separates the Caerfai and Porth-y-rhaw groups. (A) Pen-y-Cyffrwy - contact between the Cwm Mawr Member and the Porth Clais Sandstone Formation. (B) Newgale - thick tabular beds of coarse to pebbly sandstone typical of the Porth Clais Formation. Note the well developed fining upward character. (C) Porth Clais - purple silty sandstones of the Porth Clais Formation pass into a unit of thickly bedded pebbly sandstones that mark the top of the Caerfai Group. (D) Details of the contact between the Caerfai and Porth-y-rhaw groups. Note the thin dark laminae. This organic-rich sediment characterizes most of the Porth-y-rhaw Group.

*Type section:* The type section is at Porth Clais where the formation is fully exposed. Reference sections occur along cliff sections south of Trelerw between Carreg-y-Barcud and Ogof-y-Ffos, and on the foreshore and low cliff at the northern end of Newgale Sands. The latter section offers the best opportunity to study the sedimentology of the formation, as it is relatively unbioturbated.

*Thickness:* The type section attains a measured thickness of 156 m, a figure considerably lower than previously reported. Harkness and Hicks (1871, p. 390) for example, estimated the sequence between Porthstinian and Point St John to be 1500 ft (456 m). A comparable thickness has been suggested for the area around Solva (Rushton 1974). Although there is some evidence to suggest thickening of the formation from west to east, which may account in part for the figure determined from Solva, the previous lithological distinction based on diagenetic purple colouration may have led to an overestimation of thickness, as purple bands occur at very different levels across the region (see above).

*Lithology and process sedimentology:* Immediately east of Cwm Mawr, the facies present are generally more varied and coarser than those developed on the St David's Peninsula. Medium- to coarse-grained amalgamated sandstones are dominant (Fig. 2.7B), although pebbly sandstones form an important constituent. Beds are tabular in geometry, medium to thickly bedded (maximum thickness 1.5 m), and typically devoid of internal stratification. Floating rip-up clasts are common, as are water escape structures such as elutriation pipes and dish structures. Most of the beds are massive, ungraded, structureless, but grading though uncommon, is extremely variable and includes normal, inverse, inverse to normal, and normal to inverse profiles. Load casts and ball and pillow structures are well developed when sandstones are interbedded with dark-grey mudstone. All of these features together suggest rapid emplacement from high-density turbidity currents. Massive bedding in sandstone has been modelled by Kneller and Branney (1995) who proposed a mechanism of gradual aggradation beneath sustained quasi-steady currents like those developed at the mouths of high gradient mountainous streams (Mulder and Alexander 2000).

Throughout much of the St David's Peninsula, the Porth Clais Formation is a dull-grey and dull-purple monotonous succession of tabular, medium to thinly bedded fine- to rarely coarse-grained well graded sandstones, interbedded with structureless dark grey, purple and green silty mudstone. Bioturbation is ubiquitous in the silty mudstones and common in sandstones, with *Planolites*, *Teichichnus*, *Sinusites* and

*Chondrites* being the main burrow types (Crimes 1970a). These are spectacularly preserved on vertical bedding planes immediately west of Porth Clais. Sedimentary structures are difficult to identify due to the effects of bioturbation, but where apparent conform to Bouma divisions Tb, Tc, and Td. Structureless graded divisions are equated with Bouma division Ta. Hummocky cross-stratification and climbing ripple cross-lamination occurs sporadically in the lower beds of the formation. Load casts and flute casts are well exposed in the section at Porth Clais and Ogof Blawd Ceirch. Concretionary horizons and phosphate nodules have been documented at a number of levels in the upper part of the formation west of Porth Clais and northeast of Point St John. Most of the features can be equated with deposits of fine-grained, typically low-density turbidity currents, and represent the distal expression of the coarser grained facies recorded at Cwm Mawr. The type of bioturbation and rare HCS are typically associated with mid-shelf water depths.

In all localities on the St David's Peninsula (but faulted out at Cwm Mawr) the uppermost part of the formation is composed of erosively based pebbly sandstones (Fig. 2.7C and D and Fig. 2.8B) similar to those described from the Newgale Formation. This unit attains a maximum thickness south of Trelerw of 3.5 m, thins to 2.5 m at Porth Clais (Fig. 2.7C), and to less than 1.5 m at Whitesand Bay (Fig. 2.8B). The presence of inverse grading, floating rip-up clasts, a(p)a(i) clast imbrication, and pebbly sandstone–coarse sandstone couplets identify these deposits as coarse-grained turbidites emplaced by high-density turbidity currents. The lower contact of this pebbly unit is interpreted as an unconformity (or correlative conformity) based on the sharp contact between pebbly sandstone and bioturbated silty mudstone, significant basal erosion, and a clear facies dislocation. In most respects this surface is identical to the one identified at the base of the Cwm Mawr Member and likewise is considered an important marker horizon across the region. The upper boundary of this pebbly unit is also relatively sharp (Fig. 2.7D), forming a recognizable surface that separates the Caerfai Group from the overlying dominantly fine-grained Porth-y-rhaw Group.

*Lower Boundary:* The junction between the underlying Newgale Formation and the Porth Clais Formation is abrupt but conformable (Fig. 2.7A and Fig. 2.2E), and is defined at the contact between coarse-grained thickly bedded sandstones amalgamated along uneven erosion surfaces and more thinly bedded fine- to medium-grained sandstones with tabular amalgamation surfaces. The contact is well displayed at Pen-y-Cyffrwy (Fig. 2.7A) and Porth Clais. At Cwm Mawr, the junction is faulted out.

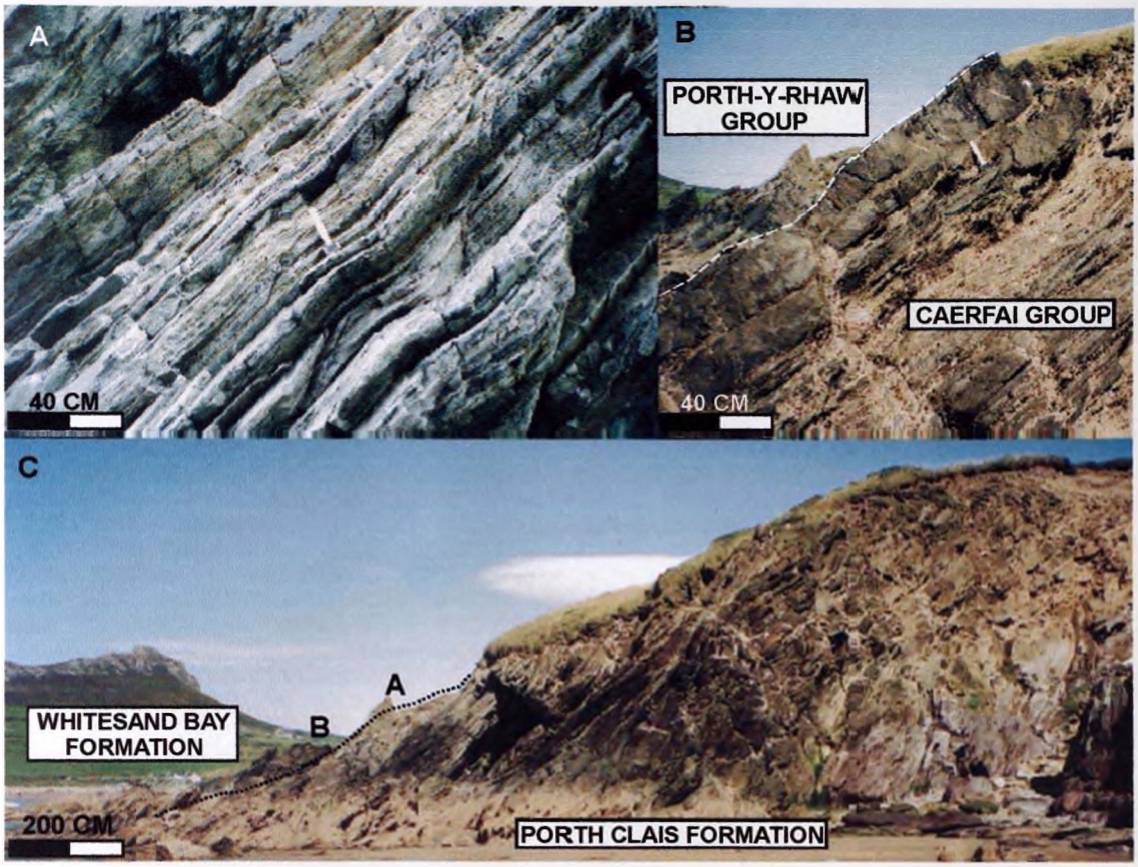



**Fig. 2.8.** Lithological characteristics of the Whitesand Bay Formation at the type locality of Whitesand Bay. (A) Thinly bedded fine-grained sandstones interbedded with bioturbated silty mudstone. (B/C) The contact between the Caerfai Group and Porth-y-rhaw Group. Notice that the beds are significantly thinner than the same unit exposed at Porth Clais (Fig. 2.7C).

*Distribution:* In addition to the type and references sections outlined above, easily accessible exposures of parts of the formation occur on the eastern and western sides of Solva Harbour, and on the extreme headland of Pen-y-Cyffrwy although faulting appears to replicate the succession somewhat and a strong cleavage obscures many of the lithological characteristics. Additional exposures not as readily accessible include the eastern side of Caerfai Bay (Fig. 2.2F), the western side of Caerbwdy Bay, immediately below the lifeboat station at Porthstinian, and in the higher grounds of Solva Valley (Jones in Cox *et al.* 1930a, p. 417). A small section (c. 15 m) of grey and purple fine-grained sandstones faulted against the Precambrian Pebidian Supergroup immediately north of Ogof Golchfa is also referred to the Porth Clais Formation. This exposure was previously mapped as "St Non's Sandstone" by Stead and Williams (1971, p. 195) and by the B.G.S. (1973) as "Solva Beds" (undifferentiated). About 120 m of green and purple silty mudstones recorded by Williams (1934) at Tancredston in the Tremaenhir syncline probably represent part of the Porth Clais Formation. Apart from at Newgale Sands, the formation is poorly developed in the Haycastle inlier, but may be represented in the east by grey flaggy sandstones overlying the "Musland Grit".

*Biota and age:* Fossils are very infrequent, especially in the lower part of the formation, but an immature cranidium apparently from Porth Clais (Loc. 3 of Farshori 1962, p. 150), and figured and identified in Lewis (1987) as *Paradoxides* (*Hydrocephalus*) cf. *sjoegreni* Linnarsson may indicate a late *P. oelandicus* (*P. pinus*) Biozone for the lower part of the formation. From beds higher up, Hicks (in Harkness and Hicks 1871, p. 390) recorded *Ctenocephalus (Hartella) solvensis* (Hicks), *Lingulella ferruginea* Salter, and *Paradoxides* (*Eccaparadoxides*) *harknessi* Hicks from a temporary exposure on the roadside between Whitchurch and Upper Solva Village. *C.* (*H.*) *solvensis* occurs in the upper part of the Porth Clais Formation on Ramsey Sound where it is associated with *Bailiaspis aff. dalmani* (Angelin), *Parasolenopleura*? Sp. and *Paradoxides ramsayensis* sp. nov. The latter species has been previously identified as *P. sjoegreni* Linnarsson (Farshori in Smith and White 1963, p. 404) which, together with Hicks' identification of "*P. harknessi*", has contributed to these strata being assigned a late *P. oelandicus* Biozone age. The one specimen of *B. aff. dalmani* was considered by Lewis (1987) to be too imperfectly preserved for positive identification, but in Sweden the species is not recorded from beds older than of the *P. gibbus* Biozone. Furthermore, it seems apparent that throughout most of the Acado-Baltic region *Hartella* is found only in beds of this age. The upper part of the Porth Clais Formation may therefore tentatively be referred to

the Zone of *Ptychagnostus gibbus*. The *P. gibbus* Biozone is also represented by the lower part of the Whitesand Bay Formation stratigraphically above.

### 2.2.2. PORTH-Y-RHAW GROUP (new)

*General:* The Porth-y-rhaw Group (Table 2.1) is a new collective term for strata previously assigned by Hicks (1881) to the "Upper Solva" and "Menevian Group", and by Harkness and Hicks (1871) to the "Lingula Flags". The group also includes the "Treffgarne Bridge Beds" of Cowie *et al.* (1972). None of these units has ever been formally defined or their boundaries described. Since the studies of Harkness and Hicks (1871) and Hicks (1881), the "Menevian" and "Lingula Flags" have been considered separate lithological units although no boundary or distinctive feature has been published to warrant this. In the stratigraphic scheme erected by Cowie *et al.* (1972), the junction between the two was taken as the boundary between the Middle Cambrian (St David's Series) and Upper Cambrian (Merioneth Series).

Lewis (1987) identified *Agnostus pisiformis* (Wahlenberg) in beds exposed at Loch Warren (north-northeast of Cradle Rock, Fig. 2.1C)), which were mapped by the B.G.S. (1973) as "Menevian". These beds, which are 500 m east of Porth-y-rhaw and were considered "Middle Lingula Flags" by Hicks and Salter (1866) are, based on the presence of *A. pisiformis*, basal Upper Cambrian in age. The Middle–Upper Cambrian boundary must therefore lie within beds formerly referred to as "Lingula Flags". The mapping of Upper Cambrian strata as "Menevian" by the B.G.S. also highlights the strong lithological similarities between the "Menevian" and succeeding beds. The boundaries of the Porth-y-rhaw Group are in fact those originally defined as "Lingula Flags" in the earliest stratigraphic scheme for the area constructed by Salter (1864). These boundaries also corresponds closely to those of the Mawddach Group of the Harlech Dome (Allen *et al.* 1981), with which the Porth-y-rhaw Group shares many lithological similarities.

*Name:* From the small coastal inlet of Porth-y-rhaw (Fig. 2.1C).

*Subdivisions:* The Group is divided into five formations (Table 2.1): the Whitesand Bay Formation (new) which equates to the "Upper Solva" of Hicks (1881); the Menevia Formation (new) which corresponds to the "Lower Menevian" and "Middle Menevian" of Hicks (op. cit); the Aber Llong Formation (new), which was formally the "Upper Menevian" of Hicks (op. cit) and the lower part of the "Lingula Flags" as

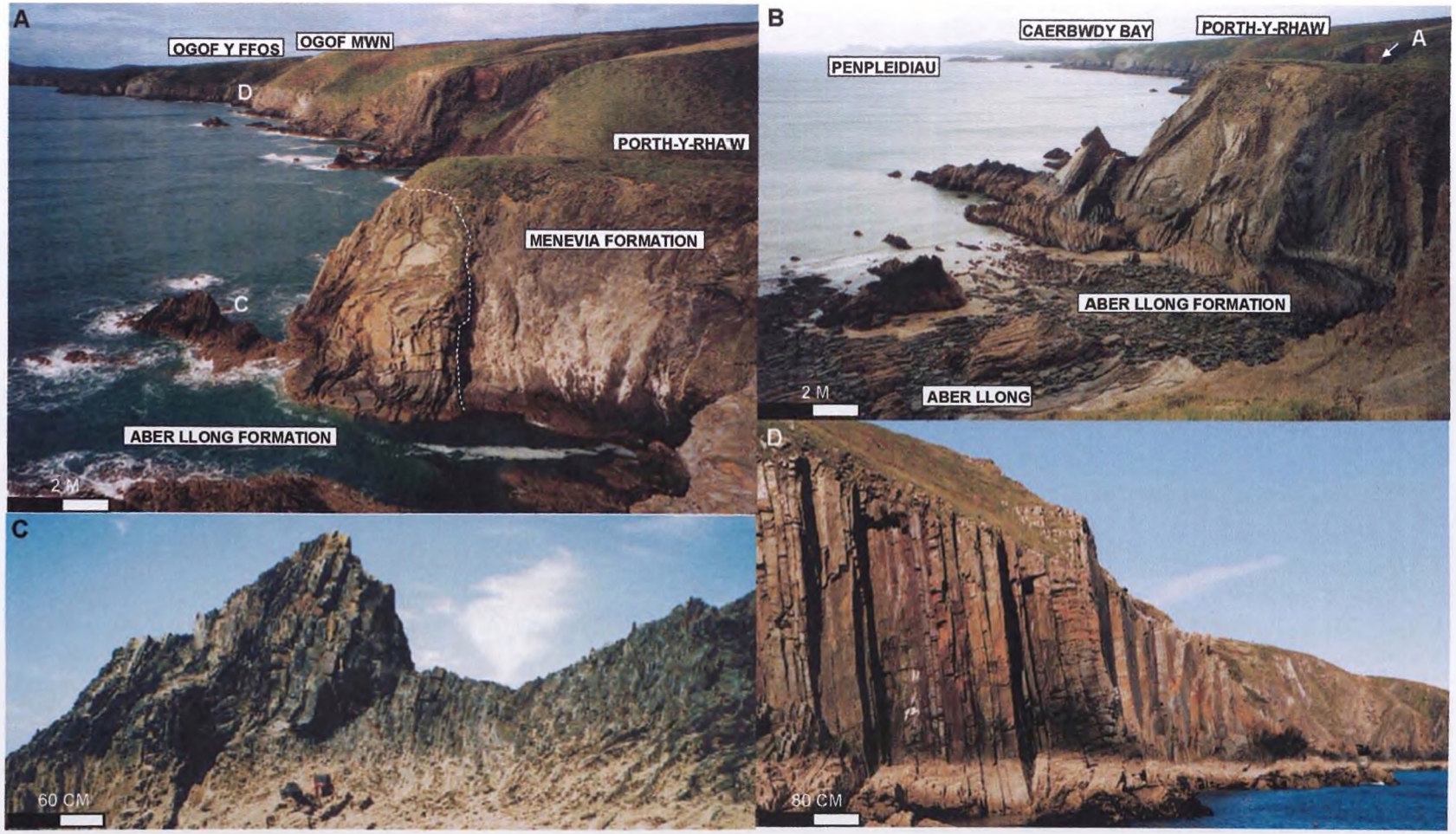



**Fig. 2.9.** Sedimentological and stratigraphic features of the Porth-y-rhaw Group exposed from Ogof y Ffos to Aber Llong. (A). View of the Porth-y-rhaw Group from an unnamed bay immediately east of Porth-y-rhaw. The contact between the Menevia Formation and Aber Llong Formation is highlighted. (B) View of the Aber Llong Formation at its type locality. (C) Arenaceous basal unit of the Aber Llong Formation. (D) Tabular sandstone beds of the Whitesand Bay Formation exposed between Ogof y Ffos and Ogof Mwn.

defined by Harkness and Hicks (1871) or the "Middle Lingula Flags" of Salter (1864) and Hicks and Salter (1866); the Ogof Velvet Formation, a term used by Kokelaar *et al.* (1985) but without formal definition, and the Treffgarne Bridge Formation (revised after Cowie *et al.* 1972). The group is unconformably overlain by fine-grained sediments of the Ogof Hen Formation that yield a fauna of early Arenig age.

*Type area:* The coastal cliffs east and west of Porth-y-rhaw (Fig. 2.9A and B), from 50 m east of Ogof y Ffôs (SM 7770 2432) to Cradle Rock (SM 7883 2372). The lower three formations are exposed in full, and the contact with Ogof Velvet Formation also occurs. Important reference sections include Whitesand Bay (Fig. 2.2B), Porth Gain and Aber Mawr (Granston area) for the Ogof Velvet Formation, while Treffgarne (9594 2287) is the only known locality that exposes the Treffgarne Bridge Formation.

*Thickness:* In the type area the group attains a measured thickness of 405 m although over 600 m of section is actually exposed through structural repetition. A further 260 m is exposed at Porth Gain and Aber Mawr and 22 m at Treffgarne, which gives a conservative estimate for the group as greater than 687 m.

*Lower and upper contact:* The group rests conformably upon the Porth Clais Formation at Whitesand Bay, Porth Clais, Point St John, and between Ogof-y-Fos and Ogof Enyon (Fig. 2.7D and Fig. 2.8C). The unconformable contact with the Gwynedd Supergroup (Arenig) may be studied at both Whitesand Bay and Porth Gain, but at both localities the junction (marked by a thin pebble lag) is cryptic due to very similar lithologies on either side.

*Dominant lithology:* The group is predominantly composed of very fine-grained quartzose sandstones and siltstones interbedded with dark-grey to black laminated mudstone. Pale weathering metabentonite horizons are present in the Menevia Formation. Carbonate concretions, nodular limestones and phosphate nodules occur throughout the lower 3 formations, which are mud-dominated, high in organic carbon (Price 1963, p. 196) and typically pyritous. The Ogof Velvet Formation is significantly more arenaceous, and black mudstone typical of the preceding formations is replaced by light blue silty mudstone. Large- and small-scale soft sediment deformation is common in both the upper part of the Whitesand Bay Formation and throughout the Ogof Velvet Formation (Kokelaar *et al.* 1985).

*Distribution:* The Porth-y-rhaw Group forms a distinctive fine-grained, dark weathering and cliff-forming unit across 7 km of coastline between Ogof y Ffôs and Ogof y Cae (SM 8218 2322), where the upper beds are faulted against Caerbwdy Sandstone. In addition to the type area, good exposure of the Menevia and Aber Llong Formations occur on the eastern and western sides of Solva Harbour. The greater part of the Cambrian outcrops in Pembrokeshire belong to the Aber Llong and Ogof Velvet formations (formally the "Lingula Flags"), which occur on both flanks of the St David's and Haycastle Anticlines, occupy the core of the Mabws Anticline and an extensive tract southeast of Granston. A small inlier also occurs on Ramsey Island.

*Biota and age:* The Porth-y-rhaw Group is composed of strata of late St David's to mid-Merioneth age. The faunal assemblage is relatively diverse and allows correlation into the Scandinavian sequences (Table 2.1). Proven biozones include those of: *Tomagnostus fissus*, *Hypagnostus parvifrons*, *Ptychagnostus punctuosis* (from the St David's Series) and the *Agnostus pisiformis* and upper *Olenus* (from the Merioneth Series). The presence of the *Ptychagnostus gibbus* Biozone is suspected, while the *Solenopleura brachymetopa* and *Lejopyge laevigata* are unproven.

### 2.2.2.1. Whitesand Bay Formation (new)

*General:* This formation corresponds to strata previously assigned by Hicks (1881) to the "Upper Solva". It also includes approximately 20 m of strata previously defined as "Lower Menevian".

*Name:* From Whitesand Bay, situated northwest of St David's.

*Type section:* On the southern side of Whitesand Bay immediately north of Ogof Golchfa (Fig. 2.8B and C). This section was mapped by Williams (in Owen and Williams 1971, fig. 5, p. 30) and Stead and Williams (1971, fig. 8, p. 195) as "St Non's Sandstone" and by the B.G.S. (1973) as "Solva Beds" (undifferentiated). Stead and Williams (*op. cit.*, p. 194–195) noted that the sequence includes "laminated dark mudstone bands which exhibit a variety of sedimentary structures", but that the rocks "are of rather different aspect to the green [St Non's Formation] sandstones at Caerfai Bay". On lithological grounds these beds are typical Whitesand Bay Formation, as exposed in the historical type locality west of Porth-y-rhaw (Fig. 2.9A) between Ogof y Ffôs and Ogof Eynon (SM 7839 2427) (Fig. 2.9D). This section is

largely inaccessible but is retained as an important reference section due to the fossiliferous localities recorded by Hicks (in Hicks and Salter 1866, p. 283) and Lewis (1987). A further reference section occurs at the inland end of Porth-y-rhaw (SM 7846 2430).

*Thickness:* At its type locality, the Whitesand Bay Formation attains a thickness of 118 m. In the cliff sections west of Porth-y-rhaw, this increases to 136 m. Previous estimates based on the latter exposure range from 46 m (Hicks 1881, p. 298) to 106 m (Jones in Cox *et al.* 1930a, p. 254), the thickness variation clearly depending upon arbitrary boundaries.

*Lower contact:* The base of the formation is taken at the first siltstone bed that occurs above the prominent pebbly sandstone unit at the top of the Porth Clais Formation. This junction, which is well exposed at both Porth Clais (Fig. 2.7C and 7D) and Whitesand Bay (Fig. 2.8B and C), also coincides with the first appearance of dark organic-rich laminae that characterise much of the Porth-y-rhaw Group.

*Lithology and process sedimentology:* The lithology is fairly uniform across the St David's Peninsula, varying from light grey, medium to thinly bedded or flaggy sandy siltstones and mudstones in the lower part (Fig. 2.7D and Fig. 2.8A) to a facies of interbedded thin dark mudstones and light grey, very fine-grained sandstones and siltstones at the top. Sandstones are generally tabular with sharp erosive basal contacts and gradational upper surfaces (Fig. 2.9D). Siltstones, particularly in the upper 15 m of the formation, are lenticular and may be better described as fading ripples (Stow and Shanmugam 1980). Dark, organic-rich mudstones occur throughout the sequence but increase in abundance and average thickness towards the top of the formation. Much of the sequence is intensely bioturbated, with *Planolites* and *Sinusites* burrows particularly common. Sedimentary structures are difficult to determine, but parallel lamination overlain by ripple cross-lamination is the dominant profile in sandstones, while siltstones document only the rippled upper division. With the additional presence of load casts and flute casts, both the sandstones and siltstones display the salient characteristics of fine-grained turbidites. A mid- to outer-shelf depth may be inferred based on palaeontological evidence.

Towards the contact with the overlying Menevia Formation, the rock takes on a banded appearance that appears cyclic in origin. The base of each banded unit is composed of a thin (0.2–2.1 cm thick) rippled siltstone that may be massive or consist of fading ripple cross-lamination. Basal boundaries are slightly erosional and

commonly loaded. This siltstone is succeeded by a graded green to grey silty mudstone, which may have a mottled appearance suggesting bioturbation (Prigmore and Rushton 2000). This horizon varies between 1–5 cm thick, and may be diffusely laminated, convoluted or structureless. This is in turn overlain by a massive or diffusely laminated, largely unbioturbated black mudstone. This banded facies is similar to the so-called "Zebra facies" (Baird and Brett 1991) commonly described from pro-delta–outer shelf environments when oxygen-carrying low-density turbidity currents enter the "dysaerobic" facies zone (Rhoads and Morse 1971).

*Distribution:* In addition to the type and reference sections outlined above, the Whitesand Bay Formation also forms part of the headland of Penpleidiau at the extreme eastern point of Caerfai Bay (Fig. 2.1C), and in the low cliffs extending south-westwards from the lime kilns in Solva Harbour. The darker banding which characterizes the division elsewhere is absent at Solva, but it appears that all originally dark mudstones in this side of the harbour, including those of the succeeding Menevia Formation, have acquired a greenish colouration due to thermal alteration by a large intrusive body (Jones in Cox *et al.* 1930a, p. 417).

*Biota and age:* Hicks (in Hicks and Salter 1866, p. 283) recorded "*Paradoxides aurora*", a new "*Conocoryphe*" and other fossils from the lowermost beds of the division. Hicks (in Salter and Hicks 1869) described the "*Conocoryphe*" as *C. bufo* Hicks, which Lake (1940, p. 283) considered a junior subjective synonym of *Bailiaspis dalmani* (Angelin). Harkness and Hicks (1871, p. 390) also listed "*Agnostus cambrensis* Hicks", *Theca antiqua* Hicks, *Theca penultima* Hicks, *Discina pileolus* Hicks, *Obolella sagittalis* Salter, and *Lingulella ferruginea* Salter. The "*Agnostus cambrensis*" was identified by Lake (1906, p. 18) as *Agnostus integer* Beyrich (now *Peronopsis integra*), but a reassessment of this specimen by Lewis (1987, pl. 5, fig. 2) showed it to be referable to *Peronopsis redita* (Pek and Vaněk 1971). Lake (1935) also described *Paradoxides intermedius* Cobbold from these beds but, according to Lewis (1987), the one cranidium differs from those of the English form illustrated by Cobbold (1913c), and was instead referred to *Paradoxides* aff. *intermedius* Cobbold. Fossils collected by Lewis (1987) from the banded facies near the top of the division at Porth-y-rhaw include *Bailiaspis* cf. *dalmani*, *Tomagnostus fissus* (Linnarsson), *Paradoxides hicksii*, *Phalagnostus* sp., *Ptychagnostus* sp. and *Phalacroma*? sp.

The Whitesand Bay Formation is conventionally referred to the biozone of *Paradoxides aurora* (following Hicks 1881). A re-examination of the type specimens by Lewis (1987) showed the species to be a probable junior subjective synonym of *P.*

*Hicksii*, and called for the term "*Paradoxides aurora* Biozone" to be abandoned. The lower part of the formation has been tenuously equated with the *P. gibbus* Biozone (Rushton 1974; Prigmore and Rushton 2000). The upper part of the formation was assigned an early *T. fissus – P. atavus* age by Lewis (1987) based on the first appearance of *T. fissus*.

#### 2.2.2.2. Menevia Formation (new)

*General:* This formation corresponds to strata previously assigned by Hicks (1881) to the "Lower Menevian" and "Middle Menevian" (Table 2.1). Following suggestions by a number of authors (e.g. Lewis 1987; Prigmore and Rushton 2000), sandstones of the "Upper Menevian" as defined by Hicks (1881) are excluded from the entirely mud-dominated Menevia Formation.

*Name:* The name "Menevian" has been employed in various senses both as a rock-formation and a biostratigraphical term (see Stubblefield 1959); in the latter context it always refers to the biozones of *Paradoxides hicksii* and *Paradoxides davidis* (Table 2.1).

*Type section:* The historical type section at Porth-y-rhaw (Fig. 2.1C and Fig. 2.10A) exposes the formation in its entirety and is designated stratotype. This SSSI is a classic geological locality of international importance. The locality is mentioned in accounts of the St David's area, notably by Cox *et al.* (1930a, b), who described the succession in detail, and in guides to the area (Owen *et al.* 1971, Williams and Stead 1982).

*Thickness:* At the type locality, the formation has a measured thickness of 97 m. This is less than half the thickness of strata that was previously assigned to the "Menevian Group" estimated by Hicks (1881, p. 299) and Stead and Williams (1971, p. 181).

*Lower contact:* At both Whitesand Bay and Porth-y-rhaw, the contact between the "Zebra facies" of the upper Whitesand Bay Formation and diffusely laminated black mudstones typical of the Menevia Formation is gradational over approximately 7 m. In these transitional beds, rippled siltstones and mottled green silty mudstone decrease in thickness as the black mudstone division increases over each cycle. The base is drawn at the first unit where the black mudstone division forms over 50% of couplet thickness.

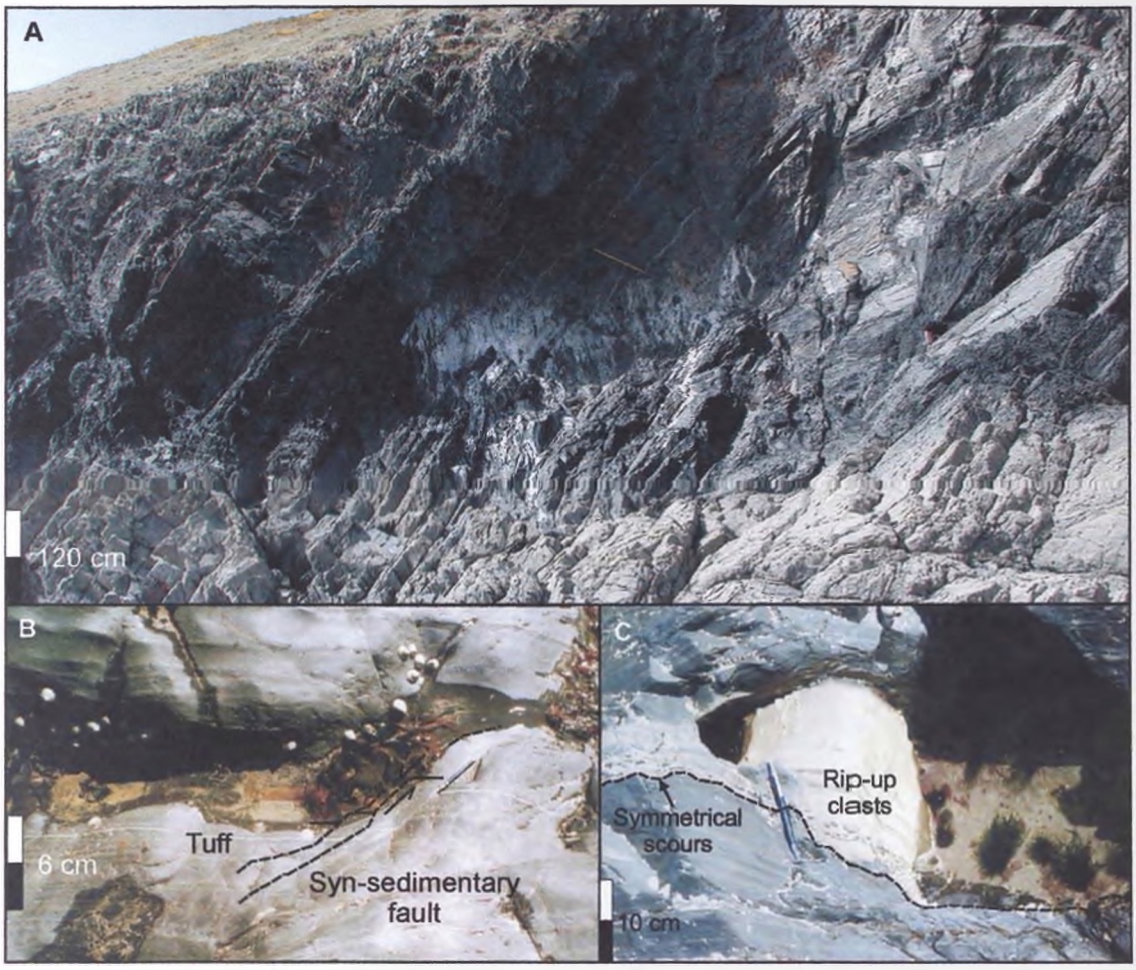



**Fig. 2.10.** Lithological characteristics of the Menevia Formation at the type locality of Porth-y-rhaw. (A) Black pyritous mudstone and thin interbedded pale bentonite horizons. (B) Details of above, with evidence of small scale micro-faulting. (C) Phosphate and mudstone rip-up clast horizon interpreted as a diastem formed by internal waves.

*Lithology:* The formation predominantly comprises massive or diffusely laminated dark-grey to black mudstones (Fig. 2.10) with occasional very thinly bedded, laterally persistent graded fine siltstones. Silt horizons contain no evidence for traction deposition and display non-erosional bases and gradational tops. Discontinuous limestone beds composed almost entirely of ferroan calcite occur lower in the formation. Pale weathering, tabular bedded metabentonites also occur (Fig. 2.10A and B). Large spheroidal carbonate concretions lower in the formation are replaced higher up by phosphate nodules. Framboidal pyrite is common throughout. Approximately 14 m above the base of the formation occurs a very conspicuous erosion surface characterised by gentle symmetrical scours overlain by a laterally persistent concentration of very well rounded phosphate and mudstone rip-up clasts (Fig. 2.10C). This horizon is of some stratigraphic importance as an identical layer has been recorded from coeval strata in the Manuals River Formation in southeastern Newfoundland (bed 115 of Howells 1925, p 36). Soft sediment deformation occurs throughout the division but is particularly prominent lower in the formation. Evidence for bioturbation is confined to the lowermost 30 m, but nowhere does it occur extensively.

The general lack of infauna, sparse epifauna (see below), the laminated texture and very dark grey to black colouration suggest low levels of dissolved oxygen, possibly bordering on complete anoxia (Arthur *et al.* 1991). The uniform composition, lack of primary sedimentary structures and inferred low sedimentation rates (based on the presence of carbonate concretions, Raiswell 1987) suggest hemipelagic sedimentation (Stow *et al.* 1996). Although the common presence of pyrite does not necessarily imply anoxic conditions on the sea floor, it does suggest that sufficient metabolizable organic matter remained during burial to promote sulphate reduction within the sediment and sulphate mineralisation (Berner 1978). The framboidal state implies early diagenetic formation at very shallow depth (Love 1967), forming in muds of soupy consistency (O'Brien 1995). This is consistent with the presence of the controversial echinoderm-like organism *Protocystites menevenis* Hicks, which Jefferies *et al.* (1987) considered particularly adapted to staying upright on extremely soft (watery) muds. The origin of the thin silt bands is uncertain, but they clearly represent a type of "event" sedimentation deposited out of suspension that punctuated an environment usually associated with intense condensation.

*Distribution:* In addition to the type section outlined above, Menevia Formation strata also occur at Penpleidiau, Dwrhyd Pit (SM 7914 2477) (see Prigmore and Rushton 2000 for site description) and Solva Harbour. Other outcrops occur at Tancredston

and in the Haycastle inlier where they constitute the upper division of the "Ford Beds" (term abandoned) described by Thomas and Jones (1912). The formation is not known from north of the St David's Peninsula, where it appears to be faulted out (Owen *et al.* 1971, p. 29).

*Biota and age:* The section through the Menevia Formation at Porth-y-rhaw, supplemented by evidence from other sites close by (Dwrhyd Pit, Penpleidiau and Solva Harbour), provides the most complete zonal sequence for the St David's Series in Britain, ranging from the base of the *fissus* Biozone up to the *punctuosus* Biozone (Prigmore and Rushton 2000). It is the type locality for several trilobite and other species and is famous for yielding *Paradoxides davidis* Salter. References covering the most important faunas include: Salter (1863, 1864, 1866), Salter and Hicks (1867, 1869), and Hicks (in Harkness and Hicks 1871). Most of the trilobites were later redescribed by Lake (1906–1946; see Thomas *et al.* 1984 for updated nomenclature). The most important contribution to the fauna of the Menevia Formation since the late 19$^{th}$ Century is undoubtedly the systematic account of Lewis (1987), on which the summary below is based.

The lower part of the Menevia Formation (beds previously referred to as "Lower Menevian" and correlated with the *T. fissus* Biozone of Scandinavia) on the western side of Porth-y-rhaw (Loc. PR–6 in Lewis 1987) have yielded *Paradoxides hicksii* Salter, *Eodiscus punctatus* (Salter) s.l., *Peronopsis scutalis* (Hicks) s.l., *Jincella applanata* (Hicks), *Linnarssonia sagittalis* (Davidson), *Protospongia* sp. and *Hyolithes* sp. Harkness and Hicks (1871, p. 396–397) also listed the following species: "*Conocoryphe" humerosa* Salter, *Agraulos* ["*Arionellus*"] *longicephalus* (Hicks), *Onymagnostus* ["*Agnostus*"] *davidis* (Hicks), *O* ["*A*"] *barrandei* (Hicks), *Protospongia diffusa* Salter, *Protocystites menevensis* Hicks, hyolithids and bradoriids. Middle *T. fissus* Biozone faunas are better known from Penpleidiau (Locs. CF–1 to CF–6 in Lewis 1987), and include *Paradoxides hicksii*, *P. illingi* Lake, *Luhops pugnax* (Illing), *Parasolenopleura elegans* (Illing), *Holocephalina incerta* Illing, *Tomagnostus fissus* (Linnarsson), *T. westergaardi* sp. nov., *Condylopyge* cf. *rex* (Barrande), *Pleuroctenium granulatum* (Barrande) s.l., *Peronopsis scutalis* (Hicks) s.l., *Onymagnostus barrandei* (Hicks) and *Eodiscus punctatus scanicus* (Linnarsson).

The upper of the formation (previously assigned to the "Middle Menevian" and correlated with both the *H. parvifrons* and *P. punctuosus* Biozones) on the western side of Porth-y-rhaw have yielded *Hypagnostus* cf. *parvifrons* (Linnarsson), *Pleuroctenium granulatum scanense* (Westergård), *Tomagnostus perrugatus*

(Grönwell), *Agraulos longicephalus* (Hicks), *Ptychagnostus cicoroidos* (Mathew), *Solenopleura applanata* (Salter), *Ptychagnostus davidis* (Hicks), *Condylopyge rex* (Barrande), *Grandagnostus* sp. B, *Phalagnostus* sp. B, *Pleuroctonium tubercalatum* (Illing), *Ptychagnostus punctuosis affinis* (Brögger), *Ptychagnostus* (*Onymagnostus*) sp., *Aconthous* sp. nov., *Anopolenus* sp. A, *Anopolenus* sp. B, *Clarella* sp. nov., *Clarella* sp. A, *Dasomatopus* sp. nov., *Hartshillia inflata* (Hicks), *Hartshillia spinate* (Illing), *Eodiscus punctatus punctatus* (Salter), *Meneviella venulosa* (Salter) and *Peronopsis Scutalis Scutalis* (Hicks). Additional collections from Solva Harbour and Ogof Eynon can be found in Lewis (1987).

### 2.2.2.3. Aber Llong Formation (new)

*General:* The Aber Llong Formation (Table 2.1) is a term applied to strata previous defined as "Upper Menevian" (*or* "*Orthis hicksii* Beds") (Harkness and Hicks 1871, Hicks 1881) and "Lingula Flags" (Harkness and Hicks 1871) (lower part). The "Middle Lingula Flags" of Salter (1864) and Hicks and Salter (1866), and the "Maentwrog Group" of Hicks (1881) roughly correspond to the part of the "Lingula Flags" that is included in the Aber Llong Formation.

*Name:* From the small bay of the same name immediately east of Porth-y-rhaw (Fig. 2.1).

*Type section:* The formation is well exposed at low tide from the southernmost point of Porth-y-rhaw eastwards (Fig. 2.9B) across the small bays and headlands as far as Loch Warren (Fig. 2.1C). Although almost continuous exposure exists, and the section is the best candidate for stratotype, small parts between Porth-y-rhaw and Aber Llong are inaccessible. An important reference section for this lower part, which also exposes the contact with the underlying Menevia Formation, occurs on the western side of Solva Harbour, although again this is tide dependent.

*Thickness:* A minimum thickness for the formation at the type locality is 172 m, but the section is structurally complex and this estimation is open to further revision. At least 100 m of continuous section occurs on the western side of Solva Harbour.

*Lower contact:* The contact between the Menevian Formation and Aber Llong Formation is sharp and marked by a unit (approximately 2.2 m thick) of thickly bedded coarse sandstone overlying black mudstone (Fig. 2.9A). According to Stead

and Williams (1971, p. 188) the junction is conformable, but Taylor and Rushton (1972, p. 9) suggested the possibility of a non-sequence as there is a general absence of higher Middle Cambrian biozones throughout Avalonia due to a widespread regression during the time of the *Solenopleura brachymetopa* Biozone. In all areas where the relevant beds are exposed, there is an abrupt lithological change at approximately the same level as that seen at Porth-y-rhaw (see Fig. 2.13). The sharp junction between mid- to outer shelf mudstones and shoreface sandstones (discussed below) is a characteristic commonly associated with forced regressions (Posamentier and James 1993; Fitzsimmons 1994; Ainsworth and Patterson 1994). The clear facies dislocation between offshore muds and nearshore sands is therefore interpreted as an unconformity or its correlative conformity (Posamentier *et al.* 1992).

*Lithology and process sedimentology:* The Aber Llong Formation, like the preceding formation, is dominated by diffusely laminated or massive pyritous black mudstone. The lower 15–18 m (Fig. 2.9A) comprise interbedded sandstones and mudstones (Fig. 2.9C), including the basal 2.2 m unit of thickly bedded medium- to coarse-grained sandstones exhibiting rare cross-bedding and symmetrical ripples. Above the basal unit, sandstones thin and fine markedly, rarely attaining a thickness greater than 15 cm, and typically falling within the fine sand to coarse silt fraction. Beds with these finer grain sizes display more variable internal stratification including hummocky cross-stratification, micro-hummocky cross-stratification, wave ripple lamination, parallel lamination and rare trough cross-bedding (restricted to medium sand). Wave ripples, interference ripples (Fig. 2.11E) and current ripples are spectacularly exposed on gently dipping bedding planes at Aber Llong. Soft sediment deformation associated with water escape often forms convolute lamination, particularly in the thicker beds. Bed geometry is extremely variable ranging from tabular (Fig. 2.9C) to highly lenticular (Fig. 2.11D). The latter is a depositional rather than erosional feature, with lenticels existing as "starved hummocks" (Myrow 1992a; Brenchley *et al.* 1993). Interbedded black mudstones may be massive, but are more commonly wavy, lenticular or flaser bedded.

Above this arenaceous lower part, the rest of the formation is almost identical to the Menevia Formation, and it is hardly surprising that parts of this succession were originally mapped as such by the B.G.S. (1973). Mudstones are typically colour banded (Fig. 2.11A), with a thin starved ripple train of siltstone, overlain by a green silty mudstone that culminates in black laminated mudstone. Tabular beds of nodular limestone (Fig. 2.11B) composed of amalgamated carbonate concretions are rare but highly conspicuous, while concretions that are not amalgamated but developed along

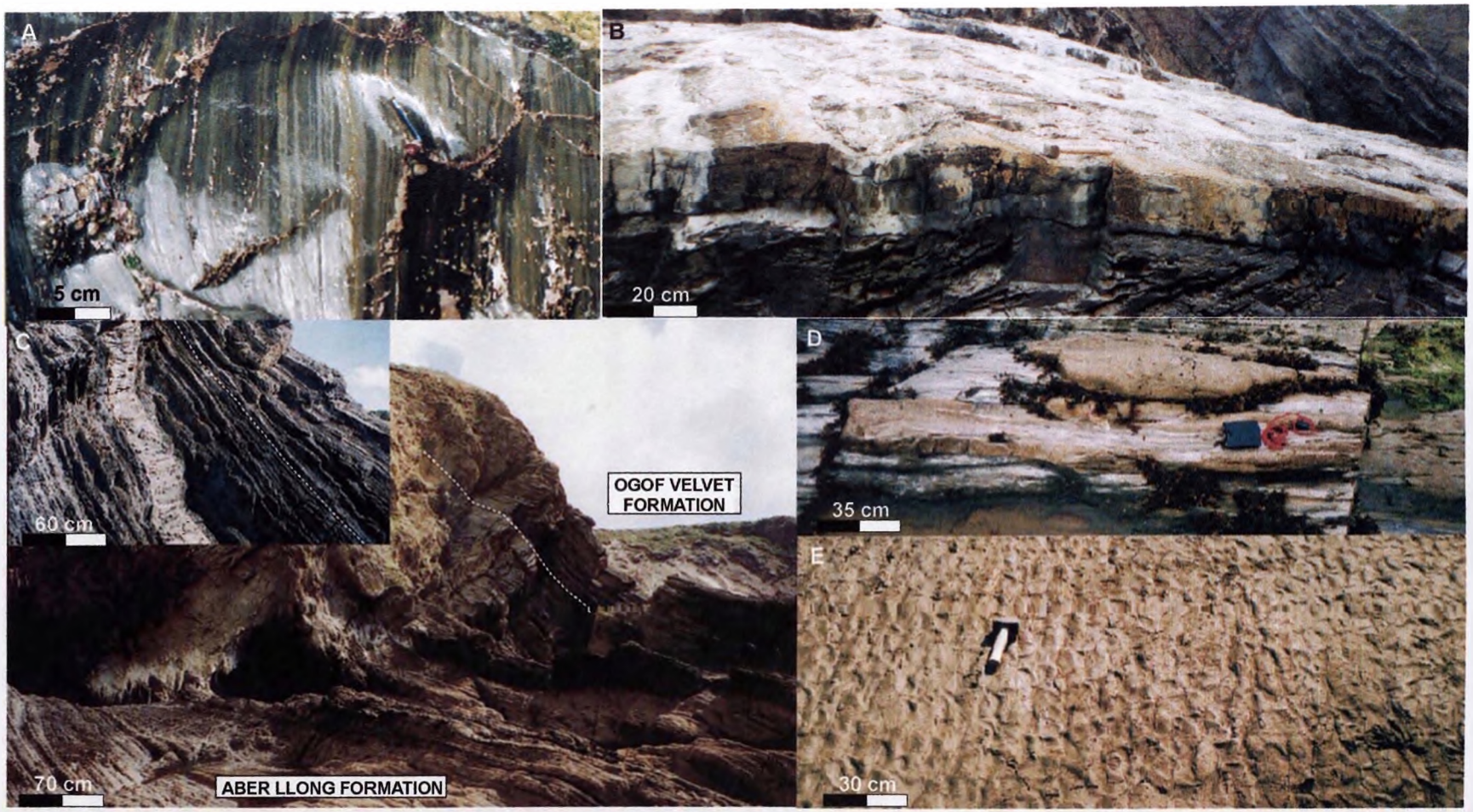



**Fig. 2.11.** Sedimentological and stratigraphical features of the Aber Llong Formation. (A) Aber Llong - colour banded siltstone and mudstone. (B) Aber Llong - nodular limestone above black mudstone. (C) Loch Warren - gradational contact between black mudstone of the Aber Llong Formation and lenticular sandstone and grey mudstone of the Ogof Velvet Formation. (D) East of Porth-y-rhaw - starved hummocks at the base of the Aber Llong Formation. (E) Aber Llong – combined-flow ripples in fine grained sandstone.

certain horizons are common. Bioturbation is completely absent. The overall fining-upward trend culminates in a distinctive black mudstone unit exposed at Loch Warren that is devoid of silt but rich in nodular limestone and carbonate concretions. This section was previously mapped as "Menevian" and is the locality where Lewis (1987) collected specimens of *Agnostus pisiformis*. The uppermost beds, which include the transition into the overlying Ogof Velvet Formation (Fig. 2.11C), mark the return of starved ripple trains and thinly bedded fine-grained sandstones. The latter become dominant in the succeeding formation.

The sedimentological characteristics outlined above are consistent with deposition on a transgressive–regressive fine-grained storm-dominated shelf (Crimes 1970a). Deposition of organic-rich mud in nearshore settings is typical of highly dissipative coastal profiles where severe wave attenuation is a common feature (Orton and Reading 1993). A good modern example of a highly dissipative shoreline exists between the Orinoco and Amazon deltas on the Surinam coast (Wells and Coleman 1981; Nittrouer *et al.* 1986), where waves neither reach the shoreline nor break. This results in the predominantly onshore transport of muds, insignificant nearshore erosion, and restricted dispersal of sand/silt grade material onto the shelf. Intense condensation on the mid- to outer shelf is represented in the Aber Llong Formation by nodular limestone and carbonate concretions. The conspicuous nodular limestone bed and abundant carbonate concretions at Loch Warren may represent the maximum flooding surface, documenting the period of most intense condensation during peak transgression.

*Distribution:* Apart from the type locality and reference sections, the Aber Llong Formation is elsewhere poorly exposed. Approximately 100 m of black mudstone with subordinate sandstone, the latter displaying very well preserved hummocky cross-stratification and starved hummocks occurs at Gwadn (SM 8032 2374), a small bay on the eastern side of Solva Harbour, where neither upper nor lower contact is exposed. Transitional beds into the overlying Ogof Velvet Formation occur in a small quarry on the path leading to Aber Mawr (SM 8802 3457). Although no contact is exposed, these dark mudstones with abundant starved ripples outcrop roughly 120 m below beds of the Ogof Velvet Formation, which form the headland at Aber Mawr. Approximately 90 m of black mudstones with starved siltstone ripples exposed at Porth Glastwr (SM 8692 3420) 1.5 km southwest of Aber Mawr were mapped as Arenig (Ogof Hen Formation) by the B.G.S. (1973). Faulted upper and lower contacts were either observed or inferred: the latter is suspected as the section is only accessible from the sea. Although some displacement of the section is evident, this

clearly occurs within beds identified as Aber Llong Mudstones. Lithological features share little in common with the shallow water facies typical of the Ogof Hen Formation. This locality also exposes the transitional contact into the Ogof Velvet Formation.

*Biota and age:* Fossils have previously been collected at only two localities. Beds previously referred to as "Upper Menevian" have at Porth-y-rhaw yielded to Harkness and Hicks (1871): *Conocoryphe* sp., *Agnostus scutalis* Salter, *Lingulella ferruginea* Salter, *Discina pileolus*, *Billingsella*? *hicksii* (Davidson), "*Orthis" hicksii* Salter, *Theca corrugata* Salter, *Protospongia fenestrata* Salter and *Protospongia flabellata* Hicks. Unfortunately the trilobites were never illustrated to confirm their identities. *"Billingsella" hicksii* and *P. fenestrata* are also recorded from beds stratigraphically lower, while the stratigraphic ranges of the remaining species are unknown. Hicks (1892) record of *Paradoxides* and "*Conocoryphe*" (specimens which have never been described) may partly correspond to the *Paradoxides forchhammeri* (*Solenopleura brachymetopa?*) zonal group of the Scandinavian sequence (Rushton 1974). Deposition during this widespread regressional phase, with the development of a falling stage systems tract (Plint and Nummedal 2000), would add significant weight to the interpretation of this arenaceous unit as a forced regression. The occurrence of *Agnostus pisiformis* at Loch Warren (Lewis 1987) in sediments deposited close to maximum flooding, places the intervening *Lejopyge laevigata* Biozone in transgressive sediments, a feature present throughout Avalonia and Sweden (Rushton 1978, p. 248; Allen *et al.* 1981, p. 307).

### 2.2.2.4. Ogof Velvet Formation (revised)

*General:* Traditionally the "Upper Lingula Flags" of Salter (1864) and Hicks and Salter (1866), and the "Ffestiniog Group" of Hicks (1881), these beds were formally defined by Kokelaar *et al.* (1985) as the "Ogof Velvet Formation" based on an 87 m thick succession of "Lingula Flags" found beneath the Ogof Hen Formation (Arenig) on Ramsey Island. Lithologically, the Ogof Velvet Formation is very similar to the Ffestiniog Flags Formation exposed in North Wales (Allen *et al.*. 1981).

*Name:* After the coastal section of the same name (SM 7090 2528) situated on the eastern headland of Bae Ogof Hên, at the most north-eastern point of Ramsey Island (see Kokelaar *et al.* 1985).

*Type locality:* The largest continuous exposure through the formation occurs in the Granston Area from Aber Mawr (SM 8800 3448) to Penmorfa (SM 8672 3466), but parts of the section are inaccessible from land and the unconformable junction with the Arenig has yet to be identified. Over 250 m of well-exposed and continuous section outcrop on both sides of Porth Gain Harbour (SM 8038 3261). As this locality best displays the junction with the Arenig, this section is designated stratotype. The succession at Aber Mawr is retained as a reference section and complements strata exposed on the Trwynhwrddyn promontory on the northern side of Whitesand Bay (Fig. 2.1B), where the unconformable contact with the Arenig is again exposed.

*Thickness:* A minimum thickness of 260 m occurs in the base-absent sequence at the type locality. A similar figure is estimated for the top-absent sequence between Aber Mawr and Penmorfa.

*Lower and upper contacts:* The lower contact with the Aber Llong Formation is well exposed immediately east of Loch Warren (Fig. 2.11C) and at Porth Glastwr (access from the sea only). In both sections the junction is entirely gradational over approximately 4 m, and is marked by a fairly rapid increase in the abundance of thin, laterally persistent fine-grained sandstone beds with a concomitant decrease in dark grey mudstone, which is replaced by light grey and dark blue silty mudstone (Fig. 2.11C). The base is drawn where sandstone forms a greater proportion than dark grey mudstone. The upper contact with the Ogof Hen Formation (Arenig) is at most localities faulted, but at Whitesand Bay (Pringle in Cox *et al.* 1930a, p. 422, 431; Jones 1940, p. 407; Evans 1948), Ramsey Island (Kokelaar *et al.* 1985), and Porth Gain, the junction is marked by very slight angular bedding discordance and a thin (2–7 cm) conglomerate horizon composed of angular volcanic and metamorphic clasts. The record of conglomerate in the Ogof Velvet Formation at Porth Gain (Cox 1915) is probably erroneous, more likely being the first recorded observation of this extremely cryptic unconformity. At Whitesand Bay, Evans (1948) also documented channel and karst-like features, but even with photographic evidence, this is difficult to verify.

*Lithology and process sedimentology:* The formation generally comprises light-grey weathering quartzose fine-grained sandstones with interbedded light blue silty mudstone. Bed thickness, sandstone to shale ratio, and average grain size all increase up section, continuing a trend begun in the underlying formation. Silty mudstones are either laminated or massive lower in the sequence but become wavy,

lenticular and flaser bedded half way up (Fig. 2.12C). Wave, interference and current ripples are commonly associated with these structures. Cross-lamination is typically bi-directional, and displays evidence for continued reactivation. Loading of ripple forms suggests deposition on a low strength substrate. All of these structures are beautifully preserved in the wave-weathered section at Whitesand Bay. Bioturbation is extremely rare, but *Planolites* burrows occur occasionally higher in the succession at both Whitesand Bay and Porth Gain.

Sandstones are tabular towards the base, but become increasing lenticular higher up, culminating in intensely amalgamated channels incised into wavy bedded silty mudstone (Fig. 2.12A). Internal stratification is extremely well developed throughout, and particularly well preserved at Whitesand Bay and Porth Gain. The lower beds record a stratification sequence comparable to Bouma divisions Ta–Td, with erosive bases, gradational tops, and well developed sole structures including load casts and flute casts. These beds pass gradationally into hummocky cross-stratified sandstones that become amalgamated higher up (Fig. 2.12D) and replaced by trough cross-bedding and quasi-planar lamination (cf. Arnott 1993).

Channels that form the upper part of the sequence may be hummocky cross-stratified, trough cross-bedded or quasi-planar laminated, with trough cross-bedding dominating the medium fraction. Grading is particularly common. Each channel unit is completely encased in silty mudstone, and is typically composed of at least 14 discrete depositional episodes (Fig. 2.12A). Channel margins are typically steep, occasionally overhanging, with no evidence for lateral accretion. Convolute lamination is particularly well developed in channel units exposed at Whitesand Bay, with excellent preservation of various types of water escape structure. Sinuous and straight gutter casts are also extremely abundant, with good examples exposed at Aber Mawr and Porth Gain. Although well developed throughout the succession, they are quite distinctive when associated with channel units, particularly at Aber Mawr. Sediment slides, although relatively uncommon, are a conspicuous feature of the formation, with good examples exposed at Whitesand Bay, Porth Gain (Fig. 2.12B), and according to Kokelaar *et al.* (1985), on Ramsey Island.

On both palaeontological and sedimentological grounds, Turner (1977) concluded that the Ogof Velvet Formation represented intertidal and subtidal deposition. The presence of wavy, lenticular, and flaser bedding, coupled with reactivation surfaces, bi-directional cross-bedding, hypersaturated low strength muds, and the quartzose nature of the sediments higher in the formation are certainly consistent with this interpretation (Reineck and Wunderlich 1968; Visser 1980; Yeo and Risk 1981). However the incised channel units, and the amalgamated




**Fig. 2.12.** Lithological features of the Ogof Velvet Formation. (A) Channelized medium- to fine-grained sandstones encased in wavy bedded silty mudstones at Whitesand Bay. These amalgamated channel units are interpreted as nearshore conduits that bypass sand-grade material through a dominantly fine-grained coastal setting out onto a sandy inner shelf. (B) Slump horizon in hummocky cross-stratified sandstones at Porth Gain. (C) Wavy, flaser and lenticular bedding at Whitesand Bay. This is a classic tidal heterolithite. (D) Amalgamated hummocky cross-stratified and quasi-planar laminated fine sandstones at Porth Gain. This inner shelf deposit is the main depositional zone located at the mouth of the nearshore conduits illustrated in (A).

| Characteristics of a fine grained subaqueous delta | Ogof Velvet Formation |
|---|---|
| 75-95% clay, silt and very fine sand | * |
| Little or no subaerial expression | * |
| Nearshore grain size profile may be inversely graded | * |
| Well developed bypass - deposition - condensation zonal scheme | * |
| Muddy nearshore prone to bypass (low accumulation rates). | * |
| High energy tidal currents and expanded intertidal zone | * |
| Moderate mass movement and resedimentation | * |
| Dissipative shoreline (high wave attenuation) | * |
| Low salinity water column | * |
| Association with shore attached mud banks (Aber Llong Mst Fm) | * |
| Large low gradient catchment draining a passive margin | * |

**Table 2.2.** Summary of the main characteristics of large fine-grained subaqueous delta platforms based on studies by Nelson (1982), Nittrouer *et al.* (1986), Alexander *et al.* (1991), Michels *et al.* (1998), and Hill *et al.* (2001). Evidence for a low salinity water column is uncertain, but this feature may account for the almost complete exclusion of biogenic activity, body fossils, and the unusual distribution of bioturbation in the Welsh Basin. See text for further details. * = present.

sandstones and interbedded sandstones and mudstones lower in the sequence, are not compatible with deposition under the modulating affect of tides. Instead, the presence of hummocky cross-stratification, quasi-planar lamination, combined flow ripples, gutter casts, flute casts, and the unpredictable frequency of bedding are typical features of inner to mid-shelf storm deposits (Harms *et al.* 1975; Brenchley 1985; Arnott 1993; Myrow and Southard 1996).

A rather unusual feature of this storm- and tide-dominated shoreline sequence is the occurrence of fine-grained sediment in the nearshore. Proximality trends such as grain size and sandstone to shale ratio actually decrease in the nearshore, the exact opposite to that recoded on most modern and ancient storm-influenced shelves (Brenchley 1985; Swift *et al.* 1988; Johnson and Baldwin 1996). The presence of gutter casts and channels in the nearshore (Fig. 2.4) is consistent with the only tempestite model developed for fine-grained shorelines. According to Myrow (1992a) and Perez-Lopez (2001) these features act as sediment conduits that bypass sand grade material through the nearshore and out onto the inner shelf. Identical facies in the Ffestiniog Flags Formation in North Wales were interpreted by Allen *et al.* (1981) as being deltaic in origin. A comparison of the salient attributes of the Ogof Velvet Formation with accepted features of subaqueous delta platforms associated with large fine-grained rivers like the Amazon and Ganges is presented in Table 2.2., and reaffirms this conclusion.

*Distribution:* In addition to the type and reference sections outlined above, the formation occurs extensively to the east and west of Solva Harbour, but access is difficult, and in cliff sections at Porth Dwfn (SM 8041 3253) to the west and Trwyn Elen (SM 8192 3281) and Trwyn Llwyd (SM 8331 3293) to the east of Porth Gain.

*Biota and age*: Fossils in the Ogof Velvet Formation are extremely rare and are not considered age-diagnostic. Disarticulated shells of the brachiopod *Lingullella davisii* (M'Coy) are abundant at certain horizons at several localities including Whitesand Bay and Porth Gain. As this is a facies-dependant species, previous suggestions of correlation with *L. davisii* bearing sediments of the Ffestiniog Flags Formation cannot be assumed (Rushton 1974). The only other collection of note are well preserved *Hymenocaris*-like crustacea obtained from Whitesand Bay by Lewis (1987).

### 2.2.2.5. Treffgarne Bridge Formation

*General:* Dark laminated mudstones exposed in the Treffgarne area assumed importance when Upper Cambrian trilobites of the *Olenus* Biozone were discovered there (Lake 1906–1946, pp. 10, 58). Fossils include *Lingulella davisii* and the trilobites *Homagnostus obesus* (Belt), *Olenus cataractes* Salter and *Olenus mundus* Lake, the latter two of which Rushton (1983) considered to be conspecific. The local name "Treffgarne Bridge Beds" was proposed for these strata by Cowie *et al.* (1972), and the general geology of the area was described by Thomas and Cox (1924). Because the section is poorly exposed (intermittently exposing only 20 m of strata), and fault bounded by Precambrian and Arenig Volcanics, its relationship to the Ogof Velvet Formation is unknown. An upper *Olenus* age (*cataractes* Biosubzone) places it stratigraphically above the Aber Llong Formation, but it contains lithofacies that are different from both the upper part of the formation and the whole Ogof Velvet Formation. Based on the age and lithological characteristics of the Ffestiniog Flags Formation in North Wales (Allen *et al.* 1981), and sediment dispersal patterns (Crimes 1970a) that suggest a south to north migration of facies belts across Wales (Prigmore and Rushton 2000) culminating in shallow water sedimentation in North Wales by the uppermost *Olenus* and *Parabolina spinulosa* Biozones (Allen *et al.* 1981), it is difficult to imagine Ogof Velvet sedimentation being any younger than the *O. cataractes* Biosubzone. The Treffgarne Bridge Formation is therefore tentatively equated with the Ogof Velvet Formation, and may simply record more distal

deposition away from the main axis of deltaic sedimentation, a view shared with Prigmore and Rushton (2000).

*Type section:* In cutting along the roadside and in a quarry next to Treffgarne Bridge (SM 9594 2287).

*Lithology:* This predominantly argillaceous formation shares many lithological characteristics with the Aber Llong Formation like colour banding (green, dark grey and black mudstones), starved siltstone ripples, convolute lamination and rare cross-lamination. Hard fine-grained siliceous sandstones occur as both lenticels and 1–6 cm thick tabular beds. Parallel lamination is occasionally preserved in the latter, but always slightly convoluted by water escape. These beds are interpreted as distal storm deposits laid down on the mid- to outer-shelf.

## 2.3. THE CONCEPT OF A UNIFIED AVALONIAN CHRONOSTRATIGRAPHY

Avalonia (Fig. 2.1E) is one of several exotic terranes within the Appalachian-Caledonide orogen that are interpreted to have evolved along an active margin of Neoproterozoic Gondwana (Nance *et al.* 1991, 2002). Extending from New England and Atlantic Canada (West Avalonia) to southern Britain (East Avalonia), Avalonia is the largest of these peri-Gondwanan terranes, all of which are characterized by Neoproterozoic histories of continental margin subduction, and by the peri-Gondwanan affinity of their early Palaeozoic shallow marine succession (Nance and Thompson 1996; Landing 1996).

The remarkable lithological and palaeontological similarities between Cambrian successions in East and West Avalonia have long been appreciated (e.g. Mohr and Allen 1965), but up until the late 1970's, work on the Avalonian cover sequence was dominated by macrofossil studies and generalized lithostratigraphic descriptions from small areas (Landing 1996). With the birth of high-resolution sequence stratigraphy and precise U-Pb radiometric dating techniques, a picture of a unified Avalonian cover sequence has emerged by extrapolating chronostratigraphically significant, unconformity-bounded depositional sequences identified in the type-Avalonian succession in SE Newfoundland, into coeval sections in Nova Scotia, southern New Brunswick, eastern Massachusetts, Rhode Island, Cape Breton Island, the Carolina Slate Belt, and parts of Southern Britain (Landing *et*

*al.* 1980; Landing 1988, 1991, 1992, 1994, 1996; Landing and Benus 1988; Brasier 1989, 1992; Landing and Westrup 1996; Landing *et al.* 1998; McIlroy *et al.* 2000).

Cambrian palaeogeographical reconstructions based on west–east transects across these Avalonian cover sequences apparently define a marginal (western) and inner (eastern) platform (Fig. 2.1A) (Landing 1994, 1996; Landing and Westrop 1996). In the sedimentary record, these broad geographical locations are apparently defined by their depositional response to the timing and scale of epeirogenic activity (Landing 1992, 1996). Marginal platform successions such as those on the Burin Peninsula (SE Newfoundland), St John's (New Brunswick), Cape Breton Island and Nova Scotia typically demonstrate: (1) a thick lower Placentian Series that extends downwards into the latest Neoproterozoic (e.g. the Rencontre–Random formations on the Burin Peninsula, Fig. 2.13) and, (2) a dominantly arenaceous Branchian–middle Acadian (St David's) Series punctuated by large unconformities (e.g. St John's, New Brunswick, Fig. 2.13). These features are comparable with Cambrian successions in the Bangor area and Caernarfonshire Slate Belt in southern Britain (which are situated on the northwestern periphery of the British Avalonian Superterrane (Fig. 2.1A); a location consistent with the marginal platform of West Avalonia (Landing 1996).

These characteristics may be contrasted with successions on the eastern inner platform of Avalonia in locations such as Trinity Bay (SE Newfoundland, Fig. 2.13) and Cradle Brook (New Brunswick), which typically demonstrate: (1) a thin lower Placentian Series with an unconformable contact with the latest Precambrian (e.g. the Random Formation at Trinity Bay, Fig. 2.13) and, (2) a shale-dominated middle Lower Cambrian–upper Middle Cambrian that contains units of limestone (e.g. the Bonavista and Brigus groups and Chamberlain's Brook Formation at Trinity Bay, Fig. 2.13). The dominantly fine-grained succession at Nuneaton on the eastern part of the Midland Platform defines the inner platform in southern Britain (Brasier 1989; Landing 1996).

Based on a comprehensive synthesis of local studies, Landing (1996) proposed 9 epeirogenically-controlled depositional sequences that are apparently recognized in the Dyfed Supergroup of southern Britain (Fig. 2.13). As this sequence framework was principally developed from sections in West Avalonia, and has yet to be applied in detail to any sections in southern Britain (Landing relied almost entirely on secondary accounts), this contribution to Cambrian stratigraphy in SW Wales presents an opportunity to test the applicability of a unified Avalonian stratigraphy to Cambrian sections in southern Britain. Although Pembrokeshire exposes one of the most complete successions of Cambrian rocks in southern Britain, it was overlooked

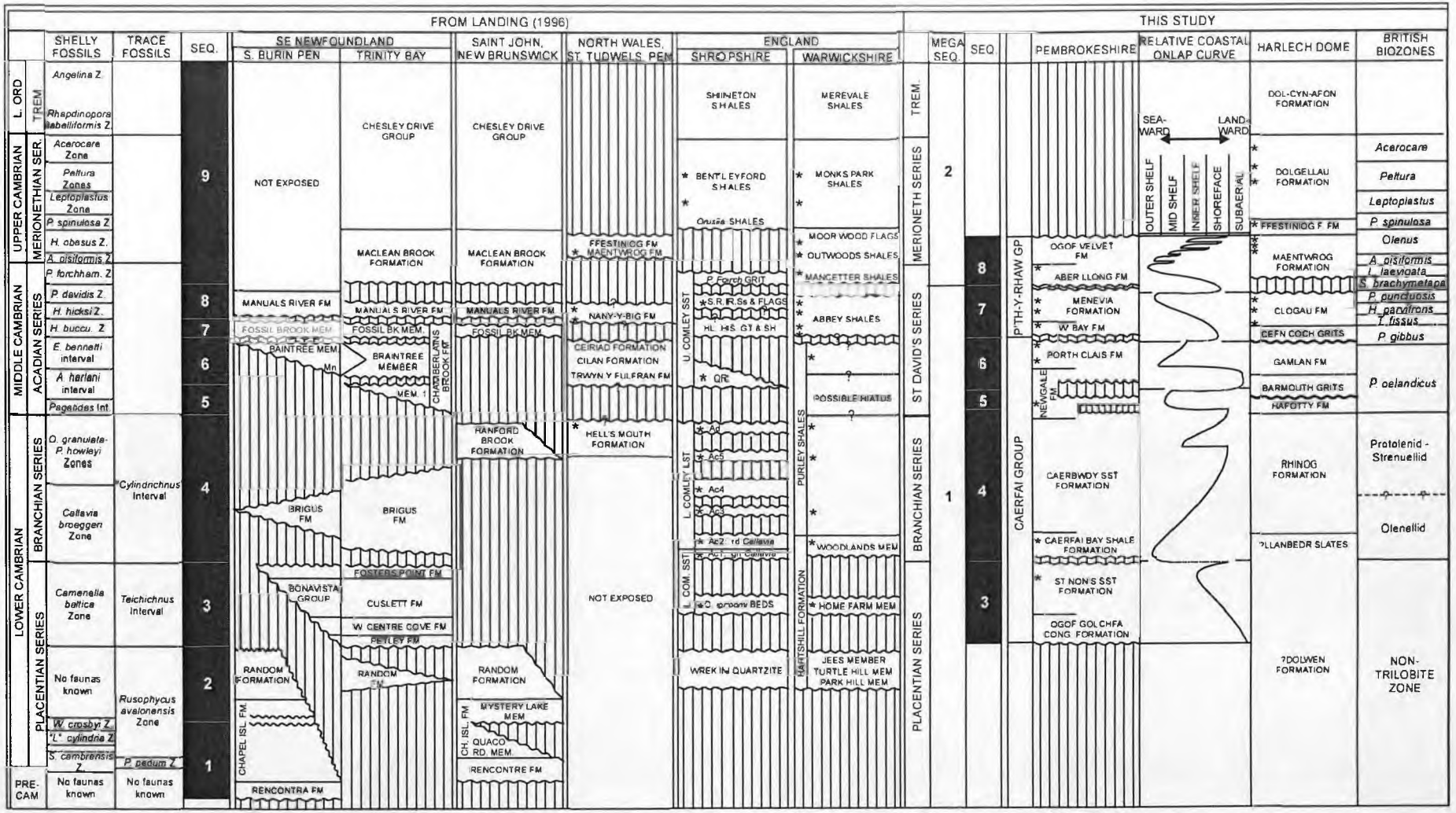



**Fig. 2.13.** Cambrian sequence stratigraphy across the Avalonian platform. Fossil zonation from Atlantic Canada taken from Landing (1992), and southern Britain from Cowie *et al.* (1972). Biostratigraphy follows Cowie *et al.* (1972), Rushton (1972), Allen *et al.* (1981), Brasier (1989), Young *et al.* (1994), Landing (1996) and Rushton *et al.* (2000). * = biostratigraphically constrained.

in Landing's (1996) synthesis of Avalonia stratigraphy. This may be because geographically, Pembrokeshire is located between the inner and marginal platform (Fig. 2.1A), and contains a succession not as easily incorporated into Landing's broad overview.

## 2.4. SEQUENCE STRATIGRAPHY

Sequence stratigraphic nomenclature used here follows that of Vail *et al.* (1977) modified by Van Wagoner *et al.* (1988). Sequence boundaries are placed at surfaces showing substantial fluvial incision and/or a significant basinward translation of coastal onlap (see Fig. 2.14) (Van Wagoner *et al.* 1988; Posamentier and James 1993). Utilising these basic principles, the Dyfed Supergroup is divided into 8 unconformity bounded depositional sequences (Fig. 2.14), which correlate both lithologically and chronologically with epeirogenically-controlled sequences identified by Landing (1996) throughout Avalonia (Fig. 2.13). Sequences 1 and 2 of the Avalonian stratigraphic scheme (latest Neoproterozoic to the mid Placentian Series of the Lower Cambrian) are not recognized in the Dyfed Supergroup of SW Wales, a feature typical of successions situated on the Avalonian inner platform (Landing 1996; Landing and Westrop 1996). These sequences are only fully developed on the marginal platform, which in Eastern Avalonian corresponds roughly to localities in North Wales. Examples of sequence 1 and 2 deposits include the Fachwen Formation and lower Llanberis Slates in the Caernarfon Slate Belt (Crimes 1970a, Rushton 1974), and the Dolwen and Llanbedr formations around the Harlech Dome (Allen and Jackson 1978, 1985).

For a detailed overview of biostratigraphical correlation, the reader is referred to excellent review papers by Brasier (1989) and Landing (1991, 1992, 1995, 1996). Detailed faunal correlations are not discussed further here.

### 2.4.1. Depositional sequences

#### *2.4.1.1. Sequence 3*

Sequence 3 extends from the base of the Ogof Golchfa Formation to the base of the Caerfai Bay Formation (Fig. 2.14), attaining a maximum thickness of 195 m. The basal unconformity that separates arc-related Precambrian sediments from basal Cambrian conglomerates demonstrates slight angular discordance and is interpreted

as a type-1 sequence boundary. The overlying 41 m consists almost exclusively of poorly sorted cobble-pebble conglomerates of the Ogof Golchfa Formation (Fig. 2.3), interpreted as lowstand alluvial fan and gravelly braided stream deposits (Fig. 2.4). These are in turn overlain by transgressive nearshore marine sandstones of the St Non's Formation. A wave ravinement surface (transgressive surface of erosion) (Fig. 2.3C) separates syn-tectonic lowstand deposits from post-tectonic onlap strata of the transgressive systems tract. A 1.5 m thick unit of intensely bioturbated mid-shelf silty mudstones mark the maximum flooding surface at Porthselau. A return to nearshore sedimentation is evident in the uppermost 7 m of the St Non's Formation with the replacement of *Teichichnus* burrows with *Skolithus* burrows. This rapid shallowing is interpreted as an attenuated highstand systems tract.

A U-Pb radiometric date from the base of the overlying Caerfai Bay Formation places sequence 3 at the top of the Lower Cambrian Placentian Series (Landing *et al.* 1998), and coeval with the Bonavista Cycle (Fig. 2.13) in SE Newfoundland (Landing 1996). A strong tectonic control on sequence development and sedimentation is evident throughout Avalonia. Good examples include sediment-filled fissures along the sub-Bonavista unconformity in SE Newfoundland interpreted by Landing (1996) as recording active extension, while compressional tectonic regimes appears dominant in both the Lower Comley Sandstone of Shropshire and the condensed limestones of the Home Farm Member (Hartshill Formation) at Nuneaton (Brasier 1989; Landing 1996). The occurrence of alluvial fan and gravely braided stream deposits at the base of sequence 3 in NW Pembrokeshire is consistent with syn-tectonic sedimentation. The presence of blue and green amphibole, mylonite, and medium to high-grade metamorphic lithic fragments throughout sequence 3, coupled with westerly-derived palaeocurrent patterns (Fig. 2.15) suggest sediment was shed from a southerly extension of the Monian Superterrane (Fig. 2.1A), implying fault-accommodated subsidence along the Menai Straits Fault System.

The recognition of sequence 3 in North Wales is severely hampered by a complex and poorly documented lithostratigraphy, as well as few fossiliferous horizons. Based solely on shared lithological characteristics, Landing (1996) correlated the Bonavista cycle with the Dwndwr Grits (a subdivision of the Llanberis Slates) of the Caernarfon Slate Belt. This unit, like sequence 3 in NW Pembrokeshire was sourced from the Monian Superterrane to the west (Crimes 1970a). Thus movements along the Menai Straits Fault System that led to basin inception in Pembrokeshire may also account for the sudden influx of coarse detritus in the otherwise uniform mudstones of the Llanberis Slates, making the lithological correlation of Landing (1996) more secure. The Lower Cambrian successions of the

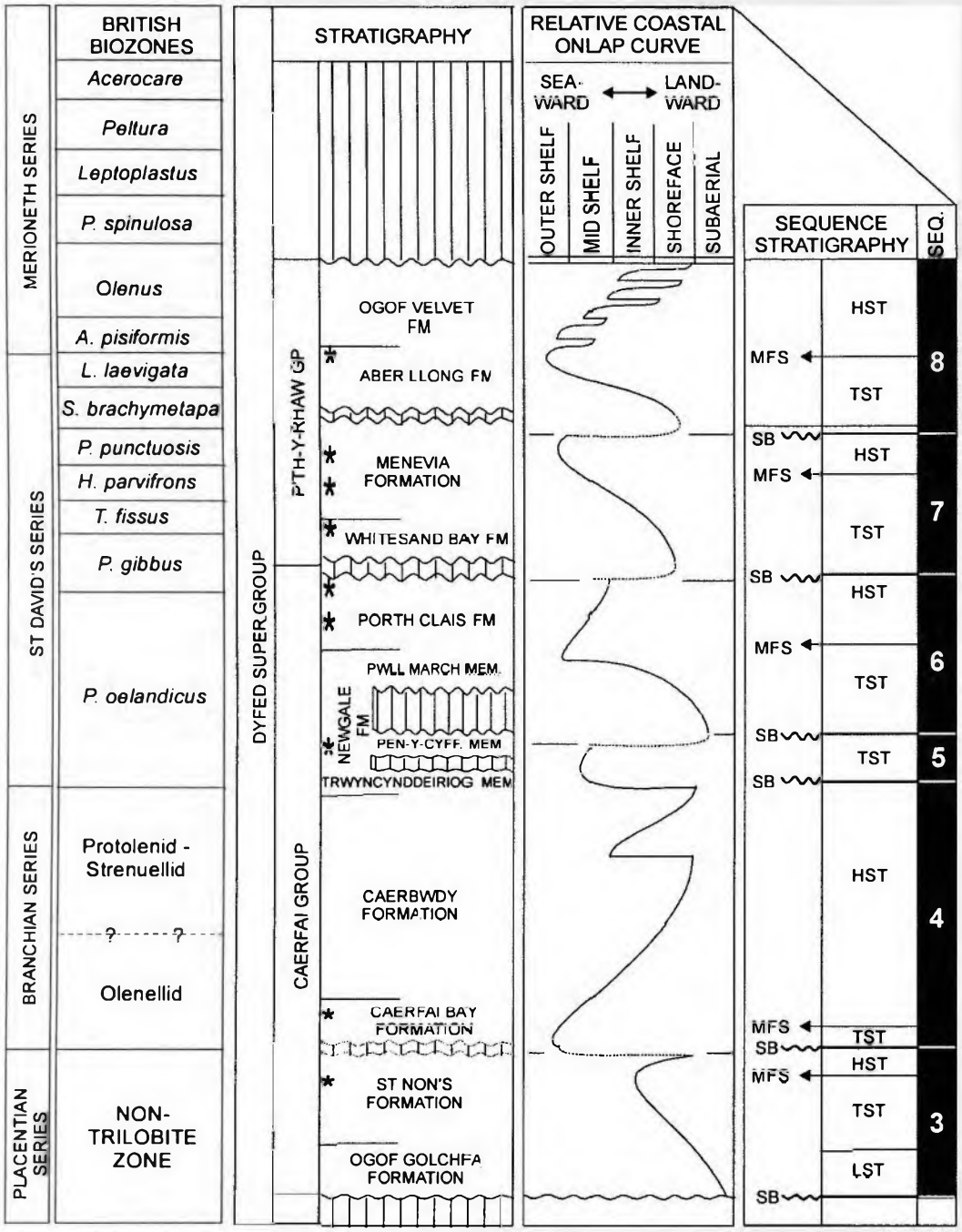



**Fig. 2.14.** Sequence stratigraphy of the Dyfed Supergroup exposed in SW Wales. * = biostratigraphic control.

Harlech Dome are extremely poorly understood in terms of facies and stratal stacking patterns, and ultimately it is not yet possible to determine depositional sequence stratigraphy.

*2.4.1.2. Sequence 4*

Sequence 4 (Fig. 2.14) attains a maximum thickness of 179 m and includes the red shales and tuffs of the Caerfai Bay Formation, the purple muddy sandstones of the Caerbwdy Formation, and the pebbly sandstones and coarse sandstones of the Trwyncynddeiriog Member (basal division of the Newgale Formation). This lithostratigraphy is very similar to the Hanford Brook Formation (New Brunswick) and other successions on the marginal Avalonian platform (Landing and Westrop 1996). The paraconformity at the top of the St Non's Formation is considered a "drowning paraconformity" (cf. Proust and Hosu 1996) based on rapid deepening rather than the more commonly documented shallowing/emergence. This surface is correlated with the type-2 unconformity that separates the pre-trilobitic Placentian Series from the trilobitic Branchian Series at the top of the Bonavista Group in SE Newfoundland (Landing 1996, Landing *et al.* 1998) (Fig. 2.14), and records a major phase of tectonic reorganization of basins across Avalonia. Depocenter migration, a change in provenance and an easterly switch in sediment source are features that characterize this sequence boundary in West Avalonia (Landing 1996; Landing and Westrop 1996), while post-Home Farm and "*Obolus*" *groomi* bed emergence at Nuneaton and Shropshire respectively (Fig. 2.13) suggest a compressional regime on the Midland Platform (Brasier 1989; Landing 1996).

Rapid deepening across this sequence boundary in Pembrokeshire is interpreted as the local expression of basin reorganization based on: (1) a similar switch from westerly derived sediment in the St Non's Formation to easterly derived in the Caerfai Bay Formation (Fig. 2.15), (2) the instant shut down of arenaceous sedimentation, this being a typical syn-tectonic lithological expression (the "anti-tectonic cycles" of Paola *et al.* 1992 and Gorden and Heller 1993), and (3) the abundance of thick, coarse-grained feldspathic tuff (Fig. 2.2A). The tectonic reorganization evident in Shropshire suggests that fault rejuvenation along the Welsh Borderland Fault System (Fig. 2.1A) may be responsible for the easterly switch in sediment source, a conclusion consistent with the apparent lack of upper Lower Cambrian and Middle Cambrian strata to the southeast in the Carmarthen area and Malvern Hills (Fig. 2.1A) (Cope and Rushton 1993).

The base of the Brigus Formation in SE Newfoundland (Fig. 2.13) is marked by a rapid west to east onlap typical of the transgressive systems tract (Landing 1996), a retrogradational motif mirrored in the distal tempestites and condensed shales of the Caerfai Bay Formation. The rest of Brigus cycle deposition compares well with the inner platform Purley Shales at Nuneaton (Brasier 1989), both of which continue a retrogradational (transgressive) trend. In SW Wales, the Caerbwdy

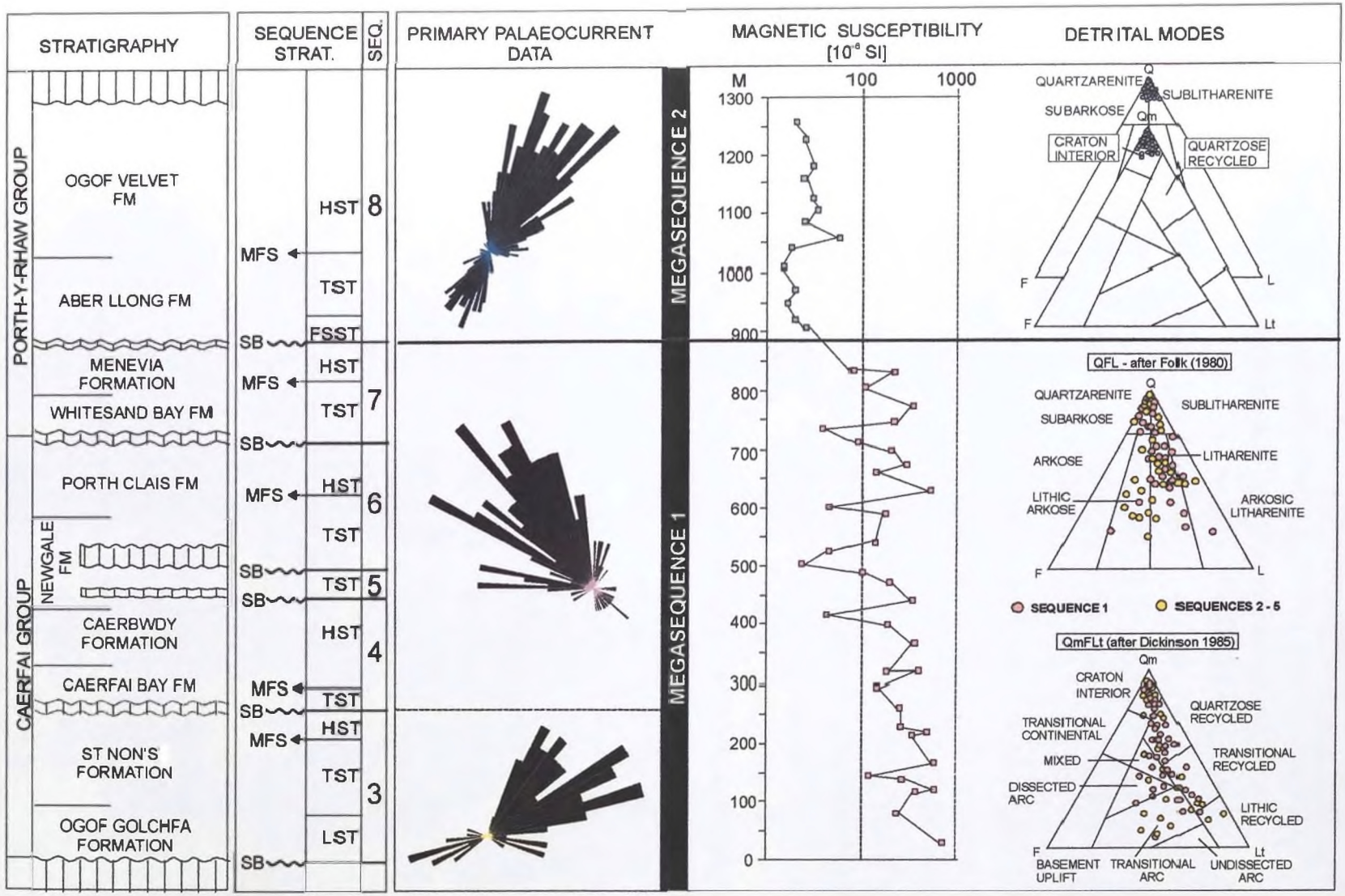



**Fig. 2.15.** Definition of megasequences based on palaeocurrent data, magnetic susceptibility and petrography. See text for details.

Formation and Trwyncynddeiriog Member form a 157 m thick coarsening and shoaling upwards sequence (a classic highstand systems tract) from bioturbated muddy shelf sandstones at the base to coarse-grained fan-delta front turbidites towards the top. The latter record reworking of their upper surfaces by tidal currents, thus a position above fairweather wave base is considered likely. A parallel change in lithology and depositional environment occurs in the Hanford Brook Formation on the marginal platform in southern New Brunswick (Landing and Westrop 1996), while in Shropshire the Lower Comley Limestone (Fig. 2.13) comprises five unconformity-bounded units (Ac2–Ac5, Ad) that record epeirogeny of the Longmynd and other blocks (Brasier 1989).

This variability in sequence 4 across Avalonia can be accounted for if we consider major fault-block rotation in what appears to be a dominantly extensional "rift" regime. In this model (Fig. 2.16), successions punctuated by hiatuses would occupy tilt-block highs (e.g. Shropshire, Carmarthen and the Malverns), while thick sand-rich strata form progradation clastic wedges sourced from the elevated tilt-block. Due to typical low clastic penetration away from the fault (a result of the direction of depositional slope), much of the half graben will be relatively condensed and mud-rich, accounting for the sections in SE Newfoundland and at Nuneaton. This interpretation of the inner Avalonian platform is consistent with: (1) stratal thickening into faults evident on seismic profiles across the Midland Platform (Smith and Rushton 1993), (2) a rapid phase of differential subsidence apparent in subsidence curves constructed from Lower and Middle Cambrian successions throughout southern Britain (Prigmore *et al.* 1997), (3) a thin transgressive systems tract and thick highstand systems tract in NW Pembrokeshire, reflecting initial rapid subsidence (fault activation and block rotation) followed by clastic wedge progradation during relative tectonic quiescence (the anti-tectonic cycle), and finally (4) the onset of fan-delta sedimentation during clastic wedge outbuilding, a classic depositional system response to fault activation (Massari and Colella 1988).

Sequence 4 in North Wales comprises the red and green slates of the upper Llanberis Slates, which are similar in lithology to the Brigus Formation and Purley Shales (Landing 1996), and coarse-grained turbidites of the Hell's Mouth and Rhinog formations of St Tudwal's Peninsula (Fig. 2.1A) and the Harlech Dome respectively. The regressive trend that characterizes sequence 4 in locations proximal to active fault zones (essentially the marginal platform) is evident in both formations (Crimes 1970a), but most notably in the Hell's Mouth Formation, where supposed deep water turbidite fan deposits (Bassett and Walton 1960; Crimes 1970a; Young *et al.* 1994) pass rapidly into gravelly turbidites with interference, asymmetrical and symmetrical

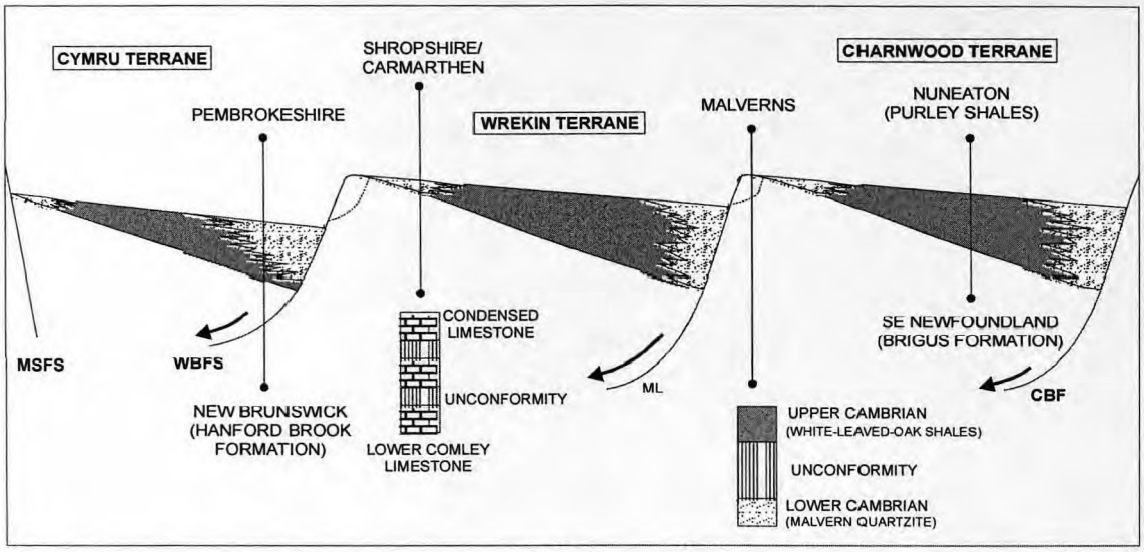



**Fig. 2.16.** Structural model to account for facies distribution, sequence architecture and location of unconformities in the successions in SW Wales, Shropshire, Malvern and Nuneaton (see text for details). Fault block rotation with tilt-block highs also explains the temporal and spatial distribution of these features in SE Newfoundland. Cross section is shown as X–Y in Fig. 1A. Abbreviations of faults are the same as Fig. 2.1A.

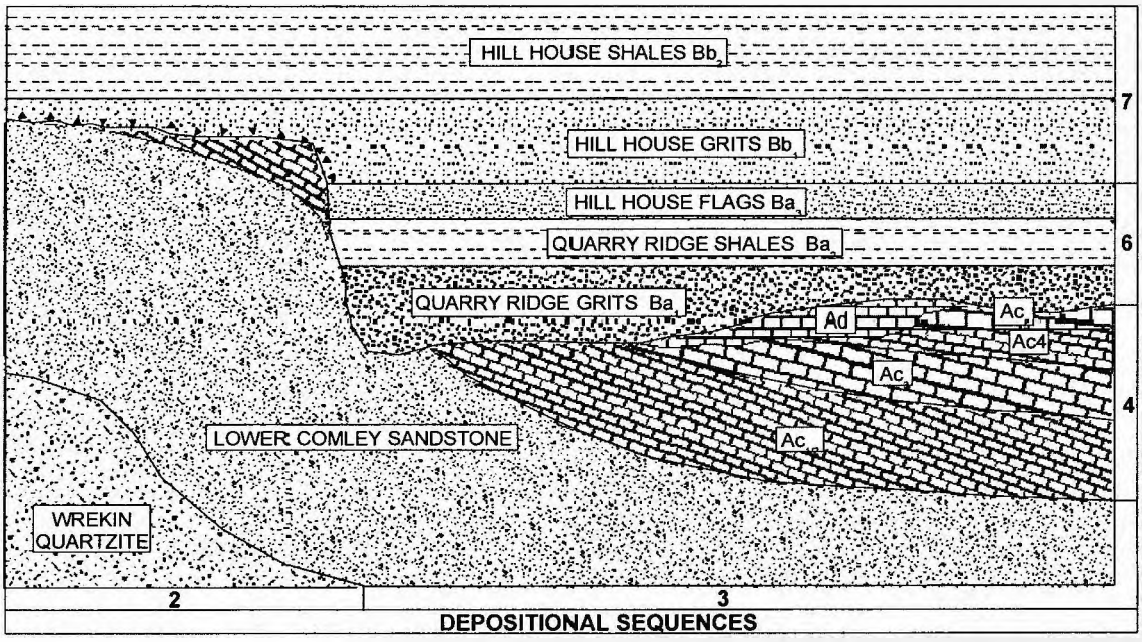



**Fig. 2.17.** Cross section and depositional sequence stratigraphy of the succession exposed at Comley, Shropshire.

rippled tops (Bassett and Walton 1960). These are virtually identical to the pebbly sandstones of Trwyncynddeiriog Member, which may suggest that these turbidites are Gilbert-type fan-delta deposits (cf. Postma 1990) rather than deep-sea fan. Although the dominant source for both formations was the Monian Superterrane to the north (Bassett and Walton 1960), Crimes (1970a) identified pebbles in easterly-derived turbidites that he correlated with the Uriconian Volcanics of Shropshire. This provides a critical link between fault rejuvenation on the Midland Platform and turbidite deposition in North Wales.

*2.4.1.3. Sequence 5.*

The base of sequence 5 is drawn at the flooding surface within the Newgale Formation between the pebbly sandstones of the Trwyncynddeiriog Member and the dark grey phosphatic shales of the Pen-y-Cyffrwy Member (Fig. 2.5D and E). This condensed sequence attains a thickness of 13 m in sections south of St David's, thinning dramatically to less than 1.5 m at Newgale, and spans the whole of the dominantly transgressive Pen-y-Cyffrwy Member. The rapid onset of condensed shale deposition follows a prolonged phase of fan-delta progradation (clastic wedge penetration from the basin margin fault in the east) that is evident in the upper part of sequence 4. This flooding surface is similar to the drowning paraconformity recorded at the top of the St Non's Formation. The occurrence of slump structures (Fig. 2.5C) immediately below the sequence 4–5 boundary in successions at Newgale and Caerfai Bay, as well as the almost instantaneous increase in accommodation space that led to drowning of the fan-delta environments, strongly suggests a renewed phase of fault-block downwarping and consequent "in place drowning" (cf. Sanders and Kumar 1975, Swift 1975) of the delta system. This phase of rapid subsidence accounts for the low clastic penetration into the basin as coarse material is trapped close to the fault scarp, and the initiation of condensed shale sedimentation in more distal locations.

The sparse trilobite fauna recovered from the Trwyncynddeiriog Member enables correlation with the condensed manganiferous shales (Member 1) of the Chamberlain's Brook Formation of SE Newfoundland (Fig. 2.13). In correlating sequence 5 across Avalonia, Landing (1996) highlighted three definitive characteristics: (1) argillaceous sedimentation with high levels of manganese and phosphate, (2) intense condensation associated with rapid flooding of basin margins (rapid coastal onlap) and, (3) a strong syn-tectonic element to deposition. All of these

characteristics are clearly evident in the Trwyncynddeiriog Member and are quite conspicuous in inferred sequence 5 strata throughout southern Britain.

In North Wales, the manganiferous shales of the Hafotty Formation (Matley and Wilson 1946; Allen and Jackson 1985) abruptly overlie the Rhinog Grits in the Harlech area (Fig. 2.13). This transition is similar to the one recorded in Pembrokeshire, with a sudden switch from rapidly accumulating turbidite deposits to condensed shales. The enrichment in manganese has been related to submarine exhalative hydrothermal solutions (Bennett 1987), which suggests an important tectonic element. This phase of active tectonism is also obvious in the succession at Shropshire (Fig. 2.13) where sequence 5 approximates to an angular unconformity between the *Lapworthella* Limestone (Ad) at the top of sequence 4 and the Quarry Road Grits which form the base of sequence 6 (Landing 1996). This unconformity is highlighted in a cross section from the Comley area of Shropshire in Figure 2.17. The transition was interpreted by Cobbold (1925) as recording uplift, tilting, and erosion of the Lower Comley Limestone and Lower Comley Sandstone, characteristics now understood to be compatible with fault-block rotation and an extensional tectonic regime (Fig. 2.16.). A discontinuous 1–2 cm thick phosphatic horizon that occurs in some locations in the Comley area between the *Lapworthella* Limestone and basal conglomerate of the Quarry Road Grits (Cobbold 1933) may represent an erosional remnant of sequence 5 onlap and sediment condensation prior to emergence of the tilt-block high.

An unconformity of similar magnitude occurs between the Hanford Brook Formation of sequence 4 and the Fossil Brook Member (Chamberlain's Brook Formation) of sequence 7 in New Brunswick (Fig. 2.13), which may similarly be located on a tilt-block high. This may also account for the lack of significant sequence 4 deposition and the large unconformity that separates the Random Formation (sequence 2) from the Hanford Brook Formation. Sequence 5 at Nuneaton is represented by the upper part of the Purley Shales (Fig. 2.13). The stratigraphy is poorly known because of limited outcrop, and no evidence has been reported for a sequence 4–5 boundary. A similar setting to that outlined for the lower Purley Shales of sequence 4 may be concluded (Fig. 2.16).

#### *2.4.1.4. Sequence 6*

This sequence in SW Wales (Fig. 2.14) forms a 172 m thick fining then coarsening upward motif from the base of the Cwm Mawr Member (Newgale Formation) (Fig. 2.6A) to the base of the pebbly sandstone unit that defines the top of the Porth Clais

Formation (Fig. 2.7C and D). The sequence boundary is marked by a change from mid-shelf mudstones and thin sandstone turbidites of sequence 5 to alluvial fan and fan-delta conglomerates (Fig. 2.4), pebbly sandstones and tidal heterolithics of the Cwm Mawr Member (Fig. 2.6A). This rapid alluvial incursion is associated with deep erosional incision and is interpreted as a type-1 sequence boundary based on a major basinward shift in facies as well as subaerial exposure and concurrent subaerial erosion (Van Wagoner *et al.* 1988). This initial, abrupt downward shift in coastal onlap (Fig. 2.14) is followed immediately by channel backfilling and general retrogradation of facies belts forming a 60 m thick transgressive tracts that culminates in dark grey shales of the prodelta. A phosphatic horizon characterized by black organic-rich laminae separates retrogradational from progradational strata at Newgale, and may represent the maximum flooding surface. The overlying progradational sandstones and occasional pebbly sandstones record a sustained phase of delta front outbuilding, and the development of a 100 m thick highstand systems tract (Fig. 2.14).

Sequence 6, like sequence 4, is lithologically variable across the Avalonian platform. Locations on the inner platform such as Trinity Bay in SE Newfoundland, and Nuneaton are characterized by shale deposits of the Braintree Member (Chamberlain's Brook Formation) and upper Purley Shales respectively (Fig. 2.13), and mark a period of condensed sedimentation (Landing 1996). The marginal platform on the other hand is typically represented by a hiatus such as that recorded at St John's (New Brunswick), Fortune Bay (SE Newfoundland) and probably in the Caernarfonshire Slate Belt in North Wales (Crimes 1970a). Rapidly deposited conglomerate, pebbly sandstone, and medium–coarse sandstone appears to characterize locations intermediate between the inner and marginal platforms. Examples include the fan-delta deposits of Pembrokeshire, the nearshore conglomerates and sandstones of the Quarry Ridge Grits in Shropshire (Fig. 2.17), the coarse-grained turbidites of the Cilan Formation on St Tudwal's Peninsula (Fig. 2.13), and its proximal equivalent, the Barmouth Formation of the Harlech Dome (Crimes 1970a; Allen and Jackson 1985). Landing's (1996) correlation into Shropshire is biostratigraphically secure, but his inclusion of the turbidite fan deposits of the Cilan and Ceiriad formations remains unclear, but appears to be based solely on their stratigraphic position beneath the fossiliferous sequence 7 deposits of the Nant-y-big Formation.

The sharp contact between the Cilan Formation and the underlying condensed manganiferous shales of the Trwyn y Fulfran Formation (sequence 5) marks a significant change in the shelf regime that should be recognized in coeval

shallow marine successions elsewhere in the Welsh Basin. The importance of thick, rapidly deposited turbidite fan complexes in basin analysis has only been fully appreciated since the birth of sequence stratigraphy. The definition of systems tracts (Brown and Fisher 1977; Posamentier and Vail 1988) was of particular importance as it provided a critical link between the shelf and the basin, enabling deep marine sediments to be incorporated into a basinwide sequence framework. The majority of large submarine fans are generally considered coeval with the generation of type-1 sequence boundaries in paralic successions and are thus intimately associated with periods of relative sea level fall at the offlap break (Mitchum *et al.* 1977a, b; Vail and Todd 1981; Posamentier and Vail 1988). During progressive sequence boundary development, the shelf becomes incised and acts as a sediment bypass/transfer zone (Mutti *et al.* 1999), where erosional rather than depositional processes dominate. Consequently, depositional zones that once operated on the shelf are displaced beyond the offlap break resulting in deep marine sedimentation either directly through flood-generated hyperpycnal flows or indirectly through resedimentation processes (Mutti *et al.* 1999). As both the Cilan and Barmouth Formations were derived from the southern margin of the Welsh Basin (Crimes 1970a), a correlation with the type-1 sequence boundary at the base of sequence 6 in SW Wales is proposed.

The relationship between sequence boundary development, shelf transfer, depositional zone translation, and submarine fan construction is summarized in Figure 2.18. Important sedimentological features that strengthen this model are as follows: (1) similar palaeocurrent directions on the shelf and in the basin (essentially defines the system tract), (2) a type-1 sequence boundary in the paralic succession in Pembrokeshire (Fig. 2.6A) that demonstrates significant shelf incision, erosion and sediment bypass, and (3) an extension of the transfer zone beyond the offlap break during peak lowstand conditions. Evidence for the latter includes considerable canyon erosion prior to deposition of the Barmouth Formation (Crimes 1970a) and a thicker fan sequence in the more distal Cilan Formation (Young *et al.* 1994; Pratt 1995) suggesting considerable bypass prior to Barmouth Formation sedimentation (Mutti *et al.* 1999).

Stage 1 of this model occurs during a fall in relative sea level at the offlap break that enables the efficient transfer of clastics from the source area to shelf break created by the previous highstand clinoform slope. The inherent instability leads to large-scale slope failure and generation of accumulative (cf. Kneller 1995), and thus highly erosive high-density turbidity currents that erode canyons (in the Harlech Dome) and transfer their load out onto the basin plain (at St Tudwal's Peninsula).

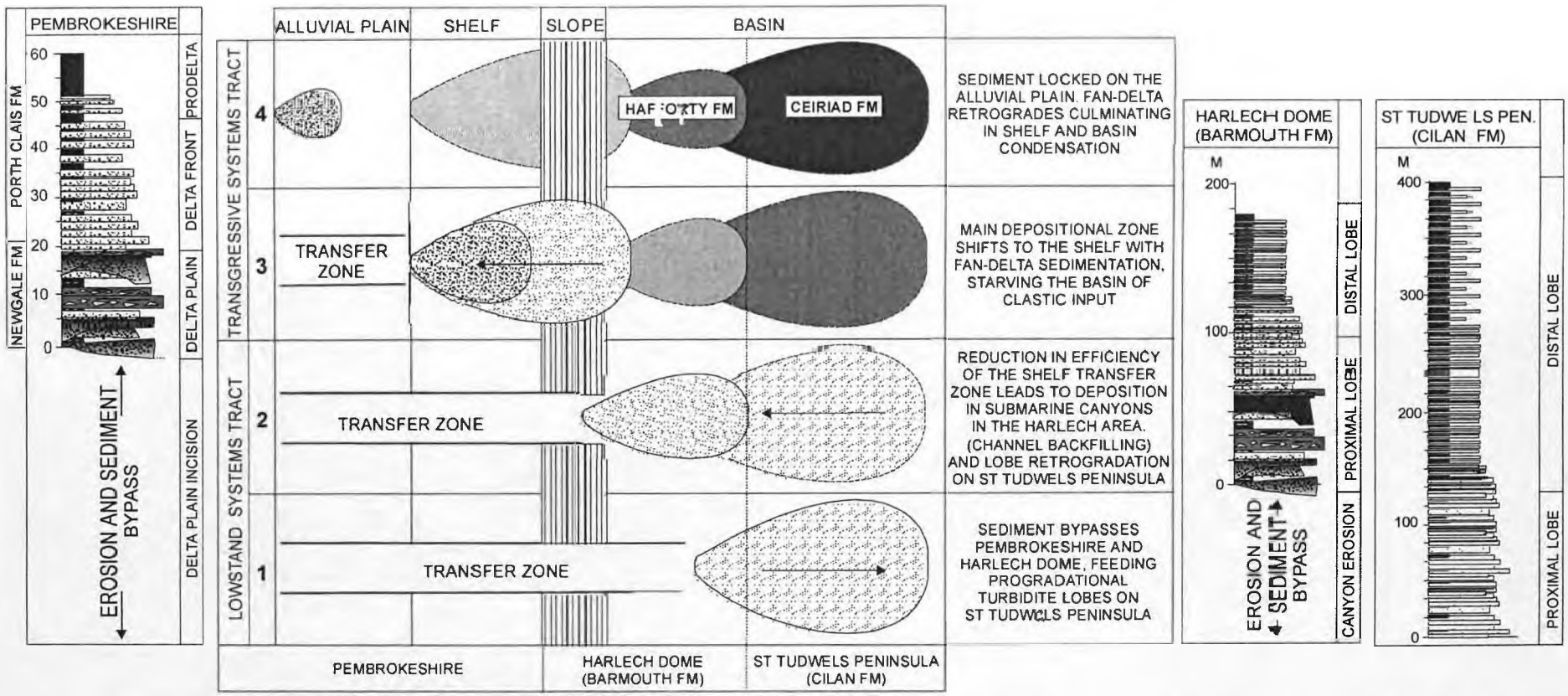



**Fig. 2.18.** Depositional model and systems tract linkage between SW Wales and North Wales during the formation of sequence boundary 3–4. See text for discussion.

The progradational character of coarse-grained lobes at the base of the Cilan Formation (Crimes 1970a) records migration of the depositional zone during the early lowstand systems tract, which place these turbidtes in a similar evolutionary stage to the "basin floor fan units" of Van Wagoner *et al.* (1988). Stage 2 is marked by deposition in canyons at Barmouth and lobe retrogradation on St Tudwal's Peninsula (Crimes 1970a), representing a reduction in the efficiency of sediment transfer across the shelf. Channel backfilling and lower clastic penetration into the basin is typically associated with small rises in relative sea level, and the filling of accommodation created on the outer-shelf (Mutti *et al.* 1999). This shift in the main depositional zone to the base of slope during the late lowstand systems tract is similar to the "slope fan units" of Van Wagoner *et al.* (1988).

Sedimentation during stages 3 and 4 occurs principally on the shelf and records basin margin onlap during a rapid rise in relative sea level associated with the transgressive systems tract. Fan-delta plain and fan-delta front deposits above the sequence boundary in Pembrokeshire suggest that the main depositional zone had migrated as far as the inner shelf, while the transfer zone is restricted to the alluvial plain. As most of the sediment liberated on the alluvial plain remains on the shelf, the basin becomes undersupplied and retrogradation of facies belts occur in both the Barmouth and Cilan formations. The final stage of transgressive sedimentation occurs almost entirely on the alluvial plain, culminating in fan-delta front flooding and ultimately shelf and basin condensation. The latter is recorded in the condensed mudstones of the Ceiriad Formation (Young *et al.* 1994) and the Lower part of the Gamlan Formation (Crimes 1970; Allen and Jackson 1985) at St Tudwal's Peninsula and the Harlech Dome respectively (Fig. 2.13). The upper part of the Gamlan Formation includes a number of sandstone turbidites (Matley and Wilson 1946) that suggest coarser material was again finding its way to the shelf edge, albeit in a greatly reduced amount. This appears roughly coeval with fan-delta progradation across the shelf during the highstand systems tract in Pembrokeshire.

The widespread unconformity at the base of sequence 6 across Avalonia (Fig. 2.13) was construed as representing a further phase of Avalonia epeirogenesis by Landing (1996). While it is often difficult to separate the effects of varying eustatic sea level from active tectonism, there are a number of features evident in sequence 6 that are more consistent with the former controlling parameter. Firstly, sea level curves determined from Middle Cambrian sequences on the tectonically stable Baltic shield demonstrate a major sea level lowstand in the middle *Paradoxides oelandicus* biozone (drafts of this curve were kindly supplied by Prof. A. Neilson, 2003, 2004, 2005). Secondly, epeirogenically controlled sequences on the Avalonia platform are

typically associated with minor volcanic activity such as tuffaceous horizons, lahars and pillow basalts, none of which can be allied with sequence boundary development. Thirdly, unconformities appear most prominently on the Avalonian marginal platform in the west, yet little sediment appears to be shed from that direction. This is not consistent with major fault-block movements, which would create highlands conducive to the liberation of vast quantities of sediment. Fourthly, if epeirogenesis was indeed occurring across the Avalonian platform, one might expect either condensation or hiatus in sections at Shropshire considering its location on a tilt block high (Fig. 2.16). In fact, the Quarry Ridge Grits–Hill House Shales of sequence 6 (Landing 1996) attain a thickness in excess of 120 m. Finally, development of the type-1 sequence boundary is associated with exposure, incision, and stripping of the shelf during a fall in relative sea level that ultimately led to the construction of a coarse-grained turbidite fan. This system response is the opposite of what would be expected during a syn-tectonic phase of sedimentation (Blair and Bilodeau 1988), instead being typical of passive margin basin evolution during a fall in eustatic sea level (essentially the Exxon model for lowstand and transgressive systems tracts, see Van Wagoner *et al.* 1988).

*2.4.1.5. Sequence 7*

The base of sequence 7 is drawn at a facies dislocation in the uppermost part of the Porth Clais Formation (Fig. 2.7C and 2.8B) where thickly bedded turbidites of the fan-delta plain sharply overly stratified sandstones and bioturbated shales of the distal fan-delta front. This rapid downward shift in coastal onlap (Fig. 2.14) involves subaqueous rather than subaerial erosion, a feature that typifies type-2 sequence boundaries (Van Wagoner *et al.* 1988). In SW Wales, sequence 7 extends to the top of the black mudstone dominated Menevia Formation, attaining a maximum thickness of 215 m. Of this, 208 m are transgressive deposits, culminating in black laminated prodelta mudstones (Fig. 2.10). The return of thin sandstone beds in the uppermost 7 m may be construed as facies belt progradation and development of a thin highstand systems tract.

Faunal and lithological variations through sequence 7 can be directly matched with the middle Middle Cambrian stratigraphy of West Avalonia (Fig. 2.13). The fine sandstones, bioturbated mudstones and occasional discontinuous limestones of the Whitesand Bay Formation also occur in the Fossil Brook Member of the uppermost Chamberlain's Brook Formation (Landing and Benus 1988), while the black laminated mudstones with pale weathering bentonites are mirrored in the Manuals

River Formation (Poulsen and Anderson 1975). According to Landing (1996), an unconformity exists at the base of the Manuals River Formation, which he correlated across the Avalonian platform (his depositional sequence 8 in Fig. 2.13). This sequence is not recognized in the succession in SW Wales, and there is some evidence to suggest possible misidentification. Firstly, Landing (1996) bases his interpretation on an apparent thickness variation in a single bentonite bed (which he takes to signify basin margin onlap), and a change in trilobites. Variations in bentonite thickness occur many times in the succession in Pembrokeshire, and are entirely depositional features, while other workers on the faunal transition in SE Newfoundland regarded it simply as a biofacies change into a more dysaerobic environment (Hutchinson 1962; Fletcher 1972). A similar biofacies transition occurs in the sequence in Pembrokeshire (Jefferies *et al.* 1987; Prigmore and Rushton 2000). Secondly, there is very little evidence for sequence boundary development in coeval sections across Avalonia (Fig. 2.13). For example, no evidence has been published for an erosion surface between the Hill House Shales and Hill House Sandstones in the succession at Shropshire (Rushton 1974, Fig. 2.17), or similarly between the Ceiriad Formation and the Nant-y-big Formation on St Tudwal's Peninsula, both of which are unconformable contacts according to Landing (1996). Continuous uninterrupted sedimentation across this supposed sequence boundary is also evident in the black mudstones of the Clogau Shales exposed in the Harlech Dome (Allen *et al.* 1981) and to the south of the Mawddach Estuary (Pratt *et al.* 1995).

The base of sequence 7 forms a readily recognisable surface across the Avalonian platform (Fig. 2.13) and has been interpreted by Landing (1996) as signifying a major phase of basin reorganization. In SE Newfoundland, a *Glossifungites* ichnoassemblage has been observed within the onlap deposit of the Deep Cove Limestone (Chamberlain's Brook Formation) (Landing 1996), which suggests burrowing of an overcompacted mud exposed by marine erosion. This intimates that this erosion surface was also a type-2 sequence boundary. Volcanism associated with sequence boundary development includes a 4.5 m thick volcaniclastic debris flow and a 60 m thick pillow basalt (Fletcher 1972), both of which are roughly coeval with a switch in sediment source from the inner to the marginal platform.

In southern Britain, this phase of tectonic reorganization is more subtle, but comprises: (1) numerous bentonites prior to and after sequence boundary development. Examples include the upper part of the Porth Clais Formation and the Menevia Formation in Pembrokeshire (Fig. 2.10), the Ceiriad Formation (upper part)

and the Nant-y-big Formation on St Tudwel's Peninsula (Young *et al.* 1994), and the Gamlan Formation (upper part) and Clogau Formation of the Harlech Dome (Allen *et al.* 1981, Pratt *et al.* 1995). (2) Enrichment in manganese at the top of the Gamlan Formation, interpreted as submarine exhalative hydrothermal solutions by Bennett (1987), and (3) a northerly switch in sediment source in the upper part of the Ceiriad Formation on St Tudwel's Peninsula (Crime and Oldershaw 1967; Crimes 1970a; Young *et al.* 1994), suggesting similar uplift of the marginal platform as that recorded in West Avalonia. This uplift continued throughout sequence 7, as witnessed by the regressive trend in the Nant-y-big Formation (Young *et al.* 1994) during a period when locations away from the platform were undergoing widespread and continued transgression (see Rushton 1974).

An erosion surface towards the base of the Abbey Shales (Fig. 2.13) may mark sequence boundary development at Nuneaton (Illing 1916). Although Rushton (1974, p 110) dismissed the surface as having no known stratigraphic significance, its position in the *Ptychagnostus gibbus* biozone places it very close to the base of sequence 7. In Shropshire, Landing (1996) correlated his sequence 6–7 unconformity with the base of the Hill House Grits, which sharply, and possibly unconformably overly the Hill House Flags. This surface, like that in SE Newfoundland also records an abrupt change in trilobites (Landing 1996). The significance of this sequence boundary in terms of tectonic regime is uncertain. There is no evidence for an angular unconformity and thus fault-block rotation prior to deposition of the Hill House Grits (Fig. 2.17) but conversely, the local development of the so-called Comley Breccia Bed (Cobbold 1913a, b) composed of fragments of Lower Comley Sandstone may be construed as representing some type of fault rejuvenation. Alternatively, and probably most likely, the Hill House Grits mark a rapid eustatic lowstand, with the Breccia Bed forming a local onlap deposit. This interpretation better fits the cross section outlined in Figure 2.17, with the timing consistent with a prominent erosion surface and abrupt change in fauna recognised worldwide at the base of the *Ptychagnostus gibbus* Biozone (Henderson and Southgate 1978; Rowell *et al.* 1982; Robison 1984; Evans *et al.* 1995). The eustatic sea level rise that followed (Rowell 1982; Prof. A. Nielson 2004, 2005) would then account for the apparent onlap and erosion of the Lower Comley Sandstone at Shropshire, as well as the transgressive nature of coeval formations that occur away from the rising marginal platform.

The position of the sequence boundary in the Harlech Dome succession is not constrained biostratigraphically, except that it is situated somewhere below the Clogau Formation (represented by the *Tomagnostus fissus* biozone [Allen *et al.*

1981], which correlates with part of the Whitesand Bay Formation). The most likely position based purely on facies development is below the coarse-grained turbidites that form the top of the Gamlan Formation (previously the Cefn Coch Grits of Matley and Wilson 1946). The sharp contact between these thickly bedded turbidites and the underlying shales is similar to that recorded at the base of the Barmouth Formation, and again records a significant change in the shelf regime to the south. This is most readily accounted for by matching turbidite deposition with a downward translation in coastal onlap on the shelf. The restricted vertical and lateral extent of the turbidite fan, which attains a maximum thickness of 17 m when associated with a canyon in the succession at Fairbourne, may be more typical of type-2 sequence boundaries where shelf transfer zones do not migrate as far as the offlap break.

The appearance of organic-rich black shales above the zone of *P. gibbus* has been considered by some (e.g. Pratt 1995) as marking a major event in the evolution of the Welsh Basin. The reason for the onset of anoxic sedimentation after such an extended period of strongly oxidized conditions has never been accounted for, but is most easily explained in terms of tectonic reorganization of the Avalonian platform with concomitant changes in basin morphology and water circulation (Thickpenny and Leggett 1987). Although it not possible to rule out other factors such as upwelling of nutrient-rich water masses (e.g. Chamley 1989) or the existence of an oxygen minimum zone (e.g. Rhoads and Morse 1971), narrowing of the basin through marginal platform uplift and the restriction on circulation that this would ultimately produce provides a more than satisfactory explanation. There is also additional evidence compiled from palaeocurrent patterns in fine-grained turbidites of the Clogau Formation (at Fairbourne) that the basin may have been closing from the southwest. This suggests linkage of the marginal and inner platforms to the southwest, and the development of a near land-locked basin similar to the modern anoxic Black Sea basin (Stow *et al.* 1996). This analogue may be extended to account for the erosion surface found within the Menevia Formation (Fig. 2.10C). This has been interpreted as recording the interception of a pycnocline (and internal waves) with a gentle prodelta slope, a process that is intensified by the density stratification typical of basins with restricted circulation (Stow *et al.* 1996).

#### *2.4.1.6. Sequence 8*

Sequence 8 in SW Wales attains a minimum thickness (below the Arenig unconformity) of 432 m and includes the black transgressive mudstones with subordinate sandstones and limestones of the Aber Llong Formation, and the

regressive stratified sandstones and blue silty mudstones of the Ogof Velvet Formation (Fig. 2.14). This transgressive–regressive motif, which spans the *Lejopyge laevigata* to *Olenus* biozones in Pembrokeshire, is also recognized in the Maclean Brook Formation in SE Newfoundland (Landing 1996), the Maentwrog to Ffestiniog formations in North Wales, and the Mancetter Shales to Moor Wood Flags at Nuneaton (Fig. 2.13). In North Wales and at Nuneaton, this regressive trend continues well into *Parabolina spinulosa* biozone (Allen *et al.* 1981; Landing 1996). Highly condensed black mudstone deposition, which affected all locations in Avalonia during the development of sequence 7 ended abruptly with the rapid influx of large quantities of well sorted, compositionally mature fine sand and silt (Fig. 2.19). The sharp contact between mid- to outer-shelf mudstones and nearshore to inner-shelf sandstones is everywhere unconformable based on a significant facies dislocation and basinward shift in coastal onlap (Fig. 2.14). Examples include surfaces between the Menevia and Aber Llong formations in SW Wales (Fig. 2.9A), the Nant-y-big and Maentwrog formations on St Tudwel's Peninsula (Crimes 1970a; Young *et al.* 1994), and the Abbey Shales and Mancetter Shales at Nuneaton (Taylor and Rushton 1971). In the Harlech Dome of North Wales, this influx of sand is represented by the deposits of high-density turbidity currents at the base of the Maentwrog, which sharply overlie condensed basinal shales of the Clogau Formation (Allen *et al.* 1981; Pratt *et al.* 1995).

The cause of sequence boundary development on the Avalonian platform is uncertain. Taylor and Rushton's (1972, p 9) suggestion "that a single tectonic event affected sedimentation in the whole Anglo-Welsh area (and south-eastern Newfoundland)" in the late Middle Cambrian appears prescient, as the most significant unconformities occur in successions located on the uplifted marginal platform (e.g. St Tudwel's Peninsula, see Fig. 2.13). Marked facies changes in the Maentwrog and Ffestiniog Flags formations across the Cwm Pennant Fracture Zone west of St Tudwels Peninsula provides some evidence for fault controlled sedimentation (Wilkinson and Smith 1988). There is also a large unconformity in Shropshire, which may suggest reactivation of fault-blocks and relative uplift of the tilt-block high. Tectonic reorganization of basin geometry is also indicated by the rapid change in provenance recorded across Avalonia (Thorogood 1990; Landing 1996, see Fig. 2.15), as well as a shift in palaeocurrent patterns in southern Britain from an easterly to a southwesterly source (Crimes 1970a, see also Fig. 2.15). Eustatic sea level may also have played a fundamental role in the facilitation of a more arenaceous style of sedimentation. A global lowstand during the *Solenopleura brachymetopa* biozone followed immediately by a eustatic sea level rise in the

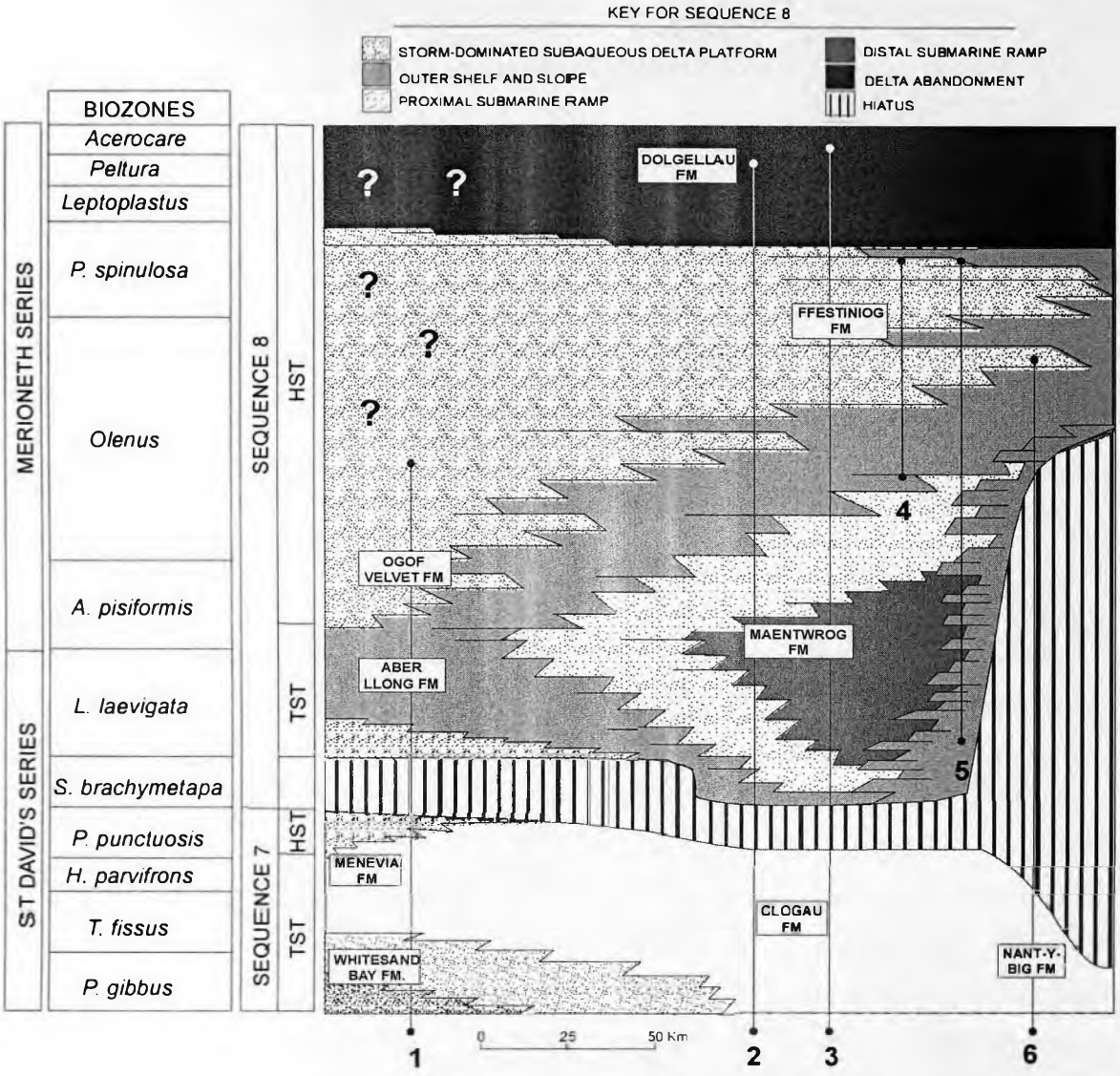



**Fig. 2.19.** Chronostratigraphic chart for the upper Middle Cambrian and Upper Cambrian of SW Wales and North Wales. Section numbers: (1) Pembrokeshire, (2) Fairbourne, (3) Harlech Dome (from Crimes 1970a and Allen and Jackson 1985), (4) Borth-y-Gest, (5) Black Rock Sands, and (6) St Tudwel's Peninsula (from Crimes 1970a and Young *et al.* 1994).

*Lejopyge laevigata* biozone is now well documented in many parts of the world (Rushton 1978; Rankey *et al.* 1994; Artyushkov *et al.* 2000; Prof. A. Nielson pers. comm. 2003). Retrogradation of facies belts following sequence boundary development is well recorded in southern Britain at the base of the Maentwrog in North Wales (Crimes 1970a; Allen *et al.* 1981), in the Mancetter Shales at Nuneaton (Rushton 1978), and in the dark mudstones of the Aber Llong Formation in SW Wales (Fig. 2.11).

The occurrence of numerous forestepping parasequences in the Ogof Velvet (Fig. 2.14) and Ffestiniog Flags formations in SW Wales and North Wales respectively suggests major highstand sedimentation during the *Olenus* and

*Parabolina spinulosa* biozones (Fig. 2.19). The origin of these parasequences is again uncertain, but considering their scale (typically <30 m thick) and frequency, they are probably driven by secular variations in eustatic sea level and/or sediment flux. Similar progradational parasequences have been reported from coeval strata on the tectonically stable Baltic Platform (Arne Nielson, pers. comm. 2003, 2004) and other locations around the world (Leggett *et al.* 1981, Conway Morris and Rushton 1988), while variations in sediment supply, although difficult to quantify, should not be discounted considering the deltaic nature of sedimentation in both formations (see below).

The Lower and Middle Cambrian successions on the Avalon Peninsula of SE Newfoundland are duly considered the type-Cambrian sections for Avalonia because of their good continuous exposure, diverse fauna, and numerous datable volcanic ash horizons (Landing 1994, 1996). Conversely however, sections through the uppermost middle Cambrian and Upper Cambrian (essentially all of sequence 8) are generally fragmentary, discontinuous, and comprised principally of fault bounded inliers. This has severely hampered any meaningful sedimentological analysis, and thus invariably, little is known about Upper Cambrian basin across the Avalonian platform in terms of their size, depositional environments and sediment sources. Sections that comprise the Welsh Basin in southern Britain offer the potential to ratify this anomaly, as continuous exposure in excess of 600 m are not uncommon ( see Fig. 2.20). The depositional environments of the Aber Llong and Ogof Velvet Formations have been previously outlined, and interpreted as a storm-dominated, tide-influenced subaqueous delta platform (Fig. 2.4). This system is most characteristically developed during the progradational stage associated with deposition of the Ogof Velvet Formation (Fig. 2.14). Detailed sedimentary logging of the latest Middle Cambrian and Upper Cambrian of North Wales demonstrates a strong systems link with deltaic sedimentation in SW Wales (Fig. 2.19), a conclusion also held by Crimes (1970a) based on a study of depositional environments and palaeocurrent patterns.

The most complete section through sequence 8 anywhere in Avalonia occurs along the coastal section at Fairbourne in North Wales (Fig. 2.1A) (Pratt *et al.* 1995). The main sedimentological characteristics of the Maentwrog to Dolgellau formations are presented in Figures 2.20 and 2.21. Similar features have been reported from coeval strata in the Harlech Dome area by Crimes (1970a) and Allen *et al.* (1981). The Ffestiniog Flags Formation, which has been interpreted by Allen *et al.* (1981) as deltaic in origin, can be matched lithologically with the Ogof Velvet Formation (compare Fig. 2.12A, C and D with Fig. 2.21A, B and C). The bypass-zone

tempestite model used to interpret the spatial and temporal distribution of facies in the Ogof Velvet Formation can also be applied to the Ffestiniog Flags, and this correlation into North Wales suggests a major phase of delta front progradation tracking northwards during the Olenus biozone (Fig. 2.19). This is consistent with a detailed palaeocurrent analysis on these Upper Cambrian sediments discussed by Crimes (1970a).

Subaqueous delta platform sedimentation of the Ffestiniog Flags is preceded in North Wales by the Maentwrog Formation (the Vigra Flags and Penrhos Shales of Matley and Wilson 1946), a thick sequence of monotonously bedded fine sandstone turbidites and dark mudstones (Crimes 1970a; Allen *et. al.* 1981; Pratt *et al.* 1995) that are time equivalent to deltaic sedimentation in South Wales (Fig. 2.19). The Maentwrog Formation has been notoriously difficult to classify in terms of depositional processes and environments, with previous interpretations ranging from deep-sea turbidite fan (Crimes 1970a; Allen *et al.* 1981; Pratt *et al.* 1995) to shelf storm deposits (Young *et al.* 1994). Redistribution by persistent contour currents has also been suggested based on the occurrence of wavy and lenticular bedding (the ripple drift bedding of Crimes 1970a) with unimodal cross-lamination (Allen *et al.* 1981, see Fig. 2.21E).

The canyon-fed submarine fan model proposed by Crimes (1970a) and endorsed by Pratt *et al.* (1995) is not easily reconciled with the lithofacies identified in the Maentwrog Formation at Fairbourne (Fig. 2.20). Problems with this interpretation include: (1) the lack of evidence for a single large feeder canyon that could have served as a point source for turbidity current generation, (2) a slope facies that appear abbreviated, suggesting only minor bathymetric relief, (3) a slope traversed by multiple shallow channels or gullies, that lack any type of levee deposit, (4) a turbidite sequence that lacks the pronounced differentiation into distinct channels, interchannel and overbank areas and, (5) the lack of asymmetrical cycles, which suggests spatially random sedimentation without the construction of discrete lobate bodies. Additionally, the canyon-fed turbidite model does not readily account for extremely well sorted turbidites. Redistribution by deep basinal contour currents has also been criticized by Fitches and Woodcock (1987) who found no evidence for a deep basin setting. Although the wavy and lenticular bedding does require persistent low energy unidirectional currents, the contourite interpretation favoured by Crimes (1970a) and Allen *et al.* (1981) fails to explain: (1) why the distribution is confined to the most proximal locations such as the slope and outer shelf, (2) why wavy beds are associated with trace fossils more typical of the shelf (e.g. *Rusophycus*, Crimes 1970a), and (3) why contour currents would be important in a basin that was

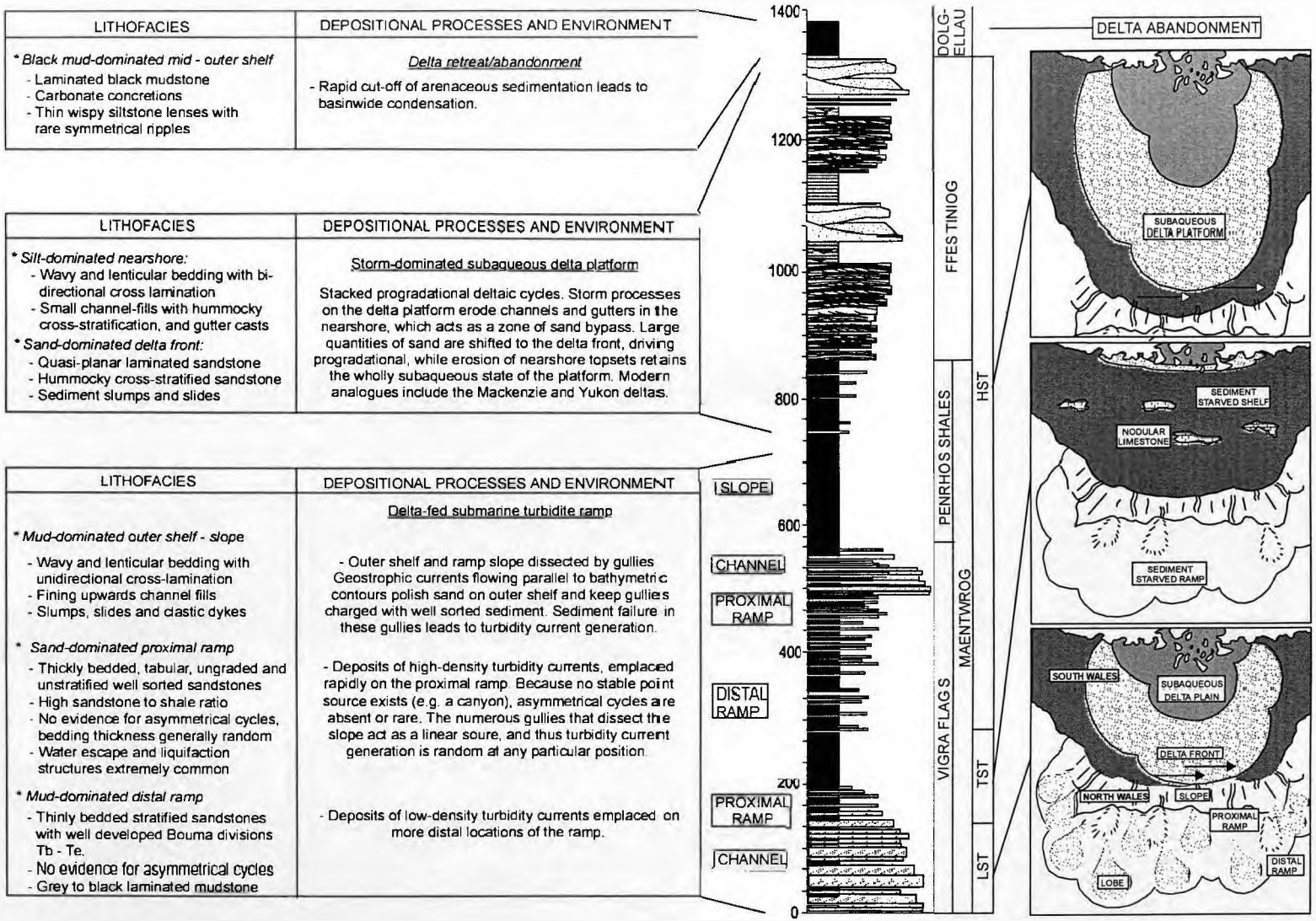



**Fig. 2.20.** Lithofacies, processes and depositional model for the Maentwrog through Dolgellau exposed at Fairbourne, North Wales. See text for details.

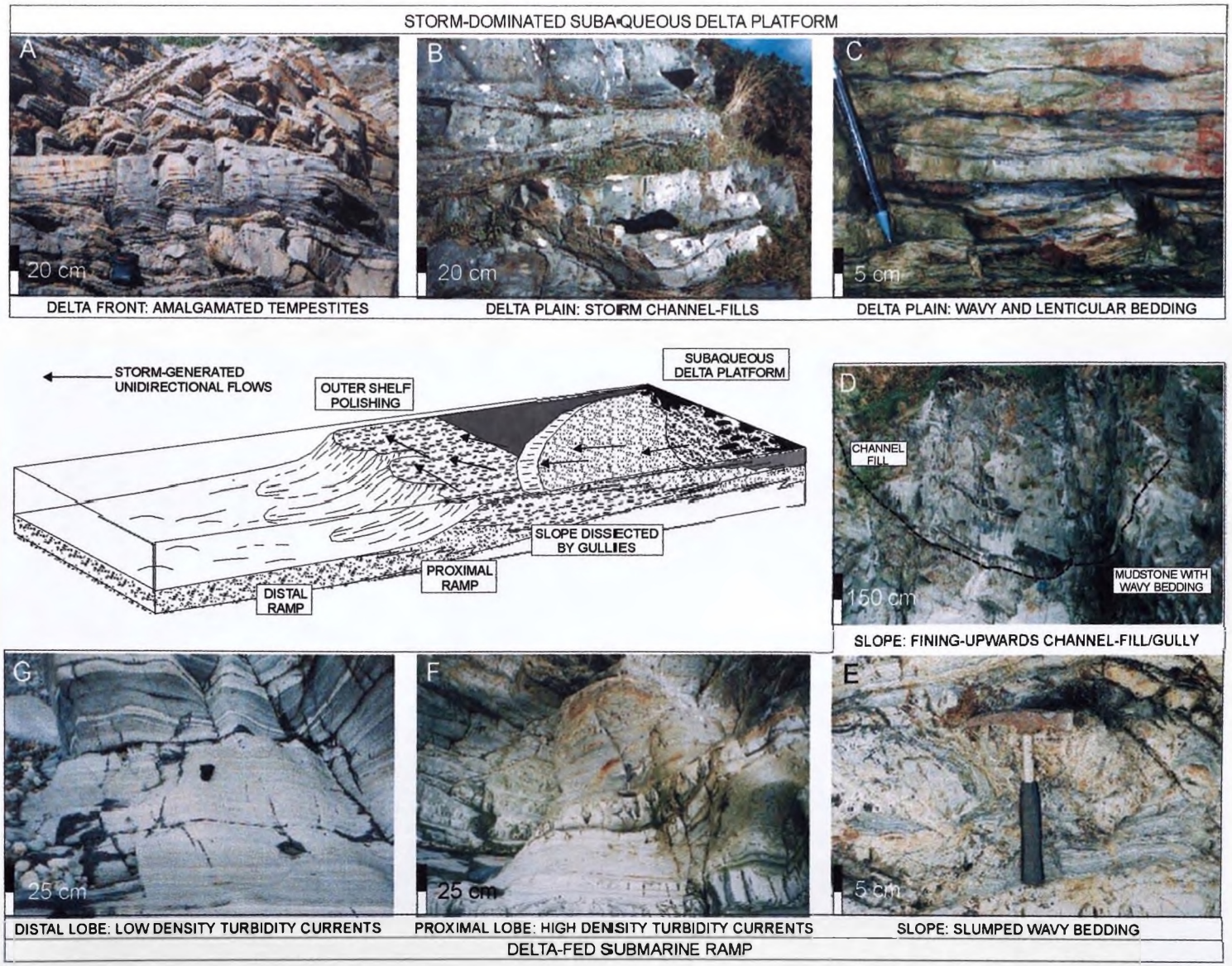

STORM-DOMINATED SUBAQUEOUS DELTA PLATFORM
A
20 cm
DELTA FRONT: AMALGAMATED TEMPESTITES
B
20 cm
DELTA PLAIN: STORM CHANNEL-FILLS
C
5 cm
DELTA PLAIN: WAVY AND LENTICULAR BEDDING
STORM-GENERATED UNIDIRECTIONAL FLOWS
OUTER SHELF POLISHING
SUBAQUEOUS DELTA PLATFORM
SLOPE DISSECTED BY GULLIES
PROXIMAL RAMP
DISTAL RAMP
D
CHANNEL FILL
MUDSTONE WITH WAVY BEDDING
150 cm
SLOPE: FINING-UPWARDS CHANNEL-FILL/GULLY
G
25 cm
DISTAL LOBE: LOW DENSITY TURBIDITY CURRENTS
F
25 cm
PROXIMAL LOBE: HIGH DENSITY TURBIDITY CURRENTS
E
5 cm
SLOPE: SLUMPED WAVY BEDDING
DELTA-FED SUBMARINE RAMP

**Fig. 2.21.** Depositional model for the Maentwrog and Ffestiniog Flags formations in North Wales (see text for details). (A) Quasi-planar lamination in the depositional zone of the Ffestiniog Flags at Borth-y-Gest. (B) Channels incised into wavy bedding in the bypass-zone of the Ffestiniog Flags at Black Rock Sands. (C) Wavy bedding in the bypass-zone of the Ffestiniog Flags at Fairbourne. (D), (E), (F) and (G) are all from the Maentwrog at Fairbourne, and generally comprise high- and low-density fine-grained and very well sorted sandstone turbidites with interbedded dark micaceous mudstones.

relatively small, restricted and possibly land-locked on three sides (Crimes 1970a; Brasier *et al.* 1992, Map 2a).

More recently, Young and Dean (1995) speculated on the possible role of storm-generated combined-flows in deposition of the Maentwrog, although they gave no evidence for this interpretation. The lack of symmetrical ripples, elliptical scours and hummocky cross-stratification effectively rule out combined-flow processes, while ungraded and unstratified thickly bedded sandstones with floating rip-up clasts imply a non-Newtonian rheological state that requires sediment concentrations at least an order or magnitude greater than that usually associated with storm erosion and sedimentation (Lowe 1988).

In terms of process sedimentology, the sandstones beds in the Maentwrog are compatible with the deposits of high- and low-density turbidity currents (Lowe 1982). It is not surprising that Crimes (1970a) opted for the point-sourced canyon-fed turbidite model, as only recently have advancements led to the realization that this system is but one member in a spectrum of submarine fan depositional styles. All of the characteristics highlighted in Figure 2.20 are instead compatible with the delta-fed submarine ramp model (Table 2.3) first described by Heller and Dickinson (1985). This model, with some amendments based on characteristics of the Maentwrog (discussed below), is displayed in Figure 2.21. In ramp systems, detritus is transported off the shelf through numerous channels (Fig. 2.21D), with no individual channel serving as a point-source for sedimentation. The network of channels instead acts as a linear-source for turbidites that are deposited continuously along the base of slope to form an aggrading ramp-like depositional feature. As many slope gullies are available for turbidity current transport, no single channel is preferentially developed into a larger canyon feeder system, hence the network is maintained, and there is a less pronounced differentiation into distinct channel, interchannel or overbank areas. This random juxtaposition of confined and unconfined flow reflects the disorganized nature of the depositional system, with each flow being an independent event starting at any point along the linear-source region. Asymmetrical cycles representing lobe construction and abandonment are thus poorly developed (Fig. 2.21F).

Although the Heller and Dickinson (1985) model in its original state offers a good approximation of the Maentwrog and Ffestiniog depositional system, there is one major modification that is required. The deltas in both examples presented by Heller and Dickinson (1985) have a significant subaerial component (similar to the Nile and Mississippi deltas) that once at the shelf break provides an extremely efficient mode of sediment transfer onto the ramp slope. The delta that characterises the Ogof Velvet and Ffestiniog formations is instead a wholly subaqueous platform (Fig. 2.4), analogues to the Amazon and Ganges-Brahmaputra deltas (Nittrouer *et al.* 1986). Sediment must therefore be transported to the ramp slope by currents acting on the shelf. Based on palaeocurrent data from the Ogof Velvet Formation, the delta platform can be divided into two broad zones (Fig. 2.4). The friction zone, which occupies the inner- and mid-shelf, is characterized by storm-generated unidirectional currents that are orientated perpendicular to the shoreline. On the outer-shelf, these offshore-directed flows are balanced by the Coriolis force (Duke 1990) resulting in shore-parallel flows that define the geostrophic zone on modern shelves (Swift *et al.* 1985). The occurrence of weak, but persistent geostrophic currents provides a means by which gullies are continuously charged with fine, very well sorted sediment, and also accounts for the proximal location on the outer-shelf of wavy and lenticular bedding. This process appears to be analogous to the outer-shelf polishing discussed by Stow (1998) and Stow and Mayall (2000), and has been reported by Stauffer (1967) from a succession later interpreted as a ramp system by Heller and Dickinson (1985).

Overlying the Ffestiniog Flags Formation in North Wales is the Dolgellau Formation (Fig. 2.20), a c 60 m thick succession of dark laminated mudstones with carbonate concretions and thin wispy siltstone beds. In a sequence stratigraphic interpretation of the Welsh Basin, Woodcock (1990) proposed, without discussion of the evidence for its identification, a sequence boundary immediately below the base of the Tremadoc (the Dol-cyn-afon Formation in North Wales). Two amalgamated medium- to coarse-grained, erosively based tuffaceous sandstones (Allen *et al.* 1981) were interpreted by Landing *et al.* (2000) as marking this unconformity at Bryn-llyn-fawr (Fig. 2.1A). These sandstones, which display internal sedimentary structures typical of the shoreface record the sudden appearance of high energy waves in what was prior to their deposition, a deep shelf environment (Landing *et al.* 2000). This facies dislocation and rapid basinward shift in coastal onlap is typical of forced regressions (Posamentier and James 1993; Ainsworth and Patterson 1994). This interpretation is consistent with a proposed eustatic sea level lowstand close to

the Cambrian–Ordovician boundary recognized in many parts of the world (Fortey 1984; Landing 1988, 1993).

The transition from progradational subaqueous delta platform sedimentation of the Ffestiniog Flags Formation to condensed deep shelf black shales of the Dolgellau Formation is not easily explained. Clearly, the rate of sediment supply suddenly fell below the rate of accommodation space creation, leading to either delta retrogradation, or more likely considering the rapid onset of condensed sedimentation (Allen *et al.* 1981), complete delta abandonment through in-place drowning (Sanders and Kumar 1975). Woodcock (2000) interpreted this deepening as signifying a renewed phase of active tectonism, with fault controlled subsidence accommodated along the Menai Straits and Welsh Borderland fault systems (Fig. 2.1A). The problem with this view is that these areas were either below or very close to sea level throughout the latter part of the Upper Cambrian (Brasier *et al.* 1992), as well as there being no evidence for any coarse clastic wedge progradation away from active scarp zones. The highly quartzose composition and fine grain sizes are not at all consistent with sedimentation during active rifting. In fact, the composition is no different from that recorded in the Maentwrog and Ffestiniog formations (Allen *et al.* 1981), which based solely on palaeocurrent patterns was not sourced from either the Midland Platform to the east or the Irish Sea Platform to the northwest (Crimes 1970a). Instead, deepening and condensation following delta progradation in the Ffestiniog Flags Formation can be more readily accounted for by assuming a rapid decrease in sedimentation rate set against a highstand in Cambrian eustatic sea level, the latter of which is suggested in most of the available sea level curves for the time period in question (Leggett *et al.* 1981; Conway Morris and Rushton 1988; Popov and Koren 1996; Prof. A. Nielson pers. comm. 2004).

The development of submarine ramp systems is closely aligned to high sedimentation rates, as rapid delta progradation with concomitant deeper basin aggradation (Fig. 2.19) are prerequisites for loss of structural relief along basin flanks (Heller and Dickinson 1985; Surlyk 1987). Rapid accommodation space creation during the Upper Cambrian highstand in sea level would render the system susceptible to rapid transgression as soon as sediment supply began to fall below accommodation creation. A change in this equilibrium may simply reflect lateral movements of the main fluvial feeder channels or the complex feedback mechanisms associated with delta autoretreat (Muto and Steel 1992, 1997). The autoretreat effect, which is the inbuilt tendency for strongly regressive shorelines (particularly deltas) to turn around to transgression, is especially appealing as it is caused by the inability of sediment supply to fill the ever increasing area behind the regressive/aggrading delta

| Depositional features of delta-fed submarine ramp systems | Maentwrog/Ffestiniog |
|---|---|
| Abbreviated section of mud-rich slope deposits traversed by multiple shallow channels or gullies | * |
| Channels are transient features rather than stable canyons, thus levee deposits are not found. | * |
| No prenounced differentiation into distinct channel, interchannel or overbank areas | * |
| Ramp has a linear rather than a point source | * |
| Absence of a channalized inner fan and middle fan environment | * |
| Asymmetrical cycles are absent or rare due to the lack of point source | * |
| System is generally sandy with sandstone to shale ratios > 3:1 | * |
| Proximal ramp dominated by thick sandstones emplaced by high-density turbidity currents | * |
| Distal ramp is more argillaceous, with thin sandstones emplaced by low-density turbidity currents | * |
| Ramp turbidites are generally very well sorted due to outer shelf polishing | * |
| Fed by a large sandy deltaic system | * |
| System typically progrades rapidly from ramp, through abbreviated slope to sandy deltaic sediments, as sedimentation rates are typically high | * |

**Table 2.3.** Depositional features of delta-fed submarine ramp systems after Heller and Dickinson (1985) and Surlyk (1987), and their occurrence in the Maentwrog and Ffestiniog Flags formations in North Wales.

front (Cattaneo and Steel 2003). Although this naturally occurs on any type of delta, the subaqueous delta platform with its nearshore zone of sediment bypass (Fig. 2.4) must be particularly susceptible.

## 2.5. TECTONOSTRATIGRAPHY, PROVENANCE AND BASIN ANALYSIS

To place Avalonian chronostratigraphy into a wider tectonostratigraphic framework requires the identification of megasequences, which are unconformity-bounded lithotectonic units deposited during a distinct phase of tectonic evolution (Hubbard 1988). The only previous tectonostratigraphic interpretation of the Avalonian cover sequence was that described by Woodcock (1990), who utilised rock preservation curves to tentatively subdivide Welsh Basin stratigraphy (Cambrian–Devonian) into three megasequences. Due to many previous uncertainties involving Welsh Cambrian stratigraphy, Woodcock (1990) favoured a conservative approach that equated all of the Dyfed Supergroup with ensialic intra-shelf sedimentation on a passive continental margin, which he defined as megasequence 1. Of some significance however is his suggestion that the late Middle Cambrian unconformity in the "Menevian" (which equates to sequence boundary 7–8 in this study) may be a candidate megasequence boundary (Woodcock 1990, p 540). In the sequence

stratigraphic framework presented in Figure 2.13, this regional unconformity separates tectonically active basin forming regimes (demonstrated in sequences 1–7) from tectonically quiescent, passive margin sedimentation (that characterizes sequence 8). This is essentially the definition of a megasequence boundary *sensu* Hubbard (1988). Megasequence definition based on depositional environments and tectonic regime are presented in Figure 2.4 and Figure 2.22 respectively. This is supplemented by palaeocurrent data, whole rock magnetic susceptibility (as an indicator of petrophysical properties), and sandstone framework composition utilising the detrital modes of sandstone (cf. Dickinson *et al.* 1983; Dickinson 1985) in Figure 2.15. Two distinct lithotectonic packages can be clearly identified, which are discussed separately below.

### 2.5.1. Megasequence 1

Evidence for mechanical subsidence under a dominantly extensional tectonic regime has been previously highlighted in the analysis of sequences 3–7, and includes (1) fault-block rotation on the Avalonian inner platform, (2) numerous intra-formational unconformities, some of which demonstrate angular discordance (e.g. Fig. 2.17), (3) in-place drowning of depositional systems during active phases of fault-block downwarping, (4) coarse-grained feldspathic tuffs located within these syn-tectonic transgressive facies and, (5) the proliferation of coarse-grained depositional systems such as alluvial fans and fan-deltas (Fig. 2.4), which due to piedmont requirements are almost always associated with tectonically active basins (McPherson *et al.* 1987; Postma 1990; Blair and McPherson 1994).

In West Avalonia, evidence for depocenter migration and alternating periods of extension and compression has led to a refinement of this interpretation, with transtensional regimes in a dominantly strike-slip or pull apart tectonic setting favoured by Murphy *et al.* (1985), Keppie and Murphy (1988) and Landing (1996). A similar conclusion for East Avalonia was tentatively proposed by Prigmore *et al.* (1997) based on subsidence curves from Lower and Middle Cambrian successions throughout southern Britain. These authors relate this tectonic regime to the transform termination of Cadomian/Avalonian subduction and the suturing of arc related terranes to form the Avalonian Superterrane (Fig. 2.1A), a suggestion also proposed by Murphy and Nance (1989), Nance (1990), and Nance *et al.* (1991, 2002) for West Avalonia.

The recognition of strike-slip basins even from well exposed basin-fill sequences is often difficult because depositional and structural histories are complex

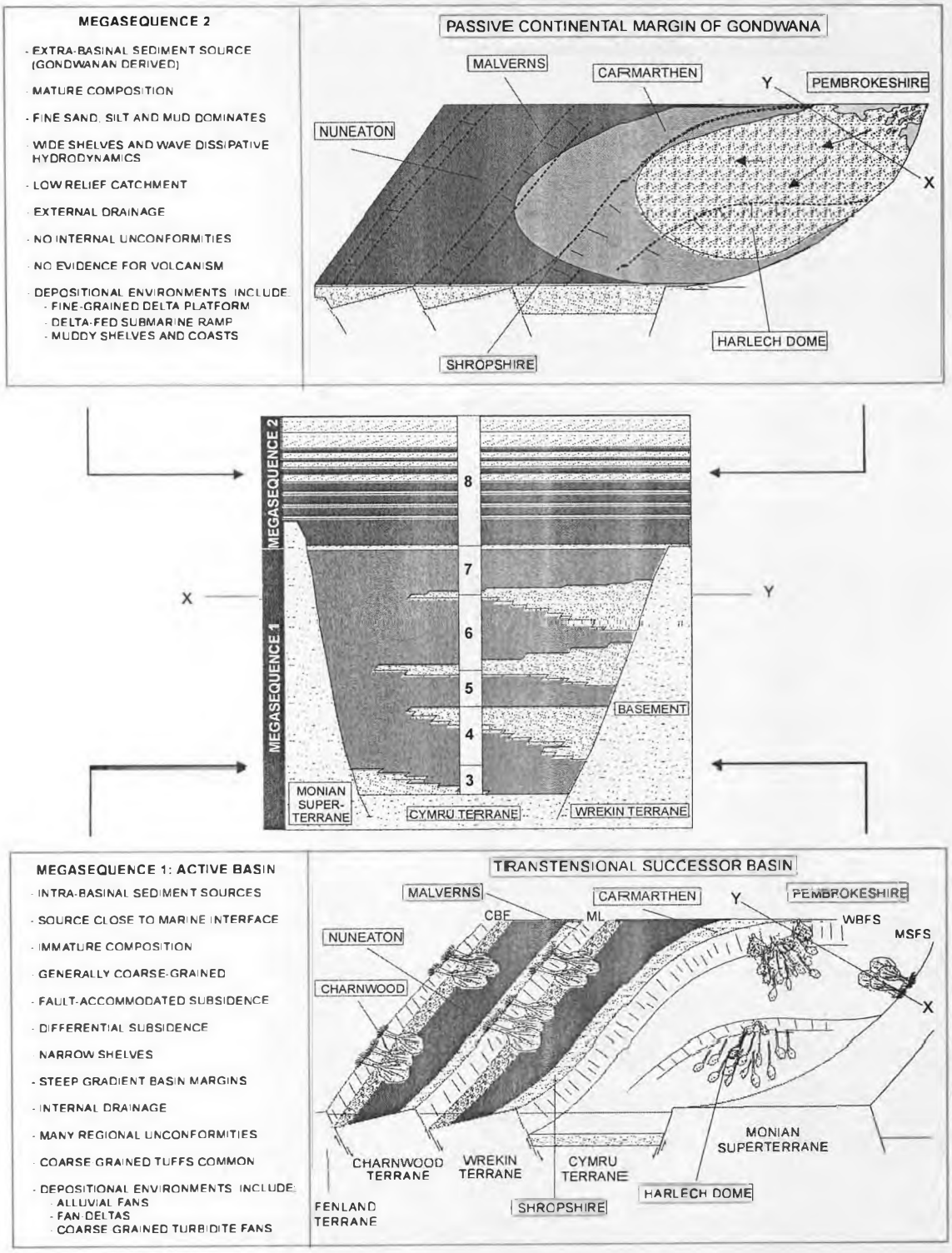



**Fig. 2.22.** Megasequence definition based on tectonic setting and basin characterization. See text for details.

(Nilsen and Sylvester 1999). However, many features thought typical of strike-slip regimes by Reading (1980), Steel and Gloppen (1980) and Miall (2000) are evident in the East Avalonian sequences of megasequence 1. These include: (1) fault-

accommodated subsidence along major structural lineaments with known strike-slip displacement (Menai Straits and Welsh Borderland fault systems), (2) unconformity-bounded sequences which record twin phases of extension and compression (e.g. the Hartshill Formation at Nuneaton; Brasier 1989 and Bridges *et al.* 1998), (3) intense reworking and cannibalization of basin margins (see Fig. 2.17), (4) sparse igneous activity except locally in zones of transtension (e.g. bentonites in transgressive facies associated with in-place drowning) and, (5) bentonites with intra-plate geochemical signatures (e.g. the Clogau Shales in North Wales; Roberts and Merriman 1990)) typical of pull apart rifts (Keppie *et al.* 1997).

Petrological characteristics of the basin-fill and relationship to tectonic setting during megasequence 1 are highlighted in Figure 2.15. Composition is typically immature, with lithic arkoses and arkosic litharenites dominant (QFL after Folk 1980). These are typical framework modes for alluvial fan and fan-delta systems deposited in tectonically active basins (Corcoran *et al.* 1999). Relatively high feldspar, volcanic lithics and magnetic susceptibility are typical properties of sediment derived from juvenile basement (Dickinson 1985; Floyd and Trench 1989; Piper *et al.* 1996). As a tectonic provenance indicator, megasequence 1 is extremely diverse and thus difficult to classify (QmFLt after Dickinson 1985). Detrital modes plot within both the magmatic arc and recycled orogen global sandstone provenance fields, a tectonic setting consistent with the abundance of sedimentary and volcanic lithic fragments. These framework modes clearly record recycling of a diverse source area that originated in a number of semi-discrete plate tectonic provinces, and is consistent with derivation from the structurally accreted terranes that form the basement of Avalonia and from late Precambrian sedimentary basins inverted during final terrane accretion (Nance 1990).

Similar model compositions have been reported from a number of basin-fills sourced from discrete allochthonous terranes incorporated within suture zones (Graham *et al.* 1993; Trop and Ridgeway 1997; Robinson 2003). These basins, which are commonly referred to as "late-stage" successor basins, are typically developed during terminal phases of long-lived orogenic cycles. The most distinguishing characteristic of successor basins, and one that defines their position in long-lived orogenic cycles, is the recycling of detritus from older basins developed earlier in the cycle into younger successor basins. Examples of this in East Avalonia include the recycling of the late Precambrian Arvonian Basin (Arfon Group) into the Dolwen Basin (Dolwen Formation) (sequence 1) in North Wales (Allen and Jackson 1978), and the uplift and inversion of the Monian Basin (Monian Supergroup of Anglesey), which was a source for sequence 3 sediments in both SW Wales, and

North Wales. This process of compositional inheritance from juvenile Precambrian basins is also supported by Sm-Nd isotope values from Lower and Middle Cambrian sediments presented by Thorogood (1990).

These petrographic properties of the basin-fill tie in megasequence 1 to terminal phases of Avalonian subduction and orogenesis. The structural inversion of Precambrian basins and the opening of transtensional successor basins appear related to the suturing of volcanic arc terranes during the transform termination of Avalonian subduction and microcontinent formation (Fig. 2.23), a tectonostratigraphic interpretation mirrored in coeval successions in the Avalonian belt of North America (Nance 1990; Nance *et al.* 1991).

### 2.5.2. Megasequence 2 (sequence 8)

The sudden arrival of huge quantities of fine-grained, very well sorted sediment during sequence 8 (Fig. 2.19) heralds a new phase of Cambrian sedimentation across the Avalonian platform (Fig. 2.22). Sequence architecture (Fig. 2.19) and depositional environments (Fig. 2.4 and 2.20) are more consistent with the mature passive margin ensialic intra-shelf sedimentation proposed by Woodcock (1990) for the whole Dyfed Supergroup. Secular variations in eustatic sea level and sediment supply are inferred to be the principle controlling mechanisms on the nature of the basin-fill stratigraphy (2.19). Although subsidence does not appear to be uniform across Avalonia (Prigmore *et al.* 1997), there is little evidence for significant accommodation creation along major basin bounding faults. For example, deep shelf mudstones of Maentwrog age occur in the Caernarfonshire Slate Belt (Crime 1970a) suggesting marine overstep of the Menai Straits Fault System, while coeval mudstones in Shropshire, the Malverns and Carmarthen indicate a similar setting for the Welsh Borderlands Fault System and the Malvern Line (Fig. 2.22). The Upper Cambrian highstand in eustatic sea level therefore appears to have produced sedimentary basins that are more extensive than the internal platforms that are the most obvious sediment source (Soper and Woodcock 1990).

This change in tectonic regime and provenance is well illustrated by the change in depositional environment (Fig. 2.4), palaeocurrent direction, magnetic susceptibility and sandstone composition (Fig. 2.15) at sequence boundary 7–8. Detrital modes reveal a dominantly quartzose detritus typical of the continental interior global provenance field, suggesting a rapid switch from juvenile basement to long established continental crust. This evolution is evident in both magnetic susceptibility (Fig. 2.15) and Sm-Nd isotope values (Thorogood 1990), the former of

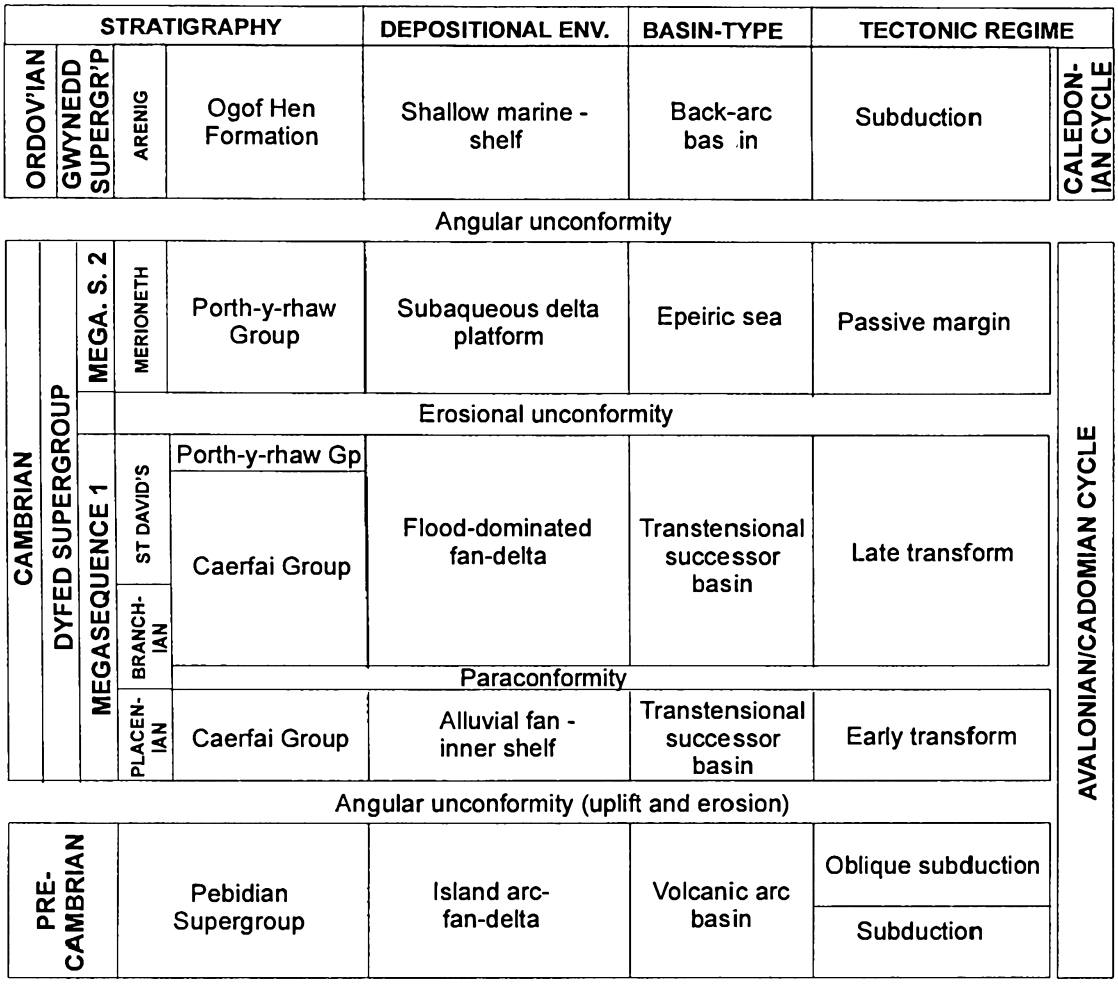



**Fig. 2.23.** Tectonostratigraphy of the late Precambrian to Ordovician succession exposed in SW Wales. The Pebidian and Dyfed supergroups record sedimentation during the Cadomian/Avalonian orogenic cycle, with the accretion of Avalonian island arcs to the northern periphery of Gondwana. Megasequence 1 of the Dyfed Supergroup records the transform termination of Avalonian subduction following oblique convergence. Megasequence 2 reflects passive margin sedimentation with Avalonia acting as a sediment sink to vast quantities of fine-grained sediment transferred off Gondwana by large, mature fluvial systems. Renewed subduction in the Ordovician (Caledonian orogenic cycle) led to rifting of Avalonia from Gondwana and ultimately its collision with Laurentia.

which records a change from magnetite-bearing (highly susceptible) juvenile basement to less susceptible phyllosilicate-bearing (mica-rich) quartzose detritus (Floyd and Trench 1989). Woodland (1946) considered this change as reflecting nothing more than the increased topographic maturity of the flanking margins of Avalonia, while Cope and Bassett (1987) concurred with this view by referring to a supposed metamorphic source in the now submerged Bristol Channel, which they termed Pretannia. Although some input from a metamorphic source is likely considering the high levels of muscovite encountered in all sequence 8 sediments (Allen *et al.* 1981; Cope and Bassett 1987; Pratt et al 1995), a source in close

proximity to basin margin flanks is not consistent with: (1) the subaqueous delta platform interpretation of the Ogof Velvet and Ffestiniog Flags formations, which are depositional systems that require fluvial networks similar in aerial distribution to the Amazon and Ganges, (2) the total exclusion of coarse-grained detritus, (3) the extremely high sedimentation rates, (4) rounded quartz grains and a mature suite of heavy minerals (Woodland 1946; Allen *et al.* 1981), (5) the total exclusion of juvenile detritus typical of the Avalonian basement and, (6) Sm-Nd isotope values that indicate derivation from a large area of long-established continental crust (Thorogood 1990).

A solution is that large volumes of very fine clastics were supplied to the region from a major continent to which Avalonia was attached. Based on lithotectonic correlations and facies indicators (Schenk 1997), faunal provinces (Fortey and Cocks 1992), palaeomagnetic data (McNamara *et al.* 2001), and provenance studies (Thorogood 1990), this land mass was the supercontinent of Gondwana, more specifically the West African craton which formed its northeastern periphery. This interpretation accounts for: (1) the high levels of muscovite and occasional oligoclase (Allen *et al.* 1981), which are grains consistent with erosion of the metamorphic and granitic core of Africa (Schenk 1997), (2) the construction of a subaqueous delta platform, as a fluvial system of such great aerial extent would produce at its terminus, a delta to rival the present day Amazon and Ganges-Brahmaputra, (3) the extremely high sedimentation rates required for the construction of a ramp margin (Heller and Dickinson 1985) that through northerly progradation during the *Olenus* biozone almost filled the Welsh Basin during the *P. spinulosa* biozone (Fig. 2.19) and, (4) the continental interior provenance signal determined from sandstone detrital modes (Fig. 2.15).

Although the connection between Avalonia and North Africa has been challenged by some authors, most notably Landing (1996) who argued for insular Avalonia by the latest Precambrian, there is a remarkably good stratigraphic correlation between the northern Gondwanan margin (Mali, Mauritania, and Morocco) and peripheral outboard terranes such as Avalonia (Fig. 2.24), Armorica (Noblet and Lefort 1990), the Meguma Zone and Arabian Peninsula (Schenk 1997). The Avalonian connection via the northern peneplained land surface of Gondwana (Mali to Morocco) is well illustrated in Figure 2.24. Unconformity-1 (which separates Tremadoc shales and Lower Cambrian sandstones in Morocco) marks a time of significant Middle and Upper Cambrian crustal stripping of the huge Sahara Platform (Schenk 1997), with efficient bypass of fine-grained material to sedimentary sinks like

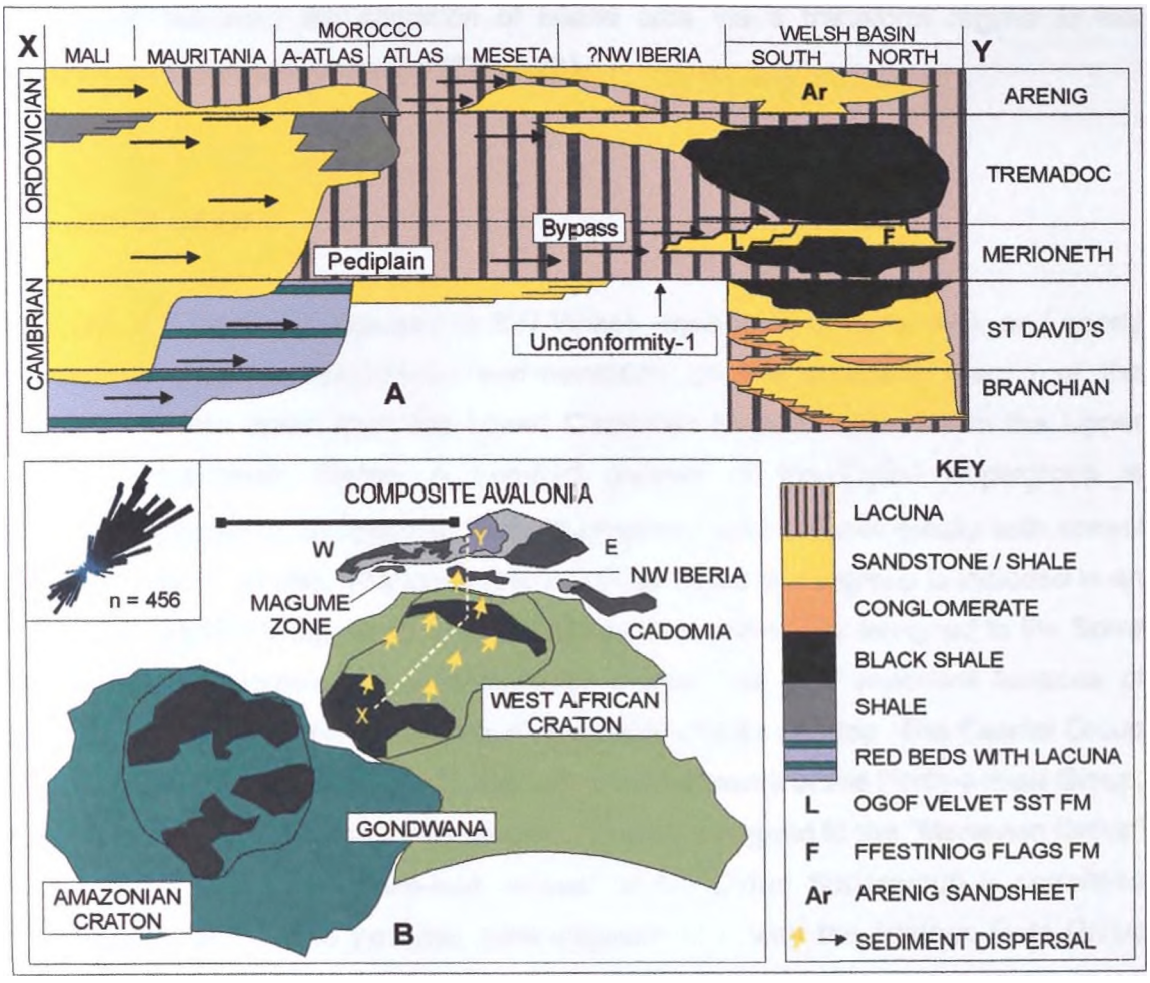



**Fig. 2.24.** The subaqueous delta platform of the Upper Cambrian Welsh Basin: its palaeogeography as a sediment sink on the northern periphery of Gondwana. (A) Stratigraphic correlation between the West African craton of North Gondwana and the peripheral outboard terrane of Avalonia based in part on Schenk (1997). Unconformity-1 is a major regional pediplain that bypassed fine sediment from the continental interior to the northern margin. The terminus of this huge fluvial system, like the Amazon and Ganges rivers, is represented by a large fine-grained subaqueous delta. (B) Sediment dispersal patterns and relationship between source and sink for some northern peri-Gondwanan terranes. Continental positions after Nance and Murphy (1994) with modifications from Gutiérrez-Alonso *et al.* (2003).

Avalonia situated on the north Gondwanan periphery. The entire expanse of North Africa thus became a vast pediplain and an extensive zone of erosion and bypass. This previously unrecognised Avalonian fine-grained sand-sheet is one of two that stretched as far as the Welsh Basin prior to opening of the Rheic Ocean and dispersal of Avalonia in the Middle Ordovician (Cocks *et al.* 1997). The second sheet is Arenig in age (Fig 2.24A) and is a correlative of the extensive Grès Armoricain Formation (Williams *et al.* 1972), which occurs over large areas of northern Gondwana (Noblet and Lefort 1990). Passive margin sedimentation during megasequence 2 therefore marks the culmination of Avalonian–Cadomian

orogenesis following the accretion of island arcs via a transform regime to the northern periphery of Gondwana (Fig. 2.23).

## 2.6. CONCLUSIONS

The Dyfed Supergroup exposed in SW Wales represents an extended, and nearly continuous phase of siliciclastic sedimentation on the southern margin of the Cambrian Welsh Basin from the Lower Cambrian Placentian Series to the Upper Cambrian Merioneth Series. A two-fold division of the Dyfed Supergroup is recognized, which is comparable both lithologically and chronologically with coeval sections in North Wales. The lower 564 m of the Dyfed Supergroup is included in an extended Caerfai Group, which now includes strata previously assigned to the Solva Group. This lithological unit is dominantly arenaceous with important horizons of conglomerate and pebbly sandstone at the base, middle and top. The Caerfai Group is overlain by 687 m of dominantly argillaceous sediments of the Porth-y-rhaw Group, a newly erected unit that includes strata previously assigned to the "Menevian Group" and "Lingula Flags". This two-fold division of the Dyfed Supergroup is correlated lithologically, and where possible biostratigraphically, with the Harlech Grits Group and Mawddach Group exposed around the Harlech Dome.

The relative ease in which Cambrian sediments in southern Britain can be integrated into an Avalonian sequence stratigraphic framework reflects the shared epeirogenic history, sediment sources and accumulation history of a microcontinent unified by the Early Cambrian. The occurrence of lithologically similar and coeval depositional sequences may be relied upon to determine the limits of the Avalonian Superterrane in the Acadian-Caledonian orogen.

The gross lithological similarities that exist between Cambrian successions across Avalonia, and between SW Wales and North Wales in particular, are better understood when basin chronostratigraphy is placed within a sequence stratigraphic framework defined by systems tracts. This is particularly evident during the Middle and Upper Cambrian when clear system links are demonstrated between paralic deposition environments in SW Wales and deeper basin turbidites in North Wales.
Lower and Middle Cambrian sequences 1 through 7 were dominated by siliciclastic deposition on an epeirogenically active platform. An extensional rift-like tectonic regime is proposed, where shale basins are coeval with areas of apparent uplift that were probable locations of tilt-block highs. The principle factor that determined the accumulation history, development of regional unconformities, extent of marine

onlap, and secular successions of lithofacies was phases of fault accommodated-subsidence along northeast trending lineaments that defined elongate basins and intervening horsts or platforms. In southern Britain, movements first along the Menai Straits Fault System then the Welsh Borderlands Fault System (both of which are terrane boundaries, Fig. 2.1A) were responsible for the dominantly coarse-grained arenaceous style of Lower and Middle Cambrian sedimentation. The rapid switch from marginal to inner platform source areas accompanied a major phase of tectonic reorganization of the Avalonian Superterrane during sequence boundary 3–4 development. In the Welsh Basin, this is highlighted by change in sediment source from the Monian Superterrane to the Wrekin Terrane. Although Landing (1992, 1996) dismissed the role of secular variations in eustatic sea level as a control on sequence development and architecture, the most prominent Lower and Middle Cambrian lowstands such as those recorded during the mid *P. oelandicus*, basal *P. gibbus* and *S. brachymetopa* biozones also influenced the depositional sequence stratigraphy.
The arrival of huge quantities of fine-grained quartzose sediment during sequence 8 heralds a new phase of Cambrian sedimentation across Avalonia. Sequence architecture and depositional environments differ markedly from those generated previously, and in contrast to the view perceived by Landing (1996), there characteristics can not be reconciled with active tectonism and an epeirogenically active platform. Instead, secular variations in eustatic sea level and/or sediment supply appear to be the main controlling mechanisms.

This broad subdivision of Cambrian Avalonian stratigraphy into tectonically active and passive phases of sedimentation fulfils the requirements for megasequence distinction. Megasequence 1 (sequences 1–7) records the transform termination of Avalonian subduction following oblique convergence, and the accretion of island arcs to the northern periphery of the supercontinent Gondwana. Under transpressional regimes, late Precambrian arc-related basins were inverted and recycled into Lower and Middle Cambrian pull-apart successor basins. Megasequence 2 (sequence 8) reflects passive margin sedimentation, with Avalonia acting as a sediment sink to vast quantities of fine-grained sediment transferred off Gondwana by large, mature fluvial systems. This marked the culmination of the Avalonian-Cadomian orogenic cycle.

*CHAPTER 3*

# BASIN MARGIN SEDIMENTOLOGY AND TECTONIC IMPLICATIONS OF EARLY CAMBRIAN RIFTING IN EASTERN AVALONIA (SOUTHERN BRITAIN): TRANSTENSIONAL SUCCESOR BASIN DEVELOPMENT IN THE LOWER CAMBRIAN (CAERFAI GROUP) OF SW WALES, UK.

## 3.1 INTRODUCTION

Avalonian-Cadomian and related terranes of the circum-North Atlantic (Fig. 3.1A) constitute portions of an accretionary orogen that developed on an active Gondwanan margin at the periphery of the Neoproterozoic supercontinent Vendia (Murphy *et al.* 2000). These peri-Gondwanan terranes are defined by their Neoproterozoic evolution on an active continental margin, and by the peri-Gondwanan "Acado-Baltic" fauna of their Cambrian–Ordovician overstep sequence (Nance *et al.* 1991; Landing 1996). They include (Fig. 3.1A): (1) the Avalonian Superterrane of southern Britain (e.g. Thorpe *et al.* 1984; Pharaoh *et al.* 1987; Gibbons and Horák 1996; Pharaoh and Carney 2000), referred to as "East Avalonia"; (2) the pre-drift continuation of this superterrane in New England and Atlantic Canada (e.g. Murphy and Nance 1989; Nance 1991; Nance *et al.* 1991, 2002), referred to as "West Avalonia"; and (3) the North Armorican Superterrane in the Cadomian orogenic belt of northwestern France and Bohemia (e.g. Chaloupsky 1990; Dupret *et al.* 1990).

The tectonostratigraphic evolution of the Avalonian Superterrane provides a record of Neoproterozoic subduction along an active continental margin of Gondwana until Avalonian rifting in the Early Ordovician (Prigmore *et al.* 1997) led to the inception of Iapetus subduction and oblique collision with Laurentia during the Early Silurian (Nance *et al.* 2002). In East Avalonia, the late Neoproterozoic (ca 700–570) history is characterized by voluminous arc-related volcanic and cogenetic plutonic rocks, by coeval sedimentary successions deposited in a variety of volcanic arc basins (Thorpe *et al.* 1984; Gibbons and Horák 1996; Compston *et al.* 2000), and

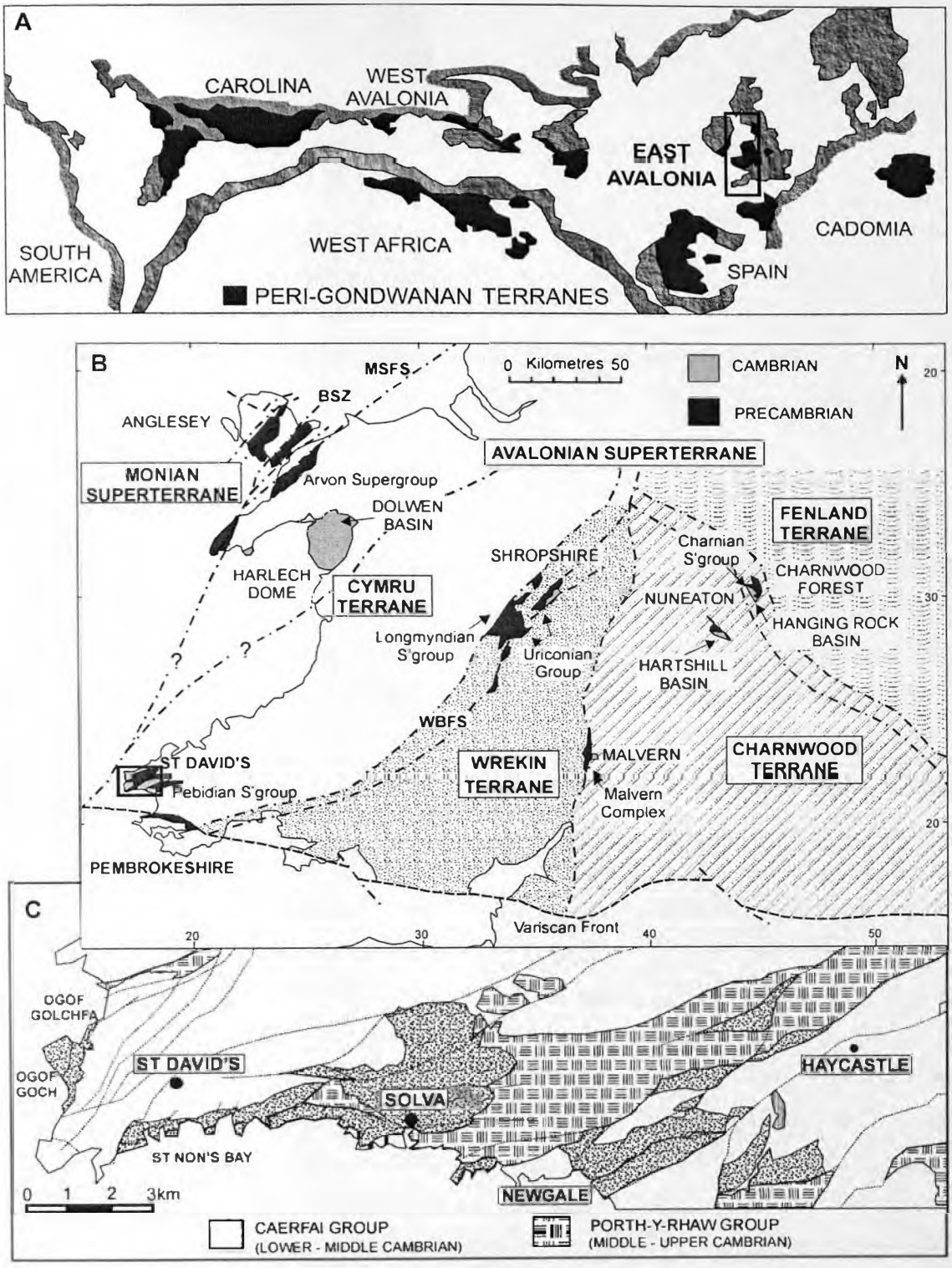



**Fig. 3.1.** (A) Early Mesozoic reconstruction of the North Atlantic showing the location of Avalonia and related peri-Gondwanan terranes of the Neoproterozoic (modified after Nance and Murphy 1994). (B) Geological map of Wales showing terrane assemblage and Precambrian/Cambrian outcrops. MSFS = Menai Strait Fault System. WBFS = Welsh Borderland Fault System (modified after Pharaoh and Carney 2000). (C) Geological map of NW Pembrokeshire showing locations of Cambrian outcrops and study areas discussed in the text.

by latest Neoproterozoic (ca 570–550) intra- and inter-arc extension and the development of arc-related successor basins (e.g. Reedman *et al.* 1984; Pauley 1990). This transition, as well as its diachroniety across Avalonia (Gibbons and Horák 1996) is consistent with the evolution from orthogonal to increasingly oblique subduction.

Unlike most recent studies on the early evolution of Avalonia, this contribution focuses on the Lower Cambrian platformal succession (other recent contributions include Brasier 1989, Landing 1996 and McIlroy 2000). Historically, the base of the Cambrian in southern Britain is taken at a regionally extensive basal conglomerate that typically rests with slight angular discordance on Precambrian arc-related rocks (Rushton 1974). The almost universal interpretation of this conglomerate as a transgressive shoreface sequence deposited during sea level encroachment across a stable, tectonically quiescent platform, has led to a view of Precambrian and Cambrian rocks as two mutually exclusive lithotectonic packages, a perception reinforced by the prominence of the sub-Cambrian unconformity. The transition from active subduction to stable cratonic platform has been variously termed the Avalonian or Cadomian orogeny (Rast 1979; Rast and Skehan 1983), a perception of collision upheld despite the lack of compelling evidence for regional orogenesis, crustal shortening/thickening, and widespread metamorphism (Nance 1991, Nance *et al.* 1991; Gibbons and Horák 1996).

This simple view of the late Neoproterozoic–Cambrian evolution of Avalonia has been recently challenged, with the extensive documentation of strike-slip tectonics in both the latest Proterozoic (Murphy and Nance 1989; Nance 1991) and Lower and Middle Cambrian (Murphy *et al.* 1985; Keppie and Murphy 1988; Landing 1996) successions in West Avalonia, and the realization that in northwest Wales at least, there is no prominent break between latest Precambrian events and Lower Cambrian sedimentation (Gibbons and Horák 1996). In addition, a number of basal Cambrian "nearshore marine" conglomerates have been reinterpreted as alluvial fan and fan-delta complexes, which are depositional systems with strong genetic ties to various syn-tectonic frameworks (McPherson *et al.* 1988; Massari and Colella 1988; Blair and McPherson 1994).

Although the importance of regional strike-slip tectonics in the Precambrian succession of East Avalonia is now well documented (Pauley 1990; Gibbons and Horák 1996), no study has yet demonstrated any influence on Cambrian sedimentation patterns. This is surprising if one consults the extensive "local" literature (see review in Rushton 1974), which consistently demonstrates a number of characteristics compatible with local phases of transtension and transpression

(Reading 1980). They include: (1) alternating periods of extension and compression, (2) differential subsidence, (3) coarse-grained feldspathic tuffs in syn-tectonic sediments, (4) depocenter migration, (5) basin margin cannibalization, and (6) numerous local and regional scale unconformities, some of which display angular discordance. Subsidence curves presented by Prigmore *et al.* (1997) from Cambrian sequences throughout East Avalonia also record rapid pulses of differential subsidence throughout the Lower and Middle Cambrian. According to those authors, profiles are indicative of transtensional regimes operating during the transform termination of Avalonian subduction. The widespread occurrence of strike-slip tectonics in both late Neoproterozoic and Cambrian successions in West Avalonia similarly led Murphy and Nance (1989), Nance (1991) and Nance *et al.* (1991, 2002) to propose termination of Avalonian subduction by transform development along the Gondwanan margin. This by default would classify the Lower Cambrian basins of Avalonia as "late-stage" successor basins (Graham *et al.* 1993; Trop and Ridgeway 1997) due to their evolution during the terminal phase of a long-lived orogenic event.

The Lower and Middle Cambrian Caerfai Group of NW Pembrokeshire (Fig. 3.1C) forms part of the Dyfed Supergroup (Woodcock 1990), a lithostratigraphic package that includes all Cambrian and Tremadoc rocks in southern Britain. The stratigraphic position of the Caerfai Group between arc-related environments of the late Precambrian Pebidian Supergroup and stable cratonic regime of the Upper Cambrian Porth-y-rhaw Group place the sequence in the tectonostratigraphic position of the arc-platform transition (Nance 1991). This detailed tectonosedimentological study of basin margin evolution focuses on the boulder–pebble conglomerates and coarse- to medium-grained sandstones of the Ogof Golchfa and St Non's formations, which are situated immediately above the angular unconformity with Precambrian arc-related sediments (Fig. 3.2). The principle outcrops discussed herein occur along cliff sections between Whitesand Bay and Porthselau and at St Non's Bay and Caerfai Bay (Fig. 3.1C).

Although the wider implications of this investigation relate specifically to the Neoproterozoic–Cambrian evolution of southern Britain, other topics addressed include: (1) sedimentary facies, stratal architecture, and depositional processes on debris flow-dominated alluvial fans and gravelly braided streams, (2) the details of an alluvial fan to braided stream transition within a temporal framework of evolving tectonic and morphological constraints, (3) an examination of some of the classic tenets of the relationship between tectonic movement and sedimentary response, with particular reference to "anti-tectonic cycles" (Paola *et al.* 1992; Gordon and Heller 1993), (4) to highlight the controls that rift-related tectonics can exert on stratal

architecture and depositional processes within the tectonostratigraphic framework of syn-extensional, transitional extensional, and post extensional phases, and finally (5) a comprehensive study of syn-tectonic sandstone composition (detrital modes) with a view to determining the origin and tectonic setting of the basin fill.

## 3.2. BASIN MARGIN SEDIMENTOLOGY AND LITHOFACIES ASSOCIATIONS

Detailed sedimentary logging of cliff sections northwest and southeast of St David's has led to the identification of three discrete facies associations based on lithology, bed thickness and geometry, grain size, and internal sedimentary structures. These facies associations (Fig. 3.2), labelled A to C, range from gravel to fine sand-dominated, and are described in ascending stratigraphic order. Each facies association is built up of a number of component lithofacies, which are described and interpreted separately, and serve as the basis for the interpretation of depositional processes and palaeoenvironment.

### 3.2.1. Lithofacies Association A

The poorly accessible cliffs sections at Ogof Golchfa (Fig. 3.1C) provide the only exposure available through Facies Association A sediments, where they rest with slight angular unconformity on the local Precambrian basement. Polymictic pebble-cobble conglomerates account for over 95% of the 24 m thick section (Fig. 3.2), the rest is composed of red, haematite-rich silty mudstone. The latter is most prominent in separating two very well defined coarsening-upwards sequences. Two types of bedding profile occur. Sheet-like forms are dominant, while amalgamated, lenticular channel profiles are subordinate. The whole facies association is referred to the Ogof Golchfa Formation.

#### *3.2.1.1. Facies A1: unstratified, tabular, clast-supported conglomerate*

##### *3.2.1.1.1. Description*

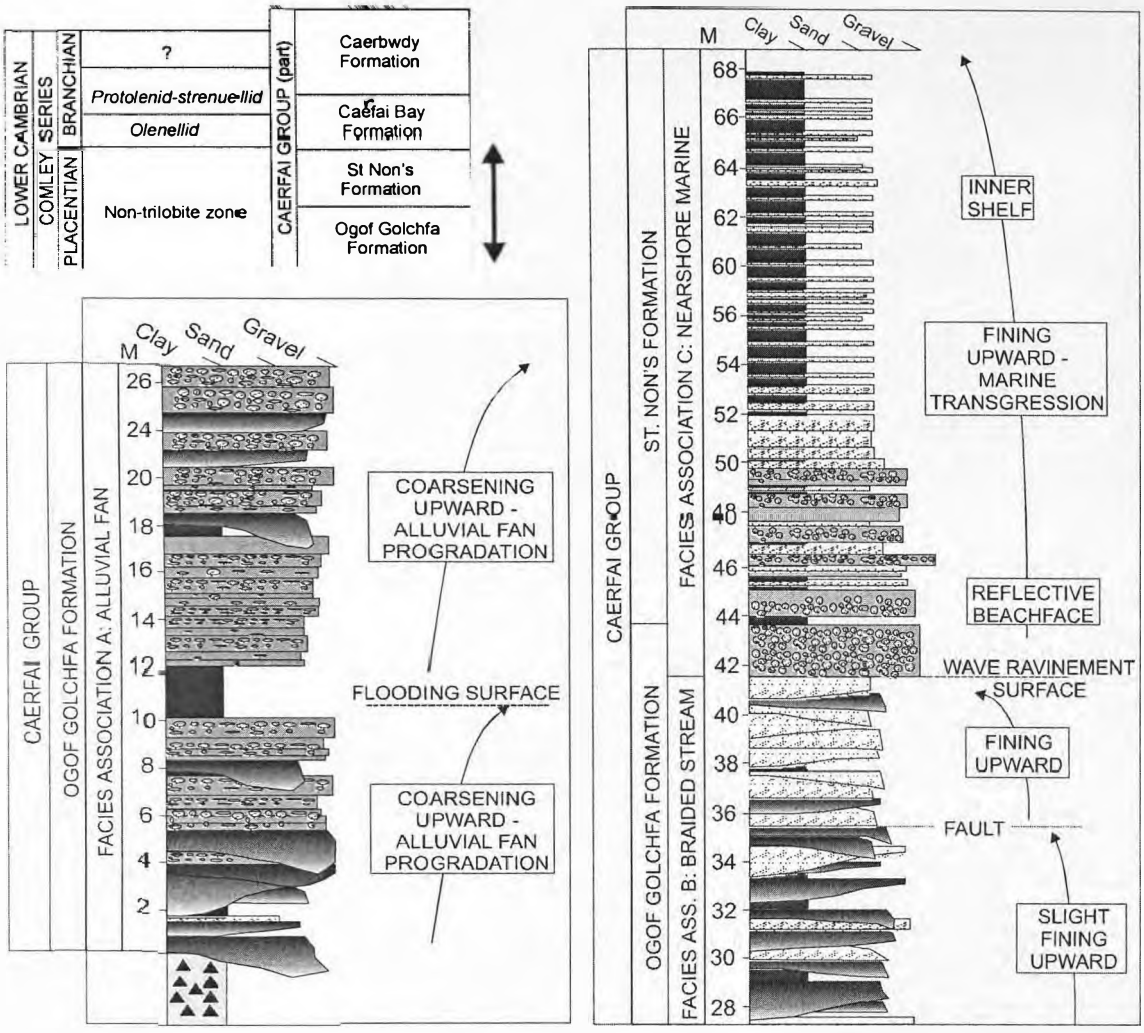



**Fig. 3.2.** Stratigraphy and detailed sedimentary log of the coastal section between Ogof Golchfa and Porthselau illustrated in Fig. 3.1B.

This lithofacies consists of medium bedded (7-115 cm thick) broadly tabular units of clast- to matrix-supported polymictic cobble conglomerate (Fig. 3.3C). Clast size ranges from small pebbles to boulders, set in a poorly sorted coarse-grained sandy matrix. Clasts are dominantly sub-rounded but varies to sub-angular. Matrix content is extremely variable but commonly forms less than 15%. Red colouration of this matrix is due to haematite staining, particularly of quartz. Pebbles of metasedimentary origin are the dominant clast type (Fig. 3.3B and D) and include (in decreasing abundance): quartzite, slate, schistose quartzite, schistose greywacke and mylonite. Felsic volcanics are subordinate (Fig. 3.3B) but are readily matched with the underlying local Precambrian arc volcanics of the Pebidian Supergroup. Bed boundaries are difficult to identify due to poorly organized texture and fabric, but where visible are planar and non-erosive. General features include poor sorting, lack of internal stratification, and a polymodal texture. Two sub-facies have been

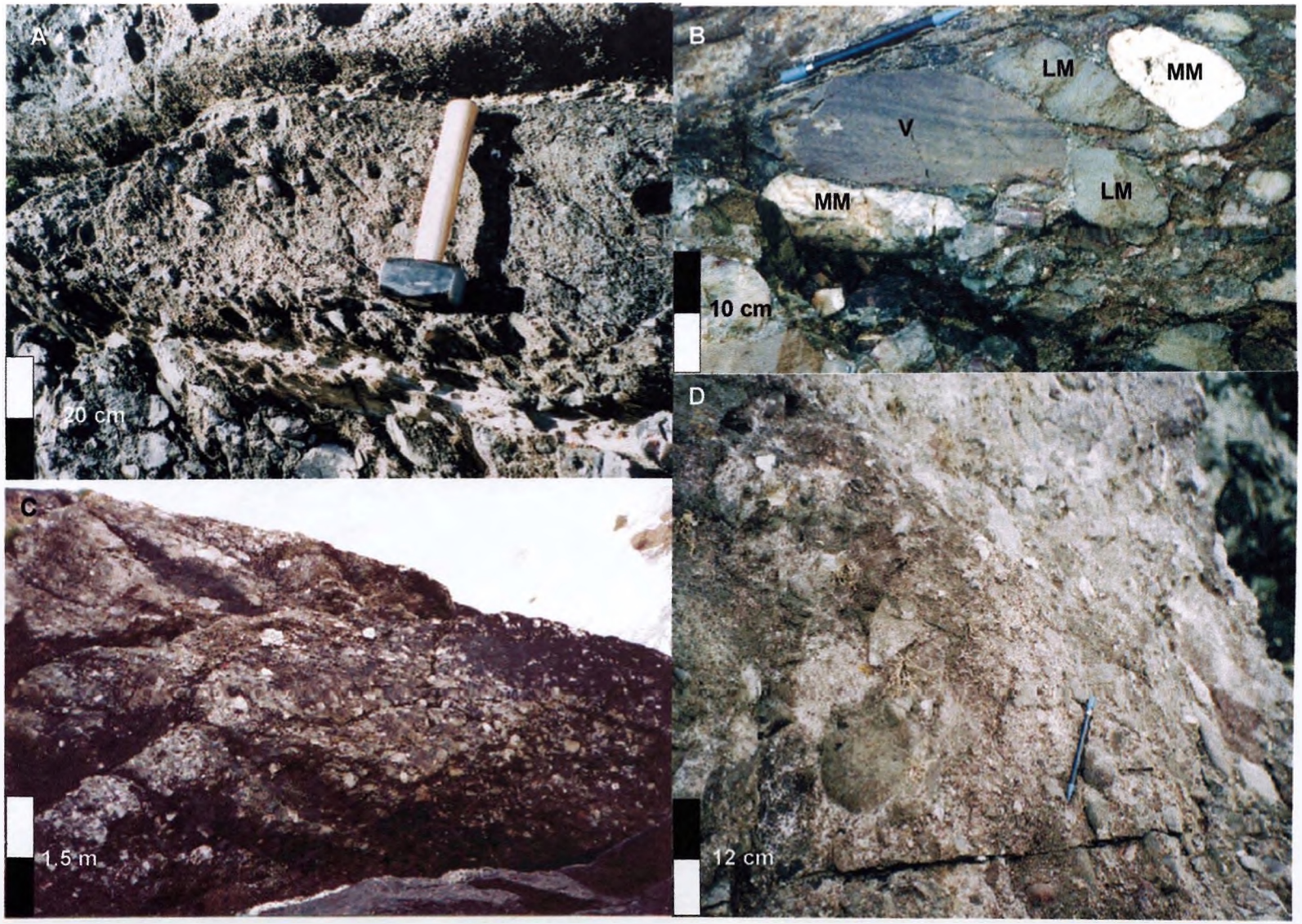

A
20 cm
B
LM
MM
V
MM
LM
10 cm
C
1.5 m
D
12 cm

**Fig. 3.3.** Sedimentological features of Facies Association A sediments (alluvial fan) exposed at Ogof Golchfa. (A). Facies A3 – HFF deposit. Note the general angularity of clasts, a(p)a(i) imbrication, and step-wise configuration of the basal erosion surface. (B) Facies A3 – Clast composition typical of HFF deposits. There is a mixture of low- and medium-grade metamorphic clasts (LM and MM respectively) exotic to SW Wales and volcanic clasts (V) comparable with the local Precambrian basement (Pebidian Supergroup). (C) Facies A1 – Clast supported non-cohesive debris flows. Note the general clast rounding, chaotic fabric, and lack of clear basal erosion surfaces. (D) Facies A1 – Clast composition typical of debris flows. Note the absence of volcanic clasts and dominance of greenschist.

determined based on differences in internal organisation of fabric. By far the most abundant, reflecting 80% of Facies A1 are profiles displaying well developed inverse grading throughout the bed, and a pervasive a(p)a(i) clast fabric (notation after Walker 1975). The second bed-type has a more chaotic and disorganised texture, although base-only inverse grading is locally present. Clasts are either randomly orientated, often in sub-vertical positions, or display weak a(p) planes with rare imbrication. To aid interpretation of depositional processes, a quantitative analysis of maximum particle size (MPS, here expressed as the mean of the long axis of the 10 largest visible clasts) and bed thickness (BTh) has been undertaken (Fig. 3.4). For both subfacies (inversely graded and chaotic, Fig. 3.4A and B), there is a significant linear correlation (correlation coefficient (r) = 0.84 for inversely graded, and 0.75 for chaotic beds) between these two variables, which is interpreted below.

*3.2.1.1.2. Interpretation*

Despite evidence for clast rounding, traction influenced sedimentation is an unlikely depositional processes for facies A1 considering the absence of stratification, matrix support, poor sorting, a(p)a(i) clast fabric (indicative of strongly sheared laminar flow, Rees 1968), insignificant basal erosion, and unstable pebble orientations. These features, in addition to well developed inverse grading and significant relationship between MPS and MTh instead suggest a sediment gravity flow origin (Bluck 1967a; Lowe 1982; Nemec and Steel 1984; Massari 1984; Kim *et al.* 1995). The polymodal grain size distribution (reflecting the transport of sand and gravel together) and lack of internal stratification suggests that deposition occurred *en masse*, and thus may be modelled on the inertia grain flows of Tokahashi (1978), where deposition occurred once the applied shear fell below the yield strength, resulting in grain interlocking and frictional freezing. Low levels of mud in the matrix suggests deposition by cohesionless debris flows (the grain flows of Lowe 1982), in which clast support was accomplished by a combination of intragranular dispersive pressure

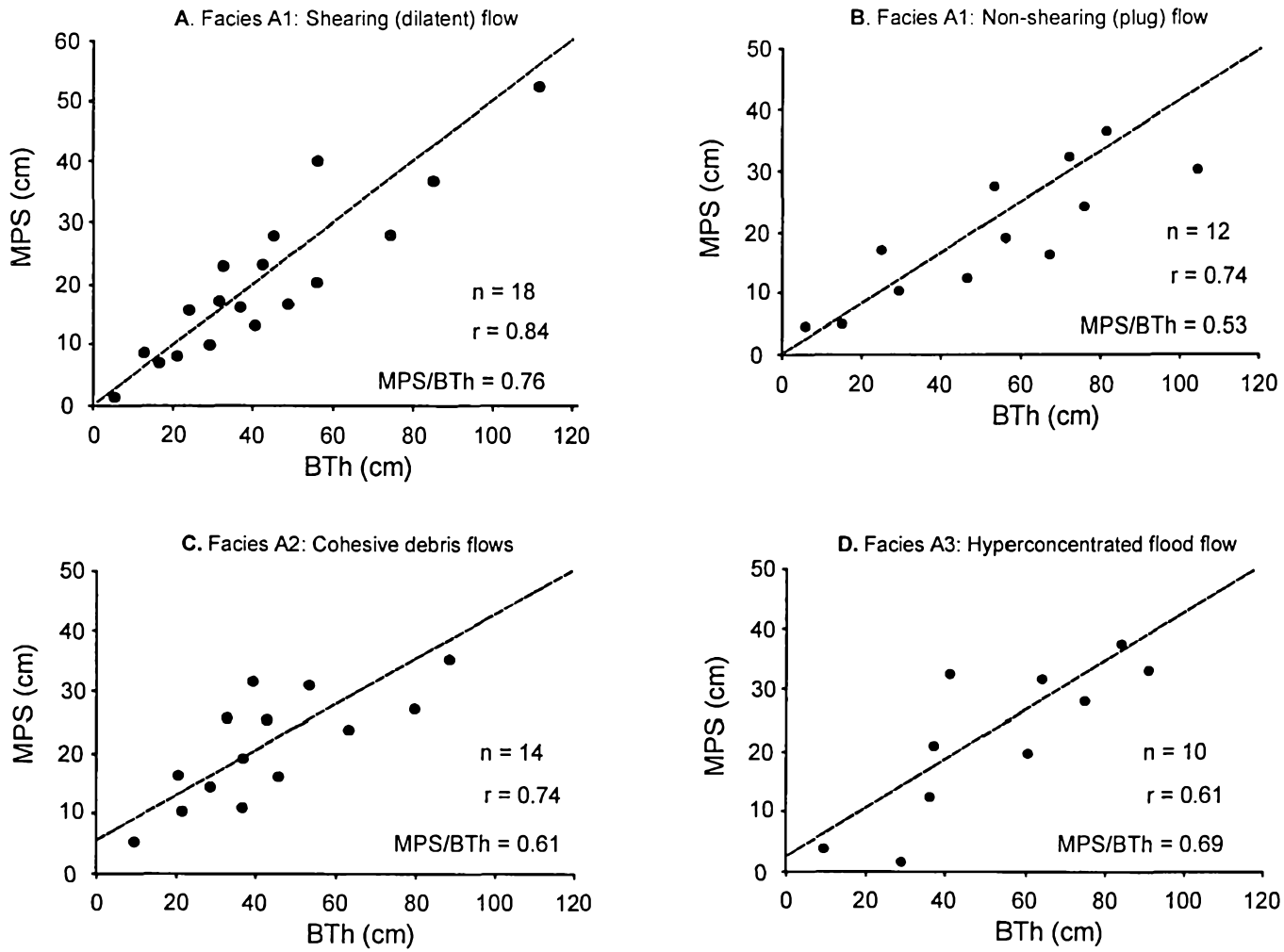



**Fig. 3.4.** Plot of maximum particle size (MPS) against bed thickness (BTh) from conglomerate lithofacies of Facies Association A. Explanation of symbols: n = number of readings, r = correlation coefficient, MPS/BTh = ratio of MPS to BTh.

formed by grain collision (Bagnold 1954), enhanced buoyant lift provided by excess pore pressure and the dense interstitial matrix of water and sand (Middleton 1970), and the vertical movement of intergranular fluid (hindered settling) (Middleton 1993). The different internal clast arrangements (inversely graded and ungraded) are probably a consequence of differences in the clast support mechanisms prior to deposition (Lowe 1982).

Beds displaying a chaotic fabric suggest a highly concentrated dispersion of high viscosity and strength that underwent little laminar shearing prior to deposition. This is evidenced by the weak clast fabric and lack of inverse grading reflecting static grain-to-grain interaction, as opposed to a collisional regime that gives rise to dispersive pressure. These rheological characteristics are frequently observed in the inert plug region of cohesionless debris flows (Chen 1988), which develop once the applied shear falls below shear strength. Due to inelastic grain collision with the substratum, a zone of basal shear develops upon which the inert plug is passively rafted (Johnson 1970). This zone of active grain collision (shear greater than strength) is likely to produce dispersive pressure, which may account for the locally developed base-only inverse grading. Beds displaying a preferred clast orientation originate from strongly shearing laminar flow where clasts were free to move and interact. Inverse grading associated with this more organised fabric similarly reflects grain collision, with the additional development of dispersive pressure. This dilation of the flow hinders the development of an inert plug (Chen 1988), and dispersions are instead referred to as dilat nt debris flows (Kim *et al.* 1995).

The variable flow properties between shearing (dilat nt) and non-shearing (plug) debris flows appear to be environmentally dependent, as they rarely occur together in the stratigraphic section. Shearing flows dominate the coarsening-upward profiles, while non-shearing flows are most abundant in strata transitional into Facies Association B (Fig. 3.2). In an attempt to understand this connection, the relationship between MPS and BTh has been utilised as advocated by Bluck (1967a); Steel (1974); Larson and Steel (1978); Nemec *et al.* (1980, 1984); Gloppen and Steel (1981); Nemec and Steel (1984); Mustard (1991); Kim *et al.* (1995), and Martins-Neto (1996). Scatter plots for both dilatant and plug debris flows (Fig. 3.4A and B) show a positive linear correlation between MPS and BTh, a feature typical of sediment gravity flows (Gloppen and Steel 1981; Nemec and Steel 1984). This correlation reflects the dependence of both flow competence and flow thickness on the internal regime (clast support mode) (Gloppen and Steel 1981), and is a relationship atypical of traction-influenced sedimentation where bed accretion is grain-by-grain. The higher correlation coefficient in dilat nt debris flows is consistent with published

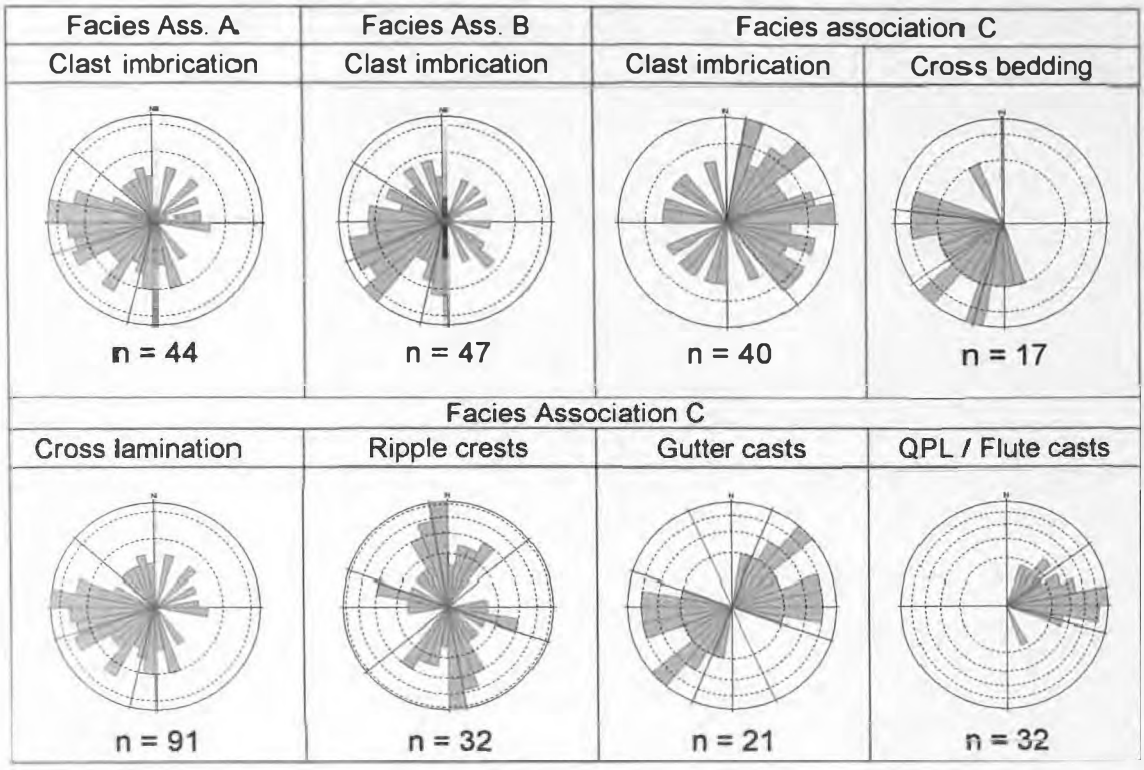



**Fig. 3.5.** Palaeocurrent data from the Ogof Golchfa Formation and lower St Non's Formation exposed between Ogof Golchfa and Porthselau.

accounts summarized in Nemec and Steel (1984), and is related to a greater equilibrium between competence and thickness, a feature apparently diagnostic of flow with a high component of dispersive pressure. The y-intersect value on MPS/BTh diagrams defines the "cohesive strength factor" (outlined in Nemec and Steel 1984), a characteristic that has been used successfully in distinguishing cohesive from non-cohesive flows (e.g. Nemec *et al.* 1984). The negligible y-intersect value for both shearing and non-shearing debris flows (Fig. 3.4A and B) suggests a thickness-dependent support mechanism and thus a cohesionless rheology according to Nemec and Steel (1984). An additional criterion useful in flow reconstruction is the ratio between MPS and BTh, understood to be a measure of relative competence (Nemec and Steel 1984; Kim *et al.* 1995). The higher value obtained from shearing flows (Fig. 3.4A) suggests a greater competence than unshearing dispersions. Based on Johnson's (1970) model, Shultz (1983) suggested that relative competence is inversely proportional to the density contrast between clast and matrix, and positively proportional to slope angle. The higher relative competence in dilatent flows can therefore be attributed either to a smaller density contrast or deposition on a steeper slope. There is no evidence for a significant change in density contrast between these flows as the matrix percentage and

composition are similar. Thus changes in depositional slope appear to influence debris flow properties, a conclusion consistent with the apparent environmental control deduced from stratigraphic relationships.

*3.2.1.2. Facies A2: muddy-matrix-supported conglomerate*

*3.2.1.2.1. Description*

Beds of matrix-supported conglomerate are composed mainly of angular to sub-rounded cobbles and pebbles randomly distributed in a very poorly sorted matrix of mud to coarse sand. Beds are between 10 and 91 cm thick, sheet-like in geometry, unstratified, and with clasts commonly in unstable sub-vertical positions. In contrast to facies A1, most clasts can be matched with the local volcaniclastic bedrock. There is again a good correlation between MPS and BTh (Fig. 3.4C).

*3.2.1.2.2. Interpretation*

The lack of internal stratification and clast imbrication, insignificant basal erosion, clasts orientated in unstable sub-vertical positions, and grain size bimodality excludes traction influenced sedimentation, while considerable amounts of clay in the matrix points to a cohesive character suggesting deposition by pseudo-plastic debris flows (Nemec and Steel 1984; Horton and Schmitt 1996; Benvenuti 2002). This is reaffirmed by the positive linear correlation ($r = 0.74$) between MPS and MTh (Fig. 3.4C) and the significant y-intersect value reflecting a thickness independent component (the matrix strength factor of Nemec and Steel 1984). Although matrix strength appears to be the main grain support mechanism, experiments by Hampton (1975) suggested that matrix strength is only capable of fully supporting particles up to coarse sand grade, so many of the larger clasts must have been supported by high local pore pressure (Iverson *et al.* 1997) and buoyancy (Major and Iverson 1999). Although a disorganized fabric may simply reflect a short travel distance, it is more often suggestive of non-sheared (high strength) 'plug' flow or weakly sheared (high viscosity) flow. Deposition occurs through cohesive freezing when the force related to the shear resistance of the flow (mainly controlled by viscosity and friction) becomes equal to the force due to gravity, i.e. when the shear stress drops below the yield strength (Johnson 1970).

*3.2.1.3. Facies A3: unstratified, lenticular sand-matrix supported conglomerate*

*3.2.1.3.1. Description*

Facies A3 forms a distinctive amalgamated unit (3.1 m thick) at the base of the succession, which is composed of a number of discrete beds deeply incised into the Precambrian bedrock. Elsewhere in Facies Association A, these beds occur both individually and as thinner (1.3-2.4 m thick) amalgamated units. This facies is characterized by angular to subrounded granules and pebbles set in a very poorly sorted medium- to coarse-grained sandy matrix. The amount of matrix is extremely variable, ranging from less than 10% to nearly 35%. Lower bounding surfaces are highly erosional and characterized by multiple concave profiles (Fig. 3.3A) with a relief of up to 60 cm, producing a stepwise configuration reflecting channel geometries with deeper and shallower parts. Internal texture and fabric display many of the characteristics of Facies A1: poor sorting, bimodal texture, lack of internal stratification, a(p)a(i) clast fabric, and inverse grading. The last two characteristics differ slightly in being more variable, with imbrication angles typically steepening towards the top of the bed (Fig. 3.3A), and inverse grading often overlying an ungraded region. Clast lithology is also more diverse, with a small percentage of local bedrock incorporated with metasandstone (Fig. 3.3B). The correlation coefficient between MPS and BTh (Fig. 3.4D) is considerably weaker ($r = 0.61$) than that reported for the cohesionless debris flows of Facies A1. Amalgamated beds were not used for MPS/BTh purposes due to the obvious reduction in BTh by erosion of successive flood events.

*3.2.1.3.2. Interpretation*

The very well defined channelized geometry, with steep margins, textural immaturity, internal scouring, and lack of lateral accretion, along with the coarse relatively poorly sorted nature of the fill, suggests deposition from high-energy sediment-charged flows in relatively short-lived, low sinuosity, well incised channels (Marzo and Anadon 1988; Jo *et al.* 1997). Some of these channels were filled during a single sedimentation event, others by successive erosional and depositional episodes. The configuration of the lower surfaces into a curved step-like profile is a feature commonly described from braided channel systems, reflecting the characteristic combined effect of both entrenchment and avulsion (Soegaard 1990).

The defining characteristic of this lithofacies is that it shows a combination of features associated with both stream-flow and debris flow processes. The poorly sorted polymodal texture, lack of internal stratification, a(p)a(i) imbrication, and the massive to inversely graded profiles are features associated with frictional freezing of cohesionless debris flows that experienced full laminar shear prior to deposition. This suggests a highly concentrated water-sediment mixture and high apparent viscosity, far above the concentration values set as the Bagnold limit for turbulence (Bagnold 1954). Although there is no evidence to suggest turbulent conditions operated during deposition, fully turbulent traction conditions must have operated prior to deposition to scour and confine the flow. This early stage of turbulence is atypical of cohesionless debris flows, which are driven almost entirely by gravitational forces, where fluid plays only a minor role in the transportational-depositional event (Mulder and Alexander 2001). They are therefore unlikely to develop turbulent eddies prior to deposition and are thus floored by essentially non-erosive surfaces. Debris flow properties therefore appear to document a transient condition in the depositional regime while the long-range transport regime was dilute and dominated by fluid turbulence. The most likely mechanism for producing transient debris flow-like properties is gravity transformation of a fully turbulent flow resulting in a density stratified bipartite structure (Sohn *et al.* 1997; Sohn 1999; Kneller and Buckee 2000).

The formation of a non-linear particle concentration gradient results in a flow with two-phase characteristics (Sohn 1999), with coarser clasts forming a concentrated solid phase (sand and gravels), overlain by a fluid component comprising water, silt and clay. A consequence of density stratification is a layered flow with discrete interfaces between components with different sediment concentrations, rheologies, and sediment support mechanisms (Postma *et al.* 1988). The flow thus becomes partitioned into a highly concentrated bedload zone where turbulence is dampened and the fluid takes on Bingham properties (Mingfu *et al.* 1983), and an overlying turbulent suspension cloud. The shear stresses necessary to maintain an active bedload zone are provided tangentially from the overlying turbulent portion of the bipartite flow (Lowe 1982) and basal shear stresses created by the weight of the flow due to gravity (Postma *et al.* 1988). Changes in imbrication angle, and degree of inverse grading may document the passage of the non-depositional liquid phase, which would induce a zone of maximum shear (and thus maximum grain interaction) high in the flow. This is atypical of debris flows, where single phase characteristics induce maximum shear at the flow base (gravitational weight).

These characteristic essentially defines the response of the flow to hyperconcentration as outlined by Sohn (1997) and Manville and White (2003), and thus the sediments of Facies A3 may be referred to as hyperconcentrated flood-flow (HFF) as proposed by Smith (1986). Due to the transient properties of HFF and still considerable uncertainties surrounding their rheological character during hyperconcentration, inferences based on MPS/BTh are tentative. Firstly the correlation coefficient ($r = 0.61$) is significantly lower than that recorded from the debris flows of Facies A1 (contrast Fig. 3.4A and D), which may imply a difference in rheology, but this is countered somewhat by the similar ratio of MPS:BTh. It is impossible to account adequately for the differences in the correlation coefficient based on the present understanding of hyperconcentrated flow except that flow properties are different from those that occur in debris flows. The similarity in MPS/BTh ratio between HFF and dilatent debris flows (compare Fig. 3.4B and D), both of which are considered high (compared with ratios presented in Nemec and Steel 1984), may reflect elevated dispersive pressure enhanced by shear stresses exerted tangentially from onto the basal inertia layer by the turbulent overflow.

#### *3.2.1.4. Facies A4: purple and red silty mudstone*

##### *3.2.1.4.1. Description*

This subordinate facies forms a highly conspicuous, broadly tabular, fine-grained unit 1.8 m thick separating two well defined coarsening-upward sequences. The lower boundary of this unit is very well defined, easily identifiable in the field by a sharp break in topography caused by differential erosion. Thinner horizons (1–7 cm) also occur between Facies A1, A2, and A3 (see Fig. 3.7B). These fine-grained intervals are dominated by red to dull-purple silty mudstone that contain undisturbed coarse siltstone laminae and pebbly lenses. There is no evidence for bioturbation.

##### *3.2.1.4.2. Interpretation*

The fine grain size and laminated appearance suggest deposition out of suspension without the influence of traction currents. Conglomerate lenses contain a clast assemblage identical to that described from Facies A1/A2, and may represent the distal expression of higher energy proximal flows. The red colouration, lack of bioturbation, and stratigraphic association with fluid and sediment gravity flows suggests a non-marine setting, possibly lacustrine or shallower ephemeral ponds

(Corcoran *et al.* 1999). Whatever their exact classification, these standing bodies of water must have been quite extensive, as bed thickness is maintained without obvious thinning across the length of the outcrop (>10 m).

### 3.2.2. Lithofacies Association B

There is no complete section through Facies Association B, but relatively good exposures occur at Ogof Golchfa and Ogof Goch. The section at Ogof Golchfa (Fig. 3.2) is the most complete, with 17 m of pebble-cobble polymictic conglomerate and subordinate sandstone and red silty mudstone. All Facies Association B sediments are referred to the Ogof Golchfa Formation. A strike-slip fault of unknown displacement occurs 37 m above the base that may have removed a significant amount of section. This may be demonstrated by the sudden decrease in clast size and percentage conglomerate in sediments above the structure (Fig. 3.2). Therefore 17 m is a minimum value, particularly as only 7 m of identical conglomerate is exposed at Ogof Goch, which forms a base-truncated sequence lying with angular unconformity on Precambrian basement (Fig. 3.6). The boundary between Facies Association A and B is gradational over 3–4 m, with typical intercalations of non-sheared debris flow deposits of Facies A3 defining the transition. Geometrically, these beds are broadly lenticular and form numerous small scale (1–2 m) fining-upward sequences (Fig. 3.7). In the wider sense, bed stacking patterns are at first aggradational, followed by retrogradational (rapid fining-upward).

#### *3.2.2.1. Facies B1: graded pebble conglomerates*

##### *3.2.2.1.1. Description*

The clast-supported conglomerates of Facies B1 form the bases of crude fining upwards sequences (Fig. 3.7B). They are normally graded, broadly lenticular in geometry with an erosive basal contact and a gradational upper transition into Facies B2. Clast sizes are the coarsest recorded in this facies association, with pebbles and small cobbles dominant, set in a moderately sorted matrix of coarse sand and granules. Matrix never exceeds 15%, and is more commonly less than 10%. Bed thickness is quite regular, ranging from 0.25 – 0.6 m. Clasts are reasonably well imbricated with an a(t)b(i) fabric (after Walker 1975). Subangular to well rounded quartzite, greenschist, phyllite, slate, schistose quartzite, and jasper, form the

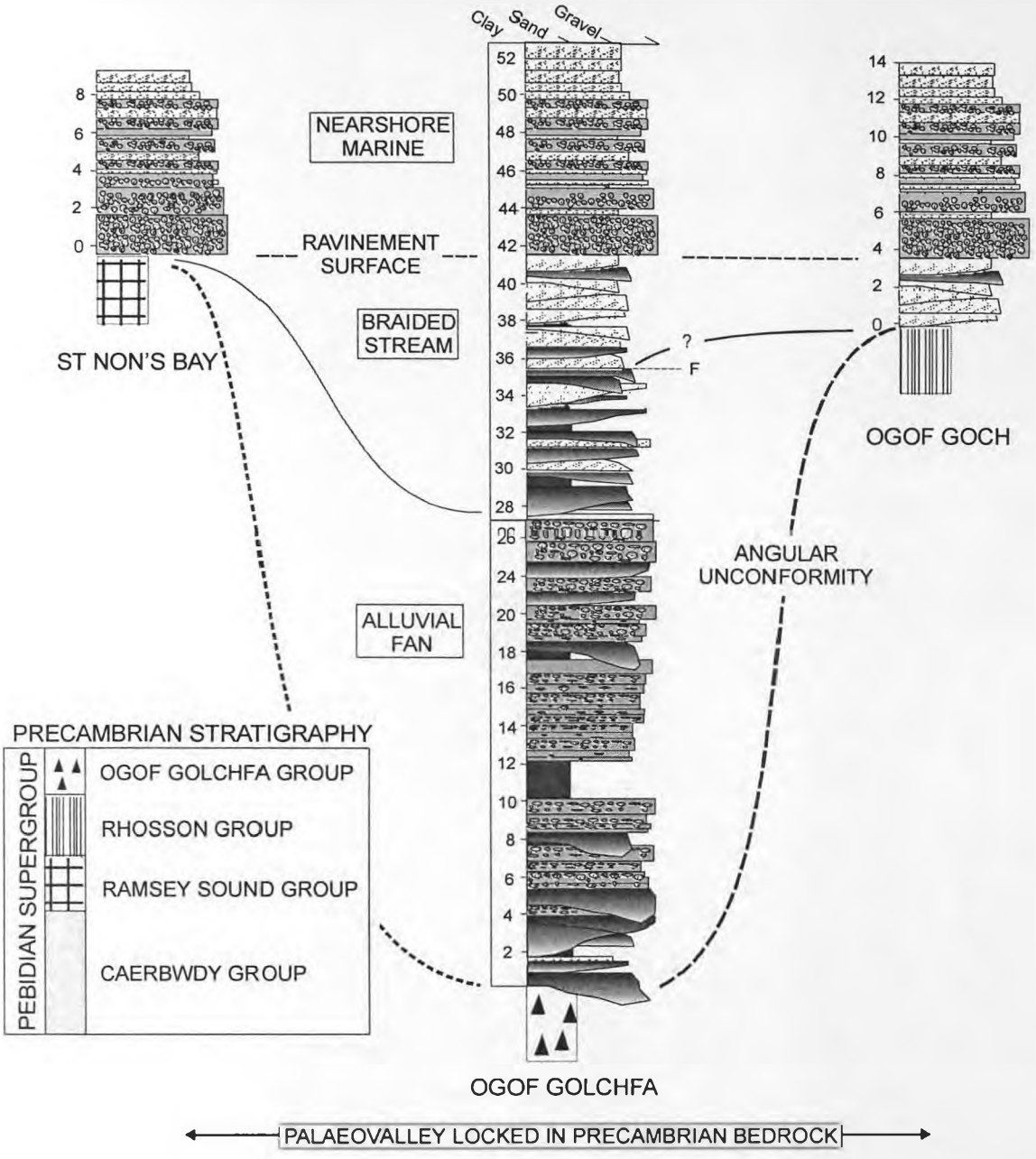



**Fig. 3.6.** Schematic cross-sectional representation of basal Cambrian overstep sequence in NW Pembrokeshire. Alluvial fan conglomerates are restricted to Ogof Golchfa suggesting deposition in a confined palaeovalley flanked by topographic relief at St Non's Bay to the SE and Ogof Goch to the NW. The presence of highlands in the latter localities is also suggested by the greater depth of erosion seen as an unconformable junction with Cambrian sediments and older divisions of the Precambrian Pebidian Supergroup.

dominant pebble types, a considerably more diverse suite than that recorded from Facies Association A.

*3.2.2.1.2. Interpretation*

The clast fabric, erosive base, and normal grading suggest fully tractional conditions operated during deposition, a conclusion consistent with the relatively well sorted texture. These characteristics, as well as the gradational contact with stratified conglomerates of Facies B2 (discussed below), are identical to the channel floor lag deposits described by Nemec and Postma (1993), Vincent (2001) and Wysocka and Swiezewska (2003). These lags typically comprise the coarsest and least mobile bedload material deposited on the stream floor immediately after the erosion maximum of channel peak-flood phase (Nemec and Postma 1993). The clast size grading and tractional fabric suggest deposition as a pavement or stream floor armour layer. Poor definition of channel margins probably reflects the highly mobile nature of the sediment load and thus very wide, shallow channels. The absence of scour and fill structures, and a more sheet like geometry are traits typical of pre-vegetative bedload streams (Fuller 1985). Smith (1976) concluded that loose, non-vegetated sediment could be 20,000 times less stable than the same sediment with 16-18% by volume plant root. The lack of land plants may suggest that channel widening rather than incision would be the expected response to fluctuating flow conditions, a conclusion consistent with empirical data presented by Fuller (1985) for the lower reaches of the Yellow River, which has a width/depth ratio of 900:1.

*3.2.2.2. Facies B2: stratified pebble conglomerate*

*3.2.2.2.1. Description*

Facies B2 dominates volumetrically (Fig. 3.7A) and consists of reasonably well sorted clast- to matrix-supported pebble conglomerate and rare pebbly sandstone in gradational lower contact with Facies B1. This relationship defines these conglomerates as broadly lenticular in geometry. Clast shape, composition, and tractional a(t)b(i) fabric are features shared with Facies B1, but bed thickness is substantially greater, ranging from 0.4 to 1.6 m. Most beds are weakly graded (Fig. 3.7A), with a matrix filled framework, but units with a lower openwork and upper sand-filled distribution are not uncommon. Upper contacts may be erosional with Facies B1 (signifying another fining upwards sequence), sharp with sandstones of Facies B3, or sharp or erosional with apparent replication of another graded unit of Facies B2 (i.e. a composite unit of amalgamated beds). These conglomerates are distinguished by their variably developed stratification, a characteristic made obvious by small changes in clast size, sorting and matrix percentage. Crude sub-horizontal stratification is the dominant form (Fig. 3.7A), but solitary sets of low angle (<15°)

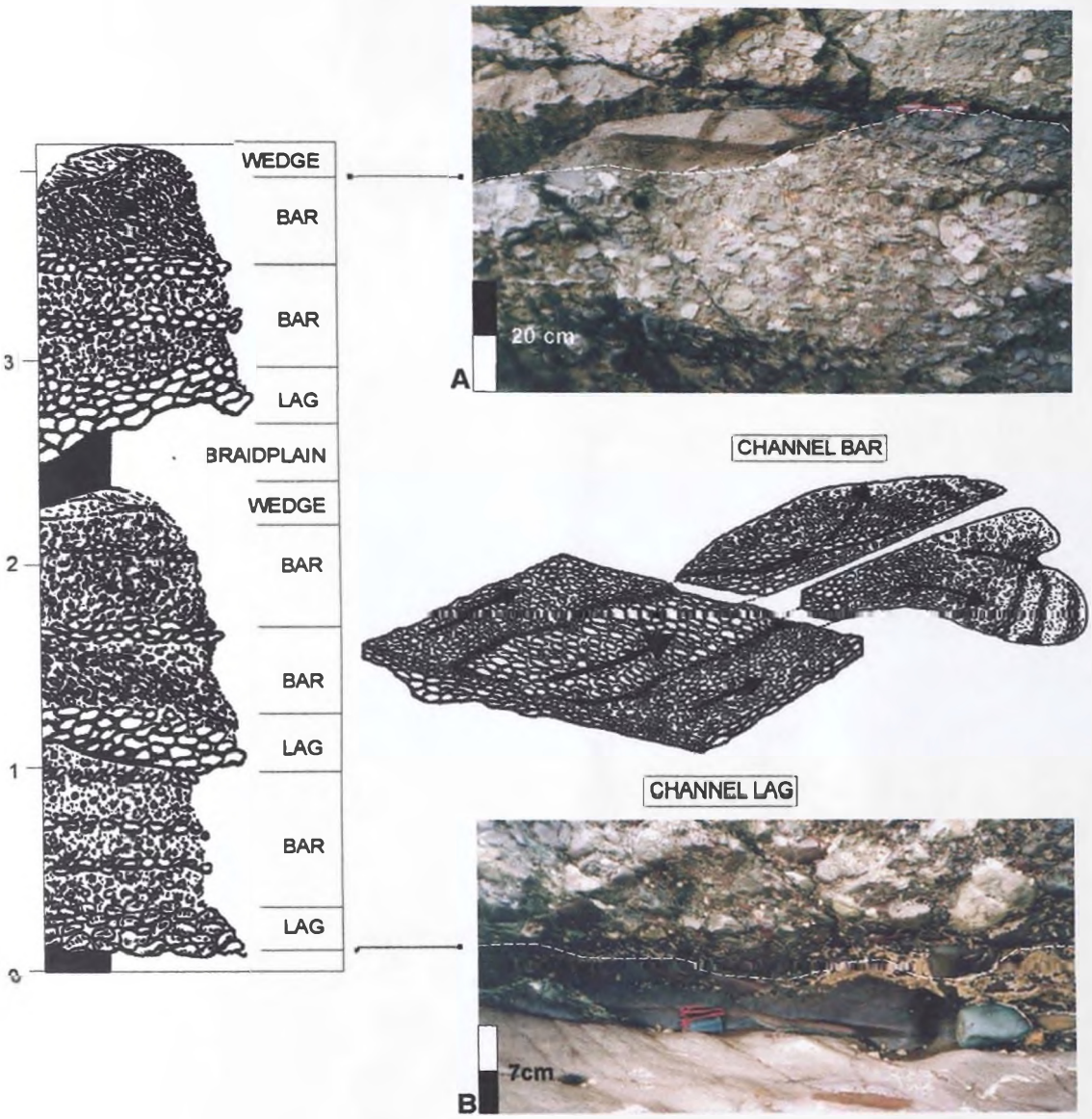



**Fig. 3.7.** Detailed log of braided stream facies exposed at Ogof Golchfa. Channel lag, channel bar and bar wedge correspond to Facies B1, B2, and B3 respectively. (A) Channel bar sheet and bar wedge – poorly developed parallel stratification and weak grading in bar sheet with some clasts in unstable positions. Bar wedge lies above a minor erosion surface and displays trough cross-bedding. (B) Channel lag sheet – pebble armour layer including purple rip-up clasts overlying purple braidplain sediments.

planar cross strata also occur. The latter typically displays a lateral transition to sub-horizontal stratification over a few metres. The direction of foreset migration is generally opposite to the direction of imbrication recorded in sub-horizontally stratified conglomerate, suggesting down stream accretion of the bedform. Two beds, one of which was figured by Crimes (1970a, fig. 3B), show large-scale (> 1m thick) foreset migration perpendicular to channel geometry and direction of imbrication, suggesting epsilon cross-bedding (lateral accretion).

*3.2.2.2.2. Interpretation*

The relative textural maturity, tractional clast fabric, stratification and gradational contact with channel lag deposits of Facies B1 strongly suggest a stream flow origin for the conglomerates. Well imbricated, sub-horizontally stratified conglomerate suggests sedimentation under high discharge levels as low relief bedforms such as longitudinal bars (Smith 1974, Boothroyd and Ashley 1975, Rust 1978) or diffuse gravel sheets (Hein and Walker 1977) deposited in an active channel tract. The lack of high-angle cross-stratification in this case indicates that the bars did not develop avalanche slip-faces, a characteristic common in shallow, powerful streams on relatively steep gradient slopes (Nemec and Postma 1993). In general, slip face foreset margins develop only if the flow depth/grain size ratio is >10 (Smith 1985), and therefore for Facies B2 gravels with an average grain size of 5 cm (max 19 cm), flow depth only averaged <0.5 m (max <1.9). An alternative explanation was offered by Hein and Walker (1977), who suggested that a period of reworking under lower flow conditions (when the rate of aggradation exceeds the rate of progradation) was necessary for the development of foreset margins. Thus rapid deposition of gravels under high flow conditions may not develop bedforms with foresets. Sedimentation under dominantly high stage conditions is also suggested by the consistency in direction of clast imbrication (Fig. 3.5), which has a high vector magnitude. Relatively low directional variance of gravel fabric was also noted by Bluck (1974), which he interpreted as a high stage indicator, when gravel is transported over channel bars with minimum deflection from the downslope direction. Weak grading reflects sedimentation under waning flow conditions by continuous accretion of progressively smaller clasts onto the bar. The openwork lower, and matrix-filled upper, framework reflects matrix winnowing and bypass during high stage, followed by falling-stage matrix infiltration (Bluck 1974).

Subordinate planar tabular cross-beds may have originated as either falling stage modification of longitudinal bars (Rust 1978; Maejima 1988) or as the internal

structure of migrating bedforms (typically medial and transverse bars) that were stable under flood conditions (Smith 1974; Rust 1978). The common transition into parallel-stratified conglomerate and the low dip angle of foresets favours development during falling stage modification (Kraus 1984). Epsilon cross-bedding was interpreted by Crimes (1970a) as evidence for point bar development in highly sinuous tidal channels. Considering the grain size of bank material and the lack of stabilising vegetation, long-term migration and progressive accretion in a meandering channel is considered unlikely (Long 1978). Instead, lateral accretion probably reflects rare instances of across-channel falling-stage accretion of a bar, a commonly reported feature in some pre-Devonian fluvial sequences (e.g. Long 1978; Allen 1983; Fedo and Cooper 1990). Although most bar forms overlie coarser grained channel lag deposits, implying a genetic link between channel scour and bar growth, there are instances when one bar directly overlies another. These bars without channel lags may record either unconfined flows (Massari *et al.* 1993) or development of secondary bars within the same channel tract. Where these bars are separated by an erosion surface (Fig. 3.7A), we can infer that another discrete flood event occupied the same channel. When the boundary is gradational or very weakly erosional, the bar probably developed as a secondary bedform in response to multiphase flooding, and became welded to the primary bar as outlined by Nemec and Postma (1993, p. 253).

*3.2.2.3. Facies B3: stratified lenticular sandstone and massive silty mudstone*

*3.2.2.3.1. Description*

This subordinate facies consists of trough cross-bedded, lenticular, coarse to granular sandstones that sharply and sometimes erosively overlie longitudinal bar conglomerates of Facies B2 (Fig. 3.7A). Upper surfaces are often truncated by the basal erosion surface of Facies B1, and they thus form the tops of fining-upward sequences. Bed thickness never exceeds 35 cm, and averages around 18 cm. In rare instances, these sandstones may in turn be overlain by red silty mudstone identical to the alluvial plain sediments of Facies A4 (Fig. 3.7B). At St Non's Bay, a silty mudstone horizon contains a thin lenticular mass of detrital haematite (Jones 1911). Sandstones are either wedge-shaped when positioned on the stoss side of longitudinal bars (as slip face accretionary bedforms) or channelled when eroded into the bar crest. In a number of examples, multiple wedges (Fig. 3.7A) develop that appear to "grow" up the lee side of the gravel bar.

*3.2.2.3.2. Interpretation*

Lenticular stratified sandstones, occurring as both wedges and small channels, are commonly documented features associated with deposition of flood-stage longitudinal bars in both modern and ancient fluvial sequences (Rust 1972, 1975; Fernandez *et al.* 1988; Marzo and Anadon 1988; Maejima 1988; Massari *et al.* 1993). By comparison with the Donjek River (Rust 1972, 1975), the sandstone wedges are low flood stage or normal discharge, perennial flow features developed at the lateral margins of exposed gravel bars. Rare preservation is a feature also consistent with the Donjek, where Rust (1972) reported wedges that failed to survive a later flood. Small channel-fills are also interpreted as relatively low discharge features and represent bar top or bar margin channels (chutes) incised during either late falling stage or early low stage flooding. Deposition of silt may record the eventual migration of the active tract of sedimentation away from the area, a feature characteristic of fine-grained deposition on the Donjek River (Rust 1978).

### 3.2.3. Lithofacies Association C

Good exposures of Facies Association C sediments occur at Ogof Golchfa (complete section, Fig. 3.2), St Non's Bay, and Ogof Goch (both top-truncated sections, Fig. 3.6). At all three localities, a cobble conglomerate lag deposit forms an abrupt base to the sequence, which locally lies with significant erosional relief on pebbly sandstones of Facies Association B (Fig. 3.8). A clear fining-upward motif is demonstrable (Fig. 3.2), from rounded polymictic conglomerate to well sorted fine-grained sandstone. Above the conglomerate, the sandstone takes on a green colouration, a diagnostic feature of the St Non's Formation.

*3.2.3.1. Facies C1: well segregated pebble conglomerate and coarse sandstone*

*3.2.3.1.1. Description*

This facies is represented by a 1.8–2.3 m thick, tabular sequence of stratified pebble-cobble conglomerate interdispersed with massive, sometimes pebbly very coarse to granular sandstone (Fig. 3.8). Conglomerate may be matrix or clast supported, with the latter dominant. The lower contact of this sequence is sharply erosional on either braided stream conglomerates of Facies Association B at Ogof Golchfa and Ogof

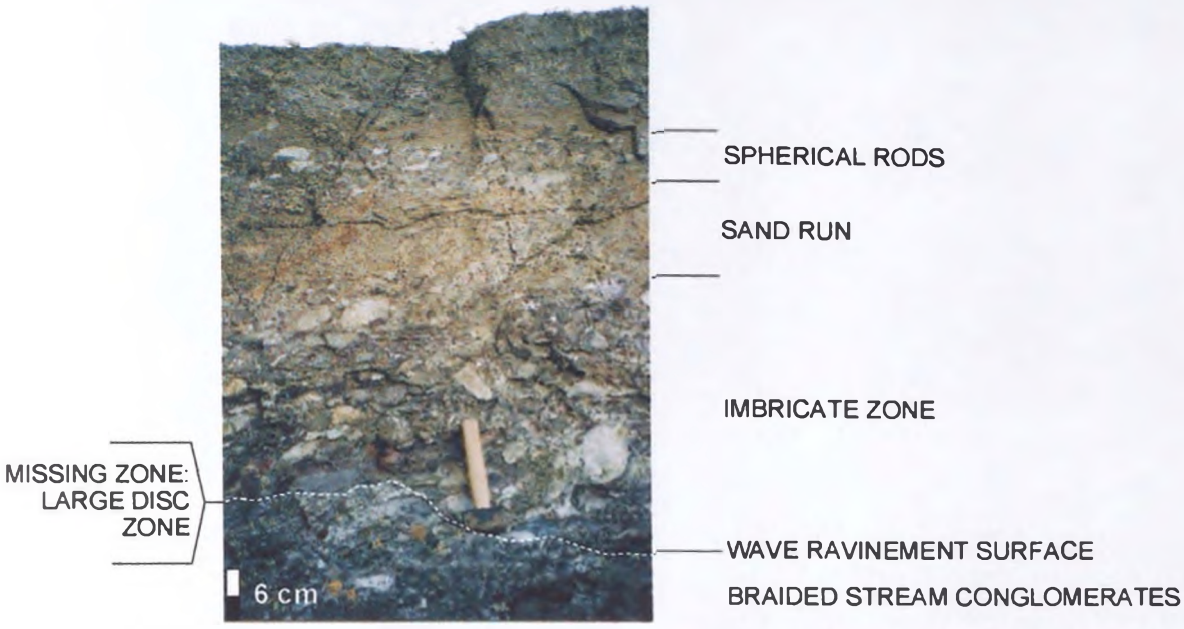



**Fig. 3.8.** Zonation of beach conglomerate above braided stream sediments at Ogof Goch.

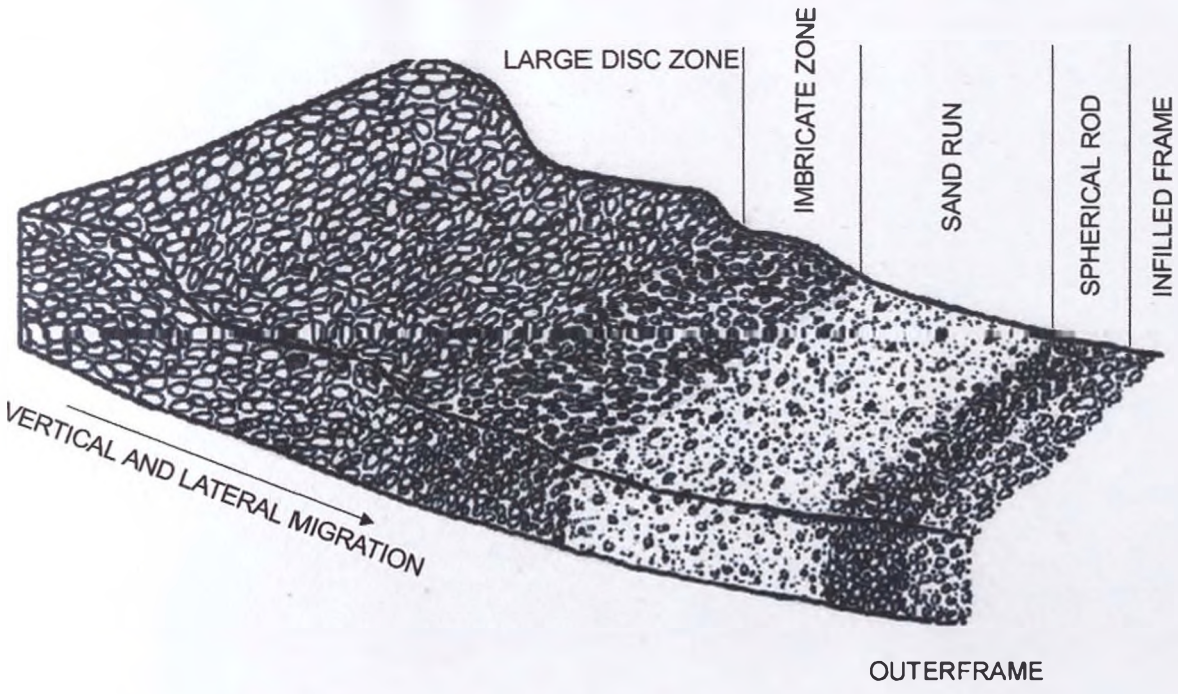



**Fig. 3.9.** Textural zonation of beach gravels at Sker Point, Wales (from Bluck 1967).

Goch (Fig. 3.8), or directly upon local Precambrian basement at St Non's Bay. The latter contact is an angular unconformity. The erosion surface is planar in some parts, but deeply scoured in others (Fig. 3.8), often with scour walls well above the angle of repose. Sediments above this surface are the coarsest in the whole facies association, forming a basal lag to the sequence. Internal erosion surfaces are infrequent lower in the profile, but relatively common towards the transition with Facies C2. Clast composition is directly related to the lithology beneath the erosion surface. This is demonstrated by comparing Figure 3.8 and Figure 3.10B, where the former (from Ogof Goch) contain quartz-rich metasedimentary clasts (e.g. quartzite, greenschist, schistose quartzite, and jasper), which are the most resistant lithologies from Facies association B, while the latter (from St Non's Bay) is composed entirely of purple and pink fragments of local Precambrian bedrock. Although both localities generally contain rounded clasts, the conglomerate above Facies Association B are exclusively very well rounded (Fig. 3.8) compared with a more mixed subangular to well rounded assemblage at St Non's Bay (Fig. 3.10B). This is due to the second cycle nature of the former, a conclusion verified by the presence of half rounds.

Beds are typically well sorted and extremely well segregated into horizontal horizons (9–38 cm thick) that show distinct vertical variations in the shape and size sorting of clasts (Fig. 3.8). This sorting has produced layers dominated by either disc and rod shapes or spheres and blades. Disc shaped clasts typically have a-axis parallel to bedding planes, and well developed easterly dipping imbrication (Fig. 3.5), opposite to that seen in the fluvial deposits of Facies Association B. A second mode exists towards the northeast. Stratification and grading are generally absent except for the overall fining upwards of the sequence, and one bed at Ogof Golchfa (figured in Crimes 1970a, his fig. 3A), which displays large scale (set height of 1.1 m) planar cross-stratification. This bed occurs beneath a conspicuous coarser grained unit that interrupts the general fining-upward. Massive sandstone interbeds have gradational upper and lower contacts with conglomerate, and are generally well sorted. Bioturbation by vertical burrowing organisms (*Skolithus*) are a conspicuous feature, although tube density never exceeds ichnofabric index 2 of Droser and Bottjer (1989). Another feature of these sandstones are delicate, roughly horizontal laminae rich in mica and heavy minerals (Fig. 3.10B), particularly haematite-rimmed magnetite.

*3.2.3.1.2. Interpretation*




**Fig. 3.10.** Sedimentological features of Facies Association C sediments. (A) Facies C2 (Ogof Golchfa) – low-angle onshore-directed cross-bedding in pebbly sandstones. These are interpreted as onshore-migrating megaripples deposited on a reflective high-energy shoreline. (B) Facies C1 (St Non's Bay) – beach conglomerates composed entirely of clasts of local Precambrian basement (Pebidian Supergroup). Pebbly sandstones interpreted as the sand run zone (see Fig. 3.9) contain biotite and muscovite laminae typical of high wave shear environments.

The accumulation of these beds in a shallow marine environment is unquestionable in the light of palaeontological evidence. The record of *Skolithus* suggests shallow, well-oxygenated water affected by persistent, relatively high-energy currents above a mobile substrate (Frey and Pemberton 1984). The laterally continuous bedding, excellent size and shape sorting, segregation of imbricated disc shaped pebbles and more spheroidal clasts, and the degree of clast rounding, reflect prolonged reworking and redistribution of sediment under high wave energy conditions (Clifton *et al.* 1971; Clifton 1973; Nemec and Steel 1984; Bourgeois and Leithold 1984; Hart and Plint 1989). Micaceous laminae rich in heavy minerals suggest wave shear (Clifton 1981), and deposition within the zone of breaking waves. By comparison with the features outlined in Table 3.1, Facies C1 is interpreted as a high gradient gravelly beachface (Bourgeois and Leithold 1984). East dipping imbrication is therefore considered as seaward inclined, suggesting east to west marine transgression at a high angle to braided river flow. The secondary mode to the northeast may reflect oblique wave approach; a characteristic previously noted from other modern (Ogren and Waag 1986) and ancient (Hart and Plint 1989) conglomerate beaches.

Vertical variation in shoreline gravels was studied by Bluck (1967b) in a number of gravelly beaches in South Wales. He recognised 4 main zones (Fig. 3.9) based on clast size, shape, sorting, and fabric: (1) an outer (seaward) frame, infilled with pebbles and sand, (2) an infill zone, with a frame of spheroidal clasts infilled and overlain by coarse sand devoid of pebbles termed the "sand run", (3) an imbricate zone, with imbricated disc shaped particles, and (4) an inner (landward) zone containing well sorted large discs. This vertical profile has been recognised in a number of modern and ancient beach successions (e.g. Marzo and Anadon 1988; Hart and Plint 1989; Rasmussen 2000). None of the studied localities preserve a complete sequence comparable to that outlined by Bluck (1967b). Instead the profile is "base-absent" (Fig. 3.8), with the imbricated zone directly overlying a very prominent erosion surface. This variation from the ideal sequence is probably related to the transgressive nature (fining-upward) of Facies C1 compared to the progradation (coarsening-upward) model outlined by Bluck (1967b). The missing "large disc zone" (Fig. 3.9) roughly equates to the washover deposit (Massari and Parea 1990), which lies landward of the zone of maximum wave activity. During transgression, erosion in the imbricate and infill zones will progressively remove facies in the landward direction producing a wave ravinement surface (Cattaneo and Steel 2003) as demonstrated in Figure 3.8. The amount of erosion that has taken place during ravinement is difficult to determine but may have been significant considering the "facies jump" from coarse-grained "medial" braided stream facies to

nearshore marine. Of particular significance is the total lack of sandy braided stream facies typical of more distal fluvial settings. The relatively steep irregular contact between Facies association B and Facies Association C, with scour walls in excess of the angle of repose has been used by some authors (e.g. Cheel and Leckie 1992) to suggest partial lithification of the sediment being eroded. If this is the case, then the ravinement surface may be better described as a diastem, of quite significant magnitude.

Based on a study of the Yallah's Fan Delta, Wescott and Ethridge (1980, 1982) devised a simple classification of beaches based on grain size, slope, width, sediment origin, and sediment supply rate. Their depositional beaches were preferentially located on active segments of the delta front, and were characterised by broad, gentle sloping foreshores with low gravel/sand ratios. In contrast, their erosional beaches (analogues of the destructive beaches of Vos and Eriksson 1977) are similar to those described here, with steep gradients and high gravel/sand ratios. As they are supplied solely by erosion of fluvial deposits (through ravinement), composition and grain size are inherited from the material being eroded (Wescott and Ethridge 1982). This is clearly the case in Facies C1, where clast roundness and composition are controlled by the geology beneath the ravinement surface (Fig. 3.8). Another important aspect of destructional onlap is the effect of transgression over a steep basin margin. The relatively high gradients inferred from Facies Association B would have lead to low rates of shoreline retreat, which significantly increases the depth of wave ravinement (Cattaneo and Steel 2003). This may account for the apparent jump in facies between Facies Associations B and C.

As a consequence of the relatively high depositional gradient, and the coarseness of much of the material being eroded, erosional profiles tend to induce reflective conditions on the foreshore (Wescott and Ethridge 1982). Steep inshore gradients substantially reduce the width of the zone of shoaling wave effects, so the incoming waves suffer little frictional attenuation and break directly on the shoreline with significant power (Reading and Collinson 1996). This reflective behaviour accounts for the excellent shape sorting, a feature related to the enhanced suspension potential of discs thrown onto the upper beachface during swash, and the greater pivotability of spheres rolled down the lower beachface during backwash (Bluck 1967b). Minor internal erosion surfaces may also be a consequence of direct wave impact. Similar scours have been recorded from modern beaches following storm events (Hart and Plint 1989). This documents an important phase of the beach cycle (Sonu and van Beck 1971) where the gravelly beach is degraded and clasts redistributed onto the shoreface during storms, only to be built up again by the

onshore asymmetry of wave-induced oscillatory flow. Although the backwash on gravelly beaches is significantly reduced through swash percolation, and therefore onshore flow greatly predominates (Fig. 3.5), the section at Ogof Golchfa records an anomalously coarse grained horizon in possibly the most distal location on the beach profile (interrupting the fining-upward sequence, Fig. 3.2). The association of this bed with large-scale cross-bedding (Crimes 1970a) suggests the existence of a plunge step cut into the base of the beachface, separating it from the shoreface. Cross-bedding formed by temporary migration of this step has been reported from reflective shorelines by Short (1984), Forbes and Taylor (1987), and Hart and Plint (1989). This depression tends to act as a locus for deposition of spheroidal pebbles rolled down the upper beachface during wave backwash.

*3.2.3.2. Facies C2: Trough cross-stratified coarse-grained sandstone*

*3.2.3.2.1. Description*

Facies C2 comprises amalgamated beds of tabular, coarse to granular sandstone characterised by trough cross-stratification (Fig. 3.10A). Set heights vary between 7–22 cm, while bed thickness ranges from 10–36 cm. Basal surfaces are either planar, or scoured into elliptical depressions (Fig. 3.10A). Although pebbles are not common in the sequence, occasional clasts occur on the lower foresets of trough cross beds. Micaceous laminae as well as vertical burrows are again common features, with the latter attaining a bioturbation index value of 3 in some of the thicker beds. Cross-bedding is unimodal towards the WSW (Fig. 3.5), which is onshore with respect to beach deposits of Facies C1

*3.2.3.2.2. Interpretation*

The abundance of cross-bedding, lack of mudstone interbeds, vertical burrows, and scoured erosion surfaces indicate strong traction currents in a shallow marine environment. The transitional contact with foreshore deposits of Facies C1, as well as onshore-directed palaeocurrents, micaceous laminae, and occasional pebbles indicate deposition in the zone of breaking waves, probably on the upper to lower shoreface (Clifton *et al.* 1971; Bourgeois and Leithold 1984; Leithold and Bourgeois 1984). Trough cross-stratified sandstones record the onshore migration of lunate megaripples above wave-base (Clifton *et al.* 1971; Bourgeois and Leithold 1984). In the high-energy nearshore environment of the modern Oregon coast, Clifton *et al.*

(1971) observed shoreward migration of lunate megaripples in medium to coarse sand. These bedforms were interpreted to have formed as the result of onshore-directed velocity asymmetry associated with long period swells. Under such conditions, the near bottom oscillatory currents are modified, with the shoreward flow under the wave crest becoming stronger and of shorter duration than under the wave trough, resulting in net landward translation (Komar 1976) and ultimately building of the beach of Facies C1. Vincent (1986) regarded shorewards bedload transport due to wave asymmetry as only important in water depths less than 10 m deep.

*3.2.3.3. Facies C3: hummocky cross-stratified sandstone*

*3.2.3.3.1. Description*

Facies C3 is composed of fine- to medium-grained sandstone either amalgamated into composite units (Fig. 3.11C) or rhythmically alternating with strongly bioturbated silty mudstone (Fig. 3.11B). The degree of bioturbation often reaches ichnofabric index 4 of Droser and Bottjer (1989) resulting in partial homogenization of sandstone as well as silty mudstone interbeds. The type of burrowing is difficult to determine but horizontal forms appear dominant with vertical burrows subordinate (Fig. 3.11B). Thin to medium bedded sandstones are broadly tabular (Fig. 3.11C), appear laterally extensive, and are composed of normally graded sandstone 5–33 cm thick. Sandstone bases are typically sharp and planar with no obvious large-scale relief or basal sole structures. Upper boundaries are invariably sharp, and display an overall hummocky topography with antiformal crest spacing ranging from 1–4 m. These large-scale symmetrical domal structures are largely non-erosional and appear to represent the original profile of preserved 3D bedforms. Internal stratification displays a fairly consistent three-fold internal division above the lower bounding surface. A complete vertical sequence contains the following gradational series of structures: parallel lamination; undulating lamination displaying low angle intersecting arches and troughs interpreted as hummocky cross stratification (HCS) (Fig. 3.11A); and small scale 2D wave and ripples. The hummocky cross-stratified division can often be traced laterally into parallel lamination.

Analysis of the hummocky cross-stratified division allows two types of cross-strata to be discerned. The commonest involves the vertical growth of a depositional hummock from parallel lamination (Fig. 3.11A). Growth continues over time by thickening of laminae over the aggrading antiform, and is similar to the accretionary HCS described by Cheel and Leckie (1993). The second bed configuration

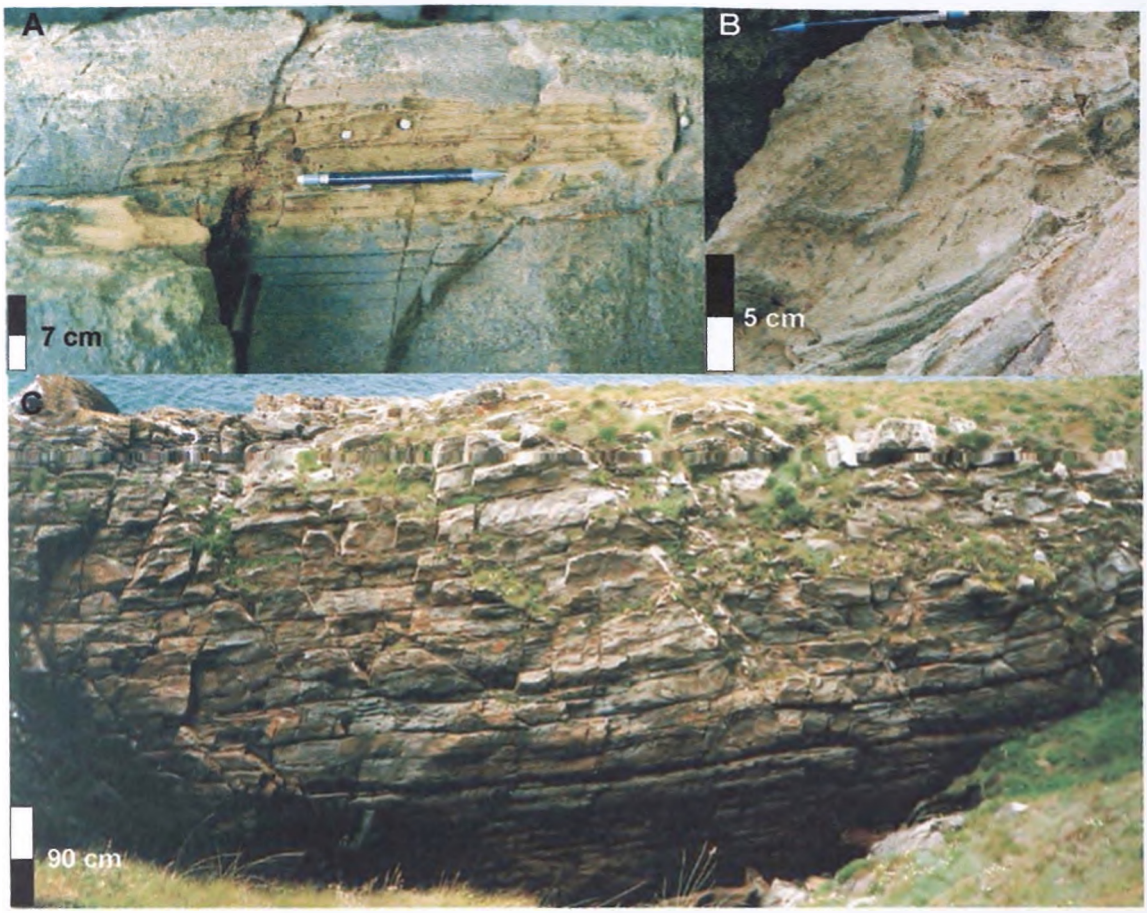



**Fig. 3.11.** Sedimentological features of Facies C2 at Ogof Golchfa. (A). Accretionary hummocky cross-stratification. Note the upward accretion of a depositional hummock by thickening of laminae over the growing antiform. (B) Horizontal and vertical burrows. (C) Amalgamated beds of hummocky cross-stratification. Note the bed thinning-upward trend typical of transgressive sequences.

commences with an undulating second-order internal erosion surface (Dott and Bourgeois 1982), which truncates parallel lamination below and forms a mantle for concordant laminae. A characteristic feature of this flat bed drape is thickening of laminae from domal highs into troughs, resulting in gradual infilling of the depression and ultimately a return to parallel lamination. Therefore the antiformal and synformal configuration is an inherited signature from the second order erosion surface that mimics the morphology of a stable bedform. Repeated scour and drape with several second-order erosion surfaces produces the morphological and geometrical characteristics that define scour and drape HCS (SD-HCS), as originally outlined by Harms *et al.* (1975).

*3.2.3.3.2. Interpretation*

The occurrence of hummocky cross-stratified sandstone alternating with bioturbated silty mudstone suggests a juxtaposition of contrasting energetics that is commonly associated with the alternation of fairweather suspension sedimentation and powerful storm-generated processes (Harms *et al.* 1975; Hamblin and Walker 1979; Dott and Bourgeois 1982; Brenchley 1985; Duke 1985, 1990; Duke *et al.* 1991). The preservation of fairweather fines reflects deposition in a more distal location than Facies C1, probably on the lower shoreface to inner-shelf (Harms *et al.* 1975; Brenchley 1985), a conclusion consistent with the dominance of horizontal over vertical burrows (Pemberton *et al.* 1992) and the greater degree of bioturbation (Hunter *et al.* 1979). Hummocky cross-stratified beds are similar to the idealised sequence (and its variants) proposed by Dott and Bourgeois (1982). HCS is considered to form under conditions of strong storm-wave oscillatory flow with a superimposed unidirectional geostrophic current, but disagreement exists concerning the relative magnitude of these currents (Leckie and Krystinik 1989; Duke 1990; Duke *et al.* 1991; Myrow and Southard 1996). A study of bed configurations by Arnott and Southard (1990) produced accretionary forms of HCS with form-concordant laminae thickening over stable antiforms under purely oscillatory or very oscillatory-dominant combined-flows. The addition of even a very weak unidirectional component resulted first in bedform migration, and under higher net flow velocities, total bedform washout forming an unusual quasi-planar lamination. The lack of anisotropic forms of HCS reflecting bedform migration argues against any significant unidirectional flow during deposition. The mode of emplacement of sand onto the inner shelf under very oscillatory-dominant combined-flows is adequately accounted for by the model for storm sedimentation proposed by Duke *et al.* (1991).

| Characteristic features | Alluvial fan | Beach |
|---|---|---|
| Sorting | Poor | Good |
| Clast segregation (disc/blades, spheres/rods | Poor | Good |
| Bed continuity | Broadly lenticular | Continuous |
| Interbedded pebbly sandstones | Common | Rare |
| Erosional basal contact | Rare/common | Rare |
| Imbrication | Landward | Seaward |
| Sphericity | High | Low |
| Rounding | Low | High |
| Heavy mineral and mica concentrations | Rare/common | Very common |
| Thickness | > 3 m | < 3 m |
| Preservation potential | Moderate | Very low |
| Clast composition | Exotic or local | Local |
| Repetitive small fining-upward sequences | Rare/common | Rare |
| Bioturbation (Cambrian examples) | Never | Common |
| Lower flow regime stratification | Very rare | Common |
| Correlation coefficient between MPS/BTh | High - Low | Very low |
| Palaeocurrents | Unimodel and divergent | Bimodel (onshore-dominated) |

**Table 3.1.** Contrasting features of beachface and alluvial fan facies based on studies by Wescott and Ethridge (1980, 1982), Bourgeois and Leithold (1984), Leithold and Bourgeois (1984), Nemec and Steel (1984), and Hart and Plint (1989).

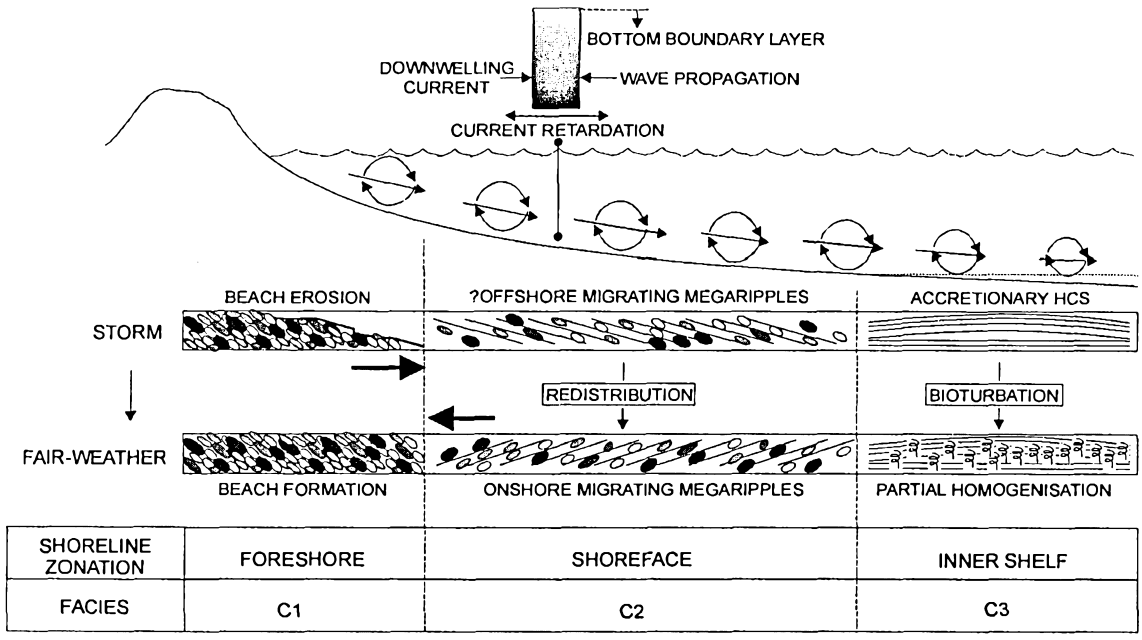



**Fig. 3.12.** Storm flow hydrodynamics on a high-energy gravelly reflective shoreline based on features present in Facies Association C.

| Characteristic features | Alluvial fan | Beach |
|---|---|---|
| Sorting | Poor | Good |
| Clast segregation (disc/blades, spheres/rods | Poor | Good |
| Bed continuity | Broadly lenticular | Continuous |
| Interbedded pebbly sandstones | Common | Rare |
| Erosional basal contact | Rare/common | Rare |
| Imbrication | Landward | Seaward |
| Sphericity | High | Low |
| Rounding | Low | High |
| Heavy mineral and mica concentrations | Rare/common | Very common |
| Thickness | > 3 m | < 3 m |
| Preservation potential | Moderate | Very low |
| Clast composition | Exotic or local | Local |
| Repetitive small fining-upward sequences | Rare/common | Rare |
| Bioturbation (Cambrian examples) | Never | Common |
| Lower flow regime stratification | Very rare | Common |
| Correlation coefficient between MPS/BTh | High - Low | Very low |
| Palaeocurrents | Unimodel and divergent | Bimodel (onshore-dominated) |

**Table 3.1.** Contrasting features of beachface and alluvial fan facies based on studies by Wescott and Ethridge (1980, 1982), Bourgeois and Leithold (1984), Leithold and Bourgeois (1984), Nemec and Steel (1984), and Hart and Plint (1989).

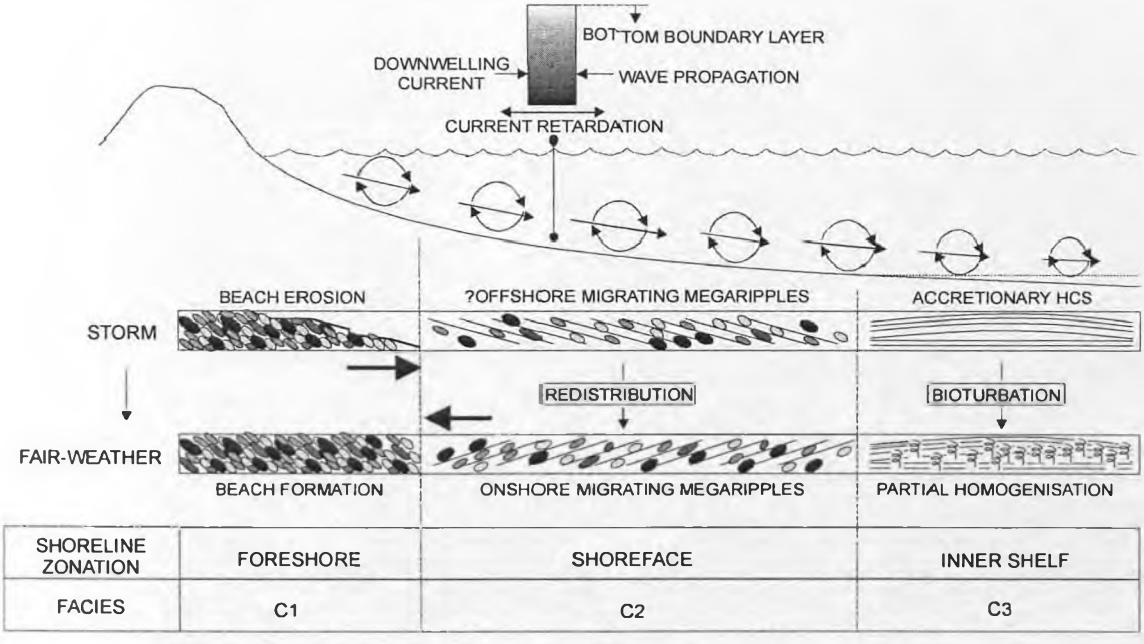



**Fig. 3.12.** Storm flow hydrodynamics on a high-energy gravelly reflective shoreline based on features present in Facies Association C.

Parallel lamination found below HCS is more difficult to quantify in terms of relative combined-flow components (Myrow and Southard 1991), as the flat bed depositional regime may develop under purely oscillatory flow, purely unidirectional flow, or a full range of intermediate combined-flows if the flow components are sufficiently powerful. Purely oscillatory, or very oscillatory-dominant combined-flows are preferred due to the vertical and lateral association with isotropic HCS (Craft and Bridge 1987), and the lack of flute casts, a common unidirectional flow indicator in storm deposits (Myrow and Southard 1996). Like parallel lamination, SD-HCS is difficult to interpret, as the synformal and antiformal configuration is inherited from second-order erosion surfaces that only mimic the morphology of a stable bedform. Because laminae are flat bed drapes, they have more in common with upper flow regime plane bed depositional regimes than either oscillatory or unidirectional bedforms, and subsequently cannot be modelled in terms of bed configurations produced experimentally. Therefore, the transition from parallel lamination to SD-HCS does not signify an appreciable change in flow regimes, and both are interpreted as high-energy oscillatory-dominant combined-flow structures. The difference in stratification is solely the result of irregular second order internal erosion surfaces. These may simply record the temporary development of exceptionally high constructive waves, as reported from the mid-Atlantic shelf by Swift *et al.* (1983).

## 3.3. PALAEOENVIRONMENT AND IMPLICATIONS FOR BASIN MARGIN EVOLUTION

### 3.3.1. Facies Association A: alluvial fan sedimentation

The interbedded assemblage of fluid gravity flow (HFF) and sediment gravity flow (debris flow) deposits is consistent with the unique hydraulic properties created by the geomorphological setting and composite morphology of alluvial fans (Blair and McPherson 1994). The major attributes of the alluvial setting that promote these hydraulic conditions include high gradient slopes (symptomatic of their linkage between tectonically controlled upland drainage basins and lowland sedimentary basins), a mantle of poorly sorted colluvium derived from upland weathering, and heavy rainfall events. These features strengthen the role of catastrophic flooding and supercritical flow conditions resulting in deposits that are coarse, texturally immature, and with few sedimentary structures attributable to traction flow.

The two coarsening-upward sequences (Fig. 3.2) with debris flows preferentially occupying the upper reaches is consistent with two discrete phases of progradation (Nemec and Steel 1984). Although polydirectional palaeocurrent data from clast imbrication are slightly biased towards WSW dipping (Fig. 3.5), suggesting fan progradation roughly to the east. The dominance of cohesionless debris flows and HFF provides evidence for: (1) presence of a feeder channel draining a small steep hinterland catchment area (Stokes and Mather 2000), (2) intense but infrequent precipitation (flash floods in a semi-arid climatic belt), (3) a source area conducive to the production of clay deficient colluvium (Blair 1999), and (4) steep fan gradients to maintain grain dispersions (typically between 5–15°, Blair and McPherson 1994). The restricted clast assemblage documented in Facies Association A is consistent with a small catchment area, while their psammitic origin would not produce significant quantities of clay. Haematite staining on both quartz grains (in thin section) and clasts also suggests a semi-arid climate. Although steep gradient slopes are a prerequisite for debris flow formation, the occurrence on the fan surface of ephemeral ponds at the base of the second coarsening upward-sequence (Fig. 3.2), and plug debris flows towards the top, imply periods of both rapid reductions in gradient (in the case of ponding) and more gradual flattening of the depositional profile (in the case of plug debris flows). Deposition of shales associated with the development of standing water suggests rapid alluvial plain downwarping (Crews and Ethridge 1993), while the gradual reduction in slope is the typical alluvial fan response to radial extension (essentially the stage 2 to 3 transition outlined in Blair and McPherson 1994, fig. 20), supporting the inference of progradation during upwards coarsening.

These features are comparable to the debris flow fans of Harvey (1984), the Type I alluvial fans of Blair and McPherson (1994), and the footwall derived fans of Gawthorpe and Colella (1990). According to Blair and McPherson (1994), these characteristics delineate specific palaeotectonic conditions including: (1) the geomorphic juxtaposition of a bedrock block and an actively subsiding basin (i.e. a piedmont setting), (2) presence of a zone of regional subsidence associated with either crustal extension or transtension, (3) presence of a dip-slip or strike-slip fault at the boundary between the bedrock block and the sedimentary basin, and (4) close proximity (<5-10 km) to the basin margin fault. Although there is no evidence in the field for a once active fault scarp, palaeocurrent data combined with the likely lateral sediment derivation with respect to the fault, imply a source located west of Pembrokeshire (see Fig. 3.1B). The lack of local basement clasts in over 90% of Facies Association A conglomerates suggests that the fault may have been a major

structural lineament juxtaposing blocks of greatly different lithological and metamorphic character.

The significance of cohesive debris flows derived from colluvium shed from local bedrock is more difficult to determine because the source clearly played no obvious role in the generation of over 90% of deposits on the alluvial fan surface. As cohesionless dispersions are the dominant mode of transport, it must be assumed that the basin margin fault block yielded very little clay, a conclusion consistent with the metasedimentary clast assemblage. Cohesive debris flows by contrast demand sufficient clay in the dispersion to provide matrix strength, the main clast support mechanism. This was probably accomplished by weathering of the local Precambrian volcaniclastics, and particularly the breakdown of plagioclase, thus yielding sufficient amounts of clay to produce colluvium that would readily transform into a cohesive debris flow upon failure (Blair 1999). The apparent lack of mixing between these 2 disparate source areas raises the question of where did this local topographic expression lie with respect to the basin margin fault? Due to poor exposure of the Ogof Golchfa Formation throughout the region, only a tentative suggestion can be proposed. A basic cross section (Fig. 3.6) from St Non's Bay in the southeast, to Ogof Goch in the southwest (roughly 90° to the direction of fan progradation), suggests that these localities may have been minor topographic highs during alluvial fan sedimentation. It is conceivable that cohesive debris flows were shed from relief unrelated to the main fault activity, and dispersed at a high angle across the trend of main fan progradation. Cohesionless debris flows may therefore have been preferentially directed into a small pre-existing valley following the first episode of major fault activation. Although the lack of palaeocurrent data from cohesive flows prevents verification of this process, this interpretation may explain why the Ogof Golchfa Formation lies on Precambrian rocks of such varied age (Green 1908, p. 376). Localities such as St Non's Bay record a Cambrian overstep sequence resting on far older Precambrian arc volcanics than for example at Ogof Golchfa (Fig. 3.6). This would be expected from areas acting as palaeovalley walls where deeper-seated erosion would occur.

An interesting feature of Facies Association A conglomerates is the occurrence of partially rounded clasts in cohesionless debris flows (Fig. 3.3D). This poses a problem in interpretation as the processes inherent to debris flow deposition do not lead to clast rounding (Martins-Neto 1996). This problem is compounded by the presence of angular clasts of identical composition dispersed with partially rounded types, and the fact that HFF deposits contain a less rounded clast assemblage (Fig. 3.3B) despite turbulent conditions being operational in the earliest

phase of their flow evolution (Todd 1989). It is clear that some of the material incorporated into debris flows underwent prior reworking, but the lack of half-rounds and clasts of conglomerate indicate that these characteristics were not inherited from a previously deposited conglomerate. These features can be accounted for by Schumm's (1973) concept of geomorphic threshold. If we consider a poorly sorted (in this case sand to boulders) mass of colluvium collecting in a feeder canyon, the coarsest material (cobbles and boulders) will only be mobilised during the most catastrophic rainfall events (Levson and Rutter 2000) or after sufficient time has elapsed to make the pile susceptible to failure (Heward 1978). It follows therefore that cobbles and boulders have a higher residence time in the canyon than the more easily liberated sand, granules and pebbles. Therefore smaller magnitude trigger events may induce a fluid gravity flow, or a small debris flow that transforms (*sensu* Fisher 1983) into a fluid gravity flow, while at the same time rounding cobbles and boulders trapped in the feeder canyon. These more frequent and thus less concentrated flows will not only contain a greater proportion of angular to rounded clasts but also produce a deposit with abundant sandy matrix, an observation consistent with HFF deposits of Facies A3 (Fig. 3.3A). During a more catastrophic rainfall event or after a protracted period of cobble-boulder build-up, the whole mass of colluvium (including reworked cobbles and boulders and fresher, angular material added since the last flood) would fail together, producing a sediment gravity flow ranging in clast size from pebbles to boulders. Considering the multiple phases of prior reworking, the debris flow deposit is typically matrix poor, has a high percentage of rounded clasts, but at the same time contains some angular material.

This detailed account of Facies Association A provides compelling evidence for alluvial fan sedimentation at the base of the Cambrian in SW Pembrokeshire. As it is widely recognized that alluvial fans are preferentially located in areas of active tectonism (Massari and Colella 1988, and references therein), and thus delineate specific palaeotectonic elements applicable to the early evolution of the Welsh Basin, the previous, widely accepted interpretation of the sequence as a simple transgressive beachface (Crimes 1970a; Rushton 1974; Cope and Bassett 1987; Prigmore and Rushton *et al.* 2000) requires further discussion. This is particularly so as that interpretation leads to a picture of overall tectonic quiescence, a traditional viewpoint still upheld in recent textbooks (e.g. Woodcock 2000). A list of common features typical of beachface and alluvial fan deposits are presented in Table 3.1. The beachface interpretation offered by Crimes (1970a) relies heavily on clast rounding and bioturbation, but his account does not specify where in the 45 m+ conglomerate succession bioturbation occurs. In fact, the lower 40 m (Facies

Associations A and B in this study) contain no evidence of biogenic activity. The mechanism for clast rounding outlined above has been reported from other alluvial fan successions (e.g. Wasson 1977; Desloges and Gardner 1984; Martins-Neto 1996), while poor sorting, positive linear correlations between MPS and BTh, unimodal palaeocurrents, exotic clasts, and lack of significant amounts of local bedrock material are not consistent with derivation from ravinement processes associated with marine transgression. There are no known occurrences of 40 m thick gravelly beach sequences (Stokes pers. comm. 2001), while northwest dipping imbrication (also reported by Crimes 1970a) suggests a beach facing a basin to the southewest, the complete reverse of that expected from Welsh Basin palaeogeography (Jones 1938; Crimes 1970a; Rushton 1972; Brasier *et al.* 1992). If clast imbrication is taken as "upstream dipping", a feature typical of alluvial environments (Nemec and Steel 1984), the source block lay to the southwest and basin to the northwest, which is consistent with Welsh Basin dimensions and the location of the proposed source area based on detailed petrography (discussed below). By way of contrast, true gravel beach sequences deposited during Lower Cambrian transgression in the Welsh Basin were described by Cope and Rushton (1992), Wright *et al.* (1993), and Rushton *et al.* (2000).

### 3.3.2. Facies Association B: braided stream sedimentation

The observed variety of deposits and their vertical arrangement resemble those described from modern and ancient proximal gravelly braided streams (Boothroyd and Ashley 1975; Miall 1977, 1978; Rust 1978; Allen 1983; Kraus 1984; Nemec and Steel 1984; Fernandez *et al.* 1988; Marzo and Anadon 1988; Nemec and Postma 1993). In particular, Facies Association B sediments closely resemble deposits of the Scott glacial outwash model (Boothroyd and Ashley 1975) established by Miall (1977, 1978), and the proximal Donjek River sediments described by Rust (1972, 1975). A proximal location with respect to the drainage basin is suggested by the coarse clast size, the lack of significant sand facies, and the exclusion of well-developed trough cross-stratified conglomerate. Sedimentation is inferred to have taken place within a distributary network of shallow channels that repeatedly divided and rejoined due to the formation of low relief longitudinal bars. This network style is promoted by bank instability, high water discharge, steep gradients, and large bedload, features consistent with both the unvegetated setting of the Cambrian, and the stratigraphic association with alluvial fan sediments. These factors may have also contributed to

the effective bypassing of fines through the system, although the lack of clay in particular must also have influenced by the quartz-rich source area.

The small-scale fining-upward sequences (Fig. 3.7) are the typical stratigraphic expression of variable water discharge braided streams, and record either gradual channel abandonment or simple waning-flow (Nemec and Steel 1984). The interaction of channel scour (Facies B1) and bar growth (Facies B2), as well as the texture and fabric inherent to these processes are consistent with waning flow sedimentation from a discrete flooding episode (Nemec and Postma 1993). Recorded phases include peak flood stage (channel lag), high flood stage (bar accretion), falling flood stage (bar modification) and low flood stage (sand wedge and bar dissection). It is difficult to ascertain whether low water features are strictly low flood and thus entirely ephemeral, or if a modifying perennial component exists. The lack of compound cross-bedding (Massari *et al.* 1993), evidence for sand wedge reactivation either as separate bedforms or foreset erosion, apparent semi-arid climate, and association with high gradient alluvial fan sediments are features more consistent with ephemeral conditions, although some perennial modification cannot be discounted.

The transition from alluvial fan to braided stream (Fig. 3.2) clearly records a profound change in sediment dispersal processes and water/sediment discharge ratios. Apart from the obvious switch to confined flow and fully Newtonian, sub-critical processes, this evolution also includes a significant increase in clast variability and thus erosion of a more varied source area, a greater degree of clast rounding, better sorting, higher compositional maturity, and an overall reduction in percentage conglomerate and clast size, particularly MPS. These features are consistent with a less catastrophic response to flood trigger mechanisms, reflecting flood episodes with longer duration and significantly lower discharge peaks (Blair and McPherson 1994). Although the transition from alluvial fan to braided stream appears to be a common evolutionary phase, and has been recorded from a number of modern and ancient basin margin settings (Marzo and Anadon 1988; Nava-Sanchez *et al.* 1995; Kostachuck *et al.* 1986; Rasmussen 2000; Stokes and Mather 2000; Benvenuti 2002; Cox *et al.* 2002), the fundamental controls that promote these changes are complex and poorly understood (Collinson 1996).

Contributing factors that may increase the water/sediment ratio and thus induce a more fluvial-style of deposition include a switch to longitudinal drainage with significantly lower gradients and larger hinterlands (Gawthorpe and Colella 1990), recession of the watershed through catchment enlargement (Orton 1988; Stokes and Mather 2000), or a regional climatic change from semi-arid to more humid conditions

(Benvenuti 2002). Entrenchment of the fan surface by braided distributaries may also be promoted by a change in source rock geology (Collinson 1996), or a reduction in gradient (Kostachuck *et al.* 1986) induced by either a protracted period of alluvial fan progradation (Blair and McPherson 1994), or source area denudation and scarp retreat (Heward 1978, fig. 6B). The apparent ephemeral nature of braided stream deposition, as well as red siltstones and a mass of detrital haematite suggests continuation of semi-arid conditions into Facies Association B, and thus a significant change in climatic conditions may be rejected as a primary control. The same can be said for source rock geology, which although clearly more varied, is unlikely to have imparted a major change in transport load. A change from transverse to longitudinal drainage is a well documented phase in rift basin evolution (Gawthorpe and Colella 1990; Wescott and Ethridge 1990), but is considered an unlikely scenario in the present study considering similarities in palaeoflow (Fig. 3.5) and source rock lithology.

Instead, the evolution to braided streams appears to be a direct consequence of catchment area expansion aided by a significant reduction in overall gradient and source area denudation (scarp retreat). This is suggested by the more varied clast assemblage in Facies Association B, the fining-upwards trend (Cox *et al.* 2002), and the stratigraphic position of braided stream conglomerates above a major phase of alluvial fan progradation (Fig. 3.2). This reduction in gradient may also account for the increase in sorting, clast rounding, and compositional maturity, as the residence time for material on the surface is greatly expanded, with the likelihood of repeated transport and storage cycles (Jo *et al.* 1997). All these factors, together with the geomorphic maturity of the hinterland, imply declining tectonic activity after the phase of tectonism that initiated alluvial fan sedimentation.

### 3.3.3. Facies Association C: transgressive marine sedimentation

The temporal evolution of depositional environments evidenced in Facies Association C sediments record simple marine transgression over a coarse-grained and relatively high-gradient braidplain. This developed roughly east to west, with the coastline orientated north-south, perpendicular to fluvial channels. The nature of destructive onlap, as outlined by Vos and Eriksson (1977) and Wescott and Ethridge (1980, 1982) dictates the character of the nearshore in terms of gradient, grain size, and the coastal response to fairweather and storm waves. The well segregated gravelly beach, onshore-directed currents, narrow shoreface (based on the stratigraphic thickness of Facies C2, Fig. 3.2), and negligible tidal signature are features typical of

high-gradient reflective shorelines, where waves break directly on the coast. The hydrodynamic regimes experienced on these coastlines are controlled principally by the steep gradient and pebbly foreshore. By limiting frictional attenuation and thus enhancing the velocity asymmetry of orbital currents, and reducing the significance of backwash through high swash percolation, currents across the shoreface have a strong onshore component, particularly during storms, when sediment is more likely to be mobilized.

There are surprisingly few published accounts of coarse-grained storm deposits, and even fewer examples from reflective coastal profiles. Case studies from dissipative shorelines highlight the role of powerful unidirectional currents in sediment transfer offshore (Hamblin and Walker 1979; Galli 1989; Myrow 1992a; Arnott 1993; McKie 1994; Siringan and Anderson 1994; Perez-Lopez 2001). In cases where coarse-grained material is available on the foreshore, these currents are capable of transporting pebbles and coarse sand beyond the fairweather wave-base and out onto the shelf (e.g. DeCalles 1987; Galli 1989). Sedimentary structures such as cross-bedding (Swift *et al.* 1983), quasi-planar lamination (Arnott 1993), anisotropic HCS (Midtgaard 1996), and flute casts (Myrow and Southard 1996) in the resultant deposit clearly record the interplay between waves and powerful unidirectional currents in variably developed combined-flows. The importance of net offshore flow on reflective coastlines is less certain but, based on the restriction of conglomerates to the shoreface and above fairweather wave-base, and the dominance of accretionary forms of HCS in this study and others (e.g. Leithold and Bourgeois 1984; Cheel and Leckie 1992), it appears likely that unidirectional currents are less significant in a hydrodynamic regime dominated by oscillatory motion.

This inverse correlation between wave power and unidirectional flow velocity appears counter intuitive, but oceanographic data from analogous shoreface and inner-shelf settings summarized by Snedden and Swift (1991), and theoretical considerations by Grant and Madsen (1979) suggest that in wave-dominated cases, offshore current flow is actually retarded in the wave boundary layer by asymmetrical (onshore) wave orbital motion. A simple model outlining foreshore, shoreface, and inner shelf dynamics during storm and fairweather conditions on a reflective coastline is presented in Figure 3.12. During set up phases, an oscillatory dominant combined-flow develops with an overall net offshore component, as depleted unidirectional currents slightly amplify the offshore wave stroke (Duke 1990). This oscillatory-dominant combined-flow drives pebbles and sand offshore, possibly as megaripples (Cheel and Leckie 1992), as far as fairweather wave-base, while fine to medium sand is transported onto the shelf and reworked into purely oscillatory or very oscillatory

dominant combined-flow structures such as accretionary HCS. Post-storm reworking and redistribution by fairweather waves drives the coarse material on the shoreface back towards the shoreline forming steady state megaripples, while at the same time rebuilding the beach after storm erosion.

The stratigraphic association of braided stream conglomerates and nearshore marine deposits, might suggest that the sediments of Facies Association C formed part of an actively transgressing braid delta complex. Because these systems, like alluvial fans, require unique geomorphological and hydrological constraints, and are thus associated with certain palaeotectonic elements, it is critical for palaeogeographical reconstructions that the distinction is made between deltaic and non-deltaic coastlines. One might assume that a coastal perturbation built exclusively by fluvial processes would be readily determinable in ancient successions. Although this is generally the case in progradational sequences were fluvial discharge tends to dominate over marine processes, transgressive sequences, due to reduced sediment flux, have delta front coastal facies indistinguishable from those of wave-dominated non-deltaic shorelines. Examples include the destructive beachfaces of the Yallah's Delta (Wescott and Ethridge 1980, 1982) and numerous small fan-deltas off the Baja California Peninsula (e.g. Nava-Sanchez *et al.* 1995, 1999). In these instances, low sediment flux to the delta front encourages almost complete reworking of fluvially derived material by fairweather waves, resulting in coastlines dominated by steady-state features similar to those recorded on non-deltaic shorelines.

To qualify the coastal system as a braid delta (*sensu* McPherson *et al.* 1988), we would ideally require evidence for interfingering of fluvial processes (including those developed in the subaqueous realm through flow transformation) with nearshore marine dynamics. For example, the friction-dominated mode of sediment dispersal common in braid deltas (Martinsen 1990) would be expected to produce frequent, but rather inefficient (*sensu* Mutti *et al.* 1996, 2000) hyperpycnal underflows, that build either mouth bars or Gilbert-type foresets (depending upon water depth in the receiving basin) through rapid flow deceleration at the river mouth. We might also expect some evidence of marine encroachment onto the braid plain during active channel dissection (Fedo and Cooper 1990), although the preservation potential of these sediments would be low during transgressive phases if ravinement processes were active. Additional features typical of coastal systems experiencing some form of modification by fluvial discharge events include a high directional variance in palaeoflow due to shoreline protrusion, a strong aggradational element even during retrogradation (e.g. backstepping parasequences) as sediment supply will often exceed rates of accommodation space creation (Cattaneo and Steel 2003),

secondary resedimentation processes and slope failure (Colmenero *et al.* 1988), high and low density hyperpycnal turbidity currents preserved below fairweather wave-base (Mutti *et al.* 2000; Mulder and Alexander 2001), incised channels dissecting the beachface acting as feeders to the delta front and slope (Martinsen 1990), and finally, in Cambrian examples, an additional stress for nearshore organisms of fluctuating salinity levels associated with high magnitude flood discharge events. The latter may result in a low bioturbation index.

As none of these features are present in Facies Association C sediments, we can say with some certainty that there is no genetic relationship between fluvial and nearshore marine systems, and they appear quite separate in both time and space. Indirectly of course, marine encroachment of the coarse-grained, high gradient braid plain controls the shoreline response to shoaling waves, leading to reflective coastal behaviour. As outlined in Figure 3.12, this essentially dictates shelf dynamics and the character of nearshore deposits. Finally, this interpretation also solves the problem of the apparent facies jump at the wave ravinement surface, where beachface sediments directly overlie medial braided stream deposits (Fig. 3.2). This unconformable relationship in terms of facies belts must be expected if the environments above and below the ravinement surface have no genetic linkage.

## 3.4. PETROGRAPHY AND PROVENANCE ANALYSIS

### 3.4.1. Methodology

This petrographic study was conducted on 29 samples spanning lithofacies A through C as exposed in the cliff sections between Ogof Golchfa and Porthselau. A minimum of 400 framework grains were counted per thin section to ensure a two-sigma confidence range of 5% or less of the whole rock for any calculated model percentage (van der Plas and Tobi 1965). In addition, 100 quartz grains in each section were counted to determine quartz type as outlined by Basu *et al.* (1975) and Tortosa *et al.* (1991). Cement and (pseudo)matrix (<0.03 mm) were not counted (Dickinson 1970), while slides with more than 20% matrix were omitted (Dickinson 1985). Feldspar was recognised on the basis of its cloudy appearance, cleavage, twinning, and diagenetic alteration rather than utilising staining techniques, as this was found to obscure important metamorphic textures, a problem encountered in a number of other studies (Dorsey *et al.* 1988). Feldspar and lithic grains, regardless of their degree of alteration or replacement were classified as these grain types if they

could be positively identified on the basis of remnant extinction and texture. Recognition of such altered grains is critical in provenance studies because diagenetic processes can alter the depositional composition of sand (Cox *et al.* 2002). Although many authors recommend the universal application of the Gazzi-Dickinson (GD) point-counting method for determining model composition, as the counting of minerals >0.63 mm within lithic fragments as monomineralic grains reduces the model dependency on grain size (Dickinson and Suczek 1979, Ingersoll *et al.* 1984), the traditional method (Zuffa 1985) is preferred in this study following considerations by Decker and Helmond (1985), Suttner and Basu (1985), and von Eynatten and Gaupp (1999). This approach better accounts for the variety of lithoclast types, especially in coarse-grained syn-orogenic deposits (von Eynatten and Gaupp (1999), where even the GD method is not truly independent of grain size (Bangs Rooney and Basu 1994). Therefore the focus is on maximum source rock information (that is, the variety of lithoclast types), while the problem of grain size is minimised by restricting sampling to coarse-grained sandstones as proposed by Zuffa (1985), and Decker and Helmond (1985).

Framework modes have been summed through recalculation and normalization into 8 grain categories widely used for purposes of comparative petrography. These categories and recalculated percentages of different detrital modes are described in Table 3.2. The relative percentages of recalculated parameters that are used to determine provenance are displayed in Table 3.3, and may be divided into grain assemblages (QFL, QmFLt, Folk 1980, Dickinson 1985), and framework lithic grains (QpLvmLsm, Dickinson and Suczek 1979; Ingersoll and Suczek 1979). Note that Samples 21 through 29 (Table 3.3) have a total lithic component too low for meaningful framework analysis thus QpLvmLsm recalculations were deemed unnecessary. Following standard convention, model data are presented on ternary diagrams (Fig. 3.13) with superimposed plate tectonic provenance fields devised by Dickinson *et al.* (1983) with some minor modifications by Dickinson (1985). The QFL data emphasise framework grain stability by grouping all quartzose types together, while provenance is emphasized by recasting the data with polycrystalline quartz and chert included in lithic fragments (QmFLt). Following recommendations proposed by Graham *et al.* (1976) and Ingersoll and Suczek (1979), sedimentary and metasedimentary lithic grains were included together as Lsm, because of the operational difficulties in consistently differentiating, as end-member types, grains that belong to a continuum. Although in many cases differentiation is possible by the alignment of certain crystals such as mica (tectonite

Q–F–L:

Q = Qm + Qp, where:
Q = Total quartz grains
Qm = Monocrystalline quartz
Qp = Polycrystalline quartz (including chert)

F = P + K, where:
F = Total feldspar grains
P = Plagioclase
K = Potassium feldspar

L = Lvm + Lsm, where:
L = Total lithic fragments (including metamorphosed lithic fragments)
Lvm = Total volcanic and metavolcanic lithic fragments
Lsm = Total sedimentary and metasedimentary lithic fragments

Qm–F–Lt:

Qm = Monocrystalline quartz
F = Total feldspar
Lt = Total lithics (including polycrystalline quartz)

Qp–Lvm–Lsm:

Qp = Polycrystalline quartz
Lvm = Total volcanic and metavolcanic lithic fragments
Lsm = Total sedimentary and metasedimentary lithic fragments

Qp2-3–Qp>3–Qnu–Qu:

Qp2-3 = Polycrystalline quartz with 2-3 crystals
Qp>3 = Polycrystalline quartz with >3 subcrystals
Qnu = Non-undulatory monocrystalline quartz
Qu = Undulatory monocrystalline quartz.

**Table 3.2.** Framework grains and recalculated parameters used in this study.

of some authors), and this would certainly yield much richer provenance information (Ingersoll 1990), the advantage is offset by the inevitable increase in subjectivity due to subtle and often arbitrary distinctions between textural features. Even with the inclusion of sedimentary and metamorphic lithics in Lsm, QpLvmLsm recalculations are still considered highly sensitive indicators of provenance and plate tectonic setting (Ingersoll and Suczek 1979). Accessory minerals were not included in detrital mode recalculations, but the abundance of important "tracer elements" (Johnsson 1993) such as detrital blue and green amphibole and epidote were noted as a percentage of the whole rock composition for specific provenance purposes.

| Petrofacies and sample numbers | QFL % | | | QmFLt % | | | QpLvmLsm % | | |
|---|---|---|---|---|---|---|---|---|---|
| | Q | F | L | Qm | F | Lt | Qp | Lvm | Lsm |
| **Petrofacies A1** | | | | | | | | | |
| 1 | 34 | 48 | 20 | 10 | 48 | 42 | 19 | 41 | 40 |
| 2 | 30 | 43 | 27 | 19 | 42 | 39 | 16 | 40 | 44 |
| 3 | 29 | 41 | 30 | 8 | 41 | 51 | 20 | 33 | 47 |
| 4 | 31 | 35 | 34 | 16 | 35 | 49 | 32 | 24 | 44 |
| 5 | 18 | 42 | 40 | 6 | 43 | 51 | 22 | 33 | 45 |
| 6 | 28 | 32 | 40 | 12 | 33 | 55 | 24 | 12 | 64 |
| 7 | 44 | 32 | 24 | 29 | 33 | 38 | 30 | 17 | 53 |
| 8 | 48 | 13 | 39 | 25 | 13 | 62 | 52 | 9 | 39 |
| Mean | 33 | 35 | 32 | 16 | 36 | 48 | 26 | 28 | 45 |
| SD | 9.53 | 10.6 | 7.57 | 8.3 | 10.76 | 8.22 | 11.52 | 12.23 | 8.14 |
| **Petrofacies A2** | | | | | | | | | |
| 9 | 49 | 3 | 48 | 19 | 3 | 78 | 58 | 9 | 33 |
| 10 | 47 | 19 | 34 | 21 | 19 | 60 | 25 | 9 | 66 |
| 11 | 56 | 32 | 12 | 38 | 30 | 32 | 52 | 7 | 41 |
| 12 | 48 | 9 | 43 | 24 | 11 | 65 | 48 | 12 | 40 |
| 13 | 50 | 24 | 26 | 27 | 26 | 47 | 37 | 17 | 46 |
| 14 | 59 | 16 | 25 | 38 | 16 | 46 | 32 | 13 | 55 |
| 15 | 66 | 21 | 13 | 50 | 20 | 30 | 50 | 12 | 38 |
| 16 | 54 | 12 | 34 | 16 | 12 | 72 | 30 | 17 | 53 |
| 17 | 61 | 20 | 19 | 34 | 19 | 47 | 56 | 8 | 38 |
| 18 | 57 | 21 | 22 | 44 | 21 | 35 | 12 | 8 | 80 |
| 19 | 77 | 5 | 18 | 70 | 5 | 25 | 44 | 2 | 54 |
| 20 | 72 | 12 | 16 | 53 | 25 | 22 | 65 | 8 | 27 |
| Mean | 57 | 17 | 26 | 37 | 17 | 46 | 42 | 10 | 48 |
| SD | 9.94 | 8.23 | 11 | 16.17 | 8.18 | 18.75 | 15.63 | 4.4 | 15.38 |
| **Petrofacies B** | | | | | | | | | |
| 21 | 76 | 9 | 15 | 71 | 8 | 21 | | | |
| 22 | 89 | 9 | 2 | 84 | 10 | 6 | | | |
| 23 | 79 | 16 | 5 | 74 | 16 | 10 | | | |
| 24 | 93 | 4 | 3 | 87 | 4 | 9 | | | |
| 25 | 95 | 4 | 1 | 88 | 4 | 8 | | | |
| 26 | 95 | 4 | 1 | 90 | 5 | 5 | | | |
| 27 | 93 | 5 | 2 | 88 | 6 | 6 | | | |
| 28 | 91 | 8 | 1 | 87 | 8 | 5 | | | |
| 29 | 88 | 8 | 4 | 85 | 6 | 9 | | | |
| Mean | 91 | 6 | 3 | 85 | 6 | 9 | | | |
| SD | 1.88 | 1.48 | 1.46 | 6.11 | 4.16 | 4.77 | | | |

**Table 3.3**. Recalculated parameters used for composition and provenance analysis.

### 3.4.2. Framework grains

*3.4.2.1. Texture*

Textural characteristics (sorting, matrix content, roundness, and mineralogical maturity) vary considerably up through the section. A rapid estimation of sorting was made by comparison with visual textural patterns such as those of Beard and Weyl (1973). Utilising these visual aids, sandstones vary from very poorly sorted with occasional dispersed pebbles (Fig. 3.14D and E) to well sorted (Fig. 3.14C). Grains are angular to well rounded, while matrix, consisting of small orientated clay minerals such as chlorite, high birefringent illite/montmorillite, and sericite (as an alteration product of feldspar), typically amount to less than 20% of the whole rock composition. Samples with excess of 15% matrix are invariably higher in feldspar and unstable lithics (typically of volcanic parentage) which suggests much of this matrix may be of secondary diagenetic origin (pseudomatrix) rather than a primary (depositional) constituent of the rock. Haematite staining in the matrix is also a feature of samples obtained from Facies Associations A and B.

*3.4.2.2. Quartz*

Although quartz is the principle framework grain when averaging recalculated modes over the entire studied section ($Q_{60}F_{19}L_{21}$), individual samples record a great diversity in abundance (ranging from 18–97% as %QFL) (Table 3.3). Grains are angular to well rounded, and comprise monocrystalline (ranging from 6–90%, mean 46%) and polycrystalline (ranging from 12–65%, mean 34%) varieties. Abraded overgrowths of silica common to both quartz types suggest second cycle input from a sedimentary or metasedimentary source.

Monocrystalline quartz of probable volcanic origin is represented by clear euhedral crystals with idiomorphic resorption embayments (Fig. 3.14D and E), non-undulatory extinction, and a lack of internal strain, vacuoles, and prominent fluid inclusions (Folk 1980). Similar quartz grains present in felsic, and rarely vitric volcanic lithic fragments further suggest their volcanic parentage. Plutonic varieties are determined by traces of vacuoles, fluid and heavy mineral inclusions (zircon, tourmaline, and rutile needles), along with weak undulatory extinction. Where abundant fluid inclusions give a turbid aspect, this "bubbly quartz" (Folk 1980) may be of hydrothermal origin, a conclusion consistent with vermicular chlorite and epidote inclusions (Folk 1980). Monocrystalline grains with strong undulatory extinction and deformation lamellae (Fig. 3.14E) record internal strain and a probable metamorphic origin. This metamorphic source also appears to contribute most, if not all of the polycrystalline quartz (Fig. 3.14B and F), based on strong grain elongation, preferred crystallographic orientations, and intense intercrystalline suturing (Blatt *et*

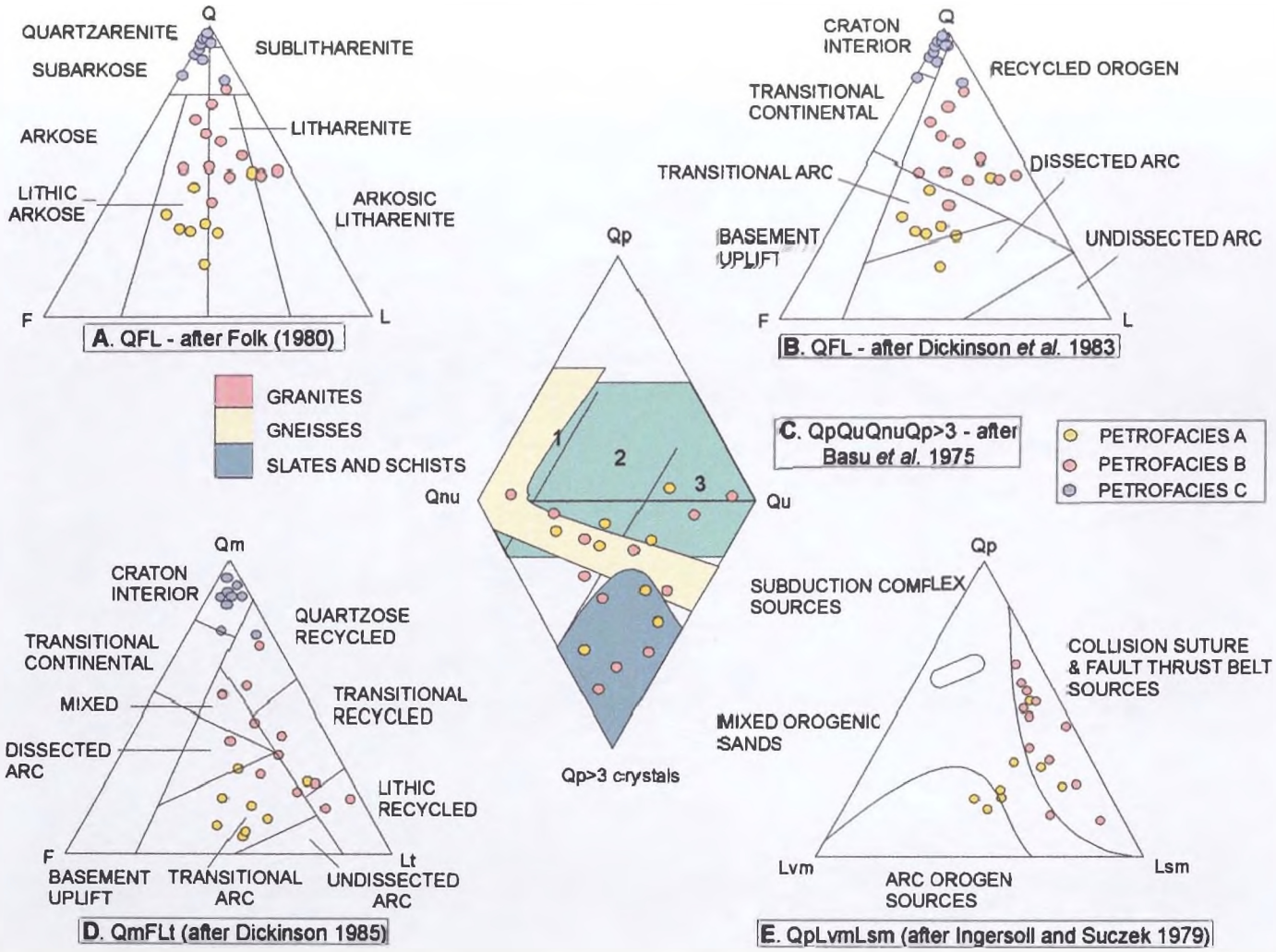



**Fig. 3.13.** Ternary diagrams from Facies Associations A, B and C describing sandstone composition and interpreting tectonic setting. Fields in (C) are (after Basu *et al.* 1975): 1 – plutonic, 2 – middle and upper rank metamorphic, and 3 – low grade metamorphic.

*al.* 1980). Polycrystalline quartz is particularly diagnostic of low and medium grade metamorphic source rocks (Basu *et al.* 1975). Microcrystalline grains (Fig. 3.14D) with weakly sutured (protomylonite), strongly sutured (mylonite) or unsutured (chert) fabrics occur sporadically. Mylonite is typically micaceous, but where strongly aligned mica constituents more than 10% of the total composition, these are instead classified as lithics (mylonitic schist).

The grain size of crystals that constitute polycrystalline quartz has been used to determine likely origin (Basu *et al.* 1975). Coarsely crystalline types are likely to be plutonic in origin, while finely crystalline varieties imply a gneissic source. Although both of these grain types occur, the dominant varieties by some considerable margin are grains of intermediate size considered typical of schistose basement. Although these conclusions are based on oversimplified reasoning, this interpretation of the origin of polycrystalline quartz is consistent with the abundance of associated metamorphic lithics (see below).

*3.4.2.3. Feldspar*

Both plagioclase (Fig. 3.14E) and K-feldspar are present and included as feldspar. The total percentage of feldspar ranges from 2–48%, but averages less than 20% over the whole section. This range in feldspar is principally due to variations in plagioclase, as K-feldspar is only ever found in trace amounts (less than 5%) throughout. On the basis of refractive index, plagioclase lies in the albite-andesine range and is usually twinned, with repeated (sometimes chessboard) and Carlsbad twinning. Orthoclase and microcline are the most abundant variations of K-feldspar. Feldspar grains may be subangular and clear, to well rounded and altered/partially replaced. Commonly observed etched and corroded grains are due to partial replacement by clay minerals and sericite dust. The highest recorded levels of feldspar lie in samples immediately above the unconformable contact between Cambrian sediments and Precambrian arc volcanics (Samples 1–7 in Table 3.3). A correspondence with abundant volcanic lithics (Lvm in Table 3.3) suggests local basement erosion as a source for most of the angular plagioclase. Rounded and highly altered grains are not found with lithics that can be matched with local sources, and instead may be exotic to the area.

*3.4.2.4. Lithics*

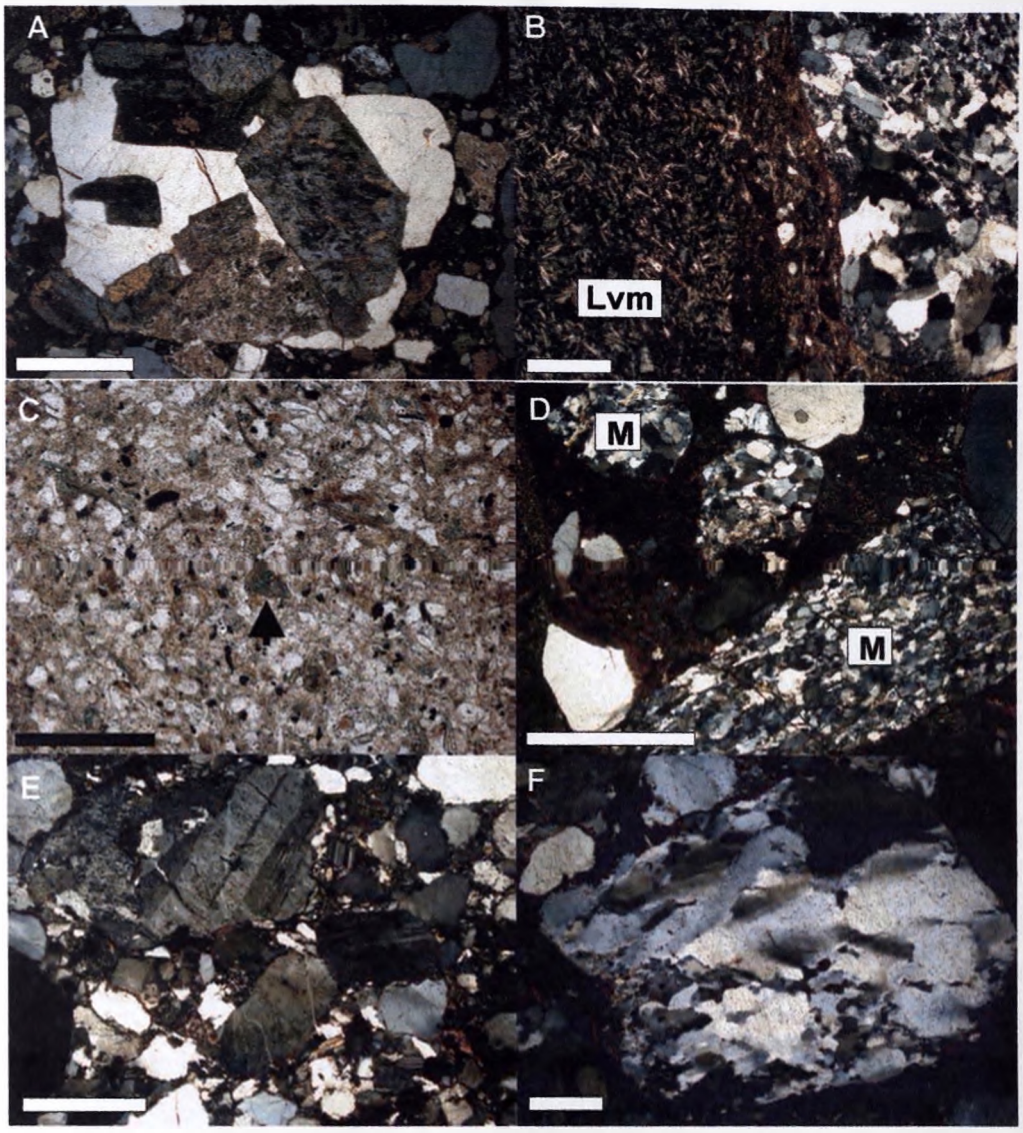



**Fig. 3.14.** Photomicrographs of principle grain types present in the Ogof Golchfa and St Non's formations. All cross nicols except C. Scale bar = 1 mm. (A) Petrofacies A2 – large euhedral plagioclase feldspar and optically clear quartz interpreted as a granitic lithic fragment. (B) Petrofacies A1 – the grain on the left (Lvm) is a fine-grained plagioclase-rich volcanic lithic, probably basalt. The grain on the right is strained polycrystalline quartz of metamorphic origin with preferential orientation of elongated crystals with sutured boundaries (hyperconcentrated flood-flow deposit). (C) Petrofacies B – angular to well rounded monocrystalline quartz and angular first cycle blue amphibole (arrowed) in moderately well sorted quartz arenites (storm deposit). (D) Petrofacies A2 – fine-grained polycrystalline quartz with minor plagioclase interpreted as mylonite (M) based on the degree and consistency of grain elongation (braided stream deposit). (E) Petrofacies A1 – optically clear non-undulatory monocrystalline quartz of volcanic origin and highly strained monocrystalline quartz of metamorphic origin are the dominant quartz types. The abundance of plagioclase feldspar classifies this poorly sorted rock as an arkose (hyperconcentrated flood-flow deposit). (F) Petrofacies A2 – quartzite lithic fragment showing preferred elongation and suturing of quartz crystals and alignment of mica (debris flow deposit).

After quartz, lithic fragments (excluding polycrystalline quartz) are the most common constituents of the analysed sandstones with abundance (as %QFL) ranging from 1-48% averaging 21% for the whole section. Fourteen types of lithic fragment have been identified. The most common types are low grade (quartzite and slates) and medium grade (phyllite-schist, phyllite-quartzite, phyllite, and greenschist) metamorphic grains (Lsm in Table 3.3), followed by (in decreasing abundance), felsic volcanics and tuffs, mafic volcanics (Lvm in Table 3.2), and shales and arenites. Sedimentary grains probably represent intrabasinal rip-up clasts. Subsidiary grain types include quartz-feldspar aggregates, with both granitic (Fig. 3.14A) and gneissic texture, and mafic glass shards.

Quartzite is mica bearing (Fig. 3.14F) with strongly orientated muscovite and chlorite with fine-grained polygonal quartz. Greenschist is a collective term used to describe aggregates of chlorite-quartz-albite, chlorite-albite-magnetite, and quartz-epidote-albite. Slates are characterised by their conspicuous slatey cleavage, this being an undulating to planar foliation defined by alternating domains of dark organic-rich clays, recrystallised muscovite and chlorite, and partially recrystallised elongate and lenticular quartz and feldspar. The latter is apparently a result of pressure solution and, in some cases, local recrystallisation of quartz in pressure shadows during lower greenschist facies metamorphism (Dorsey 1988). Phyllite-schist fragments contain clear, euhedral micas that commonly alternate with thin bands highly recrystallised quartz in a strongly preferred planar foliation, while phyllite-quartzite fragments contain roughly 75% fully recrystallised quartz ± albite, with lesser amounts of well crystallised mica. These phyllite grains equate to the quartz-mica tectonite of other workers. Relict crenulation cleavage in some of these phyllite grains indicates polyphase deformation in the source area.

Volcanic lithic fragments are characterised by microlithic (lathlike) (Fig. 3.14B), microgranular, felsitic, ophitic, and vitric textures, although sericitization and replacement by silica-rich minerals often destroy the original fabric. Felsitic fragments are often difficult to tell apart from chert, unless microphenocrysts present in the groundmass are coarse enough to show contrasts in refringence between quartz and feldspar crystals.

*3.4.2.5. Accessory minerals*

Important tracer elements include detrital blue and green amphibole (euhedral crystals with green or lavender blue and purple rhombic crystals), and epidote, all of which are metamorphic grade indicators. Blue amphibole (Fig. 3.14C) is only known

from high pressure/low temperature metamorphic rocks of "blueschist facies" and is considered a 1st cycle mineral due to its instability with respect to chemical and mechanical abrasion (Shoa *et al.* 2001). Epidote marks the threshold of change from "greenschist" to "epidote-amphibolite" metamorphic facies, and is more resistant, being able to suffer more than one sedimentary cycle (von Eynatten and Gaupp 1999). Samples high in blue amphibole also tend to have abundant green amphilbole and epidote, suggesting a common source. Other accessory minerals (in decreasing abundance) include detrital chlorite, muscovite, haematite, zircon, chloritized biotite, clinopyroxene, and tourmaline.

### 3.4.3. Petrofacies discrimination

On the basis of compositional similarities, sandstones can be classified into 2 broad petrofacies. The mineralogically immature "high-lithic petrofacies" (Petrofacies A1 and A2 in Fig. 3.15) corresponds to alluvial fan and braided stream deposits of Facies Associations A and B. Recalculated mean values (Table 3.3, Fig. 3.15) of %QFL ($Q_{45}F_{26}L_{29}$) and %QmFLt ($Q_{26}F_{26}Lt_{47}$) clearly distinguish this petrofacies from the "high-quartz petrofacies" (Petrofacies B in Fig. 3.15) with recalculated mean values of %QFL ($Q_{91}F_{6}L_{3}$) and %QmFLt ($Q_{85}F_{6}Lt_{9}$) (contrast Fig. 3.14E with Fig. 3.14C). This quartzose petrofacies corresponds to nearshore marine deposits of Facies Association C.

Based on relative percentages of feldspar (as %QFL) and volcanic lithics (as %QpLvmLsm) (Table 3.3, Fig. 3.15), the "high-lithics petrofacies" may be subdivided into the "volcanic lithics petrofacies" (Petrofacies A1, %QFL: $Q_{26}F_{29}L_{26}$, and %QpLvmLsm: $Qp_{34}Lvm_{19}Lsm_{46}$) and the high metasedimentary lithic petrofacies (Petrofacies A2, %QFL: $Q_{57}F_{17}L_{26}$, and %QpLvmLsm: $Qp_{42}Lvm_{10}Lsm_{48}$). Petrofacies A1 corresponds to the deeply incised basal unit of HFF deposits (Fig. 3.2), while Petrofacies A2 is principally debris flow and gravely braided stream sediments. When model data is plotted on the ternary diagrams of Dickinson and Suczek (1979), Dickinson *et al.* (1983), and Dickinson (1985) (Fig. 3.13), petrofacies fields clearly occupy semi-discreet regions. While there is a clear distinction at the marine ravinement surface (Fig. 3.8) between Petrofacies A2 and B (Fig. 3.13 and Fig. 3.15), some overlap is apparent between Petrofacies A1 and A2, a transitional phase replicated in the stratigraphic succession where HFF pass transitionally into debris flow deposits. Salient attributes of these petrofacies as well as there evolution through time is discussed below.

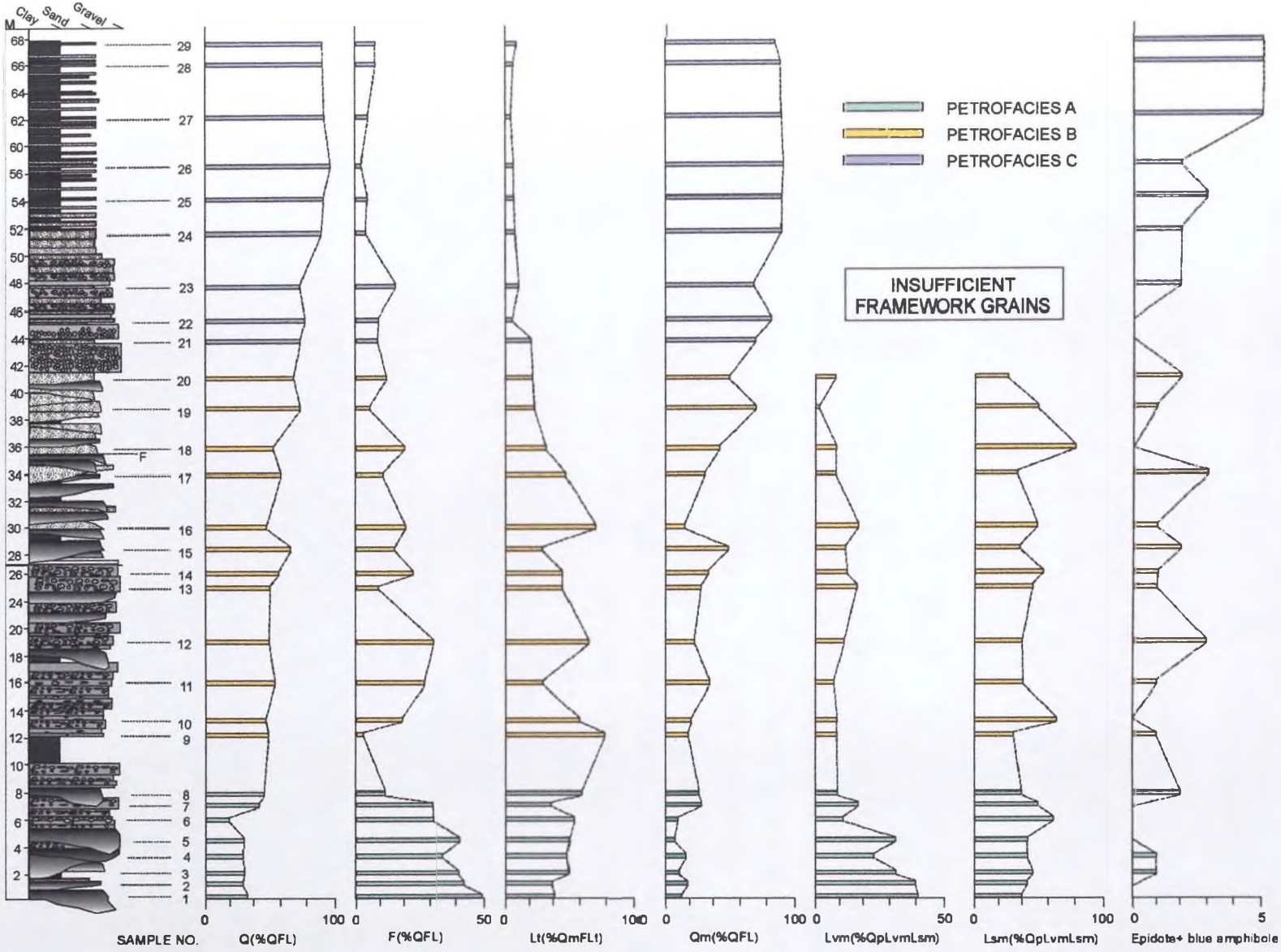

Clay
Sand
Gravel
M
68
66
64
62
60
56
54
52
50
48
46
44
42
40
38
36
34
32
30
28
26
24
20
18
16
14
12
10
8
6
4
2
F
29
28
27
26
25
24
23
22
21
20
19
18
17
16
15
14
13
12
11
10
9
8
7
6
5
4
3
2
1
SAMPLE NO.
Q(%QFL)
F(%QFL)
Lt(%QmFLt)
Qm(%QFL)
Lvm(%QpLvmLsm)
Lsm(%QpLvmLsm)
Epidote+ blue amphibole
0
100
50
5
PETROFACIES A
PETROFACIES B
PETROFACIES C
INSUFFICIENT
FRAMEWORK GRAINS

**Fig. 3.15.** Summary of sandstone compositional data and petrofacies discrimination (see text for details).

### 3.4.4. Petrofacies

#### *3.4.4.1. Petrofacies A1: volcanic lithic petrofacies*

##### *3.4.4.1.1. Description*

Roughly equal percentages of quartz, feldspar, and lithics (Table 3.3) define the volcanic lithic petrofacies as lithic arkoses (Fig. 3.14E), and arkosic litharenites (Fig. 3.13A). The dominant feldspar is plagioclase, while significant proportions of the total quartz population is polycrystalline quartz, a factor that accounts for the shift in data points towards the L pole in the QmFLt plot (Fig. 3.13D). Monocrystalline quartz types are principally metasedimentary (with abraded overgrowths and undulatory extinction) and volcanic, which corresponds well with a lithic population characterised by felsic volcanics/tuffaceous material, and low to medium grade metasedimentary fragments (quartzite, slate, phyllite-schist). Temporal variations in framework grains (Fig. 3.15) include an upward decrease in feldspar and volcanic lithics with a concomitant increase in metasedimentary fragments. The proportion of volcanic lithics must be considered as an absolute minimum as relatively high pseudomatrix (>15%) suggests preferential breakdown of these most labile grains. Accessory minerals include trace amounts of detrital epidote, muscovite, chlorite, and biotite.

##### *3.4.4.1.2. Interpretation*

As a provenance indicator, Petrofacies A1 is extremely diverse and thus not easily characterized. Detrital modes plot within both the magmatic arc and recycled orogen global sandstone provenance fields (Fig. 3.13B, D and E) and display a relatively wide spread of data points (Standard Deviation (SD) averaging 9.76) when compared with other published examples (contrast with data presented by Dickinson and Suczek 1979, and Dickinson *et al.* 1983). The magmatic arc signature (high feldspar and volcanic lithics) is largely confined to the basal 5 m of the section (Fig. 3.15), and records erosion of the local Precambrian volcanics by hyperconcentrated flows. This provenance signal is clearly "counterfeit" (*sensu* Graham *et al.* 1993 and Hendrix *et al.* 2000) with respect to plate tectonic setting, in that it records erosion from a *relict* arc terrane rather than an active orogenic phase. Similar problems with inherited

signatures have been documented by number of authors (e.g. Mack 1984; Dorsey 1988; Graham *et al.* 1993; Trop and Ridgeway 1997; Hendrix 2000), and appear particularly prevalent when associated with 1st and 2nd order drainage systems such as those active during incipient stages of alluvial fan evolution (Blair and McPherson 1994).

Relatively high quartz values ($Q_{33}F_{35}L_{32}$) when associated with typical arc derived detritus (F and Lvm) define the dissected arc province (Fig. 3.13B and D) of deep-seated pluton erosion (Dickinson and Suczek 1979). Again this tectonic setting appears incorrect, based on the almost total exclusion of plutonic lithics, particularly those comparable to the local Dimetian granophyre. Instead, abraded overgrowths and undulatory extinction suggest mixing of relict arc detritus with a more exotic metasedimentary source, one that presumably also supplied metasedimentary lithics, detrital muscovite, and epidote.

This progressive dilution of one source by another can only be determined in QpLvmLsm plots (Fig. 3.13E), with basal samples grouping in the arc orogen field while those associated with lesser amounts of volcanic lithics plot on the edge of the collisional suture field. This distinction, which is clearly beyond the resolution of QPL and QmFLt model recalculations (Fig. 3.13B and D), strengthens claims by Suttner and Basu (1984) that lithic-based provenance studies (aided by traditional point-counting methods) offer far greater resolution in determining temporal phases of source area evolution. The abundance of polycrystalline quartz indicate that metamorphic source rocks were proximal to the site of deposition as the low durability of mineral interfaces causes fragments to be broken up during prolonged or aggressive transport (Johnsson 1993). This evidence combined with high levels of feldspar and unstable lithics is consistent with the footwall derived alluvial fan interpretation determined from sedimentological features of Facies Association A (Blair and McPherson 1994), while conflicting strongly with the beach interpretation previously offered (Crimes 1970a).

#### *3.4.4.2. Petrofacies A2: metasedimentary lithic petrofacies*

##### *3.4.4.2.1. Description*

This petrofacies includes relatively quartz-rich, lithic bearing compositions that average $Q_{57}F_{17}L_{26}$ (Table 3.3) that coupled with a high standard deviation, ranging from 9 to 11 (%QFL) with a maximum of 18.7 (for Lt as %QmFLt) defines a variability in sandstone classification from immature lithic arkoses and arkosic litharenites to

relatively mature sublitharenites (Fig. 3.13A). Metasedimentary grains dominate the lithic component ($Qp_{42}Lvm_{10}Lsm_{48}$), and include greenschist, phyllite-schist, phyllite-quartzite, phyllite, slate, and quartzite, with subsidiary mylonite, jasper, and chert. Volcanic lithics are principally felsitic with lesser amounts of tuffaceous material, of which some grains are well rounded. Plutonic fragments (granite and gneiss) are rare. Quartz type also indicates a dominantly metasedimentary source, with monocrystalline grains exhibiting undulatory extinction and abraded overgrowths dominant, followed closely by strongly sutured and elongate polycrystalline varieties. Volcanic quartz is rare, while plutonic quartz is difficult to distinguish from metamorphic quartz (Basu *et al.* 1975), but is considered negligible based on plutonic lithic abundance. Plagioclase again dominates the feldspar mode. Accessory minerals such as muscovite, clinopyroxene, epidote, and blue and green amphibole generally form a greater proportion of the total framework composition (Fig. 3.15).

The increase in lithic variability is essentially a temporal variation up through the petrofacies rather than a sudden change from Petrofacies A1. Additional variations include an increase in grain rounding and monocrystalline and total quartz, at the expense of total lithics and feldspar (Fig. 3.15). This obvious increase in maturity parallels similar trends in conglomerate clast composition and shape, and records differences in sediment transport processes between debris flow-dominated alluvial fans and gravely braided streams.

*3.4.4.2.1. Interpretation*

Qualitative analysis of framework modes (Fig. 3.13) yields a similar spread in data (SD from 4.4 to 8.75) comparable to that described from Petrofacies A1, which again makes interpretation difficult. The standard QFL diagram of Dickinson *et al.* (1983) classifies all but one sample as recycled orogenic, a conclusion that appears consistent with the high percentage of metasedimentary fragments relative to volcanic grains (Table 3.3) (Dickinson and Suczek 1979). Problems in interpretation arise when model data are recast in more sensitive (lithic-based) provenance diagrams such as QmFLt and QpLvmLsm (Figs 16D and E respectively), where the true nature of source variability may be acknowledged by the breakdown of general plate tectonic settings into more detailed orogenic provinces.

Because recycled orogenic settings invariably recycle metasediments originally deposited along passive margins (Dickinson and Suczek 1979; Dickinson 1985), the sandstones contain too many volcanic fragments and feldspar (Table 3.3) to have been derived exclusively from a recycled orogen, yet too few volcanic

fragments and feldspar to have been derived from an arc orogen (Dickinson and Suczek 1979; Ingersoll and Suczek 1979; Mack 1984; Graham *et al.* 1993; Trop and Ridgeway 1997; Corcoran *et al.* 1999). Chert, blue and green amphibole, jasper, and epidote may reflect derivation from a subduction complex (Dickinson and Suczek 1979; Dickinson 1985), yet the data points do not plot near the subduction derived samples of Dickinson and Suczek (1979) and Ingersoll and Suczek (1979) (Fig. 3.13E). With the addition of low, medium, and high-grade metamorphic rocks, as well as mylonite and trace amounts of granite, these sandstones clearly originate from a mixture of source rocks and plate tectonic provinces. This detrital composition may have been produced by rapid superposition in time of a collisional orogen, subduction complex, and arc orogen, or more likely by a collisional event that juxtaposed some combination of these source rock provinces into a single orogenic belt. A source area composed of disparate allochthonous (suspect) terranes, where sandstone composition reflects the characteristics of a previously assembled collage also explains the lack of a clear unroofing history (Graham *et al.* 1993) as well as the abundance of mylonite, as major lithological boundaries are typically highly tectonized ductile shear zones. This collisional episode marking the accretion of suspect terranes may be locally represented by the angular unconformity at the base of the studied sequence that separates Precambrian arc volcanics from Cambrian sediments. Similar framework compositions have been reported from piggyback basins (thrust top basins) and late-stage successor basins by Dickinson *et al.* (1983), Graham *et al.* (1993), Trop and Ridgeway (1997), Corcoran *et al.* (1999), Robinson *et al.* (2003), and are clearly plate tectonic settings not yet adequately accounted for in global sandstone provenance schemes (a problem foreseen by Mack 1984).

Although no predictable unroofing history is apparent, there are a number of important temporal variations in framework composition that illustrate important sedimentological features. The transition from alluvial fan to braided stream sedimentation accounts for the decrease in more labile fragments such as lithics, polycrystalline quartz, and feldspar, and the concomitant increase in monocrystalline quartz, as dominantly quartzose labile fragments break up. This evolution in framework modes to heightened maturity is typical of alluvial fan to braided stream transitions (Wysocka and Swierczewska 2003), and essentially records aggressive denudation of the post-tectonic landscape. This period of catchment area expansion also readily accounts for the increase in lithic variability as recession of the watershed incorporates more varied source terranes.

*3.4.4.3. Petrofacies B: high quartz petrofacies*

*3.4.4.3.1. Description*

Sandstones in this petrofacies are dominantly quartz arenites ($Q_{91}F_6L_3$) (Fig. 3.14C) with minor subarkoses and sublitharenites (Fig. 3.13A). Irrespective of the relative abundance of labile components, rounded monocrystalline quartz dominates the model composition ($Qm_{85}F_6Lt_9$). Authigenic chlorite is an important accessory mineral and may form up to 20% of the whole rock composition giving the rock a greenish tinge in hand specimen. Unlike petrofacies A1 and A2, samples are generally winnowed and well sorted, a characteristic consistent with their marine aspect. Unstable framework grains such as feldspar, lithics, and polycrystalline quartz are greatly reduced (Table 3.3), although basal samples in close proximity to the wave ravinement surface record $Q_{79}F_9L_{21}$, with $Lt_{21}$, where sands are associated with conglomerates. For this reason, it made no statistical sense to recalculate modes as %QpLvmLsm. Although greatly reduced in abundance, lithic grains remain remarkably diverse, with most of metasedimentary rock types documented in Petrofacies A2 present in variable degrees. What is most surprising and difficult to interpret is the actual increase in accessory minerals such as blue amphibole and epidote (Fig. 3.15).

*3.4.4.3.2. Interpretation*

Considering the position of Petrofacies B above a wave ravinement surface, the most logical source of these wholly marine quartz arenites is erosional reworking and winnowing of Petrofacies A2 sediments. In shallow marine environments, prolonged residence periods improves the chances of considerable wave reworking and consequent elimination of labile grains, shifting the resultant sand composition towards the mature quartz-rich end of the spectrum (Mack 1984; Johnson 1993; Espejo and Lopez-Gamundi 1994; Marenssi *et al.* 2001). Feldspar grains are reduced due to fracturing along cleavage and twinning plains making them susceptible to chemical weathering, while quartzose lithics and polycrystalline quartz breaks up to form monocrystalline quartz. Quantitative analysis of framework modes (Fig. 3.13), if interpreted without consideration for depositional processes, would imply a craton interior province, and a switch to a mature, high order drainage network sourced by quartzose lowlands (Dickinson and Suczek 1979; Dickinson 1985). Because certain lithic and accessory minerals can be detected throughout the section, this almost instantaneous increase in maturity is unlikely to reflect any

dramatic change in provenance. Deposits that have been significantly modified by depositional processes have been said to show "environmental" (Marenssi *et al.* 2001) or "depositional" (Espejo and Lopez-Gamundi 1994) signatures, because the environmental effects largely obscured the original provenance signal.

### 3.4.5. Quartz type

The characteristics of quartz types have been used in the inference of provenance (Basu *et al.* 1975; Young 1976; Girty 1987; Girty *et al.* 1988; Tortosa *et al.* 1991; Lee and Sheen 1998; Wysocka and Swierczewska 2003). Basu *et al.* (1975), with later modifications by Tortosa *et al.* (1991), introduced a diamond plot and defined fields corresponding to specific parent rocks. Point-counting data derived from the various quartz types from the studied section were plotted on this provenance discrimination diagram (Fig. 3.13C). Both low-grade and middle- to upper-grade metamorphic source rocks are evident. This is clearly corroborated by the types of lithoclasts present, principally phyllite, schist, greenschist, and quartzite, as well as muscovite, epidote, and blue and green amphibole. Monocrystalline and polycrystalline quartz with abundant fluid inclusion trails, chlorite and muscovite inclusions, are typical of quartz veins developed parallel to predominant foliation, particularly during greenschist facies metamorphism (Lee and Sheen 1999). Abundant mylonite is typical of low-grade ductile shear zones (Tortosa *et al.* 1991). The record of a major plutonic source is clearly incorrect based on both clast composition in conglomerates and lithic characteristics in thin section. This anomaly is well documented (Girty *et al.* 1988) and arises through problems in classifying volcanic/metavolcanic grains which are difficult to distinguishing from quartz populations derived from middle- to high-grade metasedimentary rocks.

### 3.4.6. Controls on sandstone composition

Sandstone composition can be visualized as an open system, where the final product is the result of provenance, (lithology, relief, and climate of the source area) and grain size (Folk 1980; Johnsson *et al.* 1988; 1991, Johnsson 1992, 1993; Espejo and Lopez-Gamundi 1994; Cox and Lowe 1995). The resultant composition can be modified, or in some cases drastically changed by mechanisms operating during sediment transport and during, and after, deposition (e.g. diagenesis) (Mack 1984; Cox *et al.* 2002). Only after fully accounting for the effects of these additional factors can sandstone framework composition be considered to be a confined system in

which the only variable involved is the source area lithology. Consequently, a careful analysis must be carried out to evaluate fully the relative importance of the factors controlling sandstone composition. Temporal changes attributable to parallel changes in depositional setting have been outlined previously. Out of the three petrofacies determined, only Petrofacies A2 is considered a possible reflection of source area composition and Lower Cambrian tectonic setting. Petrofacies A1 contains a strong inherited signature, an artefact of a long extinct tectonic cycle, while Petrofacies B has been heavily modified in the depositional environment with the resultant breakdown of the original labile components. Therefore, analysis of the effects of diagenesis and climate/relief on the framework mode composition is restricted to Petrofacies A2.

*3.4.6.1. Compositional variations due to diagenetic alteration*

Burial diagenesis commonly results in the destruction of feldspar and lithic grains, dissolution of unstable phases, the growth of authigenic phases, and cementation (Folk 1980; Johnsson 1993). Without the use of geochemical techniques, and considering the variability in original textural features of the deposit (a parallel to variable depositional processes), it is very difficult to differentiate between original and diagenetically modified petrofabrics. Secondary pseudomatrix formed by *in situ* mechanical and chemical alteration of labile framework grains (Dickinson 1970) is considered the main diagenetic process based on the following textural characteristics: (1) the deformation of weak detrital grains (mainly fine lithics) through mechanical action, resulting in their being squeezed into the interstices between more stable grains (mono-crystalline and polycrystalline grains of quartz); (2) matrix that occurs as interstitial clots occupying spaces equivalent to the preserved detrital grain; (3) areas of relict chlorite grain-rimming reflecting original grain boundaries; (4) detrital grains "floating" in sericitic pseudomatrix that preserves relict lithic textures (Cox *et al.* 2002); and finally (5) relatively high percentages of matrix which is often inconsistent with the depositional environment. This is well illustrated with up to 19% matrix in sandstone tempestites, which contrasts with the expected amount of 1-4% based on the degree of sorting indicated by internal sedimentary structures (Visher 1969).

*3.4.6.2. Compositional variations due to climate and relief in the source area*

Climate can be a primary control on sand mineralogy (Suttner *et al.* 1981; Mack 1984; Johnsson 1992, 1993; Corcoran *et al.* 1999). Climatically controlled weathering in the source area, collectively known as palaeoweathering, modifies the primary composition prior to introduction of the weathered assemblage into the dispersal system (Velbel and Saad 1991). It has been suggested that palaeoweathering in humid climates may significantly reduce the content of labile sand-sized components (Suttner *et al.* 1981), leading to a "palaeoweathering" signature in the framework composition recognized in resulting quartz-rich sandstones. Although intensive forms of palaeoweathering have been documented from a host of post-Silurian depositional environments, the lack of vegetation in older sediments enables particles freed from the host rock to almost immediately enter the transport phase of the sedimentary cycle (Fuller 1985), resulting in detrital modes that better reflect source area characteristics.

Although the influence of climate and relief on sandstone composition has long been known, its exact quantification remains a problem even in modern sedimentary systems (e.g. Ibbeken and Schleyer 1991). Grantham and Velbel (1988) defined a simple weathering index (wi):

$$wi = c \times r$$

where c is the rate of weathering ("climate") and r is the residence time of the sediment in the weathering environments ("relief"). In ancient systems the variables c and r cannot be determined accurately. Weltje (1994) introduced a semi-quantitative approach, which is based on modern fluvial sands with known source rock lithologies and different climatic and physiographic conditions. A semi-quantitative weathering index is calculated from the above formula using estimates for c and r (Fig. 3.16A). The compositional data of the modern sands were plotted in the logratio diagram ln(Q/F) vs. ln(Q/L) and each sample group was combined with its specific weathering index. The resulting compositional trend defines a clear relationship between sandstone composition, weathering index, and source rock lithology (Fig. 3.16B).

The compositional framework grain data for Petrofacies A2 (Table 3.2) are plotted into the diagram ln(Q/F) vs. ln(Q/L) (Fig. 3.16B). Most of the samples plot into the upper field of wi=0 indicating a detrital spectrum with very low degrees of weathering and a mainly metamorphic parentage. Because the diagram is solely based on data from modern sediments, post-sedimentary processes have not been considered. The effect of diagenetic modification has been discussed previously, and would generally be expected to reduce feldspar and lithoclast concentration. This would shift the composition to higher quartz content and, consequently, higher

**A**

| Semi-quantitative weathering index (wi = c x r) (Weltje 1994) | | RELIEF | | |
|---|---|---|---|---|
| | | High, mountains | Moderate, hills | Low, plains |
| CLIMATE | Semi-arid, mediterranean | 0 | 0 | 0 |
| | Temperate, subhumid | 0 | 1 | 2 |
| | Tropical, humid | 0 | 2 | 4 |

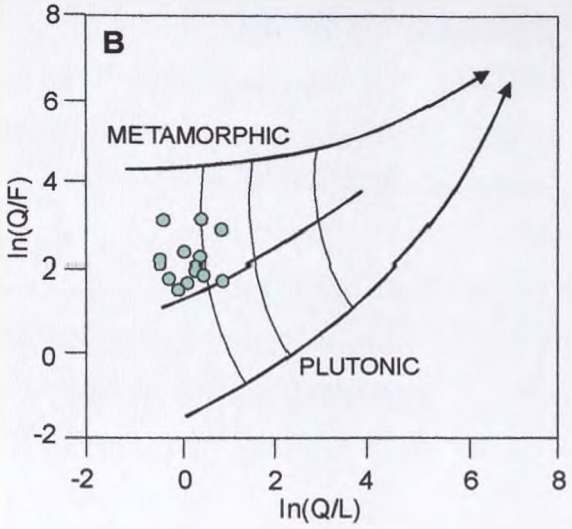



**Fig. 3.16.** (A) Semi-quantitative weathering index based on semi-quantitative estimates for climate and relief. (B) The analyzed samples indicate a very low weathering index (wi = 0). See text for further discussion.

| Terrane | Description | Interpretation | Specific source rock indicators | Reference |
|---|---|---|---|---|
| Coedana Terrane (Holland Arms Gneisses) | Slivers of granotoid and gneissic rocks, sometimes converted to mylonitic schists. | Late Precambrian arc pluton. Frontal slivers dissected during obilque convergence. | Granite, gneiss, clinopyroxene, mylonite, plagioclase, polycrystalline quartz | Greenly (1919) Beckinsale and Thorpe (1979) Gibbons *et al.* (1994). |
| Aethwy Terrane (Anglesey Blueschist) | Phengitic mica schist and crossitic/glaucophanic metabasite, with minor lawsonite schist and spessartine-rich metasediments. | Fragments of accretionary prism caught between slivers of dismembered arc. | Blue and green aphibole, epidote, mylonite, greenschist, muscovite, polycrystalline quartz. | Gibbons and Mann (1983) Gibbons and Gyopars (1986) Dallmeyer and Gibbons (1987) |
| Monian Supergroup | Polydeformed psammites and pelites with horizons of pillow basalt erupted into jaspery and micritic sediments. Ultra mafic rocks, capped by a regional scale olisthostrome. | Forearc basin, ophiolite complex, and pillow lava melange. | Low-grade metasandstone, slate, chert, jasper epidote, chlorite, muscovite, reworked volcanic lithics, plagioclase, mylonite. | Greenly (1919) Wood (1974) Gibbons and Horak (1990) Phillips (1990b) |

**Table 3.4**. Specific source rock indicates yielded from the main tectono-metamorphic units associated with the Berw and Llyn shear zones on Anglesey.

apparent weathering indices. Therefore the observed low weathering indices cannot be explained by post-sedimentary processes.

Palaeoclimatic indicators throughout the section studied consistently indicate semi-arid conditions during sedimentation, a conclusion consistent with the high

latitudinal position of Avalonia in palaeogeographical reconstructions (Torsvik *et al.* 1996). Figure 3.16A is unable to quantify residence time in the weathering environment (relief) as low weathering indices (w=0) when combined with a semi-arid climate may develop on steep ("mountain") or low ("plain") gradient slopes. Significant topographic relief is instead suggested by alluvial fan, and to a lesser degree gravelly braided stream deposits, and the angularity of much of the sediment incorporated into debris flows and hyperconcentrated flows. As steep slopes correlate with rapid downslope transport rates, minimal alluvial storage and rapid burial, weathering-limited conditions are favoured, resulting ultimately in little chemical or physical alteration to original sandstone framework composition.

### 3.4.7. Source area

Sandstone framework modes reflect recycling of an extremely diverse source area that originated in a number of semi-distinct plate tectonic provinces. Low- and medium-grade metasandstones are the principle source rocks, supplemented by high-grade metamorphics, granite, mylonite, blueschist, jasper and chert. This very distinctive compositional assemblage has been identified from a number of roughly coeval Lower Cambrian successions in North Wales, and matched both petrographically (Nicholas 1915; Greenly 1919; Gibbons 1983) and geochemically (Roberts and Merriman 1990) with components of the Monian Superterrane (Gibbons and Horák 1996) exposed on Anglesey (Fig. 3.1B).

This tectonic collage, which is separated from the type-Avalonian Superterrane by a network of steep sinistral shear zones and brittle faults, the Menai Strait Fault System (Gibbons 1983, 1987; Gibbons and Horák 1990), has been divided into three tectono-metamorphic terranes (Pharaoh and Carney 2000) incorporating: (1) a belt of blueschist facies rocks (Aethwy Terrane) composed of phengitic mica schist and crossitic/glaucophanic metabasite, with minor lawsonite schists (Gibbons and Mann 1983; Dallmeyer and Gibbons 1987), (2) high-grade gneisses and granite (Coedana Terrane), in places converted to mylonitic schists (Greenly 1919; Beckinsale and Thorpe 1979), and (3) a thick sequence of low-grade metasediments (Monian Supergroup), with horizons of pillow basalts and ultra mafic rocks, capped by a regional scale olisthostrome (Wood 1974; Phillips *et al.* 1991b; Gibbons *et al.* 1994). The contacts between all these units are defined by faults. In most cases these are ductile dip-slip faults and strike-slip shear zones (Gibbons 1987), the oldest movements of which pre-date the late Lower Cambrian (Gibbons 1987). The most prominent early mylonitic belt within the Menai Strait Fault System is

the Berw Shear Zone, which runs for some 25 km across Anglesey before joining the Llyn Shear Zone on the Llyn Peninsula (Fig. 3.1B).

The main tectono-metamorphic units associated with the Berw and Llyn shear zones are presented in Table 3.4. These terranes clearly yield a number of specific source indicators that can be matched directly with grain types occurring in the Ogof Gochfa and St Non's formations. This juxtaposition of radically different metamorphic terranes along steep tectonic lines is a characteristic of obliquely colliding active plate margins (Graham *et al.* 1984), a tectonic setting consistent with the component elements of the Monian Superterrane: (1) frontal arc slivers (Coedana Complex), (2) fragments of accretionary prism (Aethwy Terrane), (3) trench-forearc sediments, (4) ophiolite complex, (5) deformed olisthostrome (all from the Monian Supergroup) and (6) mylonitic ductile shear zones. Detrital modes in the studied section reflect this diversity in the source area by plotting within both the "magmatic arc" and recycled orogen" global sandstone provenance fields (Fig. 3.16B and D).

Similar model compositions have been reported from a number of basin fills that were derived from structurally accreted oceanic and volcanic rocks incorporated within suture zones (Graham *et al.* 1993; Trop and Ridgeway 1997; Ridgeway *et al.* 2002; Robinson *et al.* 2003). These basins, which are classified as "late-stage" successor basins, typically develop during terminal phases of long-lived orogenic cycles, an example being the transform termination of subduction after ridge-trench collision. This invariably results in recycling of detritus from older basins developed earlier in the orogenic cycle into younger basins, a good example being the uplift, erosion, recycling and ultimate destruction of the Monian Supergroup trench-forearc basin (Gibbons 1983). The "counterfeit" magmatic arc signature evident from provenance discrimination diagrams clearly records erosion of a relict arc terrane, rather than an active-arc tectonic setting. This by-product of basin recycling is one of the more readily identifiable characteristics of successor basins (Graham *et al.* 1993).

The position of the Monian Superterrane with respect to NW Pembrokeshire is problematic, as any evidence for continuation of the Berw/Llyn Shear Zone south of the Llyn Peninsula is lost beneath the Irish Sea (Fig. 3.1B). Sediment dispersal patterns determined from palaeoflow indicators (Fig. 3.5) are consistent with Monian-like source rocks positioned immediately west of Pembrokeshire during the Lower Cambrian (Fig. 3.1B). Therefore the Monian Superterrane has either been displaced transcurrently to its present position after the Lower Cambrian, or has a southern continuation that extends beyond SW Wales. The first scenario is incompatible with shear sense markers present throughout the Menai Strait Fault System, which consistently indicate a sinistral shearing component and thus a southeastward

displacement of terranes towards Pembrokeshire. The striking similarities between the Late Precambrian and Early Cambrian geology of Anglesey and the Rosslare Complex in southeastern Ireland (Baker 1955; Crimes and Dhonau 1967; Gibbons and Horák 1990) lends credence to the second scenario, and a south-southeastern extension of the Monian Superterrane, west of Pembrokeshire and across the Irish sea to the southeasternmost point of Ireland (Fig. 3.1B). This palaeogeographical setting for the Monian Superterrane was depicted for the latest Precambrian by Anderton *et al.* (1992, Precambrian map 3b).

## 3.5. TECTONOSTRATIGRAPHY

### 3.5.1. Stratal architecture and controlling mechanisms

The lithofacies described and interpreted above form a +68 m thick coarsening-upward–fining-upward sequence (Fig. 3.2) analogous to the megasequence outlined by Heward (1978). Coarsening upward in the basal 32 m is arranged into two higher order coarsening upward cycles composed exclusively of prograding coarse-grained continental deposits separated by a distinctive silt-dominated "flooding surface" interpreted as ephemeral pond/lacustrine sediments. The arrangement of lithofacies, and their progradation and retrogradation through time indicate both rapid and prolonged variations in the ratio between sediment supply and the rate of accommodation space creation (Revnas and Steel 1998). These two variables, which ultimately control sediment transfer processes and depositional architecture (Stokes and Mather 2000), develop in response to a number of internal (autocyclic) and external (allocyclic) controls, which operate over a variety of spatial and temporal scales. Typical allocyclic mechanisms include syn-depositional tectonism and climate change, while source rock lithology and lateral switching of the alluvial tract constitute the most important autocyclic controls (Collinson 1996).

The palaeotectonic inferences of mass flow-dominated alluvial fan sedimentation have been previously highlighted. The required piedmont setting with juxtaposition of bedrock block and actively subsiding valley is the most commonly invoked allocyclic control in coarse-grained largely continental sequences (Eliet and Gawthorpe 1995; Martins-Neto 1996; Ryang and Chough 1999; Stokes and Mather 2000; Benvenuti 2002), as both accommodation space and sediment flux are generated simultaneously with either valley subsidence (in extensional regimes) or source uplift (in compressional regimes). Evidence for phases of syn-orogenic

sedimentation in the studied section include: (1) rapid vertical facies changes and an unconformable basement-cover relationship (Mueller and Corcoran 2001), (2) a coarse grain size, high lithic content and immature composition, coupled with mixing of local and more exotic source terranes (Lee and Sheen 1999; Hendrix 2000; Qayyum *et al.* 2001; Lawton *et al.* 2003; Robinson *et al.* 2003), (3) evidence for tilting of the fan surface commonly reflected in deeply incised basal units (Ryang and Chough 1997, 1999; Stokes and Mather 2000), (4) footwall derived alluvial fans and a consequent drainage system (Leeder *et al.* 1988), and finally (5) a sharp flooding surface reflecting almost instantaneous cut-off of sediment flux to the fan surface (Crews and Ethridge 1993; Graham *et al.* 1993; Benvenuti 2002).

Clay-dominated intervals sharply overlying phases of alluvial fan progradation are generally considered excellent indicators of syn-orogenic sedimentation, having been documented in rift, transtensional, and foreland basin settings (Blair and Bilodeau 1988; Steel 1988; Crews and Ethridge 1993; Martins-Neto 1996; Mutti *et al.* 1996, 2000). This stratal architecture of coarsening upward separated by flooding surfaces has been linked specifically to the balance between fault-controlled subsidence (accommodation space creation) and relative source uplift (sediment flux) by a number of authors (e.g. Paola *et al.* 1992; Crews and Ethridge 1993; Gordon and Heller 1993; Benvenuti 2002). A graphic interpretation of the coarsening-upward sequences recorded in the section at Ogof Golchfa along with the inferred response of the alluvial system to tectonic activity (fault rejuvenation) is presented in Figure 3.17. The coarsening-upward phases (designated phase 2 and 4 in Fig. 3.17) correspond to periods of increasing ratios of sediment flux to subsidence rate, resulting in basinward growth (progradation) of the alluvial fan. This increase in the ratio of sediment flux to subsidence rate was probably driven solely, at least during phase 2, by a decrease in the rate of accommodation space following initial fan surface incision. The second coarsening upward profile (phase 4 in Fig. 3.17) may have been further influenced by an increase in sediment flux, as evidenced by a more varied clast and lithic composition, and inferred drainage basin expansion (Facies Association B, Petrofacies A2). Coarsening-upward successions therefore appear to record the transition from tectonically active to tectonically quiescent stages, a depositional signature commonly referred to as "anti-tectonic" cycles (Heller *et al.* 1988; Paola *et al.* 1992; Gordon and Heller 1993). Conversely, finer grained intervals (phase 3 in Fig. 3.17) are known to represent periods of rapid differential subsidence, which counters the tendency of sediment shed from rapidly rising uplands to prograde across the adjacent basin by absorbing sediment and lowering or reversing the depositional slope (Blair and Bilodeau 1988; Crews and Ethridge

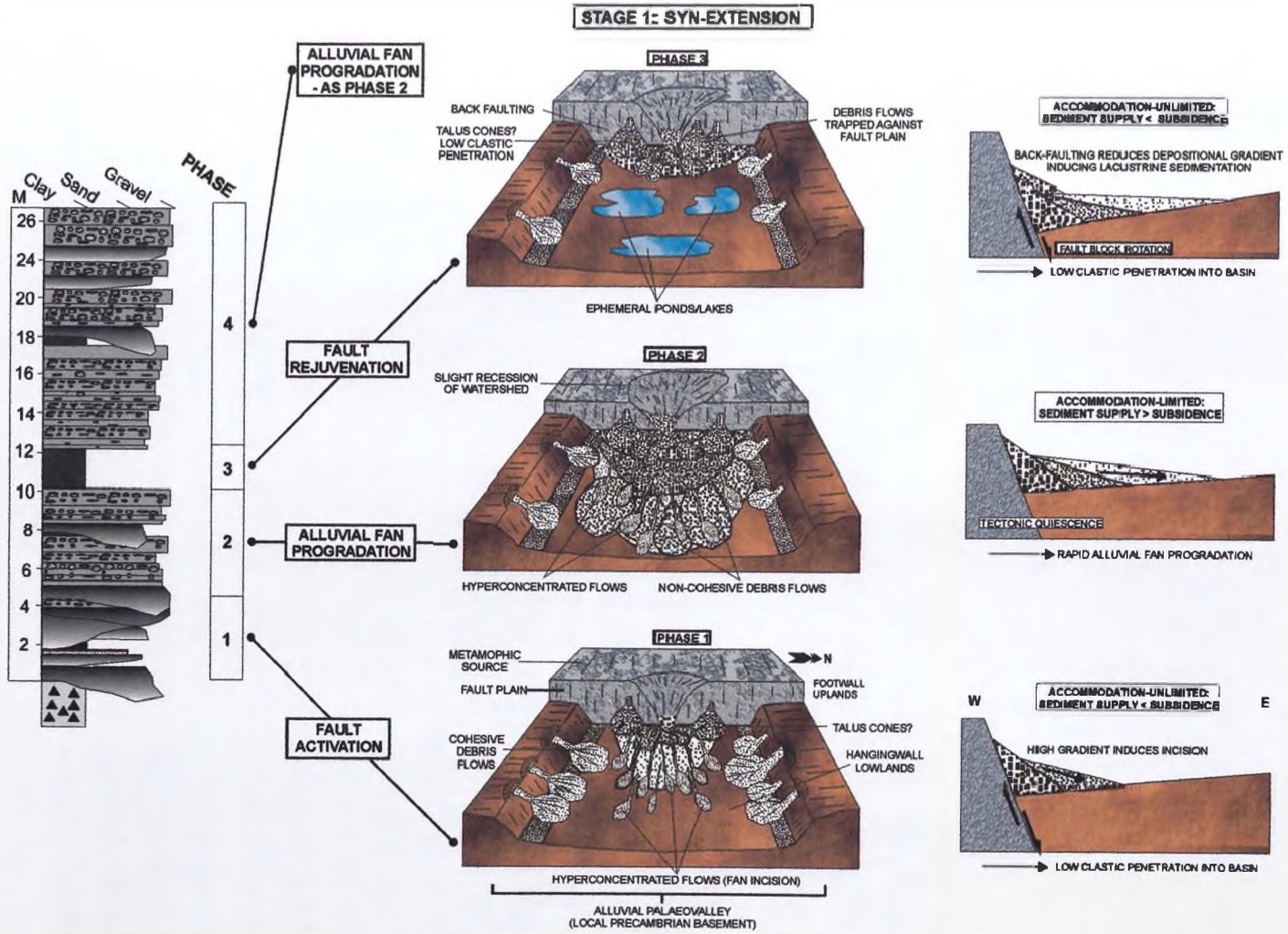



**Fig. 3.17.** Tectonosedimentary model for syn-orogenic (Stage 1) alluvial fan deposits of the Ogof Golchfa Formation (see text for discussion).

1993). The sedimentary response to source rejuvenation is therefore delayed, resulting in low clastic penetration into the basin, and the phase of maximum subsidence being relatively starved of sediment.

Although the lack of regional exposure severely hinders detailed analysis of palaeoslope trends, and thus evidence for lowering or reversal of depositional slopes during fault rejuvenation is limited, fault block rotation may explain the almost instantaneous switch from alluvial fan sedimentation in the form of steep gradient debris flows to substantially lower gradient ephemeral pond deposits. A similar transition involving identical facies was reported by Ryang and Chough (1999) from well-exposed alluvial fan and braided stream deposits of the Eumsung Basin in Korea. According to these authors, the transition from debris flow to ephemeral pond/lacustrine sedimentation can be most adequately accounted for by assuming differential subsidence with a zone of maximum downwarping proximal to the fault plane. As illustrated in Figure 3.17 (phase 3), fault block rotation will most likely counteract the depositional slope constructed by alluvial fan processes, and in doing so, allow areas of the largely inactive alluvial plain to become locations of standing bodies of water.

The fining-upward that characterizes the upper part of the megasequence (Fig. 3.18) implies a more prolonged variation in the ratio between sediment supply and accommodation space. The position of the inflection point between coarsening upwards and fining upwards lies close to the transition between alluvial fan and braided stream sedimentation (phase 5 in Fig. 3.18), implying a common causal factor in both process and stratigraphic architecture. A quantitative measure of relative rates of subsidence and sediment flux from an alluvial fan to braided stream transition was reported by Soegaard (1990), who concluded that the required reduction in gradient necessary to induce a more fluvial style of sedimentation necessitates a supply of sediment in excess of accommodation space creation. This increase in the ratio between sediment supply and subsidence can most adequately be accounted for by assuming waning tectonic influence coupled with recession of the watershed (phase 5 in Fig. 3.18), a feature consistent with the more varied clast composition evident in braided stream deposits. A waning tectonic influence and aggressive source area denudation without repeated reactivation of the source will ultimately lead to a diminished siliciclastic input and fining-upward (Crews and Ethridge 1993).

Although evidence for a piedmont setting maintained over more than one cycle strongly implies a tectonic control on depositional architecture (Benvenuti 2002), it is difficult to determine whether highlands were initiated by basin subsidence

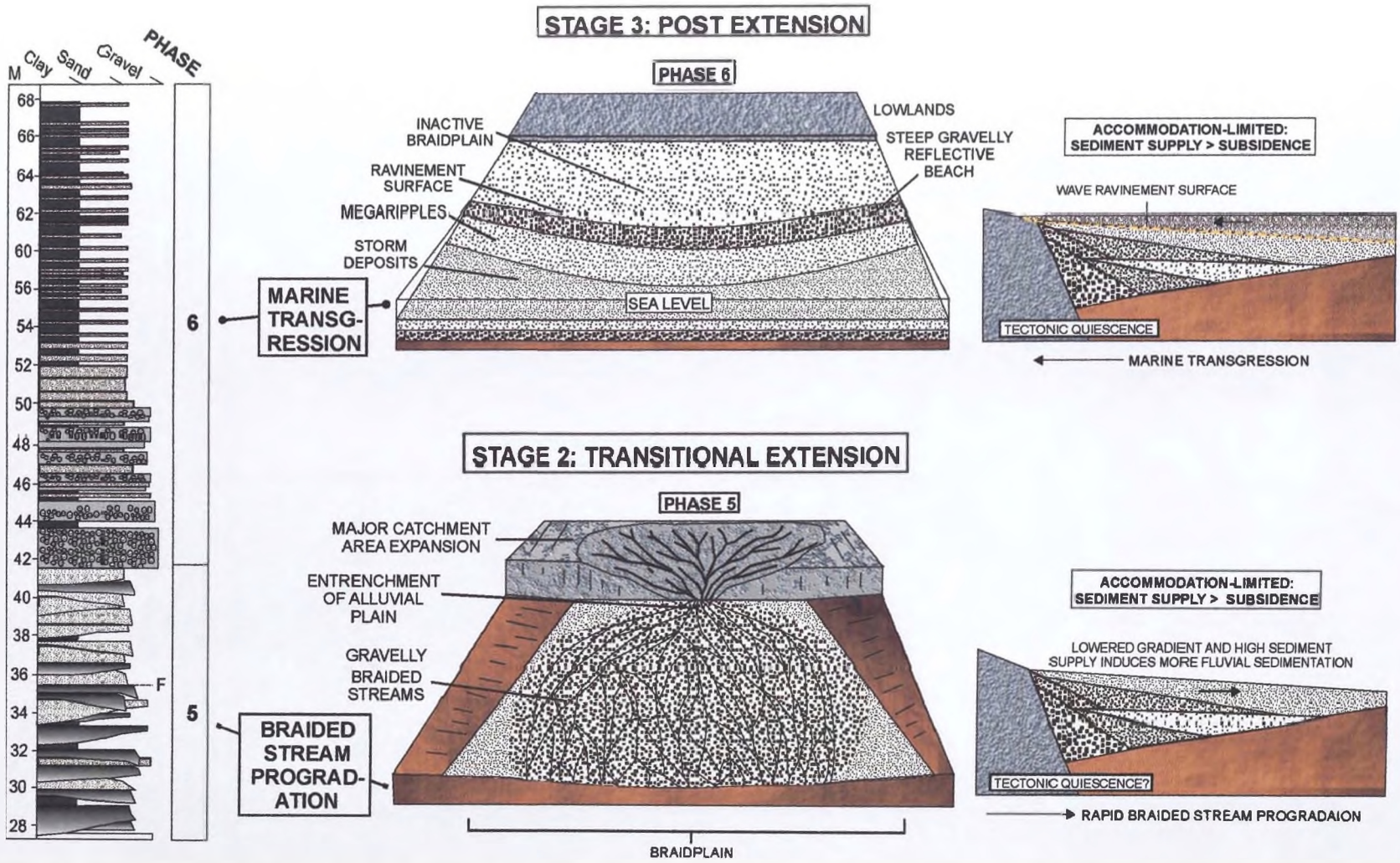



**Fig. 3.18.** Tectonosedimentry model for transitional (Stage 2) and post-orogenic (Stage 3) sedimentation in the Ogof Golchfa and St Non's formations.

(extensional regime) or source uplift (compressional regime). Evidence for fault-block rotation would favour a purely extensional setting, an interpretation consistent with the lack of internal angular unconformities within the sedimentary succession (Martins-Neto 1996). Subsidence analysis conducted on outcrops throughout the Cambrian Welsh Basin (Prigmore *et al.* 1997) also indicate a protracted period of regional extension (transtension) during the time the Caerfai Group was deposited. Evidence for compressional tectonics remains speculative, with possible Early Cambrian folding and thrusting with associated low-grade metamorphism during accretion of the Monian Superterrane (Gibbons 1987).

The above discussion argues for a strong tectonic control on sedimentation, one that influences both depositional processes and stratigraphic architecture. Although periodic changes in climate and source rock lithology are known to generate cyclic patterns similar to those recorded herein (Mutti *et al.* 1996, 2000), conglomerate facies consistently indicate similar (semi-arid) climatic conditions e.g. mass flow-dominated alluvial fans, ephemeral braided streams, red haematite staining, and discrete masses of detrital haematite, while a dramatic change in source rock lithology is unlikely considering the similarity in clast and lithic composition, and palaeocurrent direction throughout the section. The most likely autocyclic process that may have generated the observed cyclicity is lateral switching of the main alluvial tract. Although the effects of this mechanism are difficult to assess due to outcrop restrictions, the sharp flooding surface that separates two discrete phases of alluvial fan progradation is difficult to account for by any other means than fault-accommodated tectonically-induced subsidence, while evidence for the alluvial palaeovalley locked in bedrock (Fig. 3.6) suggests a relatively confined alluvial tract, with restrictions on the possible scale of active zone switching.

### 3.5.2. Tectonosedimentary model and basin margin evolution

Assuming the megasequence and higher order internal cycles in the studied section were formed in response to variations in fault-accommodated subsidence, a 3-stage (6-phase) tectonosedimentary model is proposed to account for the observed vertical evolution in lithofacies and clast composition. In recognition of this tectonic element, variations in sediment flux and accommodation space through the megasequence may be expressed in terms of syn-extension, transitional extension, and post-extension (here referred to as stages 1–3) as advocated by numerous authors e.g. Dietrich *et al.* (1993) and Rainbard *et al.* (2003). These stages of basin margin evolution are highlighted in a series of palaeoenvironmental reconstructions

displayed in Figures 3.17 and 3.18, and a schematic cross sectional representation (Fig. 3.19).

*3.5.2.1. Stage 1: syn-extension (phases 1–4).*

Syn-extensional sedimentation at the base of the Cambrian in NW Pembrokeshire is similar to numerous other examples of tectonically active stages of basin evolution in being composed exclusively of alluvial fan deposits (Facies Association A). In phase 1 (Fig. 3.17), intense bedrock incision by hyperconcentrated flow marks the onset of piedmont generation in the study area, and is a typical basal signature associated with initial phases of fault controlled subsidence (Ryang and Chough 1999; Hendrix 2000; Lawton 2003), when accommodation space creation outstrips sediment flux, resulting in increasing fan gradient, and sediment bypass. This phase of bedrock incision results in the inherited magmatic arc signature recorded in Petrofacies A1, as local sediment eroded from the relict arc terrane of the Pebidian Supergroup is incorporated with detritus shed from the fault scarp. Cohesionless, and to a lesser extent cohesive debris flows are the main elemental components of alluvial fan sedimentation during phase-2, and engineer a prolonged period of alluvial fan construction, expansion, and drainage basin enlargement. This essentially corresponds to stages 1 and 2 of alluvial fan evolution outlined by Blair and McPherson (1994). Evidence for cohesive debris flows sourced from local bedrock implies some topographic expression on the footwall lowlands (Fig. 3.18). As there is no evidence for later rejuvenation of this local source, these "highlands" probably represent a pre-existing structure generated prior to Cambrian sedimentation. The strongly progradational character of phase 2 signifies a reversal in the ratio between sediment flux and accommodation space, a feature dually controlled by expansion of the drainage area and waning of fault-accommodated subsidence.

The flooding surface that forms the base of phase 3 heralds a second pulse of tectonic subsidence that reset the gradient established during alluvial fan progradation. Rapid backfaulting allows ephemeral lakes to become established on the alluvial plain, while rapid accommodation space creation results in low clastic penetration into the basin, with the probable development of talus cones close to the mountain front. Phase 4, like phase 2, records a protracted period of alluvial fan progradation away from the now inactive fault plain (Fig. 3.18). The high run-out capabilities of debris flows and continual recession of the watershed results in an overall decrease in depositional gradient (Blair and McPherson 1994), a conclusion

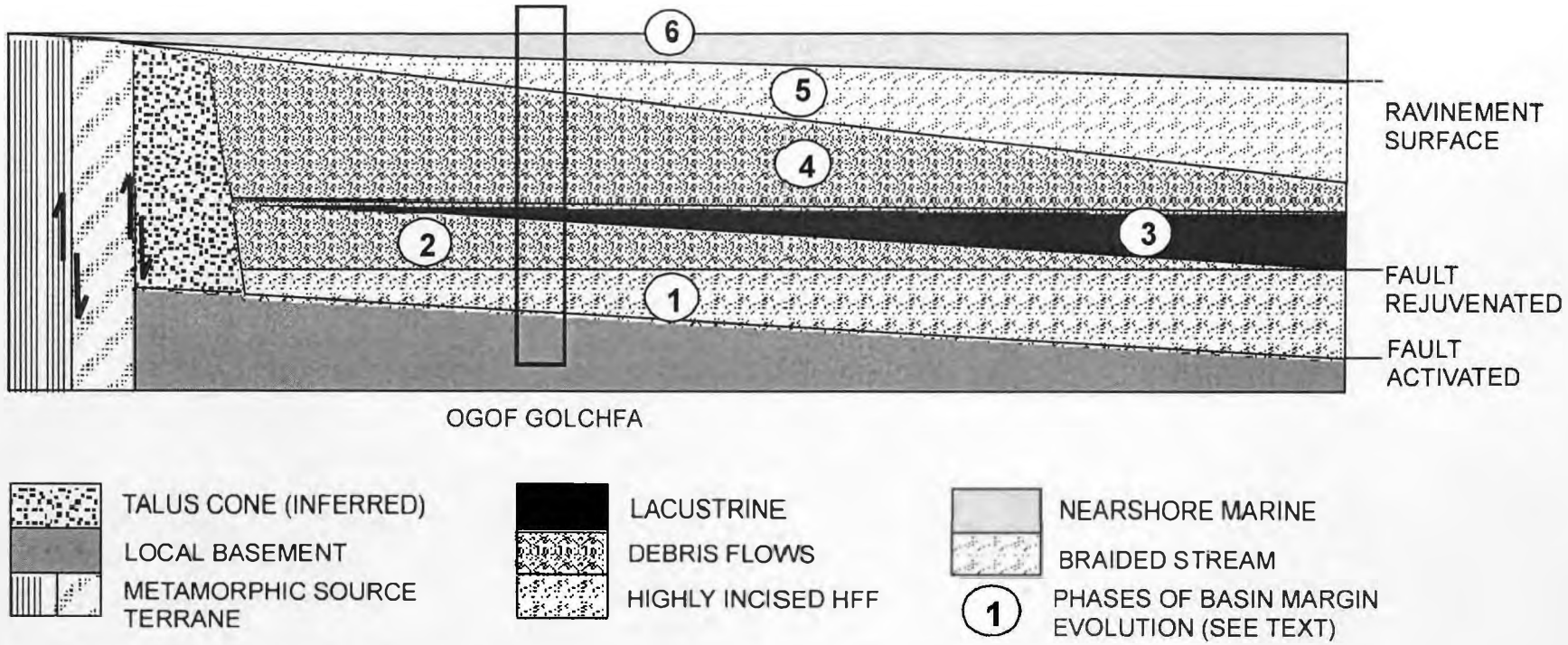



**Fig. 3.19.** Schematic cross sectional representation of basin margin evolution (see text for details).

consistent with the dominance in phase 4 of non-shearing debris flows (Kim *et al.* 1995), as well as an increase in water/sediment discharge that ultimately leads to a switch to braided stream deposition that characterises sediments of stage 2.

*3.5.2.2. Stage 2: transitional extension*

Due to uncertainties regarding the evolution of basin margins from syn-orogenic to post orogenic stages (see Ravnas and Steel 1998 for discussion), the admittedly vague term "transitional extension" is used to describe those sediments passively shed from already established topography that displays no evidence for rejuvenation (Pavelic 2001; Rainbird *et al.* 2003). The switch from alluvial fan to braided stream sedimentation records this passive phase of hinterland erosion and drainage basin expansion, as relief is worn down and depositional gradients reduced (Fig. 3.18). The decrease in labile fragments and increase in monocrystalline quartz documented in the transition from Petrofacies A1 into A2 (Fig. 3.15) is consistent with denudation of the post tectonic landscape associated with syn-orogenic to transitional orogenic phases (Cox *et al.* 2002; Arribas *et al.* 2003).

*3.5.2.3. Stage 3: post-extension (phase 6)*

The final stage of the model corresponds to the "destructive onlap phase" of Eriksson (1978), and records marine inundation and reworking of transitional orogenic material under highly reflective nearshore conditions, on crust that has become relatively stable (Fig. 3.18). Based on similarities in clast composition between transitional and post orogenic detritus, sediment supply appears tied to ravinement processes, while accommodation space creation was likely created by thermal contraction of the lithosphere following active extension, as well as contributions from a rise in eustatic sea level (Conway Morris and Rushton 1988). A steep reflective shoreline and narrow littoral zone are typical geomorphologic expressions of post-tectonic nearshore sedimentation, particularly after fault block rotation (Massari and Colella 1988).

The rise in whole rock percentages of amphibole and epidote (Fig. 3.15) during post extensional sedimentation remains problematic and cannot be solely accounted for by ravinement processes, as amphibole particularly is considered a first-cycle mineral based on its instability with respect to chemical and mechanical abrasion (Arribas *et al.* 2003). The only way one could imagine first-cycle material in transgressive shoreline deposits is through direct erosion of the original amphibole-

bearing source terrane. This would not only account for the increase in these tracer minerals up through Petrofacies B, as the sea progressively encroached the once active fault scarp to the west (Fig. 3B), but also the return to more feldspathic sandstones in the uppermost part (beyond the studied section) of the St Non's Formation (Crimes 1970a; Rushton 1974; Prigmore and Rushton 2000). If we accept this interpretation, the post orogenic phase of uniform thermal subsidence is directly comparable with other fault overstep sequences described extensively in the literature (see review in Ravnas and Steel 1998).

### 3.5.3. The extensional regime

#### *3.5.3.1. General*

The tectonostratigraphic model presented above argues for a dominantly extensional tectonic regime to generate the required piedmont setting necessary for alluvial fan and gravelly braided stream sedimentation. If we accept that the source area existed as a southerly extension of the Monian Superterrane, then fault-accommodated subsidence must have taken place along the Menai Strait Fault System (Fig. 3.1B). This terrane boundary has a protracted history of strike-slip displacement and contains kinematic indicators that record substantial pre-Ordovician sinistral shearing combined with dip-slip movement (Gibbons 1990). Syn-extensional downwarping in locations adjacent to this basement lineament in both North Wales (Harlech Dome, Fig. 3.1B) and NW Pembrokeshire is most likely to have occurred under transtensional regimes, with mechanical subsidence accommodated along high-angle oblique-slip normal faults. The kinematic indicators described are similar to those reported from pull-apart rift basins (Nance *et al.* 1991; Dorsey *et al.* 1995).

Subsidence analysis reported by Prigmore *et al.* (1997) from Cambrian sequences throughout East Avalonia suggest a regional phase of transtension accompanied by periods of more local transpression during the Lower and Middle Cambrian. These authors relate this tectonic regime to the transform termination of Cadomian/Avalonian subduction and the suturing of arc-related terranes to form the Avalonian Superterrane (Fig. 3.1B). We may further this conclusion by suggesting that transtensional basins proximal to the Menai Strait Fault System record pull-apart rifting associated with the final docking of the Monian Superterrane to the Avalonian Superterrane (Fig. 3.1B).

#### *3.5.3.2. The basin-fill*

The recognition of strike-slip basins even from well exposed basin-fill sequences is often difficult because depositional and structural histories are complex (Nilsen and Sylvester 1999). Accepted features of strike-slip basins (Reading 1980; Steel and Gloppen 1980; Miall 2000) such as: (1) alternating periods of transtension and transpression, (2) basin asymmetry, (3) differential subsidence, (4) syn-depositional tectonism, (5) sparse igneous activity, except locally in zones of transtension, (6) basin margin cannibalisation, (7) depocenter migration, (8) lateral offset of the basin from its source, and (9) a restricted basin size, are difficult or impossible to determine from the succession in Pembrokeshire because of limited outcrop and lack of an exposed fault and source. There is some evidence for a common variant on the transtensional-transpressional cycle, with the syn-, transitional and post-extensional stages evident in the Ogof Golchfa and St Non's formations interrupted by a renewed phase of extension (rapid deepening) rather than compression (rapid shallowing). A sudden switch to an easterly-derived depositional system during sedimentation of the overlying Caerfai Bay Formation and the occurrence of numerous coarse-grained feldspathic tuff is consistent with a phase of major basin reorganization generated under transtensional regimes (point 5, above).

Many of the listed features of strike-slip basins are evident in the Lower and Middle Cambrian successions analyzed by Prigmore *et al.* (1997). Excellent examples of transtensional-transpressional cycles occur at Shropshire and Nuneaton (Fig. 3.1B). The basal sequence evident in the Hartshill Formation at Nuneaton (Brasier 1989; Landing 1996; Bridges *et al.* 1998) is a good example of the "type" strike-slip depositional sequence outlined by Massari and Colella (1988), with syn-extensional Gilbert-type fan-deltaic sediments (Boon's Member), overlain by post extensional marine clastics (Park Hill, Turtle Hill and Jee's members), followed by post Jee's Member uplift, erosion and deposition of highly condensed carbonates (Home Farm Member). These sequences also record intense reworking and cannibalization along the basin margin (Rushton 1974), differential subsidence (Smith and Rushton 1993), and an eastward shift in the principle depocenter (Landing 1996). Evidence for syn-depositional tectonism include intraformational folds in the Middle Cambrian Newgale Formation of NW Pembrokeshire, Middle Cambrian bentonites in North Wales with intra-plate geochemical signatures (Roberts and Merriman 1990) typical of pull-apart rifts (Keppie *et al.* 1997), and manganese precipitated from metal-bearing submarine exhalative hydrothermal solutions in ore beds at the base of the Middle Cambrian in North Wales (Bennett 1987).

## 3.6. CONCLUSION: IMPLICATIONS FOR THE LATE NEOPROTEROZOIC–CAMBRIAN TECTONO-STRATIGRAPHIC EVOLUTION OF EASTERN AVALONIA

Evidence for strike-slip tectonics during basal Cambrian sedimentation in East Avalonia requires a revaluation of the relationship between the late Precambrian magmatic arc complex and Cambrian overstep sequence. The association of two discrete lithotectonic packages has previously defined this tectonic evolution in southern Britain. The first comprise late Precambrian, calc-alkaline, granitoid bodies and cogenetic terrestrial volcanics and volcaniclastics (see reviews in Pharaoh and Gibbons 1994; Gibbons *et al.* 1994; and Pharaoh and Carney 2000). This package is attributed to the development of a magmatic arc and associated intra-arc, interarc, and back-arc basins during the late Precambrian Avalonian orogenic cycle (Allen and Jackson 1978; Reedman *et al.* 1984; Pauley 1990; Cope and Bevins 1993; Compston *et al.* 2000). The second consists of Cambro-Ordovician platformal overstep sequences, deposited during passive overlap of the decayed magmatic arc (Woodcock 2000; Compston *et al.* 2002). Critical to this simple two-phase interpretation is the almost universal recognition of a supposed nearshore deposited basal conglomerate (e.g. Crimes 1970a, Rushton 1972). This has been taken to signify a wholly passive Early Cambrian tectonic regime, with accommodation generated solely by thermal rather than mechanical (fault-accommodated) subsidence. The transition from magmatic arc (subduction) to stable cratonic platform has been variously termed the Avalonian or Cadomian orogeny (Rast 1979; Rast and Skehan 1983), a general perception of collision upheld despite the lack of compelling evidence for regional orogenesis, crustal shortening/thickening, and widespread metamorphism (Nance 1991; Nance *et al.* 1991; Gibbons and Horák 1996).

The role of strike-slip tectonics in the diachronous cessation of arc volcanism in West Avalonia is well documented (Nance 1991; Murphy and Nance 1989, 1991; Nance *et al.* 1991, 2002), with sedimentation during the Lower and Middle Cambrian principally confined to pull-apart rift basins on an epeirogenically active platform (Murphy *et al.* 1985; Barr *et al.* 1993; Landing 1992, 1996; Keppie *et al.* 1997). To account for this transition from subduction-related to wrench-related tectonism in the apparent absence of a major collisional episode, Murphy and Nance (1989) proposed that Avalonian subduction was terminated as a result of transform activity. Murphy *et al.* (1999) later postulated ridge-trench collision as a mechanism for the diachronous cessation of arc volcanism, and the initiation of the continental transform.

The tectonostratigraphic model presented for basal Cambrian sedimentation in SW Wales as well as evidence for strike-slip tectonics from other parts of southern Britain is compatible with the subduction–oblique subduction–continental transform model proposed for West Avalonia. Strike-slip faults such as the Menai Strait Fault System and the Welsh Borderland Fault System were probably initiated as trench-linked strike-slip faults (cf. Woodcock 1986; Sylvester 1988), a suggestion first proposed by Reading (1980). The NE-SW trend of these faults (Fig. 3.1B) orthogonal to the SE polarity of Avalonian subduction (Thorpe *et al.* 1984) (thus parallel to the trench) is consistent with this interpretation (Sylvester 1988).

A "late-stage" transform regime during Lower Cambrian sedimentation also accounts for the gross similarities between the detrital mode data described above, and modal compositions described from "late-stage" successor basins developed during terminal phases of orogenic cycles. The most distinguishing characteristic of successor basins, and one that defines their position in long-lived orogenic cycles, is the recycling of detritus from older basins developed earlier in the cycle into younger successor basins (Graham *et al.* 1993; Trop and Ridgeway 1997; Robinson *et al.* 2003). In the succession in NW Pembrokeshire, the stage of subduction and oblique convergence is recorded in the sedimentation of the Pebidian Supergroup of the Avalonian Superterrane (Pharaoh and Gibbons 1994; Compston *et al.* 2002), and the formation and dissection of more outboard parts of the subduction system (e.g. frontal arc slivers and accretion prism) to form the Monian Superterrane. The angular unconformity that separates arc-related volcanics of the Pebidian Supergroup from pull-apart sediments of the Lower Cambrian may record either the ridge-trench collision proposed by Murphy *et al.* (1999) and the initiation of the continental transform, or the docking of the Monian Superterrane to the Avalonian Superterrane. Irrespective of origin, this collisional event appears to have inverted the forearc sediments of the Monian Supergroup (and related terranes) (Gibbons 1983), which under a transform regime were then recycled into transtensional successor basins during sinistral strike-slip displacement on the Menai Strait Fault System.

Cambrian pull-apart basins appear to be generally coincident in space with Precambrian basins throughout East Avalonia (Fig. 3.1B), suggesting a strong degree of inheritance. In North Wales, the Lower Cambrian "Dolwen Basin" was sourced by the late Precambrian "Arfon Basin" (Allen and Jackson 1978), while in the English Midlands, the "Hartshill Basin" and "Hanging Rock Basin" (Charnian Supergroup) were both sourced by the late Precambrian "Mapellwell Basin" (Charnian Supergroup) (Bridges *et al.* 1998; McIlroy *et al.* 1998). The position of these basins (Fig. 3.1B) seemingly corresponds to the boundaries of underlying

accreted terranes, another characteristic typical of successor basins (Graham *et al.* 1993; Trop and Ridgeway 1997). The structural inversion of Precambrian basins and the opening of transtensional successor basins throughout East Avalonian appears related to the suturing of volcanic arc terranes during the transform termination of Avalonia subduction and microcontinent formation, a tectonostratigraphic evolution mirrored in coeval successions in the Avalonian belt of North America.

*CHAPTER 4*

# THE ANATOMY OF A FLOOD-DOMINATED FAN-DELTA FROM THE MIDDLE CAMBRIAN (ST DAVID'S SERIES) OF SW WALES, UK: PROCESSES, FACIES, AND CLASSIFICATION

## 4.1. INTRODUCTION

Sediment delivery and dispersal patterns on modern inertia-dominated small and medium sized mountainous rivers draining tectonically active margins have received increasing attention in recent years (Mulder and Syvitski 1995; Wheatcroft *et al.* 1996, 1997; Mulder *et al.* 1998, 2001, 2002; Wheatcroft 2000; Wright *et al.* 2002). These so-called 'dirty rivers' (cf. Mulder and Syvitski 1995), with bulk densities of riverine outflow exceeding that of the oceanic ambient, are dominated by hyperpycnal underflows (*sensu* Bates 1953) (Fig. 4.1) which exist as quasi-steady turbidity currents (cf. Kneller 1995) capable of efficient sediment dispersal across wide shelf regions (Wheatcroft *et al.* 2000). According to Parsons *et al.* (2001), 84% of the world's rivers may be classified as 'dirty' producing turbulent underflows annually, and in turn contributing 53% of the world oceanic sediment load. Similar conclusions were reported by Mulder and Syvitski (1995) where, of the 230 rivers studied, 71% produce hyperpycnal flows during floods with a return period of less than 1000 years. These figures are consistent with the frequency of cored hyperpycnal deposits recorded during the last 100 years at the mouth of the Var Canyon in the Mediterranean (Mulder and Alexander 2001).

Considering the frequency with which hyperpycnal currents are generated in modern flood-dominated dispersal systems, hyperpycnal turbidites should form a significant proportion of the basin-fill of ancient tectonically active basins (Mutti *et al.* 1996). This is particularly so because no study of flood-generated dispersal systems has yet to fully observe and document a true geologically significant catastrophic flood event (Higgs 1990). Only a few studies have invoked quasi-steady hyperpycnal currents as a mode of across-shelf transport in ancient sequences (Balance 1988; Martinsen 1990; Falk and Dorsey 1998; Mutti *et al.* 1996, 2000, 2003; Myrow *et al.*

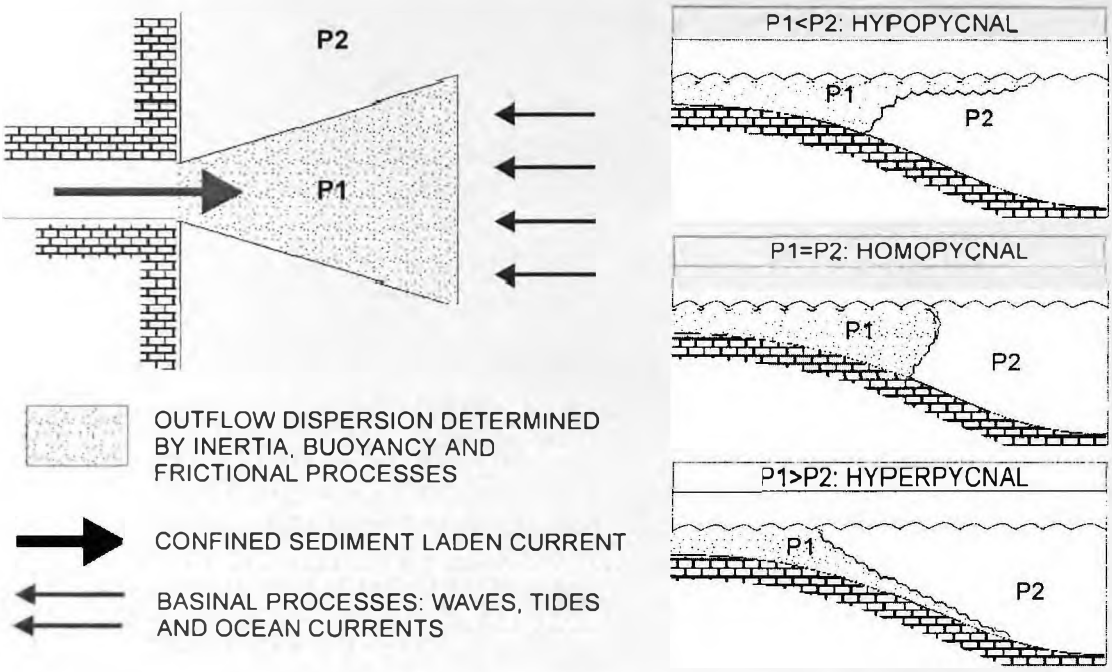



**Fig. 4.1.** Different modes of interaction between sediment-laden river water and basin water, determined by the relative density of the water bodies (modified from Orton and Reading, 1993).

2002; Plink-Björklund and Steel 2004). The catastrophic introduction of sediment into marine basins is commonly referred to as an oceanic flood (Wheatcroft *et al.* 2000). This typically occurs in physiographic settings where sediment flux to the sea is enhanced by high elevation source areas close to the shoreline, lack of extensive alluvial and coastal plains, and the periodic flooding of small and medium-sized 'mountainous' rivers and alluvial fans characterised by relatively short and high gradient transfer zones (Milliman and Syvitski 1992). On these often tectonically active margins, sediment concentration is not significantly reduced by energy dissipation and deposition on coastal plains, and therefore discharge typically arrives at the marine interface with sufficient inertia and density to underflow seawater (Mulder and Syvitski, 1995). By contrast, mature river systems draining passive margins are generally characterised by a fine-grained suspended load of low concentration, that reflects a moderate to low gradient transfer system and a less catastrophic response to short-lived flood events. Hyperpycnal flows are rare in such systems, as flood-derived sediment is commonly sequestered on coastal plains, thus reducing the concentration of river outflow and promoting hypopycnal surface plumes (McLeod *et al.* 1999) (Fig. 4.1).

This study of Middle Cambrian (St David's Series) sediments of the Caerfai Group and lower part of the Porth-y-rhaw Group (Fig. 4.2) exposed in NW

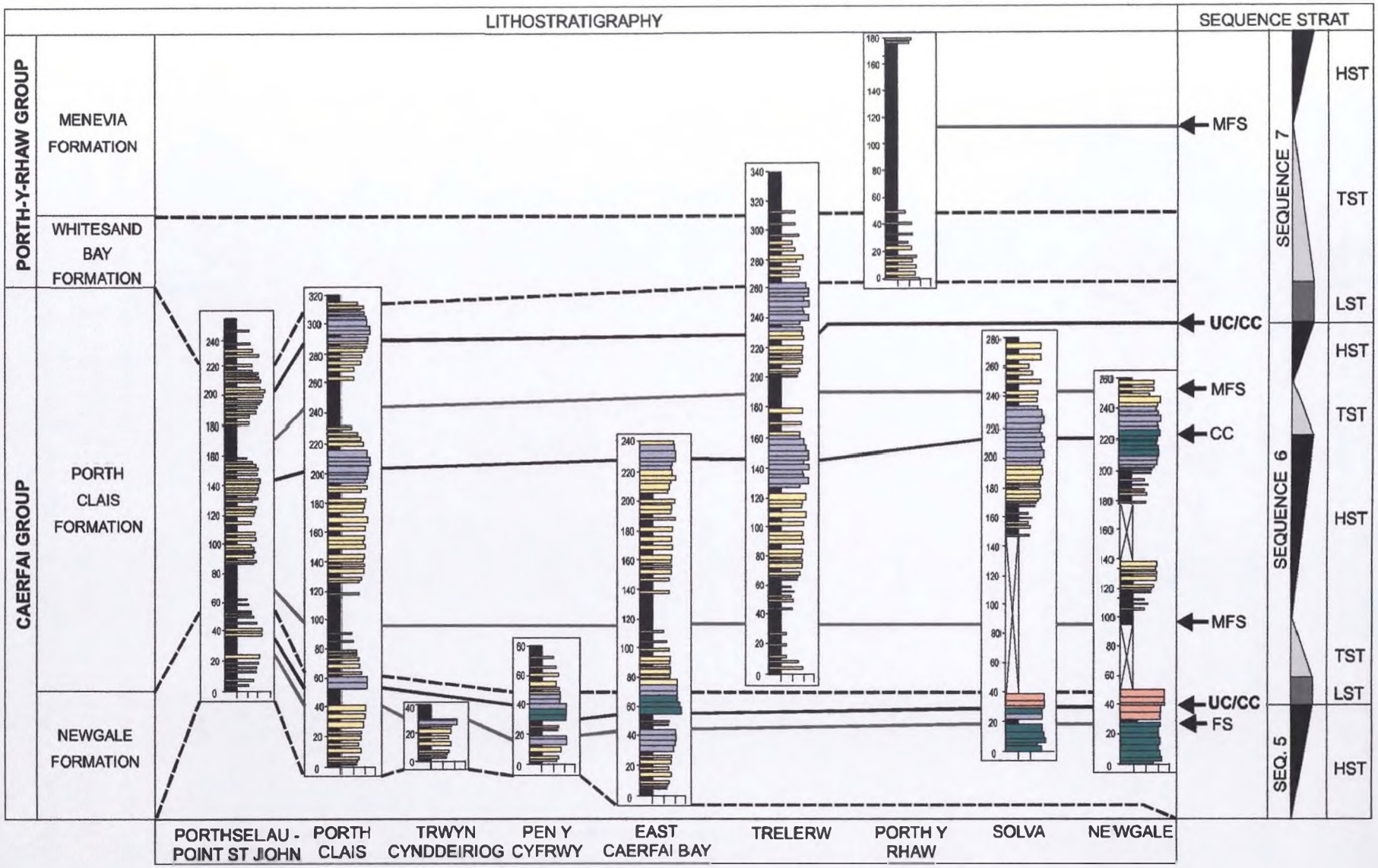

LITHOSTRATIGRAPHY
SEQUENCE STRAT
PORTH-Y-RHAW GROUP
CAERFAI GROUP
MENEVIA FORMATION
WHITESAND BAY FORMATION
PORTH CLAIS FORMATION
NEWGALE FORMATION
MFS
UC/CC
MFS
CC
MFS
UC/CC
FS
SEQUENCE 7
SEQUENCE 6
SEQ. 5
HST
TST
LST
HST
TST
HST
TST
LST
HST
PORTHSELAU - POINT ST JOHN
PORTH CLAIS
TRWYN CYNDDEIRIOG
PEN Y CYFRWY
EAST CAERFAI BAY
TRELERW
PORTH Y RHAW
SOLVA
NEWGALE

**Fig. 4.2.** Lithostratigraphy and sequence stratigraphy of the Middle Cambrian (St David's Series) exposed in NW Pembrokeshire. See Fig. 4.9 for key to lithostratigraphy. Sequence stratigraphy: LST – lowstand systems tract, TST – transgressive systems tract, HST – highstand systems tract, MFS – maximum flooding surface, CC – correlative conformity, and UC/CC – proximal unconformity/distal correlative conformity.

Pembrokeshire, Wales (Fig. 4.3C), is the first detailed investigation into the lithofacies, processes, geometry, and classification of coarse-grained deltas built exclusively by flood-generated sediment dispersal processes. It complements work on ancient flood-dominated fluvio-deltaic systems by Mutti *et al.* (1996, 2000, 2003) and Plink-Björklund and Steel (2004), who have set out preliminary criteria for their recognition and interpretation.

## 4.2. GEOLOGICAL SETTING

The conglomerates, sandstones and mudstones that comprise the upper part of the Caerfai Group and lower part of the Porth-y-rhaw Group were deposited on the southern margin of the Welsh Basin (Fig. 4.3B), a NE–SW trending structural intra-shelf basin (Crimes 1970a) initiated during transform termination of subduction associated with the late Proterozoic–Cambrian Avalonian-Cadomian orogeny (Murphy and Nance 1989, Nance 1990, Nance *et al.* 1991, 2002). Avalonia (Fig. 4.3A) is one of several exotic terranes within the Appalachian-Caledonide orogen that are interpreted to have evolved along an active margin of Neoproterozoic Gondwana (Nance *et al.* 1991). Extending from New England and Atlantic Canada (West Avalonia) into Southern Britain (East Avalonia), Avalonia is the largest of these peri-Gondwanan terranes, all of which are characterized by Neoproterozoic histories of continental margin subduction, and by the peri-Gondwanan affinity of their early Palaeozoic shallow marine successions (Nance and Thompson 1996, Landing 1996).

The late Neoproterozoic–Ordovician history of Avalonia (Fig. 4.4) includes prolonged subduction and its transition, without intervening continental collision, to a late Cambrian passive margin characterized by Acado-Baltic fauna (Keppie 1984, Murphy *et al.* 1985). To account for this transition in tectonic environment in the absence of a major collisional event, Murphy and Nance (1989) proposed that Avalonian subduction was terminated as a result of transform activity. The interaction of a continental transform with the subduction zone resulted in the termination of subduction, the structural inversion of intra-arc basins, and the formation during the

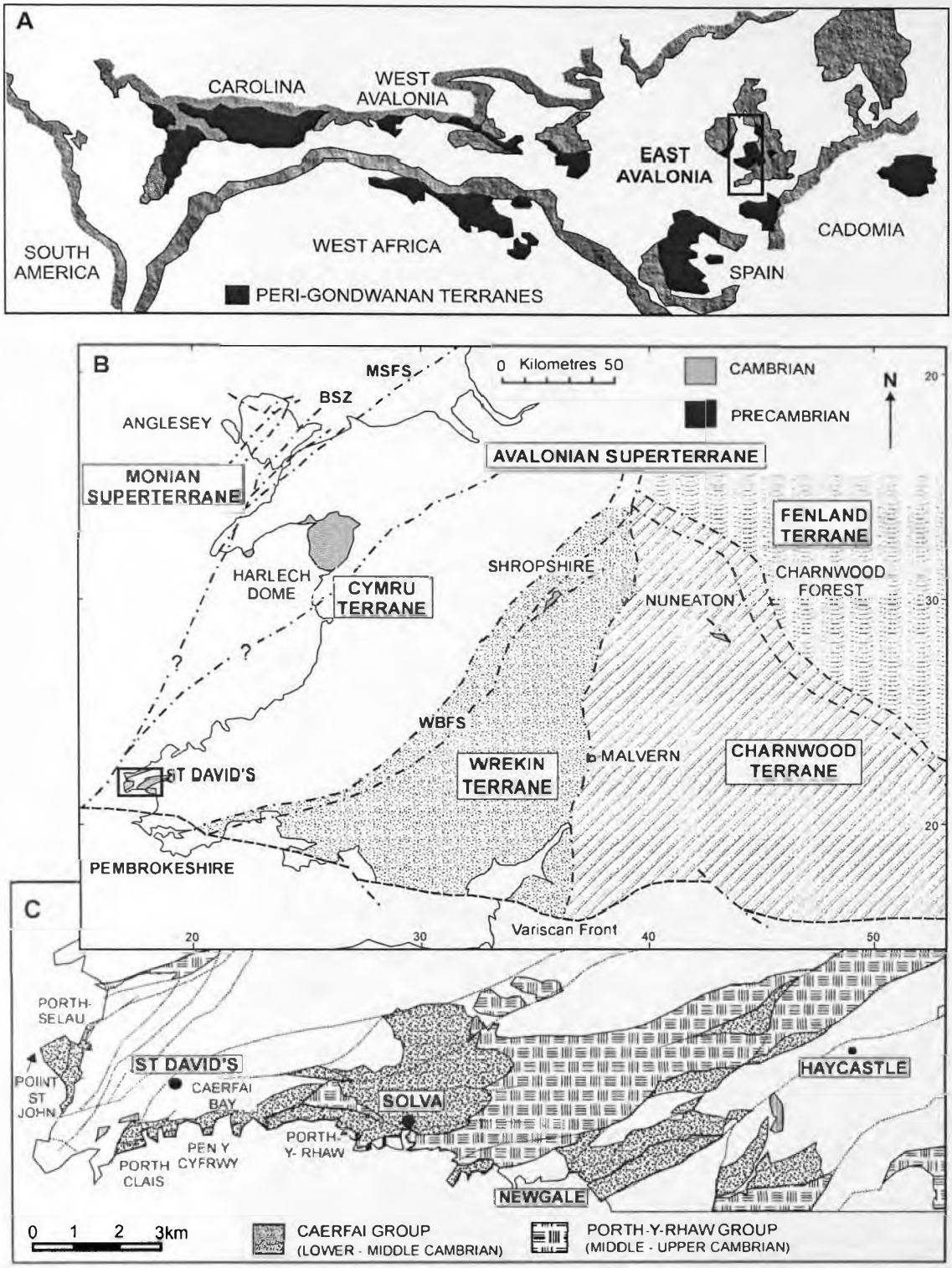



**Fig. 4.3.** (A) Early Mesozoic reconstruction of the North Atlantic showing the location of Avalonia and related peri-Gondwanan terranes of the Neoproterozoic (modified from Nance and Murphy 1994). (B) Geological map of Wales showing terrane assemblage. MSFS = Menai Strait Fault System. WBFS = Welsh Borderland Fault System (modified from Pharoah and Carney 2000). (C) Geological map of NW Pembrokeshire showing locations of Cambrian outcrops and study areas discussed in the text.

Lower and Middle Cambrian of "late-stage" transtensional successor basins (Murphy *et al.* 1985, Keppie and Murphy 1988, Landing 1996).

The early transform stage (Fig. 4.4), recorded in alluvial fan and nearshore marine sediments of the Ogof Golchfa and St Non's formations, was supplied by orogenic highlands to the west of Pembrokeshire, a probable southern extension of the Monian Superterrane (Fig. 4.3B). Oblique-slip displacement was accommodated along the Menai Strait Fault System during final docking of the Monian Superterrane with the Cymru Terrane. This study focuses on sedimentation during the late transform stage of Avalonian-Cadomian orogenesis (Fig. 4.4). Major basin reorganization at the end of the early transform stage is recognized throughout Avalonia (Landing 1996), and is locally represented by a paraconformity in the Caerfai Group (Fig. 4.4) and a rapid switch to developing orogenic highlands to the east. Three unconformity-bounded, epeirogenically controlled sequences have been recognised (Fig. 4.4). These correlate, within the constraints of presently known biostratigraphy and geochronology, with transtensional-transpressional cycles identified throughout East and West Avalonia (Brasier 1989, Landing 1996).

## 4.3. TERMINOLOGY AND DEFINITION OF PROCESSES

Both the fan-delta and turbidite concepts suffer from an extremely unstable nomenclature. It is therefore necessary to discuss how terms such as 'fan-delta' and 'turbidity current' are used here.

### 4.3.1. Fan-deltas

A fan-delta is commonly defined as a coastal prism of sediment delivered by an alluvial fan and deposited in a standing body of water (Holmes 1965). The simplicity and applicability of this definition relies entirely on how an alluvial fan is defined, and thus classification schemes for fan-deltas have concentrated principally on the alluvial feeder system (McPherson *et al.* 1988; Postma 1990), since this dictates the principle characteristics of its subaqueous parts (Dunne and Hempton 1984). If the alluvial fan is defined in a more restricted sense as essentially a transfer zone with high gradient slopes and elevated catchments (see Blair and McPherson 1994 for a detailed review), the ensuing catastrophic nature of sedimentation with ephemeral

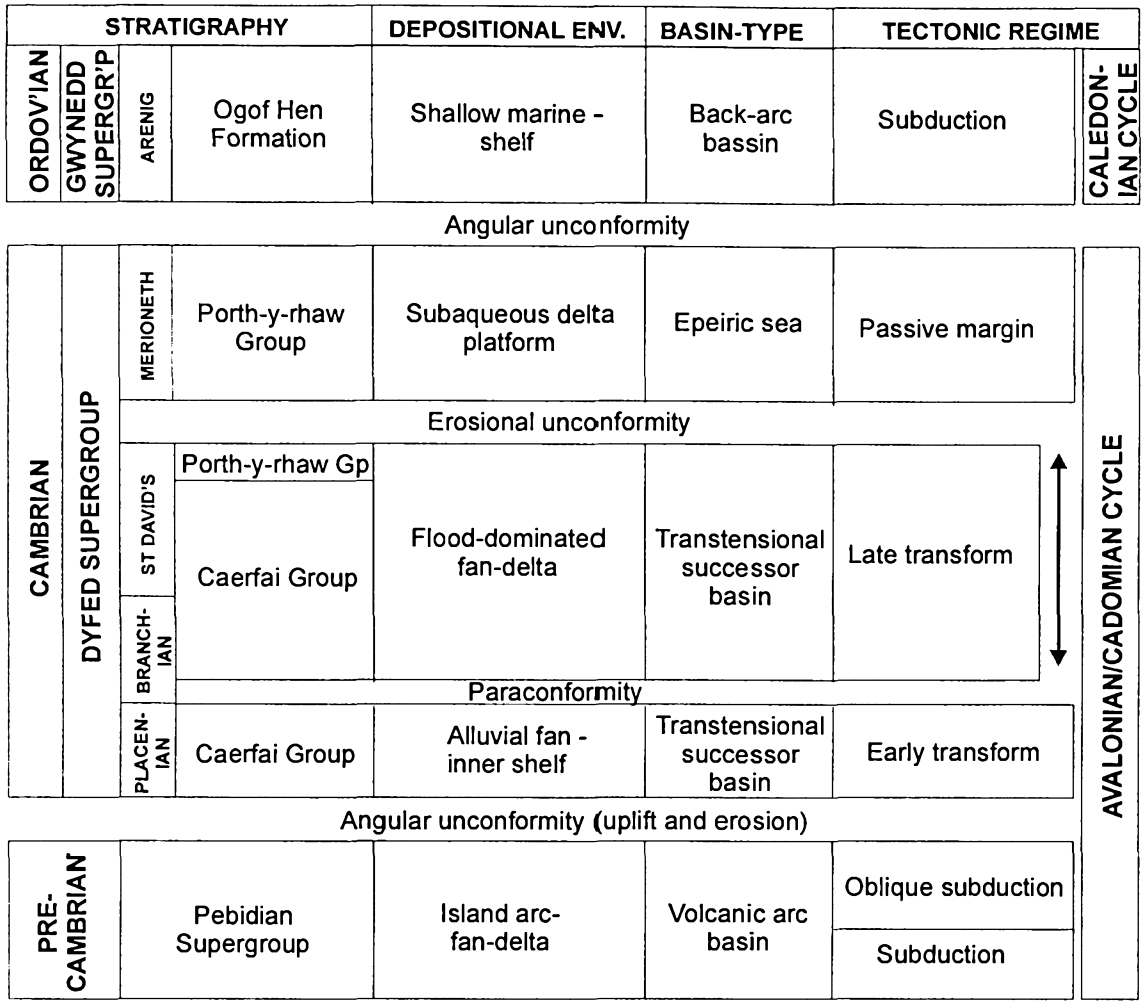



**Fig. 4.4.** Stratigraphic framework and tectono-depositional features of late Precambrian to Ordovician strata exposed in NW Pembrokeshire. The Pebidian and Dyfed supergroups record sedimentation during the Cadomian/Avalonian orogenic cycle, with the accretion of Avalonian island arcs to the northern periphery of Gondwana. Renewed subduction in the Ordovician (Caledonian orogenic cycle) led to rifting of Avalonia from Gondwana and ultimately its collision with Laurentia. Arrow = strata discussed in this study.

fluid gravity flows and sediment gravity flows, should be readily recognizable in the main depositional zones of the fan-delta plain and the fan-delta front. This restricted definition of a fan-delta essentially corresponds to the type-A feeder system of Postma (1990). Type-B, C, and D feeder systems, as defined by Postma (1990), are difficult to reconcile with alluvial fan processes (Blair and McPherson 1994). Characteristics such as stable channel-levee complexes, trough and planar-bedded sandstones, well sorted textures, and low-gradient, broad coastal plains are more often associated with a mature fluvial system, and may be better interpreted in terms of a braidplain-delta (*sensu* Orton 1988).

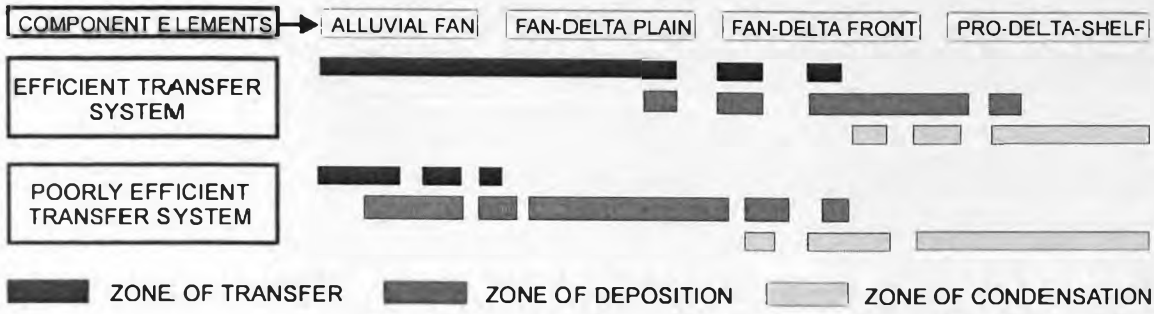



**Fig. 4.5.** Component elements of flood-dominated fan-deltas (modified from Schumm (1977) and Mutti *et al.* (1996)).

The basic component elements of a fan-delta are outlined in Figure 4.5 and consist essentially of four distinct facies belts: the alluvial fan, fan-delta plain, fan-delta-front, and prodelta – outer shelf. An essential feature of fan-deltas is the direct linkage between the alluvial feeder, the nearshore, and the receiving basin (Prior and Bornhold 1990). Following Schumm (1977, 1981), the system may be looked upon as consisting of three genetically related zones that encapsulate all sub-environments from the drainage basin to the outer shelf. This wholly dynamic system may be treated in terms of zones of transfer, deposition and condensation. For all fan-deltas (*sensu stricto*) the alluvial regime (dominated by catastrophic events) reflects the transfer zone (feeder system), while prodelta environments are associated with the zone of condensation. The location of the zone of deposition basinward of the zone of transfer depends entirely on the efficiency of transfer processes in the alluvial sub-environment (Fig. 4.5). The concept of flow efficiency has been discussed in many papers (e.g. Mutti 1992; Richards *et al.* 1998) and is defined as 'the ability of a flow to carry its sediment load basinwards, and to segregate its grain size population into distinct facies types' (Mutti *et al.* 1999). Although a fairly routine concept in the description and interpretation of deep marine turbidite systems (Pickering *et al.* 1989), its application to deltaic sequences has been extremely limited. Often the emphasis has been on single sub-environments, commonly treated as genetically independent systems (Mutti *et al.* 1996). It is demonstrated here that the efficiency of the transfer zone defines the location of the zone of deposition, and thus controls the location of sand bodies and the overall geometry of the fan-delta, as well as defining the type and distribution of lithofacies. This in turn plays a crucial role in the manner in which basin processes, particularly waves, can modify delta characteristics (Orton 1988). As a general rule, highly efficient transfer processes build elongate and widely distributed depositional zones, and the zone of transfer is expanded to include the delta plain (Fig. 4.5). Conversely,

systems of low efficiency are characterised by transfer processes that lead to rapid emplacement and narrow zones of deposition located close to the nearshore. The classification of fan-deltas is a rather complicated affair, largely due to the variability in possible feeder systems and processes acting in the basin. A classification scheme for coarse-grained deltas is presented in Figure 4.6, highlighting the main focus of this paper.

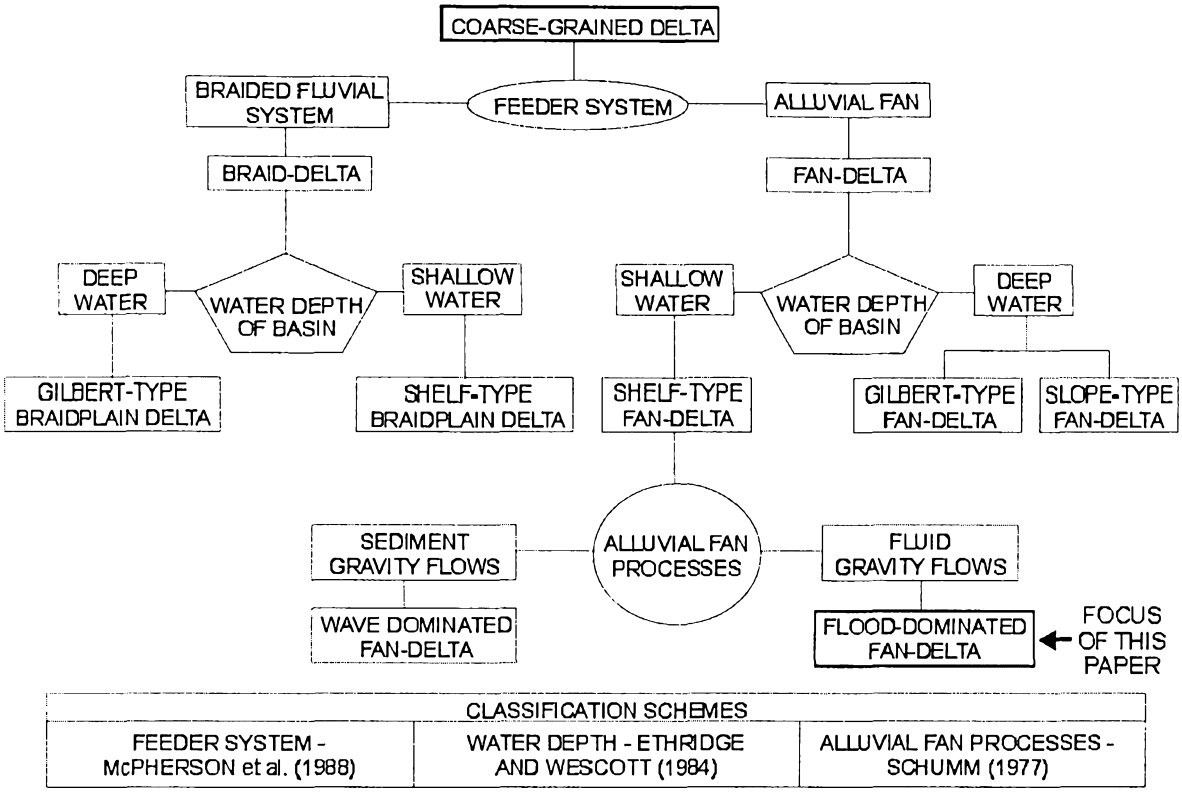



**Fig. 4.6.** Classification of coarse-grained deltas based on feeder system, water depth and alluvial fan processes.

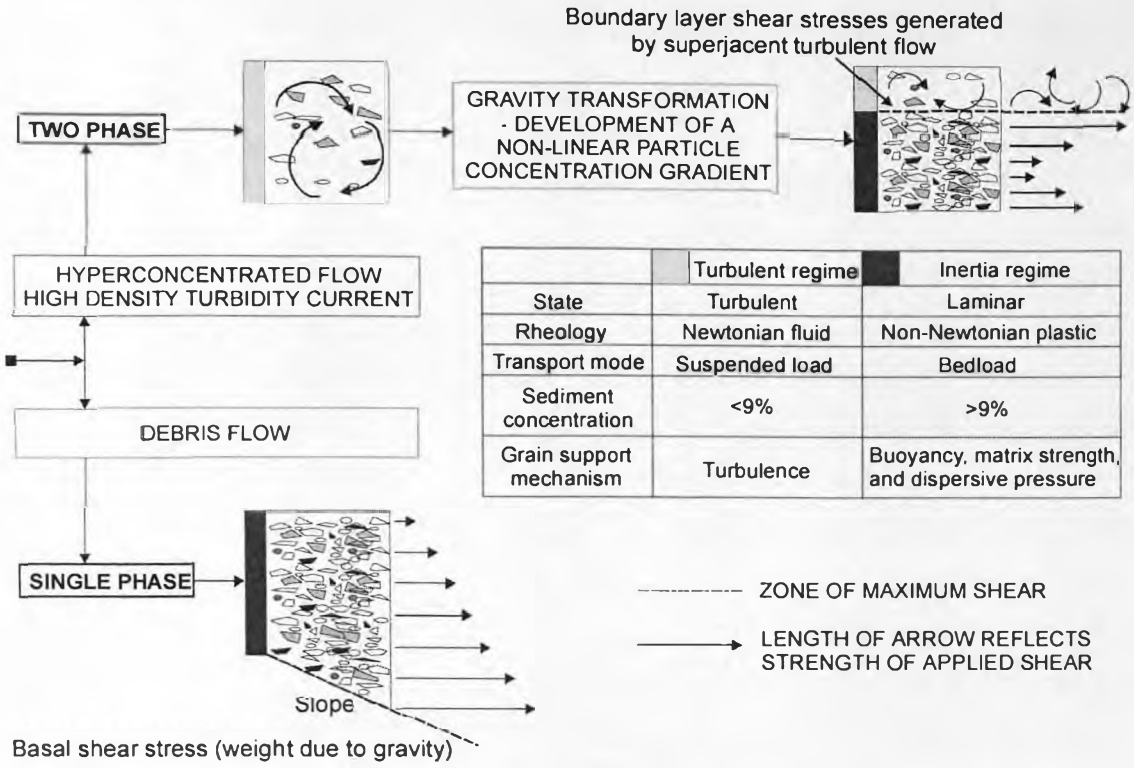
### 4.3.2. Hyperconcentrated flow

The term 'hyperconcentrated flow' as loosely defined by Beverage and Culbertson (1964) has degenerated into a 'catch-all' category for flows that appear unusual and difficult to classify. Originally proposed for subaerial flows with sediment concentrations and rheological behaviour 'intermediate' between those of plastic mudflows and fluid flows (Pierson and Costa 1987), the term has since been applied to pyroclastic flows (Smith 1986), subaqueous flows (Mulder and Alexander 2001), turbid underflows in lakes (Talbot and Allen 1996), and catastrophic flood flows in alluvial settings (Sohn *et al. 1999;* Manville and White 2003). The definition of

rheological properties varies from fully turbulent Newtonian behaviour, to non-plastic and pseudo-plastic non-Newtonian rheology (Beverage and Culbertson 1964; Mulder and Alexander 2001). Here, subaerial flood-generated deposits that display properties of both turbulent and laminar behaviour, and that would be classified under the umbrella term 'hyperconcentrated flow', are referred to as hyperconcentrated flood flow (HFF): they are strictly a result of deposition from a catastrophic, sediment-laden floods in an alluvial environment. These fluid gravity flows roughly equate to the 'incised channel floods' of Blair and McPherson (1994) and, with sheetfloods and sediment gravity flows, are the primary aggradational processes in the construction of alluvial fans (*sensu stricto*) (Sohn *et al.* 1999).

The original definition of hyperconcentrated flow, with its intermediate rheological characteristics between debris flows and stream flows, has led to much confusion. A rheology transitional between a debris flow and a stream flow suggests that there exists a transitional state between Newtonian (fluid) and non-Newtonian (plastic) behaviour when, in reality, a flow can only be one or the other. This confusion stems from the empirical data presented by Beverage and Culbertson (1964), which suggested that hyperconcentrated flow should be defined by a sediment concentration between 40-80 wt%, intermediate in sediment transport characteristics between debris flow and normal stream flow. As pointed out by Sohn (1999), at intermediate concentrations, coarse particles are not fully supported by turbulence, matrix strength or dispersive pressure, and are thus likely to undergo gravity transformation (*sensu* Fisher 1983), and develop a non-linear particle concentration gradient through settling to the base of the flow. Transitional concentrations therefore develop two-phase characteristics (Sohn 1999), with coarser clasts forming a concentrated solid phase (sand and gravel), overlain by a fluid component comprising water, silt and clay (Fig. 4.7).

A consequence of density stratification is a layered flow with discrete interfaces between components with different sediment concentrations, rheologies and sediment support mechanisms (Postma *et al.* 1988; Sohn 1999). The flow thus becomes partitioned into a highly concentrated bedload zone or 'moving bed', where turbulence is increasingly dampened and the fluid may develop Bingham properties, and an overlying fully turbulent suspension cloud. This bedload zone is commonly referred to as a traction carpet when associated with high-density turbidity currents (HDTC) (Dzulynski and Sanders 1962), and some authors have also applied this term to subaerial bipartite flows (Todd 1989). Due to the absence of turbulence, and thus traction in these concentrated zones, the term inertia carpet is preferred




| | Turbulent regime | Inertia regime |
|---|---|---|
| State | Turbulent | Laminar |
| Rheology | Newtonian fluid | Non-Newtonian plastic |
| Transport mode | Suspended load | Bedload |
| Sediment concentration | <9% | >9% |
| Grain support mechanism | Turbulence | Buoyancy, matrix strength, and dispersive pressure |

**Fig. 4.7.** Flow properties in single phase and two phase flows, and differences between turbulent and inertia regimes.

Massari 1984), as it highlights flow in the inertia regime of Bagnold (1954). The necessary shear stresses to maintain the grain dispersion are provided by tangential shear from the overlying turbulent portion of the bipartite flow (Todd 1989, Manville and White 2003), and basal shear stresses created by the weight of the flow (Postma *et al.* 1988). Density stratification or bipartite structure should be the defining characteristic of HFF, and provides a more practical criterion for its recognition, especially in ancient sequences.

### 4.3.3. High-density turbidity current

The concept of HDTC has been contentious since Sanders (1965) expressed concerns on the inclusion of the Bouma A division into a classification scheme reflecting deposition from a current where the diffusive force of turbulence was the dominant grain support mechanism. The strict definition of a turbidity current as a 'sediment gravity flow in which the sediment is supported mainly by the upward component of fluid turbulence' (Middleton and Hampton 1973) restricts flow concentration to the Bagnold limit for turbulence, which is 9% by volume (Bagnold 1962). Therefore the term 'turbidity current' (*sensu stricto*) is not compatible with the

modifiers 'high-density' or 'high concentration'. Above the Bagnold limit for turbulence grain-to-grain interaction becomes important and the flow will develop multiple grain support mechanisms including matrix strength, dispersive pressure, and buoyancy (Lowe 1982), and thus cannot be classified as turbidites *sensu* Middleton and Hampton (1973). This has led to unusual interpretations such as 'non-turbulent turbidity current' (McCave and Jones 1988) which, as pointed out by Shanmugam (1997), represents 'the ultimate in oxymoron'.

The term HDTC implies that there exists a set concentration or density for the flow when, in terms of concentration, 'high density' is often equated with 'intermediate concentration' and a value between that of a debris flow and a turbidity current (*sensu stricto*). Vague and unworkable definitions based on transitional rheologies have been discussed under 'hyperconcentrated flow', and HDTC would be better similarly defined and identified on the basis of density stratification (Fig. 4.7): this is the most obvious by-product of the concentration values characterised by HDTC (Sohn 1999). The use of the term 'turbidity current' in this paper follows the definition by Kuenen (in Sanders 1965 p. 217): 'a turbidity current is a current flowing in consequence of the load of sediment it is carrying and which gives it excess density'. This very broad definition requires some modification to allow distinction between 'turbidity currents' (*sensu lato*), debris flows, and subaerial flows. This extended definition is how the term 'HDTC' is applied in this paper: (1) flow is strictly subaqueous, and is classified as a sediment gravity flow driven by excess weight forces, (2) flow is not depth-specific (Falk and Dorsey 1998) and may travel on steep or shallow gradients (Mutti *et al.* 1999), (3) flow may demonstrate multiple grain support mechanisms expressed as flow transformations recorded by a wide range of deposits, (4) the 'transitional' concentration values make gravity transformation a likely precursor, and thus HDTC are density stratified two-phase flows (Mutti *et al.* 1999), (5) these two phases (inertia carpet and over-flowing turbulent suspension) must be mutually dependent (Sohn 1999).

These defining criteria for deposits of HDTC have two advantages concerning their natural distinction from single-phase debris flows and LDTC. As evidence for density stratification may be elucidated from the deposit, a bipartite flow with mutually dependent internal divisions does not have to be given different process names such as 'sandy debris flow' and overlying 'turbidity current' for the inertia layer and suspension cloud respectively, as advocated by Shanmugam (1997, 2000). Importantly, this allows the term 'HDTC' to be retained, as it is well entrenched in the literature. With respect to LDTC (Fig. 4.8), if the Bouma A division is restricted to beds that display normal size grading (Kuenen and Migliorini 1950) rather than

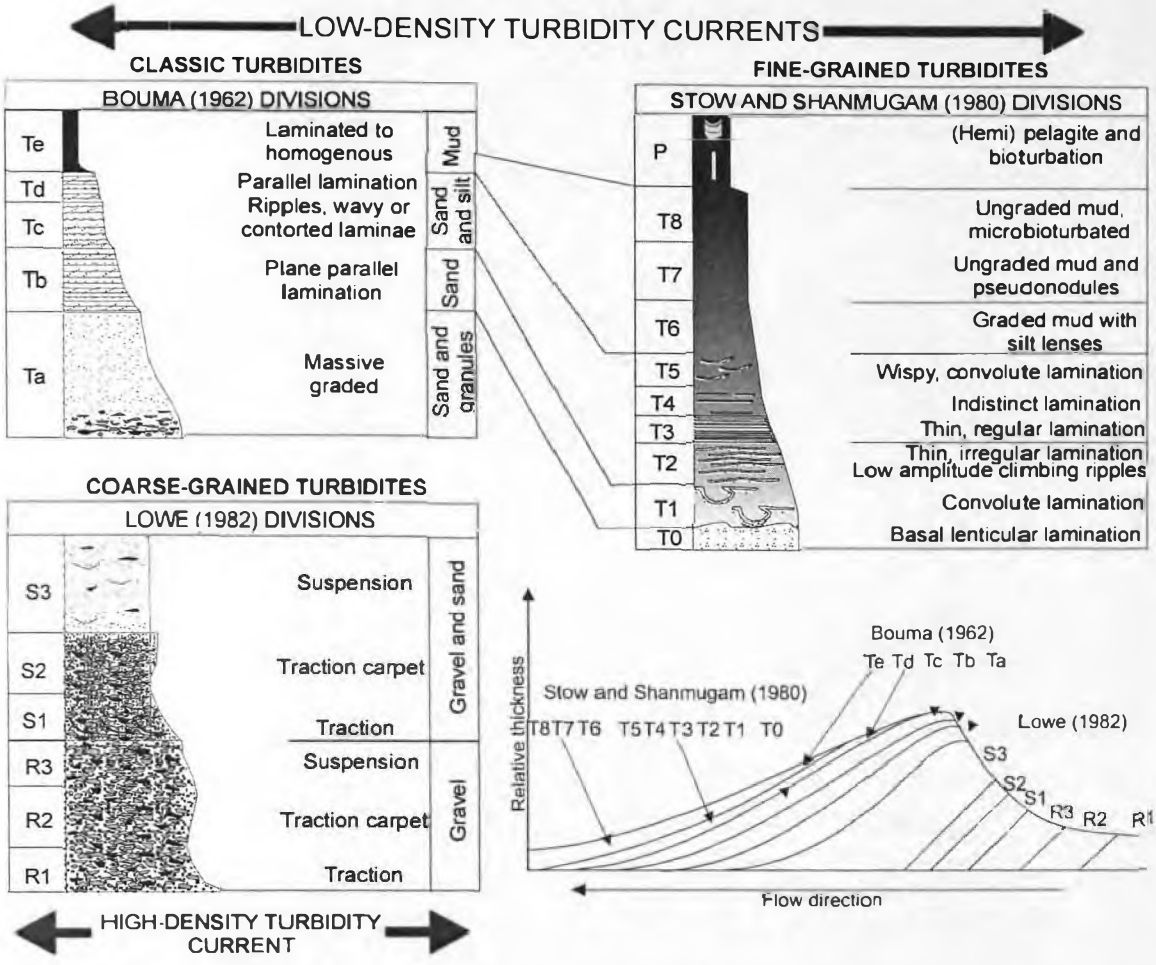



**Fig. 4.8.** Classification of turbidites based on grain size and sedimentary structures.

'ungraded and graded beds' as originally defined by Bouma (1962), then the entire Bouma sequence (Ta-Te) represent deposition from flows that are entirely fluid (Newtonian) in their rheology and thus fully turbulent with regards to grain support (Shanmugam 1997). Massive beds (here defined as ungraded and unstratified) are almost always associated with floating clasts (Shanmugam 1997), suggesting some degree of flow strength (Bingham plastic properties), and thus a grain support mechanism other than turbulence. The common practice of equating massive beds and graded beds has no foundation therefore. These obvious differences in depositional dynamics (e.g. hindered settling versus unhindered settling) ultimately reflect fundamental differences in flow state (laminar versus turbulent), rheological behaviour (non-Newtonian plastic versus Newtonian fluid) and concentration, and their distinction is warranted on the most basic principles. Massive sands/gravels are inferred to be the most distal expression of HDTC (Fig. 4.8), while graded unstratified sands/gravels represent the most proximal signature of LDTC where their common association with planar lamination and ripple cross lamination equate more readily to

the Bouma sequence. Turbidites displaying complete or partial Bouma sequences are the natural expression of LDTC when defined as 'sediment gravity flows with fluidal (i.e. Newtonian) rheology and turbulent state in which sediment is held in suspension by fluid turbulence' (Shanmugam 1997).

## 4. LITHOFACIES AND PROCESS SEDIMENTOLOGY

Detailed sedimentary logging of the cliff sections south of St David's has led to the recognition of five recurring sedimentary facies associations based on lithology, bed thickness and internal sedimentary structures (Fig. 4.9). These Facies Associations, labelled A to E range from gravel-dominated to mud-dominated and are described in the manner in which they develop in a basinward direction with facies association A being the most proximal (alluvial fan) and E the most distal (prodelta – outer shelf). Each facies association is built up of a number of component lithofacies, which are described and interpreted separately and in order of decreasing proximality. To aid large-scale interpretations, each Facies Association is illustrated by a detailed representative log from the best-exposed locality and a breakdown of its palaeoenvironmental significance and processes of deposition. Based on lateral changes in depositional environments (Fig. 4.9) and palaeocurrent data (Fig. 4.10), the system can be seen to prograde and retrograde in accordance with base level changes to the NW and SE respectively, with a fairly persistent nearshore strike running approximately NE-SW. Thus, the trend of the coastline from Porth Clais in the west to Newgale in the east (Fig. 4.9) roughly coincides with increasing proximality of the system to the sediment source.

### 4.1. Facies Association A: alluvial fan

#### *4.1.1. Facies A1: unstratified, tabular, non-erosive pebbly sandstone*

##### *4.1.1.1. Description*

This subordinate lithofacies consists of medium to thickly bedded (60–145 cm) broadly tabular units of sand-matrix-supported conglomerate and pebbly sandstone (Fig. 4.11A). General features include poor sorting, polymodal texture, lack of internal stratification and angular to subrounded pebble- to cobble-sized clasts set in a poorly sorted coarse-grained sandy matrix. Matrix content is extremely variable but

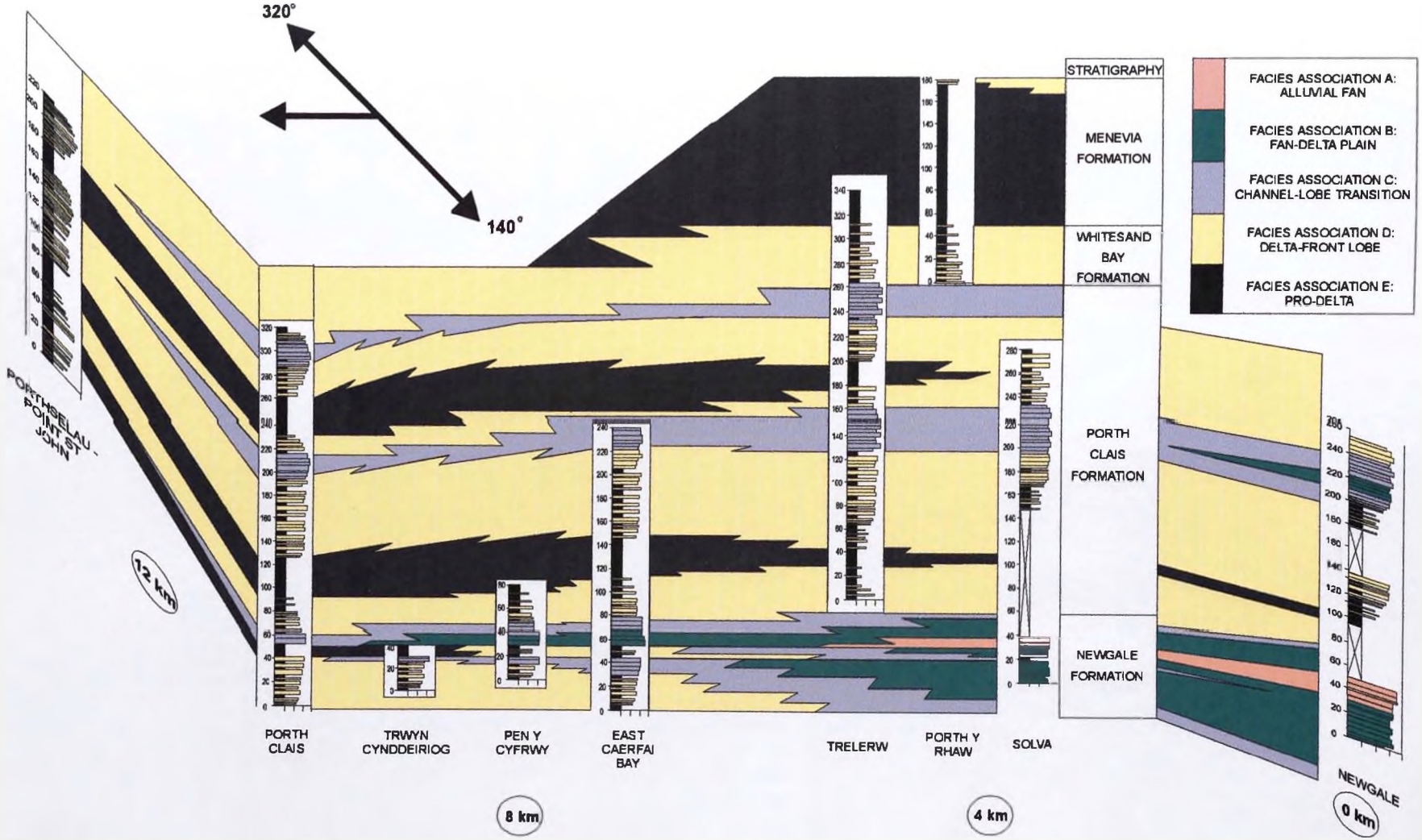



**Fig. 4.9.** Stratigraphic correlation and large-scale stacking patterns across the NW Pembrokeshire coast. See text for details.

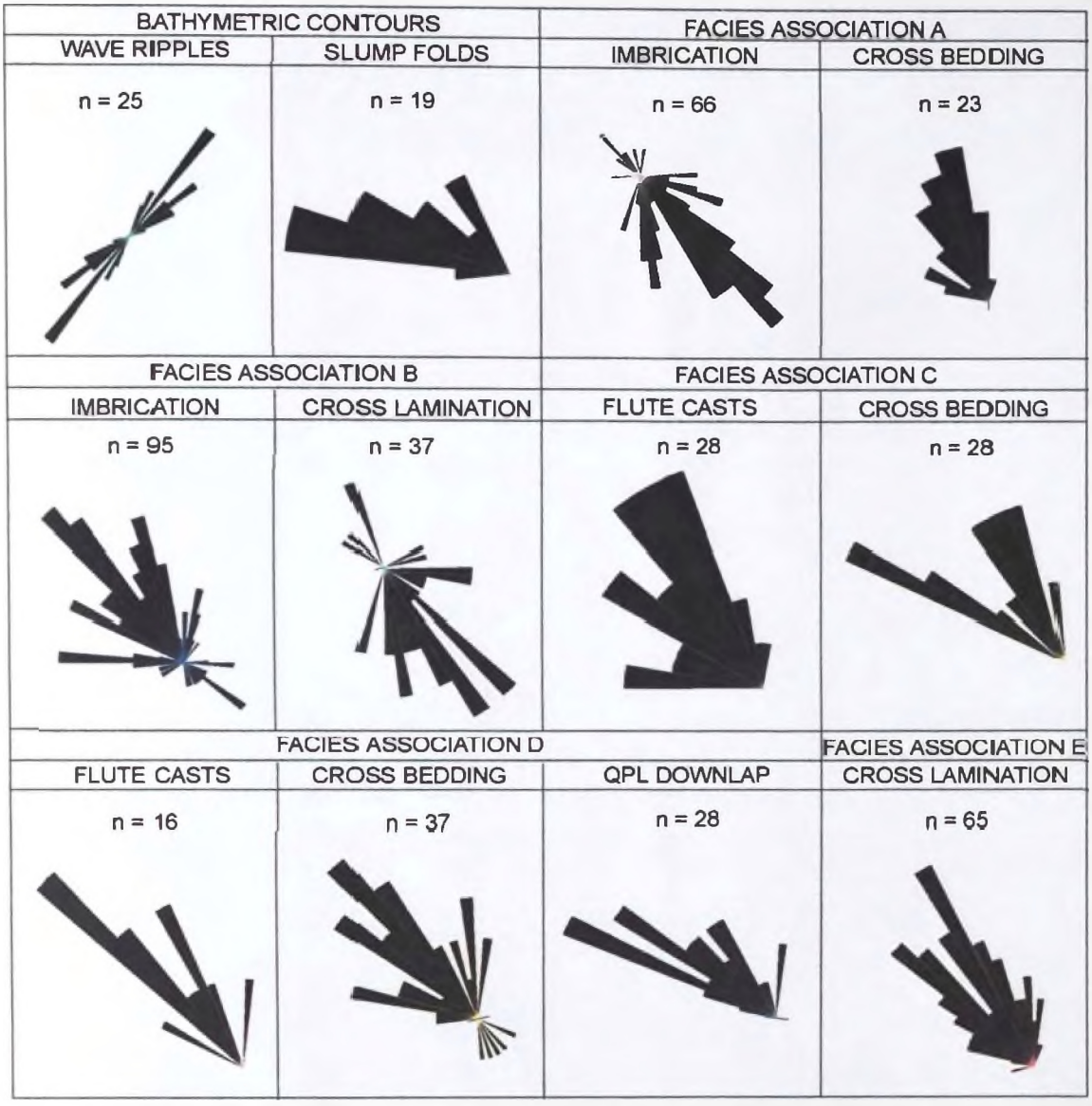



**Fig. 4.10.** Palaeocurrent data from primary sedimentary structures evident in the Caerfai and Porth-y-rhaw groups.

commonly exceeds 30% resulting in a fabric with only partial clast contacts. Bed boundaries are often difficult to distinguish due to poorly organised texture and fabric, but where visible are planar and non-erosive. Two sub-facies have been recognized based on internal fabric. Most abundant (70% of the facies) are textures that are chaotic and ungraded, with clasts orientated in unstable sub-vertical positions. These disorganized fabrics are often associated with matrix content in excess of 45%, resulting in apparently 'floating' outsized clasts. Cobble grade clasts are preferentially deposited in the lower 30 cm, locally forming a clast-supported fabric. The second bed-type has a more organized texture, with either local basal inverse grading or

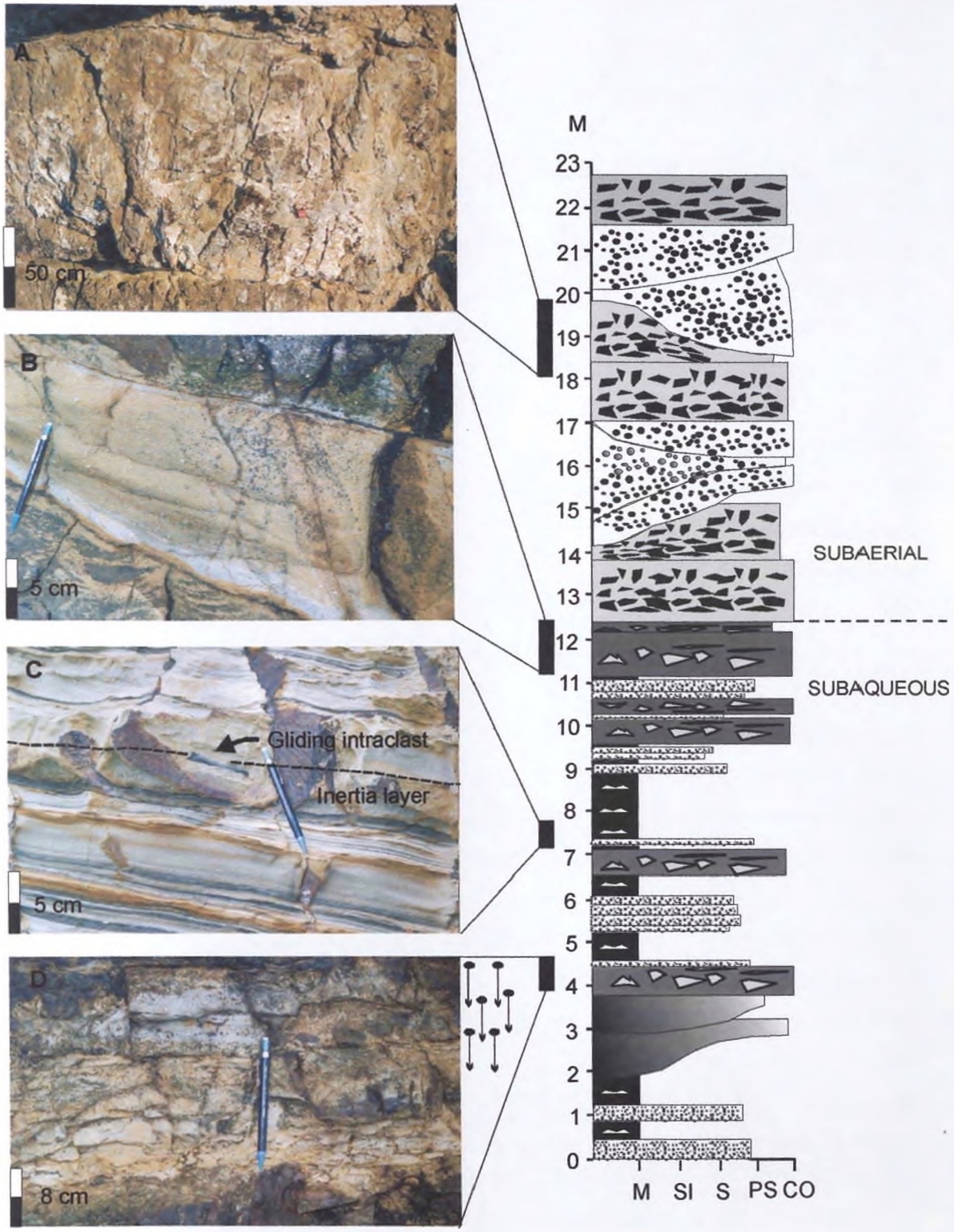



**Fig. 4.11.** Sedimentological characteristics of Facies Association A (alluvial fan) and B (fan-delta plain) at Newgale (all from the Newgale Formation). (A) Facies A1 – thickly bedded pebbly sandstone interpreted as a debris flow deposit. (B) Facies B4 – cohesive debris flow (mudflow). (C) Facies B3 – gliding rip-up clast above a basal inertia layer. Streaky mudstone and siltstone interpreted as wavy bedding of Facies B1. (D) Facies B4 – unusual matrix-supported conglomerate displaying inverse and normal grading.

crude inverse grading throughout the bed. Clast fabric is dominantly a(p)a(i) (after Walker 1975).

*4.1.1.2. Interpretation*

The lack of internal stratification and presence of unstable clast orientations excludes traction-influenced sedimentation. Instead, a sediment gravity flow origin is suggested by insignificant basal erosion, poorly sorted texture, vertically orientated and outsized clasts, local inverse grading and clast angularity (Nemec and Steel 1984; Lowe 1982; Kim *et al.* 1995). The polymodal grain size distribution (indicative of transport of sand and gravel together) and lack of internal stratification suggest that deposition occurred *en masse* and thus may be modelled on the inertia grain flows of Takahashi (1981) where deposition occurred once the applied shear fell below the yield strength, resulting in grain interlocking and frictional freezing. Low levels of mud in the matrix suggests deposition by cohesionless debris flow (the grain flows of Lowe 1982), in which clast support was accomplished by a combination of intergranular dispersive pressure formed by frictional grain interaction (Kim *et al.* 1995), enhanced buoyant lift provided by the dense interstitial matrix of water and sand (Middleton 1967) and the vertical movement of intergranular fluid (hindered settling). Angular clasts and the poorly sorted texture suggests sediment originated from fractured bedrock located only a short distance from the site of deposition (Blair and McPherson 1994). Subaerial emplacement is indicated by the poorly developed nature of grading (Nemec and Steel 1984) and the association with HFF deposits of Facies A2.

Beds displaying a chaotic fabric were deposited from concentrated dispersions that underwent little laminar shearing, suggestive of inert conditions analogous to plug flow (Johnson 1970). Clast collision may have been hampered by the watery matrix, resulting in a lack of inverse grading and clast imbrication. The main support mechanism was probably the enhanced buoyant lift of the dense sediment-water matrix and thus the disorganized flows may be classed as density-modified grain flows following Lowe (1982). Although non-sheared plug flow implies high internal viscosity and strength (Kim *et al.* 1995), the observed concentration of cobble grade material close to basal surfaces indicates that buoyant lift was not enough to prevent the largest clasts settling during deposition. Beds displaying a preferred clast orientation originate from strongly sheared laminar flow where clasts were free to move and interact (Rees 1968). Inverse grading associated with this more organized fabric similarly reflects grain collision, with the additional

development of dispersive pressure, particularly in the basal zone of inferred maximum shear (Fig. 4.7). Flows with these characteristics are indicative of dilatant cohesionless debris flows (Chen 1988), and may have resulted from the surface transformation (*sensu* Fisher 1983) of density-modified grain flows as overland floodwaters were concentrated into creeks and incisions (Smith 1986).

### *4.1.2. Facies A2: unstratified, lenticular pebbly sandstone*

#### *4.1.2.1 Description*

Pebbly sandstone units up to 3.2 m thick with irregular internal erosion surfaces that separate a series of individual depositional episodes (30-180 cm thick) are the defining features of Facies Association A. Lower bounding surfaces are highly erosional and characterised by multiple concave-up profiles with a relief of up to 1.2 m, producing a stepwise configuration reflecting channel geometries with deeper and shallower parts (Fig. 4.12B). Smaller scale asymmetrical scours on these basal surfaces are occasionally filled with crude trough cross-bedding (Fig. 4.12C). Set heights are clearly dependent upon scour relief, while lack of reactivation suggests rapid filling from a single depositional event. Internal texture and fabric displays many of the characteristics of Facies A1: poor sorting, bimodal texture, lack of internal stratification and, angular to sub-rounded clasts of pebble to cobble grade. Siltstone intraclasts often make up a considerable proportion (>25%) of this gravel fraction. Individual beds are either ungraded (40%) or display a well-defined inversely graded interval above a basal ungraded zone (Fig. 4.12B). Clast fabric is dominantly a(p)a(i) but variations in imbrication angle occur in vertical profile. Imbrication angles are highest at the top of the bed (Fig. 4.12B), with rare imbrication reversals at the highest level, that flatten out gradually towards the base. A common feature associated with basal surfaces is the occasional alignment of larger clasts, invariably cobble grade, along the scoured surface. In the few instances where clast alignment may be determined, the fabric is clearly a-axis transverse to flow, b-axis imbricated (a(t)b(i)). Coarse sandstones, usually less than 20 cm thick, commonly cap the pebbly sandstones. These sandstones are often highly lenticular, cut out by the succeeding sandstone unit. Internally, the sandstones are massive but often contain markedly outsized intraclasts up to 14 cm long apparently suspended in the sand. Clasts always display a well developed a(p) a(i) fabric (Fig. 4.12B).

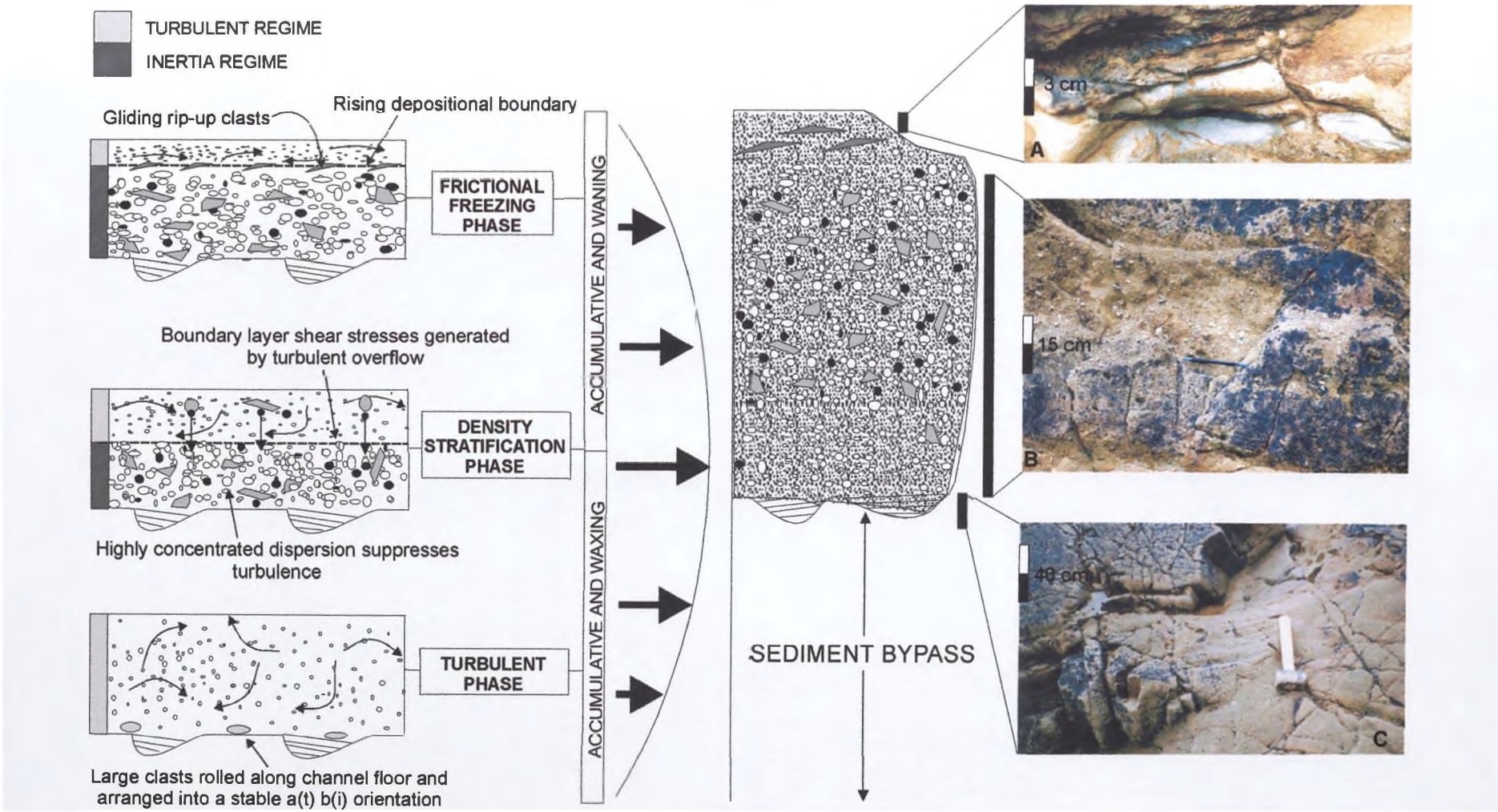



**Fig. 4.12.** Inferred mechanism for deposition of hyperconcentrated flood-flow deposits based on characteristics present in Facies A2 (all photographs are of the Newgale Formation at Newgale). (A) Gliding rip-up clast. (B) Massive to inversely graded profile and increase in clast imbrication upwards. (C) Trough cross-stratification.

*4.1.2.2. Interpretation*

The very well defined channelized geometry, with sharp steep margins, textural immaturity, internal scouring, and lack of lateral accretion, along with the coarse relatively poorly sorted nature of the fill, suggests deposition from high energy sediment-charged flows in relatively short lived, low sinuosity, well incised channels (Marzo and Anadon 1988; Jo *et al.* 1997). Some channels were filled during a single sedimentation event, others by successive erosional and depositional episodes. The configuration of the lower surfaces into a curved step-like profile is a feature commonly described from braided channel systems, reflecting the characteristic combined effect of both entrenchment and avulsion (Soegaard 1990). The defining characteristic of this lithofacies is that it shows a combination of features associated with both stream-flow and debris flow processes. The poorly sorted polymodal texture, lack of internal stratification, a(p)a(i) imbrication, and the massive to inversely graded profiles are features associated with frictional freezing of cohesionless debris flows that experienced full laminar shear prior to deposition. This suggests a highly concentrated water-sediment mixture and high apparent viscosity, far above the concentration values set as the Bagnold limit for turbulence (Bagnold 1954). Although there is no evidence to suggest turbulent conditions operated during deposition, fully turbulent traction conditions must have operated prior to deposition at an earlier stage in the transportational-depositional event to scour and confine the flow, and produce the crude trough cross-bedding documented from erosional pits on lower bedding surfaces. The abundance of intraclasts in these deposits probably testifies to this highly erosive stage. Outsized clasts littering basal surfaces may represent lag deposits formed by debris too coarse to be transported as suspended load. Instead, clasts were rolled along the channel surface as bedload, and were arranged in a stable a(t)b(i) orientation. This early stage of turbulence is considered atypical of cohesionless debris flows, which are driven almost entirely by gravitational forces, where fluid plays only a minor role in the transportational-depositional event (Mulder and Alexander 2001). They are therefore unlikely to develop turbulent eddies prior to deposition and are thus floored by essentially non-erosive surfaces. Debris flow properties therefore appear to document a transient condition in the depositional regime while the long-range transport regime was dilute and dominated by fluid turbulence. The most likely mechanism for producing transient debris flow-like properties is gravity transformation of a fully turbulent flow resulting in a density stratified bipartite structure (Sohn 1997, 1999; Kneller and Buckee 2000). This

characteristic essentially defines the response of the flow to hyperconcentration as previously outlined (Fig. 4.7).

A simple reconstruction of the flow properties and transformations during a waxing and waning flood event is presented in Figure 4.12. The rheological evolution may be framed within three stages roughly corresponding to flood waxing (turbulent phase), peak discharge (density stratified phase) and flood waning (frictional freezing stage). As predicted by the acceleration matrix of Kneller (1995; (Fig. 4.13), channelized (accumulative) flow during the rising limb of the flood hydrograph is essentially non-depositional. This early turbulent phase is instead highly erosional as indicated by scour pits, deeply incised channel margins and numerous intraclasts. This stage may be analogous to the 'tearing up of the river bed' phenomenon widely observed during hyperconcentration on the Yellow River (Chien 1989). At around peak discharge the flow reaches a critical concentration and undergoes gravity transformation with the development of a non-linear particle concentration gradient and it becomes density stratified. The newly acquired moving bed or inertia carpet is driven by tangential boundary shear stresses applied from a superjacent turbulent flow. Flood waning results in a decrease in applied shear to the bedload zone and frictional freezing of the inertia carpet. Late stage deposition is recorded by sandstone caps with gliding intraclasts (Fig. 4.12A), suggesting the maintenance of internal rheological interfaces even when discharge was greatly reduced (Postma *et al.* 1988). The maintenance of hyperconcentration even during recessional stages is a common occurrence on the modern Yellow River (Wan and Shen 1978). This reconstruction of HFF highlights some of the dangers of basing conclusions on flow properties solely on the deposit alone (also see Kneller and Buckee 2000).

### *4.1.3. Palaeoenvironment and process sedimentology*

The interbedded assemblage of fluid gravity flow (HFF) and sediment gravity flow (debris flow) deposits is consistent with the unique hydraulic properties created by the geomorphologic setting and composite morphology of alluvial fans (Blair and McPherson 1994). The major attributes of the alluvial setting that promote these hydraulic conditions include high gradient slopes mantled by colluvium and heavy rainfall events. These features strengthen the role of catastrophic flooding and supercritical flow conditions resulting in deposits that are coarse, texturally immature, and possess with few sedimentary structures attributable to traction flow. Drainage basin morphology, climate, and source rock lithology have been addressed as major factors controlling the relative proportion of various depositional processes (Schumm

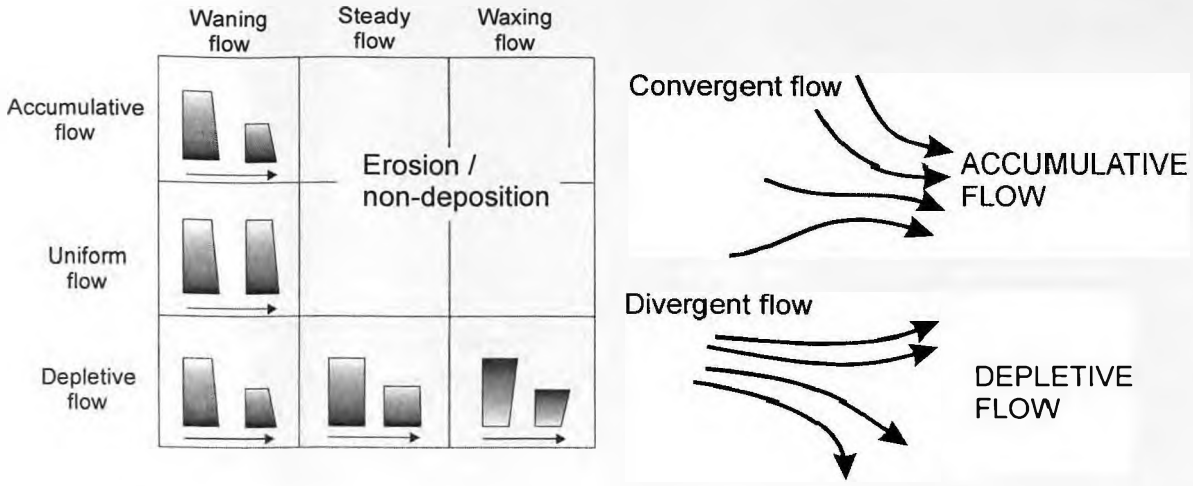



**Fig. 4.13.** The acceleration matrix (after Kneller 1995) for quasi-steady turbidity currents, with illustrative bed sequences for each field showing downstream and vertical changes in relative grain size (arrows point downstream).

1977; Blair 1999), with a traditional subdivision into fluvial dominated (wet-type) and debris flow dominated (dry-type) fans (Bull 1972). The dominance of fluid gravity flows (the Type II fans of Blair and McPherson 1994) may suggest a humid climate (Evans 1991), clay-deficient colluvial sediment (Blair 1999), or deposition at the very distal toe of the alluvial fan, as sediment gravity flows preferentially occur in the upper reaches of the system (Nemec and Steel 1984). This may be supported by dilatant debris flows, which appear to record a transitional rheology between proximal debris flow and more distal HFF. The absence of reliable palaeoclimate indicators makes it difficult to interpret the particular climatic setting, but palaeomagnetic data (Torsvik *et al.* 1996) suggest arid sub-polar conditions rather than the humid conditions that actively promote fluid based transport. It is conceivable that the dominance of HFF is solely determined by the lack of fine-grained detritus in the source area. A high proportion of quartz and granite clasts in the deposit suggest erosion of the local Precambrian Dimetian granophyre, which according to Bloxam and Dirk (1988) contains extremely low levels of feldspar, and would thus be unlikely to produce considerable proportions of clay grade material. This effectively produces colluvial sediment with high permeability and prevents the transformation of wet colluvium to a debris flow (Blair 1999).

The different rheological properties of cohesionless debris flows and HFF play a fundamental role in the assessment of flow efficiency in the alluvial environment. Mass deposition by debris flows with little evidence for sediment bypass represent an inefficient mode of sediment dispersal since they simply transfer sediment from its

source area to the closest mountain front, building elongate lobes on the fan surface (Beaty 1990). The term 'lobe' is unequivocally associated with deposition, but few equate 'channel' with transfer and bypass (Mutti *et al.* 1999). Incised channels on modern alluvial fans concentrate sediment charged flash floods on the medial parts of the fan, allowing flows to maintain velocity, depth, competence and capacity for a greater distance, thus transferring sediment to more distal locations (Blair and McPherson 1994). The main depositional zone (or lobe) is commonly made up of sheetflood deposits resulting from flow expansion and attenuation at channel mouths. The absence of sheetflood deposits from Facies Association A implies that the alluvial system was entirely bypassed prior to frictional freezing and the main depositional zone is not represented in the alluvial environment. Thus Facies Association A may be looked upon as a true transfer zone in the sense of Schumm (1977) and a highly efficient transfer zone in the sense of Mutti *et al.* (1996, 1999).

The discussion above highlights the importance of distinguishing 2-phase density stratified flows such as HFF from true single-phase debris flows (Fig. 4.7). This distinction is even more important when alluvial fans prograde into standing water, as the efficiency of the alluvial system in transferring sediment to the aqueous portion essentially defines the character of fan-deltas (Postma 1990; Mutti *et al.* 1996, 2000), and also determines the manner in which basin processes redistribute and modify these characteristics (Orton 1988). Although the definition of 'intermediate' concentration flows as structurally bipartite removes some of the ambiguity in recognizing ancient examples (Sohn 1999), distinction in practice is not straightforward, as the over-riding turbulent suspension remains a transporting medium with little preserved evidence in the depositional record (Manville and White 2003). Density stratified flows therefore record only deposition of the basal inertia layer, which in terms of rheology is essentially a debris flow (Shanmugam 2000). Therefore indirect evidence for fluid flow in the whole transportational–depositional event is necessary, as well as evidence for shear applied from above, indicating the presence of a turbulent overflow.

The most distinctive feature of 2-phase flows, and the one likely to be recorded in the rock record, is evidence for turbulent conditions (i.e. traction currents) prior to *en masse* deposition, a characteristic apparently atypical of single-phase debris flows (Mulder and Alexander 2001). This early turbulent stage, probably reflecting flood stage waxing and accumulative flow (Fig. 4.13), may be inferred from channel incision, intraclasts, cross bedded scours and channel lags recording a(t)b(i) (traction-stable) fabrics, but is unlikely to lead to significant deposition. Changes in imbrication angle within the bed may also imply a bipartite structure by demonstrating

tangential shear applied to the upper surface of the inertia layer. In this study, most of the beds interpreted as HFF are characterised by imbrication angles that are highest towards the top of the bed and flatten out gradually towards the base (Fig. 4.12B). Walker (1977) and Hein (1982), however, recorded an increase in imbrication angle towards the base of the bed and progressive flattening towards the top. Massari (1984), in a very detailed study of neritic mass flow conglomerates, described an identical imbrication pattern. The causes of changes in imbrication are poorly understood but probably relate to the intensity of grain interactions, where greatest interaction and collision results in greater angles of imbrication (Rees 1968, Hiscott and Middleton 1980). Walker's (1977) and Hein's (1982) studies were on deep marine resedimented beds associated with slope failure on a proximal turbidite fan. Highest imbrication at the base of the flow, reflecting the zone of most intense grain collisions, is consistent with maximum shear stresses rooted to the base of the inertia carpet. In the case of Massari (1984), neritic deposition probably precluded steep slopes and, as in the present study, shear stresses would not be expected to impart violent clast collision at the base of the flow. The lower fabric is therefore dominated by low angle imbrication or flat-lying clasts. An upward increase in imbrication angle suggests a greater grain interaction higher in the inertia layer, and therefore an upward velocity gradient within the flow (Mulder and Alexander 2001). This would be expected if the maximum applied shear was from above, exerted tangentially from an over-riding turbulent portion in what must be a bipartite flow. This style of imbrication may equate to the 'stratified inertia layer' of Sohn (1997), where low imbrication angles occur in the basal frictional region of non-vibrating grains (with continuous grain contacts). This is overlain by the collisional region, dominated by active grain collisions under intense shear stresses.

The development of these two regions within the inertia carpet should, based on the degree of grain interaction, also be reflected in the distribution of inverse grading. Inverse grading in bipartite flows usually occurs higher in the bed (Fig. 4.12B) while basal zones are generally ungraded (Smith 1986) suggesting static grain-grain contacts in this region (Pierson 1981). The degree of inverse grading, reflecting the strength of dispersive pressure, increases with applied shear (Pierson 1981). Therefore, in a similar manner to changes in imbrication, this style of inverse grading may reflect a dominant shear stress from above that only significantly affects the upper reaches of the bedload zone. This trend is commonly reversed in debris flows, where base-only inverse grading records violent grain interaction in the basal zone of maximum shear (Postma and Roep 1985, Martins-Neto 1996).

### 4.4.2. Facies Association B: fan-delta plain

#### *4.4.2.1. Facies B1: wavy and flaser bedded silty mudstone*

##### *4.4.2.1.1. Description*

Facies B1 is composed of rapidly alternating millimetre to centimetre thick, well sorted siltstones, interbedded with structureless dark blue mudstone (Figs. 11C and 14A). Siltstones are predominantly cross-laminated, wavy to lenticular bedded, with asymmetrical, or rarely symmetrical, rippled tops and internal flasers. These bedding geometries closely resemble the classic wavy and lenticular bedding described by Reineck and Wunderlich (1968). Convex-up lower surfaces beneath the thickest ripple forms reflect loading on a low strength, possibly hydroplastic, substrate. Asymmetrical ripple profiles display cross stratification that dips predominantly to the southeast, roughly perpendicular and offshore with respect to the palaeoshoreline (Fig. 4.10). Opposing dip directions occur sporadically. Small-scale reactivation surfaces are demonstrated by cross-laminated foresets dipping at slightly different angles broken by sub-millimetre muddy flasers, and suggest interruptions in the steady advance of a migrating ripple. A characteristic feature of Facies B1 is the partial development of microsequences (Tessier *et al.* 1995) 8–17 cm in thick, that allow the fine-grained succession to be divided into alternating 'layers' of silt-rich and mud-rich components (Fig. 4.14A). Each microsequence consists of roughly 8–13 individual depositional elements but the number is often hard to identify with any accuracy. Although structures resembling desiccation cracks have been identified from Facies B1 (Rushton 1974), no examples were documented in this study.

##### *4.4.2.1.2. Interpretation*

The origin of wavy and lenticular bedding was discussed by Reineck and Wunderlich (1968) and Yeo and Risk (1981). Both are thought to reflect small-scale alternations in slack water and current agitated conditions. The juxtaposition of sediments with these contrasting depositional energetics at a frequency demonstrated in Figure 4.14A suggests emplacement under the modulating effects of tidal currents (Reineck and Singh 1973). This is further substantiated by reactivation surfaces, bimodal cross lamination and mudstone drapes on ripple foresets which, by analogy with modern examples (Evens 1965; Yoa and Risk 1981), indicate that deposition occurred in a

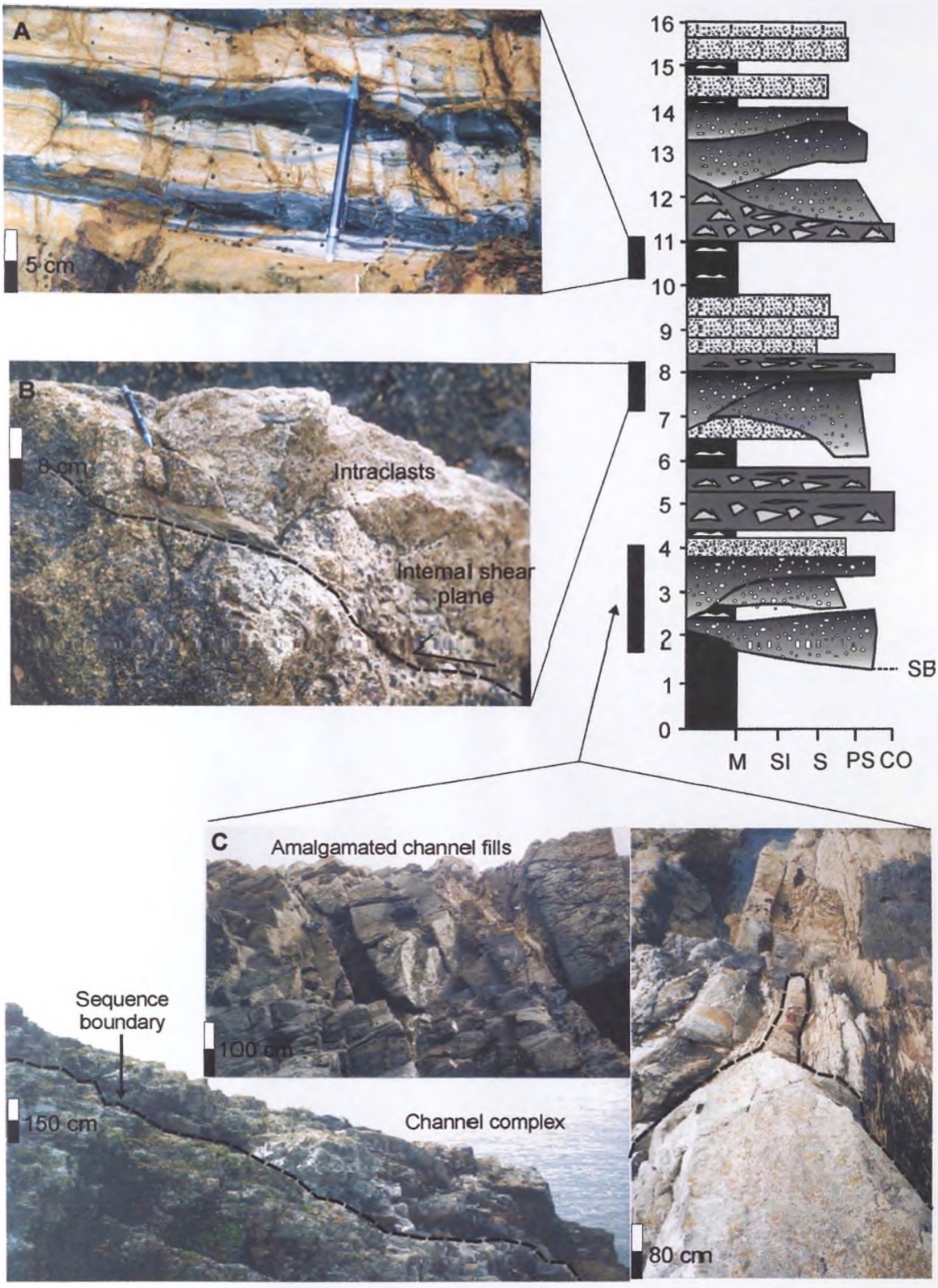



**Fig. 4.14.** Sedimentological characteristics of Facies Association B (fan-delta plain) at Pen-y-Cyffrwy (all photographs are from the Newgale Formation). (A) Facies B1 – wavy and lenticular bedding. (B) Facies B2 – internal shear plane and gliding intraclasts. (C) Facies B2 – amalgamated channel fills incised by high-density turbidity currents.

zone of short-term fluctuations in sea level, where bedforms migrated episodically under the control of base level fluctuations in a time-velocity asymmetric current (Vesser 1980). The lack of any herringbone cross-stratification or larger scale cross-bedding and the total dominance of southeast directed flows suggest weak tidal currents in an ebb-dominated regime. Evidence for microsequences displaying a similar juxtaposition of energetics is reminiscent of the tidal couplets often recorded from both modern and ancient tidal flat environments (Tessier *et al.* 1995). According to Archer *et al.* (1991) these couplets represent a lower order periodicity probably that of the spring-neap tidal cycle, enveloping the higher order semi-diurnal/diurnal cycle.

#### *4.4.2.2. Facies B2: unstratified, lenticular pebbly sandstones*

##### *4.4.2.2.1.Description*

Facies B2 consists of amalgamated pebbly sandstones that display concave-up, channelized basal surfaces (Fig. 4.14C). Bed thickness is extremely variable, ranging from 30–160 cm, averaging roughly 75 cm. Clast size is likewise variable with a maximum of 20 cm, averaging within the small pebble to coarse granule range, and set in a poorly sorted matrix of fine to coarse sand. The fabric is rather disorganized, with no sedimentary structures attributable to traction sedimentation. Numerous beds contain mudstone and siltstone intraclasts, many of which are highly deformed. These 'floating' outsized clasts tend to accumulate within certain layers of the bed and are often characterised by well developed a(p)a(i) imbrication. An unusual feature only documented in a few beds, are intraclasts aligned on what appear to be internal shear planes (Fig. 4.14B) orientated at approximately 5° to the basal erosion surface. Textural features are variable, with massive to normally graded beds (90%) or inverse to normally graded (10%). Lower divisions predominate in both cases, usually constituting more than 95% of the bed, so normal grading is only represented by a thin 2-7 cm cap. These graded caps often form a rather distinctive grain-size break. Sole marks were difficult to identify in the field, but a few load and flute casts were discerned.

##### *4.4.2.2.2. Interpretation*

This facies has many of the characteristics of non-cohesive debris flow deposits: poor sorting, inverse grading, 'floating' outsized clasts, lack of internal stratification,

and a(p)a(i) clast imbrication (Nemec and Steel 1984; Kim *et al.* 1997). The poor sorting and the outsized clasts indicate that the flow retained some viscosity and strength (Pierson 1981; Surlyk 1984). The inverse grading and a(p)a(i) clasts suggest active grain collision and the development of dispersive pressure in a sheared laminar flow. Internal shearing within the flow may explain the deformation of the more labile intraclasts (Mulder and Alexander 2001). Internal shearing prior to deposition may also account for the alignment of intraclasts along shear planes within the bed. This phenomenon was first documented and interpreted by Nemec (1990b) but has since been identified in many inferred subaqueous non-cohesive debris flow deposits (Mastalerz, 1995). Frictional freezing of the grains leads to a build up of stress as pore spaces are reduced, grains become tightly packed, and pore pressure reaches a critical value (Nemec 1990a). As modelled by Nemec (198845-46) and further developed by Nemec *et al.* (1988), the mechanical response of the flow to the build up of pressure is the development of an internal shear surface (thrust wedge of Nemec *et al.* 1988). The forward verging surface acts as a new, local sole, which eroded clasts pass upon (Fig. 4.14B).

The ungraded deposits indicate relatively low dispersive pressure and poor size sorting capabilities. The grain support mechanism was probably a combination of intragranular dispersive pressure, buoyancy caused by the density difference between the sand and clast, and pore fluid pressure. Deposition is inferred to have occurred *en masse* through frictional grain resistance (frictional freezing). The normally graded caps indicate the presence of turbulence during late-stage deposition or reworking (Hiscott and Middleton 1980). Although this facies displays many of the characteristics of cohesionless debris flows, that interpretation requires the presence of steep subaqueous slopes (estimated at 15–28° by Lowe 1982) to provide the high shear stresses needed to maintain the grain dispersion (Postma *et al.* 1988). In the absence of a significant slope (as suggested by a broad tidally influenced delta plain and lack of slump structures), it is difficult to account for the driving mechanism of the flow. Considering the normally graded top, it is more likely that these flows were density stratified, and thus rheologically similar to HFF. The debris flow characteristics therefore represent frictional freezing of a basal inertia carpet, with the necessary shear stresses prior to freezing applied tangentially from above by a fully turbulent over-flow. These characteristics in the subaqueous realm essentially define HDTC (Lowe 1982; Postma *et al.* 1988).

The interpretation of coarse-grained turbidites relies on the classification scheme proposed by Lowe (1982). This may be looked upon as an extension to the Bouma sequence (Fig. 4.10) which, as noted by many authors (e.g. Mutti and Ricci

Lucchi 1972; Walker 1978) does not adequately accommodate flows of high concentration and coarse grain size. The model and terminology proposed by Lowe (1982) for coarse-grained turbidites can be treated in terms of several distinctive but gradational dynamic grain populations deposited during discrete sedimentation waves as the relative efficiencies of different support mechanisms change with flow deceleration. The coarse-grained population (>granular) produces a sequence of sedimentary divisions termed the $R_{1-3}$ sequence, and the sand to granule population produces the $S_{1-3}$ sequence (Fig. 4.8). According to Lowe (1982), each sedimentation wave passes from an initial stage of traction sedimentation ($R_1/S_1$) to one of mixed frictional freezing ($R_2/S_2$) and the development of an inertia carpet, to a final stage of direct suspension sedimentation ($R_3/S_3$). The very coarse nature of this lithofacies, the thickness of the inertia carpet and its 'proximal' highly channelized bedding geometry suggests, by comparison with other studies (e.g. Massari 1984), that the deposits equate to the $R_2$ division with a minor $R_3$ cap. Highly channelized basal surfaces and flute casts overlain by essentially non-erosive $R_2$ sediments require fully turbulent conditions operating prior to gravity transformation and the formation of the inertia carpet. The transportational–depositional event is therefore directly analogous to the emplacement of HFF deposits as displayed in Figure 4.12, and appears to substantiate claims by many authors (e.g. Lowe 1982; Kneller and Branney 1995) that conditions of sediment transport in dense sediment gravity flows are not necessarily the same as those during their deposition. Turbulent conditions preceding the onset of inertia carpet development are in effect preparing erosional pathways for inertia flows, a process documented from a number of modern turbidite fan and fan-delta environments (e.g. Prior and Bornhold 1989).

The prominent grain size breaks between the $R_2$ and $R_3$ divisions and the poor development of the latter turbulent phase suggests effective sediment bypass of the frozen inertia carpet by the lower density overflow (Mutti *et al.* 2000). The finer grain size population in the overflow is then destined to undergo a further phase of gravity transformation forming a sandy bipartite flow (Fig. 4.15) with the depositional characteristics of the S-sequence as outlined by Lowe (1982). Therefore, both before and after gravity transformation and frictional freezing of the dense inertia layer, turbidity currents were transportational rather than depositional media, transporting sediment to more distal locations. These structureless and ungraded coarse-grained turbidites can thus be referred to as base- and top-absent sequences in the sense of Walker (1965).

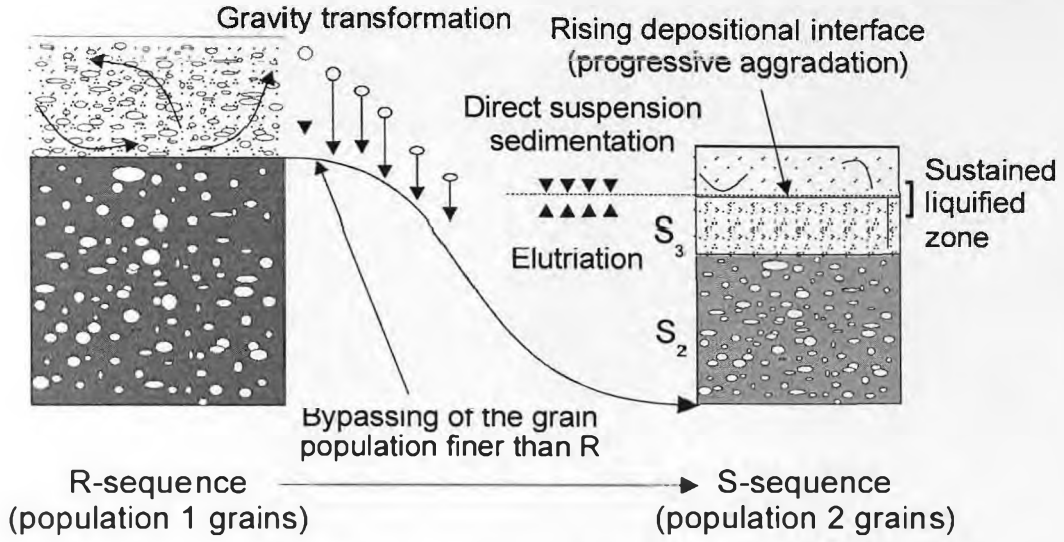



**Fig. 4.15.** Evolutionary phase in the downstream maturity of a high-density turbidity current, and mechanism for the formation of massive sandstone by direct suspension sedimentation.

*4.4.2.3.Facies B3: unstratified, tabular sandstones*

*4.4.2.3.1. Description*

This facies consists of unstratified, tabular beds of moderately sorted fine to coarse-grained sandstones. Geometry is sheet-like with lateral persistence in excess of 100 m, with little apparent thinning. Bed thickness varies between 15 and 42 cm, with no evidence for amalgamation, and beds are always enveloped by tidal heterolithic sediments of Facies B1 (Fig. 4.11C). Basal surfaces are sharp, slightly erosional and heavily loaded with flame structures in excess of 6 cm. Flute casts are also extremely abundant. Beds may be normally graded, passing upwards from either coarse or granular sandstone into fine sandstone, or massive to normally graded. Common constituents of the latter bed type are outsized rip-up clasts up to 8 cm long, apparently floating in a finer grained matrix. Positioning is usually between the massive division and the graded division (Fig. 4.11C), but many beds have clasts littered along the upper surface. All rip-up clasts display well developed a(p)a(i) imbrication. Rip-up clasts that are present on the upper surfaces of sandstone are often fragmented, cracked, and curled at the edges, which imply at least temporary subaerial exposure.

*4.4.2.3.2. Interpretation*

Scoured basal boundaries and a normally graded fabric suggest deposition from fully turbulent sediment gravity flows during waning flow conditions. Load casts with large flames reflect rapid emplacement of sediment onto a hydroplastic substrate, while flute casts are testament to high velocity unidirectional currents. Normally graded beds imply a fully Newtonian state and may be classified as LDTC (Ta Bouma division). The coarser grained massive to normally graded beds represent HDTC, where settling according to fall velocity is hindered by higher sediment concentrations. This interpretation is strengthened by the presence of outsized rip-up clasts preferentially aligned between massive and normally graded divisions. In experimental high-density turbidity currents, Postma *et al.* (1988) documented the alignment and gliding of outsized clasts along an interface separating a dense traction carpet from an overlying highly turbulent suspension. This interface is thought to represent an important physical discontinuity within the flow, reflecting an abrupt vertical gradient in flow concentration and apparent viscosity. The lower ungraded division represents a laminar inertia flow displaying a quasi-plastic rheological behaviour, with essentially non-Newtonian (stress dependent) viscometry (Postma *et al.* 1988). These inherent characteristics prevent buoyant intraclasts from sinking deeply into the inertia layer. Close inspection of Figure 4.9C reveals that the centre of mass of the intraclast is partially submerged in the coarser grained and inversely graded basal zone. A density stratified flow adequately accounts for the a(p)a(i) character of gliding clasts, which were orientated under intense laminar shear in the inertia carpet but driven by boundary shear stresses generated by the superjacent turbulent flow.

#### *4.4.2.4. Facies B4: muddy-matrix-supported conglomerates*

##### *4.4.2.4.1. Description*

This lithofacies ranges from chaotic pebbly silty mudstones to very poorly sorted, muddy-matrix supported conglomerates (Fig. 4.11B). Pebbly silty mudstones consist of pebbles, granules and rounded intraclasts randomly distributed in a muddy matrix with variably admixed silt. Beds are indistinct, sometimes graded but always internally unstratified. Basal surfaces, where visible, are planar or slightly undulose and commonly non-erosive although some basal load structures are present in intervals with interbedded tidal heterolithics. Texture may be ungraded (40%), graded (20%) or inverse graded (40%). Typical clasts are 1–4 cm across, but outsized clasts (>6 cm) are relatively common. Beds are 30–85 cm thick, and can be traced laterally

throughout the extent of the outcrop (>10 m). Important characteristics with respect to depositional processes include textural bimodality, angularity of many clasts and the disorganized fabric, often with clasts in unstable positions.

*4.4.2.4.2. Interpretation*

The lack of internal stratification and clast imbrication, insignificant basal erosion, clasts orientated in unstable sub-vertical positions, and grain size bimodality excludes traction influenced sedimentation, while the cohesive nature of the matrix suggests deposition by pseudo-plastic debris flows (Nemec and Steel 1984: Horton and Schmitt 1996, Benvenuti 2002). Pebbly silty mudstones and matrix-supported conglomerates are interpreted as mudflows (Mulder and Alexander 2001) and cohesive debris flows (Nemec and Steel 1984) respectively. The cohesive matrix provides 'matrix strength' (Lowe 1982) which is the main grain support mechanism. Experiments by Hampton (1975) suggested that matrix strength is only capable of fully supporting particles up to coarse sand grade, so many of the larger clasts must have been supported by high local pore pressure (Iverson *et al.* 1997) and buoyancy (Major and Iverson 1999). Although a disorganized fabric may simply reflect a short travel distance, it is more often suggestive of non-sheared (high strength) 'plug' flow or weakly sheared (high viscosity) flow. Deposition occurs through cohesive freezing when the force related to the shear resistance of the flow (mainly controlled by viscosity and friction) becomes equal to the force due to gravity, when the shear stress drops below the yield strength (Johnson 1970).

Some pebbly silty mudstones exhibit what appears to be well-defined normal and inverse grading (Fig. 4.11D). The apparent inverse grading in the uppermost bed in Figure 4.11D is particularly difficult to interpret as the highly viscous cohesive matrix would have prevented grain collision and inhibited the development of dispersive pressure. Cohesion would also have acted against the upward displacement of grains. These 'graded' fabrics are similar to those described by Horton and Schmitt (1996) from Miocene fan-deltas in Nevada and probably reflect water admixture into a mudflow. The main consequence of water uptake (dilution) is a decrease in matrix strength (from a plastic to pseudo-plastic rheology), which results in clasts that were previously supported sinking under gravity down through the profile. The lower normally graded bed reflects almost total restructuring of the original depositional fabric to form a basal layer dominated by coarse clasts without any inferred turbulence. The upper bed retained sufficient cohesion to maintain the

original deposition fabric. These processes have been reproduced experimentally by Baas and Best (2002).

*4.4.2.5. Palaeoenvironment and process sedimentology*

The occurrence of alluvial fan deposits conformably above coarse-grained turbidites and pseudo-plastic debris flows without an intervening beach and shoreface suggests that the catastrophic, flood-dominated character of the alluvial system determined the lithological features of the shallow to temporarily emergent nearshore (Mutti *et al.* 1996). The subaqueous environment may therefore be considered in terms of a delta associated with an alluvial fan i.e. a fan-delta (Nemec and Steel (1984). As with most proximal fan-delta deposits, it is often difficult to prove conclusively that subaqueous emplacement occurred directly from overland flows, so much of the evidence remains circumstantial. This includes an identical clast composition and unstable very angular volcanic fragments in both subaerial and subaqueous mass flows, subaerial rip-up clasts in pseudo-plastic (non-erosive) debris flows, parallelism between subaerial and subaqueous palaeocurrent indicators, and the lack of any evidence for slumping or sliding (essentially removing the most common trigger for subaqueous mass flow, Falk and Dorsey 1998). Total absence of biogenic activity may imply fluctuating salinity levels associated with flood events (Myrow *et al.* 2002). Although Crimes (1970a) preferred to invoke storm processes to account for the juxtaposition of coarse-grained event beds and fine-grained tidal heterolithics, the lack of a high-energy beach to upper shoreface is problematic, as it removes the sediment source upon which storm processes act. Storm induced combined flow regimes (Duke *et al.* 1991a) fail to account for the observed texture, clast fabric, or bedding geometries recorded from Facies Association B, and the total absence of structures attributable to traction sedimentation.

The genetic relationship between turbidity currents and catastrophic overland floods has been addressed in a number of recent publications (see Mutti *et al.* 2003 and Mulder *et al.* 2003 for comprehensive reviews). The manner in which the fluvial regime dictates delta characteristics is directly related to the physiographic and climatic features of the alluvial system (Blair and McPherson 1994). High elevation drainage basins and high gradient transfer zones located close to basin margins promote maximum sediment flux to the marine interface, allowing catastrophic flood flows to maintain sufficient velocity and retain significant concentration to form negatively buoyant plumes with excess density to underflow marine water (Mulder

and Syvitski 1995). Although the processes involved in this mode of sediment dispersal are complex because both subaerial and subaqueous flow characteristics remain poorly understood (Mutti *et al.* 2000), a framework for interpretation must be based around the fundamental flow properties inherited from the waxing and waning nature of the flood hydrograph (Mulder and Alexander 2001). This control on temporal evolution defines the flow as quasi-steady (Kneller and Branney 1995), as sediment density and thus velocity is maintained over a prolonged period by flood discharge.

Over 60% of Facies Association B consists of deeply incised coarse-grained turbidites emplaced by high-density hyperpycnal turbidity currents (Fig. 4.14C). Channel erosion (sediment bypass) followed by mass deposition may be explained by the shape of the flood hydrograph and predicted by the acceleration matrix (Fig. 4.13) of Kneller (1995). During flood waxing, fully turbulent relatively low-density flows either accelerate down pre-existing conduits on the delta plain or erode new channels. In either case incorporation of material by erosion induces positive acceleration (Kneller 1995) as density rises through flow bulking (current ignition of Parker 1982) promoting increased excess weight force and thus accumulative flow. This phase of erosion and sediment bypass during accumulative waxing flow is predicted by the acceleration matrix, as a current accelerating in space and time is destined to be erosional (Kneller 1995). During peak discharge or early waning flow, the necessary shear stresses required to maintain the grain dispersion fall below the flow yield strength and the newly formed inertia carpet freezes (Todd 1989), as predicted by accumulative (incised) waning flow in the acceleration matrix. With respect to the 'ideal' sequence for hyperpycnites outlined by Mulder *et al.* (2003), Facies B2 represents their 'base-truncated' sequence, as flow waxing and possibly peak discharge operate under accumulative (non-depositional) flow regimes. Therefore, following Mutti *et al.* (1999, 2000), accumulative flow in Facies B2 extends the zone of bypass initiated on the alluvial fan to include the delta plain, facilitating highly efficient transfer of flood-derived sediment to the delta front (true zone of deposition). This process of alluvial fan bypass feeding the delta-front has been reported from Quaternary deposits by Flint *et al.* (1991). Coarse-grained base-absent hyperpycnites incised into low energy fan-delta plain deposits have been recorded from the Recent by Weirich (1989) and Prior and Bornhold (1989), while ancient examples include those of Martinsen (1990), McCallum and Robertson (1995), and Mutti *et al.* (1996).

The origin of cohesive debris flows on the subaqueous plain is not clear, as there is no evidence in the field for either gravitational collapse or a high gradient

slope. The lack of cohesive debris flows in the subaerial environment argues against direct emplacement into the submarine realm, although rounded intraclasts, identical to those described from Facies Association A suggest some common link. The textural bimodality, apparent grading, variable cohesive strength and evidence for water admixture can all be accounted for by textural inversion (Larson and Steel 1978, Nemec *et al.* 1984), where subaerial flood flows invade and mix with water saturated heterolithic fines to produce bimodal, mud-rich pebbly beds (Martins-Neto 1996; Benvenuti 2002). This process of coarse clastic invasion of unconsolidated fine-grained sediment promotes water uptake and significantly reduces the cohesive strength of the matrix. Thus, pebbles and granules originally deposited towards the top of the heterolithic sequence may pass down through the profile under gravity, forming an apparently normally graded fabric. During invasion events with only minor mixing, higher cohesive matrix strength supports all but the densest clasts thus accounting for apparent inverse grading.

This process of textural inversion is promoted on the subaqueous plain by depositional characteristics during background sedimentation. Although some similarities exist between modern tidal flats and the broad expanse of the tidally influenced delta plain, the lack of tidal channels must have led to extremely poor drainage, facilitating 'ponding' of water between ebb and flood cycles (Yeo and Risk 1981). An environment where the thin surface veneer was permanently hyper-saturated, not only accounts for textural inversion, but also the high degree of load and flame structures commonly encountered on the basal surface of thick turbidites, and the patchy occurrence of desiccation cracks. Commonly desiccated upper surfaces of hyperpycnites (e.g. Facies B3) presumably brought the upper surface of the bed above the ponded water line. Occasional dark laminae with flecks of organic matter in fine-grained heterolithics (Fig. 4.11C) may imply that the subaqueous plain had undergone periods of temporary stagnation.

### 4.4.3. Facies Association C: channel–lobe transition

#### *4.4.3.1 Facies C1: tabular, unstratified pebbly sandstone*

##### *4.4.3.1.1. Description*

Facies C1 comprises tabular, thickly bedded (30–145 cm), poorly sorted, massive to normally graded, and rare inverse to normally graded pebbly sandstone beds (Fig. 4.16A). Clasts up to 4 cm long occur randomly scattered throughout the bed. No

internal stratification has been identified. These characteristics are virtually identical to Facies B2, differing only in their slightly finer grain size, better representation of normal grading and apparent lateral continuity. Beds have irregular erosive bases with well-developed flute casts and scoured pits up to 30 cm in depth. Despite a local pinch and swell morphology caused by post-depositional erosion, beds may be traced for over 200 m with little overall thinning. The upper 4–6 cm often consists of small overturned fold structures while bedding planes record irregular ripple-like forms (Fig. 4.16B). The latter resemble the kinneyia ripples of Martinsson (1965) and Dzulynski and Simpson (1966).

*4.4.3.1.2. Interpretation*

Poor sorting, absence of mud from the matrix, lack of internal stratification, erosive bases and the styles of graded fabric suggest deposition from density stratified, coarse grained HDTC similar to those that deposited Facies B2. Rare inverse grading and lack of internal shear planes reflect lower dispersive pressure and pore fluid pressure, while thicker intervals of normal grading imply at least partly turbulent flow conditions, particularly in the later stages of deposition. Although the grain populations in some beds may correspond to the S-sequence (Fig. 4.8) as defined by Lowe (1982), the generally massive, disorganized nature of the fabric contrasts with the well developed grain size segregation usually associated with sandy HDTC (Mastalerz 1995, Falk and Dorsey 1998), and therefore deposition is considered in terms of the R-sequence. Massive and inversely graded divisions reflect frictional freezing of a basal inertia carpet ($R_2$), while normal grading suggests high-rate fallout from a dense suspension ($R_3$). Small-scale folds and kinneyia ripples record the passage of HDTC (Bose *et al.* 1997). The development of a highly concentrated, non-turbulent basal carpet prevents significant erosion (Hsu 1959) but the high velocity and thus high applied shear may deform and roll the upper reaches of the bed below (Dzulynski and Simpson 1966). Although debris-flow-like conditions dominated during deposition, in a similar manner to Facies B2, the highly erosive bases, presence of mudstone intraclasts, and well developed flute casts are testament to earlier, powerful, fully turbulent unidirectional currents operating prior to supercritical concentrations and development of an inertia carpet ($R_2$ division). This evidence for continued erosion and sediment bypass during at least waxing of the flood hydrograph suggests continuation of accumulative flow conditions downcurrent from the incised delta plain. This intimate association upstream with channelized high-density turbidites of Facies B2 (a little over a kilometre in the proximal direction),

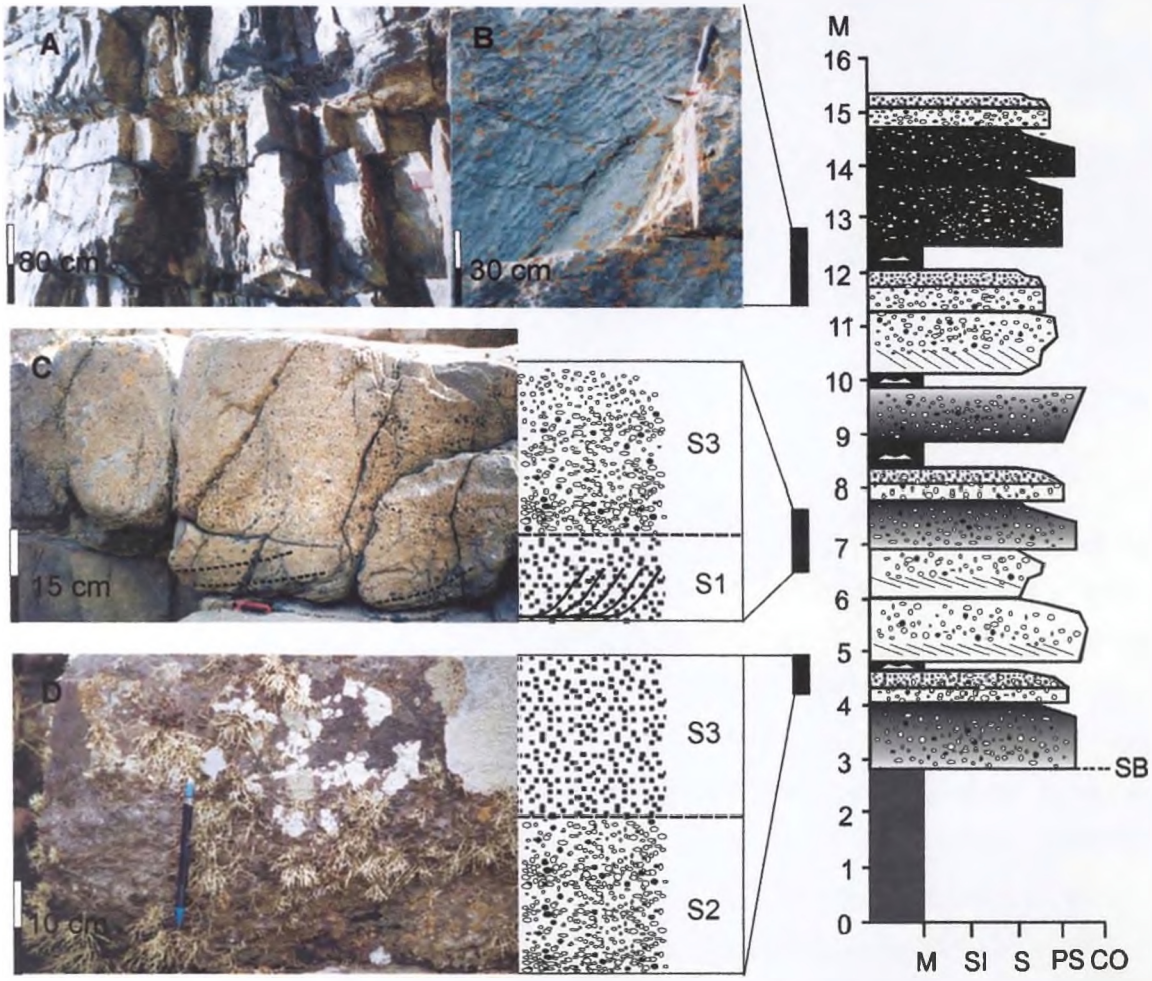



**Fig. 4.16.** Sedimentological characteristics of Facies Association C (channel-lobe transition) at Porth Clais (all photographs are from the Newgale Formation except (C), which is from the Porth Clais Formation). (A) Facies C1 – thickly bedded massive sandstone interbedded with wavy beds of Facies B1. (B) Facies C2 – kinneyia ripples formed by deformation of a passing high-density turbidity current. (C) Facies C2 – $S_1/S_3$ divisions of a high-density turbidity current. (D) Facies C2 – $S_2/S_3$ divisions of a high-density turbidity current.

suggests that this facies originated in a high sediment accumulation zone at the front of the shallow subaqueous channels.

*4.4.3.2. Facies C2: massive to normally graded, crudely stratified pebbly sandstone*

*4.4.3.2.1. Description*

This consists of poorly sorted, medium to thickly bedded (10–95 cm) coarse and pebbly sandstones characterised by sharp, planar surfaces, with abundant and diversified sole marks including load and flute casts. Lateral persistence is high, and beds can be traced for over 200 m. The most distinguishing characteristic of this facies is the well developed bipartite structure. Two varieties have been identified. The most common is a simple pebbly sandstone-coarse sandstone couplet (Fig. 4.16D). The basal pebbly division is either massive or inversely graded, with clasts displaying a(p)a(i) orientation. The upper sandstone division is either ungraded throughout or, rarely, ungraded with a thin graded cap. These massive intervals (ungraded and structureless) often display poorly developed dish structures and possible elutriation pipes. The transition to coarse sand may be gradational over a few centimetres or abrupt. Isolated outsized clasts line up between the two divisions of the bed and display a(p)a(i) orientation. The second bed type displays a lower granular cross-stratified division with small pebble alignment on foresets, overlain by a massive division identical to that described above (Fig. 4.16A and C). Cross stratification is always poorly developed and often disappears laterally. Some beds display lateral transitions from parallel stratification to cross stratification. The presence of *Skolithos* burrows on numerous bedding planes mark the most proximal evidence of biogenic activity.

*4.4.3.2.2. Interpretation*

Poor sorting, a(p)a(i) clast orientation, hydraulic sorting of pebbles, granules and sand into discrete couplets, and minor inverse grading is interpreted to reflect deposition from HDTC (Lowe 1982). The finer grain sizes, thinner bedding, occasional tractional structures, lower erosive capability, and better grain size segregation are features typical of more highly evolved turbidity currents than those that deposited Facies C1 (Falk and Dorsey 1998). These characteristics essentially define the S-sequence for sandy turbidites as outlined by Lowe (1982). Pebbly sandstone-coarse sandstone couplets record gravity transformation and flow

segregation of population 2 grains that were retained in suspension and bypassed the more proximal deposits of the R-sequence (Fig. 4.15). This restructuring of the proximal overflow into a traction carpet and distal overflow composed of population 2 grains and finer is a commonly recorded evolutionary phase in the downflow maturity of a HDTC (Falk and Dorsey 1998; Mutti *et al.* 1999).

The depleted (unsteady) character of the S-sequence overflow actively promotes direct suspension sedimentation (*sensu* Lowe 1982) out of the superjacent turbulent cloud, resulting in significant deposition ($S_3$) onto the underlying inertia carpet ($S_2$). The character of the $S_3$ division as ungraded and structureless requires a specific depositional regime to prevent turbulence and the development of traction structures as, unlike population 1 dispersions, easily suspended sand requires extremely high concentrations to dampen turbulent eddies (Lowe 1982). This problem has been addressed by Kneller and Branney (1995) who proposed a mechanism of gradual aggradation beneath a sustained quasi-steady current, particularly hyperpycnal flow (Fig. 4.1). Deposition is inferred to have occurred incrementally from the base of the flow upwards, recording gradual aggradation of a sustained liquefied zone (Fig. 4.15). This rising depositional boundary, dominated by hyperconcentration and hindered settling, is maintained for as long as deposition is balanced by grain supply from the upper turbulent portion of the flow. Because the liquefied zone spans the entire flow boundary, including both the lower dense region of the flow and the upper non-compacted part of the deposit (Fig. 4.15), there is no sharp discontinuity across the depositional flow boundary and thus no traction structures will develop (Kneller and Branney 1995). An additional process aiding the development of this liquefied zone is the elutriation of fine particles from the underlying inertia layer (Mutti *et al.* 1999). This upward motion, driven by excess pore pressure in the inertia carpet, will increase further the density of the liquefied zone, which is thus maintained from both above and below (Fig. 4.15). An origin from direct suspension sedimentation and elutriation is consistent with dish structures and elutriation pipes (Lowe 1982), recording liquefaction and fluidization as pore water is expelled during progressive aggradation (increased overburden)

Couplets with a lower cross-stratified interval represent the $S_1$ traction stage of Lowe (1982) (Fig. 4.8). This early traction phase, developed prior to the supercritical flow conditions that deposited the overlying $S_3$ division, is likely to record the most proximal expression of waxing depositional flow. These flows have been referred to as depletive by Kneller and Branney (1995), which as predicted by the acceleration matrix (Fig. 4.13), will deposit continuously irrespective of temporal variation. Therefore, the bedding sequences in Facies C2 appear to record an

important evolutionary phase in the spatial development of a quasi-steady hyperpycnal current as flow matures from an accumulative (partly erosional) to a depletive (wholly depositional) state. This transition essentially defines the zones of sediment bypass and deposition in flood-dominated dispersal systems (Mutti *et al.* 1999, 2003).

*4.4.3.3. Palaeoenvironment and process sedimentology*

In terms of sandbody geometry, the transition down-slope from the multi-event channel complexes that characterise the delta plain to sheet-like, amalgamated, very thickly bedded pebbly sandstones may be best interpreted as a channel-lobe transition or high sediment accumulation zone (Mutti and Ricci Lucchi 1972). This conclusion is strengthened by the presence of coarse-grained 3D megaripples (Mutti *et al.* 1999), abundant flute casts (Mutti and Normark 1987, Morris *et al.* 1998) and the divergent palaeocurrent pattern. The latter is the most typical facet of lobate bodies reflecting radiating flow from confined conduits (Mutti and Ricci Lucchi 1972). *Skolithos* burrows and occasional thin interbeds of wavy bedded siltstone suggest deposition in a shallow subtidal environment between low energy mudflats (Facies Association B) and higher energy cross-bedded sandstones (Facies Association D). The lack of any significant redistribution by ambient currents suggests relatively low competence background processes although low matrix content on the upper few centimetres of some beds may imply minor winnowing (Nemec and Steel 1984).

Significant deposition at the channel mouth is a function of divergent flow promoting enhanced mixing with ambient fluids and increased friction, leading to progressive deceleration and ultimately a reduction in flow competence (Mutti *et al.* 1999). This process is most evident in the preferential deposition of grain population 1 (Facies C1) and further segregation of the turbulent overflow resulting in deposits with S-sequence characteristics (Facies C2). Current divergence also promotes flow transformation from accumulative to depletive, dictating zones of bypass and deposition. This evolution must be considered as the most natural expression of the channel-lobe transition documenting a change from positive (channel incision) to negative (lobe propagation) acceleration. Although this distinction between bypass and deposition marks an important process boundary, we will later demonstrate this to be an oversimplification, as zones of sediment bypass and deposition may prograde and retrograde in space during deposition of a single bed in response to temporal changes in sediment supply.

### 4.4.4. Facies Association D: flood-generated delta-front sandstone lobe

#### *4.4.4.1. Facies D1: inverse to normal and inversely graded, unstratified sandstone*

##### *4.4.4.1.1. Description*

This facies comprises well developed inverse and inverse to normally graded (Fig. 4.17C), moderately sorted fine to very coarse sandstones. Beds range from 15–70 cm thick and are tabular, with planar non-erosive basal surfaces. A typical inverse to normally graded unit consists of fine sandstone at the base passing upwards into a thin (2–8 cm) granular layer with occasional outsized clasts displaying a(p)a(i) orientation (Fig. 4.17C). This in turn grades upwards back into medium to fine sandstone. No obvious internal stratification exists. The relative thickness of inversely graded divisions is extremely variable. The most common variant is 60% inverse but units made up of equal proportions are also very common. Wholly inversely graded beds are the subordinate type (Fig. 4.17B).

##### *4.4.4.1.2. Interpretation*

The lack of sedimentary structures, occasional a(p)a(i) imbrication, great lateral persistence and apparent 'floating' outsized clasts suggest deposition from HDTC. Although the origin of inverse grading in turbidites remains obscure (Hand 1997), it is usually attributed to dispersive pressure caused by mutual impacts of grains behaving inertially within a rapidly shearing layer. Because the effectiveness of grain inertia for transferring momentum from particle to particle diminishes rapidly with decreasing clast size (Bagnold 1954), the inverse grading that characterises Facies D1 is difficult to interpret since the sand lower in the unit is far too fine for grain collisions to produce sufficient dispersive pressure to upwardly emplace the granules illustrated in Figs. 13B and 13C. Following theoretical considerations presented by Hand (1997), the upward increase in grain size is instead interpreted as representing sustained deposition from a quasi-steady current that increases its velocity, capacity, and grain size over time. In a similar manner to deposition of the $S_3$ unit in Facies C2, sustained aggradation occurs via a liquefied zone where grains added upcurrent coarsen through time as the flow waxes. Peak velocity and carrying capacity coincide with the period of maximum erosion on the accumulative delta plain (channel incision), resulting in the emplacement of outsized rip-up clasts (Fig. 4.17C) on the

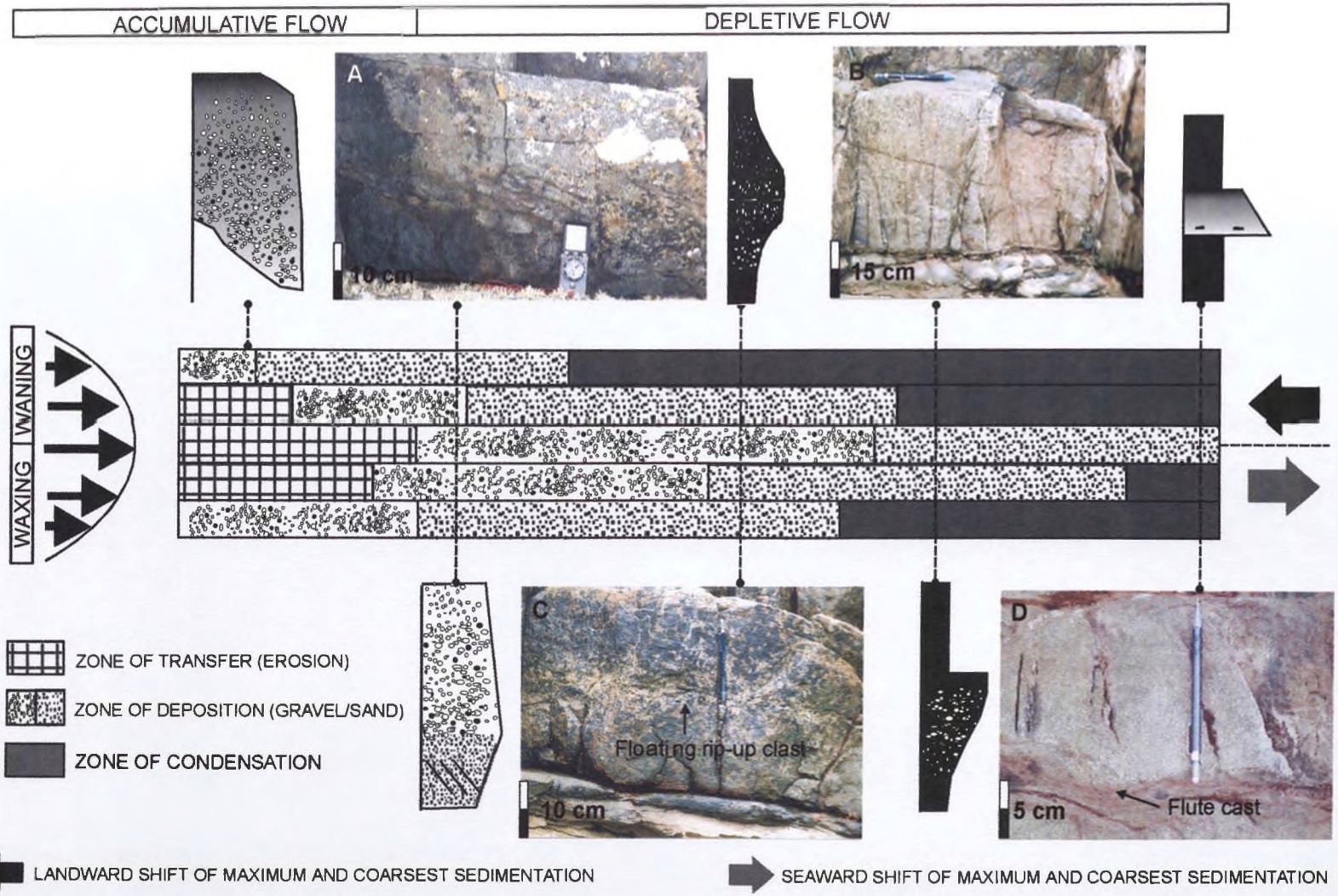



**Fig. 4.17.** Forestepping and backstepping of facies during a single flood event controlled by the flood hydrograph (all photographs are from the Porth Clais Formation). (A) Facies C2 (east Caerfai Bay) – $S_1$ and $S_3$ divisions of high-density turbidity currents. (B) Facies D1 (Newgale) – inversely graded turbidite. (C) Facies C3 (Porth Clais) – inverse to normally graded turbidite. (D) Facies D4 (Porth Clais) – normally graded turbidite.

aggrading interface of the depletive delta-front lobe. The normally graded division records flow waning, when current velocity, capacity, and grain size are reduced over time. This inverse to normally graded profile is identical to the quasi-steady hyperpycnal deposits described by Syvitski and Schafer (1996) and Mulder *et al.* (1998) and forms the most distinctive characteristic of the type hyperpycnite sequence outlined by Mulder *et al.* (2001). Computer modeling of turbidites generated by overland flood events (Skene *et al.* 1997) and the acceleration matrix proposed by Kneller (1995) also predict inversely graded profiles for a waxing depletive flow and normally graded profiles for waning depletive flow. These correspond to a depositional phase during a period of increasing then decreasing flood discharge.

#### *4.4.4.2. Facies D2: cross-stratified, well sorted sandstone*

##### *4.4.4.2.1. Description*

Cross beds rarely occur through an entire bed, but are commonly present in the upper reaches of massive or inverse to normally graded beds (Figs. 14A and 14B). The transition into this facies may be gradational or relatively sharp, and usually marks an increase in sorting and rounding of grains. Cross sets are metres long and up to 14 cm thick with abundant mudstone drapes. Reactivation surfaces within cross sets are defined by minor erosional scours occasionally aligned with mud chips (Prigmore and Rushton 2000), changes in cross stratal steepness and, in places, superimposed smaller scale sets of ripple cross lamination. The dips of both scales of cross strata are predominantly offshore despite local evidence for flow reversals, such as herringbone cross-bedding (Fig. 4.18A).

##### *4.4.4.2.2. Interpretation*

This facies records the migration of small-scale dunes similar to those recorded from subtidal (Evans 1965) or proximal storm settings (Cheel and Leckie 1992). A storm origin can probably be dismissed, as foreset angles are generally too steep and consistent compared with the low angle compound bedding formed under storm currents (Rossetti 1997). The lack of symmetrical ripples and elliptical scours also suggest dominantly unidirectional motion without a significant oscillatory component. Mud drapes within cross sets indicate episodic migration of dunes that remained stable over multiple episodes while cross lamination records the superimposition of

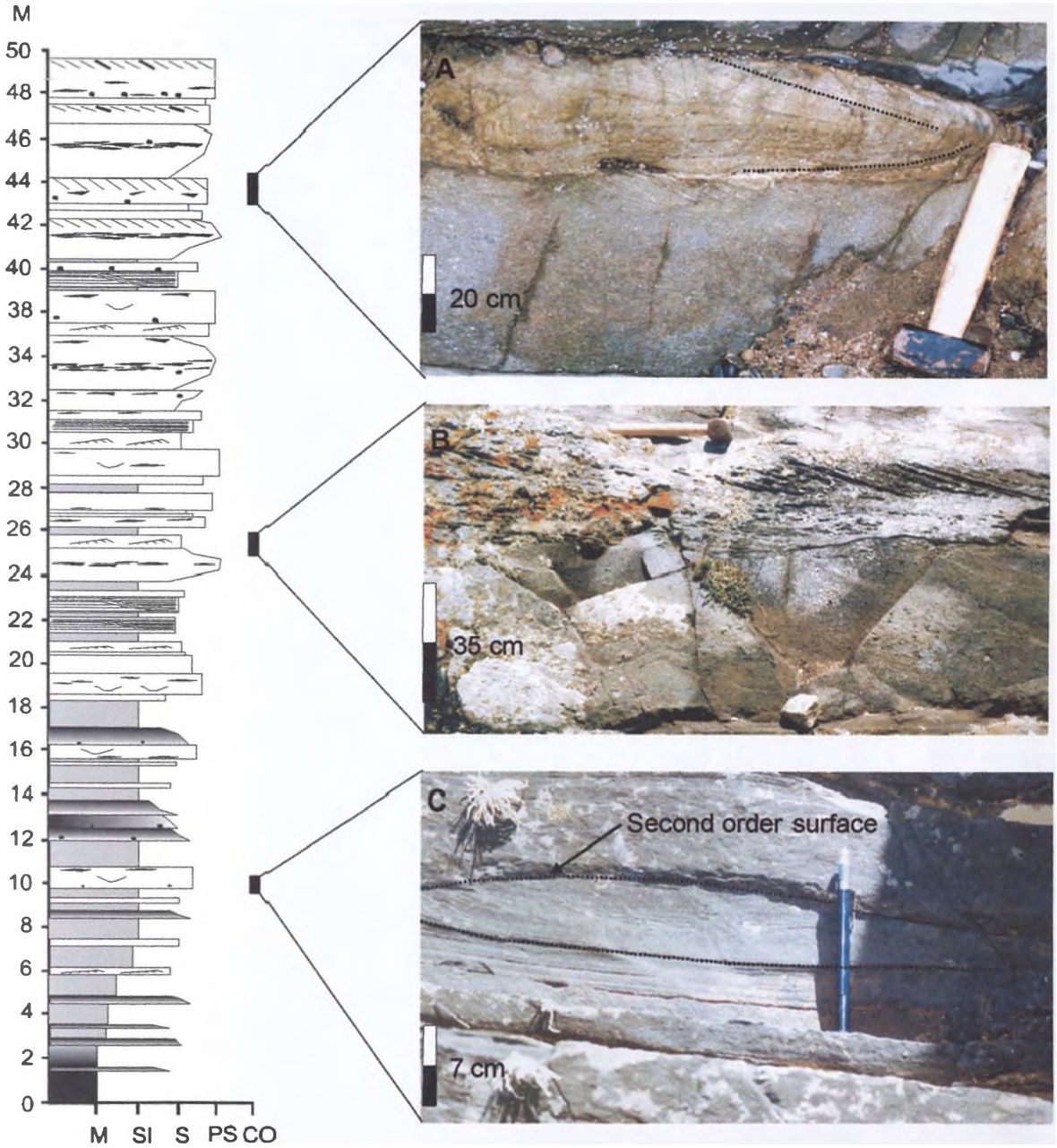



**Fig. 4.18.** Sedimentological characteristics of Facies Association D (delta-front sandstone lobe) sediments at Newgale (all photographs are from the Porth Clais Formation). (A) Facies D2 – partial tidal reworking (herringbone cross bedding) of a turbidite. (B) Facies D2 – as above but with planar unidirectional cross-bedding. (C) Facies D3 – Scour and drape hummocky cross stratification with 2nd order internal erosion surfaces.

ripples on dunes by variable strength flows. These different scale bedforms and the abundance of mudstone drapes provide evidence for regular variations in flow velocity and direction. The nearly constant offshore dips of both scales of foresets indicate ebb-dominated tidal currents. Rare herringbone cross-bedding, mud drapes capping foresets, and reactivation surfaces record the modulating influence of flood tides. The presence of cross bedded tops to massive and inverse–normally graded beds reflect tidal reworking and partial redistribution of sediment emplaced on the delta-front by HDTC. Although subtidal current velocities were clearly greater than those experienced on the delta plain, the relatively fine grain size of the reworked cross beds suggest that the tidal competence was insufficient to cause significant redistribution (Tamura and Masuda 2003). This is amply demonstrated in the coarser grained facies of C1 and C2 where there is no evidence for tidal reworking (Fig. 4.16), presumably because the grain size exceeded the carrying capacity of background processes.

#### *4.4.4.3. Facies D3: graded sandstone with HCS and climbing ripple lamination*

##### *4.4.4.3.1. Description*

Facies D3 comprises tabular, laterally extensive beds of clean, well sorted, fine to medium grained, graded sandstone 6–39 cm thick. Lower bounding surfaces are sharp and planar with well-developed and abundant flute casts. Three distinctive bedding types have been identified based on internal structure. The first contains a three-fold internal division comprising a lower normally graded structureless unit overlain by a zone of parallel lamination typified by subtle yet readily recognisable undulations (Fig. 4.19A). This lamination is identical to the quasi-planar lamination (QPL) described by Arnott (1993) and produced in flume experiments under intense unidirectional dominant combined flows (Arnott and Southard 1990). This is in turn overlain by low angle intersecting cross sets (Fig. 4.18C) that have a preferred unimodal dip direction. Asymptotic onlapping relationships of individual lamina sets are defined by very low angle second order erosion surfaces. This is interpreted as anisotropic hummocky cross stratification (HCS) (Nøttvedt and Kreisa 1987), and formed under an oscillatory-dominant combined flow with a significant unidirectional flow component. Irregular 3D combined-flow ripples with form-discordant lamination often cap HCS divisions. Wave ripples occur sporadically.

The second bed-type comprises broad (1.5-3 m), concave-up depressions or swales (Fig. 4.19B), which occasionally develop laterally into convex-up antiforms or




**Fig. 4.19.** Sedimentological features of Facies D3. (A) Porth Clais – amalgamated fine- to medium-grained sandstones exhibiting quasi-planar lamination. Note downlapping of lowermost laminae onto basal erosion surface. (B) Newgale – amalgamated fine-grained sandstones exhibiting swaley cross stratification. (C) Pen-y-Cyffrwy – inversely graded bed with a basal division of micro-hummocky cross-stratification. (A) and (B) are from the Porth Clais Formation, (C) is from the Newgale Formation.

hummocks. These swales are similar in some respects to the trough cross-bedding described in Facies A2 (Fig. 4.12), but may be differentiated on the basis of their greater trough width, lower inclination of swale margin (less than 10° compared to angle of repose), similar geometry irrespective of orientation, and most importantly, laminae that are concordant with lower bounding surfaces (typically 2nd order internal erosion surfaces) that results in thickening into swales and draping of antiforms. The latter demonstrates vertical accretion of the bedform as opposed to lateral migration which is typified by trough cross-bedding (Harms *et al.* 1975). All these features are consistent with swaley cross stratification as originally defined by Leckie and Walker (1982) with some modification by Allen and Underhill (1989). The final bed-type is composed entirely of sigmoidal, convex-up climbing ripple lamination. The geometry differs significantly from the planar to concave-up tangential foresets typical of current ripples (Allen 1970) and instead resembles combined flow ripples produced experimentally by Yokokawa (1995) and Yokokawa *et al.* (1995).

*4.4.4.3.2. Interpretation*

The most important and distinguishing characteristic of this facies is that deposition took place from a current with both unidirectional and oscillatory flow components. HCS, occasional 2D wave ripples, and the well-sorted texture reflecting winnowing and size-sorting capabilities, suggest the presence of storm-induced wave oscillations. Unidirectional flow indicators include flute casts, normal grading, planar erosion surfaces, lateral migration of hummocky bedforms to produce anisotropic HCS, and the planing-off and washout of bedforms to produce SCS (Allen and Underhill 1989) and QPL (Arnott and Southard 1990) respectively. The limited occurrence of isotropic HCS and 2D ripples, as well as the lack of recurved groove casts, modified flute casts, bi-directional prod marks and elliptical scours on basal surfaces strongly suggests that waves were subordinate in strongly unidirectional-dominant combined flows (Martel and Gibling 1994). Most sandstone beds in this facies exhibit normal grading and successions of sedimentary structures that indicate deposition from a decelerating flow. Arnott and Southard (1990) have effectively modelled the depositional transitions identified, where QPL through anisotropic HCS to combined flow ripples reflect a decrease in the unidirectional component relative to the oscillatory component with greater preservation upwards of bedforms. The lower massive division is unusual in beds deposited under combined flow regimes. The lack of traction during a period when unidirectional flow must have been close to

peak velocity (i.e. just after erosion turned to deposition), implies a highly concentrated dispersion capable of suppressing turbulent eddies.

Myrow and Southard (1996) argued that the variability in tempestites may be accounted for by considering the interplay of the three principal forcing mechanisms: wave oscillations, geostrophic currents, and excess weight forces. There are three lines of evidence that suggest deposition of Facies D3 from flows dominated by excess weight forces (flows with a strong turbidity current component). Firstly, the vertical stratification sequence reflects deposition from unidirectional dominant combined flows at or close to the upper flow regime. Velocity profiles from modern geostrophic currents (Swift *et al.* 1986), and oscillatory-dominant combined flow structures from ancient examples (Midtgaard 1996), record only a weak unidirectional component. Powerful unidirectional currents capable of flat bed structure and flute casts are instead synonymous with turbidity currents (Shanmugam and Moiola 1995). Secondly, the presence of a lower structureless division implies suppression of turbulence in a highly concentrated dispersion. Modern geostrophic currents have typical suspended sediment concentrations of between 50–150 mg $l^{-1}$ (Swift 1985, table 3) far below that required for suppression of turbulence in a high velocity flow (Lowe 1988). High angle ripple climb with convex-up sigmoidal foresets are also testament to high depositional rates (Walker 1965), and are considered indicative of flows dominated by excess weight forces (Myrow *et al.* 2002).

The third and most important line of evidence to support flow with high excess weight force is evidence for flows being driven down slope by gravity. This requires the reconstruction of flow patterns from palaeocurrent indicators (Myrow *et al.* 2002). The well publicised conflict between oceanographic and geological data sets pertaining to storm hydrodynamics (contrast Duke 1990 with Myrow and Southard 1996) highlights uncertainties surrounding the significance of certain palaeoflow indicators with regards to formative mechanisms (oscillatory vs. unidirectional flow) within combined flow. As most ancient examples are orientated at high angles to shore, Leckie and Krystinik (1989) proposed offshore-orientated unidirectional currents in oscillatory dominant combined flows. In an attempt to reconcile geological observations with modern geostrophically balanced downwelling currents directed parallel to bathymetric contours, Duke (1990), and Duke *et al.* (1991a), argued that shore normal-flow indicators are merely the product of *peak instantaneous* shear stress of wave oscillation, and bare no relation to the *time averaged* balance of gravitational and fluid forces. Because of the inherent difficulties in obtaining time-averaged flow, palaeocurrent data from sedimentary structures is supplemented with measurements of magnetic grain alignment utilising the anisotropy of magnetic

susceptibility (AMS). The use (e.g. Rees 1961, 1965; Crimes and Oldershaw 1967; Ellwood and Ledbetter 1977, 1979; Schieber and Ellwood 1988, 1993; Taira 1989; Piper *et al* 1996; Liu *et al* 2001), and reliability of AMS (e.g. Rees and Hamilton 1970; Taira and Leinert 1979; Schieber and Ellwood 1988) as a palaeoflow indicator has long been appreciated, with the method having been successfully applied to storm deposits in a number of studies (e.g. Crimes and Oldershaw 1967; Schieber and Ellwood 1988, 1993). A brief review of the methodology and parameters used to define anisotropy is presented in Appendix A.

The main advantage of grain fabric analysis is that it provides an approximation of long term (time-averaged) flow direction in sediment too fine to produce cross-bedding (Duke 1990). As the aim is to quantify the characteristics of the unidirectional component of combined flow, samples were only measured from quasi-planar laminated intervals. To ensure reliable results that represent original sedimentary fabrics rather than a secondary tectonic overprint (mechanical rotation of grains during deformation), a number of fabric tests (outlined in Hrouda 1982, and Tarling and Hrouda 1989) have been performed on the data set. These tests compare results to the known grain response to flowing water under laboratory conditions (Rees and Hamilton 1970). Fabric tests and the parameters used to define the anisotropy are located in the Appendix (Table A1 and A2). The results of 67 measurements are presented both stereographically and as a rose diagram in Figure 4.20, and clearly record time-averaged flow offshore at a high angle to bathymetric contours deduced from slump fold vergence (Fig. 4.10). The lack of Coriolis deflection implies a force balance heavily weighted towards high driving mechanisms (Myrow and Southard 1996), and a significant turbidity current component (excess weight force) to flow (Myrow *et al.* 2002). These tempestite beds therefore record deposition from offshore-directed flows with aspects of both wave oscillations and turbidity currents. These are essentially the wave-modified turbidites generated as hyperpycnal flows during marine flooding events on fan-deltas described by Myrow *et al.* (2002) and Mutti *et al.* (2003).

Although combined flow structures are commonly identified in coarse-grained delta sequences (Mutti *et al.* 1996, table 2), it has been pointed out by numerous authors (Maejima 1988; Ballance 1988) that the exact processes leading to combined flows are problematic, especially when there is no evidence for a high energy, wave-dominated coastline (Mutti *et al.* 2000). The numerous examples of flood-dominated deltas presented by Mutti *et al.* (1996, 2000) and the Cambrian examples of Myrow *et al.* (2002) all have combined flow structures, particularly HCS, dominating the delta-front. Two models presently exist for the generation of

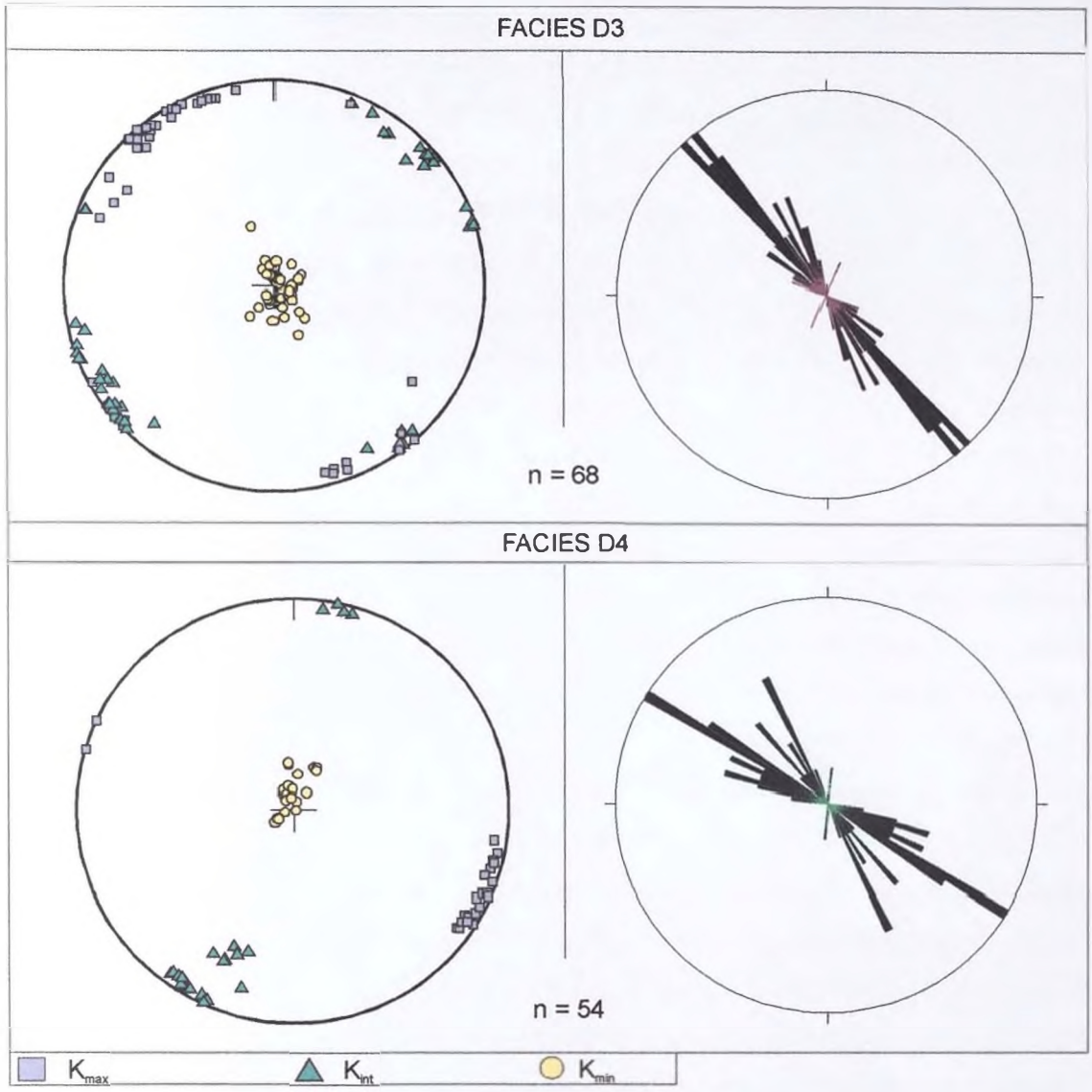



**Fig. 4.20.** Grain long axis alignment determined from the anisotropy of magnetic susceptibility. Results are presented as both equal area stereographs and rose diagrams.

combined flow on flood-dominated delta-fronts without high-energy nearshore zones. The first, proposed by Mutti *et al.* (1996) invokes internal waves generated along density interfaces within the flow. Based on the present study, this mechanism is considered unlikely, as it fails to explain the patchy occurrence of QPL and HCS. According to Higgs (1990), bedload dominated hyperpycnal flows combine with wave processes in the basin to form structures such as HCS. This combined flow model is similar to models accounting for combined flow structures in volcaniclastic mass flows, where catastrophic emplacement of sediment in marine basins during volcanic eruptions, interacts with storm processes to produce hummocky bedforms (Mangano and Buatois 1996). The interaction of fluvial discharge and storm waves has been discussed in detail by Myrow and Southard (1996). A model to account for this

interaction on flood-dominated fan-delta fronts, resulting ultimately in the deposition of a wave-modified turbidite, is presented in Figure 4.21A.

The abundance of combined flow structures on flood-dominated delta-fronts is considered to be due to the relationship between storm-induced precipitation, flood generation in alluvial feeder system, and the associated storm waves in the receiving basin. The most important prerequisite for the development of flood-dominated deltas is a high catchment area relief in close proximity to developing basins. The ensuing geomorphologic conditions of steep slopes and short sediment transport distances ensure that subaerial flood flows are capable of acquiring and maintaining sufficient sediment concentrations and inertia to form high density hyperpycnal flows (Fig. 4.1), where energy dissipation and sedimentation on coastal plains is reduced. It also means that the lag time between storm initiation (and intense precipitation) to flood flows entering the marine realm is low, and thus direct fluvial output enters the basin during storm conditions, facilitating combined flow. For this reason, Mutti *et al.* (1996) concluded that hummocky cross-stratified sandstones must represent the most genuine expression of flood-dominated delta-front sedimentation, a statement substantiated by the extremely common occurrence of HCS in fan-deltaic sequences without high-energy nearshore deposits.

The patchy occurrence of combined-flow structures in well defined progradational sequences in this study is slightly puzzling, as the minor occurrence of wave-modified turbidites would suggest that the conditions outlined in Figure 4.21A occurred at least intermittently. Emplacement below storm wave base can be ruled out as massive beds unaffected by waves occur with tidally reworked tops (Figs 14A and 14B), suggesting deposition above fair-weather wave base. Additionally, the apparently random occurrence of HCS throughout the delta lobe indicates factors other than sudden changes in water depth. The most plausible explanation for this random influence of waves on sedimentation is the development of a time lag between the storm (and the sea state it produces) and discharge of the bulk of run-off generated by the storm in the watershed: fluvial discharge effectively enters the basin during 'non-storm' conditions (Fig. 4.21B). Cacchione and Drake (1990, fig. 8) documented such a time lag for the Russian River in Northern California. Importantly, they also report occasions when there was an overlap in time between the decaying sea state and the arrival of fluvial sediment. In such cases, a relatively weak combined flow (in terms of the oscillatory component) would develop, which would adequately account for the rather poorly developed HCS documented in this study. A significant time lag is also consistent with the slightly finer grained and more thinly bedded lobe deposits encountered in this study, compared with the examples

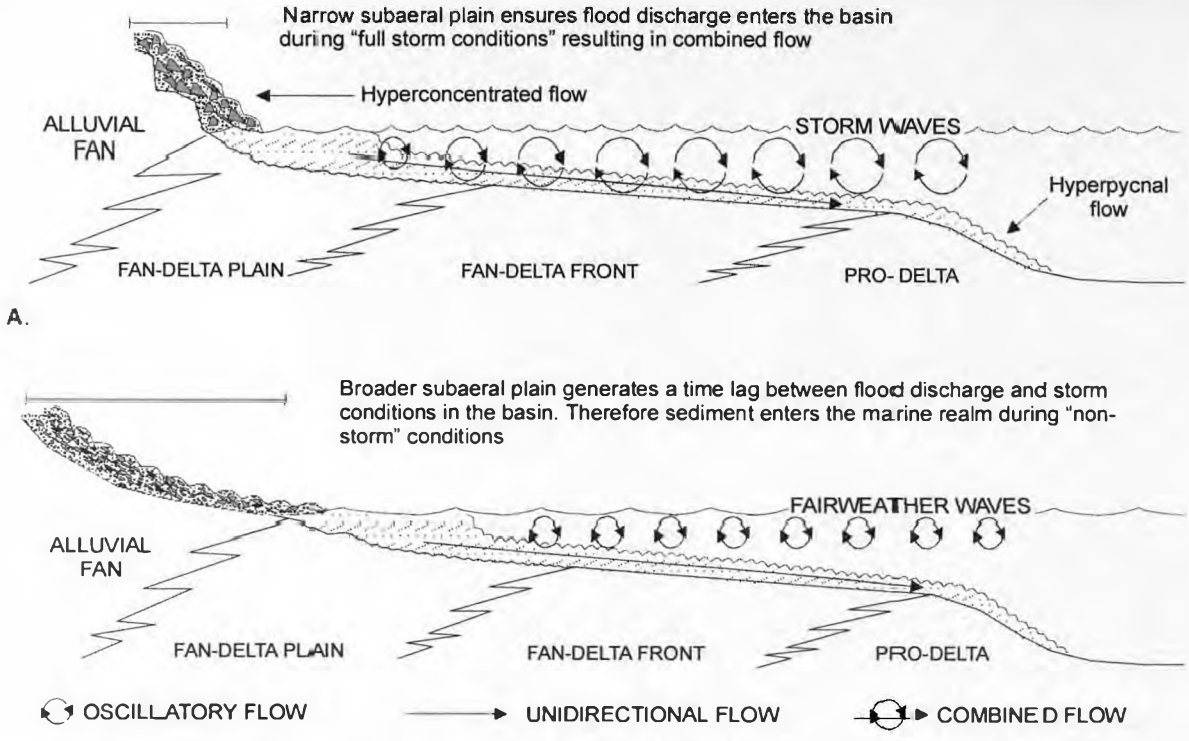



**Fig. 4.21.** The generation of combined flow on flood-dominated fan-delta fronts. (A) Fan-delta with a very narrow subaerial plain. (B) Fan-delta with a broader subaerial plain.

discussed by Mutti *et al.* (2000) and Myrow *et al.* (2002). The presence of a time lag suggests a greater distance between watershed and basin, with the probability of small amounts of sediment sequestered on the delta plain. The result would be slightly finer and thinner beds.

*4.4.4.4. Facies D4: graded, stratified, tabular sandstone*

*4.4.4.4.1. Description*

Sheet-like coarse to fine sandstones with a variably developed tripartite structure are the defining characteristics of this facies (Fig. 4.17E). Good exposure allows beds to be traced over distances in excess of 300 m without any significant change in internal stratification or bed thickness, which ranges from 6–32 cm. Beds are moderately sorted and have planar, often erosive lower contacts and gradational upper surfaces into facies D5. Sole structures are relatively common, with flute casts particularly well developed (Fig. 4.17E), and often filled with a coarse lag of angular hard clasts and rip-up clasts. On wave polished surfaces, load structures including ball and pillow morphologies and load casts with associated flames are abundant. All beds ascribed

to this facies begin with a normally graded, unstratified basal division. Roughly 30% develop parallel lamination in the upper 7-15 cm, while a further 20% have their uppermost contacts moulded into asymmetrical ripples, some with climbing ripple lamination.

*4.4.4.4.2. Interpretation*

The sharp basal contact, normal size grading and a gradational upper surface define the criteria outlined by Shanmugam (1997) for a turbidite deposited from a fully Newtonian flow. The role of significant excess weight force is reflected in palaeocurrent indicators directed at high angles to the shoreline and bathymetric contours (Fig. 4.10). Grain alignment of similar orientation (Fig. 4.20) verifies this azimuth as the direction of time-averaged flow. Well developed normal size grading particularly in the basal division reflects a fully turbulent fluid flow, where coarse and fine particles settle in accordance to their fall velocity (i.e. unhindered settling). The lack of stratification suggests direct suspension sedimentation, where sediment arrived at the depositional interface too quickly to be reworked into bedforms (Walker 1965). Rapid emplacement is also indicated by the various load structures. Parallel lamination below ripple cross lamination suggests plane bed transport of the upper flow regime through to lower flow regime and the formation of ripples. Where fallout was rapid and sustained, climbing ripples developed. Direct suspension sedimentation, through plane bed deposition; to a more dilute suspension in the presence of weak traction currents records temporal flow deceleration through well-established flow regimes (Walker 1965). The variably developed tripartite stratification readily equates to the Bouma sequence, with Ta, Tb and Tc represented (Fig. 4.8). Here, these are referred to as the most proximal deposits of low-density turbidity currents, where the grain support mechanism is solely the upward component of turbulence. This definition corresponds with the 'true' turbidites of Shanmugam (1997, 2000).

*4.4.4.5.. Facies D5: weakly graded, bioturbated silty-mudstone*

*4.4.4.5.1. Description*

This facies forms 6–120 cm thick interbeds between facies D3 and D5, and consists of structureless purple to very light grey silty mudstones, partly to fully bioturbated volcanic ashes, and occasional concretionary horizons. Horizontal burrows are

extremely common, with *Planolites*, *Teichicnus* and *Sinusites* the dominant types (Crimes 1970a). *Skolithos* and *Chondrities* burrows occur occasionally. Trilobites, although rare, have been collected (see Rushton 1974, Prigmore and Rushton 2000, for reviews on palaeontology). Although bioturbation appears ubiquitous, a very common trend is a weakly graded lower division with a higher percentage of silt and only minor apparent bioturbation, passing upwards into a truly homogenized division. Volcanic ashes that appear largely unbioturbated below, but often completely reworked above best highlight this upward trend. Carbonate concretions are also restricted to upper reworked divisions, especially the upper 6–20 cm.

*4.4.4.5.2. Interpretation*

The fine grain size, slight grading, common bioturbation and lack of internal structure are thought to reflect 'background' suspension sedimentation at a sufficient depth to be beyond the influence of ambient currents. The purple colouration suggests a well-oxygenated environment, which is reflected in high biogenic activity. The increase in the intensity of bioturbation upwards through fine-grained units probably reflects a reduced rate of sediment accumulation over time, which allowed for greater biological activity and sediment reworking (Droser and Bottjer 1986). Concretionary horizons are interpreted as representing condensation associated with minimum rates of clastic deposition, allowing early diagenetic growth at or close to the sediment-water interface (Raiswell 1987). Their occurrence exclusively in the upper reaches of silty units also indicates a decrease in sediment accumulation rates over time.

*4.4.4.6. Palaeoenvironment and process sedimentology*

The most distinguishing characteristic of this facies association is the clear interplay between fluvial and basinal processes recorded at depths between subtidal and below storm wave base, a trait most commonly associated with delta-front environments (Orton 1988; Reading and Collinson 1996). The broad divergence of palaeocurrent data, the association upstream with subaqueous channels, the sheet-like geometry, high sand content, impressive lateral distribution, well defined coarsening/thickening and fining/thinning stacking patterns (Fig. 4.9), and a turbiditic origin, fulfil all the criteria outlined by Mutti and Ricci Lucchi (1972) and Mutti and Normark (1987) for depositional lobes. Hence delta-front aggradation must be considered in terms of the coalescence of numerous sandstone lobes, probably in a similar manner to that described by Mastalerz (1995) and Mutti *et al.* (1996, 2000).

The process of sediment bypass and deposition, and its stratigraphic expression as erosive channels and depositional lobes has long been appreciated in deep marine turbidite basins (Mutti *et al.* 1999 and references therein). Only recently has this characteristic architecture sculpted by turbidity currents been identified from shallow marine settings (Ballance 1988; Martinson 1990; Dorsey *et al.* 1995; Mastalerz 1995; Mutti *et al.* 1996, 2000, 2003; Myrow *et al.* 2002). These studies equate lobe formation to HDTC ignited directly from sediment-charged flash floods, and thus justify their classification under the term 'flood-generated delta-front sandstone lobes' as proposed by Mutti *et al.* (2000). These shelfal lobes form huge sedimentary volumes in the fill of many ancient tectonically active basins (Mutti *et al.* 1996, 2000), and thus offer the greatest potential for recognition of flood-dominated dispersal systems. The fact that their stratigraphic importance has previously been largely overlooked, stems from a shared hydrodynamic regime with storm-induced geostrophic currents operating on high energy coasts, and the commonly held belief that HCS is solely a storm-generated structure. In reality, HCS is not environmentally specific (Rust and Gibling 1990; Mutti *et al.* 1996, table 2), but records the interplay between oscillatory and unidirectional currents in whatever form the unidirectional component operates, be it storm-induced geostrophic flow or flood-generated hyperpycnal flow.

Although not discussed in the most detailed study to date on flood dominated dispersal systems (Mutti *et al.* 1996, 2000), evidence for sustained deposition from a depletive (thus wholly depositional) quasi-steady turbidity current is critical to the interpretation of sand emplacement by hyperpycnal flow, and allows adequate distinction from storm-induced offshore currents. Characteristics include thickly bedded massive (Kneller and Branney 1995) and inverse to normally graded (Mulder *et al.* 1998, 2001, 2003) sandstones, extensive climbing ripple lamination with convex-up sigmoidal foresets (Myrow *et al.* 2002), and cross bedded $S_1$ divisions below either inertia carpet ($S_2$) or massive ($S_3$) sandstones (Mutti *et al.* 1999). The natural expression of quasi-steady hyperpycnal currents is not immediately obvious in the examples presented by Mutti *et al.* (1996, 2000), due to the modifying action of oscillatory currents and the resulting proliferation of combined flow structures. Their examples of delta-front sandstone lobes rarely preserve solely unidirectional flow, and therefore hyperpycnites become almost indistinguishable from tempestites.

Mutti *et al.* (1996) concluded that combined flow structures such as HCS are the most natural expression of flood-dominated dispersal systems on delta-fronts, but this is unlikely to be the case on fan-deltas where geomorphic conditions produce a time lag, and fluvial discharge enters the basin during non-storm conditions. This

scenario, which is that recorded from modern flood dispersal systems, results in depositional zones dominated by either ungraded or inverse to normally graded sandstone deposited under purely unidirectional flow. The presence of ungraded sandstone probably offers the greatest potential for distinguishing hyperpycnites from tempestites, and thus differentiating flood-dominated dispersal systems from storm systems. This premise is based on the likelihood in the former of developing and maintaining a sustained liquefied zone (Fig. 4.15) due to higher sediment concentrations and more continuous flow. Due to the relatively uniform grain size involved with storm deposition and distal hyperpycnal flow, this discrimination between ungraded and graded sandstone is not always immediately obvious. A solution is to measure the vertical variation in the rock properties that are dependent on the sandstone-shale ratio. An example of this method is presented in Figure 4.22, where vertical variations in magnetic susceptibility were obtained from a number of sandstones that appeared massive in outcrop (Floyd and Trench 1989; Piper *et al.* 1996). Most of the studied units had no predictable change in susceptibility suggesting no obvious variation in the ratio between highly susceptible magnetite-bearing sand and less susceptible phyllosilicate-bearing clay horizons. Those beds interpreted as graded in Figure 4.22 display a clear vertical variation of decreasing magnetic susceptibility towards the top of the bed, as magnetite-bearing sand is replaced, albeit in small quantities, with phyllosilicate-rich clay (Floyd and Trench 1989). The presence of shallow marine massive ungraded sandstones may provide the most reliable evidence for flood-generated dispersal processes, especially if fan-delta plain and alluvial fan sediments have been removed by later erosion.

The interpretation of a flood-dominated fan-delta system proposed here relies heavily on the premise that sediment-laden overland flows can form self-sustaining HDTC, capable of significant sediment transfer across the shelf. The early idea of shelf turbidites as depositional agents for shallow marine clastics (Hamblin and Walker 1979; Walker 1984) was dismissed shortly thereafter (e.g. Swift 1985). There seemed to be no suitable mechanism to account for the high suspended sediment concentrations necessary for autosuspension and the development of excess weight forces, on the gentle slopes that characterise most modern shelves (Pantin 1979; Parker 1983). Classic models for the energetics of sediment transport by turbidity currents (Bagnold 1962; Komar 1977) predicted that, for autosuspension to prevail, the flow velocity must be large enough for resuspension to counter deposition. On an inclined surface, flow velocity is a function of the excess weight force and the gradient of the slope (Myrow and Southard 1996). On the shallow slopes of shelf environments, autosuspension can only be accomplished by maintaining bulk density

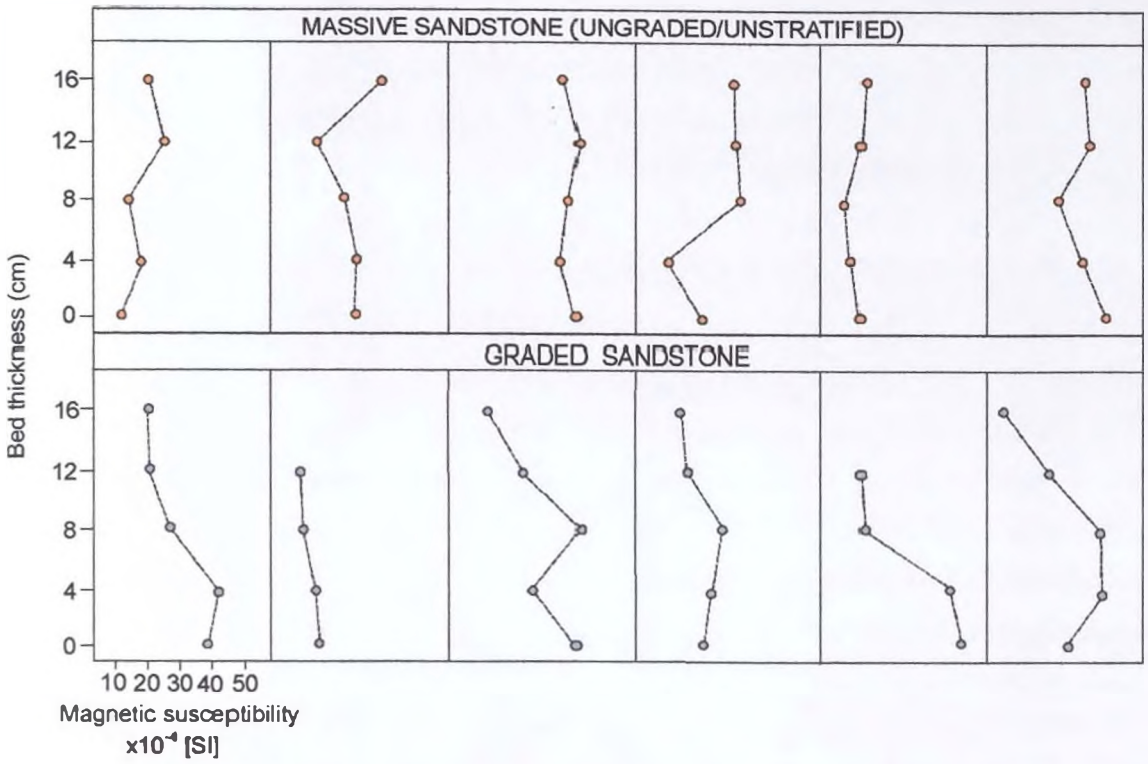



**Fig. 4.22.** Vertical variations in magnetic susceptibility from sandstones that appear ungraded and unstratified in outcrop. True massive sandstones display no consistent variation in susceptibility. Those that are subtly graded record a decrease in susceptibility up through the bed as highly susceptible magnetite-bearing sand is replaced by low susceptibility phyllosilicate-bearing clay.

at a critical value (Pantin 1979). Flows above this density threshold may increase bulk density by eroding the bed (bulking), thereby accelerating and increasing shear stresses at the base of the flow. This in turn will increase erosion, bulk density, and the excess weight force. The increase in the excess weight force through substantial bed erosion, and the subsequent acceleration of the turbid flow is commonly referred to as ignition (Normark and Piper 1991)

On flood-dominated fan-deltas, it is not necessary to invoke non-actualistic nearshore processes to account for the high sediment concentrations necessary to account for the ignition of a shelf turbidity current, as fluvial discharge provides a high density flow that may be pre-ignited with regards to autosuspension (Higgs 1990). In the present study, ignition of turbidity currents is recorded by intense basal erosion and subsequent flow confinement and the abundance of mudstone intraclasts. The zone of hyperpycnal ignition seems therefore restricted to the delta plain and the channel-lobe transition, which essentially defines the zone of transfer on modern and ancient flood-dominated fan-deltas. As hyperpycnal flows exit conduits and spread laterally, the initial reduction in bulk density leads to a different feedback mechanism

promoting deposition. Lowered density and thus excess weight force causes the flow to decelerate, with a concomitant reduction in basal shear stresses, resulting in a decrease in erosive capability and a further fall in bulk density. This mode of rapid, self-enhancing deposition was considered by Wright *et al.* (1986) as the primary cause of delta-front progradation on the modern Yellow River Delta. It also adequately accounts for significant lobe aggradation in this study and most other published examples (Mutti *et al.* 1996, 2000).

There is one significant inconsistency in applying the theory of autosuspension to account for the great lateral extent of sandstone beds on the depositional lobe. The relatively low gradient envisaged for the delta front would require significant amounts of erosion to maintain the excess weight force necessary for the continued resuspension and offshore transport. Planar bedding surfaces and relatively low abundance of mudstone intraclasts suggest that the erosive capabilities of the flow on the delta-front lobe were not particularly high, and therefore any significant reduction in bulk density through deposition would not be replenished by erosion. It is therefore necessary to explain how hyperpycnal flows had the competence to transport sand grade material over the distances defined by the distribution of the delta lobe (in excess of 10 km). Classical models for offshore sediment transport via turbidity currents do not account for the effect of basin ambient currents on the dynamic equilibrium of resuspension and deposition. Various experimental approaches have been used to study the behaviour of gravity flows on the presence of background turbulence. High levels of background turbulence supplied by powerful ambient currents act as a destructive force by promoting turbulent diffusion (Simpson 1987). Moderate ambient currents, on the other hand, provide additional boundary layer shear stresses and add viscosity, thus reducing deposition and maintaining elevated bulk density and hence excess weight force (Noh and Fernando 1991; 1992; Wright *et al.* 2001). Additional resuspension provided by background turbulence has been considered critical in the maintenance of hyperpycnal currents over 25 km offshore from the Eel River Delta in Northern California (Wheatcroft *et al.* 1997; Wright *et al.* 2001). A similar process has been inferred in ancient sequences to explain the great lateral extent of sand-rich hyperpycnal turbidites e.g. the Cretaceous Ferron Sandstone of central Utah (Mohrig 2001).

There are two important features of flood-dominated fan-deltas that actively promote resuspension and maintenance of excess weight force across the delta front. Firstly, the presence of topographical relief in the form of depositional lobes spanning the zone between fair-weather and storm wave-base. These may, in a

similar manner to modern tidal ridges (Maguregui and Tyler 1991), significantly attenuate ambient currents, resulting in low wave and tidal energy in the key area of turbidite ignition on the subaqueous delta plain. Energy levels in this zone, as suggested by deposition of delta plain shales and periods of temporary stagnation, probably fall well below the level considered destructive to turbidity currents by Foster and Stone (1963). Secondly, the time lag (Fig. 4.21B) between the storm (and the sea state it produces) and discharge of the bulk of the run-off generated by the storm in the watershed prevents the likelihood of complete turbulent diffusion of the hyperpycnal flow, as fluvial discharge is unlikely to enter the basin during peak storm conditions. Evidence for the presence of ambient currents during hyperpycnal development is suggested by the presence of combined flow structures (Facies D3), particularly on the delta lobe, recording the interplay between wave processes and offshore driven currents under excess weight force i.e. wave-modified turbidites. The study of the properties and associated structures of a combined flow resulting from the superimposition of tidal currents on a unidirectional current is still very much in its infancy (Mohrig 2001). As no criteria currently exist for the identification of this form of combined flow, its presence must be inferred from the documentation of tidally reworked turbidites.

### 4.4.5. Facies Association E: prodelta – outer shelf

#### *4.4.5.1. Facies E1: stratified fine sandstone and siltstone*

##### *4.4.5.1.1. Description*

Facies E1 comprises millimetre to centimetre thick (8 cm maximum), subtly graded, very fine sandstone and siltstone beds of restricted lateral continuity. Internal structure is dominated by ripple cross lamination, which may overlie parallel lamination. Beds with this bipartite structure are by far the most laterally persistent and tend also to be the thickest. Bases are generally planar when associated with parallel lamination, but occasional wavy bases may be scour structures. This is difficult to prove due to the homogeneity of finer grained interbeds. Horizons composed exclusively of ripple cross-lamination are better described as low amplitude – long wavelength starved or fading ripples (Stow *et al.* 1984), as they can rarely be traced as discrete beds, but instead form disconnected ripple trains. No evidence for bedform climb was documented. Sharp sunken bases to ripples may be erosional features, or may reflect loading of the bedform on a low strength substrate.

The most distinctive characteristics of this facies are the various forms of soft sediment deformation. Convolute lamination and individually contorted beds are extremely common. Small-scale slump folds with local thickening into hinges and syn-sedimentary micro-faults are also evident. Large-scale slump horizons affecting multiple facies have been observed but are less frequent.

#### *4.4.5.1.2. Interpretation*

Parallel lamination and ripple cross lamination are interpreted as reflecting deposition from unidirectional traction currents similar to those that emplaced the thicker and coarser deposits of Facies D6. Isolated starved ripple trains and the lack of climbing ripple lamination suggests dilute, low concentration turbidity currents (Basu and Bouma 2000). The density-induced nature of the flow is also indicated by the parallelism between soft sediment fold vergence and palaeocurrent data (Fig. 4.10). Deposition probably occurred in a similar manner to that described by Walker (1965) for Bouma divisions B and C, where an initial thin, persistent, parallel laminated bed was emplaced under transitional upper flow regime conditions, which was later partly or completely remoulded by lower flow regime currents. The thinner beds would tend to form isolated ripple trains. The various styles of soft sediment deformation indicate a certain degree of instability, and the presence of a relatively shallow gradient slope.

### *4.4.5.2. Facies E2: homogeneous silty-mudstone with discontinuous limestone*

#### *4.4.5.2.1. Description*

This facies is virtually identical to D5 and differs only in a greater degree of bioturbation resulting in totally homogenous silty mudstone, and far more abundant carbonate concretions (Fig. 4.23C), which often amalgamate laterally to form nodular limestones. Some nodules exhibit cone-in-cone structures. The intensity of bioturbation means that most of the burrows are unidentifiable, but rare *Planolites* and *Sinusites* may be determined. Trilobites and brachiopods are locally abundant (Lewis 1987).

#### *4.4.5.2.2. Interpretation*

In a similar manner to Facies D5, these bioturbated silty mudstones and carbonate concretions reflect very low levels of background sedimentation and periods of

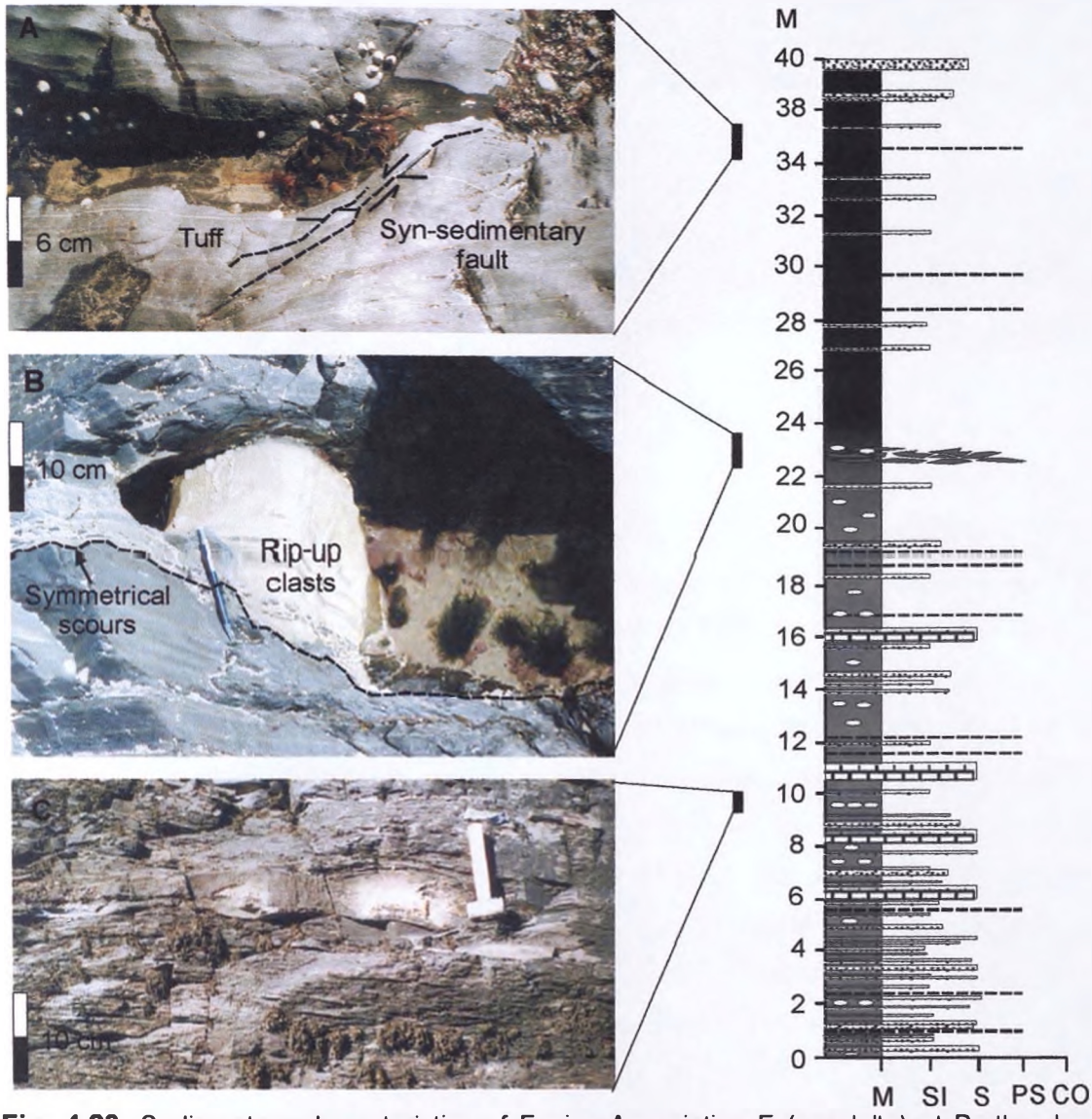



**Fig. 4.23.** Sedimentary characteristics of Facies Association E (pro-delta) at Porth-y-rhaw (all photographs are from the Menevia Formation). (A) Facies E4 – Black laminated mudstone with some soft sediment deformation. (B) Facies E3 – conspicuous rip-up clast horizon interpreted as forming through internal wave erosion along a pycnocline that intercepts a low gradient pro-delta slope. (C) Facies E2 – discontinuous horizon of carbonate concretions suggesting periods of intense sediment starvation.

extreme condensation. Cone-in-cone structures suggest relatively high pore pressures reflecting compaction and overburden (Reading and Collinson 1996).

*4.4.5.3. Facies E3: graded and banded siltstone and black mudstone*

*4.4.5.3.1. Description*

The base of Facies E3 forms an extremely conspicuous erosion surface characterised by gentle symmetrical scours overlain by a laterally persistent concentration of very well rounded phosphate and mudstone rip-up clasts (Fig. 4.23B). Sediment immediately above this surface may be divided into units 4–13 cm thick, composed of three well-defined horizons. The base of each unit is composed of a thin (0.2–2.1 cm thick) rippled siltstone that may be massive or consist of 'fading' ripple cross lamination, in which ripple crests pass gradually into ripple troughs of shale (Stow and Shanmugam 1980). Basal boundaries are slightly erosional and commonly loaded. Ripples are always low amplitude and long wavelength, and display no evidence of ripple climb. Thin siltstones are succeeded by a graded green to grey silty mudstone, which may have a mottled appearance suggesting bioturbation (Prigmore and Rushton 2000). This horizon varies from 1–5 cm thick, and may be diffusely laminated, convoluted or structureless. This is in turn overlain by a massive ungraded black mudstone devoid of structure and signs of biogenic activity. Trilobites occur in relative abundance at certain horizons.

*4.4.5.3.2. Interpretation*

This banded facies forms transitional beds between the relatively well oxygenated prodelta and the oxygen-deficient outer shelf, and is directly comparable with the so-called 'zebra facies' commonly described from such transitional settings e.g. the late Devonian Catskill prodelta environment (Baird and Brett 1991) and the Upper Jurassic Kimmeridge Clay (Wignall 1989). The lower graded silt, with ripples and evidence for rapid emplacement closely equates to the Type II turbidite silts described by Piper (1978), which form the basal division (T0) for fine grained, dilute turbidites as outlined by Stow and Shanmugam (1980). The complete sequence for muddy turbidites is outlined in Figure 4.8 and roughly corresponds to the Te division of Bouma (1962). As acknowledged by Stow *et al.* (1984), the complete set of divisions is rarely present in any one bed, which may comprise base cut-out and top cut-out sequences. The green silty mudstones with convolute lamination and diffuse

parallel lamination correspond to the T1–T3 divisions as outlined in Figure 4.8. Ungraded black mudstone is not considered to be directly related to turbidite emplacement and is better referred to as hemipelagite (P division). This is because of the sharp contact between relatively well oxygenated and sometimes bioturbated silty mudstone, and the oxygen-deficient unbioturbated black mudstone, suggesting a significant period of time had elapsed to allow for the development of oxygen deficient conditions. The turbidite deposit may thus be classed as part of a top cut-out sequence.

The variation in colour and degree of bioturbation, reflecting variations in near-bed oxygen levels (Arthur *et al.* 1984) can be most simply interpreted as reflecting temporary oxygenation of an oxygen deficient environment by turbidity currents. Fine grained sediment with these characteristics, and displaying minor bioturbation may correspond to the lower boundary of the 'dysaerobic' facies zone as discussed by Rhoads and Morse (1971). The counter-intuitive association of black shale deposition with an erosion surface is difficult to account for, but it would seem from the literature that such an association is extremely common (Baird 1981; Leckie *et al.* 1990; Wignall 1991). In a regional study of Palaeozoic black shales of North America, Baird and Brett (1991) reported that most units are marked by basal discontinuities characterised by a lag concentration of reworked pyrite and phosphate debris (see their table 1) and, like the symmetrical scours documented here (Fig. 4.23B), appear to be eroded by wave action. Possible mechanisms responsible for these features have been discussed by Baird and Brett (1986, 1991), Heckel 1991, and Schieber and Baird (2001) and are though to reflect either storm induced surface waves or deep internal waves concentrated along a density interface (pycnocline). In the latter case, significant erosion occurs when the pycnocline intercepts an accentuated slope, for example in prodelta environments.

There are three lines of evidence to suggest density stratification as the causal factor in submarine erosion. Firstly, simple reworking by surface waves implies a shallowing event, which would be expected to significantly oxygenate bottom waters, and produce to multiple erosion events. Secondly, an identical horizon has been recognised in a coeval section in the Manuels River Formation in southwestern Newfoundland (bed 115 of Howell 1925, p. 36) which, according to recent palaeogeographical reconstructions (Landing 1996) and detailed stratigraphic correlation (Brasier 1989), formed within the same intra-cratonic basin. This suggests a basinwide event rather than local storm conditions. Thirdly, Lower and Middle Cambrian palaeo-oceanographic reconstructions based on faunal barriers for circum-Iapetus intra-cratonic basins suggest the presence of a thermocline (Conway Morris

and Rushton 1988). Finally, the erosion surface signifies an important 'process boundary' separating traction deposition from deposition solely from suspension (hemipelagite of Facies E4). It is this process boundary that separates well oxygenated from oxygen deficient sub-environments. The effects of density stratification on an incoming turbidity current is discussed later, but it would seem that very few of these dilute flows had sufficient density to break through the interface and oxygenate the environment, but rather spread horizontally along the pycnocline thus depositing its load over a wider area out of suspension, accentuating condensation. A similar process has been inferred from modern (Stanley 1981, 1983) and other ancient (Baird and Brett 1991) prodelta settings.

*4.5.5.4. Facies E4: laminated black mudstone*

*4.4.5.4.1. Description*

Facies E4 forms a monotonous succession of either diffusely laminated or structureless black mudstones with intercalated thin (0.1–1.2 cm thick) graded, medium to fine silt layers with relatively sharp, but clearly non-erosional bases and gradational tops (Fig. 4.23A). Silt horizons contain no evidence for traction deposition and even the thinnest layers may be traced across the length of the outcrop (>90 m). No bioturbation is evident. Similarly, numerous volcanic ash horizons display no evidence for tractional emplacement or reworking. Black mudstones are rich in framboidal pyrite and phosphate nodules (Hicks 1875) but carbonate concretions and limestone beds have not been observed. Trilobites are rare but the controversial echinoderm-like organism *Protocystites menevenis* Hicks occurs occasionally (Jefferies *et al.* 1987).

*4.4.5.4.2. Interpretation*

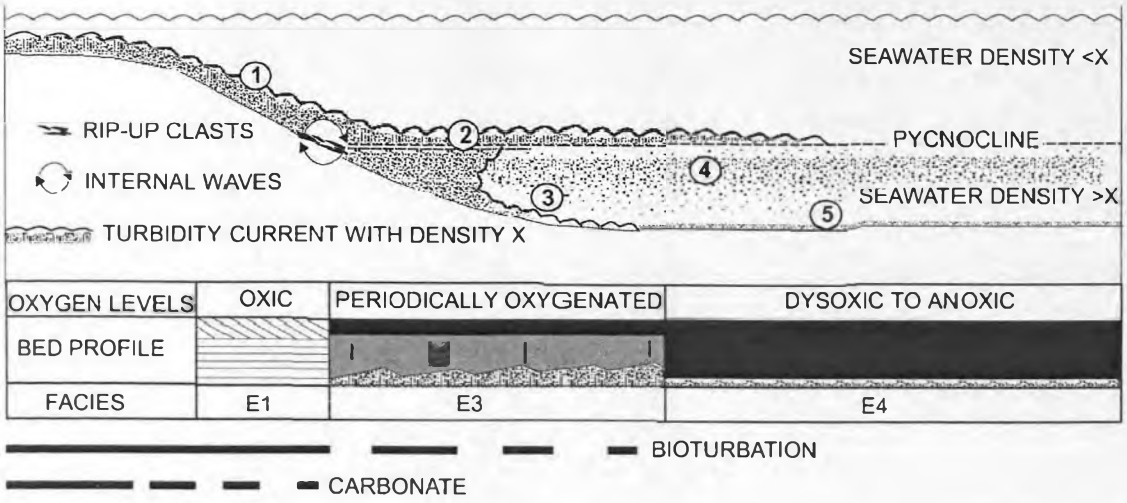
The lack of infauna, sparse epifauna, the laminated texture and very dark grey to black colouration suggests low levels of dissolved oxygen, possibly bordering on complete anoxia (Arthur *et al.* 1984). The uniform composition, lack of primary sedimentary structures and inferred low sedimentation rates suggest hemipelagic sedimentation (Stow *et al.* 1996). Although the common presence of pyrite does not necessarily imply anoxic conditions at the sea floor, it does suggest that sufficient metabolizable organic matter remained during burial to promote sulphate reduction within the sediment and sulphate mineralization (Berner 1969). The framboidal state

implies early diagenetic formation at very shallow depth (Love 1967), forming in muds of soupy consistency (O' Brien 1995). *Protocystites menevenis* was adapted to staying upright on extremely soft (watery) mud (Jefferies *et al.* 1987). The rapid decline in carbonate suggests dissolution and low pH values in bottom waters, probably due to high levels of dissolved $CO_2$ and $H_2S$ associated with oxygen depletion (McIlreath and James 1980). The origin of thin silt bands is uncertain, but they clearly represent a type of 'event' deposition that punctuated an environment usually associated with intense condensation.

*4.4.5.5. Palaeoenvironment and process sedimentology*

These fine-grained lithofacies resemble those characteristic of modern and ancient prodelta to outer shelf deposits emplaced beyond the influence of surface waves and tidal processes (Reading and Collinson 1996). Deformational features and cone-in-cone structures are a by-product of high rates of sedimentation on the delta-front leading to high pore-fluid pressures and low sediment shear strength. The relatively condensed nature typical of the distal reaches of the delta system is implied by the abundance of nodular limestone beds, carbonate concretions, starved ripples and intense bioturbation, suggesting that the ancient depositional surface remained starved of sediment for significant periods of time.

The distribution of facies and oxygen levels experienced in the prodelta – outer shelf setting can be expressed most simply as the by-product of a density stratified water column, reflecting a process boundary that separates a well oxygenated environment periodically affected by relatively dilute turbidity currents and an oxygen deficient environment below the density interface. This facies distribution with respect to a pycnocline is presented as a model in Figure 4.24. Stage 1 documents deposition on the shallow gradient prodelta slope from a LDTC producing a graded fine sand to silt layer displaying the characteristics of Bouma divisions B and C (Facies E1). Although the current is relatively dilute, flow density must be above that of the surrounding ambient fluid (Walker 1965). As the current penetrates the pycnocline (stage 2), the sharp density interface strips from the flow all the particles that have a lower density than the fluid below the interface i.e. the finest grade material, usually clay and fine silt (Rimoldi *et al.* 1996.). The denser body of the turbidity current passes through the interface (stage 3) and deposits a suite of sediments that document the passage of flow from head to tail (Stow and Piper 1984). The introduction of oxygen and entrained organisms is reflected in sediment that is green to grey and partly bioturbated (Facies E3). An important characteristic of




| STAGE | PROCESS |
|---|---|
| 1 | Low density turbidity current deposits Ta-Tc |
| 2 | Lowest density grains stripped from current at pycnocline |
| 3 | Deposition of a top absent fine grained turbidite and temporary oxygenation of the environment |
| 4 | Low-density plume travels along the pycnocline depositing over a wide expanse |
| 5 | A persistent graded bed forms due to the different settling out of the plume |

**Fig. 4.24.** Model for pro-delta sedimentation based on the characteristics of Facies Association E. See text for details.

the deposit will be the top-absent sequence (as discussed by Stow and Piper) reflecting removal of the finest material at the density interface. Stages 4 and 5 record relatively rapid deposition out of suspension from the plume concentrated along the pycnocline. Due to differential settling velocity, this initial rain of sediment will be silt-rich, forming a thin graded layer over a wide expanse (the unifites of Stanley, 1983). This horizon may be undistinguishable from the silty material laid down directly by the turbidity current in the more proximal region, but forms distinct graded lamination beyond the influence of traction currents in more distal settings (Facies E4). The light colour of the sediment indicates emplacement while oxygen conditions were still elevated. The final stage is represented by very low sediment accumulation rates throughout the prodelta-outer shelf. Oxygen-deficient conditions return below the pycnocline as minor flooding episodes do not attain sufficient density to penetrate the interface, but probably maintain sufficient turnover, and thus oxygenation of the water column above the pycnocline.

Slow sedimentation out of the plume may continue for some time, aided by continued replenishment by very dilute flood events, forming black mudstone below the pycnocline. Although this mechanism is based solely on observations in the present study, it explains the features common to the 'zebra facies' of numerous authors (e.g. Baird and Brett 1991; Schieber and Baird 2001). Although it has been

demonstrated that a density stratified water column is a basinwide feature, and therefore not restricted to flood-dominated delta systems, the catastrophic input of freshwater and sediment may have contributed significantly to the characteristics of the prodelta–outer shelf. Firstly, freshwater discharge probably augmented the already established thermocline by the establishment of a halocline (Heckel 1991). Secondly, the internal waves responsible for the characteristic diastem flooring black shale sequences, may have been magnified significantly during flood events, as sediment-charged flows displaced water in the nearshore environment, forming deep waves as observed in experiments by McLeod *et al.* (1999). This deep wave erosion may have been further intensified by internal waves formed by displacement of the pycnocline during turbidity current interaction as modelled by Rimoldi *et al.* (1996). Finally, these internal waves are more likely to erode and scour the sea bed when the pycnocline intercepts an inclined substrate (Baird 1981), an environmental constraint commonly documented from prodelta-slopes (Woodrow 1985; Baird et al. 1988; Baird and Brett 1991).

## 4.5. SEDIMENT DISPERSAL PROCESSES DEFINED BY FACIES TRACTS

The study of sediment dispersal patterns and depositional processes that ultimately define the character of the fan-delta system is best approached through the construction of facies tracts (Mutti 1992). The concept of facies tracts is here defined as the documentation and interpretation of facies types originating from the transformation of flows during their basinward motion along the erosional and depositional profile of a system. The principal facies tracts inferred from lateral and vertical lithofacies relationships are presented in Figure 4.25 and can be most simply framed in terms of hyperpycnal, hypopycnal, and homopycnal components (Fig. 4.1), with an additional mechanism not accounted for on modern river deltas, that of mass emplacement by sediment gravity flows. For ease of discussion, facies tracts are described and interpreted separately, and in the order outlined in (Fig. 4. 25 i.e. 1-4).

### 4.5.1. Hyperpycnal underflows: spatial and temporal evolution of quasi-steady turbidity currents

It has been appreciated that sediment dispersal on deltas is mainly controlled by the efficiency of the transfer system and thus sediment flux to the basin (Mulder and Syvitski 1995). The dominance of highly efficient HFF in the alluvial system is

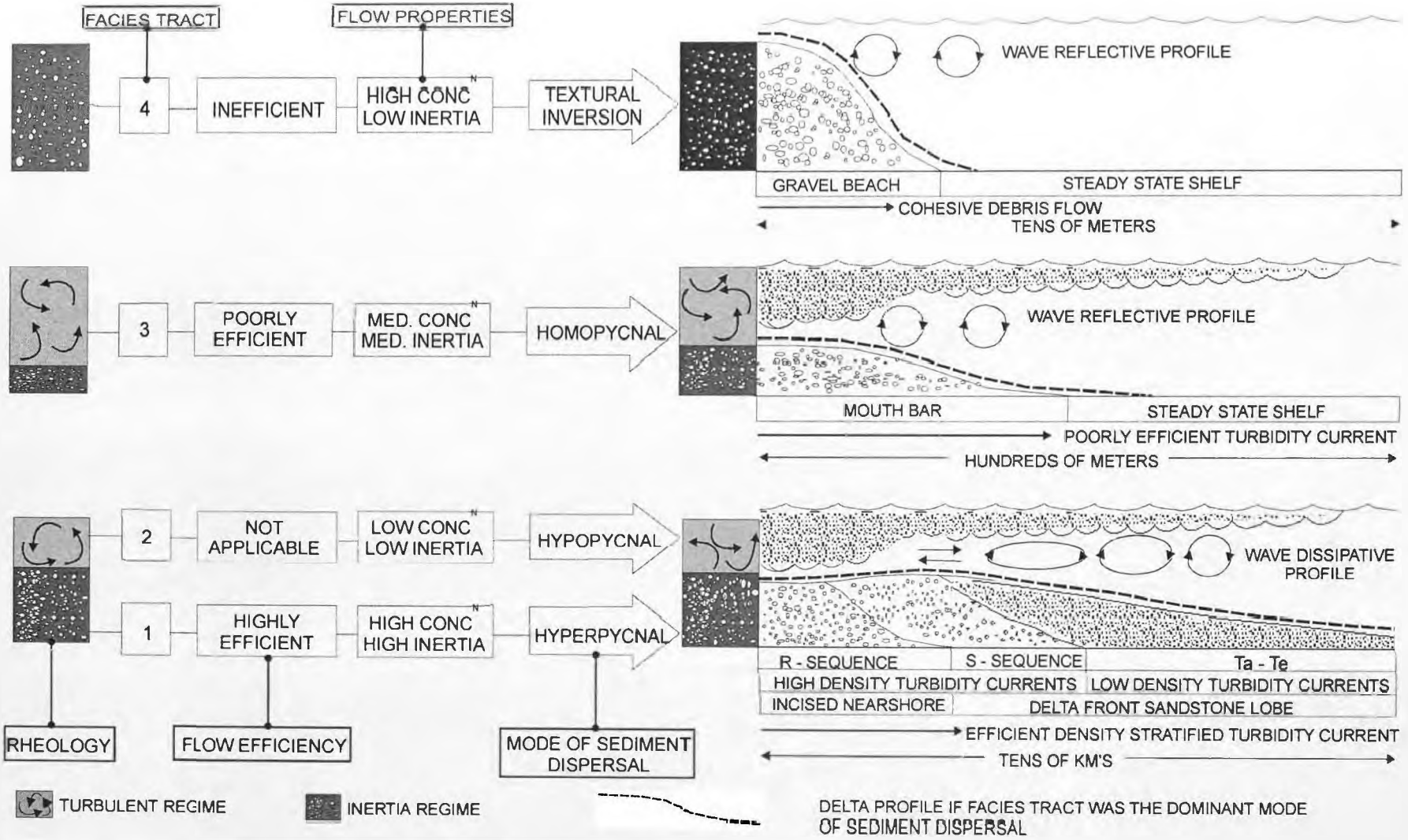



**Fig. 4.25.** Facies tracts reconstructed from lateral facies changes evident in the Caerfai and Porth-y-rhaw groups. Based on inferred flow concentration and velocity, facies tracts may be classified in terms of flow efficiency.

manifested in a fan-delta succession built almost exclusively (>70%) of high- and low-density turbidites emplaced directly from subaerial flood events (Facies Tract 1 in Fig. 4.25). A consequence of the flood hydrograph is to produce a quasi-steady turbidity current with well-defined waxing and waning phases. According to the acceleration matrix (Fig. 4.13), this variation in temporal acceleration, reflecting an increase followed by a decrease in current velocity over time, should be identifiable in the turbidite succession. While temporal acceleration is an extrinsic control on current velocity, spatial acceleration is governed primarily by the local geomorphology of the site of transport/deposition.

A common factor in promoting accumulative flow is channel incision, where lateral confinement maintains the velocity and competence of the igniting turbidity current (Mutti *et al.* 1999). Where the flow is no longer confined, increased friction and reduced excess weight force results in depletive flow (Mulder *et al.* 1998). Therefore the temporal and spatial evolution of the quasi-steady turbidity current should be demonstrated by facies that record waxing and waning of the flood hydrograph on the accumulative incised delta plain, while a different set of characteristics should define waxing and waning on the depletive delta-front lobe. The evolution of the hyperpycnal current, as defined by depositional characteristics, is discussed below in terms of increasing flood discharge (waxing flow), at peak discharge (almost steady flow), and decreasing flow discharge (waning flow). These three stages of the flood hydrograph correspond to four phases of flow evolution here referred to as the turbulent phase (waxing flow), the density stratified phase (peak discharge), the turbulent diffusion phase (waning flow) and the channel backfill phase (waning flow). The temporal and spatial evolution of hyperpycnal turbidity currents is also presented as a model in Figure 4.26.

#### *4.5.1.1. Fully turbulent phase (flow waxing)*

During lowstage waxing, relatively dilute overland floods discharge into the basin creating a fully turbulent and erosive hyperpycnal current (Fig. 4.26A). Turbidity currents ignite on the delta plain and, through the process of bulking, incise deep and narrow submarine canyons (Facies B2). The incision of deep narrow channels is aided significantly by the quasi-steady nature of the eroding current, due to prolonged passage (days to months, Mulder and Alexander 2001) of a fully turbulent (and thus erosive) body region (Alexander and Mulder 2002). This channel morphology, characterised by low width to depth ratios, has been recorded from modern (Prior and Bornhold 1988, 1989, 1990) and ancient (Martinsen 1990) fan-

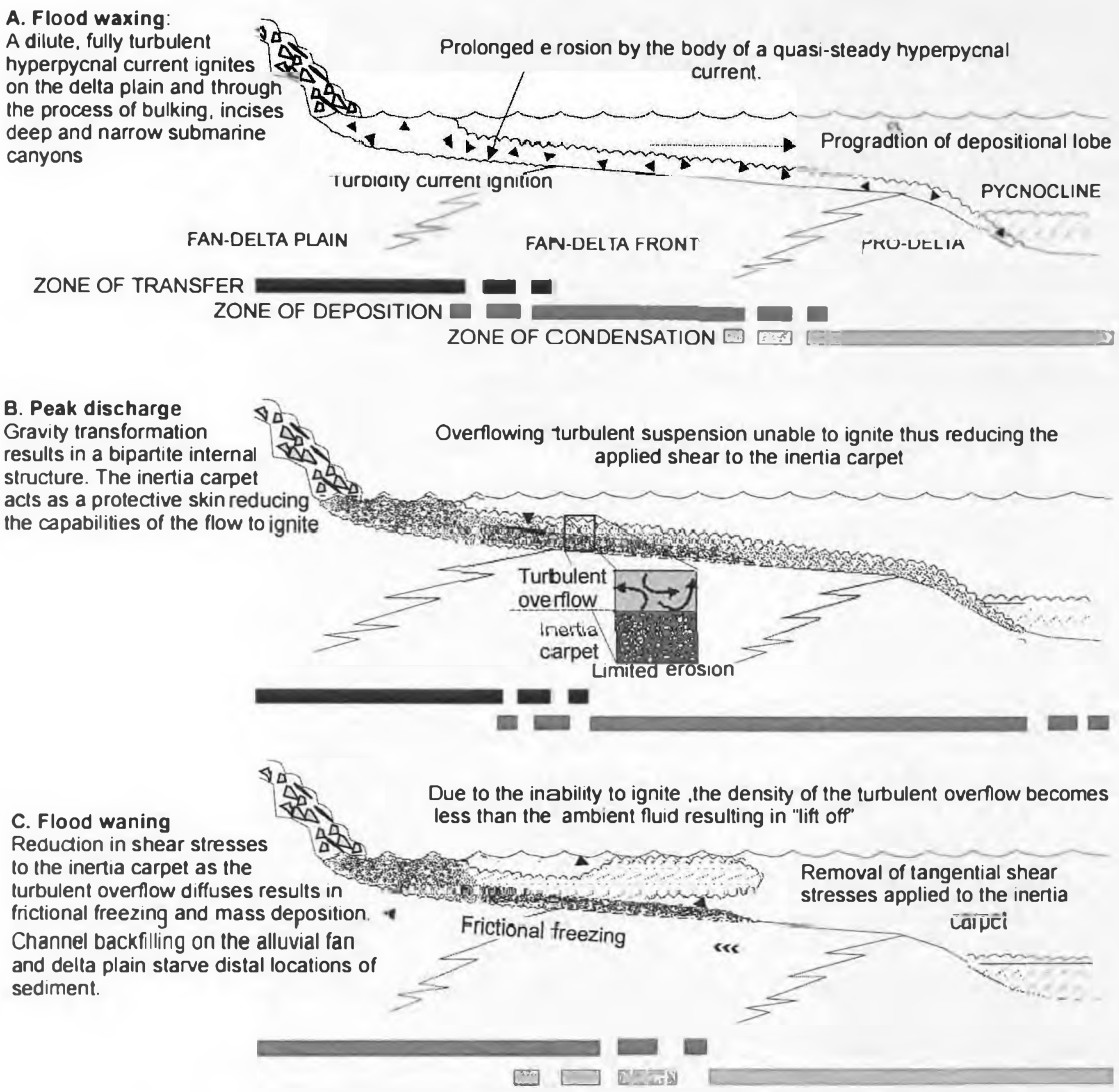



**Fig. 4.26.** Temporal and spatial phases of flow evolution during a single flood event in response to waxing and waning of the flood hydrograph.

delta bypass zones sculptured by hyperpycnal turbidity currents. Unlike surge-type turbidity currents, where the head of the flow has a major influence on flow behaviour and deposition (Alexander and Mulder 2002), quasi-steady flows will tend to be extremely dilute in their earliest phase and the passage of the flow front appears to be unrecorded. As the flow is accumulative (confined), this location acts as a zone of sediment bypass, and thus contains no preserved record of waxing flow (Fig. 4.13).

At the exit of the conduit, lateral spread of the flow promotes depletive conditions leading to progradation of a depositional lobe. In this more distal location, attenuation of small-scale fluctuations in fluvial discharge promotes a high degree of flow steadiness (Mulder *et al.* 1998), resulting in the formation and migration of megaripples ($S_1$ division in Facies C2), climbing ripples (Facies D3), massive sands (Facies C1) and coarsening-upward profiles (Facies D1). An excellent example of

depletive waxing flow is displayed in Figure 4.19C. This relatively common bedding sequence has HCS at its base passing upwards into a granular division devoid of traction structures, and is very similar to the example figured by Kneller (1995, fig. 10) for a depletive waxing flow deposit. The coarsening-upward profile records the delivery (over time) of coarser grains to the progressively aggrading depositional interface (Kneller and Branney 1995). The lower division of HCS reflects relatively low flow concentrations, deposited in the earliest stages of hyperpycnal flow evolution, where unidirectional currents operating purely under traction entered the basin while storm conditions still persisted, resulting in combined flow (Fig. 4.21D). As flood discharge increased, so did the capacity of the flow to transport coarser material, resulting in apparent inverse grading and dampening of turbulence.

*4.5.1.2. Density stratified phase (peak discharge)*

At or close to peak discharge, the sustained turbidity current develops significant bedload through gravity transformation, forming a non-linear particle concentration gradient (Fig. 4.26B) and thus may be considered in terms of a bipartite flow, similar to the hyperpycnal flows with inertia bedload or psuedo-laminar inertia flows described from Bear Creek, British Columbia by Prior and Bornhold (1988, 1989, 1990) and Bornhold and Prior (1990). In a similar manner to modern examples (*op. cit.*), evidence for this coarse inertia layer is restricted to the most proximal location, as the competence of the flow to maintain a basal carpet is restricted to locations where the flow is accumulative (Prior and Bornhold, 1990). The development of inertia bedload also signifies the end of channel incision since turbulence is dampened in the basal region and the inertia carpet essentially acts as a protective skin between the seabed and the overflowing suspension cloud (Hsu 1959). Peak stage on the delta lobe is well represented by granular grade material and abundant rip-up clasts (Fig. 4.17C) as the zone of erosion and coarsest deposition moves progressively seawards. This forestepping of erosional and depositional zones during increasing flood discharge has been documented by Mulder *et al.* (1998) from hyperpycnal turbidites deposited from the Saguenay River flood of 1663 AD.

*4.5.1.3. Turbulent diffusion phase (flow waning)*

The development of a density-stratified flow will significantly affect the efficiency and competence of the overflowing turbulent suspension cloud. The reduction in sediment concentration as fluvial discharge wanes is compounded by the inability of

the turbulent overflow to ignite on the delta-plain due to the protective barrier of the bedload zone (Fig. 4.26C). Although minor bulking may take place through elutriation (upward motion of fine particles from the inertia carpet by escaping pore fluids), it is unlikely that the critical density needed to maintain autosuspension can be accommodated solely by this process (Mutti *et al.* 1999, 2000) and thus, without erosion to maintain excess weight forces, the suspension cloud would weaken significantly. This decrease in flow competence and velocity will have a detrimental effect on the resuspension capabilities of the inertia layer as relatively large amounts of sediment will be added as the turbulent cloud begins to collapse, while shear stresses applied to this surface will decrease, resulting in greater internal friction and energy dissipation.

*4.5.1.4. Channel backfilling phase (flow waning)*

In the final stage of the flood hydrograph, the transfer zone (delta plain) becomes the depositional zone as the competence of the hyperpycnal flow is reduced, and thus the site of maximum deposition moves landward (Fig. 4.26C), and flow is accumulative and waning (Fig. 4.13). The reduction in applied shear from the rapidly dispersing turbulent cloud promotes frictional freezing of the inertia carpet. The most proximal location corresponds with the coarsest grain size, roughly within the range of grain population 1 of Lowe (1982), thus resulting in deposition of the R-sequence (Facies B2 and C1). Downcurrent, the competence of the flow was only sufficient to maintain population 2 grains, resulting in deposition of the S-sequence ($S_2/S_3$, Facies C2). The traction stage of both sequences ($R_1$, $S_1$) is considered to represent deposition during flow waxing and thus constitutes in most (but not all) cases, the basal erosion surface. As the onset of frictional freezing is directly related to the reduction in concentration of the overflowing turbidity current, freezing is inferred to occur from the most distal location affected by inertia bedload (the channel-lobe transition) landwards, as this reflects the lateral concentration gradient of the turbulent overflow. This will therefore result in backfilling of channels on the delta plain.

Waxing depletive flow on the depositional lobe is poorly represented. This is manifested in the limited occurrence of normal grading. The condensed nature of waning flow deposition, only represented by thin graded caps on far more extensive massive or inversely graded divisions suggest a significant reduction in the efficiency of the hyperpycnal flow. Most of its sediment load is sequestered on the delta plain through channel backfilling, thus essentially starving the more distal reaches of the

delta. Sediment starvation is amplified by the likelihood of flow lofting (or reversed buoyancy) of the turbulent suspension cloud as density dips below that of the ambient fluid (Sparks *et al.* 1993; McLeod *et al.* 1999). Extreme examples of this process are beds with well developed inverse grading overlain directly by fines (Fig. 4.17B).

*4.5.1.4. Temporal and spatial evolution*

The temporal and spatial evolution of a hyperpycnal current on a flood-dominated delta can be defined simply in terms of a basinward- followed by a landward-shift in the main zones of erosion and deposition. As demonstrated in Figure 4.17, during waxing flow, the depositional zone progrades (coarsening upwards) and the zone of erosion moves seawards, so that areas that were initially depositional become erosional, and the flow reworks its own deposits. As the flood wanes, the site of maximum deposition moves landwards, resulting in a fining upwards, retrogradational motif. A similar temporal and spatial evolution of depositional processes dictated by the flood hydrograph have been inferred from modern fan-deltas (Prior and Bornhold 1990) and offshore from small mountain streams (Mulder *et al.* 1998, 2001). This relationship of forestepping and backstepping may also be extended to include the alluvial environment (Fig. 4.27). This figure highlights the evolution of the flood event in terms of flow efficiency, the ability of a flow to carry its sediment in a basinward direction (Richards *et al.* 1998). The earliest stage of flood sedimentation (A to T1, in (Fig. 4. 27) is dominated by highly efficient subaerial and submarine flows resulting in erosion and sediment bypass of the alluvial environment and delta plain, with significant deposition on the delta-front lobe (forestepping of the depositional zone). During or just after peak stage (T2), sediment concentration exceeds flow competence on the shallow gradient delta plain resulting in channel backfilling. This reduction in flow efficiency means little sediment escapes the delta plain, which becomes the new depositional zone. Higher slope gradient in the alluvial environment is sufficient to maintain a certain degree of sediment bypass. The final stage of deposition occurs almost exclusively in fluvial channels with only minor sedimentation in the submarine portions of the delta. This poorly efficient flow effectively starves the delta of sediment and deposition occurs principally out of suspension from surface plumes.

This interpretation of sediment dispersal on a flood-dominated fan-delta differs significantly from that proposed by Mutti *et al.* (1999, 2000) who preferred to model facies tracts on surge-like bipartite flows, similar to slump derived debris flows

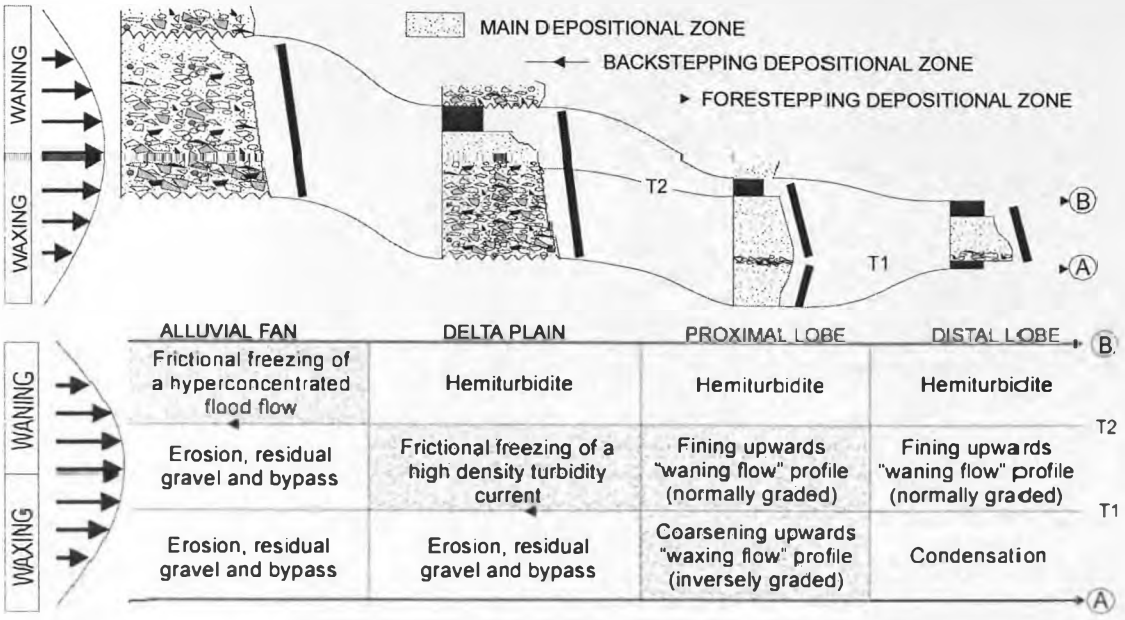



**Fig. 4.27.** Temporal and spatial changes in flow evolution during a discrete flood event. Diagram portrays this evolution as forestepping followed by backstepping of facies belts in response to waxing and waning flood discharge.

and HDTC common in deep marine systems. Although partially acknowledging a certain steadiness of flow behaviour, the model proposed by Mutti *et al.* (1999, 2000) relies almost entirely on an erosive head region to supply the density required for autosuspension. As the characteristics of hyperpycnal flows are dependent on the flood hydrograph (waxing followed by waning), the associated underflow must be quasi-steady, and the passage of the head region would thus occur very early in the flow evolution. Even with catchment basins situated in close proximity to basin margins, the time lag between storm and effluent discharge would still produce gradual waxing, and thus the early stages of hyperpycnal generation will be relatively dilute and essentially non-erosive, severely reducing the influence of the head on the long-term characteristics of the turbidity current (Mulder and Alexander 2001, Alexander and Mulder 2002). The main phase of bulking (erosion) must therefore occur during passage of the body (Alexander and Mulder 2002) which, if the flow is solely bipartite as advocated by Mutti *et al.* (1999, 2000), is floored by an essentially non-erosive (pseudo-laminar) bedload zone. For this reason, sediment transfer to the delta-front and beyond must have occurred prior to gravity transformation during a fully turbulent stage when erosion was unhindered and ignition could take place. This process, whereby turbidity currents prepare erosional pathways for inertia flows, has been documented on modern flood-dominated fan-deltas by Prior and Bornhold (1989, 1990).

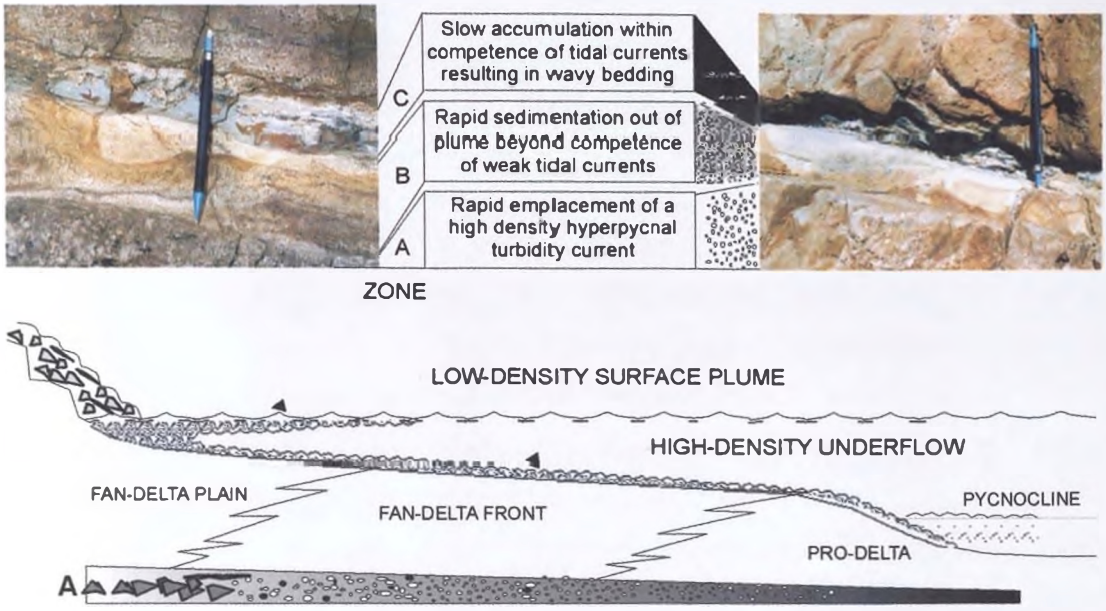
Instead of density stratified flows being the dominant mechanism of sediment dispersal as proposed by Mutti *et al.* (1999, 2000), the development of a bipartite structure is here considered to be the precursor to mass deposition and rapid channel backfilling, as it essentially cuts off the capabilities for ignition and replenishment of the over-riding turbulent suspension, leading to a reduction in tangential shear stresses and ultimately to frictional freezing of the inertia layer. This process is aided considerably by the low gradient slopes associated with shelf-type fan-deltas (Ethridge and Wescott 1984), as the shear stresses required to maintain grain resuspension are reliant entirely on those supplied by the turbulent overflow. According to Mutti *et al.* (1999, 2000), sediment dispersal in a density-stratified flow would occur principally in two phases. Initial deposition confined exclusively to the most proximal setting, will occur from a faster moving frontal inertia layer (or granular layer of Mutti *et al.* 1999). Upon frictional freezing this will be bypassed by a more dilute turbidity current, which then must account for the building of depositional lobes. It is doubtful that the coarsest particles would form the faster moving part of the flow, considering the very low gradients experienced on flood-dominated fan-delta fronts. Theoretical considerations by Hand (1997) suggest the opposite to be more likely on shallow gradients as the coarsest particles lag behind. The mechanism outlined by Mutti *et al.* (1999, 2000) resembles that deduced from field observations by Sohn *et al.* (1999) on *very steep* slopes of an alluvial fan where coarse particles *are* likely to attain sufficient momentum to form the frontal part of the flow. A further difficulty is whether a turbidity current unable to erode and thus attain self-sustainability when part of a bipartite flow, could be the transporting medium of the vast amounts of sand grade material over the distances defined by lobe distribution. The model proposed by Mutti *et al.* (1999, 2000) is not considered a likely mechanism for sedimentation from quasi-steady hyperpycnal turbidity currents based on the foregoing reasoning. Their use of transportational and depositional mechanisms obtained from studies on debris flows in high gradient alluvial fan environments may instead account for surge-type underflows generated by dam breaks and jökulhaups which do not follow the classic flood hydrograph (Mulder *et al.* 2003).

### 4.5.2. Hypopycnal surface plumes: formation and distribution of hemiturbidite

Without tidal channels to supply fine grained sediment to mudflats, and powerful storm events to resuspend and distribute sediment offshore, the origin and spatial extent of fines from the delta-plain to the outer shelf can be most adequately accounted for by flood-generated hypopycnal surface plumes (Fig. 4.1 and Facies

Tract 2 in Fig. 4.25) separated from sediment-laden overland flows during discharge into marine waters (Elliot 1986; Wright *et al.* 1986; Colella *et al.* 1987; Nemec 1995). The effect of the density contrast between salt water and complex bipartite subaerial flows on sediment dispersal in deltaic environments has been modelled experimentally by McLeod *et al.* (1999). Density stratified flows such as HFF undergo flow separation along pre-developed interfaces, where the particulate depleted turbulent cloud becomes a buoyant gravity current (hypopycnal plume), while the dense bedload develops rapidly into a negatively buoyant density current (hyperpycnal underflow). As the hypopycnal plume is directly related to the hyperpycnal underflow, and thus associated with 'event' sedimentation, the nature of suspension deposition would be expected to differ from hemipelagic background sedimentation commonly associated with open shelf dynamics. Due to the effects of bioturbation, ambient currents, and the erosive nature of event sedimentation, it is often difficult to extract any worthwhile information from fine-grained suspension deposits, so no criteria exist for the recognition of sediment emplaced by hypopycnal surface plumes. In the present study, the best evidence for this style of sedimentation is a strong non-uniformity in sedimentation rate, reflecting an early phase of rapid accumulation from a concentrated plume, which decreases over time, culminating in extreme condensation.

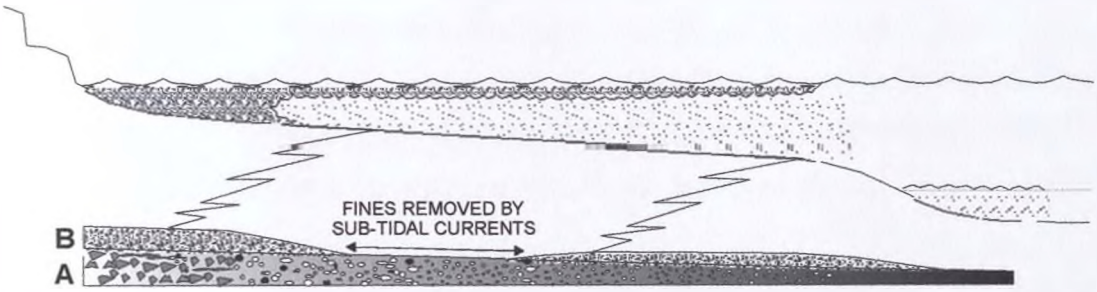
The rate of suspension sedimentation may be deduced from the presence or absence of sedimentary structures on the low energy delta-plain, and the degree of bioturbation on the delta-front. As demonstrated in Figure 4.28A, delta-plain and delta-front sedimentation may be divided into three components: (1) Component A reflects deposition from a dense hyperpycnal underflow, this is overlain by (2) a structureless graded siltstone (Component B), which is capped by (3) wavy and flaser bedded heterolithics on the delta-plain or an intensely bioturbated silty mudstone with carbonate concretions on the delta-front (Component C). A simple model has been developed to explain these characteristics (Fig. 4.28). As the stratified subaerial flood flows enters the basin, fines are separated out to form a hypopycnal surface plume, while the bedload plunges beneath the seawater to form a hyperpycnal turbidity current (McLeod *et al.* 1999), depositing Component A. Shortly after the flood event, the suspended concentrations in the surface plume are at maximum levels resulting in rapid deposition of the coarsest fraction to produce a graded siltstone (Component B). On the delta-plain, accumulation rates are greater than the competence of weak tidal currents, resulting in a structureless deposit (Fig. 4.28B). In a similar manner, rapid deposition on the delta-front must have been greater than the rate of biogenic mixing leading to a graded, partly bioturbated fabric



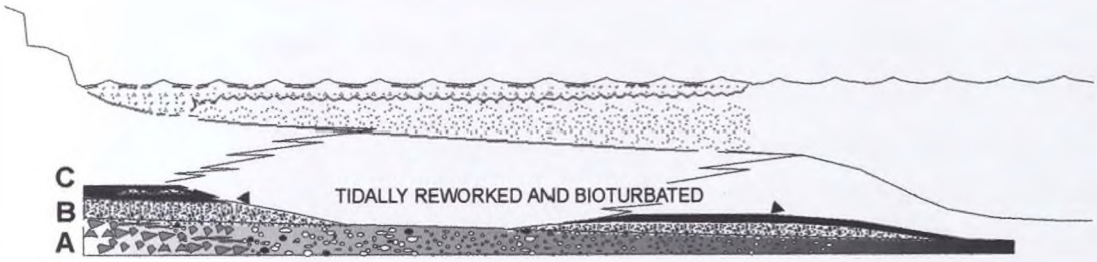




A. Flow separation of a hyperconcentrated flow into a high density hyperpycnal underflow and a hypopycnal surface plume




B. Rapid deposition out of suspension from a concentrated surface plume. High sedimentation rates result in the formation of massive sands and silts.




C. Slow sedimentation from a depleted surface plume. Accumulation rates are well within the competence of weak tidal currents and bioturbation resulting in wavy bedded silts above wave base and homogenised silts below.

**Fig. 4.28.** Mechanism for the formation of hemiturbidite through suspension sedimentation out of buoyant plume associated with a flooding event. See text for details. Both photographs are from the Newgale Formation at Newgale. Pen is 14 cm long.

(Droser and Bottjer 1986). The final stage (Component C), represents slow deposition of the finest fraction, well within the competence of weak tidal currents and biogenic mixing, resulting in wavy and flaser bedding on the delta plain and homogenized silty-mudstone on the delta-front (Fig. 4.27C). Early diagenetic carbonate concretions on the delta-front are testimony to prolonged periods of intense condensation (Raiswell 1987). The presence of sharp grain size breaks between the three components (Fig. 4.27A) also suggests that they formed during discrete phases of sedimentation, where processes across the grain size break may well have been very different (Gladstone and Sparks 2002).

Indirect evidence for flow separation includes the general lack of mud in the matrix of hyperpycnal turbidites and its presence particularly in the prodelta (Dorsey *et al.* 1995), and the high levels of silt in background sediments indicating separation of this fraction at the marine interface. As suspension sedimentation is directly related to flood events and turbidite emplacement, fine grained sediments are better referred to as hemiturbidite (*sensu* Stow and Wetzel 1990). Fine-grained accumulations similar to those described here, and implicitly related to flood events, have been described off the Washington and northern California coastlines (see review in Gorsline 1984), while anomalously thick divisions of hemipelagite between hyperpycnites in the Mediterranean (Mulder *et al.* 2001) originate from hypopycnal plumes.

### 4.5.3. Homopycnal plumes: cloud collapse or double diffusive convection

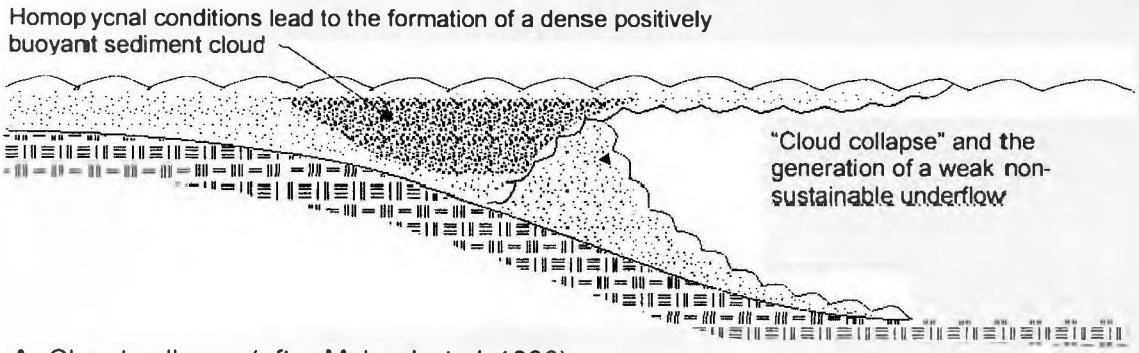
Although flood-dominated delta systems principally record efficient sediment dispersal through the generation of powerful and sustained quasi-steady hyperpycnal flows that have both the inertia and concentration to bypass the delta plain, the presence in the nearshore of thin, relatively fine grained, high and low-density turbidites suggests that not all flood events had sufficient concentration and inertia to expand the transfer zone as far as the delta-front (Fig. 4.5). Under a similar mechanism as that proposed for the modern Yellow River Delta by Wright *et al.* (1986), less catastrophic floods induce far weaker underflows that are incapable of significant erosion and channel incision, and are thus unlikely to replenish sediment lost through deposition and so maintain critical density (Pantin 1979). The reduction in basal shear stresses due to deceleration means that the current is not autosuspending and is unable to bypass the delta plain. The resultant deposit will be relatively thin, finer grained and restricted to nearshore settings (i.e. Facies B3).

Assuming that these thin turbidites are genetically related to HFF in a broadly similar manner to the highly efficient hyperpycnal flows that promote nearshore bypass, the effect of a less catastrophic flood event may be more accurately modelled not on direct hyperpycnal sediment dispersal, but rather conditions that approach a homopycnal regime (Fig. 4.1 and Facies Tract 3 in Fig. 4.25) (Mutti *et al.* 2000). In this sense, dispersal processes may have been similar to those acting on modern and ancient flood-dominated river-delta systems (Mutti *et al.* 2003) where sediment is trapped close to the river mouth (forming mouthbars) instead of escaping as hyperpycnal flows (forming shore-detached depositional lobes). At present there exist two mechanisms that may account for thin bedded fine-grained turbidites that do not attain sufficient inertia and density to autosuspend. McLeod *et al.* (1999) modelled a poorly stratified (low density) fluid entering standing water, which may approximate to a relatively dilute flood flow. Due to insignificant bedload most of the sediment load is stripped from the subaerial flow at the marine interface, resulting in three-dimensional mixing around this point and the formation of a positively buoyant cloud that engulfs the whole water column (Fig. 4.29A). As sediment is continually added during the flood event, density reaches a critical level and the cloud collapses, forming a relatively weak non-sustainable underflow (see McLeod *et al.* 1999, fig. 8).

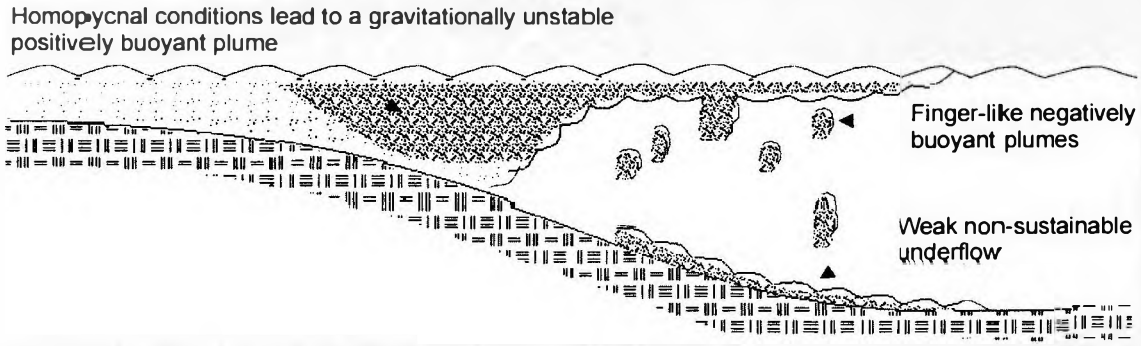
The second mechanism has been modelled experimentally by Parsons *et al.* (2001) and involves double diffusive convection (Hoyal *et al.* 1999a, 1999b), where finger-like negatively buoyant plumes detach from a gravitationally unstable concentrated layer in a developing surface plume (Fig. 4.29B). This form of 'settling convection' has been recorded by Kineke *et al.* (2000) from the mouth of the Sepik River, Papua New Guinea. Both of these mechanisms adequately account for the surge-type characteristics of Facies B3 (e.g. normal grading and lack of evidence for gradual aggradation) even though the input inducing the turbidity current is quasi-steady (flood discharge). A similar evolution of relatively low-density quasi-steady discharge into a surge-type flow has been produced experimentally by McCaffrey *et al.* (2003).

### 4.5.4. Mass emplacement and textural inversion

The final and subordinate facies tract is also the most inefficient at distributing sediment into the basin. Cohesionless debris flows are inferred to undergo a process of textural inversion as they actively invade hydroplastic 'reduced strength' muds of the delta plain, and rapidly develop into cohesive debris flows (Facies Tract 4 in (Fig. 4. 25). The extremely limited distribution and poor dispersal into the basin is primarily




A. Cloud collapse (after Mcleod *et al.* 1999)




B. Double diffusive convection (after Parsons *et al.* 2001)

**Fig. 4.29**. Mechanisms for homopycnal dispersion through positively buoyant plumes during flood discharge events. See text for details.

due to the mode of grain resuspension that characterises flows with significant cohesive matrix. As debris flows are maintained by gravitational forces and are thus reliant on basal shear stresses to maintain the grain dispersion, their propagation across the low gradient delta plain ultimately leads to rapid 'cohesive freezing' as the falling applied shear drops below the rising yield strength (Johnson 1970). The inefficiency of debris flows as sediment dispersal mechanism has also been documented on deep marine turbidite fans, even when slopes may be significant. Maar (1999) showed that the conversion of failure-related debris flows to turbidity currents is an inefficient process, which requires very large debris flows to produce relatively small turbidites. Prior and Bornhold (1990) observed relatively efficient dispersal from initial debris flows only on slopes in excess of 20°.

## 4.6. FAN-DELTA CLASSIFICATION BASED ON ALLUVIAL FEEDER SYSTEM AND FLOW EFFICIENCY

Fan-deltas (*sensu lato*) have been notoriously difficult to classify (Nemec 1990b) because of the huge variability in the alluvial feeder regime (see Postma 1990) and contrasting processes acting in the receiving basin (Orton 1988). The first step towards a classification scheme must involve the definition of a fan-delta which, as discussed above, relies entirely on the definition of an alluvial fan. Following the criteria set out by Blair and McPherson (1994), limiting alluvial fans to flood-generated and thus ephemeral sediment and fluid gravity flow processes effectively removes the confusion surrounding the distinction between a delta built by a braided fluvial system and a true fan-delta. Thus feeder systems B, C and D of Postma (1990) should, on the first tier of coarse-grained delta classification, be described in terms of a braidplain delta.

The main advantage of restricting fan-deltas to alluvial fans dominated by catastrophic flood related processes (i.e. the type A feeder system of Postma 1990) are that these processes should be readily identifiable in the subaqueous realm. It has long been appreciated that the gradient of the feeder system directly controls the nature of the fan-delta in terms of characteristic facies, facies distribution, overall geometry and the effect this has on basinal processes, particularly wave effectiveness (Dunne and Hempton 1984; Orton 1988). As an alluvial fan (*sensu stricto*) may be fluid gravity flow-dominated ('wet') or sediment gravity flow-dominated ('dry'), this distinction forms the basic subdivision of shelf-type fan deltas (Fig. 4.30). The likely characteristics of fan-deltas formed in response to these differing modes of sediment transfer in the feeder system may be obtained from the facies tracts previously discussed (Fig. 4.25). This study has demonstrated that fan-deltas fed by alluvial feeder systems dominated by fluid gravity flows develop an expanded transfer zone which not only includes the alluvial fan but also the delta plain, resulting in a broad shallow gradient profile of the nearshore and delta-front. The effect of widely distributed lobes many kilometres offshore is to severely attenuate wave processes resulting in a dissipative coastal regime, which allows for the preservation of the fan-delta as originally defined by flood related processes. In a global study of twenty flood-dominated fan-deltas ranging in age from Mesozoic to Pleistocene conducted by Mutti *et al.* (1996), not a single example demonstrated a high energy wave dominated nearshore. Similar low energy shoreline conditions have been reported from flood-dominated fan-deltas by Ballance (1988) and Dorsey *et al.* (1995).

Unlike highly sediment-charged fluid gravity flows, sediment gravity flows appear unable to generate self-sustaining hyperpycnal currents and are thus classified as inefficient distributors of sediment, as deposition occurs entirely on the

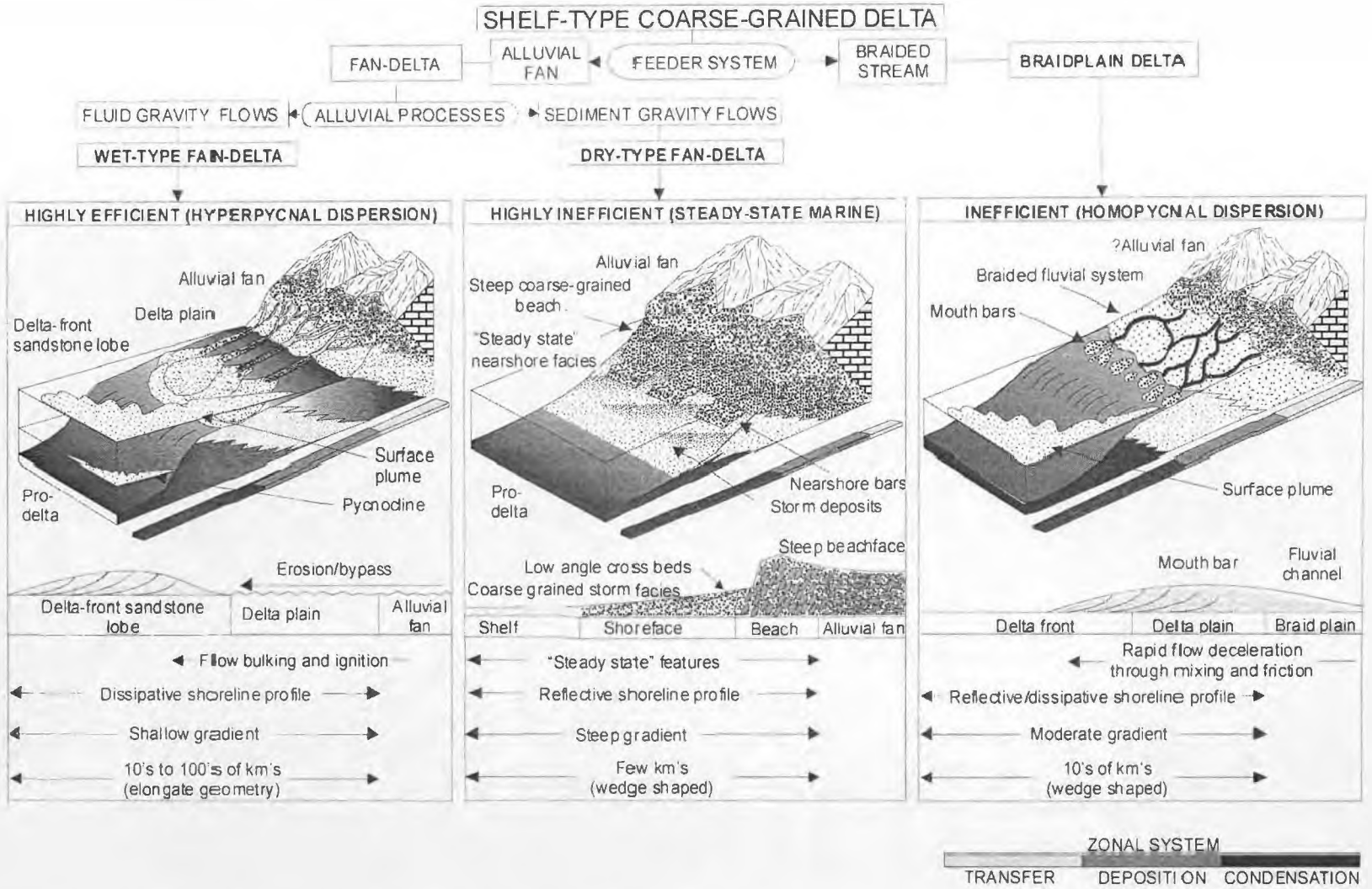



**Fig. 30.** Classification of fan-deltas based on flow efficiency (see text for details).

delta plain. Hypothetically, if cohesionless debris flows were the dominant mode of sediment transfer in the alluvial feeder system, the rapid deposition of coarse material in the nearshore would significantly affect the manner in which basin processes interact with fan-delta development (Orton 1988). This will be most simply manifested in a steep nearshore gradient developed and maintained by a wave reflective coastal regime. The result of strong nearshore circulation cells set-up through waves breaking directly on the shoreline, will be total reworking of sediment gravity flow characteristics into 'steady state' high energy marine components identical to those commonly recorded from wave dominated non-deltaic coastlines (Bardaji *et al.* 1990). Therefore, poorly efficient sediment gravity flow dominated fan-deltas should be relatively easily differentiated from highly efficient fluid gravity flow fan-deltas, both in their alluvial feeder system and the subaqueous portion. This linkage based on shared catastrophic emplacement mechanism allows for fan-delta classification and an appreciation of the alluvial system even when the feeder system is no longer exposed.

The use of flow efficiency as a tool in classification may also be extended to differentiate shelf-type fan-deltas from braidplain deltas, especially if the subaerial component is poorly exposed or removed by later erosion. The processes acting during Facies Tract 3 (Fig. 4.25) may closely approximate the sediment dispersal patterns commonly documented when braided fluvial systems enter a standing body of water. A feeder system associated with broad coastal plains, relatively shallow gradients, and a braided channel network must promote a very different mode of sediment dispersal at the marine interface (Mulder and Syvitski 1995). The ensuing reduction in fluvial inertia and sediment flux would, as outlined in Facies Tract 3, promote homopycnal and hypopycnal dispersal regimes (Fig. 4.1) and thus the main depositional zone is situated close to the sediment source. Instead of depositional lobes attached to subaqueous channels many kilometres offshore as documented by Martinsen (1990), Mutti *et al.* (2000) and this study, homopycnal flows build the nearshore equivalent, resulting in the development of mouth bars (Fig. 4.30). Mouth bars as inefficient analogues to depositional lobes reflect the inability of dilute flows without sufficient momentum to produce underflows that can undergo the important phase of turbidity current ignition and flow entrenchment on the delta plain. Highly efficient transfer zones with offshore lobes associated with alluvial fans (*sensu stricto*) have been recorded by Dabrio and Polo (1988), Prior and Bornhold (1988, 1989, 1990), Dorsey *et al.* (1995), Mastalerz (1995), McCallum and Robertson (1995), Mutti *et al.* (1996, 2000), Falk and Dorsey (1998), and Myrow *et al.* 2002, while inefficient transfer zones associated with mouth bars and a braided fluvial

system have been documented by Colmenero *et al.* (1988), Fernandez *et al.* (1988), Orton (1988) and Mutti *et al.* (1996, 2000).

This classification scheme, highlighting the fundamental control of flow efficiency on coarse-grained delta characteristics, must be treated as a preliminary step in the description and interpretation of fan-deltas. The examples quoted to support some of the conclusions are from systems dominated by either sediment gravity flows or fluid gravity flows. In reality, many alluvial feeder systems will operate under a combination of these processes (Blair and McPherson 1994) and therefore would be more likely to produce more complex geometries and facies distributions reflecting components of nearshore bypass as well as nearshore deposition (e.g. Rasmussen 2000). This can be demonstrated somewhat in the variability of facies tracts identified in the present study, although the complete dominance of HFF in the feeder system firmly places the studied system in the end member category of flood-dominated fan-deltas.

## 4.7. CONCLUSIONS

The characteristics of flood-dominated dispersal systems encapsulating facies distributions, sediment dispersal patterns, geometry and the response of basinal processes to coastal perturbations can only be truly acknowledged when the system, defined by zones of transfer, deposition and condensation is treated as a wholly dynamic integrated process-response system. Although a fairly routine concept in the description and interpretation of deep marine turbidite systems, the concept of flow efficiency when applied to deltaic systems essentially defines the location of the main zone of deposition basinward of the zone of transfer, and thus exerts the fundamental control on the location of sand bodies. In turn, this governs delta geometry and redistribution capabilities by ambient currents (Fig. 4.30).

Utilising these approaches to deltaic sedimentation may be of significant value to petroleum exploration, as detached lobate sand bodies of appreciable lateral extent offer a realistic reservoir target. Of further significance to play analysis is the likely tectonic regime promoting flood-dominated dispersal systems. Steep gradient transfer zones promoting high sediment flux situated close to basin margins are considered the main prerequisite for oceanic flooding episodes and the construction of subaqueous lobate sand bodies. The first response of the system particularly in pull-apart, rift and foreland basin-fill sequences to an episode of source rejuvenation is rapid flooding of alluvial and nearshore environments as the reaction rate of

systems to increased subsidence outstrips that of coarse clastic input associated with rejuvenated source area uplift (Blair and Bilodeau 1988). In-place flooding during transtensional tectonic regimes in the present study is manifested in thick lobe sequences blanketed by 4-12 m thick units of mudstone forming potentially effective topseals. As prodelta environments in flood-dominated systems are prone to density stratification, the lack of water column turnover below well augmented pycnoclines offer the potential for organic-rich charge systems to develop within the same depositional sequence as the potential reservoir and seal.

# APPENDIX A
# AMS IN DETRITAL SEDIMENTS

## A.1. METHODOLOGY

AMS can be defined as the intensity of magnetisation of a rock, where this intensity is a function of the direction of the applied field (Butler 1992) in accordance with the equation;

$$\underline{M} = K\underline{H}$$

where $\underline{M}$ is the acquired magnetisation, K is the susceptibility of the rock sample and $\underline{H}$ is the applied magnetic field. If a rock has a fabric related to either the orientation of grain shape or the crystallographic orientation, the susceptibility that arises will be anisotropic and is approximated by a symmetrical second-rank tensor (Hrouda 1982). This can be described as a triaxial ellipsoid with principle eigenvectors K1>K2>K3, representing the maximum ($k_{max}$), intermediate ($k_{int}$), and minimum ($k_{min}$) susceptibility axes respectively (Fig. 4.A1). Numerous parameters have been introduced both for the quantification of the magnitude of anisotropy, and for defining the shape of the ellipsoid (see table 1.1 in Tarling and Hrouda (1993) for a summery of parameters in general use). The scope of this study requires mean susceptibility ($k_{mean}$), and parameters H, F, L, u, and q (Table A1). $k_{mean}$ provides an approximation on the amount of material in the sample causing the magnetic signal. H is a measure of total anisotropy and thus fabric strength, and reflects the degree of preferred orientation of the magnetic mineral. The angle u on a magnetic lineation (L) versus foliation (F) plot (Fig. 4.A2) defines the shape of the susceptibility ellipsoid. A u angle <45° defines an oblate (disc shaped) fabric, while u = >45° is referred to as a prolate (cigar shaped) fabric. Foliation is the plane normal to the preferred direction of short axes (Kmin), while lineation corresponds to the preferred direction of long (or crystallographic) axis orientation, and represents the strength of $k_{max}$ in relation to $k_{int}$ within the plane of foliation. Parameter q is a ratio combining the three principle susceptibilities, and

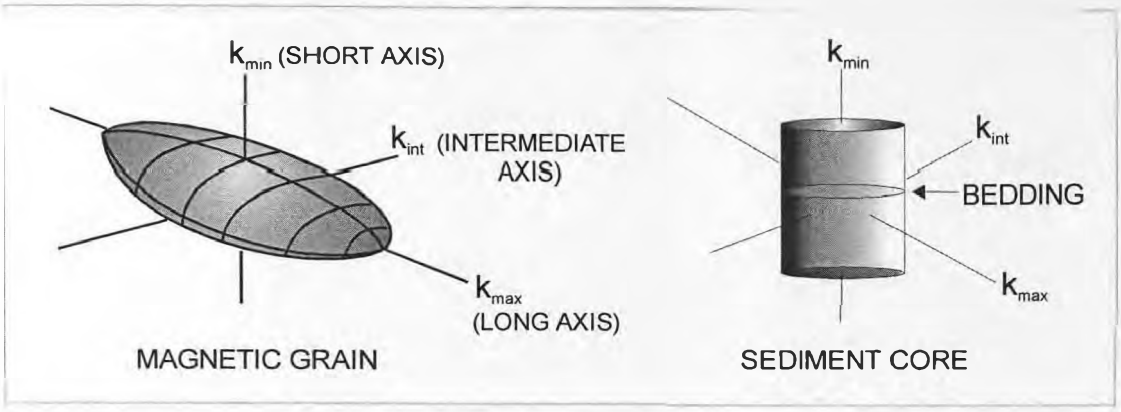



**Fig. A1.** Basic principle of magnetic susceptibility (see text for discussion). The relationship between the magnetic grain and the sedimentary core is also shown to aid visualization.

represents a ratio of linear to foliar elements in the magnetic fabric, and is thus a reflection of ellipsoid shape.

## A.2. PROPERTIES OF THE MAGNETIC FABRIC

Using the parameters listed in Table A1, a number of fabric tests have been developed based on the known grain response to flowing water under laboratory conditions (for a thorough review see Rees and Hamilton 1970). These conclusions, which are presented in column two in Table A2, define the characteristics of a depositional sedimentary fabric. Values outside of these experimental ranges usually imply mechanical rotation of grains associated with tectonic restructuring of the fabric (Parés *et al.* 1999). Additional characteristics of fluid flow alignment are a spread of $K_{max}$ orientations around the mean, and long or crystallographic alignment of axes that differ from local fold and cleavage trends.

Five sites were sampled for magnetic fabric analysis (Table A2), 3 from Facies D3 (49 subsamples), and 2 from Facies D4 (41 subsamples). To determine the petrofabric, block samples (one block per site) were orientated in the field by magnetic compass and drilled in the laboratory (Owens 1994). Specimens were measured on an AGICO KLY3 Kappabridge, and site means calculated (Jelinek 1978, Owens 2000). Specimen susceptibility axes are accurate to within 2° (95% limits), and are plotted on equal area lower hemisphere stereographs (Fig 20A) with the three principle axes presented in the manner specified by Ellwood *et al.* (1988).

| Parameter | Equation | Reference |
|---|---|---|
| Mean susceptibility ($k_{mean}$) | $k_{mean} = (k_{max} + k_{int} + k_{min})/3$ | Nagata (1961) |
| Total anisotropy (H) | $H = (k_{max} - k_{min})/k_{mean}$ | Owens (1974) |
| Magnetic foliation (F) | $F = (k_{int}/ k_{min})/k_{mean}$ | Stacey *et al.* (1960) |
| Magnetic lineation (L) | $L = (k_{max}/k_{int})/k_{mean}$ | Balsley and Buddington (1960) |
| Angle on an L/F graph (u) | $\mu = \tan^{-1} [(k_{max} - k_{int})/(k_{int} - k_{min})]$ | Jelinek (1981) |
| Shape factor (q) | $q = (k_{max} - k_{int})/[0.5(k_{max} + k_{int}) - k_{min}]$ | Granar (1958) |

**Table A1.** Parameters used in the study to define the magnetic anisotropy and fabric.

| Fabric test | Primary indicator | Reference | A1 | A2 | A3 | A4 | A5 |
|---|---|---|---|---|---|---|---|
| q | 0.06>q>0.7 | Hamilton and Rees (1970) | 0.11 | 0.36 | 0.18 | 0.21 | 0.09 |
| $k_{min}$ | <25° from vertical | Hamilton and Rees (1970) | 13 | 9 | 22 | 16 | 11 |
| L/F | u°<45° (oblate) | Owens (1974) | 14 | 24 | 22 | 18 | 9 |
| $K_{max}$ (dec) | N.A.T. 61° - 241° | Crimes and Oldershaw (1967) | 328-148 | 336-156 | 331-151 | 319-139 | 334-154 |
| H | >1 | Owens (2000) | 8.6 | 4.3 | 5.1 | 5.7 | 7.2 |

**Table A2.** Fabric tests that describe the response of grains to flowing water. Values clearly demonstrate that all samples upon which conclusions on palaeoflow are based appear to record only sedimentary characteristics, with no tectonically induced mechanical rotation. N.A.T. = not aligned to local stress field. The local cleavage direction is unpublished data from the first author, and approximates the regional Caledonian trend (Woodcock, 1984).

The susceptibility of all samples is inferred to be dominantly carried by paramagnetic phyllosilicates, in particular chlorite and muscovite. Although magnetite is often assumed to be the major contributor to the magnetic susceptibility (Hrouda 1982), no appreciable quantities have been detected in either thin section analysis or isothermal remnant magnetisation (IRM), a conclusion supported by very low bulk susceptibilities (typically 10-45 $x10^{-5}$ [SI]). Orientated thin sections demonstrate a clear alignment of large detrital chlorites and micas which according to Hounslow (1985) not only provide the susceptibility anisotropy but also significantly improve the likelihood of recovering a primary depositional fabric (Piper *et al.* 1996) as the mineral's crystallographic axis ($k_{max}$) align parallel to the long axis of quartz grains during diagenesis, a process that may destroy the less stable magnetite. Fabric tests that have a bearing on the critical assessment of the data set are presented as site means (e.g. A1, A2, etc) in Table A2. A more detailed breakdown of ellipsoidal

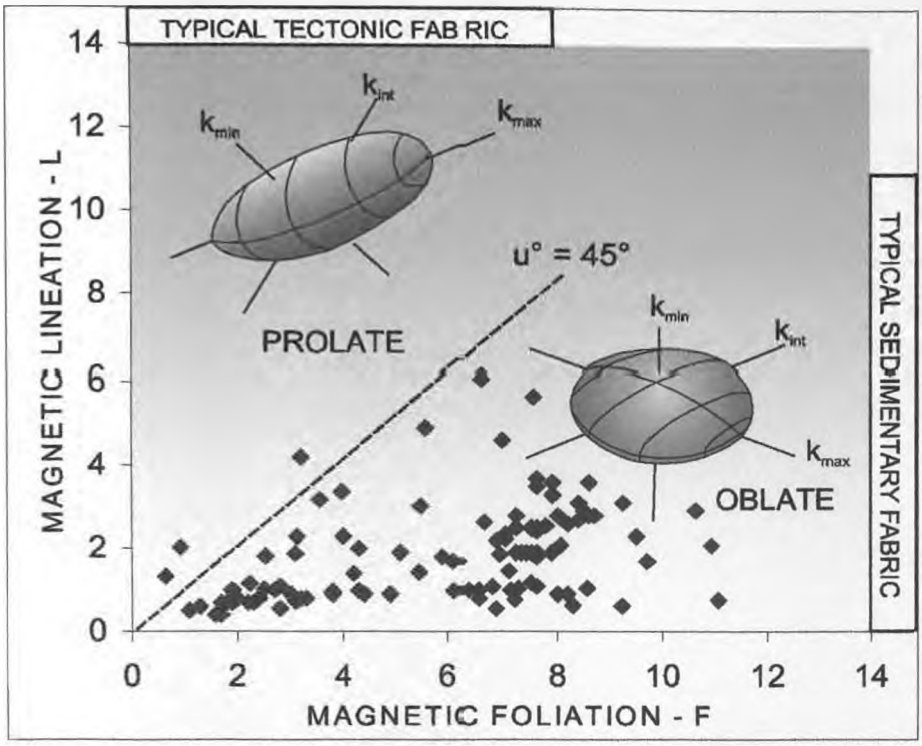



**Fig. A2.** Graphical illustration of the shape of AMS ellipsoids in an L/F-plot. Note that the shape parameter (angle u) describes the relative shape of the ellipsoids numerically. Results clearly record oblate ellipsoids, which form the typical fabric of laboratory deposited sediments (Rees and Hamilton 1970).

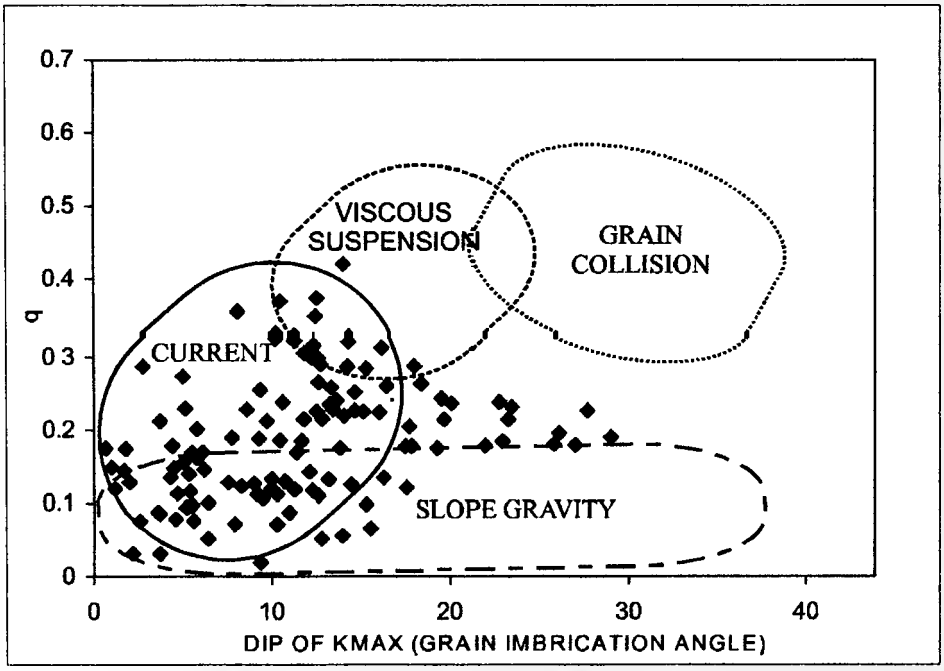



**Fig. A3.** q value vs $k_{max}$ imbrication angle plotted as means of determining the likely depositional process. Fields depict ranges obtained experimentally by Taira (1989). Low but perceptible imbrication values and low q indicate traction current deposition.

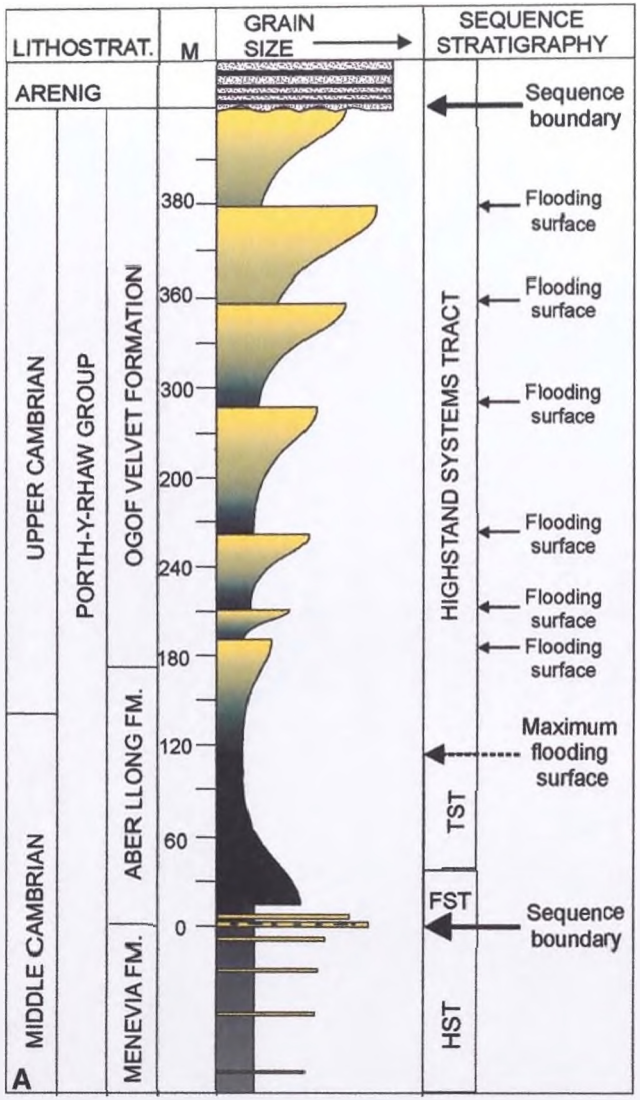
shape, in the form of an L/F diagram is presented in Figure 4.A2. Additionally, as advocated by Taira (1989), q has been plotted against the grain imbrication (inclination of $k_{max}$ axes) as a means of discriminating between the four main depositional processes responsible for three-dimensional alignment of grains in the sedimentary environment (Fig. 4.A3). Without exception, all the samples upon which conclusions on palaeoflow are based satisfy the criteria for a primary sedimentary fabric, and deposition appears largely to be under the influence of traction currents.

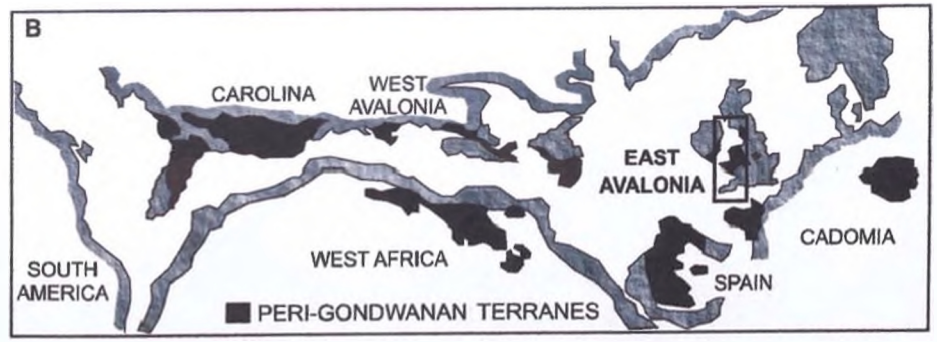
*CHAPTER 5*

# PROCESSES, DYNAMICS AND FACIES ON A MUDDY STORM-DOMINATED CAMBRIAN SHELF: NEW PERSPECTIVES ON THE BYPASS-ZONE TEMPESTITE MODEL

## 5.1. INTRODUCTION

Over the past two decades, intensive documentation of storm-dominated shelf systems from modern and ancient settings has provided a solid conceptual background and quantitative framework for understanding storm-flow dynamics. The refinement of tempestite models, where suits of sedimentary structures and palaeocurrent patterns are systematically integrated into a time-averaged force balance equation (essentially the interaction between pressure gradient, Coriolis, frictional, and excess weight forces), has led to a greater emphasis on process-based interpretations (Brenchley 1985; Craft and Bridges 1987; Leckie and Krystinik 1989; Duke 1990; Duke *et al.* 1991a; Winn Jr. 1991; Myrow 1992a; Brenchley *et al.* 1993, Jennette and Pryor 1993; McKie 1994; Midtgaard 1996; Myrow and Southard 1996; Bádenas and Aurell 2001). This new approach to a subject area that had become caught up in arguments between the relative merits of oceanographic and geological datasets is epitomised by the tempestite model proposed by Myrow and Southard (1996). There model highlights the potential multiplicity of storm-generated processes by considering the possibility of storm emplacement on ancient shelves under non-actualistic conditions, while critically maintaining firm grounding in plausible fluid dynamics and sediment transport processes. This approach is significant if we consider the *scale* of processes that must have operated on some ancient shelves to produce storm deposits that are many times thicker than their modern counterparts and appear more widely distributed across the shelf. As vertical and lateral stratification sequences in tempestites preserve a record of this changing force balance in both space and time, this simple four-part balance problem offers a powerful tool in the analysis of spatial and temporal variations in shelf dynamics (Myrow and Southard 1991).


LITHOSTRAT.
M
GRAIN SIZE
SEQUENCE STRATIGRAPHY
ARENIG
UPPER CAMBRIAN
MIDDLE CAMBRIAN
PORTH-Y-RHAW GROUP
OGOF VELVET FORMATION
ABER LLONG FM.
MENEVIA FM.
380
360
300
200
240
180
120
60
0
HIGHSTAND SYSTEMS TRACT
TST
FST
HST
Sequence boundary
Flooding surface
Flooding surface
Flooding surface
Flooding surface
Flooding surface
Flooding surface
Maximum flooding surface
Sequence boundary
A


B
CAROLINA
WEST AVALONIA
EAST AVALONIA
CADOMIA
SOUTH AMERICA
WEST AFRICA
SPAIN
PERI-GONDWANAN TERRANES

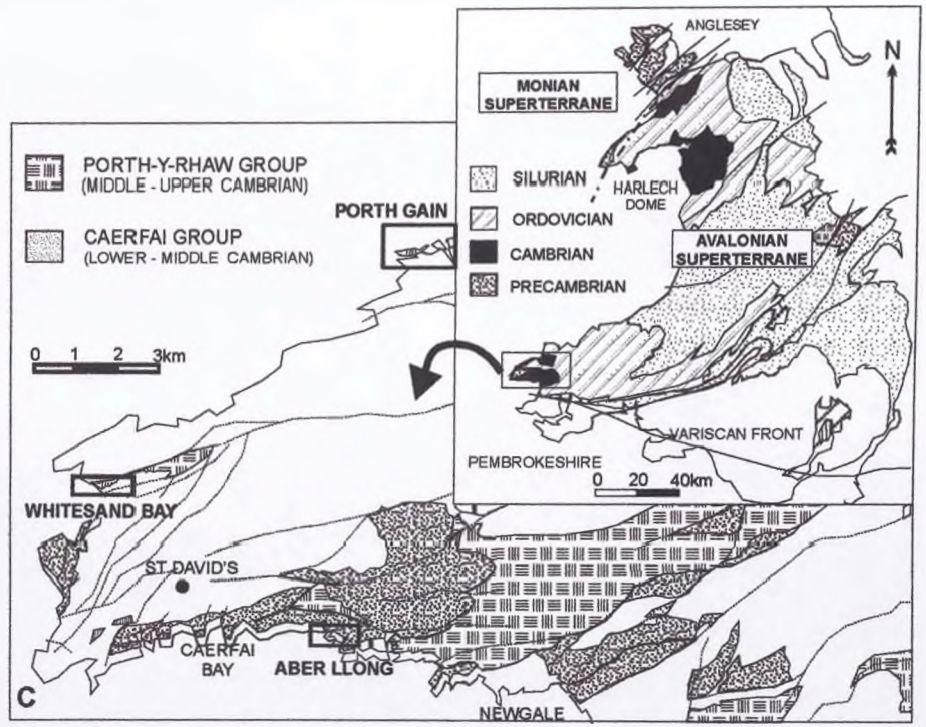

ANGLESEY
N
MONIAN SUPERTERRANE
PORTH-Y-RHAW GROUP
(MIDDLE - UPPER CAMBRIAN)
CAERFAI GROUP
(LOWER - MIDDLE CAMBRIAN)
SILURIAN
ORDOVICIAN
CAMBRIAN
PRECAMBRIAN
HARLECH DOME
PORTH GAIN
AVALONIAN SUPERTERRANE
0 1 2 3km
VARISCAN FRONT
PEMBROKESHIRE
0 20 40km
WHITESAND BAY
ST DAVID'S
CAERFAI BAY
ABER LLONG
NEWGALE
C

**Fig. 5.1.** (A) Stratigraphy of the upper part of the Porth-y-rhaw Group in SW Wales. (B) Early Mesozoic reconstruction of the North Atlantic showing location of Avalonia and related peri-Gondwanan terranes of the Neoproterozoic (modified after Nance and Murphy 1994). (C) Geological map of Wales (inset) and SW Pembrokeshire showing location of Cambrian outcrops discussed in the text.

This present investigation utilises a tempestite model devised by Myrow (1992a) to assess storm facies, processes, and dynamics on a fine-grained shelf with a muddy coastal zone. This so called "bypass-zone tempestite model", developed to account for rather unusual proximality trends recorded on fine-grained storm-dominated shelves, is a good example where a strictly uniformitarian approach is inadequate to account for the potential multiplicity of storm processes operating during the *geologically* significant storm event. Unlike facies models developed from sandy shorelines, the bypass-zone tempestite model records a shallow intertidal to subtidal zone dominated by fine-grained sediment deposited in a zone of sand bypass, where high velocity sediment-laden flows erode deep and narrow conduits (gutters) which funnel sand out onto the shelf. Time-averaged palaeocurrent indicators from the nearshore to mid-shelf are strongly aligned perpendicular to shore, suggesting the presence of unidirectional currents with a driving force balance heavily weighted towards high pressure gradient, frictional, and excess weight forces. This is in contrast to modern storm flows that are geostrophically balanced by the Coriolis Force on the inner shelf (Swift *et al.* 1987), resulting in shore oblique or shore parallel flow, and a force balance equation with low pressure gradient, minimal frictional resistance, and with an excess weight parameter considered by oceanographers to be insignificant (see discussion in Myrow and Southard 1996). The processes that lead to nearshore bypass of sand grade material through a muddy nearshore also promote expansion of the shallow water friction zone out onto the shelf, elevate storm-generated unidirectional currents, and produce proximality trends, vertical and later stratification sequences, and palaeocurrent patterns that differ significantly from those recorded on modern and some other ancient sandy shorelines.

Although the bypass-zone tempestite model represents a significant advancement in understanding storm sedimentation on fine-grained coastlines, the original investigation was, as the author acknowledged (Myrow 1992a, p. 113), incomplete. The only other studies that specifically refers to nearshore incision and sediment bypass are brief references in Kidwell (1989), Leckie *et al.* (1990), and McCormick and Grotzinger (1993), and a detailed account of gutter casts in the bypass-zone by Perez-Lopez (2001). The latter contribution is important, providing

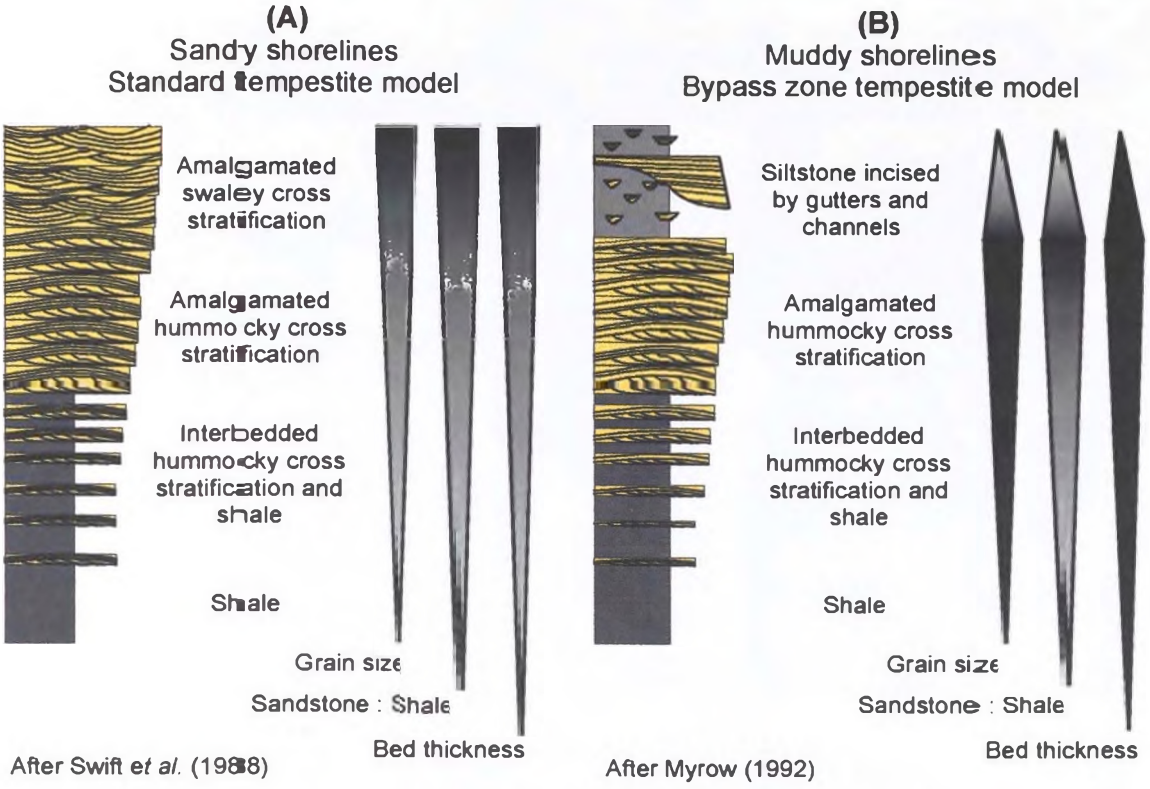



**Fig. 5.2.** Stratigraphic expression and proximality trends on prograding storm-dominated coastlines. (A) Standard tempestite model developed from sandy shorelines based on Swift *et al.* (1988). (B) Bypass-zone tempestite model recorded from a muddy coastal setting by Myrow (1992).

validation of the model and proximality trends on fine-grained carbonate platforms. Although nearshore incision and bypass are important processes on some storm affected coastlines, there are four simple fundamental questions that need to be addressed: (1) why does incision and bypass occur, (2) what are the processes involved, (3) why is it restricted to fine grained coastlines and (4), are these processes controlled by specific environmental constraints?

Well-exposed and non-bioturbated mudstones, siltstones, and fine sandstones of the Ogof Velvet Formation of SW Pembrokeshire (Fig. 5.1A and C) offer an excellent opportunity to further our understanding of bypass-zones on fine-grained storm-dominated coastlines. To fully address the questions posed above, and build up a step-by-step synthesis of processes, dynamics, and facies associated with bypass systems, the present investigation is divided into 4 sections. The first is an overview of the bypass-zone tempestite model and associated proximality trends, with a brief review of published examples to highlight recurring. This is followed by a detailed facies analysis of the Ogof Velvet Formation exposed at Whitesand Bay and Porth Gain (Fig. 5.1C), where salient attributes of the tempestite model and process

sedimentology are discussed. This understanding of basic component elements of the model leads into a synthesis of shelf dynamics, where conclusions on process sedimentology are integrated with detailed palaeocurrent analysis into a palaeohydraulic model for deposition on fine-grained storm-dominated coastlines. Because difficulties exist in discriminating between time-averaged palaeocurrent indicators and wave-induced peak instantaneous shear stresses (Duke 1990), palaeocurrent data from primary sedimentary structures are supplemented by measurements of grain fabric utilising the anisotropy of magnetic susceptibility (AMS). The final section addresses some of the broader aspects of the bypass-zone tempestite model by placing controls and processes into their wider environmental context.

## 5.2. TEMPESTITE MODEL: PROXIMALITY TRENDS AND PUBLISHED ACCOUNTS

Standard facies models for storm deposits mostly involve sandy shorelines, and incorporate proximality trends that typically show a seaward decrease in grain size, sandstone-shale ratio, and tempestite bed thickness, as sediment entrained in the nearshore is swept seawards by relaxation currents (Fig. 5.2A). The stratigraphic configuration of storm deposits from muddy shorelines often differs markedly: grain size, sandstone-shale ratio, and tempestite bed thickness actually decrease in the nearshore, which instead is characterized by a distinctive silt-dominated facies incised by sand-filled gutters cast, pot casts, and small channel fills (Fig. 5.2B). To account for these trends, particularly the inversely graded nearshore profile, the tempestite model outlined by Myrow (1992a) with some modifications by Pérez-López (2001) invokes a nearshore zone of sand bypass. The model for storm sedimentation based on a spatial reconstruction of lithofacies present in the Ogof Velvet Formation (Fig. 5.3) is an excellent example of this bypass system, where high-velocity sediment-laden flows erode gutters and channels that act as conduits for funnelling sand onto the inner shelf. Further offshore, distality trends are similar to those recorded from sandy shorelines and simply reflect progressive flow deceleration. This spatial distribution of facies therefore records zones of sediment bypass, deposition and relative condensation (Fig. 5.3).

In terms of a process-based analysis, the fundamental distinction between these two facies models is based on the relative balance between down-welling unidirectional currents and storm wave oscillatory motion in combined-flow. Most

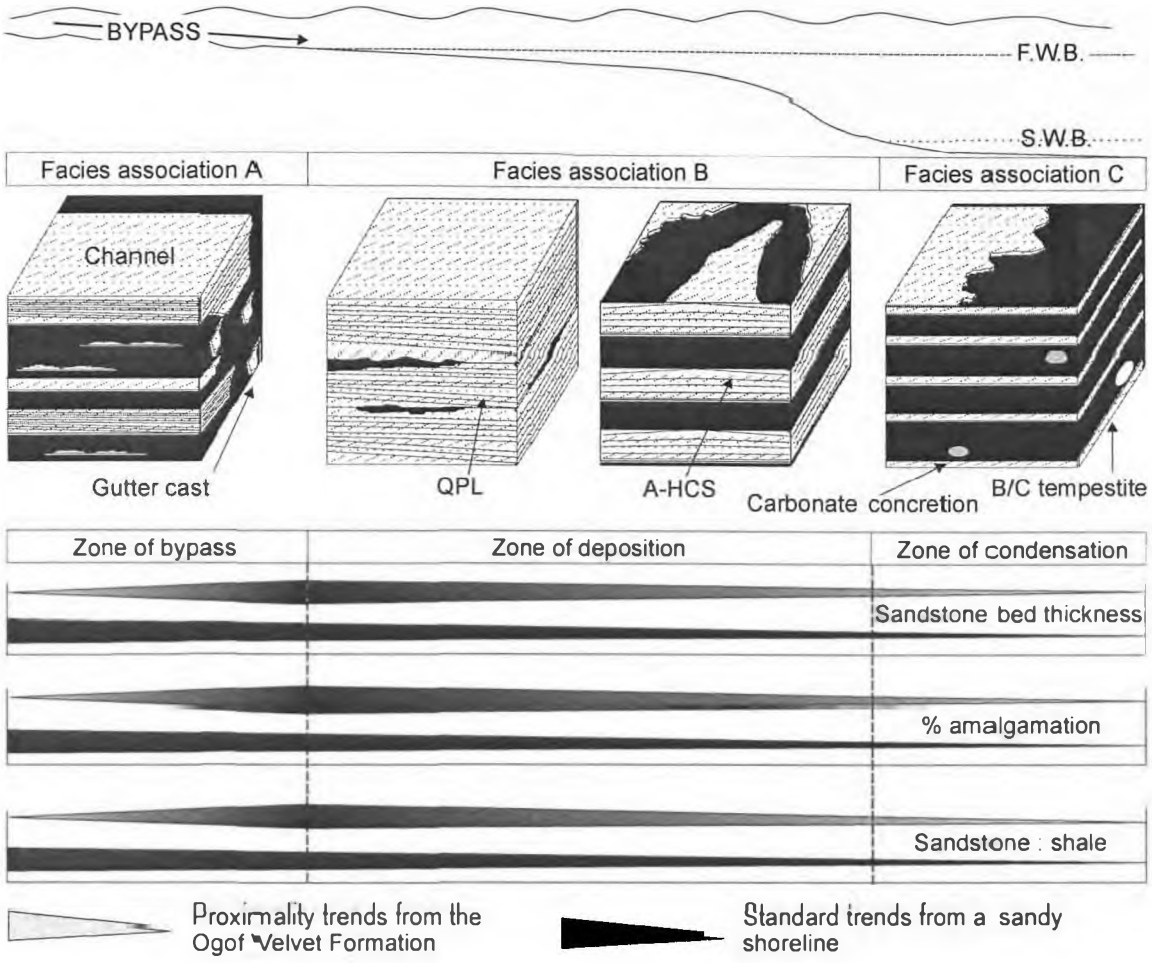



**Fig. 5.3.** Bypass-zone tempestite model and proximality trends for the Ogof Velvet Formation. For comparison, the same trends from a standard sandy storm-affected coastline (based on Swift *et al.* 1987) are also presented. The clear disparity in the nearshore between the standard trends and those from the Ogof Velvet Formation reflect bypass of sand grade material through nearshore conduits (gutters and channels) to form a high accumulation zone below fairweather wave base. The spatial distribution of facies indicates zones of bypass, deposition, and condensation (see also figs. 5.15 and 5.18) that are compatible with the bypass-zone tempestite model outlined by Myrow (1992).

recent investigations on storm hydrodynamics on sandy shorelines follow considerations offered by Duke (1990) and Duke *et al.* (1991a), and invoke oscillatory-dominant combined-flows and a weak geostrophically balanced unidirectional component. However, incision of channels and gutters on shorelines in the bypass-zone tempestite model demand unidirectional currents of significant velocity to erode and scour the nearshore. Elevated unidirectional currents in unidirectional-dominant combined-flows may also account for the dominantly offshore-directed time-averaged palaeoflow patterns recorded on shelves experiencing nearshore bypass (Myrow 1992a; 1992b; Pérez-López 2001; this study Fig. 5.12A). Weak flows with small driving forces (pressure gradient and excess

weight force) have a small friction force relative to the Coriolis force, while strong flows with large driving force have friction greatly exceeding Coriolis force (Duke 1990). Weaker currents therefore tend to be shore parallel, as experienced on most modern shelves, while stronger flows are directed at high angles to shore (Myrow and Southard 1996).

As elevated unidirectional currents appear to be the key process behind the bypass-zone tempestite model, to adequately address the questions posed in the introduction, it is necessary to understand why storms on fine-grained coastlines generate unidirectional-dominant combined-flows. Although the case study on the Ogof Velvet Formation is particularly aimed at resolving this issue, it is possible to gain a foundation for interpretation by referring to the considerable literature on fine-grained storm-dominated coastlines that experience incision. Selected examples are illustrated in Table 5.1. It is critical to define how the term "bypass" is used in here. Mutti *et al.* (1999, p 40) wrote, "Almost everybody would agree that "lobe" means deposition and therefore a bed characterised by some lateral extent. The concept of "channel" is more difficult to define. Most sedimentologists would relate the term to erosion and therefore to a convex-downward geometry of a deposit; fewer would think in terms of sediment bypass or transfer zones". All of the studies presented in Table 5.1 record nearshore incision, but only a handful were treated as sediment bypass-zones, so their applicability as examples of the bypass-zone tempestite model is not immediately obvious.

Published accounts of incision and bypass, which span the Precambrian to recent, have a number of key features in common (Table 5.1). These include bypass-zones restricted to: (1) locations affected by tidal currents, (2) accommodation-limited periods (early transgressive and late highstand systems tracts), (3) highly dissipative shorelines with high wave attenuation and low nearshore orbital velocities, and (3) extensive, very low gradient platforms developed at the mouths of very fine-grained rivers, and on carbonate platforms. The last trend is possibly the most significant as the gradient of the depositional surface in essence dictates: (1) the response of the shoreline to incoming waves, defining either dissipative or reflective behaviour, (2) controls the width and energy regimes of the intertidal zone, and (3) is a primary constraint on water depth and shelf width, thus governing available accommodation space. We can therefore hypothesize, based solely on published examples, that the bypass-zone tempestite model operates under unidirectional-dominant combined-flows, and that these intensified and highly erosive currents are promoted in settings where tidal currents are significant, nearshore wave energy attenuated, and

| Example | Storm type | Incision | Water depth | Wave energy | Systems tract | Platform | Reference |
|---|---|---|---|---|---|---|---|
| Mackenzie Delta Beaufort Sea | Winter | Gutters | 3m | Low | E - TST | Mackenzie Delta | Hill *et al.* (2001) |
| East Texas Coast, Gulf of Mexico | Winter and hurricane | Channels | Subtidal | Low | E - TST | Transgressed delta | Siringan and Anderson (1994) |
| Tibjak Beach, Beaufort Sea | Winter | Channels | Subtidal | Low | E - TST | Mackenzie Delta | Hequette and Hill (1993) |
| Cretaceous Moosebar Fm, Alberta | Winter | Channels | Shoreface | Moderate | E - TST | Transgressed delta | Taylor and Walker (1984) |
| Cretaceous Kootenai Fm, Montana | Winter | Channels | Intertidal/ subtidal | Low | E - TST | Carbonate | James (1979) |
| Jurassic Sundance Fm Wyoming | Winter | Channels | Intertidal/ subtidal | Moderate | M/L - HST | ? | Brenner and Davis (1973) |
| Jurassic Loriguilla Fm, Spain | Winter and hurricane | Channels | Mid ramp | Low | M/L - HST | Carbonate | Badenas and Aurell (2001) |
| Triassic Majanillos Fm, Southern Spain | hurricane | Gutters | Intertidal | Low | E - TST | Carbonate | Perez-Lopez (2001) |
| Triassic Durrenstein Fm, Italy | hurricane | Channels | Intertidal | Low | M/L - HST | Carbonate | Galli (1989) |
| Permian Brotherton Fm, England | hurricane | Channels | Peritidal | Moderate | M/L - HST | Carbonate | McKie (1993) |
| Silurian Whirlpool Sandstone, Ontario | Winter and hurricane | Channels | Subtidal | Low | E - TST | Transgressed delta | Cheel and Middleton (1993) |
| Silurian Medina Fm, New York State | Winter and hurricane | Channels | Subtidal | Moderate | M/L - HST | ? | Duke *et al.* (1991) |
| Cambrian Chapel Island Fm, Newfoundland | Winter | Gutters | Subtidal | Low | E - TST | Fine-grained delta | Myrow (1992) |
| Proterozoic Burnside Fm, Canada | Winter | Gutters | Subtidal | Low | M/L - HST | Sandy delta | McCormick and Grotzinger (1993) |

**Table 5.1.** Selected published examples of storm-dominated, tide-influenced coastlines where shore normal gutter casts and channels dissect the nearshore. All of these examples are from fine-grained, low-energy coastlines. For an extensive list of further examples see Cacchione *et al.* (1984).

accommodation space limited over broad areas. These relationships, as well as the wider significance of the bypass-zones, are explored below.

## 5.3. LITHOFACIES OF THE OGOF VELVET FORMATION

### 5.3.1. Facies Association A: siltstone dominated nearshore

#### *5.3.1.1. Facies A1: description*

Facies A1 comprises alternating millimetre to centimetre thick, very well sorted and mineralogically mature siltstones, very fine sandstones and silty mudstones. Two sub-facies occur. The most abundant bedding style is rapidly alternating rippled siltstones and silty mudstones of roughly equal proportions (Fig. 5.4B). Quartzose siltstones are predominantly cross-laminated, wavy to lenticular bedded, with asymmetrical or more rarely symmetrical ripple marked tops and internal flasers. These bedding geometries closely resemble the classic wavy and lenticular bedding described by Reineck and Wunderlich (1968). Convex lower surfaces beneath the thickest ripple forms reflect loading on a low strength, possibly hydroplastic substrate. Asymmetrical ripple profiles display cross-stratification that dips predominantly to the northeast, roughly perpendicular and offshore with respect to the palaeoshoreline (Fig. 5.12A). Opposing dip directions to the SE occur sporadically. A rare but significant ripple profile includes forms with flat crests that appear to have been planed off after the bedform had been created. Small-scale reactivation surfaces are demonstrated by cross-laminated foresets dipping at slightly different angles broken by sub-millimetre muddy flasers, suggesting interruption in the steady advance of the migrating ripple.

The second sub-facies is characterised by laterally persistent, normally graded, erosively based and locally scoured, thin to very thinly bedded fine sandstones, which occur intermittently throughout Facies A1 (SD in Fig. 5.4B). These thicker and coarser beds tend to protrude from this generally silt-dominated facies and are thus easily recognizable in outcrop. Basal surfaces are commonly loaded, and often display small scour features resembling flute casts. Internal stratification is

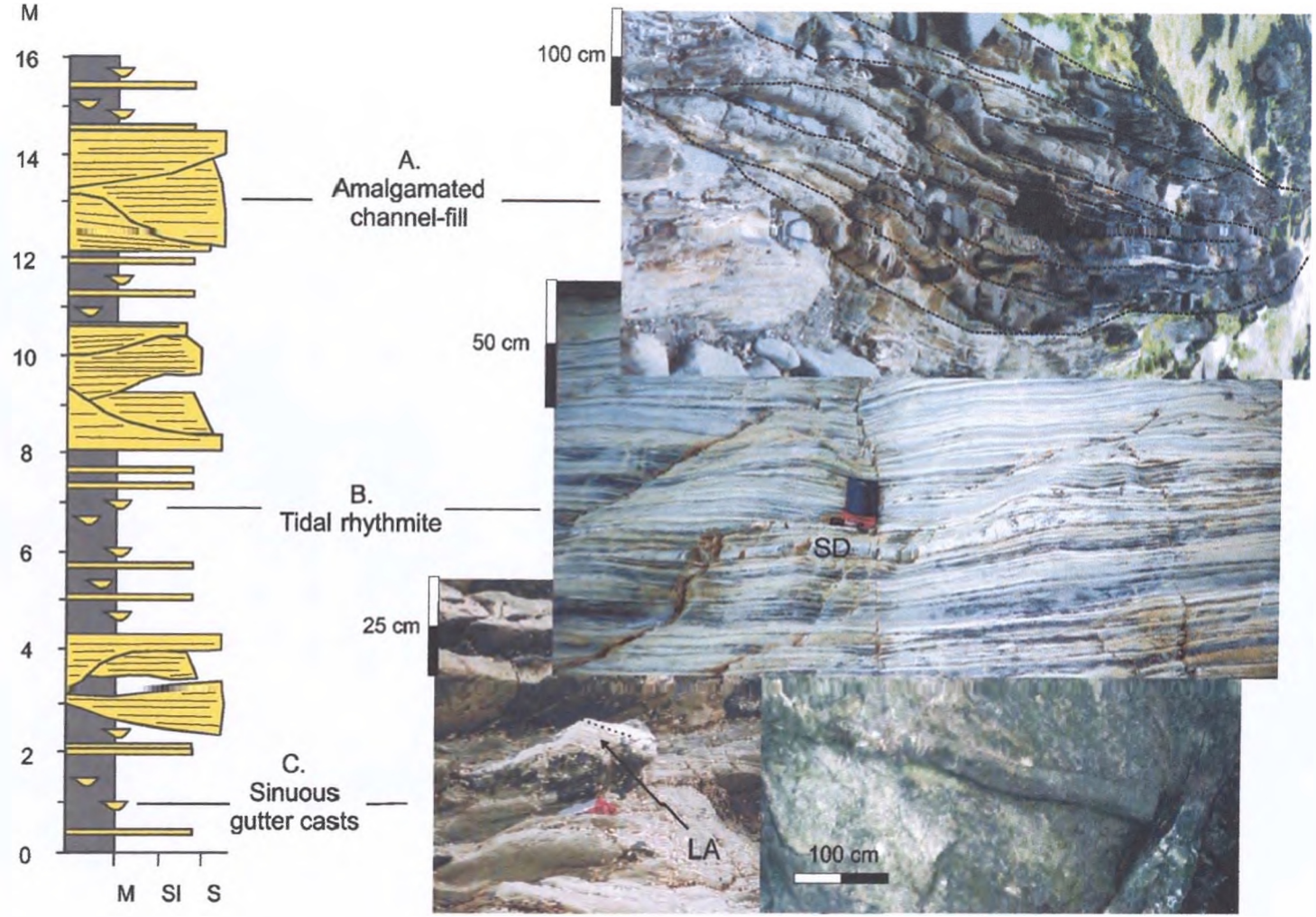



**Fig. 5.4.** Characteristic features of Facies Association A sediments. (A) Facies A3 (Whitesand Bay) – composite channel fill incised into tidally influenced deposits of Facies A1. (B) Facies A1 (Whitesand Bay) – rhythmically alternating wavy and lenticular beds interpreted as tidal deposits, punctuated by randomly distributed, thicker storm deposits (SD). (C) Facies A2 (Porth Gain) – sinuous gutter casts displaying over-steepened margins and lateral accretion (LA). A similarity in general morphology to river channels suggests incision by secondary helical flow vortices.

extremely difficult to identify due to weathering, but beds appear crudely planar laminated at the base, passing upwards into ripple cross-lamination. Upper surfaces can be gradational into wavy beds or sharp, and moulded into wave-generated vortex ripples or interference ripples

*5.3.1.2. Facies A1: interpretation*

The origin of wavy and lenticular bedding was discussed by Reineck and Wunderlich (1968) and Visser (1980). Both are thought to reflect small-scale alternations in slack water and current agitated conditions. The juxtaposition of sediments with these contrasting depositional energetics at a frequency demonstrated in Fig. 5.4B suggests emplacement under the modulating effects of tidal currents (Reineck and Singh 1973). This is further substantiated by reactivation surfaces, bimodal cross-lamination and mudstone drapes on ripple foresets which indicate, by analogy with modern examples (Evens 1965; Yoa and Risk 1981), that deposition occurred in a zone of short term fluctuations in sea level, where bedforms migrated episodically under the control of base level fluctuations in a time-velocity asymmetric current (Visser 1980). The lack of herringbone cross-stratification and the total dominance of northeast-directed flows suggest a strongly ebb-dominated tidal cycle. Symmetrical ripples indicate the presence of wave-generated oscillatory currents, while flat-topped ripples reflect deposition in very shallow to possibly emergent settings (Klein 1977). Shallow water conditions are also inferred from the localised presence of interference ripples.

In contrast to the predictable bedding sequences outlined above, the thin laterally persistent fine sandstones record rapid deposition from episodic high energy events that record waning flow characteristics (grading) and both a unidirectional (flute casts and parallel lamination) and oscillatory (wave ripples and symmetrical scours) flow component. Very similar bedding characteristics randomly distributed within wavy and lenticular beds have been recorded following storm events on tidal flats in the Bay of Fundy (Yoa and Risk 1981), the Yangtze River Delta (Xu *et al.* 1989) and the Mackenzie River Delta (Hill *et al.* 2001). Gradational upper surfaces are a characteristic of both Facies A1 storm deposits and modern examples, and reflect partial redistribution of storm-emplaced sediments by tidal currents. The preservation of delicate mud-draped ripple foresets in wavy and lenticular beds, as well as parallel lamination in some storm deposits, reflects relatively low energy fair-weather waves (Xu *et al.* 1989), even in this nearshore setting.

Although a tidal influence can be clearly demonstrated, the exact environment of deposition is somewhat problematic. The wavy and lenticular bedding were previously interpreted (Turner 1977) as reflecting deposition on an intertidal flat (his rhythmite facies). Although sediments of Facies A1 resemble recent tidal flat deposits described by Reineck (1975) from the German North Sea Bight, the lack of tidal channels conflicts with this interpretation. Absence of tidal channels, desiccation cracks and abundance of load structures on both tidally deposited and storm emplaced beds has also been recorded from other Cambrian "tidal flat" sequences (Hiscott 1984). These environments display many of the characteristics of the shore-attached muddy banks and extensive subaqueous platforms associated with large, fine-grained river deltas such as the Mississippi (Louisiana coast), Amazon and Orinoco (Surinam coast), Yellow River (Gulf of Bohai) and the Mackenzie Delta (Beaufort coast) (Wells and Coleman 1981; Wang 1983; Hill *et al.* 2002). Deposition of silt and clay in these non-barred wave-influenced nearshore settings is in response to extremely high sediment supply and rapid accumulation rates (McCave 1971). Fair-weather wave attenuation is a common feature, which induces estuarine-type circulation, where the net movement of sediment in suspension is principally onshore, and fines are trapped by the littoral energy fence (Wells and Coleman 1981). This fence is broken only during large storms (shoreface bypassing), when sediment escapes onto the shelf (Swift and Thorn 1991).

*5.3.1.3.Facies A2: description*

Facies A2 consists of small sand-filled erosive features incised into wavy and lenticular beds of Facies A1 (Fig. 5.4C). In plan view, these linear scours are clearly gutter casts (Whitaker 1973; Myrow 1992b). Cross sections range from 4–23 cm across, 2–11 cm deep and casts are a minimum of 4 m long. Cross-sectional geometry is extremely varied and ranges from asymmetrical to symmetrical, with walls ranging from steep and overhanging to shallow and scallop-like. In plan view, gutters may be straight or highly sinuous. The infill is composed exclusively of coarse silt which may be massive, parallel laminated or rarely cross-laminated perpendicular to the gutter long axis (Fig. 5.4C). This style of cross-lamination is restricted to asymmetrical cross sectional profiles and appears to record a form of lateral accretion, presumably developed on a meander bend. Upper surfaces are commonly gradational into wavy and lenticular bedding suggesting at least partial redistribution of sediment by tidal processes. A common feature of gutter casts that appears absent from Facies A2 is the proliferation of bounce and prod marks. This is to be

expected from an environment devoid of bioclastic material, and one where the substrate appears to have low shear strength, thus reducing the likelihood of tools within the flow. The long axis orientation of gutter casts is shown in Fig. 5.12A and records incision by currents flowing roughly perpendicular to the shoreline. This relationship is consistent with most published examples of gutter orientation (Myrow 1992b; Pérez-López 2001).

*5.3.1.4. Facies A2: interpretation*

Although gutter casts have been reported from a wide range of environments, including fluvial (Rust and Gibling 1990), lacustrine (Daley 1968) and submarine fans (Whitaker 1973), most published examples occur on shallow marine storm-affected shelves, and appear particularly abundant in intertidal (Flood 1981; Perez-Lopez 2001), subtidal (Myrow 1992a; Galli 1989) and inner shelf (Chakraborty 1995) environments. There is no broad consensus on the hydrodynamic conditions under which gutter casts are cut and filled but, considering their wide ranging environmental distribution, their origin is probably polygenetic, involving either purely oscillatory flows (Chakraborty 1995), purely unidirectional flows (Myrow 1992b) or a wide range of combined-flows (Aigner 1985). Formative processes commonly invoked include geostrophically balanced barometric gradient currents (Chakraborty 1995), storm waves (Aigner 1985), tidal currents (Flood 1981) and combined gradient currents/ebb tidal currents (Bridges 1973; Leithold and Bourgouis 1984).

The orientation of gutter casts normal to the shoreline in Facies A2 precludes formation by geostrophically-balanced gradient currents, while the steep, often undercut margins are difficult to reconcile with wave processes. Geometries more closely resemble gutters reported from intertidal and subtidal settings by Bridges (1973), Myrow (1992b) and Perez-Lopez (2001). A spiralling pattern of tool marks on cast bases has led to the suggestion that they were formed by secondary flow patterns of longitudinal helical flows developed at the base of storm-generated unidirectional currents directed parallel to the long axis of the gutter. Due to the lack of tool marks on the gutters of Facies A2, this process cannot be confirmed, but similarities in plan geometry between gutters and meandering rivers suggests the spiralling action of helicoidal flow as scaled down versions of those measured on modern river meander bends (Sundbourg 1956). As pointed out by Myrow (1992b), straight gutter casts may simply record higher velocity flows capable of cutting through meander bends.

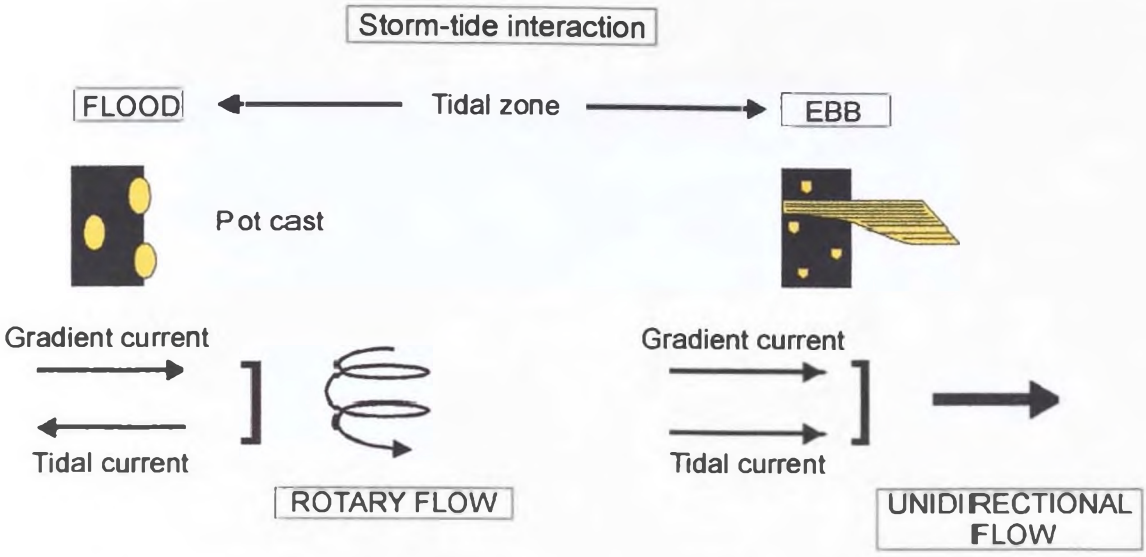



**Fig. 5.5.** Mechanism for the formation of pot and gutter casts through storm-tide interaction based on characteristics of Facies A2. See text for details

A storm origin is consistent both with the evidence of rapid cut and fill, inferred from the likely instability of undercut margins in a low strength substrate (see Facies A1), as well as the preserved record of both unidirectional and oscillatory components in what appears to be a strongly unidirectional-dominant combined-flow. Although not discussed in the detailed review of gutter casts by Myrow (1992b), the presence of a superimposed tidal cyclicity on a storm-generated combined-flow may be crucial to the formation of many gutter casts, particularly as most examples where gutter casts are abundant are reportedly incised into fair-weather sediments clearly deposited under the influence of tidal processes (see Table 5.1). The effects of tides on offshore-directed gradient currents has received little attention (Rossetti 1997), but this interaction during storm conditions may explain the distribution of gutter casts in the bypass-zone tempestite model (Fig. 5.3). In studies by Myrow (1992a) and Pérez-López (2001), abundant gutters were restricted to locations affected by tidal processes, and were shown to rapidly terminate basinward of fair-weather wave base, below which tempestites were deposited. It is therefore conceivable that storm-generated unidirectional currents were enhanced by ebb currents (Bridges 1973; Leithold and Bourgeois 1984; Rossetti 1997) leading to nearshore erosion (Rossetti 1997) and ultimately sediment bypass (Fig. 5.5). Conversely, the effect of flood tides would be expected to dampen storm-generated offshore flows, and may result in a complex "interacting" flow (Fig. 5.5). The common association of pot casts with gutter casts reported both by Myrow (1992b) and Pérez-López (2001) may reflect the interaction of flood tides and relaxation currents. As suggested by Perez-Lopez

(2001), the complex vertical rotary flow required for the formation of pot casts (Alexander 1932; Myrow 1992b) appears to develop through the interaction of two opposing currents, here considered to be relaxation and flood tidal currents. Although no palaeocurrent data for tidal cyclicity were presented by Pérez-López (2001), Myrow (1992a) documented a slight dominance of flood tides, coinciding with abundant pot casts in the tidal zone. This contrasts with the present study where a very strongly ebb-dominant tidal cycle is demonstrated, with no evidence for pot cast formation. A modern equivalent of this gutter cast facies may be the fine grained coastline of the Florida Keys (Bahia Honda Key), which is also tidally influenced, storm affected, and dissected by gutter casts orientated perpendicular to a fine grained shoreline (A. Perez-Lopez, pers. comm. 2003).

*5.3.1.5 Facies A3: description*

This consists of intensely amalgamated fine- to medium-grained sandstones that form lenticular bodies encased in wavy bedded siltstones of Facies A1 (Fig. 5.4A). In cross section, sandstones units are clearly composite channel-fills, composed of up to 18 individual depositional events. These sandstone bodies are easily recognizable due to their limited lateral extent and consistently sharp, commonly concave-upward erosional basal contacts and planar upper surfaces. Good exposures in steeply dipping strata at Whitesand Bay commonly demonstrate a ridge and platform topography (Fig. 5.4A) due to differential weathering of silt (host sediment) and sand (channel bodies). Composite units rarely exceed 10 m across (typically 5-7 m), with depths of 0.9–2.1 m. Channel margins may be smooth and symmetrical, but are more commonly uneven and slightly asymmetrical, with steep and overhanging walls. Internal amalgamation surfaces in particular may be deeply scoured. Small-scale erosional features resembling flute casts are relatively common on surfaces exposed at Porth Gain. Thin mudstone partings traceable over distances between 0.1-1.3 m often define internal amalgamation surfaces. A detailed field sketch of one of the channelized units is presented in Figure 5.6. Note the lack of any consistent trend in bed thickness, and the apparent widening of the channel during successive erosional events. This often leads to stepwise and uneven channel geometry. There appears to be no clear trend in channel distribution throughout the facies association, except a slight increase in abundance towards the inferred surface of maximum regression in each individual parasequence.

Individual beds vary in thickness between 11 and 85 cm, and are variably graded, commonly passing upwards from medium to very fine sand. Internal

stratification is dominated by parallel lamination typified by subtle yet readily recognizable undulations that display all the characteristics outlined by Arnott (1993) for quasi-planar lamination (QPL). Important features include a pinch and swell morphology in accordance with positive and negative topographic variations, and downlapping of the lowermost laminae onto the lower first order erosion surface. Arnott (1993) noted a consistent parallelism between flute cast orientation and the direction of downlap, with both recording offshore flow at high angles to the inferred shoreline. A similar trend is recorded here (Fig. 5.12A). A small percentage of quasi-planar laminated beds are overlain by hummocky lamination. This hummocky division commonly commences with a second-order erosion surface (Dott and Bourgeois 1982), which forms a mantle for concordant laminae. A characteristic feature of this flat bed drape is thickening of laminae from domal highs into troughs, resulting in gradual filling of the depression and almost planar lamination. Repeated scour and drape with several internal second-order surfaces produces the characteristic morphology and geometry that defines scour and drape hummocky cross-stratification (SD-HCS) as originally described by Dott and Bourgeois (1982). Wave formed vortex, asymmetrical and interference ripples are only occasionally recorded due to low preservation potential. Convolute lamination is a conspicuous feature throughout the facies (Turner 1977).

*5.3.1.6. Facies A3: interpretation*

The lenticular nature of Facies A3, which is clearly incised into tidally influenced sediments of Facies A1 led Turner (1977) to suggest a tidal channel origin for the amalgamated sandstone beds, which formed the basis for an intertidal flat interpretation for the Ogof Velvet Formation. Although the modulating effect of tidal processes cannot be completely discounted, as their effect on host sediment characteristics (Facies A1) implies their existence during channel formation, most of the channel-fill features are not compatible with deposition from cyclic semi-permanent currents. For instance, the lack of well defined lateral accretion surfaces is problematic: it is widely accepted that pre-Devonian tidal flats sequences are dominated by sand sheet channel elements, not steeply incised geometries with well defined channel margins (Fedo and Cooper 1990; Tirsgaard 1993). Even modern tidal channels, which benefit from increased channel stability afforded by the binding effects of vegetation, have migration rates commonly between 30 and 100 m a year (Luden 1934). Reineck and Singh (1958) calculated that 58% of a North Sea tidal flat had been reworked by rapidly migrating channels in just 68 years. The tidal geometry

described here suggests cut and fill *events* rather than long-term migration and progressive accretion in meandering channel systems. The steep and overhanging margins imply rapid deposition of the fill following the formation of the scour, as it is unlikely that vertical scour walls could exist at the sediment-water interface for extended periods of time (Goldring and Aigner 1982), especially considering the highly fluidised nature of the host sediment. The lack of slumped margins typical of semi-permanent channels also argues against a purely tidal origin (Yeo and Risk 1981). Although short-lived tidal scours appear to be rare in tidally influenced nearshore settings, Sarker *et al.* (1991) reported parabolic incisions from intertidal sediments of the Bay of Bengal that may have similar cross-sectional geometries to those described here. Although size and spacing are similar, the lack of a tidally influenced fill, particularly mud draped foresets, reactivation surfaces, bi-directional trough cross beds and thick-thin bundles, probably eliminates any primary control on formation by reversing tidal currents.

Instead, well defined grading, and stratification sequences recording upper flow regime planar, and quasi-planar lamination to lower flow regime structures such as HCS, cross-bedding and ripples, record deposition from waning flow events in both unidirectional flows (flute casts, Myrow and Southard 1996), strong unidirectional-dominant combined-flows (QPL, Arnott and Southard 1990) and rarely oscillatory-dominant combined-flows (?HCS and symmetrical scours, Rossetti 1997). These features are more consistent with deposition from storm-generated combined-flows with a particularly strong unidirectional component (Galli 1989; Arnott 1993; Rossetti 1997). As modelled by Arnott and Southard (1990), the presence of a significant unidirectional current limits the variability of stratification sequences expected from combined-flow processes, thus accounting for the dominance in channel-fill sequences of QPL. The presence of convolute lamination suggests rapid vertical expulsion of pore water through loosely compacted sand, indicating rapid deposition and high initial porosity (Lowe 1975).

Sand filled channels shallowly incised across the nearshore and inner shelf perpendicular to the coastline are a common feature of some fine-grained coastlines (Table 5.1). The most common interpretation for most occurrences (and all in Table 5.1) involves locally intensified offshore-driven bottom currents associated with storm induced coastal down-welling (Swift *et al.* 1985). In a similar manner to the formation of gutter casts in Facies A2, channel morphology is apparently controlled by the geometry of helical secondary flow circulation caused by variations in bed shear stresses (Swift and Ludwick 1976; Flood 1981; Galli 1989). The development of large scale helical flow as opposed to small-scale patterns associated with gutter casts is

probably a function of storm intensity, as large-scale helical motion can only develop when the bottom boundary layer is well mixed (Flood 1981). During less catastrophic storm events, stable layers develop within the water column, forming a lid that limits the vertical extent of helical circulation (Flood 1981), and thus linear scours are confined to small-scale geometries such as gutter casts.

An important but slightly unusual feature of the channel fills is their clear multi-event history, suggesting that storm-generated currents preferentially returned to the same location (Fig. 5.4A). This style of channel fill occurs in a number of ancient fine-grained, nearshore storm-affected sequences, for example, the Devonian Baggy Beds Formation of Devon (M. Stokes, pers. comm.) and the Upper Cambrian Maentwrog Formation of North Wales (J. Crossley, pers comm.). Examples from the literature include scour features described by Flood (1981), Leithold and Bourgeois (1984) and Cheel and Middleton (1993). Possible causal factors include the increased likelihood of eroding poorly consolidated channel fill sediment (Leithold and Bourgeois 1984), or the preferential remobilisation of the coarser grained and thus more highly erosive (previously deposited) channel-fill (Flood 1981). This process may have responsible for channel widening during successive events as displayed in Figure 5.6. An additional and possibly critical factor is the effect of partly filled depressions on the helical flow circulation, which could conceivably act as loci for the initiation of successive current vortices. This may also account for amalgamated gutter casts recorded from other nearshore storm sequences (e.g. Myrow 1992b; Chakraborty 1995; Perez-Lopez 2001).

It is clear from the channelized geometry and internal stratification sequences that unidirectional currents were significant factors in the development of Facies A3, while oscillatory currents appear to be subordinate (as envisaged from the characteristics of Facies A1 and the patchy development of HCS) in what appears to be a unidirectional-dominant combined-flows. Although a storm-generated combined-flow increases in both unidirectional and oscillatory components with proximity to the shoreline, it appears that most storm influenced shelves develop unidirectional-dominant combined-flows only when approaching storm wave base (due to exponential decay with depth of the oscillatory component), and thus nearshore areas are often strongly oscillatory-dominant (Swift and Nummedal 1987). But it is also apparent that along certain storm-affected coastlines unidirectional currents must become highly significant and locally intensified to erode the linear depressions described (Table 5.1). In a similar manner to the formation of gutter casts in Facies A2, many modern and ancient examples of large-scale storm incision into the nearshore may be associated with the superimposition and enhancement of down-

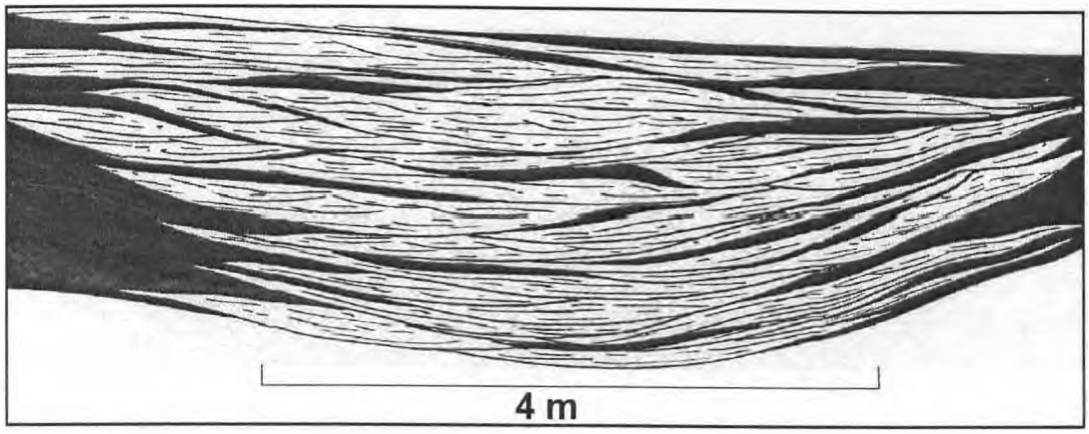



**Fig. 5.6.** Detailed field sketch of the amalgamated channel complex displayed in Fig. 5.4A. Note the general channel widening with accretion to the left over successive storm events.

welling unidirectional flow by ebb tidal currents. Table 5.1 documents some known occurrences where storm-tide interaction may have led to the development of nearshore channels. Brenner and Davies (1973, p 1689) discussed "the flushing of surge channels during storms" when tidal currents are superimposed on storm activity, while Leithold and Bourgeois (1984) recorded stratification sequences within tempestites that display features of both unidirectional amplification and retardation associated with tidal cyclicity. Channels filled with a complex array of combined-flow cross-stratification were interpreted by Rossetti (1997, p 317) to form from "storm enhanced tidal flows [that] caused the downward erosion of the mid-upper shoreface, and promoted the development of large scours".

*5.3.1.7. Summary*

The salient characteristics of Facies Association A represent a classic example of nearshore bypass on a fine-grained, wave dissipative shoreline (Fig. 5.3), under a hydrodynamic regime dominated by locally intensified storm-generated unidirectional currents. A mechanism has been proposed that accounts both for the amplification of unidirectional currents and the formation of linear scours, and the peculiar association of pot casts with bypass-zones (Fig. 5.5). The preferential incision of larger-scale channels over gutter casts represents a slight deviation from the original model outlined by Myrow (1992a). These broader helicoidal flows developed in well-mixed bottom boundary layers, also appear to dominate other bypass-zones (Table 5.1), and may simply reflect more intense storms affecting the coastline.

### 5.3.2. Facies association B: sandstone dominated inner to mid-shelf

#### *5.3.2.1. Facies B1: description*

The most abundant facies of the Ogof Velvet Formation, Facies B1, forms sheet-like amalgamated units of fine to medium grained sandstones up to 8 m thick, composed of individual beds ranging from 8-63 cm (Fig. 5.7A). In fully developed progradational parasequences, amalgamated sandstone units pass upwards into the siltstone dominated nearshore facies association, and downwards into interbedded sandstones and shales of Facies B2. Because of amalgamation, it is extremely difficult to recognise first order bounding surfaces except where relict lenses of silty mudstone are present between beds. Basal contacts are invariably sharp but, except for a few shallow scours, are generally planar. Flute casts are common, while gutter casts have been recorded from the thickest medium-grained beds.

Internal stratification is dominated by QPL; where over 80% of the beds conform to the ideal tripartite sub-divisions outlined by Arnott (1993). This simple idealized sequence consists of downlapping QPL above a planar erosion surface and below a thin veneer of 2D and 3D ripples. Simple 2D geometries are wave-formed vortex ripples. Irregular 3D crests with form-discordant lamination and lee slopes less than the angle of repose are possibly combined-flow ripples (Fig. 5.8B). Downlap and flute cast orientation are presented in Fig. 5.12A and display a similar parallelism and high angle offshore trend as the quasi-planar laminated sandstones of Facies A3. The uppermost parts of roughly 20% of beds are similar to beds described by Dyson (1996), where QPL is erosively overlain by SD-HCS (Fig. 5.7C). These rare second-order erosion surfaces are identical to those recorded in Facies A3.

#### *5.3.2.2. Facies B1: interpretation*

Based on the position of quasi-planar laminated sandstones in well defined progradational sequences (Arnott 1993; Dyson 1996), and a strong correspondence with high energy combined-flow configurations produced experimentally (Arnott and Southard 1990), this rather unusual style of stratification, has, in a similar manner to HCS, become synonymous with storm depositional processes (Arnott 1993). Amalgamation of sandstone beds is commonly associated with high intensity storm episodes in a proximal setting close to fair-weather wave base (Dott and Bourgeois 1982), a conclusion substantiated by the position of Facies B1 below tidally

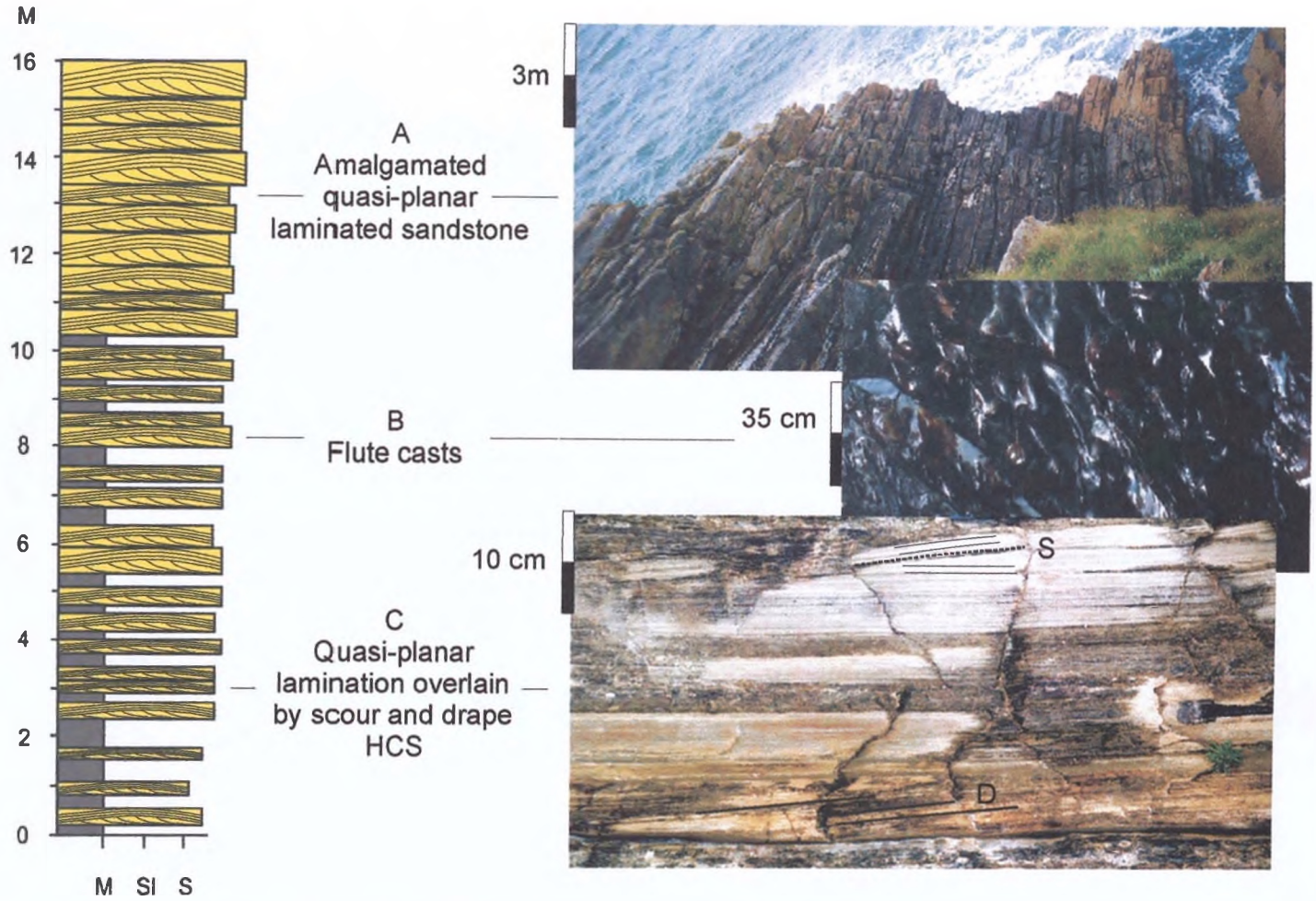



**Fig. 5.7.** Sedimentological features of Facies Association B sediments. (A). Facies B1 (Porth Gain) – coarsening and bed thickening upwards sequence (younging to the left) of amalgamated quasi-planar laminated sandstones. (B) Facies B1 (Porth Gain) – clustered flute casts on the base of a quasi-planar laminated sandstone. (C). Facies B1 (Porth Gain) – gently undulating quasi-planar lamination with distinctive downlapping laminae (D). Note the conspicuous hummocky second order erosion surface (S), which forms a mantle for concordant lamination (scour and drape HCS).

influenced sediments of Facies Association A. Although QPL represents the most abundant form of stratification in the Ogof Velvet Formation, its occurrence in the ancient record appears restricted, with only a handful of other examples known (e.g. de Raaf *et al.* 1977; Kreisa 1981; Arnott 1993; Dyson 1996; Midtgaard 1996; Rossetti *et al.* 2000), although modern occurrences have been documented (e.g. Greenwood and Sherman 1986). This suggests that the conditions necessary for its formation are for some reason unusual in storm depositional systems. This is highlighted by the apparent inverse correlation between HCS and QPL, where the latter, if present, tends to dominate the succession at the expense of other more common stratification styles, particularly those associated with stable bedforms (Arnott 1993).

A study of bed configurations under a wide range of combined-flows by Arnott and Southard (1990) produced QPL when a significant, but not necessarily high unidirectional component was added to oscillatory flow in what was described as a high energy combined-flow. The shallow but perceptible topographic relief developed in areas that were once stable hummocks. With the addition of a moderate unidirectional component to the combined-flow, 3D bedforms developed significant downstream asymmetry (possible anisotropic HCS). Higher unidirectional velocities led to bedform washout, leaving only a gentle quasi-planar morphology that was stable over the highest unidirectional velocities attainable in the flume (R. Arnott pers. comm. 2003). Therefore, irrespective of the strength of the oscillatory component, the presence of significant unidirectional flow limits the variability of stratification sequences expected from combined-flow processes, as the preservation potential of large 3D bedforms is severely reduced. Although hummocky bedforms are unstable even under combined-flow with a relatively low unidirectional component, quasi-planar downlapping onto first order erosion surfaces may record the leading edge of an offshore migrating sand-sheet (Arnott 1993), or in the case of Facies A3, a low angle in-channel bar. The parallelism between flute cast and quasi-planar downlap orientation reflects migration under the influence of powerful unidirectional currents (Myrow and Southard 1996). The sporadic occurrence of gutter casts suggests that these unidirectional currents sometimes developed a secondary helical flow during intense substrate scour.

The record of temporal variation in flow regimes during a single storm event is documented in the vertical stratification sequence (Myrow and Southard 1991). The tripartite subdivision of the idealized and most commonly recorded bed-type represents simple waning of a unidirectional-dominant combined-flow (Arnott 1993). The lack of large-scale bedform configurations is testament to persistent unidirectional currents throughout deposition. A relatively small number of beds

record an upper division of HCS. The significance of this 3D hummocky bedform in terms of temporal flow evolution is entirely dependent on the form of HCS developed. Accretionary forms (Fig. 5.8A) involve the growth of a *depositional* hummock and can therefore be modelled as a stationary or laterally accreting bedform, and integrated within a framework of experimentally produced bed configurations (i.e. as large symmetrical and asymmetrical 3D ripples, Arnott and Southard 1990, and Southard *et al.* 1990). These would form isotropic and anisotropic HCS respectively, and are typical of purely oscillatory or very oscillatory-dominant combined-flow regimes (Duke *et al.* 1991a). This style of HCS is extremely rare in the Ogof Velvet Formation due to elevated unidirectional currents. Although not abundant, the most common style of HCS is the scour and drape variety, where the antiformal and synformal configuration is inherited from the form of second-order erosion surfaces that mimic the morphology of stable bedforms (Cheel and Leckie 1993). This style of HCS is the type most commonly recorded in ancient successions (Duke *et al.* 1991a). Individual laminae have more in common with plain bed depositional regimes than either oscillatory or unidirectional bedforms, and cannot be modelled in terms of bed configurations produced experimentally. Consequently, the transition from quasi-planar laminated intervals into SD-HCS need not imply waning flow, and more importantly does not require a very oscillatory-dominant combined-flow with a low unidirectional component.

The constraints on HCS formation e.g. low unidirectional flow, and the problems associated with these constraints (see Myrow and Southard 1996 for discussion) only apply to the far more limited A-HCS. The supposed "unified concept of storm sedimentation" proposed by Duke *et al.* (1991a) has been widely accepted by the sedimentological community, and is commonly referenced to account for the formation of all forms of HCS. However, Duke *et al.* relied heavily on conclusions gathered from flume experiments (e.g. Arnott and Southard 1990), and the model is thus only strictly applicable to HCS generated by bedform growth, as Duke *et al.* acknowledged. The rarity of A-HCS in the stratigraphic record suggests that this unified concept is the exception rather than the rule, and that only rarely does the shelf experience purely oscillatory or very oscillatory-dominant combined-flow. Without the restriction on unidirectional flow velocity imposed by assuming the existence of stable bedforms, the greater thickness of ancient storm beds relative to modern examples and the wider distribution of sand across the shelf no longer appear problematic. A combined-flow with a significant unidirectional component is also more consistent with recent measurements of unidirectional current velocity on modern shelves (Hill *et al.* 2003). The transition from QPL to SD-HCS does

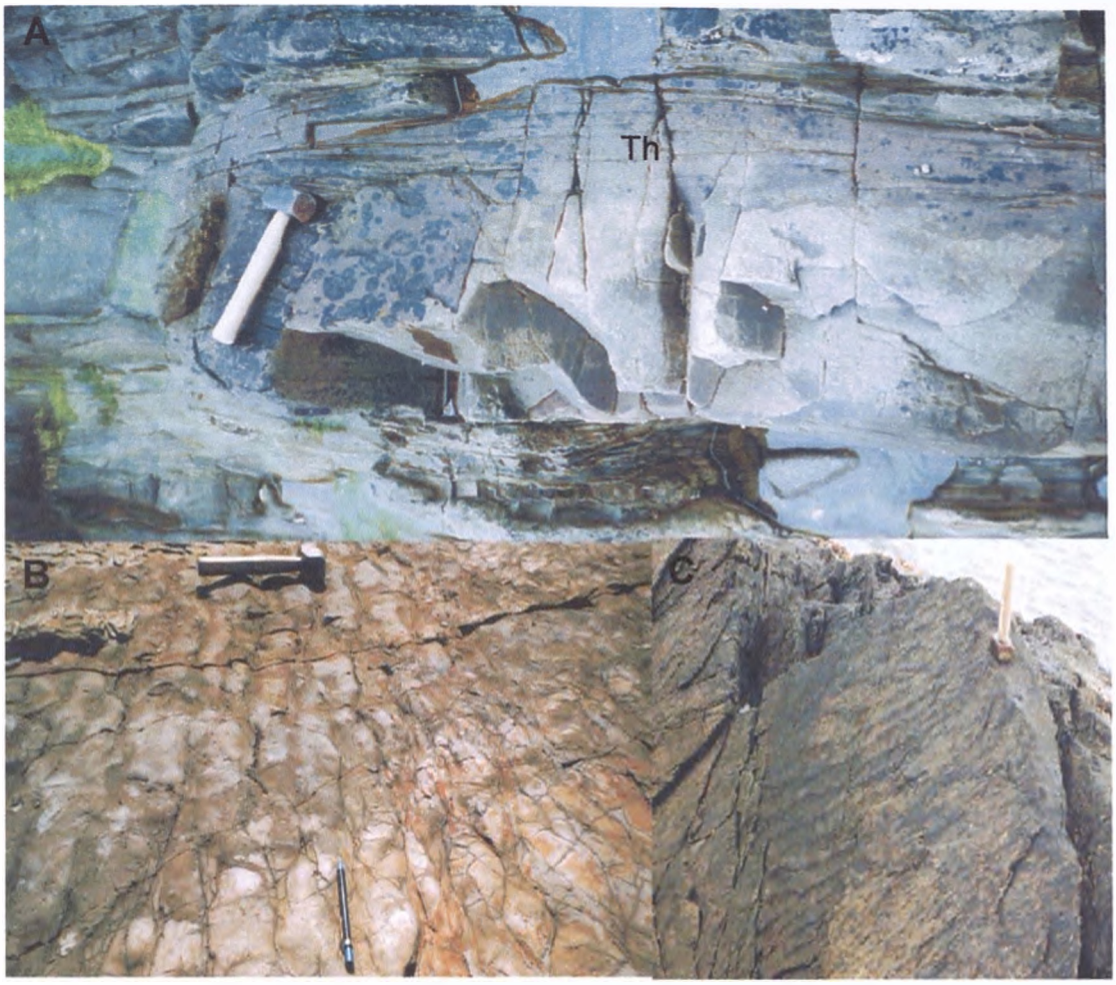



**Fig. 5.8.** Lithological features of Facies Association B sediments. (A). Facies B2 (Whitesand Bay) – accretionary HCS with a well developed domed upper surface, and internal lamination that thickens over the aggrading antiform (Th), resulting in the upwards growth of a depositional hummock. (B) Facies B1 (Porth Gain) – combined flow ripples with irregular and slightly over-steepened crests. (C) Facies B2 (Porth Gain) – wave formed vortex ripples with characteristic straight and bifurcating crests. Length of hammer = 31 cm.

not signify an appreciable change in flow regimes, and both are interpreted as high energy combined-flow structures with significant net flow. The difference in stratification is solely the result of irregular second-order internal erosion surfaces. These may simply record the temporary development of exceptionally high constructive waves, as reported from the modern Mid Atlantic Shelf by Swift *et al.* (1983).

*5.3.2.3. Facies B2: description*

Rhythmically alternating thinly bedded sandstones and shales of Facies B2 comprise less than 25% of Facies Association B but occur in every asymmetrical coarsening upwards sequence identified in the Ogof Velvet Formation. In fully developed progradational cycles, Facies B2 intervals pass gradationally into Facies Association C and amalgamated sandstones of Facies B1. Thin bedded sandstones are broadly tabular, appear laterally extensive, and are composed of normally graded fine sandstones and coarse siltstones 6–30 cm thick. Interbedded shales are more extensive in Facies Association C and are discussed in detail later. Sandstone bases are typically sharp and planar with no obvious large-scale relief or basal sole structures. Upper boundaries are invariably sharp, and display an overall hummocky topography with antiformal crest spacing ranging from 1–4 m. These large-scale symmetrical domal structures are largely non-erosional and appear to represent the original profile of preserved 3D bedforms (Fig. 5.8A). Internal stratification displays a fairly consistent three-fold internal division above the lower bounding surface. A complete vertical sequence contains the following gradational series of structures: parallel lamination with parting lineation; undulating lamination displaying low angle intersecting arches and troughs interpreted as HCS; and small scale 2D wave (Fig. 5.8C) and 3D combined-flow ripples. Roughly 30% of beds record a similar rippled division beneath the parallel laminated interval.

Analysis of the hummocky cross-stratified division allows three types of cross strata to be discerned (Fig. 5.9). SD-HCS is identified in outcrop by numerous internal second-order erosion surfaces that are draped concordantly by lamination that thicken into swales and thin over hummocks. Laminae that thicken over antiforms record the vertical growth (accretion) of a depositional hummock (Th in Fig. 5.8A), and is interpreted as A-HCS. The lack of bedform migration (i.e. its isotropic character) argues against substantial unidirectional flow, and growth probably occurred under purely oscillatory or very oscillatory-dominant combined-flow (Duke *et al.* 1991a). The third type of HCS is characterised by low angle cross strata sets that

have a preferred unimodal dip direction implying lateral migration of a bedform. Asymptotic onlapping relationships of individual laminae are defined by very low angle second-order erosion surfaces. This is interpreted as anisotropic HCS (An-HCS) (Nøttvedt and Kreisa 1987) and formed under an oscillatory-dominant combined-flow with a stronger unidirectional component than A-HCS (Midtgaard 1996).

*5.3.2.4. Facies B2: interpretation*

Evidence for combined-flow deposited sandstones rhythmically alternating with variably bioturbated silty mudstone suggests a juxtaposition of contrasting energetics that is commonly associated with the alternation of fair-weather suspension sedimentation and powerful storm-generated processes (Dott and Bourgeois 1982). The preservation of fair-weather fines reflects deposition in a more distal location than Facies B1, probably on the mid-shelf (Brenchley 1985). One of the most distinctive features of the Ogof Velvet Formation is the paucity and restricted vertical extent of HCS. A major limiting factor on the generation of large amplitude bedforms needed for A- and An-HCS is a combined-flow with a significant unidirectional component. Therefore the variability in style of cross strata in Facies B2 suggests that in this more distal setting, unidirectional currents were not as powerful, and the combined-flow appears to be oscillatory-dominant. To assess the temporal evolution of storm dynamics in this more distal location, the vertical stratification sequences previously defined may be incorporated into a bed configuration stability diagram (Fig. 5.9). This method, first utilised by Myrow and Southard (1991), is based on the present knowledge of stability fields of combined-flow bed phases in fine sand (Arnott and Southard 1991). Stability fields are framed within axes of maximum orbital velocity and unidirectional flow velocity.

Bedform configurations from vertical stratification sequences are plotted as points on the diagram, and joined by straight lines representing the evolution of flow regimes through time. As storm parameters change at a faster rate than at which beds can attain an equilibrium status (Arnott and Southard 1991), not all the theoretically expected bedforms will be generated. Also, those developed prior to plane bed conditions may be lost to subsequent erosion. Stratification generating curves for the three types of HCS present in Facies B2 are presented, as well as a comparative curve for the quasi-planar laminated bed with overlying SD-HCS. The position on the diagram of small ripples is self-explanatory. Parallel lamination on the other hand is more difficult to quantify in terms of relative combined-flow components

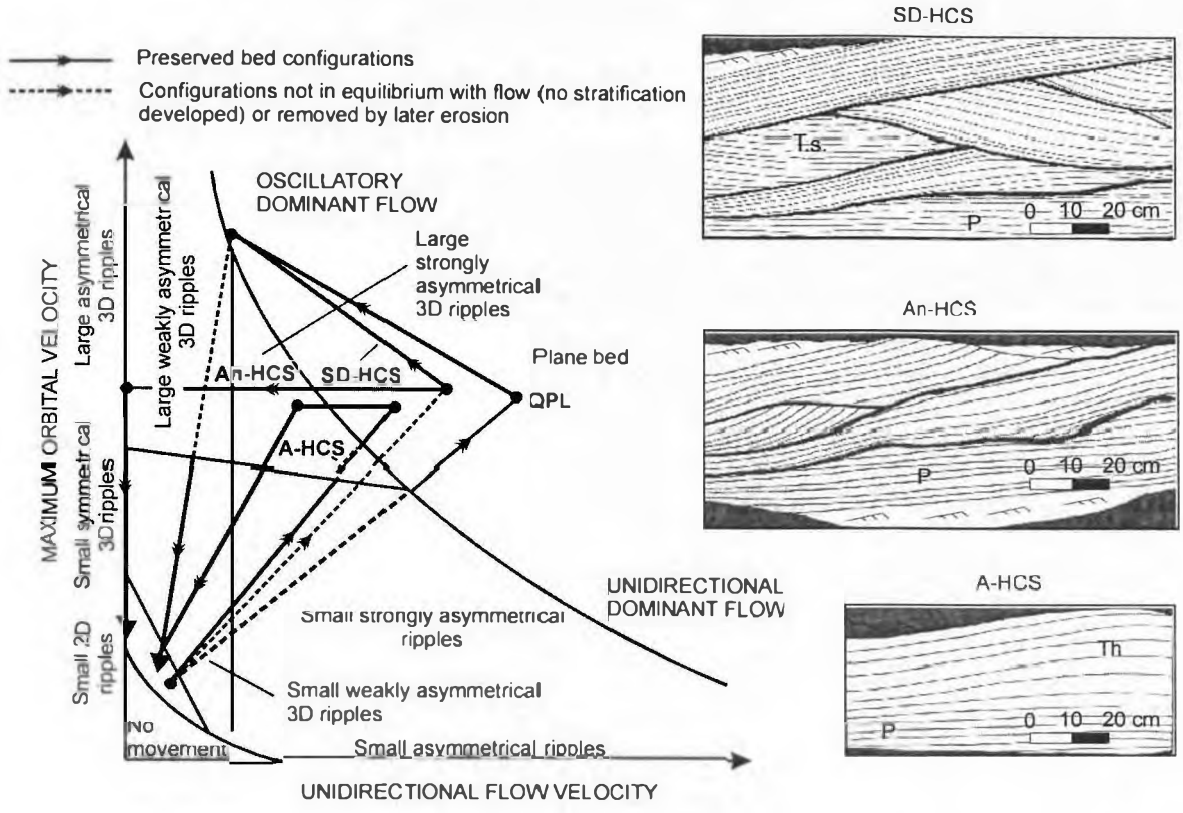



**Fig. 5.9.** Representative stratification sequences from Facies B2 plotted in a bed configuration stability diagram for combined-flow in fine sand (diagram modified after Myrow and Southard 1991). Each path reflects varying flow conditions during a single storm event as recorded from the stratigraphic record (field sketches). SD-HCS = scour and drape HCS, A-HCS = accretionary HCS and An-HCS = anisotropic HCS. T.s. = thickening of laminae into swales, P = parallel lamination, and T.h. = thickening of laminae over antiforms.

Myrow and Southard 1991), but is plotted in the mid point plane bed field between oscillatory and unidirectional-dominant as parting lineation parallel to flute cast orientation and the presence of laterally continuous lamination suggests considerable unidirectional currents, while the vertical and sometimes lateral transition into HCS indicates intense wave activity. A-HCS plots within the large 3D symmetrical ripple field, while An-HCS straddles the large weakly asymmetrical and large strongly asymmetrical ripple fields. SD-HCS is interpreted as a plane bed configuration with a lower unidirectional but higher oscillatory component than QPL.

Generating curves indicate deposition during the following flow changes: (1) SD-HCS – high energy unidirectional-dominant combined-flow which may remove waxing flow indicators, followed by a decrease in the unidirectional component as orbital velocity increases, which is succeeded by a low energy combined-flow as both components decrease; (2) A-HCS – high energy combined-flow which evolves into a very oscillatory-dominant combined-flow as unidirectional velocity decreases,

followed by a low velocity purely oscillatory flow; (3) An-HCS – low energy combined-flow which intensifies to a high energy combined-flow and then evolves to an oscillatory-dominant combined-flow with a significant unidirectional component, followed by a return to low energy combined-flow conditions. A common evolutionary trend in all curves is that unidirectional currents dominate the combined-flow during storm waxing and peak storm conditions, while storm waning operates principally under an oscillatory-dominant regime. These changing hydrodynamics compare favourably in evolution but differ in scale to those recorded on many modern shelves (e.g. Snedden and Nummedal 1991; Amos *et al.* 1996; Hill *et al.* 2003). The relatively rare occurrences of ripple cross-lamination beneath parallel lamination records a change in equilibrium state from small current ripples to plane bed, and thus an increase in current intensity. Although documented in some studies (Croft and Bridges 1987; Arnott 1993; Midtgaard 1996), waxing flow indicators will always be the exception as waxing flow generally outpaces the speed at which bedforms reach equilibrium (Arnott and Southard 1990), and any bedform is unlikely to survive subsequent reworking under plane bed conditions.

Dashed lines on Fig. 5.9 represent parts of the stratification sequence that in theory should be present but did not attain equilibrium with the flow. This appears to occur mainly during flow waxing and waning, suggesting that storm growth and depletion were periods when current parameters changed rapidly. Stratification generating curves from Facies Association B compare favourably with bed configuration stability diagrams constructed by Hill *et al.* (2003) based on oscillatory and unidirectional current reading from the shoreface of Hudson Bay, Quebec. HCS configurations operate within the same fields as moderate storms in Hudson Bay, while quasi-planar laminated intervals are remarkably similar to the record of major storms.

*5.3.2.5. Facies B3: description*

Facies B3 is a subsidiary facies that straddles the boundary between Facies Associations A and B, and is characterized by subaqueous deformational features and rare gravity flow deposits (Fig. 5.10). Deformed bedding principally affects strata assigned to Facies B2 and C1 (discussed below), but in a few cases extends to Facies B1. Although deformation is very conspicuous in outcrop, with some excellent examples particularly at Porth Gain, it characterizes only a small part (less than 4%) of the Ogof Velvet Formation. Sedimentological characteristics show considerable diversity, but five subfacies (referred to as types- A to E) can be recognized.

Type-A features are disturbed (slumped) horizons (Fig 10A) that involve up to four discrete sandstone-mudstone couplets with accumulative thickness of 80-200 cm. High angle convex-up shear zones often dissect disrupted beds. These surfaces may be traced laterally into bedding parallel décollement (tangential shear) surfaces over several metres (D in Fig. 5.10A). Internal deformation is intense and chaotic with both plastic and brittle regimes common. Folds display no preferred vergence direction. Individual décollement surfaces often terminate against another high angle shear surface producing a step-like configuration over distances in excess of 15 m. Close to these terminations, thrust slices (TS in Fig. 5.10A) and small reverse faults inclined up-slope are associated with décollment suggesting compression against high angle shear planes. These terminations are also characterized by the highest degree of internal disruption. This style of deformation is similar to slump and slide deposits reported by Postma *et al.* (1988), Nemec (1990), and Myrow and Hiscott (1991).

Type-B beds are generally more coherent with only moderate disruption and no obvious basal shear plane or décollement surface. Disrupted units contain small recumbent folds (Fig. 5.9A) with a consistent vergence direction to the ENE. These smaller scale deformational structures appear to record the plastic response of semi-consolidated sediment to gravity-driven downslope instabilities. Type-C beds are ungraded, unstratified, pebbly silty mudstones 8-34 cm thick, with large (up to 4 cm) intraclasts of siltstone and fine sandstone floating in a fine-grained matrix. The internal fabric is disorganized often with clasts in unstable positions. Bed boundaries are sometimes difficult to distinguish but appear planar and non-erosional. These features are incompatible with traction-influenced sedimentation, and deposition is inferred to have been from cohesive debris flows with grain support provided by matrix strength (Lowe 1982).

Metadepositional (and hence truncated) convolute lamination of bed-type D records the partial liquefaction of a previously deposited tempestite. Characteristic features (Fig. 5.10B) include the strengthening upwards of folds from an undeformed base, close box-like fold geometries with conjugate axial planes, and truncated convolutions with sand volcanoes overlying anticlines. At least a partially liquefied state is indicated by the smoothness of folds, extreme thickness variations shown by individual laminae, and the scarcity of microfaults. From the prominent box-like form of the convolutions, vertical deformational forces were dominant, producing an isotropic pattern of shear stress vectors in the horizontal plane. Some beds, including that in Fig. 5.10B, display fold limbs inclined from the vertical indicating a subordinate horizontally-directed force. This may represent a minor component of downslope gravity-driven instability. Sand volcanoes and box-like folds appear to form in

response to the vertical expulsion of pore fluids, as the highly fluidized sediment strives to attain closer packing and reduced pore volume. Liquefaction results from the build-up of pure pressure as the bed attempts, via fluid expulsion, to reach a stable configuration (Myrow and Hiscott 1991). Complete liquefaction resulting in a liquefied flow may occur when the effective resistance of the granular material is reduced to zero by this increase in pore pressure.

Facies-type E is composed of sheet-like beds 14-78 cm thick that lack any form of stratification or grading. These characteristics, as well as their pale colour, sharp bases and tops, anomalous thickness relative to beds in surrounding strata, and their laterally persistent nature led to an original interpretation as volcanic ashes (bentonites), deposited out of suspension below storm wave base. Later thin section analysis demonstrated that these beds were actually quartz arenites. The complete absence of grading and internal structure can most readily be accounted for by assuming flows of extreme concentration that dampen turbulent eddies, preventing the formation of traction structures (Kneller and Branney 1995). The uniform grain size and quartzose composition is consistent with deposition from a liquefied flow (Lowe 1982), formed from the spontaneous liquefaction of a previously deposited metastable quartz-rich bed.

*5.3.2.6. Facies B3: interpretation*

Facies B3 can be most simply interpreted as a process-response subsystem associated with sediment failure (subfacies types- A, B and D) and subsequent sediment flow (types- C and E). The two main prerequisites for slope- and sediment-induced deformation are: abundant and rapid accumulation of fine grained sediment particularly silt and very fine sand, which does not easily allow fluids to escape during burial; shocking of accumulated sediment (Michels *et al.* 1998). Trigger mechanisms include storm wave loading, particularly in deltaic environments, and seismic shaking (Coleman 1981, Prior *et al.* 1989). Failure occurs when sediment strength is reduced to a certain level by increasing pore pressure.

This process-response relationship between subfacies is highlighted in Fig. 5.10. Due to limited lateral exposure, these relationships cannot be recorded directly in the field, and conclusions are therefore based on relatively well-understood flow transformations or facies tracts (Mutti *et al.* 1999, Mulder and Alexander 2001) The two end products associated with sediment failure are debris flows and liquefied flows. Based on textural characteristics, a very well sorted liquefied flow is unlikely to develop from heterolithic source (types- A and B) while, conversely, a debris flow of

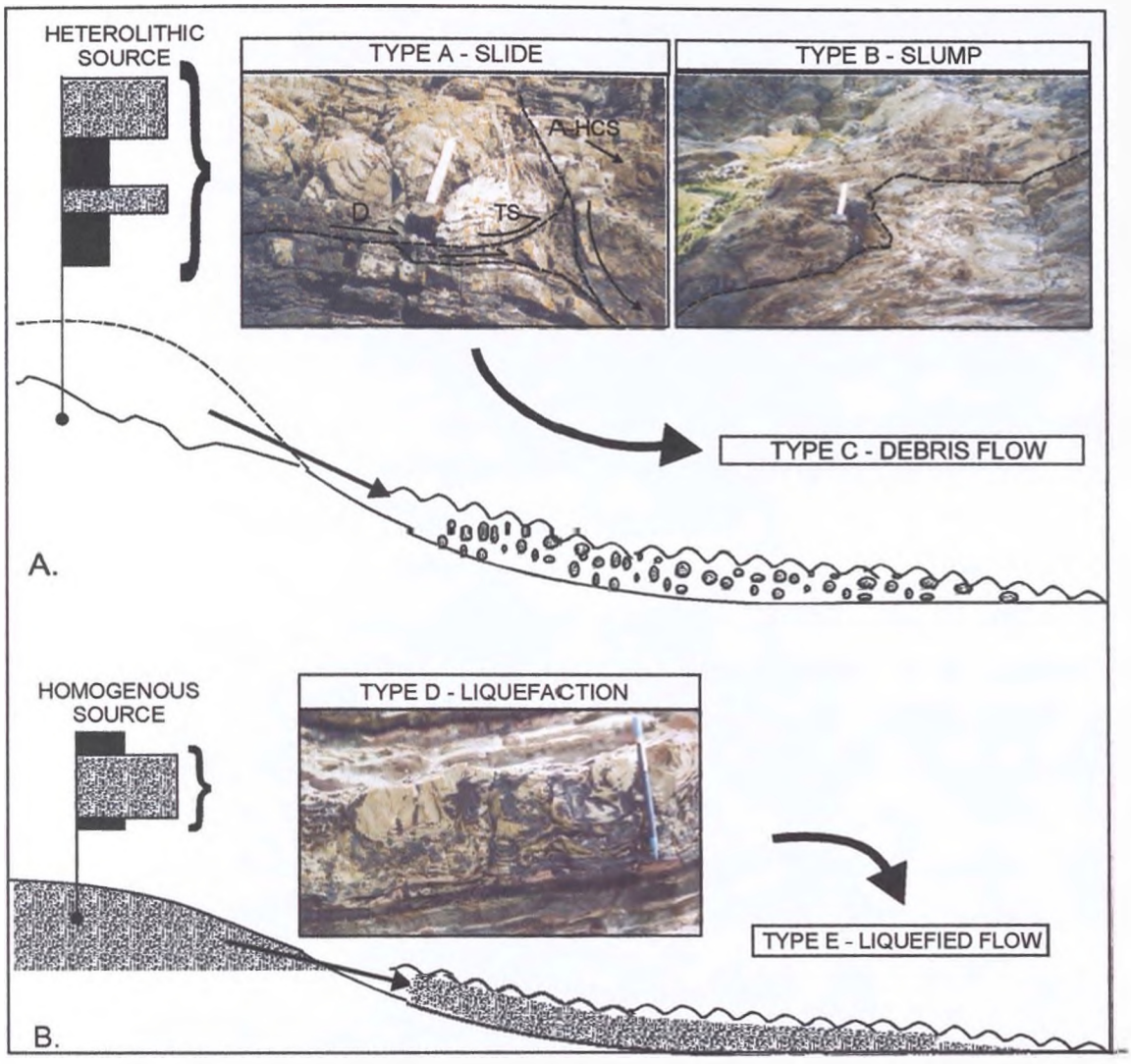



**Fig. 5.10.** Soft sediment deformation and proc-ess-response model for sediments of Facies B3. See text for details. TS = thrust slice, A-HCS = accretionary hummocky cross stratification, D = décollement surface.

variable grain size cannot form from a homogenous source like the liquefaction of a single sandstone bed (type-D). Instead it seems reasonable to assume that a heterolithic source would produce a flow of varied grain size, composed of fine matrix material and coarse grained clasts i.e. a cohesive debris flow. The instantaneous liquefaction of a storm-emplaced, and hence well sorted, sand or silt has only the grain size range to form a highly quartzose liquefied flow. Due to uptake of water (dilution) or acceleration, liquefied flows, and to a lesser extent debris flows, may undergo further transformation to high- then low-density turbidity currents (Mulder and Alexander 2001). This cannot be confirmed in the Ogof Velvet Formation because the distal toe of Facies B3, where these turbidity currents would be expected to develop, is commonly below wave base, and the deposits of low-density turbidity currents would be indistinguishable from below wave base tempestites (see Facies C1). Characteristic deposits of density-stratified (bipartite) high concentration turbidity (Lowe 1982) currents have not been recognized.

Subaqueous mass movement features are common in a wide range of environments including deep sea fans, slopes and deltaic settings (Postma *et al.* 1988, Nemec 1990). The relatively diverse suite of shallow water features evident in the Ogof Velvet Formation is very similar to that described from modern (Prior *et al.* 1984, 1986; Coleman 1981), and ancient (Martinsen 1989; Myrow and Hiscott 1991) fine grained river deltas. Of particular significance is the study by Myrow and Hiscott (1991) on the Late Precambrian-Early Cambrian Chapel Island Formation, which displays all the subfacies recognised here. The Chapel Island delta complex, like the Ogof Velvet Formation, is storm-dominated leading Myrow and Hiscott (1991) to speculate on the possible role of storm wave loading in triggering sediment failure. This argument was based on the anomalous thickness of sandstone tempestites involved in slump/slide events and the common presence of HCS. Based on this evidence, there is a good case for wave loading in the Ogof Velvet Formation. As demonstrated in Fig. 5.10A, to the right of the high angle slide scar, A-HCS is clearly recognizable, as is the anomalous thickness of the bed, which is an order of magnitude thicker than the surrounding strata. This interpretation is preferred over the one offered by Kokelaar *et al.* (1985) to account for slump horizons evident in coeval sections on Ramsey Island. Their elaborate model involves sediment deformation and slippage off a Llanvirn rhyolite intrusion, requiring the improbable scenario that the sediments remained unlithified for over 30 million years.

*5.3.2.7. Summary*

Facies Association B sediments record basinward progradation of a fine-grained sand-sheet under the influence of unidirectional-dominant combined-flows jetting from nearshore channels and gutter casts. This continuation of intensified currents appears to limit the potential variability of stratification sequences produced by combined-flow processes, commonly resulting in complete bedform washout and the formation of QPL. It is difficult to compare the characteristics of this depositional zone with other published accounts of inner- to mid-shelf facies, because few studies differentiate between the various styles of HCS. Based on limited descriptions and occasional photographs, it appears that most high accumulation zones distal to regions of bypass are dominated by either parallel lamination or SD-HCS. Both are commonly associated with flute and gutter casts, suggesting the existence of powerful unidirectional currents within the combined-flow.

### 5.3.3. Facies association C: mudstone dominated outer shelf

#### *5.3.3.1. Facies C1: description*

Facies C1 is composed of sheet-like fine to very fine sandstones displaying a variably developed bipartite structure. Good exposure at Porth Gain allows beds to be traced over distances in excess of 200 m without any significant change in bed thickness, which ranges from 2–11 cm. Beds are normally graded, well sorted and have planar, often slightly erosional lower contacts, and sharp or rarely gradational upper surfaces into facies C1 (Fig. 5.11A). Flute casts and rare load structures with tiny flames occur on the lower surfaces of the thickest beds. Internally, beds contain parallel lamination overlain by ripple cross-lamination (turbidite divisions Tb/Tc in the terminology of Bouma (1962)). Pronounced lateral heterogeneity is common, where parallel lamination passes into ripple cross-lamination over a few centimetres. Millimetre scale mud drapes identical to those described by Chakraborty and Bose (1992) are also common.

#### *5.3.3.2. Facies C1: interpretation*

The sharp basal contact with occasional flute casts, normal size grading and parallel lamination transitional to ripple cross-lamination records the temporal flow deceleration of unidirectional currents through well-established flow regimes (Walker 1965). The total exclusion of wave-generated sedimentary structures, the presence of Tb/Tc turbidite divisions and the monotonous interbedded nature of shale and

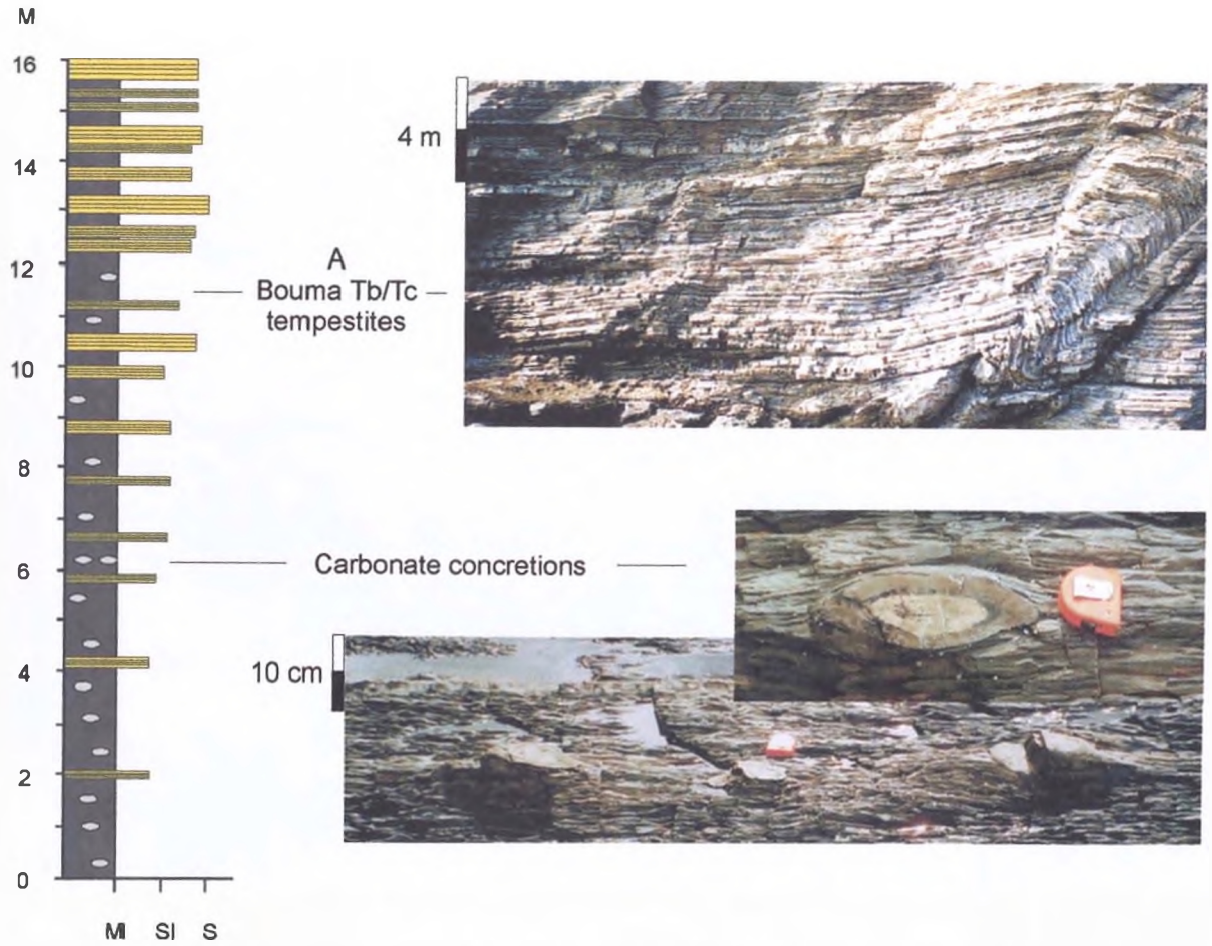



**Fig. 5.11.** Sedimentological features of Facies Association C. (A) Facies C1 (Porth Gain) – laterally persistent tabular fine-grained sandstones displaying Bouma divisions Tb/Tc, interbedded with silty mudstones of Facies C2. Note their turbidite-like appearance. (B) Facies C2 (Porth Gain) – well developed carbonate concretions typical of the lower parasequences of the Ogof Velvet Formation. Their growth along certain horizons indicates periods of condensation associated with low rates of clastic input.

sandstone led George (1970) and Stead and Williams (1971) to interpret the sequence as distal submarine fan deposits. Although there is no direct evidence for deposition above storm wave base, the pronounced lateral heterogeneity common in this facies must reflect irregular fluctuations in the strength of the depositing current, which is inconsistent with the progressive decrease in current energy associated with waning turbidity currents. High frequency fluctuations in flow velocity may also account for mud drapes on ripple foresets.

The lack of gradational upper surfaces is also inconsistent with deposition from turbidity currents. Sharp rather than gradational upper bed contacts are a feature more commonly associated with storm deposits. The sharp juxtaposition of traction deposited sand and suspension deposited mud suggests a time break across a process boundary (Gladstone and Sparks 2002), which is a feature commonly ascribed to the alternation of storm and fair-weather conditions. Beds with these characteristics (often referred to as BC tempestites) are usually interpreted as outer shelf deposits (Bourgeois 1980) and have their modern equivalents in "graded storm sand layers" reported from shelf depths in excess of 40 m (Reineck 1968).

*5.3.3.3. Facies C2: Description*

Facies C2 consists of structureless, soft, light grey to light blue silty mudstone. Typically, the facies occurs as 0.8–4.2 m thick units at the bases of coarsening upwards cycles and interbedded with Facies B2 and C1. Individual mudstone beds are 1-190 cm thick, laterally continuous at outcrop scale, and lack internal sedimentary structures. Carbonate concretions aligned along certain surfaces may occur in the lower cycles (Fig. 5.11B), but are far more common in the underlying Aber Llong Formation. Burrowing is generally sparse, of simple morphology and low diversity, but feeding traces (*Chondrites*) and large bedding parallel non-branching burrows (*Planolites*) are common along certain bedding planes at Whitesand Bay. This assemblage, along with *Cruziana* and *Rusophycus* traces reported by Crimes (1970a), is typical of the Cruziana Ichnofacies (Pemberton *et al.* 1992).

*5.3.3.4. Facies C2: interpretation*

The homogeneity of grain size and the lack of internal sedimentary structure reflect slow, uniform "background" sedimentation at sufficient depth to be beyond the influence of waves or currents. Rare concretionary horizons represent periods of condensation associated with minimum rates of clastic input, allowing early

diagenetic growth of carbonate close to the sediment-water interface (Raiswell 1987). Cruziana Ichnofacies bioturbation is associated with low energy suspension sedimentation in a well-oxygenated mid- to outer-shelf environment (Pemberton *et al.* 1992). For this reason, the complete absence of body fossils, microfossils (M. Williams pers. comm. 2001), and the extremely restricted trace fossil assemblage is surprising and difficult to account for. The nature of the seabed may have played some role in trace preservation, as there is considerable evidence throughout deposition of the Ogof Velvet Formation that this substrate existed as a hydroplastic or fluidised mud. This can be demonstrated by the common occurrence of large and small-scale slumps, ball and pillow structures, load casts, and loaded ripples (Dzulynski 1963), as well as the total absence of delicate tool marks such as prod and groove casts and rip-up clasts. A substrate with low shear strength may offer a severe limiting factor to benthic organisms and certainly would have an adverse affect on trace preservation (Kerr and Eyles 1991). The possibility of fluctuating salinity levels as an environmental stress is explored in the last section.

*5.3.3.7.. Summary*

Even below storm wave base, the hydrodynamic regime that generates a nearshore zone of sediment bypass by intensifying unidirectional currents leaves some impression on the characteristics of this most distal facies association. Beds up to 11 cm thick with basal flute casts record very efficient sediment dispersal across the shelf by traction currents of considerable velocity.

## 5.4. SHELF DYNAMICS

### 5.4.1. Palaeoshoreline orientation

Before the palaeohydraulic regime operating on the shelf can be evaluated, it is necessary to establish the trend of the shoreline during deposition. The most common means of reconstructing ancient shoreline orientations is from measurements of wave ripple crests (Potter and Pettijohn 1977). Although waves commonly approach coastlines from different directions, refraction of shoaling waves results in ripple crests that approximately parallel bathymetric contours (Komar 1976). The results of 51 measurements from Facies Association A and Facies Association B display a mean orientation roughly NW-SE (Fig. 5.12A). A similar

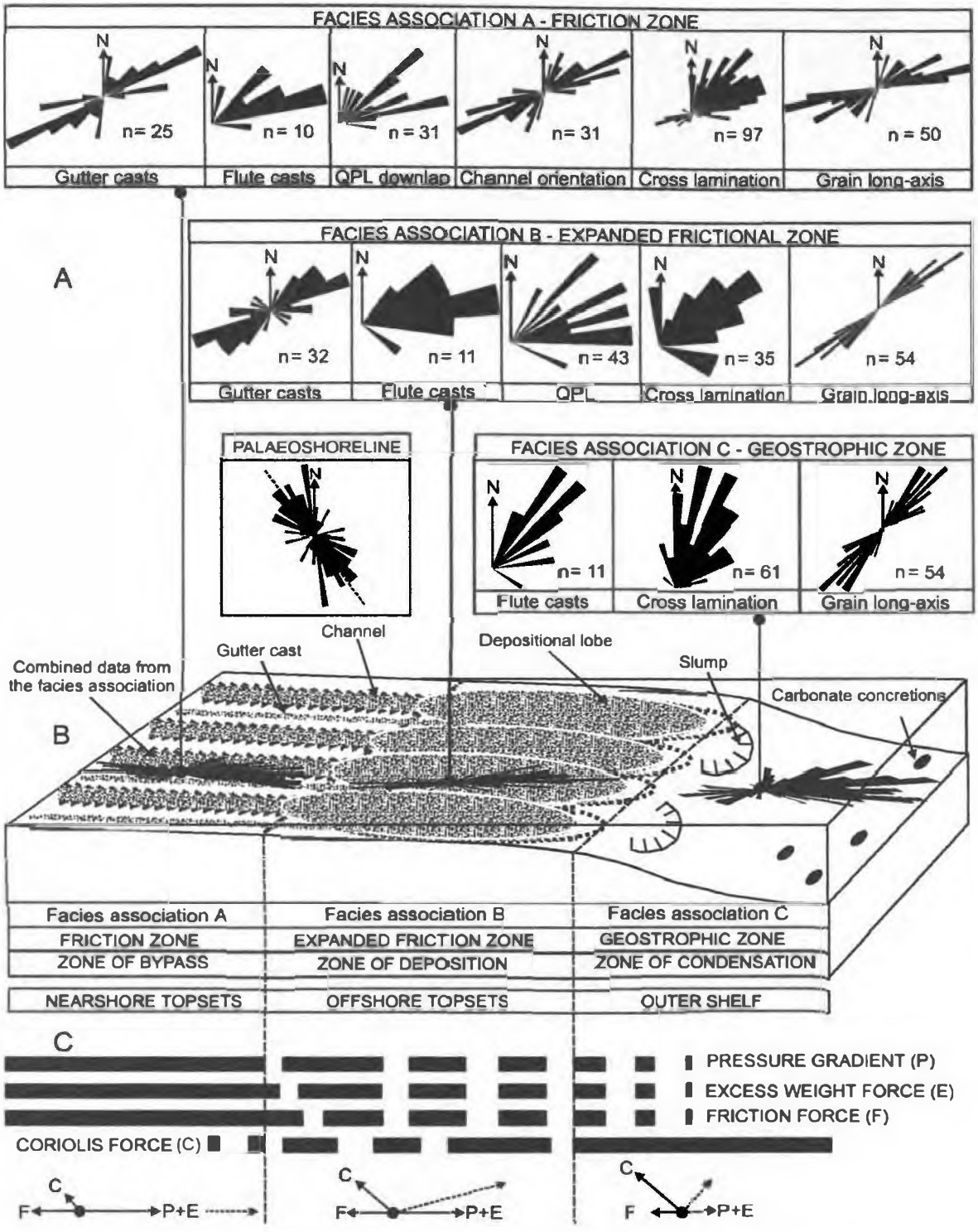



**Fig. 5.12.** Palaeohydraulic and environmental reconstruction of the Ogof Velvet Formation. (A) Summary of palaeocurrent readings. The orientation of the palaeoshoreline is also shown for ease of comparison. (B) Palaeoenvironmental reconstruction based on facies analysis and palaeocurrent data. The combined palaeocurrent readings for each facies association are presented to aid visualization of flow across the shelf. (C) The inferred contribution of the principal current forcing mechanisms (see Fig. 5.13) to the force balance equation for each facies association (see text for discussion).

shoreline orientation was reported by Crimes (1970a) from the underlying Aber Llong Formation. The presence of numerous slump horizons with consistent asymmetries in Facies B3 (type-B) may offer a reasonable estimation of shelf palaeoslope direction (Bose 1984). The vergence direction perpendicular to fold axes reflects gravity driven instability towards the ENE, suggesting bathymetric contours paralleling a NW-SE shoreline.

### 5.4.2. Current flow forcing mechanism and the force balance equation

A summary of the time-averaged balance of forces operational on the upper shoreface and shelf during storm conditions is presented in Fig. 5.13. This diagrammatically illustrates the equilibrium response of the shelf water column to an idealized storm along a straight coast in the northern hemisphere. During storm conditions, the water column is composed of three separate regions of quasi-steady circulation: a highly turbulent surface boundary layer, a core region of non-shearing, essentially inviscid geostrophic flow, and a bottom boundary layer (Fig. 5.14) (Swift and Niodorada 1985). The surface layer is wind influenced, while the frictionless core region is balanced mainly by the Coriolis Force. As the majority of the velocity shear is concentrated near the bottom (Csandy 1982), the bottom boundary layer is friction-dominated. This introduces a significant frictional term to the force balance equation (Fig. 5.13) that acts to retard geostrophic flow, resulting in it being skewed offshore parallel to the direction of the hydrostatic pressure gradient. The effect of increasing water depth with distance from the coast on the balance of forces may be analysed within the qualitative framework of shelf hydrodynamics devised by Swift *et al.* (1985) and Swift and Niodorada (1985). Seaward of the surf zone, the shoreface and shelf may be divided into two shore-parallel zones (Fig. 5.14). In the shallow water *frictional* zone, the surface and bottom boundary layers commonly overlap and occupy the entire water column. Consequently, net flow is little affected by the Coriolis Force (Swift *et al.* 1985). At greater water depths (the geostrophic zone), there is significant separation between the surface and bottom boundary layers allowing for a geostrophically balanced interior and development of Coriolis deflection.

The most controversial parameter in the force balance equation is the downslope component of excess weight of sediment-rich dispersions, termed the excess weight force by Myrow and Southard (1996). Early facies models for storm-influenced shelves concentrated on this force in isolation, essentially defining storm flows as turbidity currents. This so-called "geological viewpoint" (Walker 1984), based

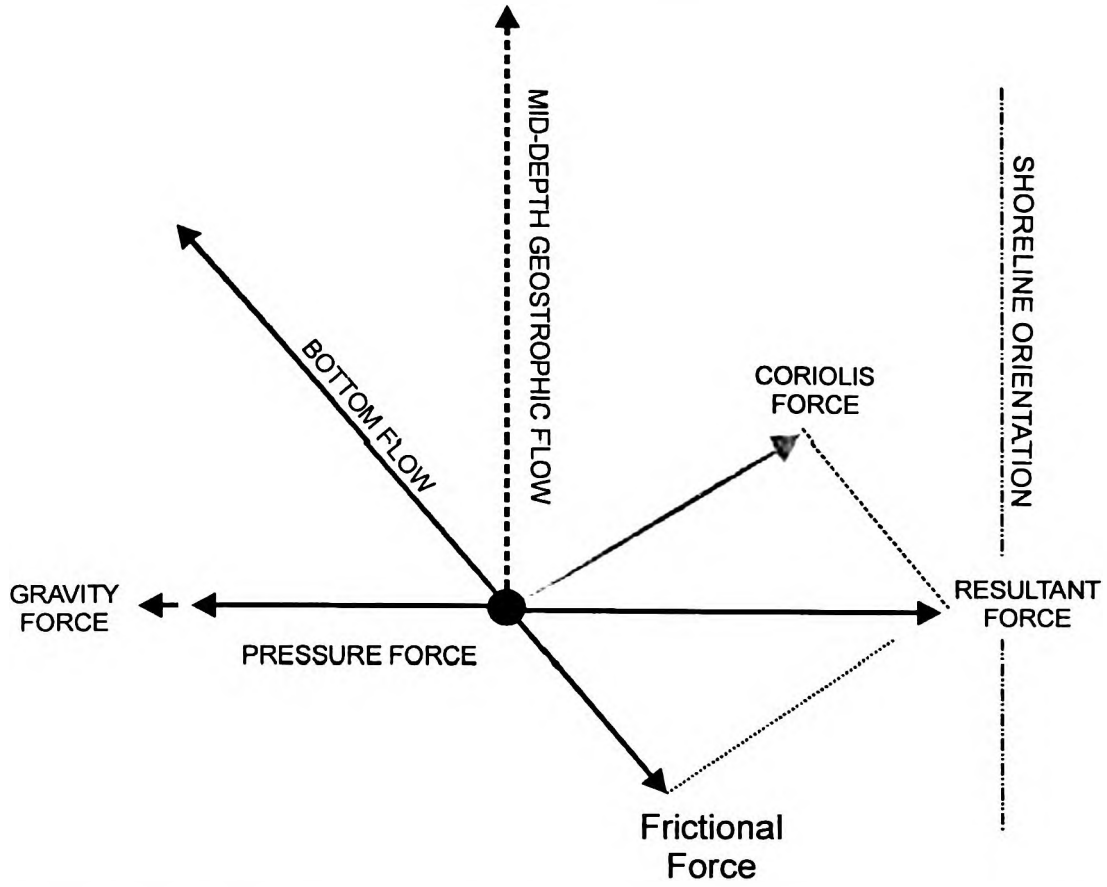



**Fig. 5.13.** Storm-induced current flow forcing mechanism over the lower shoreface and shelf in the northern hemisphere (modified from Duke 1990).

on palaeocurrent date from vertical facies sequences, clearly demonstrated offshore flow perpendicular to the shoreline and stratification sequences that resemble turbidites (i.e. waning unidirectional flow indicators). This view of storm deposition has been criticized by oceanographers (e.g. Snedden *et al.* 1988), who emphasize that modern storms generate geotropically-balanced down-welling currents that parallel the shoreline. The resulting uniformitarian dilemma became known as the "palaeocurrent problem" (Duke 1990).

As progress was made in the understanding of modern storm hydrodynamics, it became apparent that, due to the relatively low suspended sediment concentrations of geostrophic flows, excess weight forces were largely negligible in the modern force balance equation. Their role in ancient storm deposits was also questioned by Duke (1990) who drew particular attention to the fact that shore-normal flow indicators, particularly sole structures, may be merely products of the peak instantaneous shear stress of wave oscillations. This may bear no relation to the time averaged balance of gravitational and fluid forces, which would promote essentially shore-parallel flow. Following Duke (1990), excess weight forces have

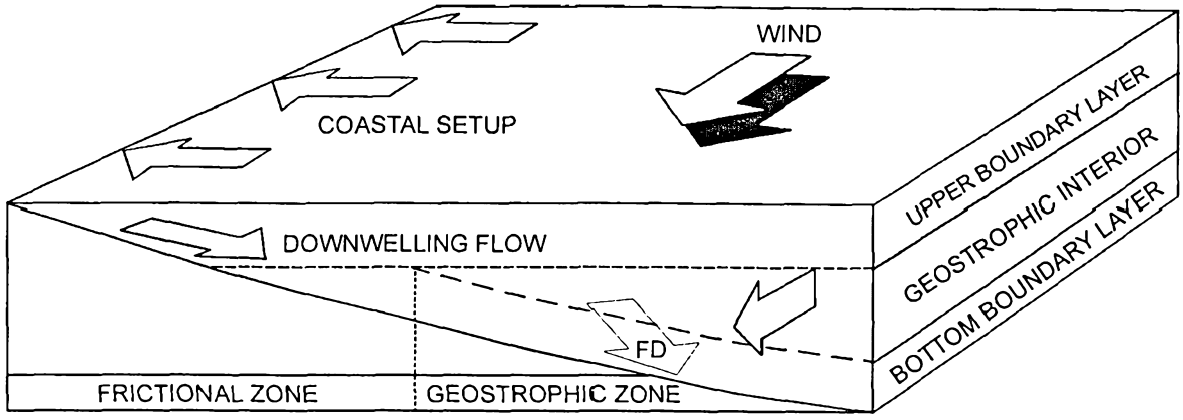



**Fig. 5.14.** Idealized diagram of motion in the coastal ocean during a downwelling event (modified after Swift *et al.* 1985). Note that the water column is composed of three layers which dictate the position of the coastal ocean dynamic zones. The frictional zone occupies the shallow nearshore where upper and lower boundary layers engulf the column, while deeper water locations (geostrophic zone) develop a significant geostrophic interior resulting in flow deflection (FD).

been largely dismissed as contributory agents in the force balance equation. A review of tempestite deposition by Myrow and Southard (1996) critically assessed the adequacy of modern oceanographic data to account for ancient storm depositional processes. This critique is significant if we consider the non-actualistic conditions that must have operated on ancient shelves to produce storm deposits that are many times thicker than their modern counterparts and appear more widely distributed across the shelf. There are also many studies that demonstrate shore-normal flow that cannot be adequately accounted for by assuming peak instantaneous shear stresses (Table 5.1).

### 5.4.3. Palaeoflow and grain fabric analysis

Although palaeocurrent analysis plays a crucial role in determining shelf hydrodynamics and palaeocirculation, it is apparent that no consensus has yet been reached on the significance of certain palaeoflow indicators. Because of the conflict between oceanographic and geological data sets, and particularly the difficulties in discriminating between time-averaged flow and peak instantaneous shear stress of wave oscillation (Duke 1990), palaeocurrent data from sedimentary structures are here supplemented by measurements of grain fabric (grain long axis alignment). Although this approach has met with considerable success in storm deposits, including significant conclusions drawn on relative combined-flow processes (e.g. Cheel 1991; Arnott 1993), its utility has too often been overlooked. This is in part due to the labour intensive point-counting method often deployed and the large data sets

required for statistically significant results (Taira and Lienart 1979). An alternative to this traditional method, and the one utilized here, is the measurement of bulk sample properties by studying the anisotropy of magnetic susceptibility (AMS). Although the use (e.g. Rees 1961; Crimes and Oldershaw 1967) and reliability of AMS (e.g. Taira and Leinert 1979; Schieber and Ellwood 1988) as a palaeoflow indicator has long been appreciated, with a considerable amount of literature built up over the last 40 years aimed at refining the method, its utility is still undervalued by sedimentologists. For this reason, it is pertinent to first briefly review the methodology of AMS and highlight the main properties of the magnetic fabric.

*5.4.3.1. AMS in detrital sediments*

It is beyond the scope of this study to delve to deeply into the methodology of magnetic fabric analysis. Excellent reviews of the application of AMS to sedimentary rocks are given in Hrouda (1982) and Tarling and Hrouda (1993), and there are detailed case studies from modern and ancient environments including fluvial (Taira 1989), beachface (Rees 1965), incised valleys (Lui *et al.* 2001), storm-dominated shelves (Schieber and Ellwood 1988, 1993), submarine canyons and fans (Piper *et al.* 1996) and abyssal plains (Ellwood and Ledbetter 1977, 1979). Because the method has such a wide-ranging application, it is fundamental that the cause of the magnetic fabric, be it sedimentary (primary) or tectonic (secondary), is first assessed (Crimes and Oldershaw 1967).

AMS can be defined as the intensity of magnetization of a rock, where this intensity is a function of the direction of the applied field (Butler 1992) in accordance with the equation:

$$\underline{M} = K\underline{H}$$

where $\underline{M}$ is the acquired magnetisation, K is the susceptibility of the rock sample and $\underline{H}$ is the applied magnetic field. If a rock has a fabric related to either the orientation of grain shape or the crystallographic orientation, the susceptibility that arises will be anisotropic and is approximated by a symmetrical second-rank tensor (Hrouda 1982). This can be described as a triaxial ellipsoid with K1>K2>K3, representing the maximum ($k_{max}$), intermediate ($k_{int}$), and minimum ($k_{min}$) susceptibility axes respectively (Fig. 5.15). Numerous parameters have been introduced to quantify the magnitude of anisotropy, and to define the shape of the ellipsoid (Tarling and Hrouda 1993, table 1.1). The scope of this study requires mean susceptibility ($k_{mean}$), and parameters H, F, L, u, and q (Table 5.2). $k_{mean}$ provides an approximation on the amount of material in the sample causing the magnetic signal. H is a measure of total

| Parameter | Equation | Reference |
|---|---|---|
| Mean susceptibility ($k_{mean}$) | $k_{mean} = (k_{max} + k_{int} + k_{min})/3$ | Nagata (1961) |
| Total anisotropy (H) | $H = (k_{max} - k_{min})/k_{mean}$ | Owens (1974) |
| Magnetic foliation (F) | $F = (k_{int}/ k_{min})/k_{mean}$ | Stacey *et al.* (1960) |
| Magnetic lineation (L) | $L = (k_{max}/k_{int})/k_{mean}$ | Balsley and Buddington (1960) |
| Angle on an L/F graph (u) | $\mu = \tan^{-1} [(k_{max} - k_{int})/(k_{int} - k_{min})]$ | Jelinek (1981) |
| Shape factor (q) | $q = (k_{max} - k_{int})/[0.5(k_{max} + k_{int}) - k_{min}]$ | Granar (1958) |

**Table 5.2.** Parameters used in the study to define the magnetic anisotropy and fabric.

| Fabric test | Primary indicator | Reference | A1 | A2 | A3 | A4 | A5 | B1 | B2 | C1 | C2 | C3 | C4 | C5 |
|---|---|---|---|---|---|---|---|---|---|---|---|---|---|---|
| q | 0.06>q>0.7 | Hamilton and Rees (1970) | 0.18 | 0.09 | 0.33 | 0.18 | 0.21 | 0.29 | 0.31 | 0.32 | 0.3 | 0.29 | 0.38 | 0.4 |
| $k_{min}$ | <25° from vertical | Hamilton and Rees (1970) | 17 | 15 | 17 | 24 | 22 | 12 | 10 | 21 | 17 | 19 | 16 | 18 |
| L/F | u°<45° (oblate) | Owens (1974) | 17 | 21 | 19 | 8 | 11 | 17 | 14 | 30 | 32 | 19 | 26 | 23 |
| $K_{max}$ (dec) | N.A.T. 61° - 241° | Crimes and Oldershaw (1967) | 40-220 | 24-204 | 21-201 | 6-186 | 8-188 | 35-215 | 34-214 | 286-106 | 332-152 | 249-69 | 259-79 | 224-44 |
| H | >1 | Owens (2000) | 5.8 | 7.8 | 6.1 | 2.4 | 3.6 | 2.5 | 3.4 | 16.5 | 11.2 | 10.8 | 9.4 | 10.8 |

**Table 5.3.** Fabric tests that describe the response of grains to flowing water. Values from the Ogof Velvet Formation clearly demonstrate that all samples upon which conclusions on palaeoflow are based appear to record only sedimentary characteristics, with no tectonically induced mechanical rotation. N.A.T. = not aligned to local stress field.

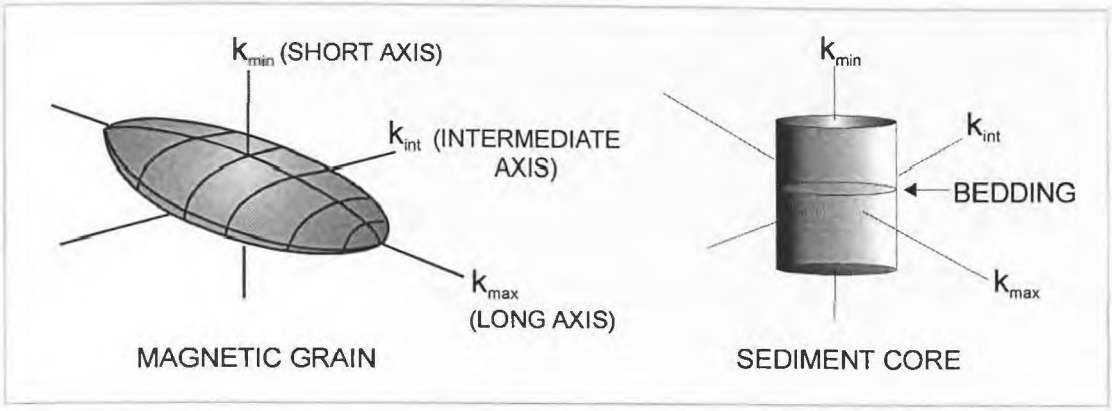



**Fig. 5.15.** Basic principle of magnetic susceptibility (see text for discussion). The relationship between the magnetic grain and the sedimentary core is also shown to aid visualization.

anisotropy and thus fabric strength, and reflects the degree of preferred orientation of the magnetic mineral. The angle u on a magnetic lineation (L) versus foliation (F) plot (Fig. 5.16) defines the shape of the susceptibility ellipsoid. A u angle <45° defines an oblate (disc shaped) fabric, while u = >45° is referred to as a prolate (cigar shaped) fabric. Foliation is the plane normal to the preferred direction of short axes (Kmin), while lineation corresponds to the preferred direction of long (or crystallographic) axis orientation, and represents the strength of $k_{max}$ in relation to $k_{int}$ within the plane of foliation. Parameter q is a ratio combining the three principle susceptibilities, and represents a ratio of linear to foliar elements in the magnetic fabric, and is thus a reflection of ellipsoidal shape.

*5.4.3.2. Properties of the magnetic fabric*

Using the parameters listed in Table 5.2, a number of fabric tests have been developed based on the known grain response to flowing water under laboratory conditions (see Rees and Hamilton 1970 for a review). These define the characteristics of a depositional sedimentary fabric (Table 5.3, column two). Values outside of these experimental ranges usually imply mechanical rotation of grains associated with tectonic restructuring of the fabric (Parés *et al.* 1999). Additional characteristics of fluid flow alignment are a spread of $K_{max}$ orientations around the mean, and long or crystallographic alignment of axes that differ from local fold and cleavage trends.

A total of 12 sites were sampled for magnetic fabric analysis (Table 5.3), 5 from Facies Association A (51 subsamples), 2 from Facies Association B (18 subsamples) and 5 from Facies Association C (50 subsamples). As the aim of the

study is to quantify the characteristics of the unidirectional component in storm-generated combined-flows, samples were collected only from stratification sequences where net flow was inferred to be significant i.e. QPL divisions above wave-base and planar laminated beds below. To determine the petrofabric, block samples (one block per site) were orientated in the field by magnetic compass and drilled in the laboratory (Owens 1994). Specimens were measured on an AGICO KLY3 Kappabridge, and site means calculated (Jelinek 1978; Owens 2000). Specimen susceptibility axes are accurate to within 2° (95% limits), and are plotted on equal area lower hemisphere stereographs (Fig 17A) with the three principle axes presented in the manner specified by Ellwood *et al.* (1988).

The susceptibility of all samples is inferred to be dominantly carried by paramagnetic phyllosilicates, particularly chlorite and muscovite. Although magnetite is often assumed to be the major contributor to the magnetic susceptibility (Hrouda 1982), no appreciable quantities have been detected in either thin section analysis or isothermal remnant magnetisation (IRM), a conclusion supported by very low bulk susceptibilities (typically 10-45 $x10^{-6}$ [SI]). Orientated thin sections demonstrate a clear alignment of large detrital chlorite and mica crystals which, according to Hounslow (1985) not only provide the susceptibility anisotropy, but also significantly improve the likelihood of recovering a primary depositional fabric (Piper *et al.* 1996) as the mineral's crystallographic axis ($k_{max}$) aligns parallel to the long axis of quartz grains during diagenesis, a process that may destroy the less stable magnetite. Confirmation of the importance of the paramagnetic contribution to susceptibility anisotropy has been determined from susceptibility versus temperature curves using the CS-3 apparatus coupled to the KLY-3 bridge (see Sagnotti *et al.* 1998 for a review of the method). Fabric tests that have a bearing on the critical assessment of the data set are presented as site means (e.g. A1, A2, etc) in Table 5.3. A more detailed breakdown of ellipsoidal shape, in the form of an L/F diagram is presented in Fig. 5.16. Additionally, as advocated by Taira (1989), q has been plotted against the grain imbrication (inclination of $k_{max}$ axes) as a means of discriminating between the four main depositional processes responsible for three-dimensional alignment of grains in the sedimentary environment (Fig. 5.17). Without exception, all the samples upon which conclusions on palaeoflow are based satisfy the criteria for a primary sedimentary fabric, and deposition appears largely to be under the influence of traction currents.

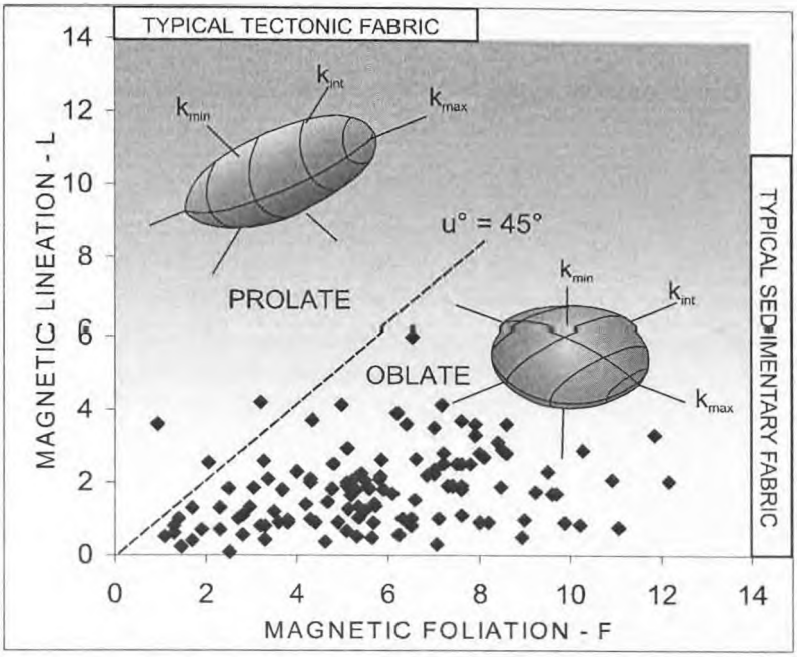



**Fig. 5.16.** Graphical illustration of the shape of AMS ellipsoids in an L/F-plot. Note that the shape parameter (angle u) describes the relative shape of the ellipsoids numerically. Results from the Ogof Velvet Formation clearly record oblate ellipsoids, which form the typical fabric of laboratory deposited sediments (Rees and Hamilton 1970).

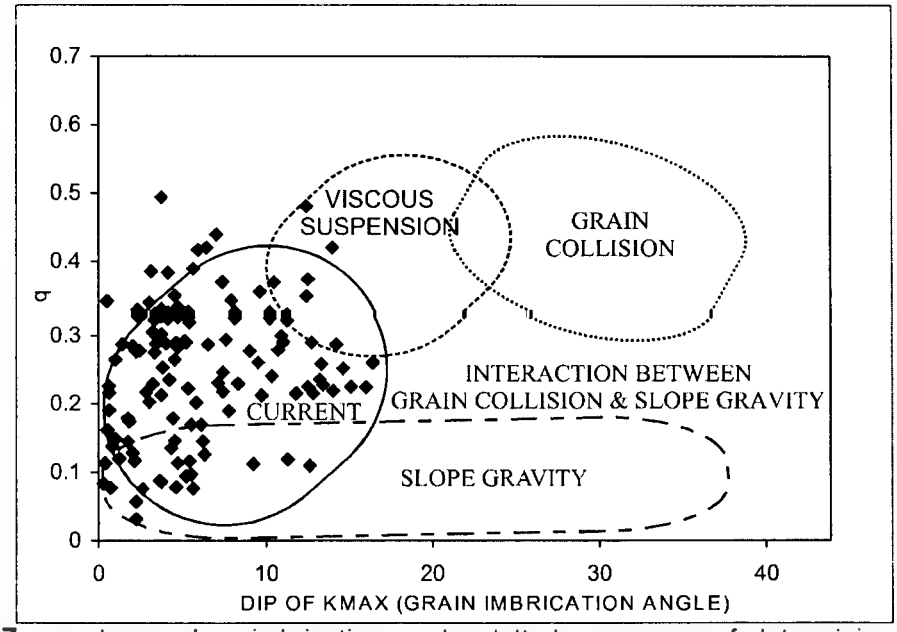



**Fig. 5.17.** q value vs $k_{max}$ imbrication angle plotted as means of determining the likely depositional process. Fields depict ranges obtained experimentally by Taira (1989). Low but perceptible imbrication values and low q indicate current deposition, which is consistent with a storm induced combined-flow.

### 5.4.4. Shelf hydrodynamics

Figure 5.12A summarizes approximately five hundred palaeocurrent readings from the Ogof Velvet Formation. The strong parallelism between AMS data and that obtained from sedimentary structures (Fig. 5.12A) is significant in two respects. Firstly, it suggests that the acquired fabric is of sedimentary origin (Liu *et al.* 2001), and secondly it endorses claims by Schieber and Ellwood (1988, 1993) that magnetic fabric analysis provides a unique and reliable tool in reconstructing ancient storm dynamics. The reconstruction and assessment of ancient shelf dynamics requires the integration of the dataset into a qualitative framework of motion based on modern storm hydrodynamics. This approach allows speculation on non-actualistic events such as geologically significant storms, whilst maintaining a firm grounding in plausible fluid dynamics and sediment transport processes (Myrow and Southard 1996). As much of our present knowledge on the forcing of currents on the continental shelf has developed from studies on the Mid Atlantic Shelf of the U.S.A. (Swift *et al.* 1983; Swift 1985; Swift *et al.* 1985; Swift and Niodorada 1985), the descriptive framework outlined in Fig. 5.14 is the obvious standard into which our data set should be integrated and conclusions on the changing force balance with depth be drawn. Palaeocurrent data integrated into this scheme is presented in Fig. 5.12B, with an additional breakdown of the inferred contribution of the main forcing mechanisms to the force balance equation (Fig. 5.12C). For convenience, palaeocurrent and grain fabric analysis is discussed within the context of zones of bypass, deposition, and condensation.

#### *5.4.4.1. Facies Association A: zone of nearshore bypass*

Palaeocurrent data from both erosional and depositional structures clearly indicate an orthogonal relationship between the inferred palaeoshoreline and current generated shear stresses (Fig. 5.12). This is the relationship widely reported from most ancient storm-affected shelves, and taken by Leckie and Krystinek (1989) as an indicator of quasi-steady shore-normal unidirectional flow. However, following Duke (1990), it is critical to establish whether the structures analysed are truly indicators of net flow rather than merely the response to peak near-bottom instantaneous shear stresses associated with orbital motion. Considering the shallow water depth inferred for Facies Association A, disregarding the modifying affect of wave processes may lead to erroneous conclusions on storm hydrodynamics.

The physical origin of channel scours, flute casts and gutter casts are admittedly problematic (Duke 1990, p 879), but can be most readily accounted for by powerful unidirectional-dominant flows (see Facies A2 and A3 for discussion). As highlighted by Myrow and Southard (1996), it has never been demonstrated experimentally that flute casts or sinuous gutter casts can form under oscillatory or combined-flows. QPL on the other hand is a poorly understood high energy combined-flow structure that may have considerable potential as a palaeocurrent indicator if it could be demonstrated that the characteristic downlapping laminae formed in response to unidirectional flows.

The three-dimensional grain fabric afforded by AMS provides an insight into the processes and flow regimes that lead to QPL. The results of fifty measurements are presented stereographically (Fig. 5.18A) and as a rose diagram (Fig. 5.12A). The bimodal data set can be divided into two distinct populations (Fig. 5.18A). Population 1 is a unidirectional fabric, with long axes of quartz grains (equivalent to the crystallographic axes of paramagnetic phyllosilicates) orientated perpendicular to the shoreline. This may suggest either shore-normal quasi-steady flow (Leckie and Krystinek 1989) or offshore-magnified wave-generated peak instantaneous shear stresses (Duke 1990). The strong parallelism between the orientation of sole structures, scours, downlap laminae and $k_{max}$ axes suggests unidirectional currents were largely responsible for grain axis alignment. This conclusion is substantiated by the direction of imbrication in Population 1. Very low angle offshore dipping imbrication is not consistent with deposition from upper flow regime (flat bed) unidirectional currents (Fig. 5.18B), purely oscillatory currents (Fig. 5.18D), or oscillatory-dominant combined-flows (Fig. 5.18E). Instead, this type of fabric displays all the characteristics of deposition on a very low angle offshore inclined surface (Rees 1965, Fig. 5.18C). This appears to substantiate claims by Arnott (1993) that QPL may record the seaward spread of a low angle sandbody, in this case an in-channel bar. Given the unidirectional downlap surface and long axis alignment, this must have migrated under the influence of substantial unidirectional currents.

Evidence for wave-generated processes, and thus a combined-flow regime is reflected in grain population 2, where bipolar long axis alignment (Fig. 5.18A) sub-parallel to the orientation of wave ripples (Fig. 5.12A) is consistent with a typical wave-generated fabric from hummocky cross-stratified beds (Cheel 1991, Fig. 5.18C). The fact that these subsamples are from the top of the cores suggests reorientation of grains during "late-stage" reworking of QPL divisions under an oscillatory-dominant combined-flow. It is interesting to note that Arnott (1993), deploying more traditional two-dimensional grain analysis, identified a very similar

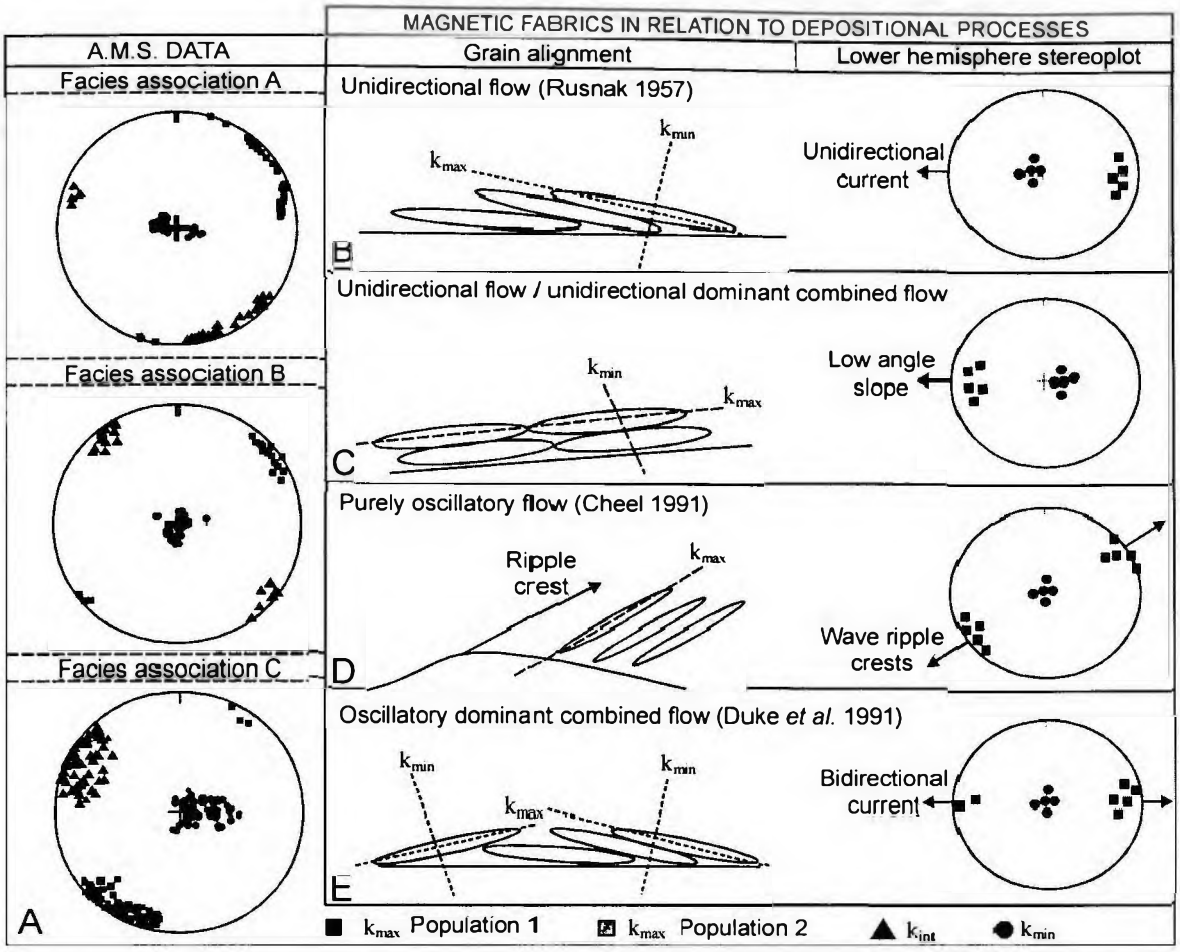



**Fig. 5.18.** (A) AMS data presented as lower hemisphere equal area stereoplots for facies associations A, B, and C. (B), (C), (D), (E) illustration of grain alignment and the expected stereographic representation for depositional process discussed in this study.

bimodal fabric in quasi-planar laminated intervals, which he also attributed to combined-flow with a significant unidirectional component.

Shore normal unidirectional currents can be most adequately accounted for by assuming close proximity to the shoreline, a conclusion consistent with the facies analysis. At these shallow water depths, not only will the pressure gradient be at its steepest (thus driving powerful offshore down-welling currents), but the limited vertical extent of the water column overlaps the surface and bottom boundary layers, resulting in no appreciable geostrophically balanced core flow (Fig. 5.14). Down-welling currents in the nearshore were also significantly affected by fair-weather processes, especially tides. The presence of gutter casts and channels imply amplification of down-welling currents in an ebb-dominated regime (Fig. 5.5). The development of secondary helical flow patterns will, assuming friction increases as the second power of current velocity (Myrow and Southard 1996), significantly

elevate frictional resistance at the base of the flow leading to channel and gutter scour. An important consequence of this in terms of the force balance equation is that, instead of sediment being lost from the flow through deposition, it is instead added through erosion as currents dissect the nearshore, thus increasing rather than decreasing the excess weight force (Fig. 5.12C). This process is essentially what has been termed "bulking" when applied to the ignition of deep marine turbidity currents that incise channels on submarine slopes. The only difference apart from scale is that enhanced erosive capacity is caused not by increased gradient but rather the superimposition of an offshore-directed tidal current. Any chance of substantial modification by the Coriolis force is further lessened as the flow would be accelerating and thus cannot be fully balanced (Duke 1990).

This process of flow bulking and the incision of nearshore channels and gutters appears to be controlled to some extent by available accommodation space. This is demonstrated in Table 5.1, where all the examples of nearshore incision coincide with periods of limited accommodation (the very early TST or mid to late HST). Forestepping shoaling-upwards cycles and a position above the transgressive shales of the Aber Llong Formation (Fig. 5.1A) suggest similar accommodation-limited conditions during deposition of the Ogof Velvet Formation. Although only a few studies have focussed on the role of relative sea level in the force balance equation (e.g. Swift and Thorn 1991; McKie 1993), the most obvious consequence of accommodation-limited conditions is an increase in friction at the base of the flow, with the likelihood of channel and gutter cast incision. This in turn should promote flows with higher than expected excess weight force. A similar occurrence of storm channelling during accommodation-limited late highstand deposition has been noted by Van Wagoner (1991), and attributed to prolonged non-deposition and erosion.

A final consideration on the shelf hydrodynamics of Facies Association A concerns the effect of very low nearshore wave energy on down-welling current velocity. The characteristics evident in this coastal facies suggest highly dissipative conditions where incoming waves are frictionally attenuated as they propagate across a very low gradient shelf. In a similar manner to the interaction of storm-generated currents and tides (Fig. 5.5), if wave orbital velocity was high, the asymmetry of motion would induce net bottom flow onshore, in the opposite direction to down-welling currents (Bowen 1980). Therefore, like the effect of strong flood tides, steady current flow in a wave-dominated nearshore is actually retarded (Grant and Madsen 1979), resulting in a significant reduction in velocity (Snedden and Swift 1991). Inverting this scenario, coastlines with low wave energy may be expected to

develop intensified offshore unidirectional flow because impedance by onshore waves is greatly reduced.

This coincidence between tidal regime, accommodation-limited conditions, wave orbital velocity, and ultimately nearshore incision and bypass are features implicit in the bypass-zone tempestite model (Table 5.1). We can therefore confidently argue that these features produce offshore-directed down-welling currents with the required velocity and frictional resistance to define a coastal zone where erosion is more significant than deposition.

*5.4.4.2. Facies Association B: Zone of inner–mid shelf deposition*

Directional trends from Facies Association B (Fig. 5.12A) are similar to those of Facies Association A, and record a dominantly offshore flow trajectory at high angles to the shoreline. Of some significance is the slight (10–20°) counter clockwise deviation of depositional flow indicators such as QPL downlap, cross-lamination, and grain long axes which appear to demonstrate a minor component of geostrophic deflection. The grain fabric from quasi-planar laminated intervals (Fig. 5.18A) again records seaward dipping imbrication reflecting the migration of a low angle bedform. The lateral continuity of bedding in outcrop suggests that foresets may represent the leading edge of an offshore migrating sand sheet as originally envisaged by Arnott (1993) for quasi-planar downlap surfaces.

The presence of offshore-directed, weakly geostrophically balanced currents operating below fair-weather wave base suggests expansion of the frictional zone beyond the limits commonly encountered on modern shelves such as the Mid North Atlantic (Swift and Niodorada 1985). This apparent non-uniformitarian dilemma has been reported from a number of ancient sequences (e.g. Duke *et al.* 1991b; Jennette and Pryor 1993), and is commonly associated with either high velocity jetting of flows from nearshore channels, limitations on accommodation space, or low Coriolis Force in equatorial latitudes (Duke *et al.* 1991b; McKie 1993). A low value for the Coriolis parameter is unlikely considering the high latitude of Avalonia during the Cambrian (Torsvik *et al.* 1996), but the effects of more proximal flow confinement (Facies Association A), and limited accommodation space in particular, offer plausible mechanisms for high angle offshore directed flow. Currents emanating from nearshore channels and gutters may be analogues of the high-speed jets described from modern settings by Csandy (1977) and Swift *et al.* (1985). A combination of storm–tide interaction, nearshore channels and subsequent high velocity jets were, according to Duke *et al.* (1991b), important prerequisites in the expansion of the

frictional zone in the Silurian Medina Formation of Ontario and New York. They likened their example to the North Sea Heligoland Bight, which is dissected by subtidal channels that are regularly flushed of sediment by coastal down-welling jets enhanced during ebb tide.

Although directional data clearly suggest a force balance firmly weighted towards high pressure gradient and elevated excess weight force (Fig. 5.12C), slight geostrophic veering, which was also reported in the example by Duke *et al.* (1991b), does imply slight modification to the force balance with increasing depth. Minor Coriolis deflection is considered a function of increased water depth and thus a greater geostrophic core flow, coupled with a slight decrease in velocity of the pressure gradient current as tidal amplification is removed (Fig. 5.12C). This reduction in flow velocity also induces a feedback mechanism of reduced excess weight force (Fig. 5.16C) as the current becomes depositional rather than erosional. The lateral spread of the flow as it exits nearshore conduits has two consequences. On the one hand, reduction in the excess weight force will promote geostrophic veering as the bulk density is reduced during progressive deposition, and additionally, the lateral spread of the flow at channel mouths will increase the surface area and thus elevate frictional resistance. In terms of architectural elements, the transition downslope from multi-event channels of Facies Association A to thick, sheet-like, amalgamated sandstones of Facies Association B. may be likened to the channel-lobe transition (high sediment accumulation zone) commonly identified in deep marine turbidite fan complexes (Mutti *et al.* 1999). The offshore migrating sand sheet envisaged for quasi-planar downlap may be more accurately described as a seaward spreading depositional lobe. The inner to mid-shelf would therefore consist of a number of coalescing sandy lobes formed at the mouths of nearshore conduits (Fig. 5.12B).

*5.4.4.3. Facies association C: zone of outer shelf condensation*

Palaeocurrent data from flute casts, cross-lamination, and grain long axes (Fig. 5.12A), record a flow azimuth oblique and to the left of shore perpendicular. This suggests that currents in this outer shelf setting operated under forcing mechanisms that more closely approximate the force balance recorded in the geostrophic zone on modern shelves. There are two reasons why the current did not attain a full geostrophic balance and thus shore parallel flow. Firstly, the forcing mechanisms were so heavily weighted towards offshore flow (high driving forces) on the inner and mid shelf that, even in more distal locations, unidirectional velocity was still

significant, as indicated by flute casts on basal surfaces and well-defined onshore dipping grain imbrication (compare Fig. 5.18A with 18B). Furthermore, the thickness of B/C tempestites suggests that excess weight forces may have been at least an order of magnitude greater than that expected from sediment-deficient modern examples. Secondly, slump structures (Facies B3) developed in roughly the location of storm wave base reflect an increase in the shelf gradient that may have accelerated flow orthogonal to bathymetric contours.

### 5.4.5. Combined-flow characteristics: the role of storm type and fetch

Two factors that have been neglected so far in the assessment of storm dynamics are the roles of storm type/intensity and fetch. The principle control on down-welling velocity is the extent of the pressure gradient developed during coastal set-up, which is in turn dependent on the intensity and duration of storm winds (Myrow and Southard 1996). Assuming that present-day atmospheric circulation patterns prevailed in the past, the storms most likely to affect shallow marine depositional environments are severe tropical cyclones (hurricanes) and mid-latitude intense winter storms (Masaglia and Klein 1983). Hurricane deposits are restricted to latitudes of about 10–45°, while intense winter storms may be expected from latitudes of 40–80° (Duke 1985, Barron 1989). Avalonia was situated at approximately 70°S during the Cambrian (Torsvik *et al.* 1996), well within the belt for intense winter storms.

Studies on the Mid Atlantic shelf (e.g. Swift *et al.* 1983 and Swift and Nummedal 1987) suggest that intense winter storms couple more effectively with the water column than hurricanes, and generate shelf flows of greater duration and spatial coherence. As a result of sustained sediment transport over great areas of the shelf, winter storms are more likely to generate combined-flows with a persistent unidirectional component (Duke 1985). This may well account for some of the more unusual features of the Ogof Velvet Formation, such as elevated bed thickness, combined-flow rather than wave-formed vortex ripples on upper bed surfaces, and the dominance of wholly quasi-planar laminated sandstones. The almost total absence of accretionary HCS suggests that at no point during storm evolution could large 3D bedforms maintain equilibrium with the flow.

This line of reasoning was applied by Duke (1985, 1987) to account for the preferred palaeolatitudinal distribution of HCS in low latitudes, as hurricanes are more likely to induce a very oscillatory-dominant combined-flow. Winter storms on the other hand would be expected to generate sedimentary structures that closely

resemble those formed under purely unidirectional flow (Duke 1985). This appears to be substantiated by the presence of "hummocky megaripples" on the Mid Atlantic (Swift *et al.* 1983) and Scotian (Amos *et al.* 1996) shelves formed under unidirectional-dominant combined-flows during intense winter storms. Although the example by Swift *et al.* (1983) was interpreted as a modern equivalent of HCS, foreset dip angles close to the angle of repose, and thinning of laminae into swales is more consistent with high angle trough cross-bedding formed under powerful unidirectional currents (Duke 1985). As many ancient storm-dominated sequences are composed almost entirely of fine sand, unidirectional-flow dunes are unlikely to be developed, as ripples pass directly into plane bed with increasing flow velocity (Middleton and Southard 1984), and thus the ancient equivalent of these largely transgressive megaripples may very well be QPL.

The contributions to elevated unidirectional currents are both varied and dynamic, but it is interesting to speculate on the possible relationship between intense winter storms and quasi-planar laminated sandstones. A good example is the study conducted by Arnott (1993) from the Lower Cretaceous (Albian-Cenemonian) Bootlegger Member of Montana. Coarsening upwards parasequences are dominated by QPL, with only two beds out of many hundreds containing HCS (R. Arnott pers. comm. 2003). This implies that unidirectional currents inhibited the development of large amplitude bedforms during practically every single storm, and in all sub-environments between storm and fair-weather wave base. Although no reason for this bias in terms of elevated unidirectional currents was offered by Arnott (1993), integration of the data set into a detailed reconstruction of Cretaceous palaeogeography and storm tracks suggests a possible link to intense winter storms.

It is well documented that occurrences of HCS in shallow marine sediments bordering the Cretaceous Western Interior Seaway (WIS) are not evenly distributed, with a very strong bias towards Late Cretaceous examples (Masaglia and Klein 1983; Duke 1985; Barron 1989). According to Barron (1989), this contrast in storm sedimentation is directly linked to the type of severe storm affecting the seaway, which in the Cretaceous was largely controlled by landmass configuration. Fig. 5.19 illustrates the difference in characteristics of the Tethys Ocean during the late Albian and early Maastrichian. A well-developed Tethys during the Albian (Fig. 5.19A) produced a very zonal subtropical high-pressure zone that steered hurricanes into the Pacific, blocking penetration and landfall in the Northern Hemisphere. The WIS was therefore protected from severe storms except in the northern segment, where coastal areas such as Montana and Alberta were profoundly affected by the Pacific winter storm track (triangles in Fig. 5.19A).

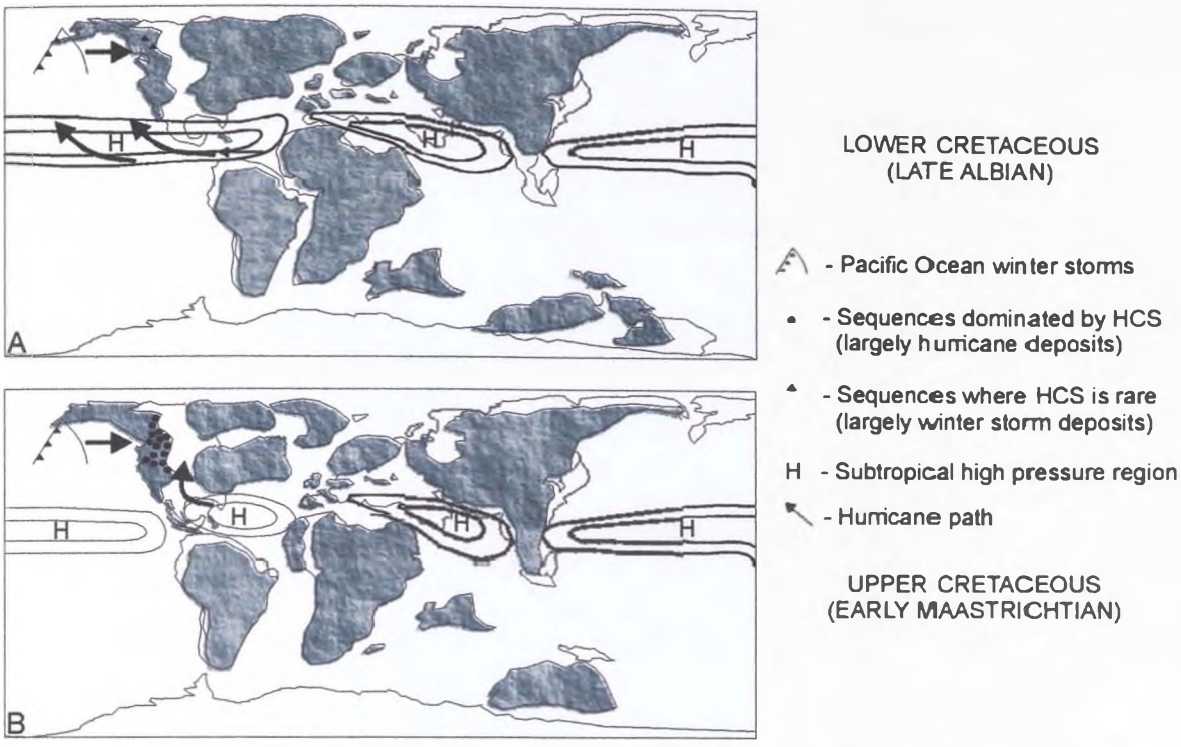



**Fig. 5.19.** Schematic position of the sub-tropical high pressure zone in the Northern Hemisphere and inferred hurricane and winter storm paths for: (A) Late Albian and (B) Early Maastrichtian palaeogeography (modified from Barron 1989). Note the wide disparity in occurrences of HCS around the Western Interior Seaway between the Early and Late Cretaceous. This according to Barron (1989) is a function of hurricane landfall down the axis of the Western Interior Seaway, which is promoted by the position of the continents in the Maastrichtian.

This conclusion is consistent with unidirectional-dominant stratification sequences in the Bootlegger Member and other more northerly Lower Cretaceous successions such as the Moosebar Formation of Alberta and the Kootenia Formation of Montana (Table 5.1). Many of these Lower Cretaceous sequences have been interpreted by Masaglia and Klein (1983) and Duke (1985) as intense winter storm deposits. In contrast, during the Maastrictian (Fig. 5.19B) the developing North Atlantic Ocean led to a more cell-like subtropical high and with a prominent Mexican Peninsula resulted in the steering of hurricanes into and down the axis of the WIS. Consistent landfall of hurricanes would account for the numerous examples of HCS during this period (Barron 1989, fig. 11).

Although it is clear from the limited occurrence of QPL that not all intense winter storms will produce this style of stratification, it is interesting to note that all the known occurrences (referenced in Facies B1) are from continents situated within the mid-latitude storm belt. This may also be extended to the examples of nearshore incision presented in Table 5.1. Out of the fourteen studies where intense unidirectional flows have been documented, nine are associated with winter storms,

four within the combined belts of hurricanes and winter storms, three within the hurricane belt.

We have presented a conceptual argument to account for storm deposited sandstones that lack vertical stratification sequences associated with migratory and non-migratory large amplitude bedforms (A-HCS and An-HCS respectively). Although persistent unidirectional currents limit the variability of possible combined-flow structures, this has no bearing on the abundance and distribution of SD-HCS, as the main prerequisite is not a stable bedform but rather a scoured (hummocky) second-order internal erosion surface. The 3D hummocky geometry of this internal erosion surface (Fig. 5.7C) suggests wave scour as the most likely generative mechanism (Duke 1985). The cycle of erosional scour and plain bed drape has been linked to alternating periods of exceptionally high waves formed by constructive interference (scour), and "normal storm waves" (plane bed drape) (Cheel and Leckie 1993). It appears likely therefore that the limited occurrence of SD-HCS in the Ogof Velvet Formation is related not to unidirectional current velocity but rather wave climate, and in particular the lack of intermittent large constructive waves.

The fundamental control on the wave system is the distance over which prevailing winds travel over a body of water (i.e. the fetch), which is largely a function of basin configuration. Shelves bordering open oceans tend to be dominated by long period swell waves (large ocean waves), while restricted basins are characterised by short period local waves (smaller sea waves) (Hill and Nadeau 1989, Hill *et al.* 2003). The restricted nature of the Welsh Basin during the Cambrian has been noted by many authors (Crimes 1970a; Pratt *et. al.* 1994*)*. Deposition of the Ogof Velvet Formation therefore probably operated under fetch-limited conditions (Hill and Nadeau 1989), and a wave regime dominated by short period local waves. Although clearly energetic enough to induce plane bed combined-flow bed configurations, the lack of long period ocean swells would reduce significantly the number of second-order internal erosion surfaces, and thus the main prerequisite for SD-HCS formation. This line of reasoning also adequately accounts for the lack of SD-HCS reported by Arnott (1993) from the Bootlegger Member, as the Lower Cretaceous western interior was also a fetch limited seaway (Duke 1987; Swift and Nummedal 1987) prior to eustatically induced expansion in the Late Cretaceous (Lemon 1993).

### 5.4.6. Temporal and spatial evolution of storm induced combined-flow

#### *5.4.6.1. The acceleration matrix*

Very few studies have attempted to reconstruct the evolution of storm-generated circulatory currents in both space and time. Notable exceptions include Allen (1984) and Myrow and Southard (1996). The approach and methodology applied in this reconstruction follows theoretical considerations of fluid motion based on simple physical equations (Kneller 1995). Although Kneller's (1995) work was designed to account for the wide range of facies associated with deposits from deep marine fully turbulent non-cohesive flows, the exact forcing mechanism does not impose a restriction to wider application.

Temporal flow evolution may be described in terms of waxing (mean velocity at a point increases with time), steady (mean velocity at a given point remains unchanged over time) and waning (mean velocity at a given point decreases with time) (Kneller 1995; Mulder and Alexander 2001). The fundamental control on temporal variation that determines whether the current displays a well-defined waxing phase is the mechanism for flow initiation. Turbidity currents for example may behave as either instantaneous surges if triggered by slope failure, or longer duration quasi-steady currents generated by hyperpycnal river effluent (Mulder *et al.* 1998; Plink-Björklund and Steel 2004). Only the latter example would display a well defined temporal variation in flow evolution (waxing-steady-waning) as the nature of the current is reliant on the steadily increasing then decreasing flood hydrograph. If we consider the storm system, variations in flow velocity and competence over time may be framed into three similar evolutionary phases (1) storm growth (waxing flow) (2) full storm (steady flow) and (3) storm decay (waning flow) (Allen 1984). This temporal variation is not only well documented from current velocity measurements on modern shelves (Hèquette and Hill 1993; Hill *et al.* 2003), but also from sedimentary structures in ancient deposits (Craft and Bridges 1987, Arnott 1993, this study - Facies B2 and Fig. 5.9).

Spatial flow variation may be referred to as accumulative (mean velocity increases in the direction of flow), uniform (velocity consistent along the flow path), or depletive (mean velocity decreases in the direction of flow), and is controlled primarily by the local geomorphology (Kneller 1995). Accumulative flow is promoted when currents are restricted laterally (convergent or channelled flow) or accelerated downslope, whereas depletive conditions are generated during flow divergence (e.g. on a depositional lobe) or at the base of slope. An additional feature in shallow marine environments is the effect of ambient currents, particularly those associated with the tidal cycle. Although not applicable to deep marine turbidite systems and so not discussed by Kneller (1995), tidal amplification of storm-induced quasi-steady flow may also promote accumulative flow although, like the channels these flows

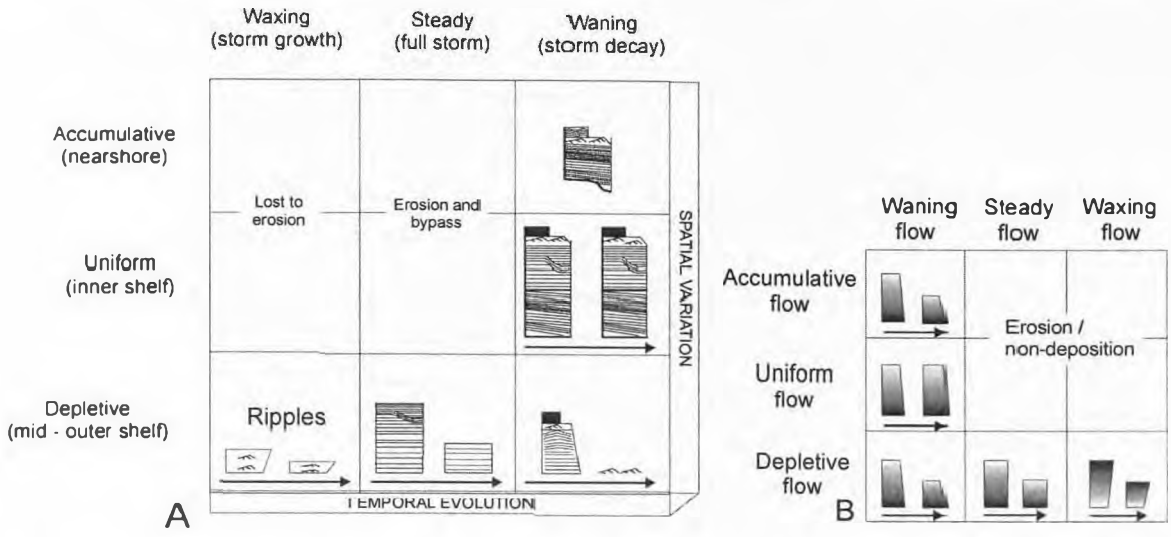



**Fig. 5.20.** Acceleration matrix, with illustrative bed sequences for each field showing downstream and vertical changes in relative grain size and sedimentary structures (arrows point downstream). (A) Acceleration matrix for quasi-steady storm-induced combined-flow based on characteristics present in the Ogof Velvet Formation. (B) Acceleration matrix for quasi-steady turbidity currents (modified from Kneller 1995).

produce, flow acceleration would be restricted to the nearshore (Facies A3). Beyond the influence of tidal enhancement (inner shelf), flow would be largely depletive forming depositional lobes (Facies Association B) at the mouths of nearshore conduits.

The time-space evolution of quasi-steady currents can be presented as a matrix diagram of spatial vs. temporal variation (Fig. 5.20). By applying simple physical equations, Kneller (1995) demonstrated that deposition may occur not only from unidirectional waning flow (modelled by the Bouma sequence) but also from steady and waxing flow. Of the nine possible fields, four are considered erosional or sites of non-deposition as none of the particles in the flow experiences any net decrease in mean stream wise velocity (Kneller 1995). In those fields that experience deposition, the deposit in terms of grain size variation is presented schematically in Fig. 5.20B by grain size logs in relative proximal (left) and distal (right) positions. These various styles of graded profile are adequate for the quantification of time-space variations in currents with a wide range in grain size, but offer only limited interpretative value in well-sorted predominantly fine-grained storm deposits. Instead, flow evolution is more adequately reconstructed from vertical stratification sequences as demonstrated in bedform stability presented in Facies B2 (Fig. 5.9). This temporal record, when integrated with lateral facies changes across the shelf, allows for full time-space analysis.

The storm-facies acceleration matrix based on characteristics of the Ogof Velvet Formation is presented in Fig. 5.20A. The qualitative differences between these deposits are outlined below:

*5.4.6.2. Depletive waxing flow*

The field of depletive waxing flow would record the earliest phase of storm growth as coastal set-up developed, and thus currents experienced on the shelf are generally of the lower flow regime. Depending on grain size variability, waxing flow velocities may be expected to produce a coarsening upwards inversely graded profile (Fig. 5.20B) coupled with a variety of ripple forms (Fig. 5.20A). Relatively common wave formed vortex ripples (Craft and Bridges 1987), asymmetrical current ripples (Arnott 1993) and 3D combined-flow ripples (Midtgaard 1996, and this study) formed at the base of storm emplaced sandstone beds suggests that these early currents existed as purely oscillatory, purely unidirectional, or variably developed combined-flows. Flow characteristics probably depend on the response time of the coastal zone to wind induced forcing mechanism (Hèquette and Hill 1993). The distal expression of depletive waxing flow would be down-current fining and sediment starvation possibly characterised by fading ripples (McCormick and Grotzinger 1993).

*5.4.6.3. Depletive steady flow*

The field of depletive steady flow would produce beds or divisions with no significant variation in grain size or flow regime (Fig. 5.20). Steady flow approximates full storm conditions where both the oscillatory and unidirectional components of combined-flow are at a maximum. This is commonly represented in both modern and ancient deposits as a plane bed configuration formed at current velocities well beyond the stability threshold for bedforms. Depending upon the frequency of exceptionally large constructive waves, and thus any limitations on fetch, the sedimentological expression of plane bed conditions may be either SD-HCS (when scoured second-order internal erosion surfaces develop) or parallel lamination (Facies B2). In more distal locations, across shelf fining would be expected, as well as a decrease in the oscillatory component (Airy wave theory) as the combined-flow becomes unidirectional-dominant close to storm wave base. This is commonly represented in ancient successions by a decrease in SD-HCS from relatively proximal to distal localities (Hamblin and Walker 1979). Depending upon the initial strength of the unidirectional currents (related to storm type) and the rate of its spatial deceleration,

the combined-flow may operate within the field of large 3D ripples and thus we might expect A-HCS and An-HCS (Facies B2). In rare circumstances such as those outlined by Myrow *et al.* (2002), persistent low energy combined-flows may form thick divisions of climbing ripple lamination. Beyond storm wave base, currents are purely unidirectional and form Tb (parallel laminated) divisions of B/C tempestites (Facies C1).

*5.4.6.4. Depletive waning flow*

Depletive waning flow produces the classic graded bed popularized in models by Bouma (1962) and Lowe (1982). Many storm depositional models are also based on the notion of temporal (waning) and spatial (depletive) deceleration (e.g. Dott and Bourgeois 1982; Walker *et al.* 1983). Vertical stratification sequences developed during temporal deceleration are generally rather variable (see Facies B2) reflecting the relative contributions and rate of deceleration of unidirectional and oscillatory currents in the combined-flow. The most commonly recorded trend on modern shelves is a rapid decrease in the unidirectional current relative to the oscillatory current as the combined-flow evolves from unidirectional to oscillatory-dominant (Hill *et al.* 2003). This trend is consistent with most ancient examples of HCS and is well recorded in Facies B2 (Fig. 5.9). In a similar manner to spatial deceleration of steady unidirectional flows, temporal deceleration of depletive unidirectional flows will promote, under an oscillatory-dominant combined-flow, the growth and possible migration of 3D hummocks from the parallel laminated division (which is an artefact of the earlier depletive steady flow at the full storm stage). Conversely, during more intense storms, or under forcing mechanisms that promote sustained unidirectional currents (e.g. intense winter storms), beds may be wholly parallel laminated as recorded by Arnott (1993) or display SD-HCS throughout most of the deposit.

The final remnants of storm-induced circulation may operate under weak combined-flows, purely oscillatory flows, or rarely purely unidirectional flows, which results in reworking of the seabed into small 2D and 3D ripples. Grain size variations across the shelf from proximal to distal locations may be modelled on the Bouma sequence, with down-current fining. The concomitant decrease in wave activity may first produce micro-HCS (Dott and Bourgeois 1982) followed by wave or combined-flow ripples. Below storm wave base, ripples are solely current generated forming the Tc division of B/C tempestites (Facies C1).

*5.4.6.5. Uniform waning flow*

The field of uniform waning flow (Fig. 5.20) demands rather unusual conditions where spatial flow remains at a fairly constant velocity resulting in no apparent distal fining or change in vertical stratification sequence. Uniform waning flow would probably develop on shelves with an incised nearshore and exceptionally strong tidally enhanced currents, occupying a position between accumulative currents in the nearshore and depletive currents on the mid-shelf. Uniformity in spatial acceleration may thus result from high speed jetting from nearshore conduits over a relatively uniform gradient. A very low gradient platform-like setting is consistent with the depositional model for the Ogof Velvet Formation discussed in the next section. In this proximal location where flows have yet to decelerate, the combined-flow is dominated by the unidirectional component. Depending upon the nature of the storm and the available fetch, plane bed configurations would be characterized by either parallel lamination, QPL, or SD-HCS (Facies B1). We would expect from the distal to proximal inner shelf, an inverse correlation between true bedform configurations such as A-HCS and plane bed structures. On shelves with similar forcing mechanisms to those identified in the Upper Cambrian Welsh Basin, the inner shelf is unlikely to be conducive to the formation of large amplitude bedforms throughout storm evolution. Kneller (1995) referred to the spatial distribution of this type of profile being generated by "slab" models (Allen 1985). This would account for the extensive across shelf distribution of the quasi-planar laminated facies in both this study and that recorded by Arnott (1993).

*5.4.6.6. Erosion and sediment bypass*

Theoretical considerations (Kneller 1995) suggest that flows that are accumulative waxing and accumulative steady, and those that are uniform waxing or uniform steady, are likely to be erosional and thus locations of sediment bypass (Fig. 5.20). I prefer to modify this conclusion and refer only to accumulative and uniform steady flows as erosive, whereas waxing accumulative and waxing uniform flow deposits are simply lost to later erosion once full storm (steady) conditions are achieved (Fig. 5.20A). It is unlikely that during the early waxing phase of current velocity (in our case storm growth), currents will be immediately capable of erosion or even non-deposition. Rather, the preservation in the rock record of a lower rippled division is a function of location, as nearshore and inner shelf settings are areas of later erosion during full storm (steady flow) conditions.

Considering that most storm deposits in proximal locations display some form of basal erosion surface suggests at least uniform conditions are attained during the full storm stage. To account for nearshore incision of gutter casts and channels it would appear that flow in the nearshore during Ogof Velvet deposition and most, if not all, of the examples in Table 5.1 must have operated under an accumulative regime. As discussed above, this is probably a function of storm flow enhancement by ebb tides as well as powerful secondary helical flows forming preferentially in pre-incised linear depressions (lateral confinement). Erosion and bypass beyond the influence of tides is probably maintained during the full storm stage by high velocity jets at channel mouths. This accounts for gutter casts at the base of Facies B1 sandstones, which are often the only remnants of uniform steady flow (bypass).

*5.4.6.7. Accumulative waning flow*

Accumulative waning flow produces grain size profiles and vertical stratification sequences that are virtually identical to those formed under uniform waning flow (compare Facies A3 and B1). The location of accumulative flow is for the most part a site of erosion and bypass (Fig. 5.20), and deposition during storm decay generally occurs within the confines of linear depressions such as gutters and channels. The efficient bypass of sediment through the nearshore and out onto the shelf results in a relatively condensed and inversely graded nearshore profile, in the sense that the coarsest material bypasses the most proximal location. Therefore proximality trends display a coarsening upwards (Facies C2–B2) then fining upwards (Facies B2–A1) motif in progradational successions (Fig. 5.3). These trends essentially define the bypass-zone tempestite model (Myrow 1992a; Perez-Lopez 2001).

*5.4.6.8. Storm flow evolution in the Ogof Velvet Formation*

The temporal and spatial evolution of combined-flow, assuming a fairly simple increasing-decreasing oscillatory component, may be analysed in terms of unidirectional flow efficiency. The concept of flow efficiency is well developed (e.g. Mutti 1992; Mutti *et al.* 1999), and is defined as "the ability of a flow to carry its sediment load basinwards" (Mutti *et al.* 1999, p. 25). Although a fairly routine concept in the description and interpretation of deep marine turbidite systems (e.g. Pickering *et al.* 1989), and to a lesser degree hyperpycnal turbidites on flood-dominated deltas (e.g. Mutti *et al.* 1996, 2000), its application to storm deposits has yet to be demonstrated.

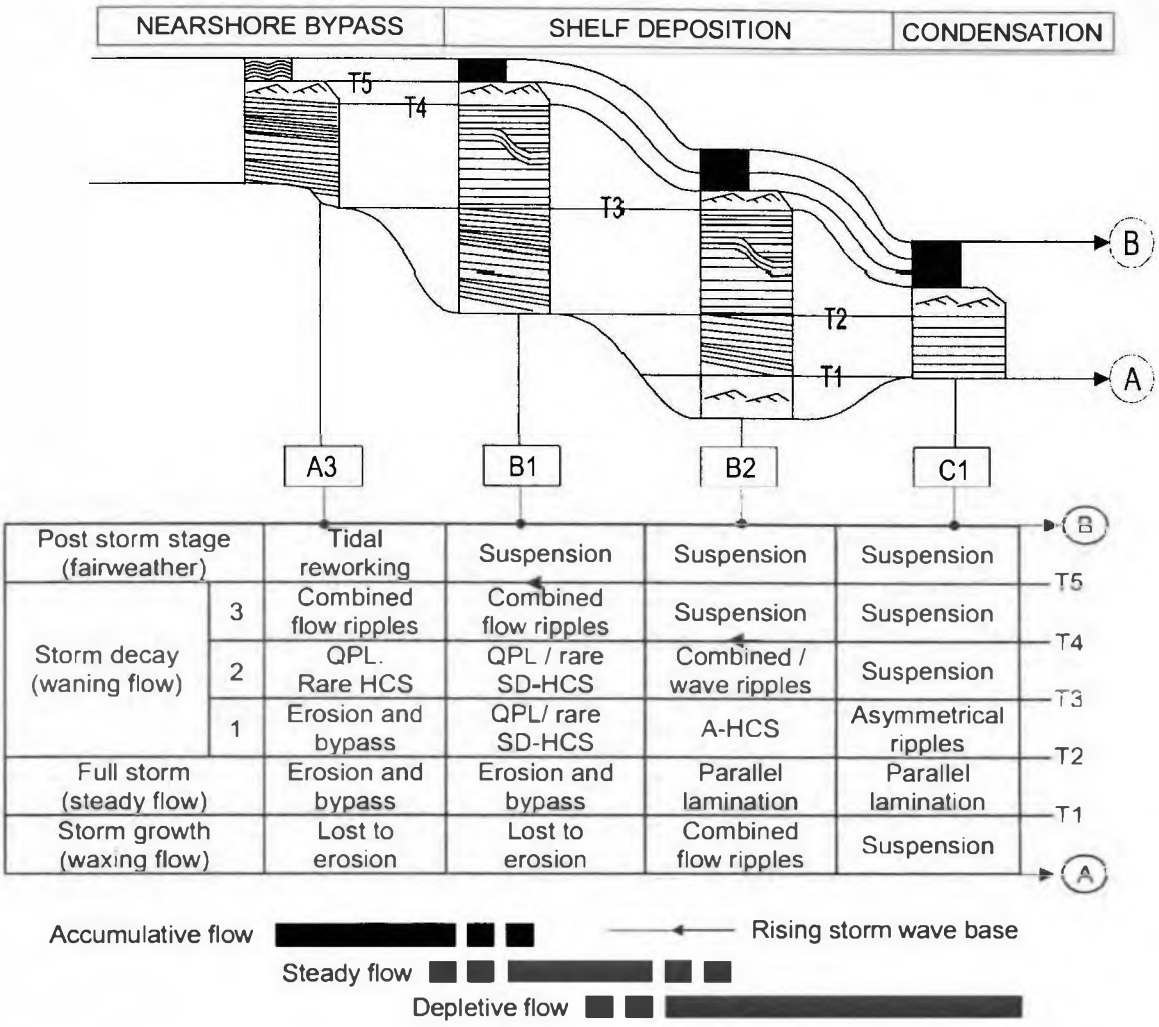



**Fig. 5.21.** Temporal and spatial evolution of storm-induced combined-flow experienced during Ogof Velvet deposition (see text for details).

Figure 5.21 displays the basic sequential arrangement of the most common facies tract identified in the Ogof Velvet Formation. The growth phase of storm sedimentation (A to T1 in Fig. 5.21) is characterized by waxing combined-flow velocities, and poorly efficient distribution of sediment across the shelf, resulting in only a thin rippled basal division irrespective of position on the shelf. Full storm conditions (T1–T2) promote very efficient unidirectional currents that induce nearshore bypass both on the accumulative nearshore (gutters and channels) and to a lesser extent the steady inner shelf (gutters). Intensive erosion in these locations reworks previously deposited sediment emplaced during waxing conditions. Decelerating (depletive) currents on the mid- to outer shelf are also predominantly unidirectional, and thus suppress bedform development resulting in parallel lamination.

The onset of waning flow conditions (storm decay 1, Fig. 5.21) marks a concomitant decrease in flow efficiency resulting in large-scale deposition, particularly in proximal facies that were former zones of bypass. The relatively condensed nature of nearshore channel fills compared, for example, to the inner shelf suggests efficient bypass continued during early storm decay (T1–T2, Fig. 5.21). On the inner shelf, QPL records the offshore migration of depositional lobes developed at the mouths of nearshore conduits (Fig. 5.12B). The spatial deceleration of unidirectional currents as the flow spreads laterally is documented by the across shelf transition from plane bed to lower flow regime configurations i.e. QPL to An-HCS and A-HCS. Below storm wave base, weak unidirectional currents reworked sand emplaced during full storm conditions into asymmetrical ripples. Continued waning of the combined-flow ultimately lead to deposition within nearshore conduits (storm decay 2, Fig. 5.21). This reduction in flow efficiency means that little sediment escapes the nearshore and inner shelf, effectively starving more distal locations (zone of condensation in Figs. 2, 11B, and 20). Low competence flow on the mid-shelf remoulds the just-deposited sandy substrate into either combined-flow or wave ripples. The outer shelf was essentially devoid of currents, resulting in post-storm fallout of fines. Although not recorded in the present study, this early fallout phase may produce graded rhythmites (Reineck and Singh 1972).

Currents in the final stage of storm decay (T4–T5, Fig. 5.21), restricted to nearshore and inner shelf locations, were weak combined-flows that remoulded sands into wave and combined-flow ripples. In greater water depths, the rising storm wave-base produces a relatively quiescent water column promoting fine-grained suspension sedimentation. Conditions during the post storm stage (T5–B) continued this trend, with suspension deposition in all environments below fair-weather wave-base. Wave attenuation across the inner shelf and nearshore is an important process during fair-weather periods. Without large breaking waves, and thus an effective nearshore circulation cell, fine-grained sediment only moved onshore, thus maintaining the fine-grained inversely graded shoreline profile.

Although these spatial and temporal trends in storm evolution are based solely on the vertical and lateral variation in stratification sequence in the Ogof Velvet Formation, the conclusions applicable to the examples of nearshore bypass listed in Table 5.1. As this type of study offers a means by which to study the potential multiplicity of storm processes by providing a workable framework of spatial and temporal flow variation, its utility may be expanded to include the storm depositional system in general.

### 5.4.7. Shelf dynamics: concluding remarks

The palaeohydraulic reconstruction of the Upper Cambrian shelf during deposition of the Ogof Velvet Formation (Fig. 5.12) differs quantitatively if not qualitatively from models developed from direct measurements on modern storm-affected shelves. Although it is critical for geologists working on ancient sequences to maintain a firm grounding in plausible fluid dynamics and sediment transport processes, it is equally important to address obvious disparities between modern and ancient deposits, and to consider processes under non-actualistic conditions. The role of excess weight of sediment-rich dispersions is an example where a strict uniformitarian approach is inadequate to account for the potential multiplicity of storm processes operating during the geologically significant event. This is not to say that offshore-directed flows are necessarily turbidity currents, but rather that tempestite deposition involves a four-part force balance problem (Figs. 12C) with variable contributions from pressure gradient, frictional, Coriolis, and excess weight forces. As demonstrated by Myrow and Southard (1996), the true variability of tempestite deposition should be studied and framed within this force balance equation.

The contributions to, and the characteristics of, storm-induced combined-flows are both varied and dynamic, but may be better understood when sedimentological data is integrated with known palaeogeographical/environmental constraints such as relative sea level changes, palaeolatitude, and fair-weather ambient processes. To illustrate this, a flow chart is presented in Fig. 5.22 that summarizes the main controls on the storm system during deposition of the Ogof Velvet Formation, as well as the key processes that dictate the force balance equation. By reversing the flow chart (thus beginning with depositional properties) and fully utilizing understanding of the balance of forces, we can adequately account for the physical and environmental factors that promote coastal bypass. As inferred from the earlier review of the literature on nearshore incision, powerful offshore-directed currents enter the realm of accumulative flow when amplified by ebb tidal currents in a low wave energy setting where impedance in the wave boundary layer is significantly reduced. The necessary shear stresses that promote incision are a function of current velocity and limitations in available accommodation space. A combination of nearshore accumulative flow and accommodation-limited conditions also dictate the flow direction, internal stratification sequence, and the extent of sand dispersion onto the shelf by expanding the friction zone while at the same time inducing a style of jet flow as currents emanate from nearshore conduits.

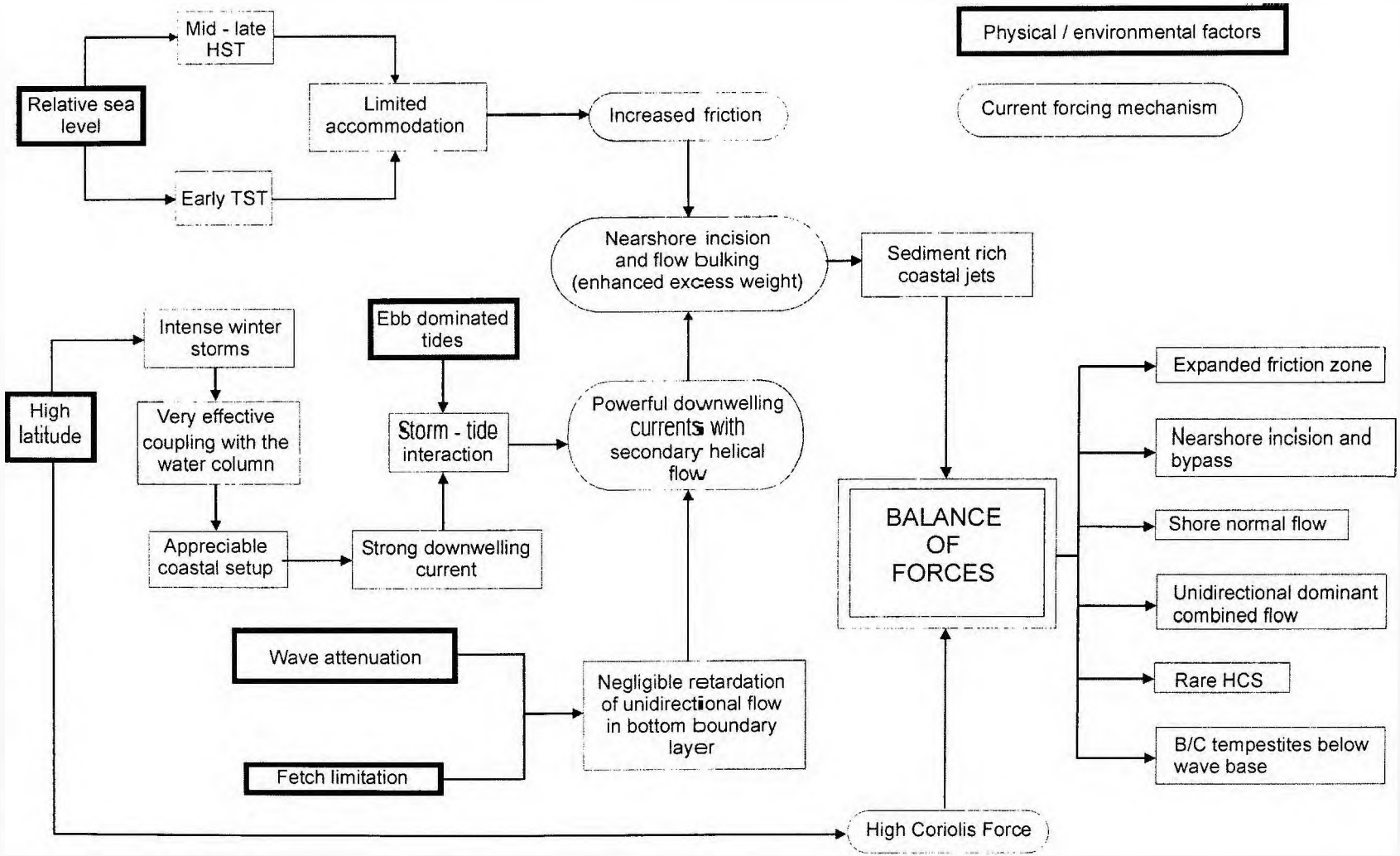



**Fig. 5.22.** Summary flow chart illustrating the main controls on the storm system during deposition of the Ogof Velvet Formation. Key processes that dictate the force balance equation are also highlighted.

## 5.5. THE BYPASS-ZONE TEMPESTITE MODEL: ENVIRONMENTAL SIGNIFICANCE

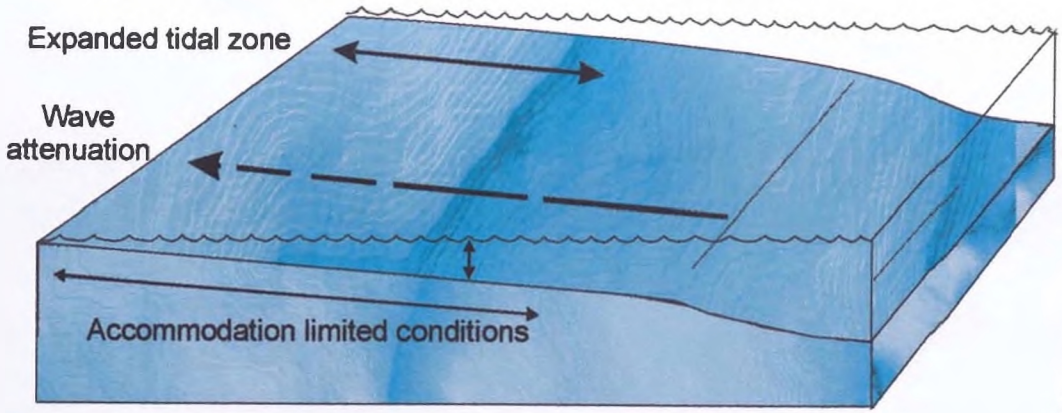
### 5.5.1. Depositional setting

The final part of this study attempts to address some of the broader aspects of the bypass-zone tempestite model by placing the controls and processes illustrated in Fig. 5.22 into their wider environmental context. According to Myrow (1992a), nearshore bypass is the typical hydrodynamic response of the shelf to storm processes acting on highly dissipative muddy shorelines, a conclusion consistent with the sedimentological features of the Ogof Velvet Formation, and all the examples presented in Table 5.1. Of particular significance, and the cause of the dissipative regime, is the restriction of sediment bypass to depositional environments associated with aerially extensive, very low gradient platforms. This is well illustrated in the examples presented in Table 5.1, where nearshore incision preferentially occurs on highstand carbonate platforms, and early transgressive/late regressive fine-grained subaqueous delta platforms. The reason for this bias, and the fundamental control of gross depositional setting on the bypass-zone tempestite model is discussed below.

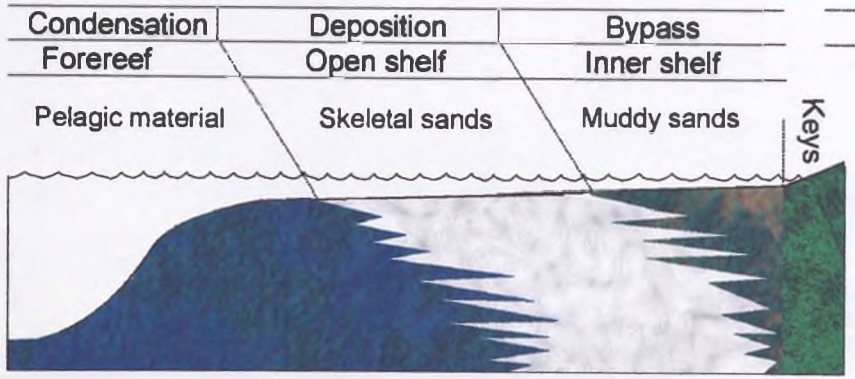
#### *5.5.1.1. Early transgressive and late highstand carbonate platforms*

There are numerous published accounts of storm-induced nearshore incision and bypass on carbonate platforms, with the most detailed studies conducted by McKie (1993), Perez-Lopez (2001), and Bádenas and Aurell (2001). On these platforms, the early TST and late HST are periods when the rate of carbonate production roughly matches the rate of accommodation space creation (McKie 1993). Shallow subaqueous platforms consequently develop over huge areas of the shelf with extremely low gradients, resulting in accommodation-limited conditions extending 10's to 100's of kilometres offshore (Wright and Burchette 1996). A consequence of these shallow gradients is a hydrodynamic regime dominated by severe wave attenuation, a high energy and aerially extensive intertidal zone, and a greatly expanded friction zone (Fig. 5.23). As illustrated in Fig. 5.22, these environmental constraints promote storm-tide interactions resulting in accumulative flow with high basal shear stresses that suffers little impedance and thus velocity reduction by onshore-directed shear stresses in the wave boundary layer. Vertical stratification sequences and palaeocurrent trends from these carbonate platforms are broadly

A. Typical hydrodynamics on a carbonate plateform




B. Facies belts on the South Florida Shelf platform




C. Bohai Key, Florida: Nearshore bypass

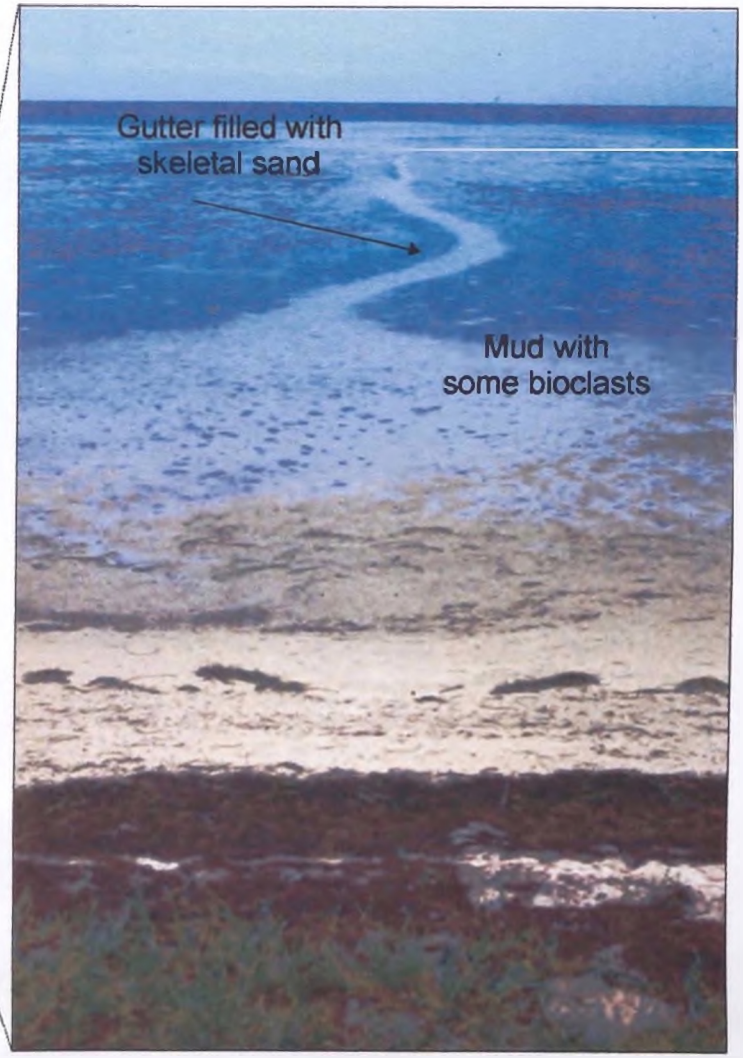


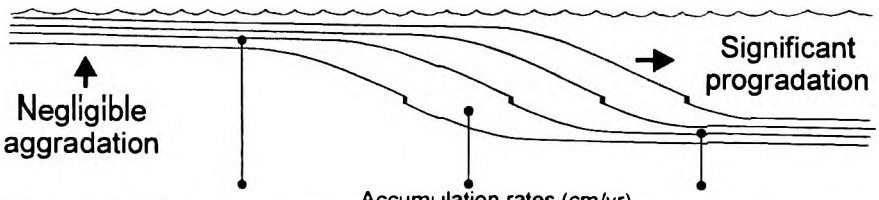
**Fig. 5.23.** Nearshore bypass on carbonate platforms. (A) Typical shelf hydrodynamics experienced on aerially extensive, low gradient carbonate platforms. (B) Simplified facies belts of the south Florida Shelf platform (after Enos, 1977, Sellwood, 1986). (C) Example of nearshore bypass from Bohai Key, south Florida (image kindly supplied by A. Perez-Lopez). Note the highly sinuous nature of gutter casts, and the fine-grained muddy nearshore. Photograph was taken 2 days after hurricane landfall.

similar to those obtained from the Ogof Velvet Formation, where combined-flows are unidirectional-dominant (e.g. Bádenas and Aurell 2001), with flow orthogonal to the shoreline (e.g. McKee 1993). An excellent modern example of nearshore bypass on a carbonate platform is the South Florida shelf (Fig. 5.23B), where the muddy shoreline is dissected by sinuous gutter casts (Fig. 5.23C) that act as conduits feeding an inner shelf composed of skeletal sand. This results in the inversely graded nearshore profile evident in Figure 5.22B.

*5.5.1.2. Fine-grained subaqueous delta platforms*

The formation of large subaqueous platforms of similar geometry to carbonate examples described above requires a very specific set of physical and environmental constraints. Firstly, sediment accumulation rates on the shelf have to be extremely high (in the order of 6–8 cm/yr, Kuehl *et al.* 1989) to raise the sediment water interface above normal shelf level. Secondly, to maintain a subaqueous state, vertical accretion must be negligible, but at the same time progradation considerable, to develop the widespread subaqueous distribution and extremely low gradient (Nittrouer *et al.* 1986). This rather unusual set of conditions is attained on aerially extensive subaqueous delta platforms developed at the mouths of large fine grained rivers that discharge into fairly energetic seas (Alexander *et al.* 1991). A good example is the subaqueous platform associated with the Amazon River, which extends some 200 km from the coast at gradients of less than half a degree (Nittrouer *et al.* 1986).

To prevent the platform accreting to sea level whilst simultaneously promoting progradation (lateral accretion), the nearshore topsets of deltas such as the Ganges-Brahmaputra (Kuehl *et al.* 1989) and Amazon (Nittrouer and DeMaster 1986; Nittrouer *et al.* 1986, 1996) are locations of high-applied shear stress and thus sediment bypass. Conversely, offshore topsets and foresets are sites of rapid accumulation (Table 5.4). As sedimentation rates then decrease rapidly on the bottom sets (Table 5.4), the subaqueous platform has a very similar zonal scheme (bypass-deposition-condensation) to that highlighted in the bypass-zone tempestite




| Example | Proximal topset (nearshore) | Distal topset/ foreset (shelf) | Bottom set (outer shelf) | Reference |
|---|---|---|---|---|
| Ganges - Brahmaputra | Negligible | 6 to 8 | Negligible | Kuehl *et al.* 1989 |
| Shandong | 0.1 | 0.4 to 0.9 | 0.03 to 0.09 | Alexander *et al.* 1991 |
| Amazon | <2 | >10 | <0.1 | Kuehl *et al.* 1982 |
| Typical gradient, 1: | 3000 | 1000 | 2000 | Nittrouer *et al.* 1986 |
| Chapel Island Formation | Wavy and lenticular bedding with gutters | Fine grained sandstone with HCS | Silty mudstone with carbonate concretions | Myrow 1992 |
| Ogof Velvet Formation | F.A.-A | F.A.-B | F.A.-C | |
| Zone | Bypass | Deposition | Condensation | |

**Table 5.4**. Sediment accumulation rates from three well studied modern subaqueous deltas. Note that the subaqueous platform has a very similar zonal scheme to both the Ogof Velvet and Chapel Island formations, the latter of which has also been interpreted as a fine-grained delta by Myrow (1992).

model (Fig. 5.3). The physical processes that apply the necessary shear stresses and induce bypass on nearshore delta topsets include hyperpycnal underflows (Mackenzie Delta, Hill *et al.* 2001), coastal current drift (Amazon Delta, Nittrouer *et al.* 1986) and tidally enhanced down-welling currents (Shandong Delta - Alexander *et al.* 1991; Ganges-Brahmaputra - Michels *et al.* 1998; and Yukon Delta - Nelson 1982). The bypass-zone tempestite model may therefore document a means by which large subaqueous deltas developed in storm belts maintain their shallow water geometry. Excellent examples of nearshore incision and bypass on ancient fine-grained river deltas include the Proterozoic Burnside Formation in Canada (McCormick and Grotzinger (1993), and Member 2 of the Lower Cambrian Chapel Island Formation of Newfoundland (Myrow 1992a) (Table 5.4). Nearshore channels filled with graded storm sand layers on the Alaskan Yukon Delta (Nelson 1982; Howard and Nelson 1982) and gutters at 3 m water depth incised into silts and clays on the Canadian Mackenzie Delta (Hill *et al.* 2001) appear to be direct modern analogues.

### 5.5.2. The Ogof Velvet Formation: palaeoenvironment and palaeogeography

Due to poor biostratigraphic control, and difficulties in tracing facies laterally across the Pembrokeshire coast, the exact depositional environment of the Ogof Velvet Formation is not immediately obvious, a factor that may explain the widely disparate interpretations previously offered by George (1970) and Turner (1977). Given the environmental significance of the bypass-zone tempestite model discussed above,

| Characteristics of a fine grained subaqueous delta | Ogof Velvet Formation |
|---|---|
| 75-95% clay, silt and very fine sand | * |
| Little or no subaerial expression | * |
| Nearshore grain size profile may be inversely graded | * |
| Well developed bypass - deposition - condensation zonal scheme | * |
| Muddy nearshore prone to bypass (low accumulation rates). | * |
| High energy tidal currents and expanded intertidal zone | * |
| Moderate mass movement and resedimentation | * |
| Dissipative shoreline (high wave attenuation) | * |
| Low salinity water column | * |
| Association with shore attached mud banks (Aber Llong Mst Fm) | * |
| Large low gradient catchment draining a passive margin | * |

**Table 5.5.** Summary of the main characteristics of a large fine-grained subaqueous delta based on studies by Nelson (1982), Nittrouer *et al.* (1986), Alexander *et al.* (1991), Michels *et al.* (1998), and Hill *et al.* (2001). Evidence for a low salinity water column is uncertain, but this feature may account for the almost complete exclusion of biogenic activity, body fossils, and the unusual distribution of bioturbation in the Welsh Basin. See text for further details. * = present.

the most logical interpretation involves progradation of a subaqueous delta. A comparison of salient attributes of the Ogof Velvet Formation with accepted features of subaqueous delta platforms associated with large fine-grained rivers like the Amazon and Ganges is presented in Table 5.5, and reaffirms this conclusion.

The question of sand source in the deltaic setting, and the bypass-zone tempestite model in general, was approached by Myrow (1992a) who proposed three alternatives: (1) erosion of tidal flat facies, (2) redistribution of distributary mouth sands, and (3) hyperpycnal underflows generated during river floods. In the example presented by Myrow (1992a) and in this study, the shoreline is not preserved, so there is no conclusive answer, but the erosion of silt-dominated tidal sediments (Facies Association A) is unlikely to liberate the required quantities of sand, while hyperpycnal currents on fine grained deltas are sand deficient. Therefore it appears likely that the sand source was a more proximal facies like channel mouth bars off the main distributaries. A key factor in erosion and transportation may be the storm-tide, which would cause coastal flooding and erosion during high water, and efficient transport offshore by down-welling current – ebb interaction during falling tide.

The north-easterly progradation of the delta system not only adequately accounts for the sedimentological characteristics of the younger Ffestiniog Flags Formation (see Fig. 5.27A) in North Wales (Allen *et al.* 1981), but also the near complete filling of the Welsh Basin during the latest Cambrian (Crimes 1970a,

Woodcock 1990). The rather unusual trace fossil distribution reported by Crimes (1970b) in North Wales may also reflect the huge quantities of fresh water delivered from the southern margin. The scale of bioturbation is ten times higher in sediments shed from the northern non-deltaic margin, even though these highly mobile coarse sandstones and conglomerates are far less conducive to trace preservation. In terms of modern analogues, the characteristics of the Ogof Velvet Formation are fairly typical of all the well-studied examples of large subaqueous deltas. The Yukon Delta in Norton Sound (Bering Sea) probably offers the closest approximation, where rapid progradation is filling an epeiric sea by efficient bypass of the nearshore topsets during intense winter storms (Nelson 1982). Passage of these storms also leads to storm wave loading of similar expression and scale to slumps and slides recoded in the Ogof Velvet Formation.

To fully understand and appreciate the wider environmental significance of the bypass-zone tempestite model, it is necessary to study the temporal phases of delta evolution within the context of changing formative parameters. Although sediment bypass is the system response to low gradient platform geometry, in siliciclastic examples, the ultimate controlling mechanisms are high sediment flux and limited accommodation. These act to maintain the extensive, but wholly subaqueous low-gradient profile. To assess temporal phases of delta evolution within these controlling parameters, we refer to theoretical considerations of facies-type in relation to sediment supply and relative sea level change discussed by Jervey (1988). Jervey focused on the effect of fluctuating sediment supply on the stratigraphic record, with relative sea level held constant. Here we consider relative sea level as a variable set against a constant sediment rate: Jervey's "rate of sediment influx" (measured as low, moderate and high) becomes our "rate of sediment influx *relative* to rate of accommodation space creation". This consideration of accommodation space vs. sediment supply in a theoretical framework for sedimentation is essentially the "regime" theory proposed by Swift and Thorn (1991). Two main shelf regimes are recognised: (1) supply-dominated regimes (rate of sediment supply exceeds the rate of accommodation space creation), and (2) accommodation-dominated regimes (rate of sea level rise and sediment dispersal exceeds the rate of sediment supply). In this study, reference to this regime model is simply accommodation-limited and accommodation-unlimited respectively. Fig. 5.24 illustrates the temporal phases of delta evolution within the context of systems tracts (i.e. the stratigraphic expression of the ratio between accommodation space and sediment supply).

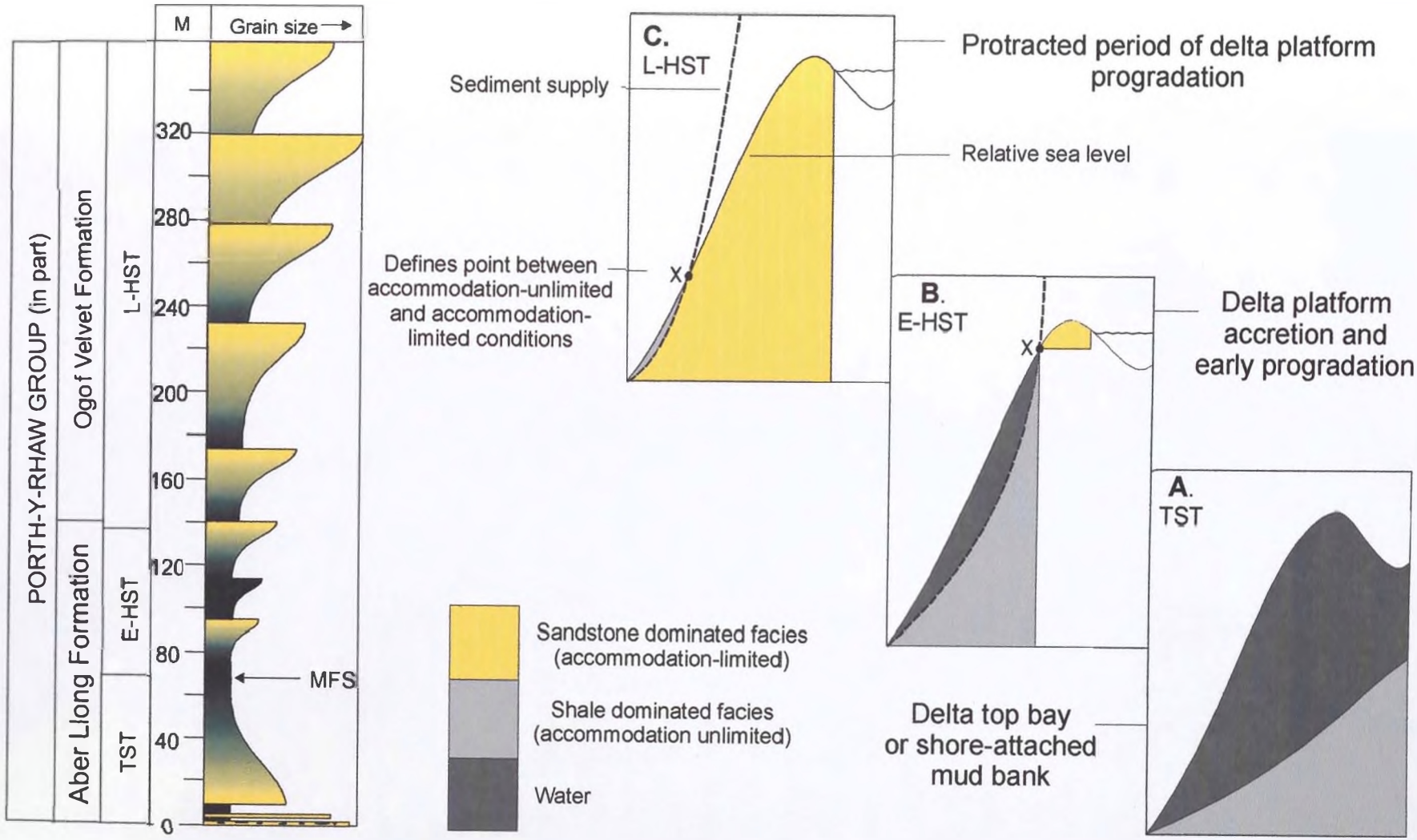

M
Grain size
320
280
240
200
160
120
80
40
0
PORTH-Y-RHAW GROUP (in part)
Aber Llong Formation
Ogof Velvet Formation
TST
E-HST
L-HST
MFS
Sediment supply
Defines point between accommodation-unlimited and accommodation-limited conditions
C.
L-HST
X
Protracted period of delta platform progradation
Relative sea level
B.
E-HST
X
Delta platform accretion and early progradation
A.
TST
Delta top bay or shore-attached mud bank
Sandstone dominated facies (accommodation-limited)
Shale dominated facies (accommodation unlimited)
Water

**Fig. 5.24.** Temporal phases of subaqueous delta platform evolution within the controlling parameters of sediment flux and relative sea level change. (A1) Rate of accommodation space exceeds sediment supply throughout the sea level cycle. (B) Rate of accommodation space exceeds sediment supply up to point X, above which sediment supply outstrips accommodation space and excess sediment is bypassed basinwards, building delta foresets. (C) Rate of sediment supply nearly always exceeds accommodation space creation, resulting in a protracted period of nearshore sediment bypass and foreset progradation. TST - transgressive systems tract, E-HST - early highstand systems tract, L-HST - late highstand systems tract, MFS - maximum flooding surface.

*5.5.2.1. Transgressive systems tract (TST)*

The Aber Llong Formation (Fig. 5.24) forms a transgressive shale sequence composed of black shales and grey varve-like shales (Fig. 5.25C and D) with occasional thin sandstone beds displaying interference ripples (Fig. 5.25A). Based on similar facies present in Member 1 of the Lower Cambrian Chapel Island Formation in Newfoundland, (Myrow and Hiscott 1991), these semi-restricted shoreline to shelf sediments may represent either delta top bay deposits like those associated with the Mississippi Delta or, more likely considering depth variations, the shore-attached mud banks developed along the Surinam Coast between the Orinoco and Amazon deltas (Wells and Coleman 1981). There is no evidence within the TST for nearshore incision and bypass, presumably because accommodation always exceeded sediment accumulation (Fig. 5.24A), resulting in accommodation-unlimited conditions throughout the sea level cycle. Consequently the physical and environmental factors that promote bypass (Fig. 5.22) were never initiated, and at no point did the shoreline prograde, so parasequences were not able to develop. Transgressive phases therefore record deposition either prior to delta formation, or when the area was down-coast from the main locus of sedimentation. This period of low sediment supply relative to accommodation space creation would also characterize delta abandonment phases, a process that may account for the shallow marine black shales of the Dolgellau Formation, which overlie delta platform facies of the Ffestiniog Flags Formation in North Wales (Allen *et al.* 1981).

*5.5.2.2. Early highstand systems tract (E-HST)*

The upper 74 m of the Aber Llong Formation consists of dark grey shales with abundant carbonate concretions interbedded with laterally discontinuous hummocky cross-stratified sandstones (Fig. 5.25B) that define three coarsening- and bed-thickening upwards parasequences. These thin, discontinuous sandstones resemble

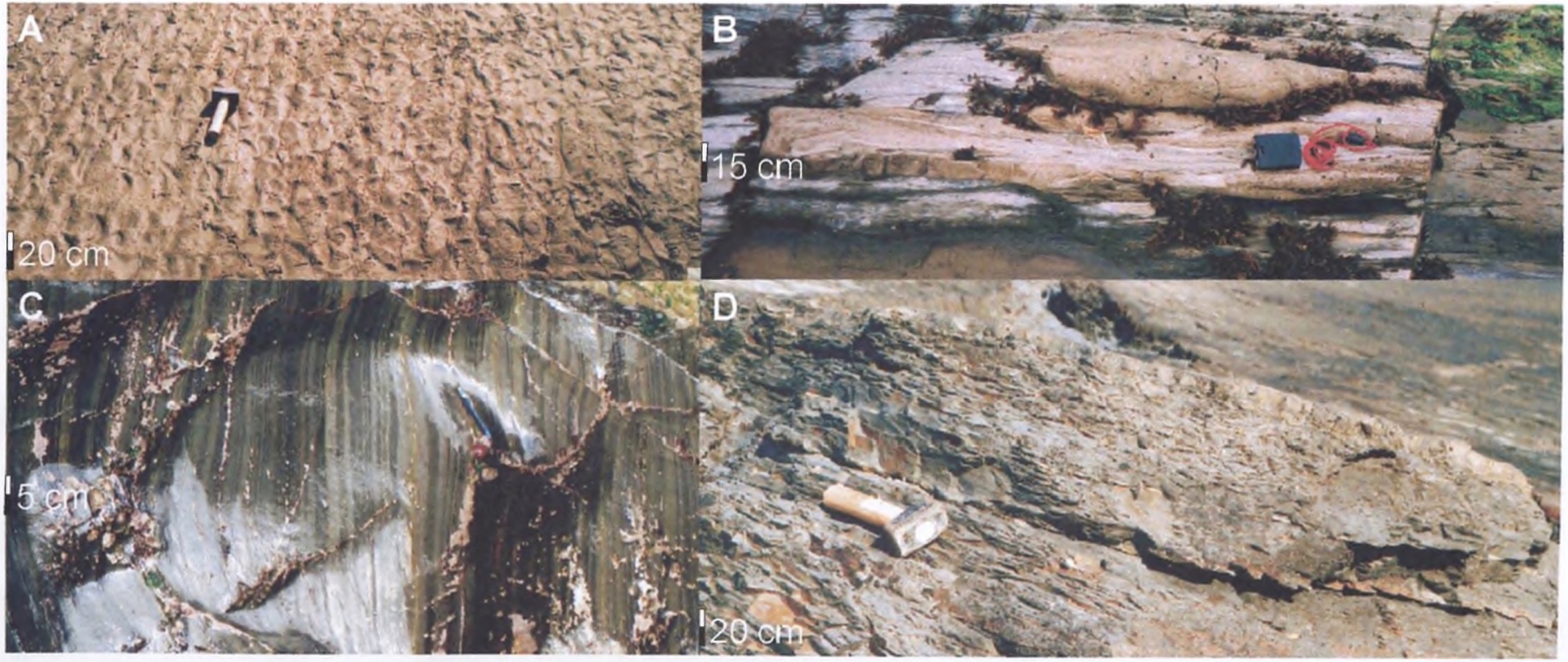


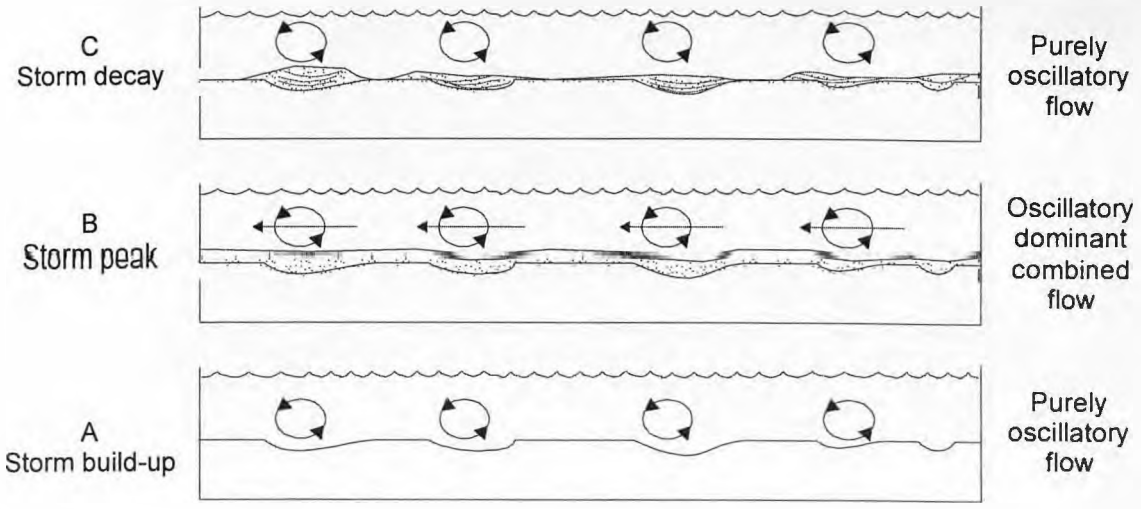

**Fig. 5.25.** Lithological features of the Aber Llong Formation. (A) Varve-like black and grey shales (Aber Llong). (B) Thin sandstone bed displaying interference ripples (Aber Llong). (C) Black shales beneath interference ripples (Aber Llong) (D) Sediment starved hummocks with SD-HCS (East of Porth-y-rhaw).

the starved hummocks of Myrow (1992a) and Brenchley *et al.* (1993), which develop when the supply of sand is low, but under wave conditions that would normally generate thicker continuous hummocky cross-stratified beds. The presence of A-HCS, SD-HCS, elliptical scours, and a non-erosional antiformal geometry suggest intense wave oscillations, while lack of QPL, An-HCS, planar erosion surfaces, gutter casts, flute casts, and very low sediment supply argue for weak unidirectional currents, a conclusion consistent with the poor distribution of sand across the shelf evidenced by the lack of B/C tempestites deposited below wave base.

A simple model for deposition of starved hummocks under very oscillatory-dominant combined-flows is presented in Fig. 5.26, which may be contrasted with bed configurations associated with the bypass-zone tempestite model in the overlying Ogof Velvet Formation (Fig. 5.9). As the most proximal sediments exposed are still some way below fair-weather wave base, bypass cannot be conclusively demonstrated, but is considered unlikely for most of the sea level cycle considering the relative insignificance of unidirectional currents. The lack of high velocity net flow and nearshore bypass may again be related to accommodation-unlimited conditions persisting throughout much of the sea level curve. Fig. 5.24B demonstrates that up to point X on the sea level curve, the rate of accommodation space creation exceeds the rate of sediment supply. Above this point, sediment supply outstrips accommodation, and only then will excess sediment bypass the nearshore onto the shelf, resulting in foreset progradation. The transition from topset aggradation to foreset progradation (at point X) signifies delta platform expansion and a change in shelf hydrodynamics from oscillatory-dominant to unidirectional-dominant combined-flows. This change from accommodation-unlimited to accommodation-limited conditions also induces shoreline progradation, and thus shoaling upwards parasequences are expected, but are likely to be poorly defined in the stratigraphic record as aggradational conditions predominate.

#### *5.5.2.3. Late highstand systems tract (L-HST)*

The final phase of delta evolution is that documented in the sediments of the Ogof Velvet Formation. These record a protracted period of foreset progradation as the rate of sediment supply almost always exceeds the rate of accommodation space creation, irrespective of relative sea level (Fig. 5.24C). The excess sediment that cannot be accommodated on delta topsets is redistributed basinwards driving progradation. The present day Amazon, Ganges-Brahmaputra, McKenzie and Yukon




A: Wave scour of the seabed into erosional hollows

B: Weak unidirectional currents deposit thin contineous sand bed on the inner to mid shelf, partly filling erosional scours

C: Waves redistribute sand into hollows on the seabed forming laterally discontineous sand patches. Further reworking forms either SD-HCS or A-HCS depending on wave climate

**Fig. 5.26.** Mechanism for the formation of starved hummocks displaying HCS under oscillatory-dominant combined-flows, based on characteristics evident in the upper part of the Aber Llong Formation.

deltas are at this stage of development, where continued outbuilding occurs despite Holocene sea level rise (Kuehl *et al.* 1989; Nittrouer *et al.* 1996; Hill *et al.* 2001).

*5.5.2.4. Sediment source and dispersal patterns*

A paradox in the geological history of Avalonia is that its sedimentary basins were apparently more extensive than the internal platforms that are the most obvious sediment source (Soper and Woodcock 1990). A solution is that large volumes of very fine clastics were supplied to the region from a major continent to which it was attached. Based on lithotectonic correlations and facies indicators (Schenk 1997), faunal provinces (Fortey and Cocks 1992), palaeomagnetic data (McNamara *et al.* 2001), and provenance studies (Thorogood 1990), this land mass was the supercontinent of Gondwana, more specifically the West African craton which formed its north-eastern periphery. This interpretation requires a river system of similar aerial distribution to the Amazon and Ganges, which at their terminus, like the Cambrian example, are prone to constructing large fine-grained subaqueous delta platforms.

Although the connection between Avalonia and North Africa has been challenged by some authors, most notably Landing (1996) who argued for insular

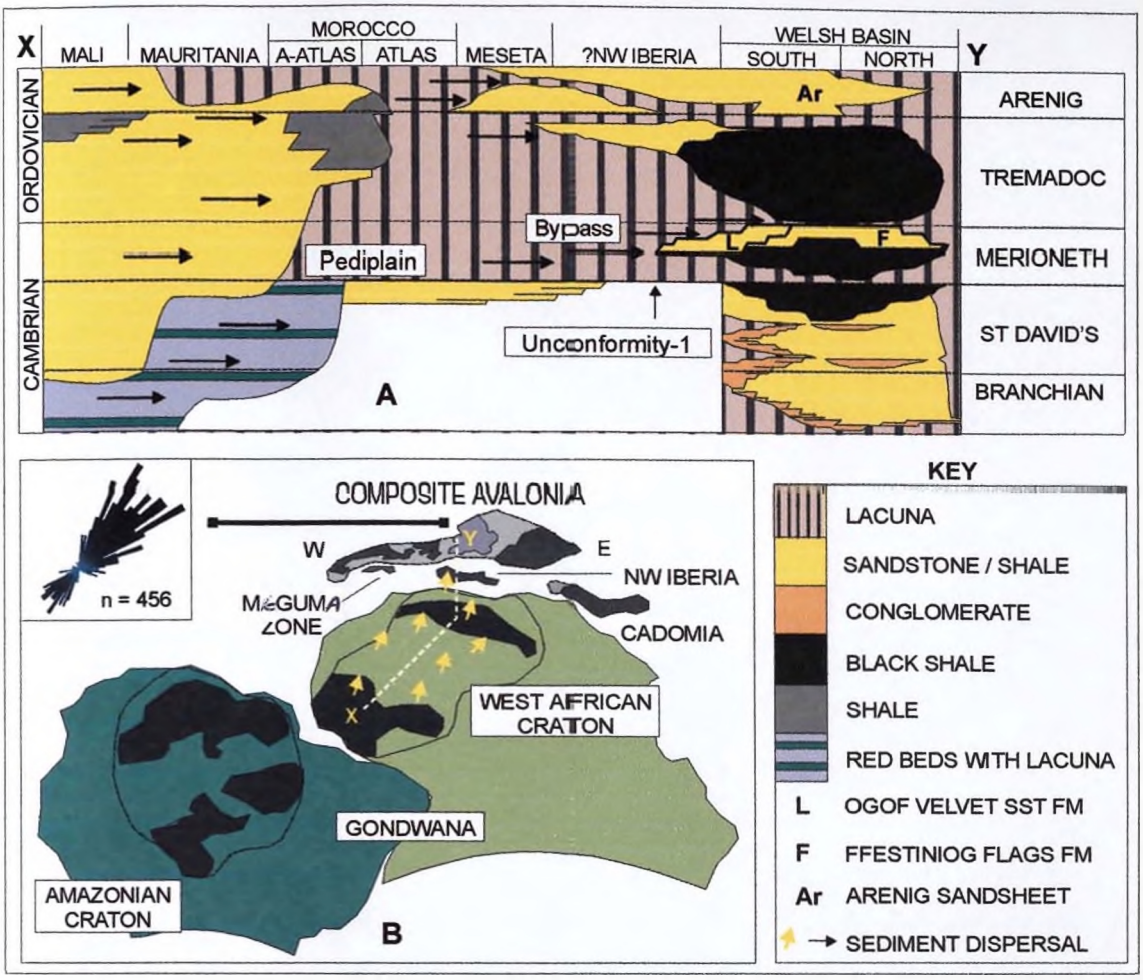



**Fig. 5.27.** The subaqueous delta platform of the Upper Cambrian Welsh Basin: its palaeogeography as a sediment sink on the northern periphery of Gondwana. (A) Stratigraphic correlation between the West African craton of North Gondwana and the peripheral outboard terrane of Avalonia based in part on Woodcock (1990), Soper and Woodcock (1990) and Schenk (1997). Unconformity-1 is a major regional pediplain that bypassed fine sediment from the continental interior to the northern margin. The terminus of this huge fluvial system, like the Amazon and Ganges rivers, is represented by a large fine-grained subaqueous delta. (B) Sediment dispersal patterns and relationship between source and sink for some northern peri-Gondwanan terranes. Continental positions after Nance and Murphy (1994) with modifications from Gutiérrez-Alonso *et al.* (2003).

Avalonia by the latest Precambrian, there is a remarkably good stratigraphic correlation between the northern Gondwanan margin (Mali, Mauritania, and Morocco) and peripheral outboard terranes such as Avalonia (Fig. 5.27), Armorica (Noblet and Lefort 1990), the Meguma Zone and Arabian Peninsula (Schenk 1997). The Avalonian connection via the northern peneplained land surface of Gondwana (Mali to Morocco) is well illustrated in Figure 5.27. Unconformity-1 (which separates Tremadoc shales and Lower Cambrian sandstones in Morocco) marks a time of significant Middle and Upper Cambrian crustal stripping of the huge Sahara Platform (Schenk 1997), with efficient bypass of fine-grained material to sedimentary sinks like

Avalonia situated on the north Gondwanan periphery. The entire expanse of North Africa thus became a vast pediplain and an extensive zone of erosion and bypass. This previously unrecognised Avalonian fine-grained sand-sheet is one of two that stretched as far as the Welsh Basin prior to opening of the Rheic Ocean and dispersal of Avalonia in the Middle Ordovician (Cocks *et al.* 1997). The second sheet is Arenig in age (Fig 5.27A) and is a correlative of the extensive Grès Armoricain Formation (Williams *et al.* 1972), which occurs over large areas of northern Gondwana (Noblet and Lefort 1990).

## 5.6. CONCLUSIONS

This high-resolution study describes and interprets the facies, processes, and dynamics evident on fine-grained storm-dominated coastlines. A review of existing literature and a case study on the Upper Cambrian Ogof Velvet Formation provides evidence for the following interpretations.

1. The bypass-zone tempestite model proposed by Myrow (1992a) adequately accounts for the spatial distribution of facies recorded from many fine-grained storm-dominated coastlines. Nearshore bypass of sand grade material through silt-dominated nearshore facies may have been overlooked in previous studies, as few authors have equated erosion and incision with sediment bypass. Based on a number of published accounts and facies relationships in the Ogof Velvet Formation, bypass-zones appear restricted to: (1) locations affected by tidal currents, (2) accommodation-limited conditions, (3) wave dissipative shorelines, and (4) extensive, low gradient platforms developed at the mouths of fine-grained rivers, and on carbonate platforms.
2. Locally intensified unidirectional currents are required for the initiation of bypass-zones, and unidirectional-dominant combined-flow structures are the most common stratigraphic expression in associated inner to mid-shelf facies. Intensified unidirectional currents record a force balance with a high driving mechanism (pressure gradient and excess weight force) and low Coriolis Force. High current velocities combined with accommodation-limited conditions lead to expansion of the nearshore friction zone out onto the shelf, resulting in highly erosive flows directed offshore at high angles to bathymetric contours

3. The Upper Cambrian Ogof Velvet Formation was deposited as a subaqueous delta platform at the mouth of a large fine-grained river system similar to the Amazon and Ganges. This huge fluvial system drained the supercontinent of Gondwana to which Avalonia was attached, and its importance in supplying sediment to the Welsh Basin provides the only sedimentological evidence for this connection during the Upper Cambrian. The Gondwanan-Avalonian connection also places an important constraint on Avalonian rifting and the opening of the Rheic Ocean. The bypass-zone tempestite model on siliciclastic platforms documents a means by which these large subaqueous deltas retain their wholly subaqueous profile by restricting topset aggradation while simultaneously promoting foreset progradation.

# *CHAPTER 6*

# CONCLUSIONS

## Stratigraphy, sedimentology and sequence stratigraphy of the Dyfed Supergroup in SW Wales

The Dyfed Supergroup exposed in SW Wales represents an extended, and near continuous phase of siliciclastic sedimentation on the southern flank of the Cambrian Welsh Basin from the Lower Cambrian Placentian Series to the Upper Cambrian Merioneth Series. A two-fold division of Cambrian strata is recognized. The lower 564 m is included in an extended Caerfai Group, which is dominantly arenaceous, with important horizons of conglomerates and pebbly sandstone. This is overlain by 687 m of fine-grained arenaceous and argillaceous sediments of the Porth-y-rhaw Group, a newly erected unit that includes strata previously assigned to the "Menevian Group" and "Lingula Flags". This two-fold division is comparable both lithologically and chronologically with the Harlech Grits Group and Mawddach Group in North Wales.

High-resolution sequence stratigraphic techniques are applied to the Dyfed Supergroup across southern Britain to facilitate integration into a unified Avalonian chronostratigraphic framework based on succession in Atlantic Canada. The relative ease of integration reflects the shared epeirogenic history, sediment sources and accumulation history of a microcontinent unified by the Early Cambrian. The occurrence of lithologically similar and coeval depositional sequences may be relied upon to determine the limits of the Avalonian Superterrane in the Acadian-Caledonian orogen.

A broad subdivision of Cambrian stratigraphy into tectonically active and passive phases of sedimentation is recognized. Megasequence 1 (sequences 1–7) records the transform termination of Avalonian subduction following oblique convergence, and the accretion of island arcs to the northern periphery of the supercontinent Gondwana. Under transpressional regimes, late Precambrian arc-related basins were inverted and recycled into Lower and Middle Cambrian pull-apart successor basins. Megasequence 2

(sequence 8) reflects passive margin sedimentation, with Avalonia acting as a sediment sink to vast quantities of fine-grained sediment transferred off Gondwana by large, mature fluvial systems. This marked the culmination of the Avalonian-Cadomian orogenic cycle.

**Basin margin sedimentology and tectonic implications of Early Cambrian rifting in Eastern Avalonia**

This detailed account of temporal variations in lithofacies, depositional processes and sandstone composition in the lower Caerfai Group presents compelling evidence for alluvial fan and braided stream sedimentation at the base of the Cambrian in SW Wales. As it is widely recognized that alluvial fans are preferentially located in areas of active tectonism, this interpretation delineates a number of specific palaeotectonic elements that are applicable to the early evolution of Avalonia. The general tectonostratigraphic evolution of the Avalonian Superterrane provides a record of Neoproterozoic subduction along an active margin of Gondwana until rifting in the Early Ordovician led to the inception of Iapetus subduction. The stratigraphic position of the Caerfai Group between arc-related environments of the late Precambrian Pebidian Supergroup and stable cratonic regimes of the Upper Cambrian Porth-y-rhaw Group places the succession in the tectonostratigraphic position of the arc-platform transition.

The role of strike-slip tectonics in the diachronous cessation of arc volcanism East Avalonia is documented, with sedimentation during the Lower Cambrian being principally confined to pull-apart rift basins on an epeirogenically active platform. To account for this transition from subduction-related to wrench-related tectonism in the apparent absence of a major collisional event, it is proposed that Avalonia subduction was terminated as a result of transform activity. The structural inversion of Precambrian basins and the opening of transtensional successor basins across East Avalonia during the Lower Cambrian appears related to the suturing of volcanic arc terranes during transform termination and microcontinent formation, a tectonostratigraphic evolution mirrored in coeval sections in the Avalonian belt of North America.

**The anatomy of a flood-dominated fan-delta from the Middle Cambrian of SW Wales**

This study of Middle Cambrian sediments of the Caerfai Group and lower part of the Porth-y-rhaw Group (Fig. 4.2) exposed in NW Pembrokeshire is the first detailed investigation into the lithofacies, processes, geometry, and classification of coarse-grained deltas built exclusively by flood-generated sediment dispersal processes. It complements work on ancient flood-dominated fluvio-deltaic systems by Mutti *et al.* (1996, 2000, 2003) and Plink-Björklund and Steel (2004), who have set out preliminary criteria for their recognition and interpretation. It has been appreciated through detailed facies analysis and understanding of process sedimentology that sediment dispersal on deltas is mainly controlled by the efficiency of the transfer system and thus sediment flux to the basin. The dominance of highly efficient HFF in the alluvial system is manifested in a fan-delta succession built almost exclusively of high- and low-density turbidites emplaced directly from subaerial flood events. A consequence of the flood hydrograph is to produce a quasi-steady turbidity current with well-defined waxing and waning phases that can be identified in the associated deposit.

The study of sediment dispersal patterns and depositional processes that ultimately define the character of the fan-delta system is best approached through the construction of facies tracts (Mutti 1992). The concept of facies tracts is here defined as the documentation and interpretation of facies types originating from the transformation of flows during their basinward motion along the erosional and depositional profile of a system. The principal facies tracts inferred from lateral and vertical lithofacies relationships can be most simply framed in terms of hyperpycnal, hypopycnal, and homopycnal components, with an additional mechanism not accounted for on modern river deltas, that of mass emplacement by sediment gravity flows.

The temporal and spatial evolution of a hyperpycnal current on a flood-dominated delta can be defined simply in terms of a basinward- followed by a landward-shift in the main zones of erosion and deposition. During waxing flow, the depositional zone progrades (coarsening upwards) and the zone of erosion moves seawards, so that areas that were initially depositional become erosional, and the flow reworks its own deposits. As the flood wanes, the site of maximum deposition moves landwards, resulting in a fining upwards, retrogradational motif. A similar temporal and spatial evolution of

depositional processes dictated by the flood hydrograph have been inferred from modern fan-deltas (Prior and Bornhold 1990) and offshore from small mountain streams (Mulder *et al.* 1998, 2001).

**Processes, dynamics and facies on a muddy storm-dominated shelf**

The bypass-zone tempestite model proposed by Myrow (1992a) adequately accounts for the spatial distribution of facies recorded from many fine-grained storm-dominated coastlines. Nearshore bypass of sand grade material through silt-dominated nearshore facies may have been overlooked in previous studies, as few authors have equated erosion and incision with sediment bypass. Based on a number of published accounts and facies relationships in the Ogof Velvet Formation, bypass-zones appear restricted to: (1) locations affected by tidal currents, (2) accommodation-limited conditions, (3) wave dissipative shorelines, and (4) extensive, low gradient platforms developed at the mouths of fine-grained rivers, and on carbonate platforms.

The palaeohydraulic reconstruction of the Upper Cambrian shelf during deposition of the Ogof Velvet Formation differs quantitatively if not qualitatively from models developed from direct measurements on modern storm-affected shelves. Although it is critical for geologists working on ancient sequences to maintain a firm grounding in plausible fluid dynamics and sediment transport processes, it is equally important to address obvious disparities between modern and ancient deposits, and to consider processes under non-actualistic conditions. The contributions to, and the characteristics of, storm-induced combined-flows are both varied and dynamic, but may be better understood when sedimentological data is integrated with known palaeogeographical/environmental constraints such as relative sea level changes, palaeolatitude, and fair-weather ambient processes.

The Upper Cambrian Ogof Velvet Formation was deposited as a subaqueous delta platform at the mouth of a large fine-grained river system similar to the Amazon and Ganges. This huge fluvial system drained the supercontinent of Gondwana to which Avalonia was attached, and its importance in supplying sediment to the Welsh Basin provides the only sedimentological evidence for this connection during the Upper Cambrian. The Gondwanan-Avalonian connection also places an important constraint on Avalonian rifting and the opening of the Rheic Ocean. The bypass-zone tempestite model on siliciclastic platforms documents a means by which these large subaqueous

deltas retain their wholly subaqueous profile by restricting topset aggradation while simultaneously promoting foreset progradation.

# REFERENCES

Aigner, T. 1985. *Storm Depositional Systems.* Springer-Verlag, Berlin Heidelberg New York. pp 170.

Aigner, T. & Reineck, H.E. (1982). Proximality trends in modern storm sands from the Heligoland Bight (North Sea) and their implications for basin analysis, *J. Sed. Petrol.* **52**, 183–215.

Ainsworth, R.B. and Pattison, S.A.J. (1994). Where have all the lowstands gone? Evidence for attached lowstand systems tracts in the Western Interior of North America. *Geology*, **22**, 415–418.
Alexander, H.S. 1932. Pothole erosion. *J. Geol.* **40**, 305–337.

Alexander, C.R., DeMaster, D.J., and Nittrouer C.A. (1991). Sediment accumulation in a modern epicontinental-shelf setting: The yellow Sea. *Mar. Geol.*, **98**, 51–72.

Alexander, J. and Mulder, T. (2002). Experimental quasi-steady density current. *Mar. Geol.*, **186**, 195–210.

Allen, J.R.L. (1983). Studies in fluviatile sedimentation: bars, bar complexes and sandstone sheets (low-sinuosity braided streams) in the Brownstones (L, Devonian), Welsh Borderlands. *Sed. Geol.*, **33**, 237–293.

Allen, J. R. L. (1984). Sedimentary structures: their character and physical basis. Developments in Sedimentology, 593 pp. Elsevier, Amsterdam. 593 pp

Allen, J.R.L. (1985). Principles of physical Sedimentology. Allen and Unwin, London, 272 pp.

Allen, P.A. and Underhill, J.R. (1989). Swaley cross-stratification produced by unidirectional flows, Bencliff Grit (Upper Jurassic), Dorset, UK. *J. Geol. Soc. Lond.*, **146**, 241–252.

Allen, P.M. and Jackson, A.A. (1978). Bryn-teg Borehole, North Wales. *Bull. Geol. Surv. G.B.*, **61**, 1–33.

Allen, P.M. and Jackson, A.A. (1985). Geology of the country around Harlech. Memoir of the British Geological Survey, Sheet 135 with part of 149 (England and Wales), HMSO, London.

Allen, P.M., Jackson, A.A. and Rushton, A.W.A. (1981). The stratigraphy of the Mawddach Group in the Cambrian succession of North Wales. *Proc. Yorkshire Geol. Soc.* **43**. 295–329.

Amos, C.L. Li, M.Z. and Choung, K.S. (1996). Storm-generated, hummocky stratification on the outer-Scotian shelf. *Geo-mar. Lett.*, **16**, 85–94.

Anderton, R., Gibbons, W. and Nicholson P.G. (1992). Precambrian. In: *Atlas of Palaeogeography and Lithofacies* (ED. By J.C.W. Cope, J.K. Ingham and P.F. Rawson). *Geol. Soc. Mem.*, **13**, 5–12.

Archer, A.W., Kvale, E.P. and Johnson, H.R. (1991). Analysis of modern equatorial tidal periodicities as a test of information encoded in ancient tidal rhythmites. In: Clastic Tidal Sedimentology (Ed. by D.G. Smith, G.E. Reinson, B.A. Zaitlin and R.A. Rahmani). *Mem. Can. Soc. Petrol. Geol.*, **16**, 189–196.

Arnott, R.W.C. 1992. Exploratory flow-duct experiments on combined flow bed configurations, and some implications for interpreting storm event stratification, *J. Sed. Petrol.* **63**. 211–219.

Arnott, R.W. and Southard, J.B. (1990). Exploratory flow duct experiments on combined-flow bed configurations, and some implications for interpreting storm event stratification. *J. Sed. Petrol.* **60**. 211–19.

Arribas, J., Alonso, A., Mas, R., Tortosa, A., Rodas, M., Barrenechea, J.F., Alonso-Azcarate, J. and Artigas, R. (2003). Sandstone petrography of continental depositional sequences of an intraplate rift basin: western Cameros Basin (North Spain). *J. Sed. Res*, **73**, 309–327.

Arthur, M.A., Dean, W.E. and Stow. D.A.V. (1984). Models for the deposition of Mesozoic-Cenozoic fine-grained organic-carbon-rich sediment in the deep sea. In: *Fine-grained sediments: Deep-Water Processes and Facies* (Ed. by D.A.V. Stow and D.J.W. Piper). *Geol. Soc. London* Spec. *Publ.*, **15**, 527–560.

Artyushkov, E.V., Lindstrom, M. and Popov, L.E. (2000). Relative sea-level changes in Baltoscandia in the Cambrian and early Ordovician: the predominance of tectonic factors and the absence of large scale eustatic fluctuations. *Tectonophysics*, **320**, 375–407.

Baas, J.H. and Best, J.L. (2002). Turbulence modulation in clay-rich sediment-laden flows and some implications for sediment deposition. *J. Sed. Res*, **72**, 336–340.

Bádenas, B. and Aurell, M. (2001). Proximal-distal facies relationships and sedimentary processes in a storm dominated carbonate ramp (Kimmeridgian, northwest of the Iberian Ranges, Spain). *Sed. Geol.*, **139**, 319–340.

Bagnold, R.A. (1954). Experiments on gravity-free dispersion of large solid spheres in a Newtonian fluid under shear. *Proc.* Roy. *Soc. London*, A265, 315–319.

Bagnold, R.A. (1962). Auto-suspension of transported sediment: turbidity currents. Proc. Roy. *Soc. London*, **A265**, 315–319.

Baird, G.C. (1981). Submarine erosion on a gentle palaeoslope: a study of two discontinuities in the New York Devonian. *Lethaia*, **14**, 105–122.

Baird, G.C., and Brett, C.E. (1986). Erosion on an anaerobic sea floor: significance of reworked pyrite deposits from the Devonian of New York State. *Palaeogeography, Palaeoclimatology, Palaeoecology*, **57**, 157–193.

Baird, G.C., and Brett, C.E. (1991). Submarine erosion on the anoxic sea floor: stratinomic, palaeoenvironmental, and temporal significance of reworked pyrite-bone deposits. In: Modern and Ancient Continental Shelf Anoxia (Ed. by R.V. Tyson and T.H. Pearson). *Geol. Soc.* Spec. *Publ.*, **58**, 223–257.

Baird, G.C., Brett, C.E. and Kirchgasser, W.T. (1988). Genesis of black shale-roofed discontinuities in the Genesee Formation, western New York State. In: *Devonian of the World* (Ed. by N.J. McMillan, A.F. Embry and D.J. Glass). *Can. Soc. Petrol. Geol. Mem.*, **14**. 357–375.

Baker, J.W. (1955). Precambrian rocks in Co. Wexford. *Geol. Mag.*, **92**, 63–68.

Balance, P.F. (1988). The Huriwai braidplain delta of New Zealand: a late Jurassic, coarse-grained volcanic-fed depositional system in a Gondwana forearc basin In: *Fan-deltas: sedimentology and tectonic setting* (Ed. by W. Nemec and R.J. Steel), Blackie and Son Ltd. London, 431-444.

Balsey, J.R. and Buddington, A.F. (1960). Magnetic susceptibility anisotropy and fabric of some Adirondack granites and orthgneisses. *Am. J. Sci.*, **258**, 6–20.

Bangs Rooney, C. and Basu, A. (1994). Provenance analysis of muddy sandstones. *J. Sed. Res*, **A64**, 2–7.

Bardaji, T., Dabrio, C.J., Goy, J.L., Somoza, L. and Zozo, C. (1990). Pleistocene fan-deltas in southeastern Iberian peninsula: sedimentary controls and sea-level changes. In: Coarse-grained Deltas (Ed. by A. Colella and D.B. Prior), *Int. Ass. Sed. Spec. Publ.*, **10**, 129–151.

Barr, S.M., Bevier, M.L., White, C.E. and Doig, R. (1993). Magmatic history of the Caledonian (Avalon) terrane of southern New Brunswick based on U–Pb (zircon) geochronology. *New Brunswick Department of Natural Resources and Energy, Mineral Resources, Information Circular*, **93–1**, 10–17.

Barron, E. J. (1989). Severe storms in earth history. *GSA Bull.*, **101**. 601–612.

Bassett, D.A. and Walton, E.K.A. (1960). The Hell's Mouth Grits, Cambrian greywackes in St Tudwel's Peninsula. *Q. J. Geol. Soc. Lond.*, **116**, 85–110.

Basu, A, Young, S.W., Suttner, L.J., James, W.C. and Mack, G.H. (1975). Re-evaluation of the use of undulatory extinction and polycrystallinity in detrital quartz for provenance interpretation. *J. Sed. Petrol.*, **45**, 873–882.

Basu, D. and Bouma, A.H. (2000), Thin-bedded turbidites of the Tanqua Karoo: physical and depositional characteristics. In: Fine-grained turbidite systems (Ed. by A.H. Bouma and C.G. Stone. AAPG Mem., 72/*SEPM* Spec. *Publ.*, **68**, 263–278.

Bates, C. C. (1953). Rational theory of delta formation. *Am. Ass. Petrol. Geol. Bull*, **37**, 2119–2162

Beard, D.C. and Weyl, P.K. (1973). Influence of texture on porosity and permeability of unconsolidated sand. *Am. Ass. Petrol. Geol. Bull* Bull., **57**, 349–369.

Beaty, C.B. (1990). Anatomy of a White Mountains Debris-Flow – The Making of an Alluvial Fan. In: *Alluvial fans: A Field Approach* (Ed. by A.H. Rachocki and M. Church), John Wiley, Chichester, 69–89.

Beckinsale, R.D. and Thorpe, R.S. (1979). Rubiduim-strongtium whole rock evidence for the age of metamorphism and magmatism in the Mona Complex of Anglesey. *J. Geol. Soc. Lond.*, **136**, 433–439.

Bennett, M.A. (1987). Genesis and diagenesis of the Cambrian manganese deposit, Harlech, North Wales. *Geol. J.*, **22**, 7–18.

Benvenuti, M. (2002). Facies analysis and tectonic significance of lacustrine fan-deltaic successions in the Pliocene-Pleistocene Mugello Basin, Central Italy. *Sed. Geol.*, **157**, 197–234.

Berner, R.A. (1969). The synthesis of framboidal pyrite. Economic *Geol.*, 64, 383–384.
Beukes, N.J. (1996). Sole marks and combined-flow storm event beds in the Brixton Formation of the siliciclastic Witwatersrand Supergroup, South Africa. *J. Sed. Res*, **66**, 567–576.
Beverage, J.P. and Culbertson, J.K. (1964). Hyperconcentrations of suspended sediment. *Proc. Am. Soc. Civil. Eng., J. Hydraul. Div.*, **90**, 117–128.

Blair, T.C. (1999). Cause of dominance by sheetflood vs. debris-flow processes on two adjoining alluvial fans, Death Valley, California. *Sedimentology*, **46**. 1015–1028.

Blair, T.C. and Bilodeau, W.L. (1988). Development of tectonic cyclothems in rift, pull-apart, and foreland basins. *Geology*, **16**, 517–520.

Blair, T.C. and McPherson, J.C. (1994). Alluvial fans and their natural distinction from rivers based on morphology, hydraulic processes, sedimentary processes, and facies assemblages. *J. Sed. Res.*, **64**, 450–489.

Blatt, H, Middleton, G.V., and Murray, R.C. (1980). Origin of Sedimentary Rocks, 2nd Edition. Prentice Hall, New Jersey, 782 pp.

Bloxam, T.W. and Dirk, M.H.J. (1988). The petrology and geochemistry of the St. David's granophyre and the Cwm Bach rhyolite, Pembrokeshire, Dyfed. *Mineralogical Mag.*, **52**, 563–575.

Bluck, B.J. (1967a). Deposition of some Upper Old Red Sandstone conglomerates in the Clyde area: a study in the significance of bedding. *Scot. J. Geol.*, **3**, 139–167.

Bluck, B.J. (1967b). Sedimentation of beach gravels: examples from South Wales. *J. Sed. Petrol.*, **37**, 128–554.

Bluck, B.J. (1974). Structure and directional properties of some valley sandur deposits in southern Iceland. *Sedimentology*, **21**, 533–554.

Boothroyd, J.C. and Ashley, G.M. (1975). Process, bar morphology and sedimentary structures on braided outwash fans, North-eastern Gulf of Alaska. In: *Glaciofluvial and Glaciolacustrine Sedimentation* (Ed. by Jopling, A.V. and McDonald). *SEPM Spec. Publ.*, **23**, 193–222.

Bornhold, B.D. and Prior, D.B. (1990). Morphology and sedimentary processes on the subaqueous Noeick River delta, British Columbia. In: *Coarse-grained Deltas* (Ed. by A. Colella and D.B. Prior). *Int. Ass. Sed. Spec. Publ.*, **10**, Blackwell Science, Oxford, 169–181.

Bose, P.K. (1983). A reappraisal of deposition of Maentwrog beds at Porth Cariad, North Wales, *Geol. Mag.*, **120**, 73–80.

Bose, P.K., Banerjee, S. and Sarkar, S., 1997. Slope-controlled seismic deformation and tectonic framework of deposition of Koldaha Shale, India. *Tectonophysics*, **269**, 151-169.

Bouma, A.H. (1962). Sedimentology of some Flysch Deposits, Elsevier, Amsterdam, 168 pp.

Bourgeois, J. (1980). A transgressive shelf sequence exhibiting hummocky cross-stratification: The Cape Sebastian Sandstone (Upper Cretaceous), southwest Oregon. *J. Sed. Petrol.*, **50**, 681–702.

Bourgeois, J. and Leithold, E.L. (1984). Wave reworked conglomerates – depositional processes and criteria for recognition. In: *Sedimentology of Gravels and Conglomerates* (Ed. by E.H. Koster and R.J. Steel). *Can. Soc. Petrol. Geol. Mem.*, 331–343.

Bowen, A.J. (1980). Simple models of nearshore sedimentation: beach profile and alongshore bars. In: *The coastline of Canada* (Ed. by S.B. McCann) *Geol.* Surv. *Can. Pap.*, **80-10**, 1–11.

Brasier, M.D. (1989). Sections in England and their correlation. In: *The Precambrian–Cambrian Boundary* (Ed. by J.W. Cowie and M.D. Brasier). *Oxford Monographs on Geology and Geophysics,* **12**, 82–101.

Brasier, M.D. (1992). Introduction. Background to the Cambrian explosion. *J. Geol. Soc. London*, **149**, 585–587.

Brasier, M.D., Ingham, J.K. and Rushton, A.W.A. (1992). Cambrian. In: Atlas of Palaeogeography and Lithofacies (Ed. by J.C.W. Cope, J.K. Ingham and P.F. Rawson). *Geol. Soc. London Mem.*, **13**, 13–18.

Brenchley, P.J. (1985). Storm influenced sandstone beds. *Modern Geol.,* **9**. 369–396.

Brenchley, P.J., Pickerill, R.K. and Stromberg, S.G. (1993). The role of wave reworking on the architecture of storm sandstone facies, Bell Island Group (Lower Ordovician), eastern Newfoundland. *Sedimentology*, **40**, 359–382.

Brenner, R.L. and Davis, D.K. (1973). Storm-generated coquinoid sandstone: Genesis of high-energy marine sediments from the Upper Jurassic of Wyoming and Montana. *GSA Bull.,*. **84**, 1685–1698.

Bridges, D., Carney, J.N., Lawley, R.S. and Rushton, A.W.A. (1998). Geology of the country around Nuneaton. *Memoir for 1:50 000 Geological Sheet 169* (England and Wales). London: The Stationary Office, 21–37.

Bridges, P.H. (1972). The significance of toolmarks on a Silurian erosional furrow. *Geol. Mag.*, **5**, 405–410.

British Geological Survey (1973). St David's. 1:25 000 special sheet.

Brown, L.F. and Fisher, W.L. (1977). Seismic stratigraphic interpretation of depositional systems: examples from Brazilian rift and pull-apart basins. *Am. Ass. Petrol. Geol. Bull* Mem., **26**, 213–248.

Bull, W.B. (1972). Recognition of alluvial fan deposits in the stratigraphic record. In: Recognition of Ancient Sedimentary Environments (Ed. by J.K. Risby and W.K Hamblin). *SEPM Spec. Publ.*, **16**, 63–83.

Burnett, D.J. and Quirk, D.G. (2001). Turbidite provenance in the Lower Palaeozoic Manx Group, Isle of Man: implications for the tectonic setting of Eastern Avalonia. *J. Geol. Soc. London*, **158**, 913–924.

Butler, R.F. (1992). Palaeomagnetism, Blackwell Scientific *Publ*ications, Boston, 266 pp.
Cacchione, D.A. and Drake, D.E. (1990). Shelf sediment transport: an overview with applications to the northern California continental shelf. In: *The Sea* (Ed. by B. LeMéhauté and M.D. Hanes). *Ocean Engineering Sci.*, **9,** John Wiley, New York, 729–733.

Cacchione, D.A., Drake, D.E., Grant, W.D. and Tate, G.B. (1984). Rippled scour depressions on the inner continental shelf off central California. *J. Sed. Petrol.*, **54**, 1280–1291.

Cattaneo, A. and Steel, R.J. (2003). Transgressive deposits: a review of their variability. *Earth Sci. Rev.*, **62**, 187–228.

Chakraborty, C. (1995). Gutter casts from the Proterozoic Bijaygarh Shale Formation, India: their implication for storm-induced circulation in shelf settings, *Geol.* J., **30**, 69–78.

Chakraborty, C. and Bose, P.K. (1992). Ripple-dune to upper stage plane bed transition: some observations from the ancient record. *Geol. J.*, **27**, 349–359.

Chaloupsky, J. (1990). Precambrian of the Bohemian Massif, Central Europe. In: Avalonian and Cadomian geology of the North Atlantic (Ed. by R.A. Strachan and G.K. Taylor). Blackie, 93–108.

Chamley, H. (1979). North Atlantic clay sedimentation and palaeoenvironments since the late Jurassic. In: *Deep drilling results in the Atlantic Ocean: Continental margins and*

*palaeoenvironments* (Ed. by M. Talwani, W. Hay and W.B.F. Ryan). *Maurice Ewing Series, Am. Geophys. Union,* **3**, 342–361.

Cheel, R.J. (1991). Grain fabric in hummocky cross-stratified storm beds: genetic implications. *J. Sed. Petrol.* **61**. 102-–110.

Cheel, R.J. and Leckie, D.A. (1992). Coarse-grained storm beds of the Upper Cretaceous Chungo Member (Wapiabi Formation), southern Alberta, Canada. *J. Sed. Petrol.*, **62**, 933–945.

Cheel, R.J. and Leckie, D.A. (1993) Hummocky cross stratification. In: *Sedimentology Review*, **1,** (Ed. By V.P. Wright), 103–122.

Cheel, R.J and Middleton, G.V. (1993). Directional scours on a transgressive surface: examples from the Silurian Whirlpool Sandstone of southern Ontario, Canada. *J. Sed. Petrol.*, **63**. 392–397.

Chen, C.L. (1988). Generalized viscoplastic modeling of debris flows. *J. Hydraul. Eng.*, **114**, 237–258.

Chien, N. (1989). A study of hyperconcentrated flows. Tsinhua Univ. Press, Beijing, (in Chinese).

Clifton, H.E. (1973). Pebble segregation and bed lenticularity in wave-worked versus alluvial gravel. *Sedimentology*, **20**, 173–187.

Clifton, H.E. (1981). Progradation sequences in Miocene shoreline deposits, southeastern Caliente Range, California. *J. Sed. Petrol.*, **51**, 165–184.

Clifton, H.E., Hunter, R.E. and Phillips, R.L. (1971). Depositional structures and processes in the non-barred high-energy nearshore. *J. Sed. Petrol.*, **41**, 651–670.

Cobbold, E.S. (1913a). Fifth Report on Excavations among the Cambrian Rocks of Comley, Shropshire, 1911. *Rep. Brit. Ass.* for 1912, 136.

Cobbold, E.S. (1913b). The trilobite fauna of the Comley Breccia-Bed (Shropshire). *Q. J. Geol. Soc. Lond.*, **69**, 27.

Cobbold, E.S. (1913c). Two species of Paradoxides from Neve's Castle (Shropshire). Q. *J. Geol. Soc. London*, **69**, 45–

Cobbold, E.S. (1925). Unconformities in south Shropshire. Proc. *Geol.* Ass. *Lond.*, **36**, 364–375.

Cobbold, E.S. (1933). Notes on Comley Quarry, near Church Stretton, Shropshire. *Brit. Ass. Reports, Section C – Geology*, 1933, 473–476.

Cocks, L.R.M., McKerrow, W.S. and van Staal, C.R. (1997). The margins of Avalonia. *Geol. Mag.*, **135**, 627–636.

Colella, A, De Boer, P.L. and Nio, S.D. (1987). Sedimentology of a marine intermontane Pleistocene Gilbert-type fan-delta complex in the Crati Basin, Calabria, southern Italy. *Sedimentology*, **34**, 721–736.

Coleman, J.M. (1981). Deltas: processes of deposition and models for exploration. Burgess, CEPCO Division, Minneapolis, 124 pp.

Collinson, J.D. (1996). Alluvial sediments. In: *Sedimentary environments: Processes, Facies, and Stratigraphy* (Ed. by H.G. Reading). *Blackwell Science*, Oxford. 37–82.

Colmenero, J.R., Aqueda J. A., Fernandez L.P., Salvador, C.I., Bahamonde, J.R., and Barba, P. (1988). Fan-delta systems related to the Carboniferous evolution of the Cantabrian Zone, northwestern Spain. In: *Fan-deltas: sedimentology and tectonic setting* (Ed. by W. Nemec and R.J. Steel), Blackie and Son Ltd. London, 267–285.

Compston, W., Wright, A.E. and Toghill, P. (2002). Dating the Late Precambrian volcanicity of England and Wales. *J. Geol. Soc. Lond.*, **159**, 323–339.

Conway Morris, S. and Rushton, A.W.A. (1988). Precambrian to Tremadoc biotas in the Caledonides. In: *Caledonian–Appalachian Orogen* (Ed. by A.L. Harris and D.J. Fettes). *Geol. Soc. London*. Spec. *Publ.*, **38**, 93–109.

Cope, J.C.W. and Bassett, M.G. (1987). Sediment sources and Palaeozoic history of the Bristol Channel area. *Proc. Geol.* Ass., **98**, 315–330.

Cope, J.C.W. and Bevins, R.E. (1993). The stratigraphy and setting of the Precambrian rocks of the Llangynog Inlier, Dyfed, South Wales. *Geol. Mag.*, **130**, 101–111.

Cope, J.C.W. and Rushton, A.W.A. (1992). Cambrian and early Tremadoc rocks of the Llangrynog Inlier, Dyfed, South Wales, *Geol. Mag.*, **129**, 543–552

Corcoran, P.L., Mueller W.U. and Padgham, W.A. (1999). Influence of tectonism and climate on lithofacies distribution and sandstone and conglomerate composition in the Archean Beaulieu Rapids Formation, Northwest Territories, Canada. *Precambrian Res.*, **94**, 175–204.

Cowie, J.W., Rushton, A.W.A. and Stubblefield, C.J. (1972). A correlation of Cambrian Rocks in the British Isles. *Geol. Soc. London*, Spec. *Report*, **2**, 2–42.

Cox, A.H. (1915). The geology of the district between Abereiddy and Abercastle (Pembrokeshire). *Q. J. Geol. Soc. London*, **71**, 273–342.

Cox, A.H. (1930). A preliminary note on the geological structure of Pen Caer and Strumble Head, Pembrokeshire. *Proc. Geol.* Ass., **41**, 274–289.

Cox, A.H., Green, J.F.N., Jones, O.T. and Pringle, J. (1930a). The St David's district. Report on the summer meeting, 1930. *Proc. Geol.* Ass., **41**, 412–438.

Cox, R. and Lowe, D.R. (1995). A conceptual review of regional-scale controls on the composition of clastic sediment and the co-evolution of continental blocks and their sedimentary cover. *J. Sed. Res*, **A65**, 1–12.

Cox, R., Martin, M.W., Comstock, J.C., Dickerson, L.S., Ekstrom, I.L. and Sammons, J.H. (2002). Sedimentology, stratigraphy, and geochronology of the Proterozoic Mazatzal Group, central Arizona. *Geol. Soc. Am. Bull.*, **114**, 1535–1549.

Craft, J.H. and Bridge, J.S. (1987). Shallow-marine sedimentary processes in the Late Devonian Catskill Sea, New York State. *GSA Bull.*, **98**, 338–355.

Crews, S.G. and Ethridge, F.G. (1993). Laramide tectonics and humid alluvial fan sedimentation, NE Uinta Uplift, Utah and Wyoming. *J. Sed. Petrol.*, **63**, 420–436.

Crimes, T.P. (1970a). A facies analysis of the Cambrian of Wales. *Palaeogeog., Palaeoclim., Palaeoecol.*, **7**, 113–170.

Crimes, T.P. (1970b). Trilobite tracks and other trace fossils from the Upper Cambrian of North Wales. *Geol. J.*, **11**, p 476–68.

Crimes, T. P. and Dhonau, N.B. (1967). The Precambrian and Lower Palaeozoic rocks of south-east Co. Wexford, Eire. *Geol. Mag.*, **104**, 213–221.

Crimes, T.P. and Oldershaw, M.A. (1967). Palaeocurrent determination by magnetic fabric measurements on the Cambrian rocks of St. Tudwels Peninsula, North Wales. *Geol. J.*, **5**, 217–232.

Csanady, G.T. (1977). The coastal jet conceptual model in the dynamics of coastal seas. In: *The Sea*, (Ed. by E.D. Goldburg, I.N. McCave, J.J. O'Brien, and J.H. Steele. John Wiley, New York. 117–144.

Csanady, G.T. (1982). Circulation in the coastal ocean. Reidel, London, 280 pp.

Dabrio, C.J. and Polo, M.D. (1988). Late Neogene fan deltas and associated corel reefs in the Almanzora Basin, Almería Province, southeastern Spain. In: *Fan-deltas: sedimentology and tectonic setting* (Ed. by W. Nemec and R.J. Steel), Blackie and Son Ltd. London, 354–367.

Daley, B. (1968). Sedimentary structures from a non-marine horizon in the Bembridge marls (Oligocene) of the Isle of Wight, Hampshire, England. *J. Sed. Petrol.* **38**. 114–127.

Dallmeyer, R.D. and Gibbons, W. (1987). The age of blueschist metamorphism in Anglesey, North Wales: evidence from 40Ar/39Ar mineral dates of the Penmynedd Schists. *J. Geol. Soc. Lond.*, **144**, 843–850.

Davies, H.G. and Downie, C. (1964). Age of the Newgale Beds. *Nature*, **203**, 71.

de Raaf, J.F.M., Boersma, J.R. and Van Gelder, A. (1977). Wave-generated structures and sequences from a shallow marine succession, lower Carboniferous, County Cork, Ireland. *Sedimentology*, **24**, 451–483.

DeCelles, P.G. (1987). Variable preservation of Middle Tertiary, coarse-grained nearshore to outer-shelf deposits in southern California. *J. Sed. Petrol.*, **57**, 250–264.

Decker, J. and Helmold, K.P. (1985). The effect of grain size on detrital modes: a test of the Gazzi-Dickinson point-counting method – discussion. *J. Sed. Petrol.*, **55**, 618–520.

Desloges, J.R. and Gardner, J.S. (1984). Process and discharge estimation in ephemeral channels, Canadian Rocky Mountains. *Can. J. earth Sci.*, **21**, 1050–1060.

Dickinson, W.R. (1970). Interpreting detrital modes of greywacke and arkose. *J. Sed. Petrol.*, **40**, 695–707.

Dickinson, W.R. (1985). Interpreting provenance relations from detrital modes of sandstones. In: *Provenance of Arenites* (Ed. by G.G. Zuffa). D. Reidel, The Netherlands, 333–361.

Dickinson, W.R. and Suczek, C.A. (1979). Plate tectonics and sandstone composition. *Am. Ass. Petrol. Geol. Bull.*, **63**, 2164–2182.

Dickinson, W.R., Beard, L.S., Brakenridge, G.R., Erjavec, J.L., Ferguson, R.C., Inman, K.P., Kneep, R.A., Lindberg, F.A. and Ryberg, P.T. (1983). Provenance of North American Phanerozoic sandstones in relation to tectonic setting. *Geol. Soc. Am. Bull.*, **94**, 222–235.

Dietrich, J.R., Higgs, R., Rohr, K.M. and White, J.M. (1993). The Tertiary Queen Charlotte Basin: a strike-slip basin on the western Canadian continental margin. *Spec.* Publ. Int. Ass. Sed., **20**, 161–169.

Dorsey, R.J. (1988). Provenance evolution and unroofing history of a modern arc-continent collision: evidence from petrography of Plio-Pleistocene sandstones, eastern Taiwan. *J. Sed. Petrol.*, **58**, 208–218.

Dorsey, R.J., Umhoefer, P.J. and Renne, P.R. (1995). Rapid subsidence and stacked Gilbert-type fan-deltas, Pliocene Loreto Basin, Baja California Sur, Mexico. *Sed. Geol.*, **98**, 181–204.

Dott, R.H. and Bourgeois, J. 1982. Hummocky stratification: significance of its variable bedding sequences. *Bull. GSA.*, **93**, 663–680.

Drosser, M.L. and Bottjer, D.J. (1986). A semiquantitative field classification of ichnofabric. *J. Sed. Petrol.*, **56**. 558–559.

Duke, W.L. (1985). Hummocky cross stratification, tropical hurricanes and intense winter storms, *Sedimentology*, **32**, 167–194.

Duke, W.L. (1987). Hummocky cross stratification, tropical hurricanes and intense winter storms: Reply. *Sedimentology*, **34**, 344–359.

Duke, W.L. (1990). Geostrophic circulation or shallow marine turbidity currents? The dilemma of palaeoflow patterns in storm-influenced prograding shoreline systems. *J. Sed. Petrol.* **60**. 870–883.

Duke, W.L., Arnott, R.W.C. and Cheel, R.J. (1991a). Shelf sandstones and hummocky cross stratification: new insights into a stormy debate, *Geology*, **19**, 625–638.

Duke, W.L., Fawcett, P.J., and Brusse W.C. (1991b). Prograding shoreline deposits in the Lower Silurian Medina Group, Ontario and New York: storm- and tide-influenced sedimentation in a shallow marine epicontinental sea, and the origin of enigmatic shore-normal channels encapsulated by open shallow marine deposits. In: *Shelf sand and sandstone bodies: Geometry, Facies and Sequence Stratigraphy* (Ed. By D.J.P. Swift, G.F. Oertel, R.W. Tillman and J.A. Thorn). *Spec. Publ. Int. Ass. Sed.*, 339–375.

Dunne, L.A. and Hempton, M.R. (1984). Deltaic sedimentation in the Lake Hazar pull-apart basin, southeastern Turkey. *Sedimentology*, **31**, 401-412.

Dupret, L., Dissler, E., Doré, F., Gresselin, F. and Le Gall, J. (1990). Cadomian geodynamic evolution in the northeastern Armorican Massif (Normandy and Maine). In: The Cadomian orogeny (Ed. by R.S. D'Lemos, R.A. Strachan, and C.G. Topley). *Geol. Soc. Lond. Spec. Publ.*, **51**, 115–131.

Dyson I.A. (1996). Significance of hummocky cross-stratification and quasi-planar lamination in the lower Devonian Wallhalla Group at Cape Liptrap, Victoria. Austr. *J. Earth Sci.*, **43**. 189–199.

Dzulynski, S. (1963). Directional structures in flysch. *Polska Akademia Nauk, Studia Geologia Polonica*, **12**, 1-136.

Dzulynski, S. and Sanders, J.E. (1962). Current marks on firm mud bottom. *Trans. Conn. Acad. Arts Sci.*, **42**, 57–96.

Dzulynski, S. and Simpson, F. (1966). Experiments on interfacial current markings, *Uniroma1*, **5,** 197—214.

Ehlers, J. (1988). The morphodynamics of the Wadden Sea. Balkema, Rotterdam, 397 pp.

Eliet, P.P. and Gawthorpe, R.L. (2000). Drainage development and sediment supply within rifts, examples from the Sperchios basin, central Greece. *J. Geol. Soc. London*, **152**, 883–893.

Elliott, T. (1986). Deltas. In: *Sedimentary environments and Facies, 2nd Edition* (Ed. by H.G. Reading). Blackwell Science, Oxford, 113–154.

Ellwood, B.B., Hrouda, F. and Wagner, J.J. (1988). Symposia on magnetic fabrics. *Physics of the Earth. and Planetary Interiors*, **51**, 249–392

Enos P. (1977). Holocene sediment accumulations of the South Florida shelf margin. In: Quaternary sedimentation in South Florida (Ed. by P. Enos amd R.D. Perkins). *Mem. Geol. Soc. Am.*, **147**, Boulder, CO., 1–130.

Eriksson, K.A. (1978). Alluvial and destructive beach facies from the Archaean Moodies Group, Barberton Mountain Land, South Africa and Swaziland. In: Fluvial Sedimentology (Ed. by A.D. Miall). *Mem. Can. Soc. Petrol. Geol.*, **5**, 287–311.

Espejo, I.S. and Lopez-Gamundi, O.R. (1994). Source versus depositional controls on sandstone composition in a foreland basin: the El Imperial Formation (mid Carboniferous – Lower Permian), San Rafael Basin, Western Argentina. *J. Sed. Res*, **A64**, 8–16.

Ethridge, F.G. and Wescott, W.A. (1984). Tectonic setting, recognition and hydrocarbon reservoir potential of fan-delta deposits. In: *Sedimentology of Gravels and Conglomerates* (Ed. by E.H. Koster and R.J. Steel). *Can. Soc. Petrol. Geol. Mem.*, 217–235.

Evans G. (1965). Intertidal flat sediments and their environments of deposition in the wash. *Q. J. Geol. Soc. Lond.*, **121**, 209–245.

Evans, J.E. (1991). Facies relationships, alluvial architecture, and paleohydrology of a Paleogene, humid-tropical alluvial fan system: Chumstick Formation, Washington State, U.S.A. *J. Sed. Petrol.*, **61**, 732–755.

Evans, K.R, Rowell, A.J. and Rees, M.N. (1995). Sea level changes and stratigraphy of the Nelson Limestone (Middle Cambrian), Neptune Range, Antartica. *J. Sed. Res.*, **B65**, 32–43.

Evans, W.D. (1948). The Cambrian–Ordovician junction, Whitesand Bay, Pembrokeshire. *Geol. Mag.*, **85**, 110– 116.

Falk, P.D. and Dorsey, R.J. (1998). Rapid development of gravelly high-density turbidity currents in marine Gilbert-type fan-deltas, Lorento Basin, Baja California Sur, Mexico. *Sedimentology*, **45**, 331–349.

Farshori, N.Z. (1962). Cambrian sediments of the St David's area, South Wales. *UnPublished Ph.D. thesis*, University of Cardiff. 298 pp.

Fedo, C.M. and Cooper, J.D. (1990). Braided fluvial to marine transition: The basal Lower Cambrian Wood Canyon Formation, Southern Marple Mountains, Majave desert, California. *J. Sed. Petrol.*, **60**, 220–234.

Fernandez, L.P., Agueda, F.A., Colmenero, J.R., Salvador, C.I. and Barba, P. (1988). A Coal-bearing fan-delta complex in the Westphalian D of the Central Coal Basin, Cantabrian Mountains, northwestern Spain: implications for the recognition of humid-type fan-deltas. In: *Fan-deltas: Sedimentology and Tectonic setting* (Ed. by W. Nemec and R.J. Steel). Blackie, 286–302.

Fisher, R.V. (1983). Flow transformation in sediment gravity flows. *Geology*, **11**, 273–274.

Fitches, W.R. and Woodcock, N.H. (1987). Sedimentation and tectonics in the Welsh Basin. *Geol. J.*, **22**, 1–5.

Fitzsimmons, R. (1994). Identification of high order sequence boundaries and land attached shoreface regressions. In: *High Resolution Sequence Stratigraphy: Innovations and Applications, Abstract Volume*, University of Liverpool, pp. 332–333.

Fletcher, T.P. (1972). Geology and Lower to Middle Cambrian trilobite faunas of the southwest Avalon, Newfoundland [Ph.D. thesis], Cambridge, University of Cambridge, 520 p.

Flint, S., Turner, P. and Jolly, E.J. (1991). Depositional architecture of Quaternary fan-delta deposits of the Andean fore-arc: relative sea-level changes as a response to aseismic ridge subduction. *Spec. Publ. Int. Ass. Sedim.* **12**. 91–103.

Flood, R.D. (1981). Distribution, morphology and origin of sedimentary furrows in cohesive sediments, Southampton Water. *Sedimentology*, **28**, 511–529.

Flood, R.D. (1983). Classification of sedimentary furrows and a model for furrow initiation and evolution. *GSA Bull.*, **94**, 630–639.

Floyd, J.D. and Trench, A. (1989). Magnetic susceptibility measurements in Ordovician greywackes of the southern uplands of Scotland. *J. Geol. Soc. Lond.*, **146**, 77–83. 45-46

Folk, R.L. (1980). Petrology of Sedimentary Rocks. Austin, Texas, Hemphill, 182 p.

Forbes, D.L. and Taylor, R.B. (1987). Coarse-grained beach sedimentation under periglacial conditions, Canadian Atlantic Coast. In: *Glaciated coasts* (Ed. by D. Fitzgerald and P. Rosen). Academic Press, New York, 51–86.

Fortey, R.A. (1984). Global earlier Ordovician transgression and regression and their biological implications. In: Aspects *of the Ordovician System* (Ed. by D.L. Bruton), Universitetsforlaget, Oslo, 37–50.

Fortey, R.A. and Cocks, L.R.M. (1992). The early Palaeozoic of the North Atlantic region as a test case for the use of fossils in continental reconstructions. *Tectonophysics*, **206**, 147–158.

Foster, D.N. and Stone, D.M. (1963). Ocean Dispersal of Ash. The University of New South Wales, Water Research Laboratory, Report, 65, 130 p.

Frey, R.W. and Pemberton, S.G. (1984). Trace fossil facies models. In: *Facies Models, Second Edition* (Ed. by R.G. Walker). Geoscience Canada Reprint Series, **1**, 189–208.

Fuller, A.O. (1985). A contribution to the conceptual modelling of pre-Devonian fluvial systems. Trans. *Geol. Soc.* S. *Afr.*, **88**, 189–194.

Galli, G. (1989). Depositional mechanisms of storm sedimentation in the Triassic Dürrenstein Formation, Dolomites, Italy. *Sed. Geol.* **61**. 81–93.

Gawthorpe, R.L. and Colella, A. (1990). Tectonic controls on coarse-grained delta depositional systems in rift basins. In: *Coarse-grained deltas* (Ed. by A. Colella and D.B. Prior). *Spec. Publ. Int. Ass. Sed.*, **10**, 113–127.

George, T.N. (1970). British Regional Geology. South Wales. H.M.S.O. (3rd Edition), 152 pp.

Gibbons, W. (1983). Stratigraphy, subduction and strike-slip faulting in the Mona Complex of North Wales – a review. Proc. *Geol.* Ass., **94**, 147–163.

Gibbons, W. (1987). The Menai Straits Fault System: an early Caledonian terrane boundary in North Wales. *Geology*, **15**, 744–747.

Gibbons, W. (1990). Transcurrent ductile shear zones and the dispersal of the Avalon Superterrane. In: *The Cadomian Orogeny* (Ed. by R.S. D'Lemos, R.A. Strachan and C.G. Topley). *Geol. Soc. London* Spec. *Publ.*, **51**, 407–423.

Gibbons, W. and Horák, J.M. (1990). Contrasting metamorphic terranes in northwest Wales. In: *The Cadomian Orogeny* (Ed. by R.S. D'Lemos, R.A. Strachan, and C.G. Topley). *Geol. Soc. Lond. Spec. Publ.*, **51**, 315–327.

Gibbons, W. and Horak, J.M. (1996). The evolution of the Neoproterozoic Avalonian subduction system: Evidence from the British Isles. In: *Avalonian and related Peri-Gondwanan Terranes of the Circum–North Atlantic* (Ed. by R.D. Nance and M.D. Thompson). Geol. Soc. Am. Spec. Pap., **304**, 269–280.

Gibbons, W. and Mann, A. (1983). Pre-Mesozoic lawsonite in Anglesey, North Wales – the preservation of ancient blueschist. *Geology*, **11**, 3–6.

Gibbons, W., Tietzsch-Tyler, D., Horák, J.M. and Murphy, F.C. (1994). Precambrian rocks in Anglesey, southwest Llyn and southeast Ireland. In: *A revised correlation of Precambrian rocks of the British Isles* (Ed. by W. Gibbons and A.L. Harris). *Geol. Soc. Lond. Spec. Rep.*, **22**, 75–84.

Girty, G.H. (1987). Sandstone provenance, Point Loma Formation, San Diego, California: Evidence for uplift of the Peninsula Ranges during the Laramide Orogeny. *J. Sed. Petrol.*, **57**, 839–844.

Girty, G.H., Mossman, B.J., Pincus, S.D. (1988). Petrology of Holocene sand, Peninsula Ranges, California and Baja Norte, Mexico: Implications for provenance discrimination models. *J. Sed. Petrol.*, **58**, 881–887.

Gladstone, C. and Sparks, S.J. (2002). The significance of grain size breaks in turbidites and pyroclastic density current deposits. *J. Sed. Res* **72**. 182–191.

Gloppen, T.G. and Steel, R.J. (1981). The deposits, internal structure and study in the significance of bedding sequences in conglomerates. In: Recent and Ancient Non-Marine Depositional Environments: Models for Exploration (Ed. by F.G. Ethridge and R.M. Flores). *SEPM* Spec. *Publ.*, **31**, 49–69.

Goldring, R. and Aigner, T. (1982). Scour and fill: the significance of event separation. In: *Cyclic and event stratification* (Ed. by G. Einsele and A. Seilacher). Springer, Berlin, 354–362.

Gorden, I. and Heller, P.L. (1993). Evaluating major controls on basin stratigraphy, Pine Valley, Nevada: implications for syn-tectonic deposition. *Geol. Soc. Am. Bull.*, **105**, 47–55.

Gordon, R.L. (1982). Coastal ocean current response to storm winds. *J. Geophys. Res.* **87**. 1939–1951.

Gorsline, D.S. (1984). A review of fine-grained sediment origins, characteristics, transport and deposition. In: *Fine-Grained Sediments: Deep Water Processes and Facies* (Ed. by D.A.V. Stow and D.J.W. Piper), *Spec. Publ. Geol. Soc. London*, **15**, 17–34.

Graham, S.A., Hendrix, M.S., Wang, L.B. and Carroll, A.R. (1993). Collisional successor basins of western China: Impact of tectonic inheritance on sand composition. *Geol. Soc. Am. Bull.*, **105**, 323–344.

Graham, S.A., Ingersoll, R.V. and Dickinson, W.R. (1976). Common provenance for lithic grains in Carboniferous sandstones from Ouachita Mountains and Black Warrior basin. *J. Sed. Petrol.*, **46**, 620–632.

Graham, S.A., McCloy, C., Hitzman, M., Ward, R. and Turner, R. (1984). Basin evolution during change from convergent to transform continental margin in central California. *Am. Ass. Petrol. Geol. Bull.*, **68**, 233–249.

Granar, L. (1958). Magnetic measurements on Swedish varved sediments. *Arkiv. F. Geofysik.*, **3**, 1–40.

Grant, W.D. and Madsen, O.S. (1979). Combined wave and current interaction with a rough bottom. *J. Geophys. Res.*, **84**, 1797–1808.

Grantham, J.H. and Velbel, M.A. (1988). The influence of climate and topography on rock-fragment abundance in modern fluvial sands of the southern Blue Ridge Mountains, North Carolina. *J. Sed. Petrol.*, **58**, 219–227.

Green, J.F.N. (1908). The geological structure of the St David's area (Pembrokeshire). *Q. J. Geol. Soc. London*, **64**, 363–383.

Green, J.F.N. (1911). Excursions to the St David's district, South Wales. *Proc. Geol.* Ass., **22**, 215–34.

Greenly, E. (1919). The geology of Anglesey. *Mem. Geol.* Surv. Great Britain, 2 volumes, London.

Greenwood, B. and Sherman, D.J. (1986) Hummocky cross-stratification in the surf zone: flow parameters and bedding genesis. *Sedimentology*, **33**, 33–45.

Gutiérrez-Alonso, G., Fernàdez-Suàrez, J., Jeffries, T.E., Jenner, G. A., Tubrett, M.N., Cox, R., and Jackson, S.E. (2003). Terrane accretion and dispersal in the northern Gondwanan margin: An Early Paleozoic analogue of a long-lived active margin. *Tectonophysics*, **365**, 221—232.

Hamilton, N. and Rees, A.I. 1970. The use of magnetic fabric in palaeocurrent estimation. Palaeogeophysics. Academic Press, London, 445–464.

Hampton, M.A. (1975). Competence of fine-grained debris flows. *J. Sed. Petrol.*, **45**, 834–844.

Hand, B.M. (1997). Inverse grading resulting from coarse-sediment transport lag. *J. Sed. Res.*, **67**, 124–129.

Harkness, R. and Hicks, H. (1871). On the ancient rocks of St David's promontory, South Wales, and their fossil contents. *Q. J. Geol. Soc. London*, **27**, 384–404.

Harms, J.C., Southard, J.B. and Walker, R.G. 1975. Depositional environments as interpreted from sedimentary studies and stratification sequences. SEPM Short Course, **2**, pp 161.

Hart, B.S. and Plint, A.G. (1989). Gravelly shoreface deposits: a comparison of modern and ancient facies sequences. *Sedimentology*, **36**, 551–557.

Harvey, A.M. (1984). Debris flow and fluvial deposits in Spanish Quaternary alluvial fans: applications for fan morphology. In: *Sedimentology of gravels and conglomerates* (Ed. by E.H. Koster and R.J. Steel). *Can. Soc. Petrol. Geol. Mem.*, **10**, 123–132.

Heckel, P.H. (1991). Thin widespread Pennsylvanian black shales of Midcontinent North America: a record of a cyclic succession of widespread pycnoclines in a fluctuating epeiric sea. In: *Modern and Ancient Continental Shelf Anoxia* (Ed. by R.V. Tyson and T.H. Pearson). *Geol. Soc.* Spec. *Publ.*, **58**, 259–273.

Hein, F.J. (1982). Depositional mechanisms of deep-sea coarse-grained sediments, Cap Enragé Formation, Québec. *Can. J. Earth Sci.*, **19**, 267–287.

Hein, F.J. and Walker, R.G. (1977). Bar evolution and development of stratification in the gravelly, braided Kicking Horse River, British Columbia. *Can. J. Earth Sci.*, **14**, 562–570.

Heller, P.L. and Dickinson, W.R. (1985). Submarine Ramp Facies Model for Delta-Fed, Sand-Rich Turbidite Systems. *Am. Ass. Petrol. Geol. Bull.*, **69**, 960–976.

Heller, P.L., Angevine, C.L., Winslow, N.S. and Paola, C. (1988). Two-phase stratigraphic model of foreland-basin sequence. *Geology*, **16**, 501–504.

Henderson, R.A. and Southgate, P.A. (1978). Middle Cambrian stratigraphy and sedimentology of the eastern Georgina basin. In: *Excursions Handbook* (Ed. by M.G. Rubenbach). 3rd Aust. *Geol.* Conv., *Geol. Soc. Aust.* (Queensland Div.), Brisbane.

Hendrix, M. S. (2000). Evolution of Mesozoic sandstone compositions, southern Junggar, northern Tarim, and western Turpan basins, northwest China: a detrital record of the ancestral Tian Shan. *J. Sed. Res*, **70**, 520–532.

Héquette, A. and Hill P.R. (1993). Storm-generated currents and offshore sediment transport on a sandy shoreface, Tibjak Beach, Canadian Beaufort Sea. *Mar. Geol.*, **113**, 283–304.

Heward, A.P. (1978). Alluvial fan sequences and megasequence models: with examples from Westphalian D-Stephanian B coalfields, Northern Spain. In: *Fluvial Sedimentology* (Ed. by A.D. Miall), *Mem. Can. Soc. Petrol. Geol.*, **5**, 669–702.

Hicks, H. (1877). On the Pre-Cambrian (Dimetian and Pebidian) of the St. David's Peninsula. *Q. J. Geol. Soc. London*, **33**, 229–241.

Hicks, H. (1881). The classification of the Eozoic and Lower Palaeozoic rocks of the British Isles. *Popular Sci. Rev.*, **5,** 289–308.

Hicks, H. (1892). The fauna of the Olenellus Zone in Wales. *Geol. Mag.*, **4**, 21–34.

Hicks, H. (1894). On some life zones in the Lower Palaeozoic rocks of the British areas, as defined mainly be researchers during the past 30 years. *Geol. Mag.*, **6,** 368–448.
Hicks, H. (1875). On the occurrence of phosphates in the Cambrian rocks. *Q. J. Geol. Soc. London*, **31**, 368.

Hicks, H. and Salter, J.W. (1866). Report on further researches in the Lingula Flags of South Wales. Report of the 35th meeting of the British Association for the Advancement of Science (Birmingham, 1865), 281–286.

Higgs, R. (1990). Is there evidence for geostrophic currents preserved in the sedimentary record of inner to middle-shelf deposits? Discussion. *J. Sed. Petrol.*, **60**, 633–635.

Hill P.R., Lewis C.P., Desmarais S., Kauppaymuthoo V. and Rais H. (2001). The Mackenzie Delta: sedimentary processes and facies of a high-latitude, fine-grained delta. *Sedimentology*, **48**, 1047–1078.

Hill, P. R. and Nadeau, O. C. (1989). Storm-dominated sedimentation on the inner shelf of the Canadian Beaufort Sea. *J. Sed. Petrol.*, **59**, 455–468.

Hill, P.R., Meulé, S., and Longuépée, H. (2003). Combined-flow processes and sedimentary structures on the shoreface of the wave-dominated Grande-riviére-de-la-Baleine delta. *J. Sed. Res.,* **73**. 217–226.

Hiscott, R.N. (1984). Tidal deposits of the Lower Cambrian Random Formation, eastern Newfoundland: facies and palaeoenvironments. *Can. J. Earth. Sci.*, **19,** 2028–2042.

Hiscott, R.N. and Middleton, G.V. (1980). Fabrics of coarse deep-water sandstones, Tourelle Formation, Québec, Canada. *J. Sed. Petrol.*, **50,** 703–722.

Holland, C.H. (1974). Cambrian of the British Isles, Norden, and Spitsbergen. A Wiley – Interscience Publication, pp. 300.

Holmes, A. (1965). Principles of Physical Geology (2nd edition). Nelson, London and Edinburgh, 1288 pp

Horton, B.K. and Schmitt, J.G. (1996). Sedimentology of a lacustrine fan-delta system, Miocene Horse Camp Formation, Nevada, USA. *Sedimentology*, **43**, 133–155.

Hounslow, M.W. (1985). Magnetic fabric arising from paramagnetic phyllosilicates minerals in mudrocks. *J. Geol. Soc. London*, **142**, 995–1006.

Howard J.D. and Nelson C.H. (1982) Sedimentary structures on a delta-influenced shallow shelf, Norton Sound, Alaska. Geol. en Mijnbouw, **61**, 29–36.

Howell, B.F. (1925). The faunas of the Cambrian Paradoxides beds at Manuels, Newfoundland. *Bull. Am. Palaeontology*, **11**, 140 pp.

Hoyal, D.C.J.D., Bursik, M.I. and Atkinson, J.F. (1999a). The influence of diffusive convection on sedimentation from buoyant plumes. *Mar. Geol.* **159**. 205–220.

Hoyal, D.C.J.D., Bursik, M.I. and Atkinson, J.F. (1999b). Settling-driven convection: a mechanism of sedimentation from stratified fluids. J. Geophys. Res., **104**, 7953–7966.

Hrouda, F. (1982). Magnetic anisotropy of rocks and its application in geology and geophysics. *Geological Surveys*. **5.** 37–82.

Hsu, K.L. (1959). Flute- and groove-casts in the Prealpine Flysch, Switzerland. *Am. J. Sci.*, **257**, 529–536.

Hubbard, R.J. (1988). Age and significance of sequence boundaries on Jurassic and Early Cretaceous rifted continental margins. *Am. Ass. Petrol. Geol. Bull*, **72**, 49–72.

Hutchinson, R.D. (1962). Cambrian stratigraphy and trilobite faunas in southeastern Newfoundland. *Geol. Survey, Can. Bull.*, **88**, 156 p

Ibbeken, H. and Schleyer, R. (1991). Source and Sediment. Springer, Berlin, 286 p.
Illing, V.C. (1916). The Paradoxidian fauna of a part of the Stockingford Shales. *Q. J. Geol. Soc. Lond.*, **71,** 386–450.

Ingersoll, R.V. (1990). Actualistic sandstone petrofacies: Disciminating modern and ancient source rocks. *Geology*, **18**, 733–736.

Ingersoll, R.V. and Suczek, C.A. (1979). Petrology and provenance of Neogene sand from Nicobar and Bengal Fans, DSDP sites 211 and 218. *J. Sed. Petrol.*, **49**, 1217–1228.

Ingersoll, R.V., Bullard, T.F., Ford, R.L., Grimm, J.P., Pickle, J.D. and Sares, S.W. (1984). The effect of grain size on detrital modes: a test of the Gazzi-Dickinson point-counting method. *J. Sed. Petrol.*, **54**, 103–116.

Iverson, R.M., Reid, M.E. and Lehusen, R.G. (1997). Debris flow mobilization from landslides. Annu. Rev. *Earth Planet. Sci.*, **25**, 85–138.

James, W.C. (1979). Limestone channel storm complex (Lower Cretaceous) Elkhorn Mountains, Montana. *J. Sed. Petrol.*, **50**, 447–456.

Jefferies, R.P.S., Lewis, M. and Donovan, S.K. (1987). Protocystites menevensis – a stem-group chordates (Cornuta) from the Middle Cambrian of South Wales. *Palaeontology*, **30**, 429–484.

Jelinek, V. (1978). Statistical processing of anisotropy of magnetic susceptibility measured on groups of specimens. *Studia Geophysica et Geodatia*, **22**, 50–62.

Jelinek, V. (1981). Characterisation of the magnetic fabric of rocks. *Tectonophysics*, **79**, 63—67.

Jennette, D.C. and Pryor, W.A. (1993). Cyclic alternations of proximal and distal storm facies: Kope and Fairview Formations (Upper Ordovician), Ohio and Kentucky. *J. Sed. Petrol.*, **63**. 183–203.

Jervey, M.T. (1988). Quantitative geological modeling of siliciclastic rock sequences and their seismic expression. In: *Sea-level Changes: An Integrated Approach* (Ed. by C.K. Wilgus, B.S. Hastings, C.G.St.C. Kendall, H.W. Posamentier, C.A. Ross and J.C. Van Wagoner). *SEPM Spec. Publ.*, **42**, 47–69.

Jo, H.R., Rhee, C.W. and Chough, S.K. (1997). Distinctive characteristics of a streamflow-dominated alluvial fan deposit: Sanghori area, Kyongsang Basin (Early Cretaceous), southeastern Korea. *Sed. Geol.*, **110**, 51–79.

Johnson, A.M. (1970). Physical Processes in Geology. Freeman Cooper, San Francisco, 577 pp.

Johnson, H.D. and Baldwin, C.T. (1996). Shallow clastic seas. In: *Sedimentary environments: Processes, Facies, and Stratigraphy* (Ed. by H.G. Reading). Blackwell Science, Oxford. 232–280.

Johnson, M.L. (1992). Chemical weathering controls on sand composition. In: Encyclopaedia of Earth Systems Science (Ed. by Nierenber, W.A.). Academic Press, Orlando, FL, 455–466.

Johnsson, M.J. (1993). The system controlling the composition of clastic sediments. In: *Processes Controlling the Composition of Clastic Sediments* (Ed. by M.J. Johnsson and A Basu). *Geol. Soc.* Am. Spec. *Paper*, *284*, 1–19.

Johnsson, M.L., Stallard, R.F. and Lundberg, N. (1991). Controls on the composition of fluvial sands from a tropical weathering environment: Sands of the Orinoco River drainage basin, Venezuela and Columbia. *Geol. Soc. Am. Bull.*, **103**, 1622–1647.

Johnsson, M.L., Stallard, R.F. and Meade, R.H. (1988). First-cycle quartz arenites in the Orinoco River basin, Venezuela and Columbia. *J. Geol.*, 96, 263–277.

Jones, O.T. (1932). On the evolution of a Geosyncline. *Q. J. Geol. Soc. London*, **47**, 1–60.

Jones, O.T. (1940). Some Lower Palaeozoic contacts on Pembrokeshire. *Geol. Mag.*, **77**, 405–409.

Jones, W. (1911). Notes on a heavy sandstone from St. David's, Pembrokeshire. Proc. *Geol.* Ass. *London*, **22**, 232-239.

Keppie, J.D. (1984). The Appalachian collage. In: *The Caledonide Orogen, Scandinavia and related areas* (Ed. by D.G. Gee and B. Sturt). J. Wiley and Sons, New York.

Keppie, J.D. and Murphy, J.B. (1988). Anatomy of a telescoped pull-apart basin: An example from the Cambrian-Ordovician of the Antigonish Highlands, Nova Scotia. *Maritime Sed. and Atlantic Geol.*, **24**, 123–138.

Keppie, J.D., Cousens, B.L., Dostal, J. and Murphy, J.B. (1997). Palaeozoic within-plate volcanic rocks in Nova Scotia (Canada) reinterpreted: isotopic constraints on magmatic source and palaeocontinental reconstructions. *Geol. Mag.*, **134**, 425–447.

Kerr, M. and Eyles, N. (1991). Storm deposited sandstones (tempesites) and related ichnofossils of the Late Ordovician Georgian Bay Formation, Southern Ontario, Canada. *Can. J. Earth Sci.*, **28**, 266–282.

Kidwell, S. (1989). Stratigraphic condensation of marine transgressive records: origin of major shell deposits in the Miocene of Maryland. *J. Geol.*, **97**, 1-24–139.

Kim, S.B., Chough, S.K., and Chun, S.S. (1995). Bouldery deposits in the lowermost part of the Cretaceous Kyokpori Formation, SW Korea: cohesionless debris flows and debris falls on a steep gradient delta slope. *Sed. Geol.*, **98**, 97–119.

Kineke, G., Woolfe, K.J., Kuehl, S.A. Milliman, J., Dellapenna, T.M. and Purdon, R.G. (2000). Sediment export from the Sepik River, Papua New Guinea: Evidence for a divergent dispersal system. *Cont. Shelf Res.*, **20**, 2239–2266.

Kneller, B.C. (1995). Beyond the turbidite paradigm: Physical models for the deposition of and their implications for reservoir prediction. In: Characterisation of deep marine clastic systems (Ed. by A.J. Hartley and D.J. Prosser), *Geol. Soc Lond. Spec. Publ.*, **94**, 31–49.

Kneller, B.C. and Branney, M.J. (1995). Sustained high-density turbidity currents and the deposition of thick massive sands. *Sedimentology*, **42**, 607–616.

Kneller, B.C. and Buckee, C. (2000), The structure and fluid mechanics of turbidity currents: a review of some recent studies and their geological implications. *Sedimentology*, **47**, (Suppl. 1), 62–94.

Kokelaar B.P., Bevins R.E. and Roach R.A. (1985). Submarine silicic volcanism and associated sedimentary and tectonic processes, Ramsey Island, SW Wales. *J. Geol. Soc. Lond.*, **142**, p 591–613.

Kolb C.R. and Van Lopik J.R. (1966). Depositional environments of the Mississippi Delta plain – southeastern Louisiana, In: *Deltas in their Geological Framework* (Ed. C. R. Kolb). Houston Geol. Soc., 17–61

Komar, P.D. (1976). Beach Processes and Sedimentation. Prentice-Hall, Englewood Cliffs, NJ. 429 p.

Komar, P.D. (1977). Computer simulation of turbidity current flow and the study of deep-sea channels and fan sedimentation. In: *The Sea* (Ed. by E.D. Goldburg, I.N. McCave, J.J. O'Brien, and J.H. Steel). *Marine modeling*, **6**, John Wiley, New York, 603–621.

Kostachuck, R.A., Macdonald, G.M. and Putnam, P.E. (1986). Depositional processes and alluvial fan drainage basin morphometric relationships near Banff, Alberta, Canada. *Earth Surf. Proces. Landforms*, **11**, 471–484.

Kraus, M.J. (1984). Sedimentology and tectonic setting of Early Tertiary quartzite conglomerates, northwest Wyoming. In: Sedimentology of gravels and conglomerates (Ed. by E.H. Koster and R.J. Steel). *Can. Soc. Petrol. Geol. Mem.*, **10**, 203–216.

Kreisa, R.D. (1981). Storm-generated sedimentary structures in subtidal marine facies with examples from the middle and upper Ordovician of south-western Virginia. *J. Sed. Petrol.*, **51**. 823–848.

Kuehl, S.A., Hariu, T.M., and Moore, W.S. (1989). Shelf sedimentation off the Ganges-Brahmaputra river system: Evidence for sediment bypassing to the Bengal fan. *Geology*, **17**, 1132–1135.

Kuenen, Ph.H. and Migliorini, C.I. (1950). Turbidity currents as a cause of graded bedding. *J. Geol.*, **58**, 91–127.

Lake, P. (1906–1946). A Monograph of the British Cambrian Trilobites. Parts 1–14. Monograph of the Palaeontological Society, London, 350 pp.

Landing, E. (1980). Late Cambrian—Early Ordovician macrofaunas and phosphatic microfaunas, St John Group New Brunswick. *J. Palaont.*, **54**, 752–761.

Landing, E. (1988). Lower Cambrian of eastern Massachussetts: Stratigraphy and small shelly fossils. *J. Paleont.*, **63**, 566–573.

Landing, E. (1991). Upper Precambrian through lower Cambrian of Cape Breton Island: Faunas, palaeoenvironments, and stratigraphic revision. *J. Paleont.*, **65**, 570–595.

Landing, E. (1992). Lower Cambrian of south-eastern Newfoundland. Epeirogeny and Lazarus faunas, lithofacies-biofacies linkages, and the myth of a global chronostratigraphy. In: *Origin and early evolution of the metazoa* (Ed by J.H. Lipps and P.W. Signor). Plenum Press, New York, pp 283–309.

Landing, E. (1993). Cambrian—Ordovician boundary in the Taconic allochthon, eastern New York, and its interregional correlation. *J. Paleont.*, **67**, 1–19.

Landing, E. (1994). Precambrian—Cambrian global stratotype ratified and a new perspective of Cambrian time. *Geology*, **22**, 179–182.

Landing, E. (1995). Upper Placentian–Branchian Series of mainland Nova Scotia (middle-upper Lower Cambrian): Faunas, palaeoenvironments, and stratigraphic revision. *J. Paleont.*, **69**, 475–495.

Landing, E. (1996). Avalon: Insular continent by the latest Precambrian. In: *Avalonian and related Peri-Gondwanan Terranes of the Circum–North Atlantic* (Ed. by R.D. Nance and M.D. Thompson). *Geol. Soc.* Am. *Spec. Pap.*, **304**, 29–61.

Landing, E. and Benus, A.P. (1988). Stratigraphy of the Bonavista Group, southeastern Newfoundland: Epeirogeny and Lazarus faunas, lithofacies-biofacies linkages, and the myth of a global chronostratigraphy. In: *Origin and early evolution of the Metazoa* (Ed. by J.H. Lipps and P.W. Signor). Plenum Press, NY, 283–309.

Landing, E. and Westrop, S.R. (1996). Upper Lower Cambrian depositional sequence in Avalonian New Brunswick. *Can. J. Earth. Sci.*, **33**, 404–417.

Landing, E, Bowring, S.A., Davidek, K.L., Rushton, A.W.A., Fortey, R.A. and Wimbledon, W.A.P. (2000). Cambrian–Ordovician boundary age and duration of the lowest Ordovician Tremadoc Series based on U–Pb zircon dates from Avalonian Wales. *Geol. Mag.*, **137**, 485–494.

Landing, E., Bowring, S.A., Davidek, K.L., Westrop, S.R., Geyer, G. and Heldmaier, W. (1998). Duration of the Early Cambrian: U-Pb ages of volcanic ashes from Avalon and Gondwana. *Can. J. Earth Sci.*, **35,** 329–338.

Larson, V. and Steel. R.J. (1978). The sedimentary history of a debris flow-dominated alluvial fan: a study of textural inversion. *Sedimentology*, **25**, 37–59.

Lawton, T.F., Pollock, S.L. and Robinson, R.A.J. (2003). Integrating sandstone petrology and non-marine sequence stratigraphy: application to the Late Cretaceous fluvial systems of southwestern Utah, U.S.A. *J. Sed. Res.*, **73**, 389–406.

Leckie, D.A. & Krystinik, Z.F. (1989). Is there evidence for geostrophic currents preserved in the sedimentary record of inner to mid shelf deposits? *J. Sed. Petrol.*, **59**, 862–870.

Leckie, D.A. and Walker, R.G. (1982). Storm- and tide-dominated shorelines in Cretaceous Moosebar-Lower Gates interval-outcrop equivalents of deep basin gas traps in western Canada. *Am. Ass. Petrol. Geol. Bull.*, **66**, 138–157.

Leckie, D.A., Singh, C., Goodarzi, F., and Wall, J.H., (1990). Organic-rich, radioactive marine shale: a case study of a shallow water condensed section, Cretaceous Shaftsbury Formation, Alberta, Canada. *J. Sed. Petrol.*, **60**, 101–117.

Lee, Y.I. and Sheen, D.H. (1998). Detrital modes of the Pyeongan Supergroup (Late Carboniferous–Early Triassic) sandstones in the Samcheog coalfield, Korea: implications for provenance and tectonic setting. *Sed. Geol.*, **119**, 219–238.

Leeder, M.R., Ord, D.M. and Collier, R.E.L. (1988). Development of alluvial fans and fan-deltas in neotectonic settings: implications for the interpretation of basin fills. In: *Fan Deltas: Sedimentology and Tectonic Setting* (Ed. by W. Nemec and R.J. Steel). Blackie, London, 173–185.

Leggett, J.K., McKerrow, W.S., Cocks, L.R.M. and Rickards, R.B. (1981). Periodicity in the early Palaeozoic marine realm. *J. Geol. Soc. Lond.*, **138**, 167–176.

Leithold, E.L. and Bourgeois, J. (1984). Characteristics of coarse-grained sequences deposited in nearshore, wave-dominated environments - examples from the Miocene of southwest Oregon. *Sedimentology*, **31**, 749–775.

Lemon, R. R. (1993). Vanished worlds: An introduction to historical geology. Wm. C. Brown. Publishers. Dubuque. 458 pp.

Levson, V.M. and Rutter, N. W. (2000). Influence of bedrock geology on sedimentation in Pre-Late Wisconsinan alluvial fans in the Canadian Rocky Mountains. *Quaternary Int.*, **68–71**, 133–146.

Lewis, M. (1987). Cambrian stratigraphy and trilobites in south-west Wales. Un*Publ*ished PhD thesis, University of Wales, Cardiff.

Liu, B., Saito, Y., Yamazaki, T., Abdeldayem, A., Oda, H., Hori, K., and Zhao, Q. (2001). Paleocurrent analysis for the Late Pleistocene-Holocene incised-valley fill of the Yangtze delta, China by using anisotropy of magnetic susceptibility data. *Mar. Geol.*, **176**, 175–189.

Long, D.G.F. (1978). Proterozoic stream deposits: some problems of recognition and interpretation of ancient sandy fluvial systems. In: Fluvial Systems (Ed. by A.D. Miall). *Can. Soc. Petrol. Geol. Mem.*, **5,** 313–341.

Love, L.G. (1967). Early diagenetic iron sulphide in Recent sediments of the Wash (England). *Sedimentology*, **9,** 327–352.

Lowe, D.R. (1975). Water escape structures in coarse-grained sediments. *Sedimentology*, **22,** 157–204.

Lowe, D.R. (1982). Sediment gravity flows: II. Depositional models with special reference to the deposits of high-density turbidity currents. *J. Sed. Petrol.*, **52**. 279–297.

Lowe, D.R. (1988). Suspended-load fallout rates as an independent variable in the analysis of current structures. *Sedimentology,* **35**, 765–776.

Lüders, K. (1934). Über das Wandern der Priele. Abhandl. Naturwiss. Ver. Bremen, 29, 19–32.

Maar, J.D.G. (1999). Experiments on subaqueous sandy gravity flows: flow dynamics and deposit structures. UnPublished MSc Thesis, University of Minnesota.

Mack, G.H. (1984). Exceptions to the relationship between plate tectonics and sandstone composition. *J. Sed. Petrol.*, **54**, 212–220.

Maejima, W. (1988). Marine transgression over an active alluvial fan: the early Cretaceous Arida Formation, Yuasa-Aridagowa Basin, southwestern Japan. In: *Fan-deltas: sedimentology and tectonic setting* (Ed. by W. Nemec and R.J. Steel), Blackie and Son Ltd. London, 303–317.

Maguregui, J. and Tyler, N. (1991). Evolution of Middle Eocene tide-dominated deltaic sandstones, Lagunillas Field, Maracaibo Basin, Western Venezuela. In: *The Three-dimensional Facies Architecture of Terrigenous Clastic Sediments, and its Implications for Hydrocarbon Discovery and Recovery*. (Ed. by A.D. Miall and N. Tyler). SEPM Concepts in Sedimentology and Palaleotology, Tulsa, **3**, 233–244.

Major, J.J., and Iverson, M.R. (1999). Debris-flow deposition: effects of pore-fluid pressure and friction concentration at flow margins. *GSA Bull.*, **111**, 1424–1434.

Mángano, M.G. and Buatois, L.A. (1996). Shallow marine event sedimentation in a volcanic arc-related setting: the Ordovician Suri Formation, Famatina Range, northwest Argentina. *Sed. Geol.*, **105**, 63–90.

Manville, V. and White, J.D.L. (2003). Incipient granular mass flows at the base of sediment-laden floods, and the roles of flow competence and flow capacity in the deposition of stratified bouldery sands. *Sed. Geol.*, **155**, 157–173.

Marenssi, S.A., Net, L.I. and Santillana, S.N. (2001). Provenance, environmental and palaeogeographical controls on sandstone composition in an incised-valley system: the Eocene La Meseta Formation, Seymour Island, Antarctica. *Sed. Geol.,* **150**, 301–321.

Marsaglia K.M. and Klein, G.D. (1983). The palaeogeography of Palaeozoic and Mesozoic storm depositional systems. *J. Geol.,* **91**. 117–142.

Martel, A.T. and Gibling, M.R. (1994). Combined-flow generation of sole structures, including recurved groove casts, associated with Lower Carboniferous lacustrine storm deposits in Nova Scotia, Canada. *J. Sed. Res*, A64, 508–517.

Martinsen, O.J. (1989). Styles of soft sediment deformation on a Namurian (Carboniferous) delta slope, western Irish Namurian Basin, Ireland. In: *Deltas: Sites and Traps for Fossil fuels* (Ed. by M.K.G. Whateley and K.T. Pickering). *Spec. Publ. Geol. Soc. Lond.*, 167–177.

Pek, I. and Vaněk, J. (1971). Revision of the genera *Peronopsis* Hawle *et Corda*, 1847 and *Diplorrhina* Hawle *et Corda*, 1847 (Trilobita) from the Middle Cambrian of Bohemia. *Vestnik Ustredniho ustavu geologickeho*, **46**, 269–276.

Martins-Neto, M.A. (1996), Lacustrine fan-deltaic sedimentation in a Proterozoic rift basin: the Sopa-Brumadinho Tectanosequence, southeastern Brazil. *Sed. Geol.*, **106**, 65–96.

Martinson, O.J. (1990). Fluvial, inertia-dominated deltaic deposition in the Namurian (Carboniferous) of northern England. *Sedimentology*, **37**, 1099–1114.

Marzo, M. and Anadon, P. (1988). Anatomy of a conglomeratic fan-delta complex: the Eocene Montserrat Conglomerate, Ebro Basin, northwestern Spain. In: *Fan-deltas: sedimentology and tectonic setting* (Ed. by W. Nemec and R.J. Steel), Blackie and Son Ltd. London, 318–340.

Massari, F. (1984). Resedimented conglomerates of a Miocene fan-delta complex, southern Alps Italy. In: Sedimentology of Gravels and Conglomerates (Ed. by E.H. Koster and R.J. Steel). *Can. Soc. Petrol. Geol. Mem.*, **10**. 259–278.

Massari, F. and Colella, A. (1988). Evolution and types of fan-delta systems in some major tectonic settings. In: *Fan Deltas: Sedimentology and Tectonic Setting* (Ed. by W. Nemec and R.J. Steel). Blackie, London, 103–122.

Massari, F. and Parea, G.C. (1990). Wave-dominated Gilbert-type gravel deltas in the hinterland of the Gulf of Taranto (Pleistocene, southern Italy). In: *Coarse-grained Deltas* (Ed. by A. Colella and D.B. Prior), *Int. Ass. Sed. Spec. Publ.*, **10**, 103–122.

Massari, F., Mellere, D. and Doglioni, C. (1993). Cyclicity in non-marine foreland-basin sedimentary fill: the Messinian conglomerate-bearing succession of the Venetian Alps (Italy). In: *Alluvial Sedimentation* (Ed. by M. Marzo and C. Puigdefábregas). *Int. Ass. Sed. Spec. Publ.*, **17**, 501–520.

Mastalerz, K. (1995). Deposits of high-density turbidity currents on fan-delta slopes: an example from the upper Visean Szczawno Formation, Intrasudetic Basin, Poland. *Sed. Geol.*, **98**, 121–146.

Matley, C.A. and Wilson, T.S. (1946). The Harlech Dome, north of the Barmouth estuary. *Q. J. Geol. Soc. Lond.*, **102**, 1–40.

McCaffrey, W.D., Choux, C.M., Baas, J.H. and Haughton, P.D.W. (2003). Spatio-temporal evolution of velocity structure, concentration and grain-size stratification within experimental particulate gravity currents. *Mar. Petrol. Geol.*, **20**, 851–860.

McCallum, J.E. and Robertson, A.H.F. (1995). Sedimentology of two fan-delta systems in the Pliocene-Pleistocene of the Mesaoria Basin, Cyprus. *Sed. Geol.*, **98**, 215–244.

McCave, I.N. (1971). Wave effectiveness at the sea bed and its relationship to bed-forms and deposition of mud. *J. Sed. Petrol.*, **41**, 89–96.

McCave, I.N. and Jones, P.N. (1988). Deposition of ungraded muds from high-density non-turbulent turbidity currents. *Nature*, **333**, 250–252.

McCormick, D.S. and Grotzinger J.P. (1993). Distinction of marine from alluvial facies in the Paleoproterozoic (1.9Ga) Burnside Formation, Kilohigok Basin, N.W.T., Canada. *J. Sed. Petrol.*, **63**, 398–419.

McIlreath, I.A. and James, N.P. (1980). Carbonate slopes. In: *Facies Models* (Ed. by R.G. Walker). Geosci. Can. Rep. Ser., **1**, 133–143.

McIlroy, D., Brasier, M.D. and Moseley, J.B. (1998). The Proterozoic–Cambrian transition within the "Charnian Supergroup" of central England and the antiquity of the Ediacara fauna. *J. Geol. Soc. Lond.*, **155**, 401–411.

McKie, T. (1994). Geostrophic versus friction-dominated storm flow: palaeocurrent evidence from the Late Permian Brotherton Formation, England. *Sed. Geol.*, **93**, 73–84.

McLeod, P., Carey, S., and Sparks, S.J. (1999). Behaviour of particle-laden flows into the ocean: experimental simulation and geological implications. *Sedimentology*, **46**, 523–536.

McNamara, A.K., Niocaill, C.M., van der Pluijm, B.A. and Van der Voo, R. (2001). West African proximity of the Avalon terrane in the latest Precambrian. *GSA Bull.*, **113**, 1161–1170.

McPherson, J.G., Shanmugam, G. and Miola R.J. (1988). Fan-deltas and braid deltas: conceptual problems. In: *Fan-deltas: sedimentology and tectonic setting* (Ed. by W. Nemec and R.J. Steel), Blackie and Son Ltd. London, 14–22.

Miall. A.D. (1977). A review of the braided river depositional environment. *Earth Sci. Rev.*, **13**, 1–62.

Miall, A.D. (1978). Lithofacies types and vertical profile models in braided river deposits: a summery. In: *Fluvial Sedimentology* (Ed. by A.D. Miall). *Mem. Can. Soc. Petrol. Geol.*, **5**, 597–604.

Miall, A.D. (2000). Principles of Sedimentary Basin Analysis. Springer, Berlin, 616 pp.

Michels, K.H., Kudrass, H.R., Hübscher, C. Suckow, A. and Wiedicke, M. (1998). The submarine delta of the Ganges-Brahmaputra: cyclone-dominated sedimentation patterns. *Mar. Geol.,* **149**. 133–154.

Middleton, G.V. (1967). Experiments on density and turbidity currents. III. Deposition of sediment. *Can. J. Earth. Sci.*, **4**, 475-505.

Middleton, G.V. (1993). Sediment deposition from turbidity currents. *Annu. Rev. Earth. Planet Sci.,* **21**, 89–114.

Middleton, G.V. and Hampton, M.A. (1973), Sediment gravity flows: mechanisms of flow and deposition. In: *Turbidites and deep-water sedimentation* (Ed. by G.V. Middleton and N.P. James), *Geol. Ass. Canada*, 119–142.

Middleton, G. V. and Southard J.B. (1984). Mechanics of sediment movement. SEPM Short Course, **3,** Tulsa, 214 pp.

Midtgaard, H.H. (1996). Inner shelf hummocky sandstone bodies with evidence for geostophic influenced combined flow, Lower Cretaceous, West Greenland, *J. Sed. Res.,* **66**, 343–353.

Miller, M.F. (1984). Distribution of biogenic structures in Paleozoic non-marine and marine-margin sequences: an actualistic model. *J. Palaeon.*, **58**, 550–570.

Milliman, J.D. and Syvitski, J.P.M. (1992). Geomorphic and tectonic control of sediment discharge to the ocean: the importance of small mountainous rivers. *J. Geol.*, **100**, 525–544.

Mitchum, R.M., Jr., Vail. P.R. and Thompson, S., III. (1977a). Seismic stratigraphy and global changes of sea-level, part 2: the depositional sequence as a basic unit for

stratigraphic analysis. In: Seismic stratigraphy – Applications to Hydrocarbon Exploration (Ed. by C.E. Payton). Mem. *Am. Ass. Petrol. Geol. Bull.*, **26**, 53–62.

Mitchum, R.M., Jr., Vail. P.R. and Sangree, J.B. (1977b). Seismic stratigraphy and global changes of sea-level, part 6: seismic stratigraphic interpretation and precedure. In: Seismic stratigraphy – Applications to Hydrocarbon Exploration (Ed. by C.E. Payton). Mem. *Am. Ass. Petrol. Geol. Bull.*, **26**, 117–134.

Mohr, P.A. and Allen, R. (1965). Further considerations on the deposition of the Middle Cambrian manganese carbonate beds of Wales and Newfoundland. *Geol. Mag.*, **102**, 328–337.

Mohrig, D. (2001). Using delta-front turbidites to assess the occurrence and properties of sand-rich hyperpycnal flows emanating from rivers. *GSA Annual Metting*, Nov. 5–8, (2001) (abstract).

Morris, S.A., Kenyon, N.H., Limonov, A.F. and Alexander, J. (1998). Downstream changes in large-scale bedforms in turbidites around the Valencia channel mouth, north-west Mediterranean: implications for palaeoflow construction. *Sedimentology*, **45**, 365–377.

Mueller, W.U. and Corcoran, P. L. (2001). Volcano-sedimentary processes operating on a marginal continental arc; the Archean Requette Formation, Slave Province, Canada. *Sed. Geol.*, **141**, 169–189.

Mulder, T. and Alexander, J. (2001). The physical character of subaqueous sedimentary density flows and their deposits. *Sedimentology*. **48**. 269–299.

Mulder, T. and Syvitski, J.P.M. (1995). Turbidity currents generated at river mouths during exceptional discharges to world oceans. *J. Geol.*, **103**, 285–299.

Mulder, T., Syvitski, J.P.M. and Skene, J.P.M. (1998). Modeling of erosion and deposition of turbidity currents generated at river mouths. *J. Sed. Res.*, **68**. 124–137.

Mulder, T., Migeon, S, Savoye, B. and Faugères, J. (2001). Inversely graded turbidite sequences in the deep Mediterranean. A record of deposits from flood-generated turbidity currents? *Geo-mar. Lett.*, **21**, 86–93.

Mulder, T., Syvitski, J.P.M., Migeon, S., Faugères, J. and Savoye, B. (2003), Marine hyperpycnal flows: initiation, behaviour and related deposits. A review. *Mar. Petrol. Geol.*, **20**, 883–899.

Murphy, J.B. and Nance, R.D. (1989). Supercontinent model for the contrasting character of Late Proterozoic orogenic belts. *Geology*, **19**, 469–472.

Murphy, J.B., Dostal, K.C., Keppie, J.D. and Hynes, A.J. (1985). Cambrian volcanism in Nova Scotia, Canada. *Can. J. Earth. Sci.*, **22**, 599–606.

Murphy, J.B., Strachan, R.A., Nance, R.D., Parker, K.D. and Fowler M.B. (2000). Proto-Avalonia: 1.2–1 Ga tectonothermal event and constraints for the evolution of Rodinia. *Geology*, **28**, 1071–1074.

Mustard, P.S. (1991). Normal faulting and alluvial-fan deposition, basal Windermere Tectonic Assemblage, Yukon, Canada. *Bull. Geol. Soc. Am.*, **103**, 1346–1364.

Muto, T. and Steel, R.J. (1992). Retreat of the front in a prograding delta. *Geology*, **20**, 967–670.

Muto, T. and Steel, R.J. (1997). Principles of regression and transgression: The nature of the interplay between accommodation and sediment supply. *J. Sed. Res.*, **67**, 994–1000.

Mutti, E. (1992). Turbidite sandstone. AGIP – Istituto di Geologia Università di Parma, 275 pp

Mutti, E. and Normark, W.R. (1987). Comparing examples of modern and ancient turbidite systems: Problems and concepts. In: *Marine Clastic Sedimentology: Concepts and case studies* (Ed. by J.K. Legget and G.G. Zuffa). Graham and Trotman, London, 1–38.

Mutti, E. and Normark, W.R. (1991). An integrated approach to the study of turbidite systems. In: *Seismic Facies and Sedimentary Processes of Submarine fans and turbidite systems* (Ed. by P. Weimer and H. Link), Ann Arbor, 75–106.

Mutti, E. and Ricci Lucchi, F. (1972). Le torbiditi dell'Appennino Settentrionale: introduzione all'analisi di facies. *Mem. Soc. Geol. It.*, **11**, 161–199.

Mutti, E., Davoli, G., Tinterri, R., and Zavala, C. (1996). The importance of ancient fluvio-deltaic systems dominated by catastrophic flooding in tectonically active basins. *Sci. Geol. Mem.*, **48**, 233–291.

Mutti, E., Tinterri, R., Benevelli, G., di Biase, D. and Cavanna, G. (2003). Delatic, mixed and turbidite sedimentation of ancient foreland basins. *Mar. Petrol. Geol.*, **20**, 333–355.

Mutti, E., Tinterri, R., di Biase, D., Fava, L., Mavilla, N., Angella, S., and Calabrese, L. (2000). Delta-front associations of ancient flood-dominated fluvio-deltaic systems. *Rev. Soc. Geol. España*, **13**, 165–190.

Mutti, E., Tinterri, R., Remacha, E., Mavilla, N., Angella, S. and Flava, L. (1999). An introduction to the analysis of ancient turbidite basins from an outcrop perspective. *AAPG, Continuing Education Coarse Note Series*, **39**, 61 p.

Myers, K.J. and Milton, N.J. (1996). Concepts and Principles of Sequence Stratigraphy. In: Sequence Stratigraphy (Ed. by D. Emery and K.J. Myers). Blackwell Science Ltd, Oxford, 11–44.

Myrow, P.M. (1992a). Bypass-zone tempestite facies model and proximality trends for an ancient muddy shoreline and shelf. *J. Sed. Petrol.* **62**, 99–115.

Myrow, P.M. (1992b). Pot and gutter casts from the Chapel Island Formation, Southeast Newfoundland. *J. Sed. Petrol.*, **6**, 992–007.

Myrow, P.M. and Hiscott R.N. (1991). Shallow-water gravity-flow deposits, Chapel island Formation, southeast Newfoundland, Canada. *Sedimentology*, **38**, 935–959.

Myrow, P.M. and Southard J.B. (1991). Combined-flow model for vertical stratification sequences in shallow marine storm deposited beds. *J. Sed. Petrol.*, **61**. 202–210.

Myrow, P.M. and Southard, J.B. (1996). Tempestite deposition. *J. Sed. Petrol.*, **66**. 875–887.

Myrow, P.M., Woodward, F., and Goodge, J.W. (2002). Wave-modified turbidites: combined-flow shoreline and shelf deposits, Cambrian, Antartica. *J. Sed. Petrol.*, **72**, 641–656.

Nagata, T. (1961). Rock magnetism. 2nd edition. Maruzen, Tokyo. 236 pp.

Nance, R.D, and Murphy, J.B. (1994). Contrasting basement isotope signatures and the palinspastic restoration of peripheral orogens: Example from the Neoproterozoic Avalonian-Cadomian belt. *Geology*, **22**, 617–620.

Nance, R.D. and Thompson, M.D. (Eds) (1996). Avalonian and Related Peri-Gondwanan Terranes of the Circum-North Atlantic. *Geol. Soc.* Am. *Spec. Paper*, **304**, 390 pp.

Nance, R.D., Murphy, J.B., Strachan, R.A., D'Lemos, R.S. and Tayler, G.K. (1991). Late Proterozoic tectonostratigraphic evolution of the Avalonian and Cadomian terranes. *Precambrian Res.*, **53**, 41–78.

Nava-Sanchez, E., Cruz-Orozco, R. and Gorsline, D.S. (1995). Morphology and sedimentology of two contemporary fan-deltas on the southeastern Baja California Peninsula, Mexico. *Sed. Geol.*, **98**, 45–61.

Nava-Sanchez, E.H., Gorsline, D.S., Cruz-Orozco, R. and Godinez-Orta, L. (1999). The El Coyote fan-delta: A wave-dominated example from the Gulf of California, Mexico. *Quaternary Int.*, **56**, 129–140.

Nelson, C.H. (1982). Modern shallow-water graded sand layers from storm surges, Bering shelf: A mimic of Bouma sequences and turbidite systems. *J. Sed. Petrol.*, **52**. 537–545.

Nemec, W. (1988). The mechanics of cohesionless sediment flows on steep subaqueous slopes: recent theoretical advances and continued sedimentological problems. In: *Abstracts Int. Workshop on Fan Deltas,. Int. Ass. Sedim.*, Univ. of Calabria, Cosenza. 45-46.

Nemec, W. (1990a). Deltas, remarks on terminology and classification. In: *Coarse-grained Deltas* (Ed. by A. Colella and D.B. Prior), *Int. Ass. Sed. Spec. Publ.*, **10**, Blackwell Science, Oxford, 3–12.

Nemec, W. (1990b). Aspects of sediment movement on steep delta slopes. In: *Coarse-grained Deltas* (Ed. by A. Colella and D.B. Prior). *Int. Ass. Sed. Spec. Publ.*, **10**, Blackwell Science, Oxford, 29–73.

Nemec, W. (1995). The dynamics of delta suspension plumes. In: *Geology of Deltas* (Ed. by M.N. Otri and G. Postma). A.A. Balkema, Rotterdam, 31–93.

Nemec, W. and Postma, G. (1993). Quaternary alluvial fans in southwestern Crete: sedimentation processes, and geomorphic evolution. In: Alluvial Sedimentation (Ed. by M. Marzo and C. Puigdefábregas). *Spec. Publ. Int. Ass. Sed.*, **17**, 235–276.

Nemec, W. and Steel, R.J. (1984). Alluvial and coastal conglomerates: their significant features and some comments on gravelly mass-flow deposits. In: Sedimentology *of Gravels and Conglomerates (Ed. by E.H. Koster and R.J. Steel). Can. Soc.* Petrol. *Geol. Mem.* 1–31.

Nemec, W., Porebski, S.J. and Steel, R.J. (1980). Texture and structure of resedimented conglomerates: examples from Ksiaz Formation (Famennian-Tournaisian), southern Poland. *Sedimentology*, **27**, 519–538.

Nemec, W., Steel, R.J., Gjelberg, J., Collinson, J.D., Prestholm, E. and I.E. (1988). Anatomy of collapsed and re-established delta front in Lower Cretaceous of eastern Spitsbergen: gravitational sliding and sedimentation processes. *Bull. Am. Ass. Petrol. Geol. Bull*, **72**, 454–476.

Nemec, W., Steel, R.J., Porebski, S.J. and Spinnangr, A. (1984). Domba Conglomerate, Devonian, Norway: processes and lateral variability in *a mass flow-dominated, lacustrine fan-delta. In: Sedimentology* of Gravels and Conglomerates (Ed. by E.H. Koster and R.J. Steel). *Can. Soc. Petrol. Geol. Mem.*, **10**.. 295–320.

Nicholas, T.C. (1915). The geology of the St Tudwel's Peninsula (Carnarvonshire). *Q. J. Geol. Soc. Lond.*, **71**, 83–141.

Nilsen, T.H. and Sylvester, A.G. (1999). Strike-slip basins: Part 1. *The Leading Edge*, 1146–1152.

Nittrouer, C.A. and DeMaster, D.J. (1986). Sedimentary processes on the Amazon continental shelf. *Cont. Shelf Res.*, **6**, 361 pp.

Nittrouer, C.A., Kuehl, S.A., DeMaster, D.J., and Kowsmann, R.O. (1986). The deltaic nature of Amazon shelf sedimentation. *Bull. GSA*, **97**, 444–458.

Nittrouer, C.A., Kuehl, S.A., Figueiredo, A.G., Allison, M.A., Sommerfield, C.K., Rine, J.M., Faria, E.C. and Silveira, O.M. (1996). The geological record preserved by Amazon shelf sedimentation. *Cont. Shelf Res.*, **16**, 817—841.

Noblet, C. and Lefort J.P. (1990). Sedimentological evidence for a limited separation between Armorica and Gondwana during the Early Ordovician. *Geology*, **18**, 303–306.

Noh, Y. and Fernando, H.J.S. (1991). Gravity current propagation along an incline in the presence of boundary mixing. *J. Geophys. Res.*, **96**, 12,586–12,925.

Noh, Y. and Fernando, H.J.S. (1992). The motion of a buoyant cloud along an incline in the presence of boundary mixing. *J. Fluid Mech.*, **235**, 557–577.

Normark, W.R. and Piper, D.J. (1991). Initiation processes and flow evolution of turbidity currents: implications for the depositional record. *SEPM Spec. Publ.*, **46**, 207–230.

Nøttvedt, A. and Kreisa, R.D. (1987). Model for the combined-flow origin of hummocky cross-stratification. *Geology*, **15**, 357–361.

O'Brien, N.R. (1995), Origin of shale fabric–clues from framboids. *Northeastern Geol. Env. Sci.*, **17**, 146–150.

Ogren, D.E. and Waag, C.J. (1986). Orientation of cobble and boulder beach clasts. *Sed. Geol.*, **47**, 69–76.

Orton, G.J. (1988). A spectrum of Middle Ordovician fan-deltas and braidplain deltas, North Wales: a consequence of varying fluvial clastic input. In: *Fan-deltas: sedimentology and tectonic setting* (Ed. by W. Nemec and R.J. Steel), Blackie and Son Ltd. London, 23–49.

Orton, G.J. and Reading, H. G. (1993). Variability of deltaic processes in terms of sediment supply, with particular emphasis on grain size. *Sedimentology*, **40**, 475–512.

Owen, T.R., Bloxam, T.W., Jones, D.G., Walmsley, V.G. and Williams, B.J.P. (1971). Summer (1968) field meeting in Pembrokeshire, South Wales. *Proc. Geol. Ass.*, **82**, 17–60.

Owens, W.H. (1974). Mathematical model studies of factors affecting the magnetic anisotropy of deformed rocks. *Tectonophysics*. **24**. 115–131.

Owens, W.H. (1994). Laboratory drilling of field-orientated block samples. *J. Struct. Geol.*, **16**, 1719–1721.

Owens, W.H. (2000). Statistical applications to second-rank tensors in magnetic fabric analysis. Geophys. *J. Int.* **142**. 527—538.

Pantin, H.M. (1979). Interaction between velocity and effective density in turbidity flow: phase plane analysis, with criteria for auto-suspension. *Mar. Geol.*, **31**, 59–99.

Paola, C., Heller, P.L., Angevine, C.L. (1992). The large-scale dynamics of grain size variations in alluvial basins: 1. *Theory. Basin Res.*, **4**, 73–90.

Parés, J.M., van der Pluijm, B.A., and Dinarés-Turell, J. (1999). Evolution of magnetic fabrics during incipient deformation of mudrocks (Pyrenees, northern Spain). *Tectonophysics*, **307**, 1–14.

Parker, G. (1982). Condition for the ignition of catastrophically erosive turbidity currents. *Mar. Geol.*, **46**, 307–327.

Parsons, J.D., Bush, J.W.M., and Syvitski, J.P.M. (2001). Hyperpycnal plume formation with small sediment concentrations. *Sedimentology*, **48**, 465–478.

Patchett, P.J. and Jocelyn, J. (1979). U-Pb zircon ages for late Precambrian igneous rocks in South Wales. *J. Geol. Soc. London*, **136**, 13–19.

Pauley, J.C. (1990). Sedimentology, structural evolution and tectonic setting of the late Precambrian Longmyndian Supergroup of the Welsh Borderland, UK. In: *The Cadomian Orogeny* (Ed. by R.S. D'Lemos, R.A. Strachan and C.G. Topley). *Geol. Soc. Lond. Spec. Publ.*, **51**, 341–351.

Pavelic, D. (2001). Tectonostratigraphic model for the North Croatian and North Bosnain sector of the Miocene Pannonian Basin System. *Basin Res.*, **12**, 359–376.

Pemberton, S. G., Reinson, G. E. and MacEachern, J. A. (1992). Comparative ichnological analysis of Late Albian estuarine valley-fill and shelf-shoreface deposits, Crystal Viking Field, Alberta. In: *Applications of ichnology to petroleum exploration--A core workshop* (Ed. by S. G. Pemberton). *SEPM Core Workshop*, **17**, 291–317.

Pérez-López, A. (2001). Significance of pot and gutter casts in a Middle Triassic carbonate platform, Betic Cordillera, southern Spain. *Sedimentology*, **48**, 1371–1388.

Pharaoh, T.C. and Carney, J.N. (2000). Introduction to the Precambrian rocks of England and Wales. In: *The Precambrian Rocks of England and Wales* (Ed. by J.N. Carney, J.M. Horák, T.C. Pharaoh, W. Gibbons, D. Wilson, W.J. Barclay and R.E. Bevins. *Geol., Cons., Rev., Series, 20, Joint Nat., Cons., Rev., Com.*, Peterborough, 1–17.

Pharaoh, T.C. and Gibbons, W. (1994). Precambrian rocks in England and Wales south of the Menai Strait fault system. In: *A revised correlation of Precambrian rocks of the British Isles* (Ed. by W. Gibbons and A.L. Harris). Geol. Soc. Lond. Spec. Rep., **22**, 85–97.

Phillips, E. (1991a). Progressive deformation of the South Stack amd New Harbour Groups, Holy Island, western Anglesey, North Wales. *J. Geol. Soc. Lond.*, **148**, 1091–1100.

Phillips, E. (1991b). The lithostratigraphy, sedimentology and tectonic settings of the Monian Supergroup, western Anglesey, North Wales. *J. Geol. Soc. Lond.*, **148**, 1079–1090.

Pickering, K.T., Hiscott, R.N. and Hein, F.J. (1989). Deep-water marine environments: clastic sedimentation and tectonics. Unwin Hyman Ltd, London, 416 p.

Pierson, T.C. (1981). Dominant particle support mechanisms in Debris flows at Mt. Thomas, New Zealand, and implications for flow mobility. *Sedimentology*, **28**, 49–60.

Pierson, T.C. and Costa, J.E. (1987). A rheological classification of subaerial sediment-water flows. In: *Debris flows/avalanches: processes, recognition, and mitigation* (Ed. by J.E. Costa and G.F. Wieczorek), *Geol. Soc. Am. Rev. Eng. Geol.*, **7**, 1–12.

Piper, D.J.W. (1978). Turbidite muds and silts on deep-sea fans and abyssal plains. In: Sedimentation in Submarine Canyons, Fans and Trenches (Ed. by D.J. Stanley and G. Kelling. Dowden, Hutchinson and Ross, Stroudsburg PA, 163–176.

Piper, J.D.A., Elliot, M.T. and Kneller, B.C. (1996). Anisotropy of magnetic susceptibility in a Palaeozoic flysch basin: the Windermere Supergroup, northern England. Sed *Geol.*, **106**, 235–258.

Plink-Björklund, P. and Steel. R.J. (2004). Initiation of turbidity currents: outcrop evidence for Eocene hyperpycnal flow turbidites. *Sed. Geol.*, **165**, 29–52.

Plint, A.G. and Nummedal, D. (2000). The falling stage systems tract: recognition and importance in sequence stratigraphic analysis. In: *Sedimentary responses to forced regression* (Ed. by D. Hunt and R.L. Gawthorpe) *Geol. Soc. Lond., Spec., Publ.*, **172**, 1–17.

Popov L.E. and Koren, T.N. (1996). Eustatic events and black shale sedimentation at the Cambrian-–Ordovician boundary. *Stratigraphy and Geological Correlation*, **4**, 419–427.

Posamentier, H.W. and James, D.P. (1993). An overview of sequence stratigraphic concepts: uses and abuses. In: Sequence Stratigraphy and Facies Associations (Ed. by H.W. Posamentier, C.P. Summerhayes, B.U. Haq and G.P. Allen). *Spec. Publ. Int. Ass. Sed.*, **18**, 3–18.

Posamentier, H.W. and Vail, P.R. (1988). Eustatic controls on clastic deposition I – sequence and systems tract models. In: *Sea-level Changes an Integrated Approach* (Ed. by C.K. Wilgus, B.S. Hastings, C.G. Kendall, H.W. Posamentier, C.A. Ross and J.C. Van Wagoner). *Spec. Publ. Soc. Econ. Paleont. Mineral.*, **42**, 109–124.

Posamentier, H.W. and Weimer, P. (1993). Siliciclastic sequence stratigraphy and petroleum geology – where to from here? *Am. Ass. Petrol. Geol. Bull* Bull., 77, 731–742.

Posamentier, H.W., Allen, H.W., James, D.P. and Tesson, M. (1992). Forced regressions in a sequence stratigraphic framework: concepts, examples and sequence stratigraphic significance. *Am. Ass. Petrol. Geol. Bull*, **76**, 1687–1709.

Postma, G. (1990). Depositional architecture and facies of river and fan-deltas: a synthesis. In: *Coarse-grained Deltas* (Ed. by A. Colella and D.B. Prior), *Int. Ass. Sed. Spec. Publ.*, **10**, 13–27.

Postma, G. and Roep, T.B. (1985). Resedimented conglomerates in the bottomsets of Gilbert-type gravel deltas. *J. Sed. Petrol.* **55**. 874-885.

Postma, G., Babic, L., Zupanic, J. and Roe, S.L. (1988). Delta-front failure and associated bottonset deformation in a marine gravely-type fan delta. In: *Fan-deltas: Sedimentology and tectonic setting* (Ed. by W. Nemec and R.J. Steel). Blackie and Son, London. 92–102.

Postma, G., Nemec, W. and Kleinspehn, K.L. (1988). Large floating clasts in turbidites: a mechanism for their emplacement. *Sed. Geol.*, **58**, 47–61.

Potter, P.E. and Pettijohn, F.J. (1977). Paleocurrents and basin analysis, Springer-Verlag, Berlin, 296 pp.

Poulsen, V. and Anderson, M.M. (1975). The Middle-Upper Cambrian transition in southeastern Newfoundland, Canada. *Can. J. Earth Sci.*, **12**, 2065–2079.

Pratt, W.T. (1995). Cambrian stratigraphy of St Tudwel's Peninsula, Gwynedd, northwest Wales: Discussion. *Geol. Mag.,* **132**, 619–622.

Pratt, H.T. Woodhall, D.G. and Howells, M.F. (1995). Geology of the country around Cadair Idris. Memoir of the British Geological Survey, Sheet 149 (England and Wales), The Stationary Office, London, 183 pp.

Price, N.B. (1963). The Geochemistry of the Menevian rocks of Wales, Un*Publ*ished Ph.D. thesis, University of Wales, 233 pp.

Prigmore, J.K. and Rushton, A.W.A. (2000). Cambrian of South Wales: St David's area. In: British Cambrian to Ordovician Stratigraphy (Ed. by A.W.A. Rushton, A.W. Owen, R.M. Owens and J.K. Prigmore). *Geological Conservation Review Series*, **18**, 51–66.

Prigmore, J.K., Butler, A.J. and Woodcock, N.H. (1997). Rifting during seperation of Eastern Avalonia from Gondwana: Evidence from subsidence analysis. *Geology*, **25**, 203–206.

Pringle, J. and George, T.N. (1948). British Regional Geology. South Wales, 2nd Edition. HMSO, London, 100 pp.

Prior, D.B. and Bornhold, B.D. (1989). Submarine sedimentation on a developing Holocene fan-delta. *Sedimentology*, **36**, 1053–1076.

Prior, D.B. and Bornhold, B.D. (1990). The underwater development of Holocene fan deltas. In: *Coarse-grained Deltas* (Ed. by A. Colella and D.B. Prior), *Int. Ass. Sed. Spec. Publ.*, 10, Blackwell Science, Oxford, 10, 75–90.

Prior, D.B., Bornhold, B.D. and Johns, M.W. (1984). Depositional characteristics of a submarine debris flow. *J. Geol.*, **92**, 707–727.

Prior, D.B., Suhayda, J.N., Lu, N.Z., Bornhold, D.B., Keller, G.H., Wiseman, W.J., Jr, Wright, L.D. and Yang, Z.S. (1989). Storm wave reactivation of a submarine landslide. *Nature*, **341**, 47–50.

Prior, D.B., Yang, Z.S. Bornhold, D.B., Keller, G.H., Lu, N.Z., Wiseman, W.J., Wright, L.D. and Zhang, J. (1986). Active slope failure, sediment collapse, and silt flows on the modern subaqueous Huanghe (yellow River) Delta. *Geo-Mar. Lett.*, **6**, 85–95.

Proust, J-N. and Hosu, A. (1996). Sequence stratigraphy and Paleogene tectonic evolution of the Transylvanian Basin (Romania, eastern Europe). *Sed. Geol.*, **105**, 117–140.

Qayyum, M., Niem, A.R. and Lawrence, R.D. (2001). Detrital modes and provenance of the Palaeogene Khojak Formation in Pakistan: Implications for early Himalayan orogeny and unroofing. *Geol. Soc. Am. Bull.*, **113**, 320–332.

Rainbird, R.H., Hadlari, T., Aspler, L.B., Donaldson, J.A., LeCheminant, A.N. and Peterson, T.D. (2003). Sequence stratigraphy and evolution of the Palaeoproterozoic intracontinental Baker Lake and Thelon basins, western Churchill Province, Nunavut, Canada. *Precambrian Res.* **125**, 21–53.

Raiswell, R. (1987). Non-steady state microbiological diagenesis and the origin of concretions and nodular limestone. In: *Diagenesis of sedimentary sequences* (Ed. by J.D. Marshall), *Geol. Soc. London* Spec. *Publ.*, **36**, 41–54.

Rankey, E.C., Walker, K.R. and Srinivasan, K. (1994).
Rasmussen, H. (2000). Nearshore and alluvial facies in the Sant Llorenç del Munt depositional system: recognition and development. *Sed. Geol.*, **138**, 71–98.

Rast, N. (1979). The Avalonian plate in the northern Appalachians and Caledonides. In: The Caledonides in the U.S.A. (Ed. by J.W. Skehan and P.H. Osberg). *Contributions to the International Geological Correlation Program (IGCP) Project 27-Caledonide Orogen: Western Massachusetts,* Boston College, 63–66.

Rast, N. and Skehan, J.W. (1983) The evolution of the Avalonian plate. *Tectonophysics*, **100**, 257–286.

Ravnas, R. and Steel, R.J. (1998). Architecture of marine rifts. *Am. Ass. Petrol. Geol. Bull*, **82**, 110–146.

Reading, H.G. (1980). Characteristics and recognition of strike-slip systems. In: *Sedimentation in Oblique-slip Mobile Zones* (Ed. by P. Ballance and H.G. Reading). *Spec. Publ. Int. Ass. Sed.*, **4**, 7–26.

Reading, H.G. and Collinson, J.D. (1996). Clastic coasts. In: *Sedimentary environments: Processes, Facies, and Stratigraphy* (Ed. by H.G. Reading). Blackwell Science, Oxford. 154–231.

Reedman, A.J., Leveridge, B.E. and Evans, R.B. (1984). The Arfon Group (Arvonian) of North Wales. *Proc. Geol. Ass.*, **95**, 313–321.

Rees, A.I. (1965). The use of anisotropy of magnetic susceptibility in the estimation of sedimentary fabric. *Sedimentology*, **4**, 257–271.

Rees, A.I. (1968). The production of preferred orientation in a concentrated dispersion of elongated and flattened grains. *J. Geol.,* **76**, 457–465.

Rees, A.I. and Woodall W.A. (1975). The magnetic fabric of some laboratory deposited sediments. Earth Planetary Sci. Lett., **25**, 121–130.

Reineck, H.E. (1958). Longitudinale Schrägschichten im Watt. Geol. Rundschau, **47**, 73–82.

Reineck, H.E. (1975). German North Sea Tidal Flats, In Tidal flats (ed. R.N. Ginsburg). Springer-Verlag, Berlin Heidelberg New York. 428 pp.

Reineck H.E. and Singh I.B. (1972). Genesis of laminated sand and graded rhythmites in storm sand layers of shelf mud. *Sedimentology*, **18**, 123–128.

Reineck H.E. and Singh I.B. (1973) Depositional Sedimentary Environments – with Reference to Terrigenous Clastics. Springer-Verlag, Berlin, 439 pp.

Reineck H.E. and Wunderlich F. (1968). Classification and origin of flaser and lenticular bedding. *Sedimentology*, **11**. 99–104.

Rhoads, D.C. and Morse, J.W. (1971). Evolutionary and ecologic significance of oxygen-deficient basins. *Lethaia*, **4**, 413–428.

Richards, M., Bowman, M., and Reading, H.G. (1998). Submarine-fan systems: characterization and stratigraphic prediction. *Mar. Petrol. Geol.*, **15**, 689–717.

Ridgeway, K.D., Trop, J.W., Nokleberg, W.J., Davidson, C.M. and Eastham, K.R. (2002). Mesozoic and Cenozoic tectonics of the eastern and central Alaska Range: Progressive basin development and deformation in a suture zone. *Geol. Soc. Am. Bull.*, **114**, 1480–1504.

Rimoldi, B., Alexander, J. and Morris, S.A. (1996). Experimental turbidity currents entering density-stratified water: analogues for turbidites in Mediterranean hypersaline basins. *Sedimentology*, **43**, 527–540.

Roberts, B. and Merriman, R.J. (1990). Cambrian and Ordovician metabentonites and their relevance to the origins of associated mudrocks in the northern sector of the Lower Palaeozoic Welsh marginal basin. *Geol. Mag.*, **127**, 31–43.

Robinson, D.M., Dupont-Nivet, G., Gehrels, G.H. and Zhang, Y. (2003). The Tula uplift, northwestern China: Evidence for regional tectonism of the northern Tibetan Plateau during the late Mesozoic–early Cenozoic time. *Geol. Soc. Am. Bull.*, **115**, 35–47.

Robison, R.A. (1984). Cambrian Agnostida of North America and Greenland, Part 1, Ptychagnostidae. The University of Kansas Paleontological Contributions, 109, 1–59.

Rossetti, D.F. (1997). Internal architecture of mixed tide- and storm-influenced deposits: an example from the Alcântara Formation, northern Brazil. *Sed. Geol.*, **114**, 163–188.

Rossetti, D.F., Góes, A.M., Truckenbrodt, W. and Anaisse J. (2000). Tsunami-induced large-scale scour and fill structures in Late Albian to Cenomonian deposits of the Grajaú Basin, northern Brazil. *Sedimentology*, **47**, 309–323.

Rowell, A.J., Robinson, R.A. and Strickland, D.K. (1982). Aspects of Cambrian Agnostoid phylogeny and chronocorrelation. *J. Paleont.*, **56**, 161–182.

Rushton, A.W.A. (1974). The Cambrian of Wales and England. In: *Cambrian of the British Isles, Norden, and Spitsbergen. Lower Palaeozoic Rocks of the World: Volume 2*, Wiley – Interscience, London, 43–122.

Rushton, A.W.A. (1978). Fossils from the Middle–Upper Cambrian transition in the Nuneaton district. *Palaeontology*, **21**, 245–283.

Rushton, A.W.A. (1983). Trilobites from the Upper Cambrian Olenus Zone in central England. Spec. Papers *Palaeontology*, **30**, 107–139.

Rushton, A.W.A. (2000). Cambrian rocks of England. In: British Cambrian to Ordovician Stratigraphy (Ed. by A.W.A. Rushton, A.W. Owen, R.M. Owens and J.K. Prigmore). *Geological Conservation Review Series*, **18**, 69–88.

Rushton, A.W.A., Owen, A.W., Owens, R.M. and Prigmore, J.K. (2000). British Cambrian to Ordovician Stratigraphy. *Geological Conservation Review Series*, **18**, 376 pp.

Rust, B.R. (1972). Structure and processes in a braided river. *Sedimentology*, **18,** 221–245.

Rust, B.R. (1975). Fabric and structure in glaciofluvial gravels. In: Glaciofluvial and Glaciolacustrine Sedimentation (Ed. by Jopling, A.V. and McDonald). *SEPM Spec, Publ.*, **23**, 238–248.

Rust, B.R. (1978). Depositional models for braided alluvium. In: Fluvial Sedimentology (Ed. by A.D. Miall). *Mem. Can. Soc. Petrol. Geol.*, **5**, 605–625.

Rust, B.R. and Gibling, M.R. (1990). Three dimensional antidunes as HCS mimic in a fluvial sandstone: the Pennsylvanian South Bar Formation near Sydey, Nova Scotia. *J. Sed. Petrol.,* **60**. 540–548.

Ryang, W.H. and Chough, S.K. (1997). Sequential development of alluvial/lacustrine system: southeastern Eumsung Basin (Cretaceous), Korea. *J. Sed. Res.*, **67**, 274–285.

Ryang, W.H. and Chough, S.K. (1999). Alluvial-to-lacustrine systems in a pull-apart margin: southwestern Eumsung Basin (Cretaceous), Korea. *Sed. Geol.*, **127**, 31–46.

Sagnotti, L., Speranza, F., Winkler, A., Mattei, M., and Funiciello, R. (1998). Magnetic fabric of clay sediments from the external northern Apennines (Italy). Phys. Earth *Planetary Inter.*, **105**, 73—79.

Salter, J.W. (1863). On the discovery of Paradoxides in Britain. Q. *J. Geol. Soc. London*, **19**, 274–277.

Salter, J.W. (1864). On some new fossils from the Lingula Flags of Wales. Q. *J. Geol. Soc. London*, **20**, 233–241.

Salter, J.W. (1866). Notes on the sections and fossils [of the Lingula Flags of South Wales]. Report of the 35th meeting of the British Association for the advancement of science (Birmingham, 1865), 284–286.

Salter, J.W. and Hicks, H. (1867). On a new Lingulella from the red lower Cambrian rocks of St David's. Q. *J. Geol. Soc. London*, **23**, 339–

Salter, J.W. and Hicks, H. (1869). On some fossils from the "Menevian Group". Q. *J. Geol. Soc. London*, **25**, 51–57.

Sanders, J.E. (1965). Primary sedimentary structures formed by turbidity currents and related sedimentation mechanisms. In: *Primary sedimentary structures and their hydrodynamic interpretation* (Ed. by G.V. Middleton), *SEPM* Spec. *Publ.*, **12**, 192–219.

Sanders, J.E. and Kumar, N. (1975). Evidence of shoreface retreat and in-place "drowning" during Holocene submergence of barriers, shelf off Fire Island, New York. *Geol. Soc. Am. Bull.*, **86**, 65–76.

Sarker, S., Banerjee, S., Chakraborty, S. and Bose, P. K. (2001). Shelf storm flow dynamics: insights from the Mesoproterozoic Rampur Shale, central India. *Sed. Geol.*, **147**, 195–205.

Schenk, P.E. (1997). Sequence stratigraphy and provenance on Gondwana's margin: The Meguma Zone (Cambrian to Devonian) of Nova Scotia, Canada. *GSA Bull.*, **109**, 395–409.

Schieber, J. and Ellwood, B.B. (1988). The coincidence of macroscopic paleocurrent indicators and magnetic lineation in shales from the Precambrian Belt basin. *J. Sed. Petrol.*, **58**, 830–835.

Schieber, J. and Ellwood, B.B. (1993). Determination of basinward paleocurrent patterns in a shale succession from anisotropy of magnetic susceptibility (AMS): A case study of the Mid-Proterozoic Newland Formation, Montana. *J. Sed. Petrol.*, **63**. 874–880.

Schumm, S.A. (1973). Geomorphic thresholds and complex response of drainage systems. In: *Fluvial geomorphology* (Ed. by M. Morisawa). SUNY, Binghamton, New York, 69–85.

Schumm, S.A. (1977). The fluvial system, John Wiley, New York, 338 pp.

Schumm, S.A. (1981). Evolution and response of the fluvial system: sedimentologic implications. In: *Recent and ancient non-marine depositional environments: models for exploration* (Ed. by F.G. Ethridge and R.S. Flores), *SEPM* Spec. *Publ.*, **31**, 19–29.

Sedgwick, A. (1847). On the classification of the fossiliferous slates of North Wales, Cumberland, Westmorland and Lancashire. *Q. J. Geol. Soc. London*. **3**. 133 pp.

Sedgwick, A. and Murchison, R.I. (1835). On the Cambrian and Ordovician systems, exhibiting the order in which the older sedimentary strata succeed each other in England and Wales. *Lond. Edin. Phil. Mag. J. Sci.*, **7**, 483–485.

Sellwood B.W. (1986) Shallow-marine carbonate environments. In: *Sedimentary Environments and Facies, 2nd edition* (Ed. by H.G. Reading). 283-342. Blackwell Science, Oxford, 283–342.

Shanmugam, G. (1997). The Bouma sequence and the turbidite mind set. *Earth Sci. Rev.*, **42**, 201–229.

Shanmugam, G. (2000). 50 years of the turbidite paradigm (1950's-(1990)'s): deep-water processes and facies models – a critical perspective. *Mar. Petrol. Geol.*, **17**, 285–342.

Shanmugam, G. and Moiola, R.J. (1995). Reinterpretation of depositional processes in a classic flysch section (Pennsylvanian Jack-fork Group), Ouachita Mountains, Arkansas and Oklahoma. *Am. Ass. Petrol. Geol. Bull*, **79**, 672–695.

Shao, L., Stattegger, K. and Garbe-Schoenberg, C-D. (2001). Sandstone petrology and geochemistry of the Turpan Basin (NW China): implications for the tectonic evolution of a continental basin. *J. Sed. Res.*, **71**, 37–49.

Short, A.D. (1984). Beach and nearshore facies: southeast Australia. *Mar. Geol.*, **60**, 261–281.

Shultz, A.W. (1983). The deposits, internal structure and geometry in six alluvial fan–fan delta bodies (Devonian—Norway) – a study in the significance of bedding sequences in conglomerates: discussion. *J. Sed. Petrol.*, **53**, 325–327.

Simpson, J.E. (1987). Gravity Currents: In the environment and laboratory. Chichester, UK, Ellis Horwood, 277 pp.

Siringan, F.P. and Anderson, J.B. (1994). Modern shoreface and inner-shelf storm deposits off the east Texas coast, Gulf of Mexico. *J. Sed. Res.,* **B64**. 99–110.

Siveter, D.J. and Williams, M. (1995). An early Cambrian assignment for the Caerfai Group of South Wales. *J. Geol. Soc. London*, **152**, 221–224.

Skene, K.I. Mulder, T, and Syvitski, J.P.M. (1997). INFLO1: a model predicting the behaviour of turbidity currents generated at river mouths. *Comp. Geosci.*, **23**, 975–991.

Smith, D.G. (1976). Effect of vegetation on lateral migration of anastomosed channels of a glacial meltwater river. *Geol. Soc. Am. Bull.*, **87**, 857–560.

Smith, G.A. (1986). Coarse-grained non-marine volcaniclastic sediment: terminology and depositional process. *Geol. Soc. Am. Bull.*, **105**, 77–100.

Smith, J.D.D. and White, D.E. (1963). Cambrian trilobites from the Purley Shales of Warwickshire. *Palaeontology*, **6**, 397–407.

Smith, N.D. (1974). Sedimentology and bar formation in the upper Kicking Horse River, a braided meltwater stream. *J. Geol.*, **82**, 205–223.

Smith, N.D. (1985). Proglacial fluvial environments. In: *Glacial Sedimentary Environments* (Ed. by G.M. Ashley). *SEPM Short Course*, **16**, 85–134.

Smith, N.J.P. and Rushton, A.W.A. (1993). Cambrian and Ordovician stratigraphy related to structure and seismic profiles in the western part of the English Midlands. *Geol. Mag.*, **130**, 665–671.

Snedden J.W. and Swift, D.J.P. (1990). Is there evidence for geostrophic currents preserved in the sedimentary record of inner- to mid-shelf deposits – Discussion. *J. Sed. Petrol.*, **61**, 148–151.

Snedden, J.W. and Nummedal, D. (1991). Origin and geometry of storm deposited sand beds in modern sediments of the Texas continental shelf. In. *Shelf sand and sandstone bodies: Geometry, Facies and Sequence Stratigraphy* (Ed. By D.J.P. Swift, G.F. Oertel, R.W. Tillman and J.A. Thorn). *Spec. Publ. In. Ass. Sed.*, 339–375.

Snedden, J.W., Nummedal, D., and Amos, A.F. (1988). Storm and fair-weather combined-flow on the Central Texas Continental Shelf. *J. Sed. Petrol.*, **58**. 580—595.

Soegaard, K. (1990). Fan-delta and braid0delta systems in Pennsylvanian Sandia Formation, Taos Trough, Northern New Mexico: Depositional and tectonic implications. *Geol. Soc. Am. Bull.*, **102**, 1325–1343.

Sohn, Y.K. (1997). On traction carpet sedimentation. *J. Sed. Res.*, **67**, 502–509.

Sohn, Y.K. (1999). Rapid development of gravelly high-density turbidity currents in marine Gilbert-type fan-deltas, Lorento Basin, Baja California Sur, Mexico. Discussion. *Sedimentology*, **46**, 757–761.

Sohn, Y.K., Rhee, C.W., and Kim, B.C. (1999). Debris flow and hyperconcentrated flood-flow deposits in an alluvial fan, northwestern part of the Cretaceous Yangdong Basin, central Korea. *J. Geol.,* **107**, 111–132.

Sonu, C.J. and van Beek, J.L. (1971). Systematic beach changes on the Outer Banks, North Carolina. *J. Geol.*, **79**, 416–425.

Soper, N.J. and Woodcock, N.H. (1990). Silurian collision and sediment dispersal patterns in southern Britain. *Geol. Mag.,* **127**, 527–542.

Southard, J.B., Lambie, J.M, Federico, D.C., Pile, H.T. and Weidman, C.R. (1990). Experiments on bed configuration in fine sand under bi-directional purely oscillatory flow, and the origin of hummocky cross-stratification. *J. Sed. Petrol.,* **60**, 1–7.

Sparks, S.J., Bonnecaze, R.T., Huppert, H.E., Lister, J.R., Hallworth, M.A., Mader, H., and Phillips, J. (1993). Sediment-laden gravity currents with reversing buoyancy. *Earth Plan. Sci. Lett.,* **114**, 243–257.

Stacey, F.D., Joplin, G., and Lindsey, J. (1960). Magnetic anisotropy and fabric of some foliated rocks from SE Australia. *Geophys. Pura. Appl.*, **47**, 30–40.

Stanley, D.J. (1981). Unifites: structureless muds of gravity flow origin in Mediterranean Basins. *Geo-mar. Lett.*, **1,** 77–83.

Stanley, D.J. (1983). Parallel laminated deep-sea muds and coupled gravity flow: hemipelagic setting in the Mediterranean. Smithsonian Contributions to Marine Science, **19**, 1–19.

Stauffer, P.H. (1967). Grain-flow deposits and their implications, Sante Ynez Mountains, California, *J. Sed. Petrol.*, **37**, 487–508.

Stead, J.T.C. and Williams, B.P.J. (1971). The Cambrian Rocks of North Pembrokeshire. In: *Geological excursions in South Wales and the Forest of Dean* (Ed. by D.A. Bassett and M.G. Bassett), Geological Association, South Wales Group, Cardiff, 180–198.

Steel, R. and Gloppen, T.R. (1980). Late Caledonian (Devonian) basin formation, western Norway; signs of strike-slip tectonics during infilling. In: *Sedimentation in Oblique-slip Mobile Zones* (Ed. by P. Ballance and H.G. Reading). *Spec. Publ. Int. Ass. Sed.*, **4**, 79–103.

Steel, R.J. (1974). New Red Sandstone floodplain and piedmont sedimentation in the Hebridean province, Scotland. *J. Sed. Petrol.*, **44**, 336–357.

Steel, R.J. (1988). Coarsening-upward and skewed fan bodies: symptoms of strike-slip and transfer fault movement in sedimentary basins. In: *Fan Deltas: Sedimentology and Tectonic Setting* (Ed. by W. Nemec and R.J. Steel). Blackie, London, 75–83.

Stokes, M. and Mather, A.E. (2000). Response of Plio-Pleistocene alluvial systems to tectonically induced base-level changes, Vera Basin, SE Spain. *J. Geol. Soc. London*, **157**, 303–316.

Stow, D.A.V. (1998). Seafloor polishing and sand spillover: reservoir potential on the upper slope. *Geoscience 98, Abstracts Volume*, p 11.

Stow, D.A.V. and Mayall, M. (2000). Deep-water sedimentary systems: New models for the 21st century. *Mar. Petrol. Geol.*, **17**, 125–135.

Stow, D.A.V. and Piper, D.J.W. (1984). Deep-water fine-grained sediments: facies models. In: Fine-grained sediments: Deep-Water Processes and Facies (Ed. by D.A.V. Stow and D.J.W. Piper), *Geol. Soc. London.* Spec., *Publ.*, **15**, 611-645.

Stow, D.A.V. and Shanmugam, G. (1980). Sequence of structures in fine-grained turbidites: comparison of recent deep-sea and ancient flysch sediments. *Sed. Geol.*, **25**, 23–42.

Stow, D.A.V. and Wetzel, A. (1990). Hemiturbidite: a new type of deep waters sediment. In: *Proc. ODP Sci. Results*, **116**, (Ed. by J.R. Cochrane and D.A.V. Stow), 25–35.

Stow, D.A.V., Alam, M. and Piper, D.J.W. (1984). Sedimentology of the Halifax Formation, Nova Scotia: Lower Palaeozoic fine-grained turbidites. In: *Fine-grained sediments: Deep-Water Processes and Facies* (Ed. by D.A.V. Stow and D.J.W. Piper). *Geol. Soc. London* Spec. *Publ.*, **15**, 127–144.

Stow, D.A.V., Reading, H.G. and Collinson, J.D. (1996). Deep seas. In: *Sedimentary environments: Processes, Facies, and Stratigraphy* (Ed. by H.G. Reading). Blackwell Science, Oxford. 232–280.

Stubblefield, C.J. (1959). Lexique stratigraphique International. Vol. 1. Europe. Fasc. 3a, England, Wales and Scotland: III Cambrian. (dated 1958).

Sundborg, A. (1956). The River Klaralven: a case study of fluvial processes. *Geogr. Ann.*, **38**, 127–316.

Surlyk, F. (1984). Fan-delta to submarine fan conglomerates of Volgian-Valanginian Wollaston Foreland Group, East Greenland. In: *Sedimentology of Gravels and Conglomerates* (Ed. by E.H. Koster and R.J. Steel). Can. *Soc.* Petrol. *Geol.* Mem., **10**, 295–320.

Surlyk, F. (1987). Slope and Deep Shelf Gully Sandstones, Upper Jurassic, East Greenland. *Am. Ass. Petrol. Geol. Bull.*, **71**, 464–475.

Suttner, L.J. and Basu, A. (1981). Climate and the origin of quartz arenites. *J. Sed. Petrol.*, **51**, 1235–1246.

Suttner, L.J. and Basu, A. (1985). The effect of grain size on detrital modes: a test of the Gazzi-Dickinson point-counting method – discussion. *J. Sed. Petrol.*, **55**, 616–617.

Swift. D.J.P. (1975). Tidal sand ridges, and shoal-retreat massifs. *Mar. Geol.*, **18**, 105–134.

Swift, D.J.P. (1985). Response of the sea floor to flow. In: Fluid and sediment dynamics on continental shelves (Ed. by R.W. Tillman, D.J.P. Swift, and R.G. Walker). Shelf Sands and Sandstone Reservoirs, *SEPM* Short Course, 13, 47–133.

Swift, D.J.P. and Niedoroda, A.W. (1985). Fluid and sediment dynamics on continental shelves. In: *Shelf Sands and Sandstone Reservoirs* (Ed. by R.W. Tillman, R.G. Walker, and D.J.P. Swift). SEPM Short Course Notes, **13**, 47–135.

Swift, D.J.P. and Nummedal, D. (1987). Hummocky cross-stratification, tropical hurricanes and intense winter storms: a discussion. *Sedimentology*, **34**, 338–344.

Swift, D.J.P. and Thorn, J.A. (1991). Sedimentation on continental margins, I: a general model for shelf sedimentation. In: *Shelf Sand and Sandstone bodies: Geometry, Facies and Sequence Stratigraphy* (Ed. By D.J.P. Swift, G.F. Oertel, R.W. Tillman and J.A. Thorn), 3–31.

Swift, D.J.P. Niedoroda, A. W. Vincent, C.E. and Hopkins, T.S. (1985). Barrier Island evolution, middle Atlantic shelf, U.S.A., Part I: Shoreface dynamics. *Mar. Geol.*, **63**, 331–361.

Swift, D.J.P., Figueiredo, A.G. Freeland, G.L. and Oertel, G.F. (1983). Hummocky cross-stratification and megaripples – a geologic double standard? *J. Sed. Petrol.*, **53**. 1295–1318.

Swift, D.J.P., Hudelson, P.M., Brenner, R.L., and Thompson, P. (1987). Shelf construction in a foreland basin: storm beds, shelf sandbodies and shelf-slope depositional sequences in the Upper Cretaceous Mesaverde Group, Book Cliffs, Utah. *Sedimentology*, **34**, 423–457.

Sylvester, A.G. (1988). Strike-slip faults. *Geol. Soc. Am. Bull.*, **100**, 1666–1703.

Syvitski, J.P.M. and Schafer, C.T. (1996). Evidence for an earthquake triggered basin collapse in Seguenay Fjord, Canada. *Sed. Geol.*, **104**, 127-153.

Taira, A. (1989). Magnetic fabrics and depositional processes. In: Sedimentary facies in the active plate margin (Ed. by A. Taira and F. Masuda), Terra Scientific *Publ*ishing Co., Tokyo, 43—77.

Takahashi, T. (1981). Debris flow. *Annu. Rev. Fluid Mech.*, **13**, 57–77.

Talbot, M.A. and Allen, P.A. (1996). Lakes. In: *Sedimentary environments: Processes, Facies, and Stratigraphy* (Ed. by H.G. Reading). Blackwell Science. Oxford. 83–125.

Tamura, T. and Masuda, F. (2003). Shallow-marine fan delta slope deposits with large-scale cross-stratification: the Plio-Pleistocene Zaimokuzawa formation in the Ishikari Hills, northern Japan. *Sed. Geol.*, **158**, 195–207.

Tarling, D.H. and Hrouda, F. (1993). The Magnetic Anisotropy of Rocks, Chapman and Hall, London, 217 pp.

Tayler, D.R. and Walker R.G. (1984). Depositional environments and paleogeography in the Albian Moosebar Formation and adjacent fluvial Gladstone and Beaver Mines formations, Alberta. *Can. J. Earth. Sci.*, **21**, 698–714.

Taylor, K. and Rushton, A.W.A. (1972). The pre-Westphalian geology of the Warwickshire coalfield. *Bulletin of the Geological Survey of Great Britain*, **35**, [dated 1971].

Tessier, B., Archer, A.W., Lanier, W.P. and Feldman, H.R. (1995). Comparisons of ancient tidal rhythmites (Carboniferous of Kansas and Indiana, USA) with modern analogues (the Bay of Mont-Saint-Michel, France). *Int. Ass. Sed. Spec. Publ.*, **24**, 259–271.

Thickpenny, A. and Leggett, J.K. (1987). Stratigraphic distribution and palaeo-oceanographic significance of European early Palaeozoic organic-rich sediments. In: Marine Petroleum Source Rocks (Ed. by J. Brooks and A.J. Fleet). *Geol. Soc. Lond. Spec. Publ.*, **26**, 231–247.

Thomas, A.T., Owens, R.M., and Rushton, A.W.A. (1984). Trilobites in British stratigraphy. Geol. Soc. Lond., Spec., Rep., **16**.

Thomas, H.H. and Cox, A.H. (1924). The volcanic series of Trefgarn, Roch and Ambleston (Pembrokeshire). *Q. J. Geol. Soc. London*, **80**, 520–548.

Thomas, H.H. and Jones, O.T. (1912). On the Pre-Cambrian rocks of Brawdy, Haycastle and Brimaston (Pembrokeshire). *Q. J. Geol. Soc. London*, **68**, 374–401.

Thorogood, E.J. (1990). Provenance of the pre-Devonian sediments of England and Wales: Sm-Nd isotopic evidence. *J. Geol. Soc. London*. **147**. 591–94.

Thorpe, R.S., Beckinsale, R.D., Patchett, P.J., Piper A., Davies, G.R. and Evans, J.A. (1984). Crustal growth and late Precambrian-early Paleozoic plate tectonic evolution of England and Wales. *J. Geol. Soc. Lond.*, **141**, 521–536.

Tirsgaard, H. (1993). The architecture of Precambrian high energy tidal channel deposits: an example from the Lyell Land Group (Eleonore Bay Supergroup), northeast Greenland. *Sed. Geol.*, **88**, 137–152.

Todd, S.P. (1989). Stream-driven, high-density gravelly traction carpets: possible deposits in the Trabeg Conglomerate Formation, SW Ireland and some theoretical considerations of their origin. *Sedimentology*, **36**, 513–530.

Tokuhashi, S. (1996). Shallow-marine turbiditic sandstones juxtaposed with deep-marine ones at the eastern margin of the Niigata Neogene backarc basin, central Japan. *Sed. Geol.*, **104**, 99–116.

Torsvik, T.H., Smethurst, M.A., Meert, J.C., Van der Voo, R., McKerrow, W.S., Brasier, M.D., Sturt, B.A. and Walderhaug, H.J. (1996). Continental break-up and collision in the Neoproterozoic and Palaeozoic – A tale of Baltica and Laurentia. *Earth Sci. Rev.* **40**. 229–258.

Tortosa, A., Palamares, M. and Arribas, J. (1991). Quartz grain types in Holocene deposits from the Spanish Central System: some problems in provenance analysis. *Geol. Soc. London* Spec. *Publ.*, **57**, 47–54.

Trop, J.M. and Ridgeway, K.D. (1997). Petrofacies and provenance of a Late Cretaceous suture zone thrust-top basin, Cantwell Basin, Central Alaska Range. *J. Sed. Res.*, **67**, 469–485.

Turner, P. (1979). Diagenetic origin of Cambrian marine red beds: Caerfai Bay Shales, Dyfed, Wales. *Sed. Geol.*, **24**, 269–281.

Turner, P. (1977). Notes on the depositional environment of the Lingula Flags in Dyfed, South Wales. *Proc. Yorkshire Geol. Soc.*, **41**. 199–202.

Vail, P.R. and Todd, R.G. (1981). North Sea Jurassic unconformities, chronostratigraphy and global sea level changes from seismic stratigraphy. In: *Petroleum Geology of the NW Continental Shelf, Proceedings,* 216–235.

Vail, P.R., Mitchum, R.M., Jr., Todd., R.G., Widmier, J.M., Thompson, S., III, Sangree, J.B., Bubb., J.N. and Hatlied, W.G. (1977). Seismic stratigraphy and sea level changes. In: *Seismic Stratigraphy – Applications to Hydrocarbon exploration* (Ed. by C.E. Payton). *Mem. Am. Ass. Petrol. Geol. Bull.*, **26**, 49–62.

Van der Plas, L. and Tobi, A.C. (1965) A chart for judging the reliability of point counting results. *Am. J. Sci.*, **263**, 87–90.

Van Wagoner, J.C., Posamentier H.W., Mitchum, R.M., Vail P.R., Sarg, J.F., Loutit, T.S., and Hardenbol, J. (1988). An overview of the fundamentals of sequence stratigraphy and key definitions. In: *Sea-level changes – an integrated approach* (Ed. by C.K. Wilgus,

B.S. Hastings, C.G. St C Kendall, H.W. Posamentier, C.A. Ross, and J.C. Van Wagoner), *SEPM Spec. Publ.*, **42**, Tulsa, 39–45.

Velbel, M.A. and Saad, M.K. (1991). Palaeoweathering or diagenesis as the principle modifier of sandstone framework composition? A Case from some Triassic rift-*valley redbeds of eastern North America. In: Developments* in sedimentary provenance studies (Ed. by A.C. Morton, S.P. Todd and P.D.W. Haughton). *Geol. Soc. London* Spec. *Publ.*, **57**, 91–99.

Vincent, C.E. (1986). Processes affecting sand transport on a storm-dominated shelf. In: Shelf Sands and Sandstone (Ed. by R.L. Knight and J.R. McLean). *Can. Soc. Pet. Geol. Mem.*, **11**, 524–132.

Vincent, S.J. (2001). The Sis palaeovalley: a record of proximal fluvial sedimentation and drainage basin development in response to Pyrenean mountain building. *Sedimentology*, **48**, 1235–1276.

Visher, G.S. (1969). Grain size distribution and depositional processes. *J. Sed. Petrol.*, **39**, 1074–1106.

Visser, M.J. (1980). Neap-spring cycles reflected in Holocene subtidal large-scale bedform deposits. A preliminary note. *Geology*. **8**, 543–546.

von Eynatten, H. and Gaupp, R. (1999). Provenance of Cretaceous synorogenic sandstones in the Eastern Alps: constraints from the framework petrography, heavy minerals analysis and mineral chemistry. *Sed. Geol.*, **124**, 81–111.

Vos, R.G., Eriksson, K.A., (1977). An embayment model for tidal and wave swash deposits occurring within a fluvially dominated middle Proterozoic sequence in South Africa. *Sed. Geol.*, **18**, 161–173.

Walker, R.G. (1965). The origin and significance of the internal sedimentary structures of turbidites. *Proc. Yorks. Geol. Soc.*, **35**. 1–32.

Walker, R.G. (1975). Generalized facies models for Resedimented conglomerates of turbidite association. *Geol. Soc. Am. Bull.*, **86**, 737–748.

Walker, R.G. (1977). Deposition of Upper Mesozoic resedimented conglomerates and associated turbidites in southwestern Oregon. *Geol. Soc. Am. Bull.*, **80**, 273–285.

Walker, R.G. (1984). Shelf and shallow marine sands. In: *Facies models* (Ed. by R.G. Walker). *Geosci. Can. Reprint Ser. 1. Geol. Ass. Can.*, Waterloo, Ontario, 141–170.

Wan, Z. and Shen, S. (1978). Hyperconcentrated flows in relation with sedimentation of the Yellow River and its tributaries. In: *Research Group of Yellow River Sedimentation* (Ed. by Z. Wan and S. Shen). Selected Research Reports on Sedimentation of the Yellow River, (in Chinese).

Wang, Y. (1983). The mudflat coast of China. Can. J. Fisheries Aquatic Sci., 40, 160–171.

Wasson, R.J. (1977). Catchment processes and the evolution of alluvial fans in the lower Derwent valley, Tasmania. *Geomorphology*, **21**, 147–168.

Weirich, F. (1989). The generation of turbidity currents by subaerial debris flows. *Geol. Soc. Am. Bull.*, **101**, 278-291.

Wells, J.T. and Coleman, J.M. (1981) Physical processes and fine-grained sediment dynamics, coast of Surinam, South America. *J. Sed. Petrol.*, **51**. 1053–1068.

Weltje, G.J. (1994). Provenance and dispersal of sand-sized sediment. *Geol. Ultaiectina*, **121**, 1–208.

Wescott, W.A. (1993). Geomorphic thresholds and complex response of fluvial systems – some implications for sequence stratigraphy. *Am. Ass. Petrol. Geol. Bull.*, **77**, 208–218.

Wescott, W.A. and Ethridge, F.G. (1980). Fan-delta sedimentology and tectonic setting – Yallahs fan-delta, southeast Jamaica. *Am. Ass. Petrol. Geol. Bull.*, **64**, 374–399.

Wescott, W.A. and Ethridge, F.G. (1982). Bathymetry and sediment dispersal dynamics along the Yallahs fan-delta front, Jamaica. *Mar. Geol.*, **46**, 245–260.

Wescott, W.A. and Ethridge, F.G. (1990). Fan-delta in coastal settings. In: *Alluvial Fans: a Field Approach* (Ed. by A.H. Rachocki and M. Church). Wiley, Chichester, 195–211.

Westergård, A.H. (1946). Agnostidea of the Middle Cambrian of Sweden. Sver. Geol. Unders. Avh., **Ser. C**, 477–

Wheatcroft, R. A. (2000). Oceanic flood sedimentation: a new perspective. *Cont. Shelf Res.*, **20**, 2059–2066.

Wheatcroft, R.A., Borgeld, J.C., Drake, D.E., Leithold, E.L., Nittrouer, C.A. and Sommerfield, C.K. (1996). The anatomy of an oceanic flood deposit. *Oceanography*, **9**, 158–162.

Wheatcroft, R.A., Borgeld, J.C., Drake, D.E., Leithold, E.L. and Nittrouer, C.A. (1997). Rapid and widespread dispersal of flood sediments on the northern California margin. *Geology*, **25**, 163–166.

Whitaker, J.H. McD. 1973. "Gutter casts" a new name for scour-and-fill structures: with examples from the Llandoverian of Ringerike and Malmoya, Southern Norway. *Norsk Geologisk Tidsskrift* , **53**, 403–417.

Wignall, P.B. (1989). Sedimentary dynamics of the Kimmeridge Clay: tempests and earthquakes. *J. Geol. Soc. London*, **146**, 273–284.

Wilkinson, I. and Smith, M. (1988). Basement fractures in North Wales: their recognition and control on Caledonian deformation. *Geol. Mag.*, **125**, 301–306.

Williams, A. Strachan, I, Bassett, D.A., Dean, W.T., Ingham, J.K., Wright, A.D. and Whittington, H.B. (1972). A correlation of Ordovician rocks of the British Isles. *Geol. Soc. Lond. J. Spec. Rep.*, **3,** 1–74.

Williams, B.P.J. and Stead, J.T.G. (1982). The Cambrian rocks of the Newgale–St David's area. In *Geological Excursions in Dyfed, South-west Wales* (Ed. by M.G. Bassett), National Museum of Wales, Cardiff, 27–49.

Williams, T.G. (1934). The Pre-Cambrian and Lower Palaeozoic Rocks of the eastern end of the St David's Precambrian area, Pembrokeshire. *Q. J. Geol. Soc. London*, **90**, 32–78.

Winn, Jr., R.D. (1991). Storm deposition in marine sand sheets: Wall Creek Member, Frontier Formation, Powder River Basin, Wyoming. *J. Sed. Petrol.*, **61**, 86–100.

Wood, D.S. (1974). Ophiolites, melanges, blueschists and ignimbrites: early Caledonian subduction in Wales? In: *Modern and Ancient Geosynclinal Sedimentation* (Ed by R.H. Dott and R.H. Shaver). *Spec. Publ. Soc. Econ. Paleont. Mineral.*, **19**, 187–194.

Woodcock, N.H. (1984). Early Palaeozoic sedimentation and tectonics in Wales. *Proc.* Geol. Ass., **95**, 323–335.

Woodcock, N.H. (1986). The role of strike-slip fault systems at plate boundaries. Royal *Soc. Lond. Phil. Trans., Ser. A*, **317**, 13–29.

Woodcock, N.H. (1990). Sequence stratigraphy of the Palaeozoic Welsh Basin. *J. Geol. Soc. Lond.*, **147**, 537–547.

Woodcock, N.H. (2000). The Cambrian and earliest Ordovician quesiscent margin of Gondwana. In: *Geological History of Britain and Ireland* (Ed. by N.H. Woodcock and R. Strachan). Blackwell Sciences, 141–152.

Woodcock, N.H. and Strachan, R. (2000). Geological history of Britain and Ireland. Blackwell Sciences, 411 pp.

Woodland, A.W. (1946). The petrology of the sediments mentioned in Matley and Wilson (1946) – the Harlech Dome. Q.*J. Geol. Soc. Lond.*, **102**, 1–40.

Wright, A.E., Fairchild, I.J., Moseley, F. and Downie, C. (1993). The Lower Cambrian Wrekin Quartzite and the age of the unconformity on the Ercall Granophyre. *Geol. Mag.*, **130**, 257–264.

Wright, L.D., Friedrichs, C.T., Kim, S.C. and Scully, M.E. (2001). Effects of ambient currents and waves on gravity-driven sediment transport on continental shelves. *Mar. Geol.*, **175**, 25–45.

Wright, L.D., Yang, Z., Bornhold, B.D., Keller, G.H., Prior, D.B. and Wiseman Jr., W.J. (1986). Hyperpycnal flows and flow fronts over the Huanghe (Yellow River) delta-front. *Geo-mar. Lett.*, **6**, 97–105.

Wright, V.P. and Burchette, T. (1996). Shallow-water carbonate environments. In: Sedimentary Environments, Processes, Facies and Stratigraphy, (Ed. by H.E. Reading). Blackwell Science, Oxford, 325–394.

Wysocka, A. and Swierczewska, A. (2003). Alluvial deposits from the strike-slip fault Lo River Basin (Oligocene/Miocene), Red River Fault Zone, north-western Vietnam. *J. Asian Earth Sci.*, **21**, 1097–1112.

Xu S., Shao X., Cheng Z. and Yan Q. (1989). Research on storm deposit sequences of Yangtze Delta. *Chinese Science*, **7**, 767–773.

Yeo, R.K. and Risk, M.J. 1981. The sedimentology, stratigraphy, and preservation of intertidal deposits in the Minas Basin System, Bay of Fundy. *J. Sed. Petrol.*, **51**. 246–60.

Yokokawa, M. (1995). Combined flow ripples: genetic experiments and applications for geological records. *Kyushu University, Faculty of Science, Memoirs, Series D, Earth and Planetary Sci.*, **29**, 1–38.

Yokokawa, M., Masuda, F. and Endo, N. (1995). Sand particle movement on migrating combined-flow ripples. *J. Sed. Res.*, **A65**, 40–44.

Young, T.P. and Dean, W.T. (1995). Cambrian stratigraphy of St Tudwel's Peninsula, Gwynedd, northwest Wales: Reply. *Geol. Mag.*, **132**, 622–623.

Young, T.P., Martin, F. Dean, W.T. and Rushton, A.W.A. (1994). Cambrian stratigraphy of St Tudwels Peninsula, North Wales. *Geol. Mag.*, **131**. 335–60.

Zuffa, G.G. (1985). Optical analysis of arenites: influence of methodology on compositional results. In: *Provenance of Arenites* (Ed. by G.G. Zuffa). D. Reidel, The Netherlands, 165–189.